

# **NOVEL CATIONIC SULFUR REAGENTS AND THEIR APPLICATION IN ELECTROPHILIC GROUP-TRANSFER REACTIONS**

Dissertation

zur Erlangung des mathematisch-naturwissenschaftlichen Doktorgrades

“Doctor rerum naturalium”

der Georg-August-Universität Göttingen

im Promotionsprogramm: Chemie

der Georg-August-University School of Science (GAUSS)

vorgelegt von

Kai Florian Gustav Averagesch

aus Essen, Deutschland

Göttingen, 2019

## Betreuungsausschuss

Prof. Dr. Manuel Alcarazo (Institut für Organische und Biomolekulare Chemie, Tammannstr. 2, 37077 Göttingen)

Prof. Dr. Franc Meyer (Institut für Anorganische Chemie, Tammannstr. 4, 37077 Göttingen)

## Mitglieder der Prüfungskommission

Referent: Prof. Dr. Manuel Alcarazo (Institut für Organische und Biomolekulare Chemie, Tammannstr. 2, 37077 Göttingen)

Korreferent: Prof. Dr. Franc Meyer (Institut für Anorganische Chemie, Tammannstr. 4, 37077 Göttingen)

## Weitere Mitglieder der Prüfungskommission:

Prof. Dr. Claudia Steinem (Institut für Organische und Biomolekulare Chemie, Tammannstr. 2, 37077 Göttingen)

Prof. Dr. Konrad Koszinowski (Institut für Organische und Biomolekulare Chemie, Tammannstr. 2, 37077 Göttingen)

Prof. Dr. Dietmar Stalke (Institut für Anorganische Chemie, Tammannstr. 4, 37077 Göttingen)

Dr. Christian Sindlinger (Institut für Anorganische Chemie, Tammannstr. 4, 37077 Göttingen)

Tag der mündlichen Prüfung: 18. Dezember 2019

I hereby declare, that this dissertation has been written independently and with no sources or aids other than those quoted. The parts performed by project collaborators have been clearly indicated.

---

Kai F. G. Aversch

## ABBREVIATIONS

°C	degree Celsius
3c-4e	three-center four-electron
9-BBN	9-Borabicyclo[3.3.1]nonane
4CzIPN	2,4,5,6-Tetra(9 <i>H</i> -carbazol-9-yl)isophthalonitrile
4POBN	$\alpha$ -(4-Pyridyl <i>N</i> -oxide)- <i>N</i> -tert-butyl nitron
A <sup>-</sup>	generic Anion
ABX	Azido-benziodoxol(on)e
Ac	acetyl
acac	acetylacetonate anion
Ad	Adamantyl
Anthr	Anthranyl
aq.	aqueous media
Am	Amyl
AMLA	ambiphilic metal ligand activation
atm	Atmosphere (unit)
ATR	Attenuated total reflectance
Å	Ångström (unit)
B	generic base
<i>B</i> -I-9-BBN	9-Iodo-9-borabicyclo[3.3.1]nonane
BDMAE	bis(2-dimethylaminoethyl) ether
BIES	base-assisted internal electrophilic(-type) substitution
Boc	<i>tert</i> -Butyloxycarbonyl
bs	broad NMR singlet
Bu	butyl
Bn	benzyl
BXs	Benziodoxol(on)es
Bz	benzoyl
ca.	circa
<i>calcd.</i>	calculated
cat.	catalytic amount
CBX	Cyanobenziodoxol(on)e
CCSD	coupled cluster single double
CDBX	Cyano-dimethyl-benziodoxol(on)e
cm	centimetres
CMD	concerted metalation-deprotonation
CTA	Chain-transfer agent
CuAAC	copper-catalyzed azide–alkyne cycloaddition
CuTC	Copper(I) thiophene-2-carboxylate
Cy	cyclohexyl
$\delta$	chemical shift
d	doublet (NMR)
DBU	1,8-Diazabicyclo[5.4.0]undec-7-ene



DCE	dichloroethane
DCM	dichloromethane
dd	doublet of doublets (NMR)
ddd	doublet of doublets of doublets (NMR)
ddt	doublet of doublet of triplets (NMR)
dddt	doublet of doublet of doublet of triplets (NMR)
deg	Degree (Angle)
DG	directing group
DIPEA	<i>N,N</i> -Diisopropylethylamine
DMA	<i>N,N</i> -dimethylacetamide
DMAP	4-Dimethylaminopyridine
DMTA	<i>N,N</i> -dimethylthioacetamide
dme	Dimethoxyethane
DMF	<i>N,N</i> -Dimethylformamide
DMTF	<i>N,N</i> -dimethylthioformamide
DMSO	dimethyl sulfoxide
dppen	1,2- <i>cis</i> (diphenylphosphino)ethylene
dt	doublet of triplets (NMR)
e <sup>-</sup>	electron
<i>e.r.</i>	enantiomeric ratio
EBX	Ethynylbenziodoxol(on)e
EDG	electron-donating group
<i>ee</i>	enantiomeric excess
EI	Electron Ionization
El	Generic Electrophile
EN	Electronegativity
equiv	equivalents
ESI	Electrospray Ionization
Et	Ethyl
<i>et al.</i>	<i>et alii</i>
eV	electronvolt
EWG	electron-withdrawing group
g	gram
GC	Gas Chromatography
GP	General Procedure
h	hour
hept	heptet (NMR)
HMBC	Heteronuclear Multiple Bond Correlation
HOMO	Highest Occupied Molecular Orbital
HRMS	High Resolution Mass Spectroscopy
HSQC	Heteronuclear Single Quantum Coherence
Hz	Herz
<i>i.e.</i>	<i>id est</i>
<i>i</i>	<i>iso-</i>
IES	internal electrophilic substitution

IR	infrared spectroscopy
<i>J</i>	coupling constant
K	Kelvin
kcal	kilocalorie
KIE	kinetic isotope effect
kJ	kilojoule
L	generic ligand
L	litre
LA	Lewis acid
LB	Lewis base
LC	Liquid chromatography
LDA	Lithium diisopropylamide
LED	Light-emitting diode
LiHMDS	Lithium bis(trimethylsilyl)amide
LR	Lawesson's Reagent
<i>m</i>	<i>meta</i> -
m	multiplet (NMR)
m/z	mass-to-charge ratio
M	molar
Me	methyl
min	minute
MS	Mass Spectrometry
NCTS	<i>N</i> -Cyano- <i>N</i> -phenyl- <i>p</i> -toluenesulfonamide
NFSI	<i>N</i> -Fluorobenzenesulfonimide
NFOBS	<i>N</i> -fluoro- <i>o</i> -benzenedisulfonimide
NMR	Nuclear Magnetic Resonance
NOE	Nuclear Overhauser Effect
Nu	generic nucleophile
NXS	N-X-succinimide
<i>o</i>	<i>ortho</i> -
oct	octet (NMR)
p	pentet (quintet)
p.t.	proton transfer
<i>p</i>	<i>para</i> -
Ph	phenyl
Piv	Pivaloyl
ppm	parts per million
Pr	propyl
pyr	pyridine
q	quartet (NMR)
R	generic substituent
RAFT	Reversible addition-fragmentation chain transfer
rt	room temperature
s	second
s	singlet (NMR)

SBM/ $\sigma$ BM	sigma/ $\sigma$ bond metatesis
sept	septet (NMR)
SET	Single Electron Transfer
sext	sextet (NMR)
Sir	Saturation-Inversion-Recovery
S <sub>N</sub> Ar	Nucleophilic aromatic substitution
t	time
t	triplet (NMR)
T	Temperature
<i>t</i>	<i>tert</i> -
TBAF	Tetra- <i>n</i> -butylammonium fluoride
TBPB	<i>tert</i> -Butyl peroxybenzoate
td	triplet of doublets (NMR)
Tf	Triflyl (trifluoromethanesulfonyl)
THF	tetrahydrofuran
TIPS	triisopropylsilyl
TLC	Thin Layer Chromatography
TM	Transition Metal
TMEDA	Tetramethylethylenediamine
TMG	1,1,3,3-Tetramethylguanidine
TMS	trimethylsilyl
Tol	Tolyl
Ts	Tosyl (toluenesulfonyl)
tt	triplet of triplets (NMR)
UV	Ultraviolet
<i>vs</i>	<i>versus</i>
X	generic halogen
Z	generic substituent



## ACKNOWLEDGEMENTS

Zuallererst gilt mein Dank Prof. Dr. Manuel Alcarazo, dafür mich in seine Arbeitsgruppe aufgenommen und mir die Gelegenheit gegeben zu haben, meine Promotion durchzuführen. Ich danke ihm dafür, mir von Anfang an die Möglichkeit gegeben zu haben, Forschung nach meiner eigenen Neugierde zu betreiben und mich dabei konsequent zu unterstützen. Weiterhin danke ich ihm für seine Unermüdlichkeit darin, trotz wechselnder Umgebung, die bestmöglichen Arbeitsbedingungen für seine Mitarbeiter geschaffen zu haben. Schlussendlich bin ich ihm dankbar für jedweden wissenschaftlichen als auch nicht-wissenschaftlichen Wissensgewinn während meiner Promotionszeit, der ohne ihn nicht möglich gewesen wäre.

Mein Dank gilt außerdem Prof. Dr. Franc Meyer, für die gewissenhafte Übernahme des Zweitgutachtens.

Ich danke den Mitarbeitern des Max-Planck Instituts für Kohlenforschung, besonders Sigrid Lutz und Gerlinde Mehler dafür, die Anfangsphase der Promotion, so leicht wie möglich gemacht zu haben. Ebenfalls bin ich den Mitarbeitern der Georg-August Universität Göttingen dankbar, zuerst für die Unterstützung während der Umzugsphase nach Göttingen und weiterhin die stetige Hilfsbereitschaft in formellen Angelegenheiten sowie die freundliche Atmosphäre am Arbeitsplatz. Hier gilt mein Dank besonders, Martina Pretor, Sabine Schacht, Dr. Christopher Golz, Dr. Sergei I. Kozhushkov und Martin Simon.

Ich danke den Serviceabteilungen des MPI, sowie der Universität Göttingen, den NMR-, Massenspektrometrie- und Röntgenkristallstruktur-Abteilungen, für ihre gewissenhafte Arbeit, die Messung zahlreicher analytischer Proben.

Ein großer Dank gilt allen momentanen und ehemaligen Arbeitskollegen der Forschungsgruppe, die meine Promotion zu einer einzigartigen Erfahrung gemacht haben: Dr. Elisa González Fernández, Dr. Hendrik Tinnermann, Dr. Lianghu Gu, Dr. Isaac Alonso, Dr. Jonathan Dube, Dr. Leo Nicholls, Dr. Alejandro García Barrado, Dr. Yin Zhang, Dr. Javier Peña, Dr. Garazi Talavera, Lukas Schaaf, Menno Hinrich, Maximilian Marx, Dr. Bernd Waldecker, Dr. Samuel Suarez Pantiga, Dr. Vijaykumar Gonela, Dr. Xiangdong Li, Dr. Jianwei Zhang, Marvin Böhm, Tim Johannsen, Thierry Hartung, Pablo Redero Garcia, Morwenna Mögel, Christian Rugen, Kristin Sprenger, Kevin Kafuta, Sebastian Kolle, Adam Zielinski, Steve Karreman und Henner Pesch.

Ich bin dankbar für all die Freundschaften die geschlossen wurden, auf dass sie lange währen.

Für das Korrekturlesen dieser Arbeit und die hilfreichen Anmerkungen danke ich noch einmal Adaś Zielinski, Dr. Bernd Waldecker und Dr. Sergei I. Kozhushkov.

Ich danke meiner Familie und meiner Freundin für die unentwegte Unterstützung, die mich bis hierhin gebracht hat. Danke Mama, danke Nils, danke Kim.

*„...and I don't care how tough you are, life will beat you to your knees and keep you there permanently if you let it. You, me, or nobody is gonna hit as hard as life. But it ain't about how hard you hit. It's about how hard you can get hit and keep moving forward; how much you can take and keep moving forward.”*

*-Rocky Balboa*

## TABLE OF CONTENTS

NOVEL CATIONIC SULFUR REAGENTS AND THEIR APPLICATION IN ELECTROPHILIC GROUP-TRANSFER REACTIONS .....	1
INTRODUCTION.....	12
NUCLEOPHILES, ELECTROPHILES AND THEIR INTERCONVERTABILITY .....	12
ELECTROPHILIC TRANSFER REAGENTS.....	15
ELECTROPHILIC CYANATION .....	18
TOLUENESULFONYL CYANIDE (TSCN) AND N-CYANOSULFONAMIDES .....	19
CYANOBENZOTRIAZOLE AND CYANO(BENZ)IMIDAZOLE .....	21
Cyano Benziodoxol(on)es (CBX).....	23
CATIONIC THIOCYANATES .....	27
ELECTROPHILIC ALKYNYLATION .....	29
N-NUCLEOPHILES .....	31
<i>P</i> -, <i>O</i> -, <i>S</i> -NUCLEOPHILES.....	35
C-NUCLEOPHILES .....	40
DITHIOESTER, THIOAMIDES AND THIONOESTERS .....	43
SYNTHESIS OF DITHIOESTERS, THIOAMIDES AND THIONOESTERS .....	46
PROPERTIES OF DITHIOESTERS, THIOAMIDES AND THIONOESTERS.....	56
APPLICATION AND REACTIVITY OF DITHIOESTERS, THIOAMIDES AND THIONOESTERS .....	58
ELECTROPHILIC ALKYNYLATION WITH TRANSITION METAL GENERATED NUCLEOPHILES .....	60
C–H FUNCTIONALIZATION .....	60
C–H FUNCTIONALIZATION -ALKYNYLATION.....	66
C–H FUNCTIONALIZATION UTILIZING ACTIVATED ACETYLENES .....	71
RESULTS AND DISCUSSION.....	77
SYNTHESIS AND EVALUATION OF NOVEL PYRIDINIUM BASED ELECTROPHILIC TRANSFER REAGENTS .....	77
PROJECT AIMS .....	77
SYNTHESIS, CHARACTERISTIC PROPERTIES AND APPLICATION OF NOVEL PYRIDINIUM-BASED ELECTROPHILIC TRANSFER REAGENTS .....	80
CONCLUSION AND OUTLOOK.....	95
C–H FUNCTIONALIZATION UTILIZING THIOIMIDAZOLONE-BASED ELECTROPHILIC TRANSFER REAGENTS .....	97
PROJECT AIMS .....	97
PRELIMINARY SCREENING.....	98
AMIDES AS WEAKLY COORDINATING DIRECTING GROUPS.....	101
MECHANISTIC INVESTIGATIONS.....	111
THE DIAZENYL FUNCTIONALITY AS A DIRECTING GROUP .....	116
CONCLUSION AND OUTLOOK.....	121

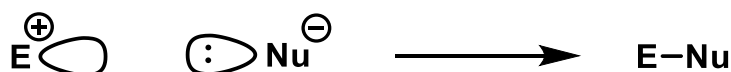
BIBLIOGRAPHY.....	123
EXPERIMENTAL.....	130
TOPIC: "SYNTHESIS AND EVALUATION OF NOVEL PYRIDINIUM-BASED ELECTROPHILIC TRANSFER REAGENTS" .....	131
TOPIC: "C–H ACTIVATION UTILIZING THIOIMIDAZOLONE-BASED ELECTROPHILIC TRANSFER REAGENTS" .....	152
NON- AND LOW REACTIVE SUBSTRATES .....	152
APPENDIX.....	174
X-RAY STRUCTURES .....	175
SPECTRA.....	234



## INTRODUCTION

### NUCLEOPHILES, ELECTROPHILES AND THEIR INTERCONVERTABILITY

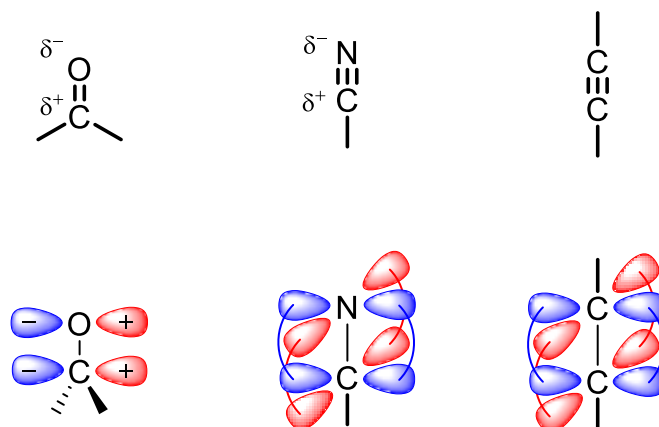
One of the most fundamental concepts of organic chemistry is the classification of organic molecules or fragments thereof into electrophiles (Greek: “electron loving”) and nucleophiles (Greek: “nucleus loving”). Nucleophiles are electron rich; they possess a filled lone pair or  $\pi$ -orbital resulting in a partial or fully developed negative charge, while electrophiles are electron deficient and are characterized by a partial or fully developed positive charge or an incomplete octet. They react with each other by donation of the electron pair from the occupied orbital of the nucleophile into the vacant orbital of the electrophile, forming a new molecular bond (Scheme 1).



Scheme 1: Reaction of a generic electrophile with a generic nucleophile in an elementary step.

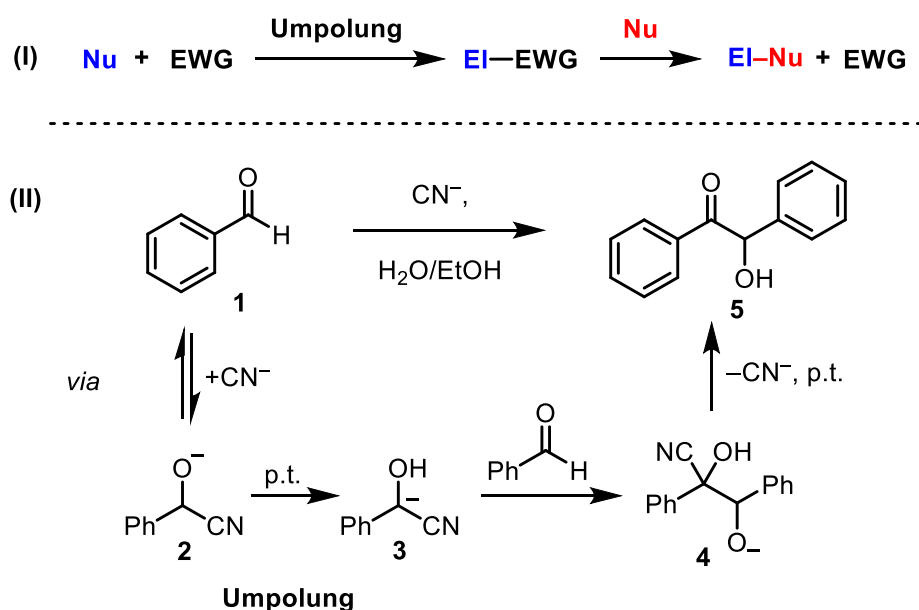
The successful identification of nucleophiles and electrophiles enables the chemist to predict the most probable outcome of an elementary step of a reaction.

In organic chemistry functional groups also can be categorized into nucleophilic and electrophilic, or ones that hold electrophilic and nucleophilic positions. Arguably, the most commonly used example is the carbonyl moiety, where a partially positive charged carbon (electrophilic) is bonded to a partially negative charged oxygen (nucleophilic) by the means of a  $\sigma$ - and  $\pi$ -bond. Similar polarization of a carbon bound to a heteroatom is found in nitriles, however, additionally, their bonding situation is resemblant to that of alkynes, since they both possess a  $\sigma$ - and two  $\pi$ -bonds (Scheme 2)<sup>[1]</sup>



Scheme 2: Partial polarization and selected orbitals of carbonyl, nitrile, and alkyne functionalities.

The fact, that the electrophilicity of the carbon in carbonyl and nitrile groups is a direct result of its electron withdrawing neighboring atom (O-, N-), can be abstracted and used as a methodology to also tune the electronic properties of other functional groups such as the aforementioned alkynes. By employing an electron withdrawing atom or electron withdrawing group (EWG) adjacent to the functional group, a partial positive charge can be induced or enhanced. In the same manner a partial negative polarization can be introduced or magnified by electron donating atoms or groups (EDG). Furthermore by employing, for example the right EWG adjacent to a partially negative charged atom, this atom can be rendered so electron poor that its reactivity is inverted, and the former nucleophile becomes an electrophile. The conversion of nucleophiles into electrophiles and *vice versa* is known as “Umpolung” or polarity inversion. The concept was originally introduced by SEEBACH and COREY.<sup>[2]</sup> The canonical Umpolung reagent is the cyanide ion, which, for example, finds application in the benzoin condensation, first observed by WÖHLER and LIEBIG.<sup>[3]</sup> Here, the cyanide anion facilitates the reversion of polarity on the carbonyl group of benzaldehyde **1** to generate nucleophile **3**, which can then undergo condensation with another equivalent of benzaldehyde, which functions as electrophile giving benzoin **5**.



Scheme 3: Depiction of a generic initial Umpolung (I) of a nucleophile and a subsequent secondary reaction, and the benzoin reaction (II) as an example for the polarity inversion of a carbonyl group. (p.t. = proton transfer)

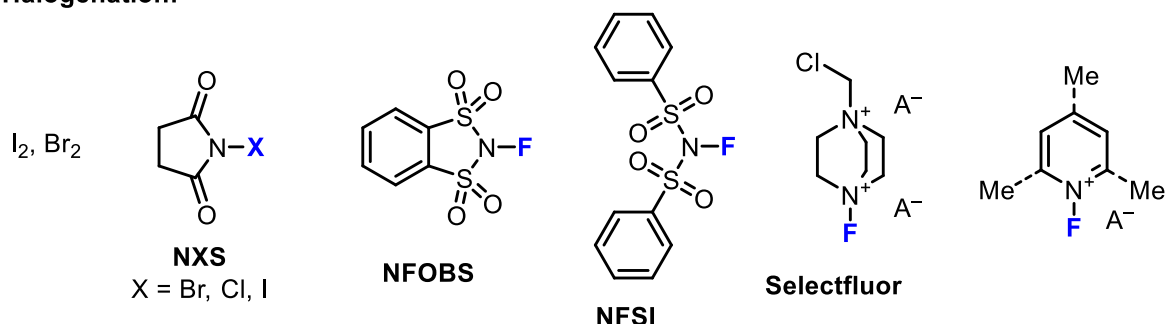
All functional groups possess an intrinsic polarization which is reflected in their most common reactivity. For example, electron rich groups like the cyano group or acetylides classically react as nucleophiles with electrophiles. As a direct result they find broad application in nucleophilic cyanation and alkynylation reactions, respectively. A general approach to broaden the scope of this type of reaction is to invert the polarization in Umpolung, as described above, generating an electrophilic fragment which then, in turn, can react with another nucleophile (Scheme 3-I).

To realize an Umpolung from nucleophile to an electrophile, various groups can be attached to the moiety that needs to be transferred. Generally, they all have electron-withdrawing properties. It is logical that atoms with high electronegativity, such as halides or well-known EWGs like tosyl or triflate, are prominent examples for the realization of Umpolung reactions. The next Chapters will cover the methods that have been developed to facilitate this kind of transformations and cover the reagents that have proven to be most successful in applications.

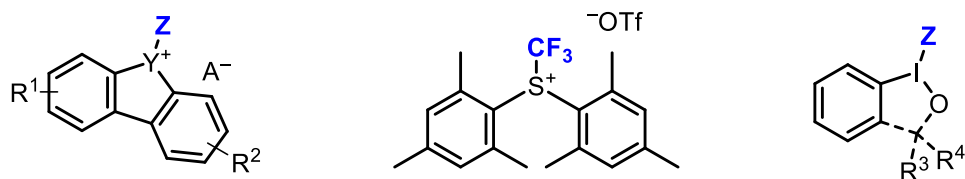
## ELECTROPHILIC TRANSFER REAGENTS

A plethora of different electrophilic transfer reagents, among these several patented and commercially available, are known and their applications have been reported in literature.<sup>[4,5]</sup> In theory, any desired organic fragment can be polarized to undergo an Umpolung and later be transferred, however selected groups are of more significance than others (Scheme 4).

### Halogenation:



### Alkylation, Thiolation:



#### Umemoto reagent and derivatives

Y = S, O, Se, Te

Z = CF<sub>3</sub>, SCF<sub>3</sub>, CN, Alkyne,

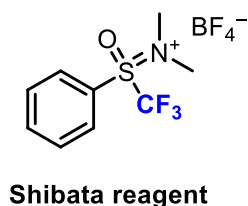
R<sup>1</sup>, R<sup>2</sup> = F, NO<sub>2</sub>, SO<sub>3</sub>, H, Me,

#### Mes-Umemoto

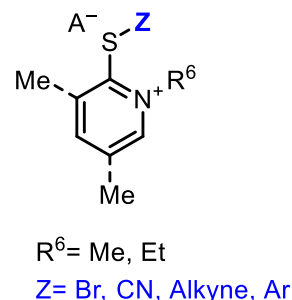
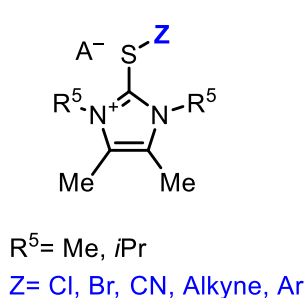
#### Togni reagent, EBX, CBX, ABX and derivatives

R<sup>3</sup> = H, R<sup>4</sup> = O or R<sup>3</sup>, R<sup>4</sup> = Me

Z = CF<sub>3</sub>, CN, N<sub>3</sub>, Alkyne



#### Reagents developed in our group:



Scheme 4: Selected electrophilic transfer reagents (NXS = *N*-X-succinimide, NFOBS = *N*-fluoro-*o*-benzenedisulfonimide, NFSI = *N*-fluorobenzenesulfonimide, EBX = ethynyl-1,2-benziodoxol-3(1*H*)-one, CBX = 1-cyano-1,2-benziodoxol-3-(1*H*)-one, ABX = 1-azido-1,2-benziodoxol-3(1*H*)-one).

As can be seen from Scheme 4, the most prevalent transferred groups are (pseudo)halogens and selected alkyl, perfluoroalkyl, thiol and alkynyl groups. Introduction of halides allows for subsequent functionalization applying classical cross-coupling reactions like the Heck

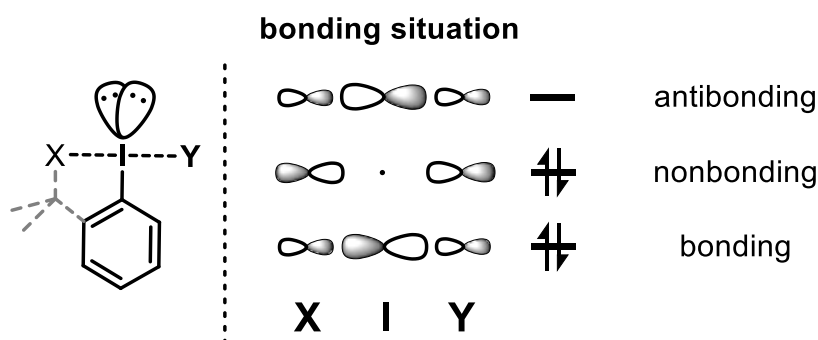
reaction, the Stille, Suzuki-Miyaura, Negishi or Sonogashira-Hagihara coupling.<sup>[6–15]</sup> Other groups like the trifluoromethyl moiety change the stability or solubility of the resulting product. Introduction of a CF<sub>3</sub> group plays a significant role in drug development to increase the stability of compounds towards metabolization and to increase the acceptor properties of hydrogen bonds. This group is normally introduced into a key structure by manipulation of trifluoroacetic acid, for example by condensation. However, the Umemoto reagent (Scheme 4) opens up new possibilities to introduce such a moiety.<sup>[16]</sup> Other functional groups such as nitriles and alkynes, which effectively are C<sub>1</sub>- and C<sub>2</sub>-synthons, but can also be modified in various other ways, are additional important motifs.

Some of the reagents presented herein possess the properties commonly described as hypervalent. It is duly noted at this point, that the term hypervalent itself and the concept of hypervalency is still a controversial topic.<sup>[17]</sup>

Nevertheless it is necessary to discuss the unique structure and properties of hypervalent compounds due to their relevance for this work. The iodonium salts discussed below, described for the first time by BERINGER in 1965,<sup>[18]</sup> have a unique structure owing to their hypervalency, which is partly reflected in their reactivity (Scheme 5). They adopt a T-shaped geometry with an almost linear **X-I-Y** triad. Stabilization is gained by electron withdrawing axial ligands, which stabilize the molecule due to the 3-center-4-electron bond (3c-4e) in which more electron density resides on the ligands at the ends (**X** & **Y**) than at the center (visualized by the node for the nonbonding orbital of the central atom). The three-centre-four electron bond, has a lower Bond Order than a normal sigma bond and is thus weaker. Attached organic groups **Y** are consequently prone to nucleophilic attack. This allows transfer of organic groups to small molecules and also advanced intermediates.

Furthermore, *trans* influences effecting their stability have been reported.<sup>[19]</sup> Manifestation of *trans* influences in general can be observed by trends in NMR, IR and solid state structures.<sup>[20]</sup> With the recent surge in the use of hypervalent iodine compounds, availability of solid state structures has also increased. Investigations of these towards *trans* influences of the ligands **X** and **Y** lead to the conclusion that combinations of ligands **X** and **Y** where one shows a strong and the other a weak *trans* influence or the scenario in which both ligands have a moderate *trans* influence seem to be favoured. Other scenarios where both ligands **X** and **Y** have strong or weak *trans* influences both result in labile compounds.

How the *trans* influence manifests itself for hypervalent iodine compounds can be explained as follows: In a linear **X-I-Y** hypervalent bonding situation the central iodine retains its 5s<sup>2</sup> lone pair and an exclusively inductive *trans* influence by the **X** ligand is transmitted through the 5p<sub>σ</sub> orbital of the iodine atom. With increasing donor ability of **X**, the **X-I** bond strength increases while the **I-Y** bond *trans* to the **X-I** bond is weakened proportionately, thus making a potential nucleophilic attack towards **Y** easier.<sup>[21]</sup>



Scheme 5: The Rundle-Pimentel orbital model for 3-center-4-electron bonds applied to hypervalent iodonium salts.<sup>[22]</sup>

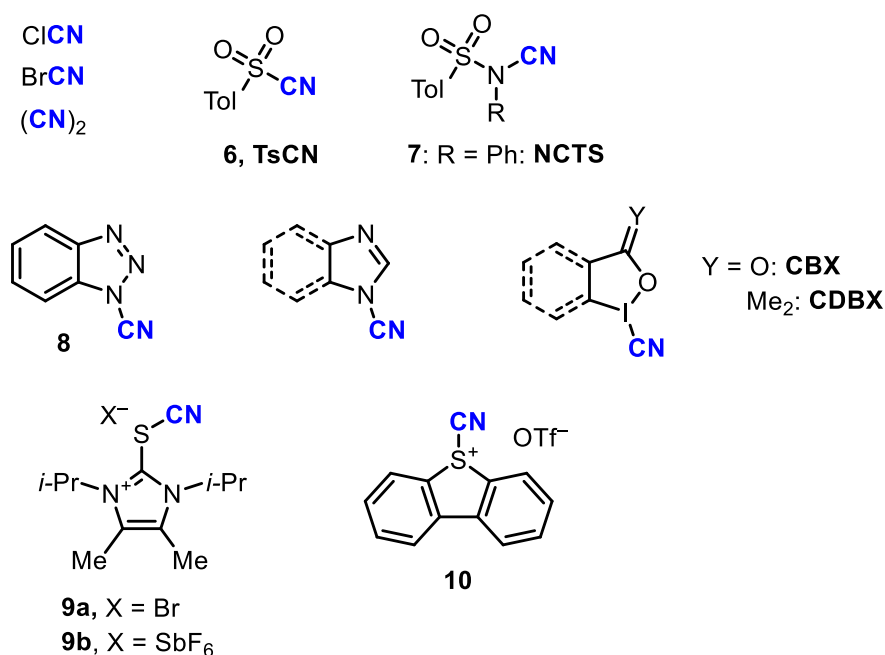
The unique properties, which enable hypervalent iodonium salts to reverse the polarity of certain organic groups in Umpolung reactions, have been unveiled, and their applicability in different research fields is documented in numerous publications. Modification of the structure from acyclic to cyclic, by introduction of an oxy-tether, gives these compounds an increased stability (Scheme 5, **X** = O). Nevertheless, thermal decomposition or decomposition in the presence of Lewis acids, bases or transition metal catalysts remains an issues for hypervalent iodonium salts.<sup>[23]</sup>

Another example for a structure exploited due to its unique properties are (perfluoroalkyl)chalcogen salts, the most prominent member of which is the Umemoto reagent. It was designed after its acyclic predecessor  $\text{Ar}_2\text{S}^+\text{CF}_3\text{SbF}_6^-$ , originally discovered by YAGUPOLSKII.<sup>[5,24,25]</sup> At first developed for electrophilic  $\text{CF}_3^+$  transfer, this motif has now found a significantly broader range of applications.

## ELECTROPHILIC CYANATION

To open up new reaction pathways and enable the synthesis of novel CN-containing compounds, numerous electrophilic cyanating reagents have been developed, commercialized and employed. While the very early reagents like cyanogen chloride, bromide, or dicyan are simple in constitution, their high toxicity in combination with their low boiling points and high vapor pressure are major drawbacks in handling these chemicals even on laboratory scale. A logic improvement consists of attaching a larger, electron withdrawing substituent to the nitrile group giving the resulting compounds a higher boiling point and thus, making them easier to handle. Ideally, with the choice of the correct polarizing group, highly stable solid compounds, which only release the desired electrophilic CN-synthon upon choice of the correct reaction conditions, can be designed.

One of the first steps towards such electrophilic cyanation reagent was taken by KURZER with the synthesis of *N*-cyanosulfonamides in 1949 (Scheme 7-I).<sup>[26]</sup> 32 years later the first successful electrophilic cyanation employing toluenesulfonyl cyanide (TsCN) **6** was reported.<sup>[27]</sup> Over the past 25 years the field experienced a renaissance, and up to today a significant amount of additional electrophilic transfer reagents were developed, underlining the demand to access and broaden this mode of reactivity (Scheme 6).<sup>[28,29–42]</sup>

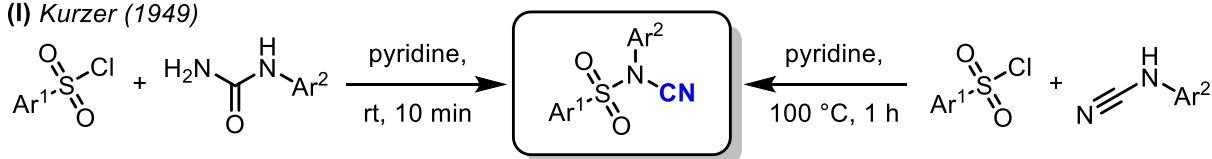


Scheme 6: A selection of electrophilic cyanide transfer reagents (Tol = tolyl, NCTS = *N*-cyano-*N*-phenyl-*p*-methylbenzenesulfonamide, CBX = cyanobenziodoxol(on)e, CDBX = cyano dimethylbenziodoxol(on)e.

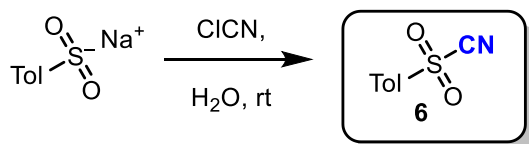
The following Sections will cover the most relevant applications of transfer reagents shown above, by highlighting selected reactions.

## TOLUENESULFONYL CYANIDE (TsCN) AND N-CYANOSULFONAMIDES

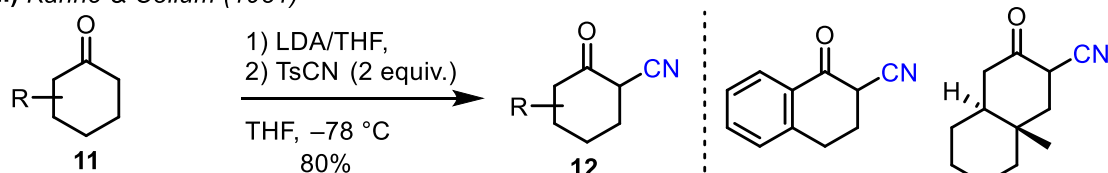
(I) Kurzer (1949)



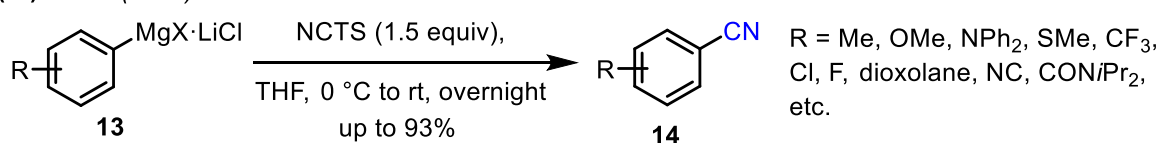
(II) Cox & Ghosh (1969)



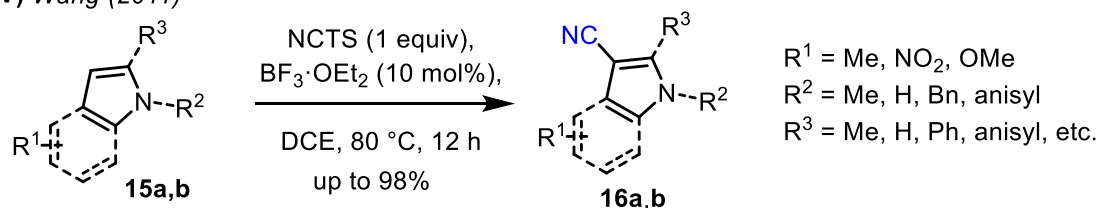
(III) Kahne & Collum (1981)



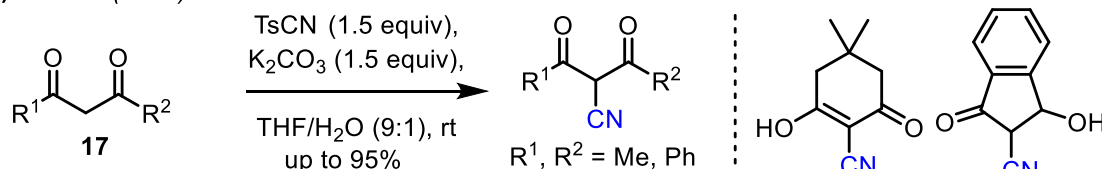
(IV) Beller (2011)



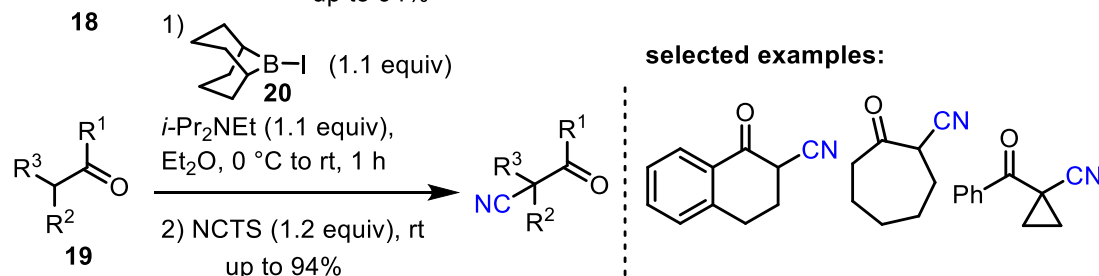
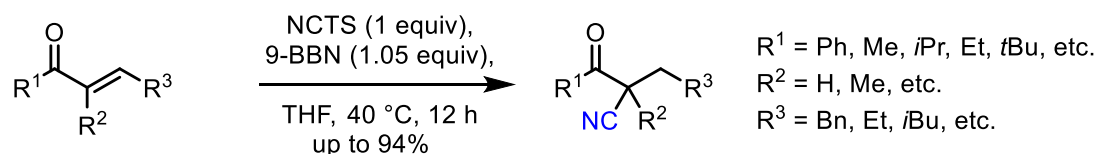
(V) Wang (2011)



(VI) Ibrahim (2013)



(VII) Minakata & Kiyokawa (2016)



Scheme 7: Electrophilic cyanation utilizing *N*-cyanosulfonamides.

A rather early example for the utilization of TsCN (6) as an electrophilic cyanating agent is given by KAHNE and COLLUM (Scheme 7-III).<sup>[27]</sup> Within the context of a natural product



synthesis study, they required a protocol to effectively cyanate a ketone moiety in compounds **11**, without compromising the integrity of an asymmetric center. After successful identification of a protocol utilizing TsCN to obtain  $\beta$ -ketonitriles **12** via lithium enolates, they could show the procedure to be general for five additional examples.<sup>[27]</sup>

30 years later, BELLER and coworkers (Scheme 7-IV)<sup>[33]</sup> realized the first electrophilic cyanation of aryl and heteroaryl Grignard reagents **13** by utilization of *N*-cyano-*N*-phenyl-*p*-methyl-benzenesulfonamide (NCTS, **7**). For selected examples they could also realize monocyantation of dibromoarenes. The relevancy for the developed procedure was further underlined by the exemplary synthesis of three different key building blocks for pharmacological and agrochemical intermediates.<sup>[33]</sup>

Using the same electrophilic cyanating reagent **7** but employing  $\text{BF}_3 \cdot \text{OEt}_2$  as a strong Lewis acid, WANG (Scheme 7-V) could show that both *N*-unsubstituted, *N*-aryl and *N*-alkyl indoles **15a** as well as pyrroles **15b** gave the corresponding heteroarylnitriles **16a,b**. The authors claim the use of an appropriate Lewis acid activates the cyanating agent; however, they do not indicate how.<sup>[34]</sup>

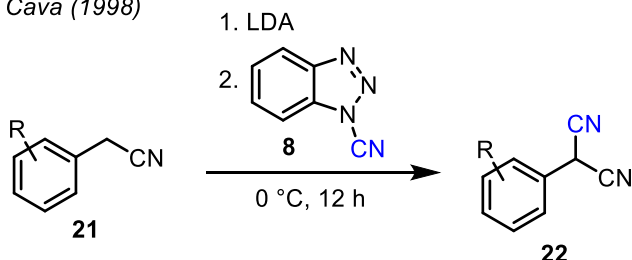
A significantly milder approach compared to that of KAHNE and COLLUM with regard to the use of a base was reported in 2013 by IBRAHIM et al. (Scheme 7-VI). With use of the mild base  $\text{K}_2\text{CO}_3$  instead of strong lithiumorganyls, they were able to cyanate both acyclic and cyclic 1,3-dicarbonyl compounds **17**. Modification of the standard reaction conditions further enabled them to develop an efficient one-pot cyanation/pyrazole formation sequence to 4-cyano pyrazoles.<sup>[31]</sup>

KIYOKAWA and MINAKATA (Scheme 7-VII) could extend the scope of modifiable substrates to  $\alpha,\beta$ -unsaturated ketones **18** by using 9-BBN as a Lewis acid to generate boron enolates via 1,4-hydroboration. Choice of the appropriate reaction temperature and solvent was crucial to facilitate complete hydroboration in this case. By switching from 9-BBN to *B*-I-9-BBN **20** and addition of a base, a protocol for saturated ketones **19** was also elaborated. The latter is remarkably orthogonal to the first system, enabling cyanation in the presence of conjugated alkene moieties with their conservation. During their studies, both TsCN and NCTS appeared to be versatile sources for electrophilic cyanation. A preliminary result with a chiral boron enolate was also reported. The cyanated product was obtained with 94% *ee*, making the reaction to be one of the few efficient examples for enantioselective electrophilic cyanation.<sup>[35]</sup>

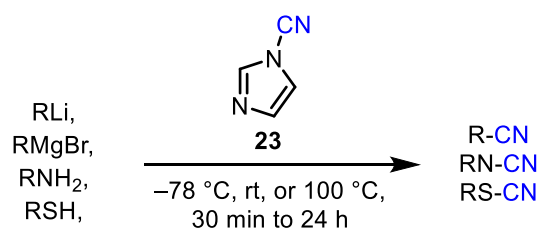
Advantages of both TsCN and NCTS are their mild reaction conditions and high reactivity towards C-nucleophiles. However, as in all nitrogen-based transfer reagents, polarization is relatively weak, and strong nucleophiles are necessary to achieve satisfying results.

## CYANOBENZOTRIAZOLE AND CYANO(BENZ)IMIDAZOLE

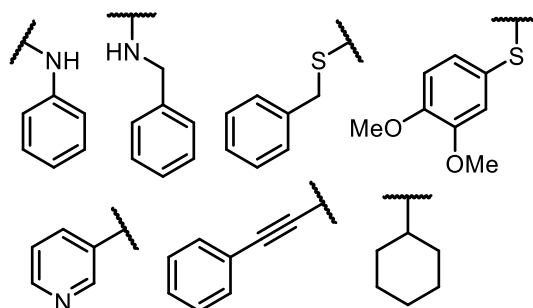
(I) Cava (1998)



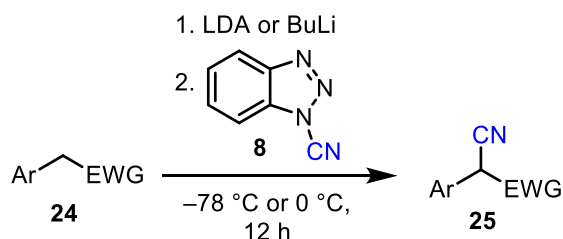
(II) Wu (2000)



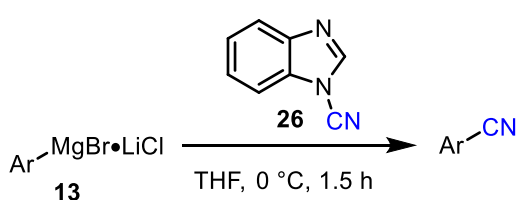
Selected examples:



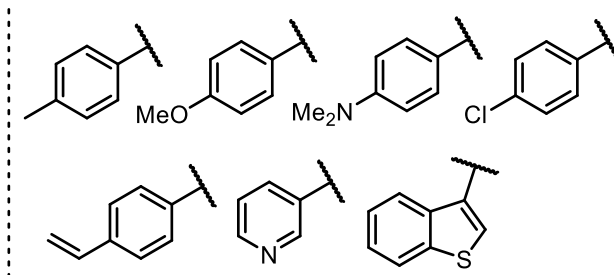
(III) Katritzky (2007)



(IV) Beller (2010)



Selected examples:



Scheme 8: Electrophilic cyanation utilizing cyanobenzotriazole or cyano(benz)imidazole.

Before CAVA et al. (Scheme 8-I) published a two-step way to access 1-cyanobenzotriazole (**8**), only syntheses which resided on the use of either cyanogen chloride or cyanogen bromide were known. In fact, the authors also postulated *in situ* formation of ClCN for their procedure, which is then consumed upon the product formation. Their synthesis, however, is significantly safer since it resides on the use of 5% sodium hypochlorite solution for the chlorination, followed by treatment with sodium cyanide to give 1-cyanobenzotriazole (**8**) after sublimation. They also found the first examples of the use of cyanating agents to obtain arylmalononitriles **22** from arylacetonitriles **21** with employment of LDA as a base.<sup>[29]</sup>

1-Cyanoimidazole (**23**), which was originally used as a coupling partner in polynucleotide synthesis, was found by Wu et al.<sup>[43]</sup> to be a potent <sup>+</sup>CN-synthon for reactions with *N*-, *C*- and *S*-nucleophiles (Scheme **8-II**). Notably, no additional base was necessary. During their experiments with thiols as nucleophiles they observed concomitant disulfide formation, which was caused by further addition of thiol to the already formed thiocyanate product. A major drawback of this reagent is the use of cyanogen bromide for the synthesis.

KATRITZKY (Scheme **8-III**) expanded the chemistry reported by CAVA and showed that not only compounds **24** decorated with EWGs such as ketones, esters, sulfoxides, but in addition also substrates with pyridyl, furyl, pyrrolyl moieties without EWGs undergo electrophilic cyanation facilitated by lithiumorganyls.<sup>[36]</sup>

In analogy to their work with NCTS, BELLER et al. (Scheme **8-IV**) also reported the reaction of arylgrignards **13** with 1-cyanobenzimidazole (**26**). To extend the developed methodology, they also showed that a domino Grignard-coupling/cyanation to give access to 2-cyano-1,1'-biaryls is feasible.<sup>[32]</sup>

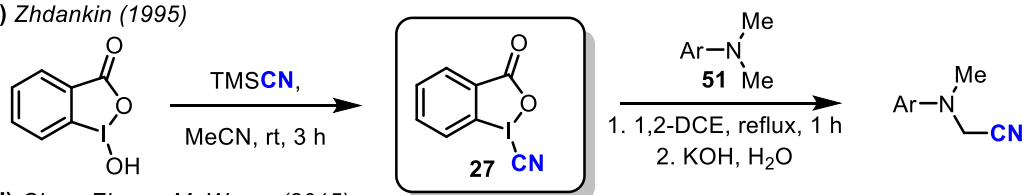
Just like TsCN and NCTS, 1-cyanobenzotriazole (**8**), 1-cyanoimidazole (**23**) and 1-cyanobenzimidazole (**26**) are nitrogen-based reagents and thus mild cyanating agents. All of which show activity with strong *C*-nucleophiles such as Grignards or lithiumorganyls; however, compounds **8**, **23** and **26** react also with *N*- and *S*-nucleophiles.

## Cyano Benziodoxol(on)es (CBX)

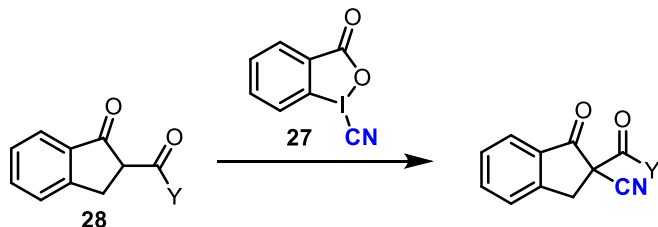
Remarkable pioneering and continued work in the field of hypervalent iodine compounds has been carried out by ZHDANKIN, OCHIAI and others.<sup>[44]</sup>

Since 2008 the field has experienced a renaissance, notably due to J. WASER and coworkers, who could clearly show that up to then, the potential of benziodoxolones (BXs) had been seriously underestimated.<sup>[45]</sup> One of the members of the BX group of compounds is cyano benziodoxol(on)e (CBX) **27**, which is used for electrophilic cyanation.<sup>[30]</sup>

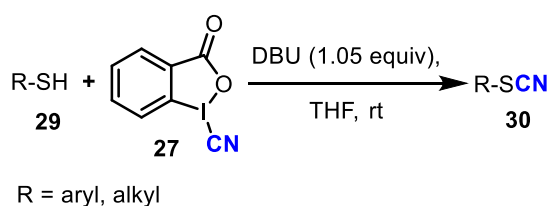
(I) Zhdankin (1995)



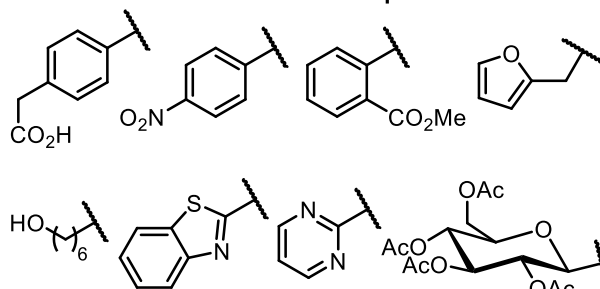
(II) Chen, Zheng, M. Waser (2015)



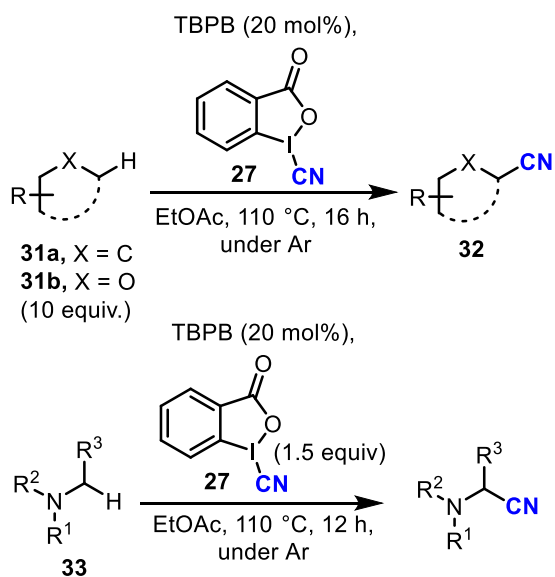
(III) J. Waser (2015)



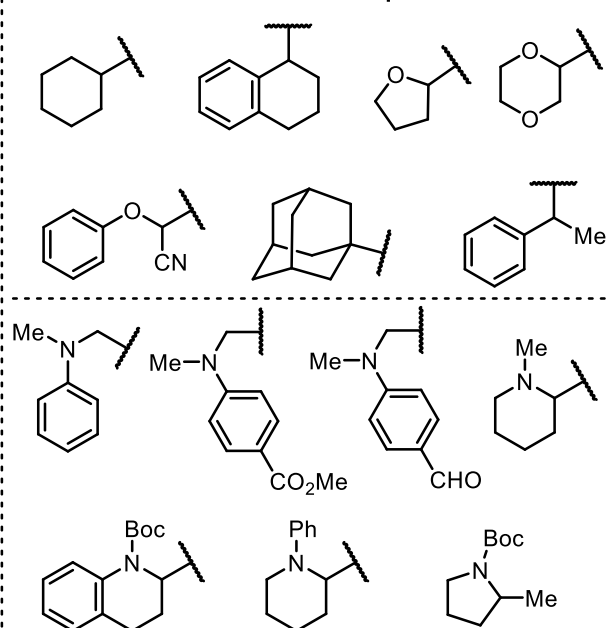
Selected examples:



(IV) Ma & Zhang (2018)

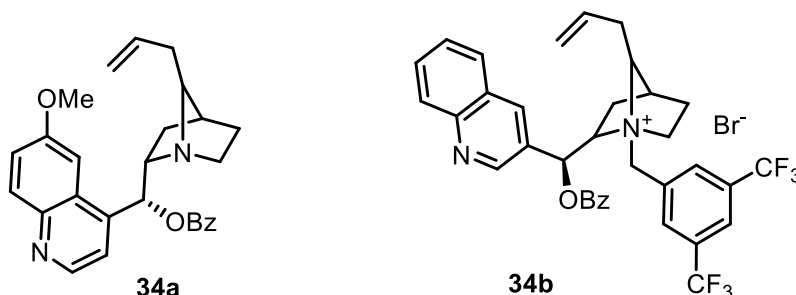


Selected examples:



Scheme 9: Electrophilic cyanation utilizing benziodoxol(on)es.

The groups of ZHENG, M. WASER and also CHEN (Scheme 9-II) all described the  $\alpha$ -cyanation of  $\beta$ -keto esters **28** with CBX **27** in 2015: [37,39,40] While CHEN et al.[37] focused on a base-free approach and also reported successful cyanation of  $\beta$ -keto amides, the main emphasis of M. WASER[39] and ZHENG[40] was on developing an enantioselective synthesis. Both groups used alkaloid-based phase transfer catalysts for the stereoselective induction.

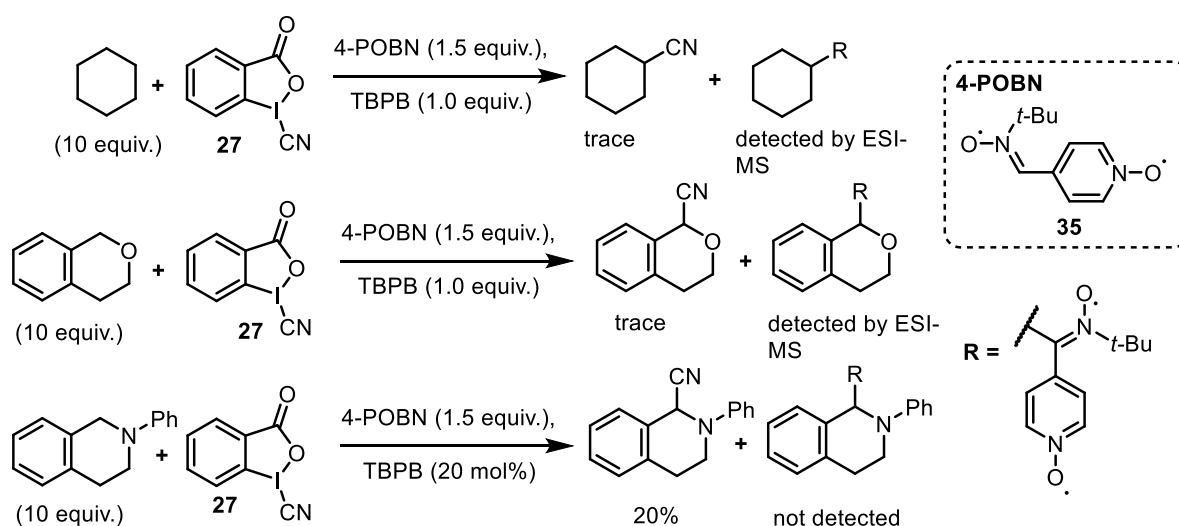


Scheme 10: Phase transfer catalysts identified to be suitable for enantioselective electrophilic cyanation.

While the group of M. WASER identified alkaloid **34a** to catalyze the reaction best in chloroform without addition of base with a maximum e.r. of 76:24, the group of ZHENG found catalyst **34b** to be the best in a solvent mixture of THF and toluene with addition of DMAP as a base, thus affording products with the highest ee of 93% (Scheme 10).

Few procedures have been proven to be straightforward for the cyanation of thiols. Among them is the reported by J. WASER (Scheme 9-III) in 2015 protocol for cyanation of compounds **29** with CBX.[38] Aliphatic and aromatic thiols **29** could be converted to thiocyanates **30** within minutes at room temperature in the presence of DBU. They have also found disulfides to be viable substrates which could be converted in up to 92% yield. Mechanistic investigations were carried out *in silico* and suggest either a SET process or a concerted transition state, both would be in agreement with the high reaction rate reported. Selected examples of significance for synthetic chemistry, chemical biology and materials science further underline the impact of this work

MA and ZHANG (Scheme 9-IV) made use of the fact that CBX is not only capable of electrophilic cyano transfer, but can also act as an oxidant. Normally an inconvenience causing undesirable side reactions, this property was used to develop a procedure for direct C(sp<sup>3</sup>) cyanation. The results from ZHDANKIN et al., who reported on azidation with azidobenziodoxole (ABX) with similar oxidative properties,[46] were applied to the cyanation protocol by MA and ZHANG.[47] Assuming a free radical chain mechanism proposed by ZHDANKIN, the groups of MA and ZHANG used *tert*-butyl-peroxybenzoate (TBPB) as the initiator. They successfully functionalized alkanes **31a**, ethers **31b** and tertiary amines **33**. To investigate the mechanism, they conducted their cyanations in the presence of *N-tert*-butyl- $\alpha$ -(4-pyridyl-1-oxide) nitron (4-POBN, **35**) as spin-trap reagent (Scheme 11).

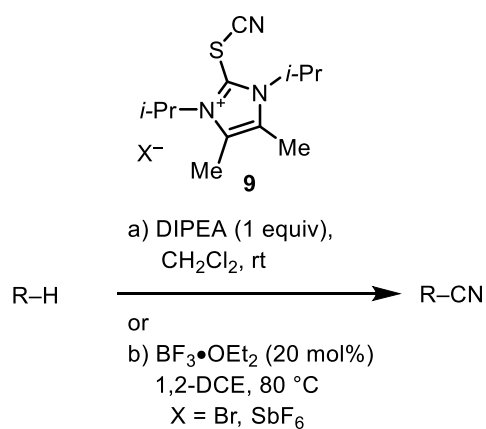


Scheme 11: Mechanistic investigations with 4-POBN as a spin trapping reagent.

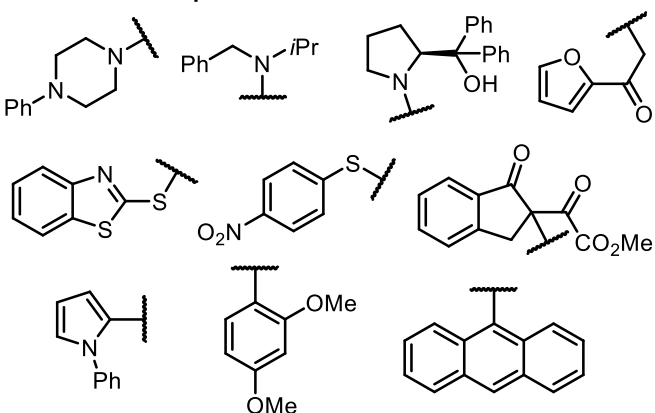
While for alkanes and ethers the reaction was completely suppressed, tertiary amines still gave moderate yields. The authors assumed an oxidative reaction process, which was tested in additional competition experiments under parallel oxidative trifluoromethylation conditions in the presence of  $\text{TMSCF}_3$  and  $\text{CsF}$ . The observation of the trifluoromethylated product verified the transient formation of an iminium cation intermediate. Based on the findings, they postulated two different mechanisms, depending on the nature of the substrate, *i. e.* alkanes and ethers *versus* tertiary amines.

## CATIONIC THIOCYANATES

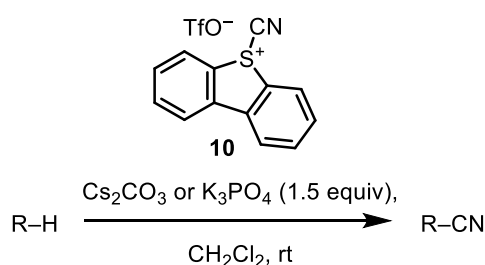
### (I) Alcarazo (2015)



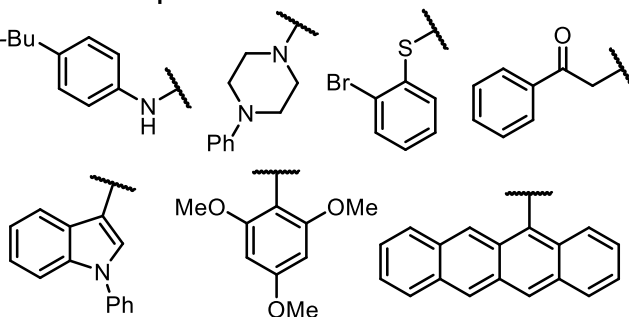
#### Selected examples:



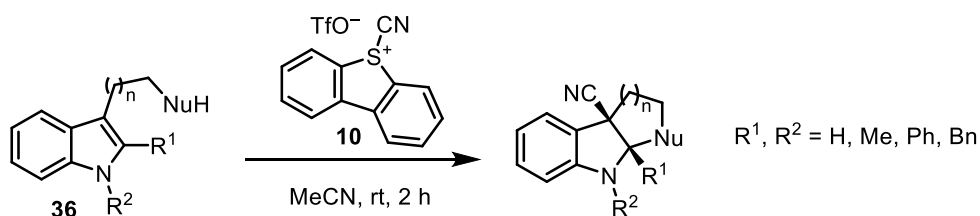
### (II) Alcarazo (2018)



#### Selected examples:



#### cyano cyclization



Scheme 12: Electrophilic cyanation utilizing imidazolium thiocyanates and dibenzothiophenium cyanates.

Based on the work of ARDUENGO & BURGESS<sup>[48]</sup> and further progressions by ROESKY,<sup>[49]</sup> ALCARAZO and coworkers were able to exploit the hypervalent character of di(halo)imidazolium salts for the synthesis of imidazolium thiocyanates **9** (Scheme 12-I).<sup>[41]</sup> These salts proved to be efficient transfer reagents for electrophilic cyanation, as *S*-, *N*- and, remarkably, also a number of *C*-nucleophiles underwent the transformation smoothly. Advantages of these reagents are the easy and short synthesis sequence, as well as their high stability.

After successful synthesis of 5-(alkynyl)dibenzothiophenium salts by utilizing the backbone, which was already popularized by UMEMOTO,<sup>[5,25]</sup> LI & ALCARAZO (Scheme 12-II)<sup>[42]</sup> could demonstrate that the cyano derivative **10** is also stable and potent in cyanation reactions. While its behavior towards nucleophiles is milder, as compared to the imidazolium thiocyanate **9**, its reactivity among electrophilic transfer reagents is unique. Thus, it shows unprecedented reactivity with indol and derivatives thereof. When 2-unsubstituted indoles



were subjected to standard reaction conditions, cyanation in 3-position with subsequent nucleophilic attack of a second equivalent of indole resulted in dimerization of the indole moiety. To make use of this observation, tryptamine derivatives **36** were employed for a cyano cyclization cascade. The methodology could even be extended to a cyanation-Povarov cascade. Noteworthy, upon cyclization of allylic indoles in which four consecutive stereocenters are generated, selective formation of only one diastereomer was observed.

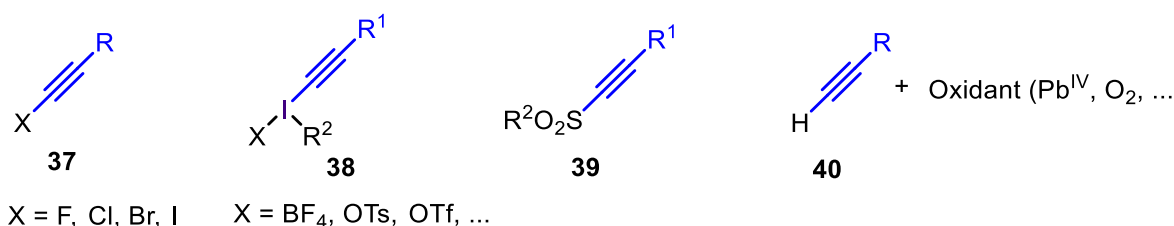
In conclusion, although various available reagents can be used to implement electrophilic cyanation, the synthetic problems remain the same. Depending on the degree of polarization of the nitrile group within a transfer reagent, diverging pathways for the functionalization of nucleophiles exist. Reagents with relatively low polarization can cleanly provide cyanated products with high selectivity, yet the employed nucleophile needs to be strong enough. Reactions of reagents with a highly polarized nitrile group can lead to diminished yields of the desired product, due to side reactions, hence reduced selectivity. Compared to other fields that explore electrophilic group-transfer reagents and reactions, electrophilic cyanations still remain relatively scarce. Finally, it is worth noting that the extension to asymmetric transformations is only known for a handful of examples.

## ELECTROPHILIC ALKYNYLATION

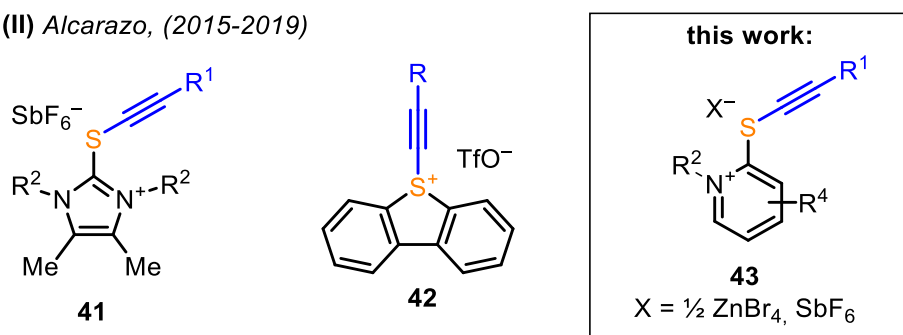
In the last Chapter the electrophilic transfer of the nitrile group was discussed. While from the first look, the transition to electrophilic alkynylation demonstrates definite similarity, the most obvious difference is the additional substitution on the opposite site of the acetylene functionality. The substitution pattern can play a vital role in the mode of reactivity and also allows tuning of it to a certain degree, as will be shown in this Chapter.

In general, the applied principles are the same as for Umpolung methodology – transmutation from nucleophiles to electrophiles. In order to discover and provide access to new reaction pathways that expand the scope of acetylene transfer reactions, complementary to nucleophilic alkynylations, electrophilic alkynylation is used. Today, it already has become an established, growing field of research. Recently, it has experienced a resurgence due to its extended application in transition metal catalysis. The most prevalent methods for the Umpolung of alkynes are the use of halogenoalkynes **37**, hypervalent alkynyliodonium salts **38**, acetylene sulfones **39** and *in situ* oxidized terminal acetylenes **40** (Scheme 13-I).

### (I) Halogens, hypervalent iodines, sulfones, oxidized terminal alkynes



### (II) Alcarazo, (2015-2019)



Scheme 13: Evolution of electrophilic alkynylation reagents.

Evaluation of the different categories of reagents reveals the halogenoalkynes **37** to be relatively mild alkynylating reagents, when used under metal-free conditions, as the next three subchapters illustrate. In addition, with the development of transition metal catalysis, the research field of haloalkyne functionalization in transition metal-mediated reactions has emerged as a much broader field. It enables access to novel products and alternatives to previously established reaction pathways (see Chapter “C–H FUNCTIONALIZATION UTILIZING ACTIVATED ACETYLENES”).

On the other hand, similar to related cyano analogs, alkynyliodonium salts **38** are inherently more reactive than haloalkynes, due to their unusual 4-electron-3-centre bond. Their applications are covered extensively in literature, and the scope of transformations is broader than that of halogenoalkynes.<sup>[50,51,52]</sup>

Sulfone-substituted alkynes are preferably used in reactions that involve radical chemistry. Terminal alkynes can effectively be oxidized to act as electrophiles, formerly by strong oxidants such as lead(IV), and more recently by mediation with transition metal catalysts combined with external oxidants such as either dioxygen or electrochemical oxidation.

Recently the group of ALCARAZO was able to expand the range of reagents by successful synthesis and application of sulfur-based reagents. A variety of these reagents could be established as platform chemicals for electrophilic cyanation,<sup>[41,42,53]</sup> alkynylation,<sup>[41,54–56]</sup> thioalkynylation,<sup>[57]</sup> alkylation and, in addition, as an aldothioketene mimetic reagent (Scheme **13-II**).<sup>[55]</sup> While the majority of the reported chemistry utilizing these reagents is metal- or at least transition metal-free, herein the expansion to transition metal catalyzed reactions is also presented (See Chapter “C–H FUNCTIONALIZATION UTILIZING THIOIMIDAZOLONE-BASED ELECTROPHILIC TRANSFER REAGENTS”).

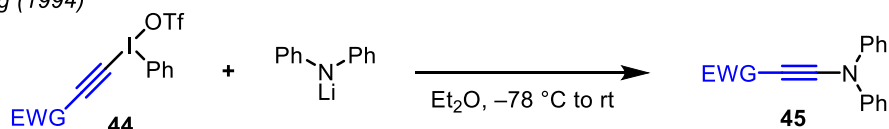
In the next three subchapters examples for electrophilic alkynylation reactions of **37-42** with *N*-, *O*-, *S*-, *P*- and *C*-nucleophiles will be covered. While reports for heteroatom-based nucleophiles, predominate, fewer examples are known for the still challenging *C*-nucleophiles.

Mechanistic proposals for the electrophilic alkynylation with hypervalent iodonium salts have been thoroughly investigated. They diverge, depending on a number of factors such as the kind of substrate, the class of hypervalent iodine compound (a differentiation between acyclic alkynyliodonium salts and cyclic ethynylbenziodoxol(on)es is necessary) and the nature of the R-substituent on the alkyne. As a result, different mechanisms have been proposed for the transformation of alkynyliodonium salts with *N*-, *S*-, *O*- and *P*-nucleophiles (see chapter next but one ‘*P*-, *O*-, *S*-Nucleophiles’ Scheme **17**) and EBX, with either *S*- or *C*-nucleophiles (Scheme **19** and Scheme **22** respectively).

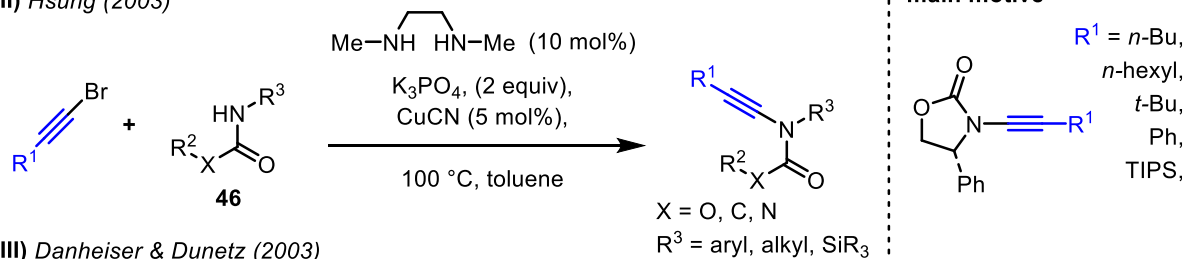
## **N-NUCLEOPHILES**

Synthesis of ynamines and ynamides is feasible by utilizing alkynyl bromides in combination with copper catalysis, hypervalent iodonium salts or, very recently, sulfur-based reagents, as well as terminal alkynes and a copper salt and dioxygen as an external oxidant.

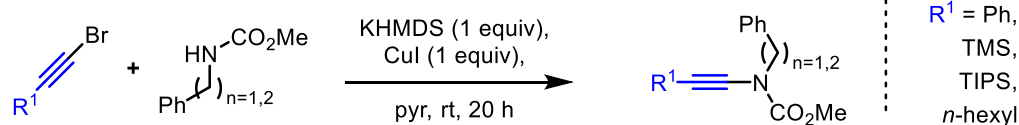
(I) Stang (1994)



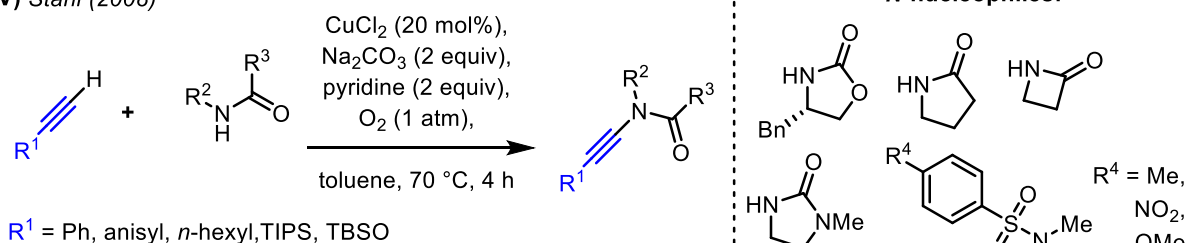
(II) Hsung (2003)



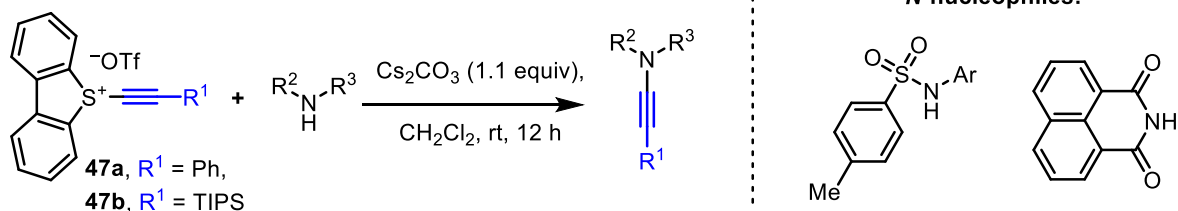
(III) Danheiser & Dunetz (2003)



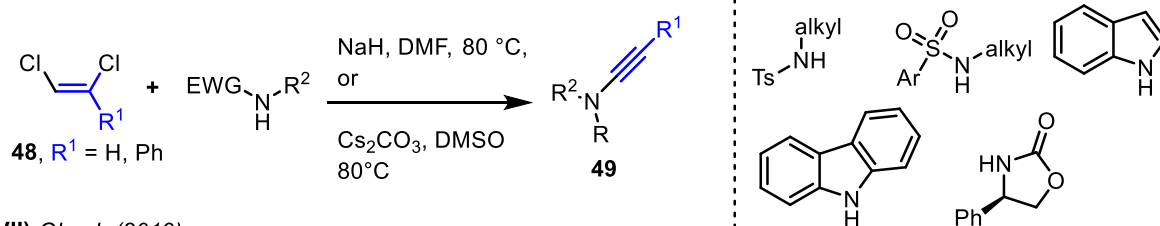
(IV) Stahl (2008)



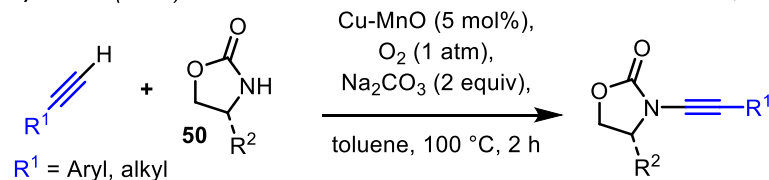
(V) Alcarazo (2018)



(VI) Zhao (2018)



(VII) Ghosh (2019)

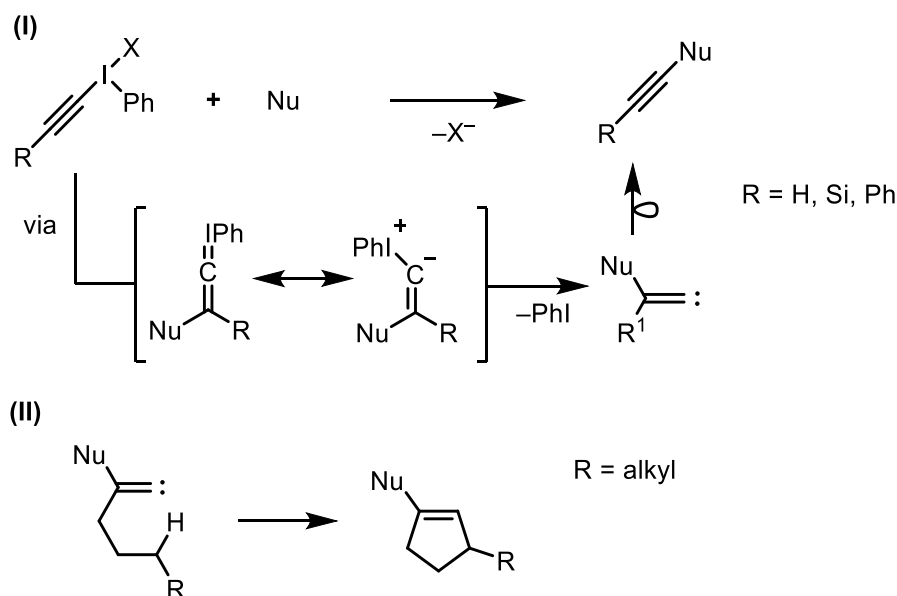


Scheme 14: Alkynylation of *N*-nucleophiles.<sup>[54,58–63]</sup>

Pioneering work was accomplished by STANG et al. (Scheme 14-I) by employing alkynyliodonium salts **44** in the successful synthesis of push-pull ynamides **45**; however, the

reaction was limited to EWG-substituted alkynes and diphenylamine as a substrate.<sup>[58]</sup> Two years later the methodology could be extended to ynamides by FELDMANN et al.<sup>[64]</sup>

FELDMAN and later WITULSKI, also proposed two mechanistic scenarios, based on migration abilities of substituents. Substitution with Si, H or Ph gives acetylenes (Scheme 15-I), while the alkyl-substituted reagents prefer an insertion pathway (Scheme 15-II).<sup>[64,65]</sup>



Scheme 15: Proposed mechanism for the nucleophilic attack on electrophilic alkynyl iodonium salts.

Similar observations were made for sulfonium reagents developed by WALDECKER & ALCARAZO (Scheme 14-V).<sup>[54]</sup>

A protocol for electron-poor amines **46** in combination with halogenoalkynes under copper catalysis was described by HSUNG et al. (Scheme 14-II).<sup>[59]</sup> They discovered that by replacement of iodoacetylenes with bromoacetylenes under their reaction conditions, homocoupling of the alkyne could successfully be diminished. While their work poses a breakthrough for the first successful employment of alkyl substituted acetylenes, further investigations showed the protocol to be less efficient when acyclic carbamates or sulfonamides were used.

An alternative approach to reduce the homodimerization of halogenoalkynes in their copper-mediated reaction, consisting in the initial generation of stoichiometric amounts of a copper-amine species and then adding two equivalents of bromoacetylenes, was selected by DUNETZ and DANHEISER (Scheme 14-III).<sup>[60]</sup> In addition, this methodology allowed the reaction to proceed at room temperature.

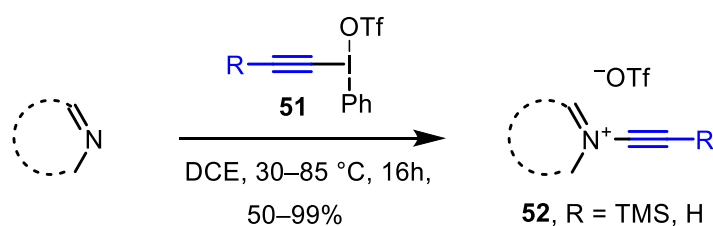
The aforementioned direct oxidation of terminal alkynes was described by STAHL et al. (Scheme 14-IV) for the optimized catalytic system utilizing one atmosphere of dioxygen to regenerate the copper catalyst. The reaction operates well with a broad scope of amides as well as acetylenes.<sup>[61]</sup>

Circumventing any potential problems of homodimerization, ALCARAZO et al. (Scheme **14-V**) have found that newly designed hypervalent benzothiophenium salts **47a** and **47b** allow alkynylation of sulfonamides and diamides. Additional investigations towards the mode of reactivity using the reagent with a  $^{13}\text{C}$ -labeled acetylene moiety gave insight into the mechanism.<sup>[54]</sup>

Another metal-free approach was reported by ZHAO et al. (Scheme **14-VI**), who used (*Z*)-1,2-dichloroalkenes **48** or alkynyl chlorides in combination with electron poor amines to elaborate an access to either terminal or internal ynamides **49**.<sup>[62]</sup>

Focusing on atom economy, the group of GHOSH (Scheme **14-VII**) reported on the heterogeneous Cu-MnO catalyst for direct oxidation of terminal alkynes using air as the sole oxidant. While they observed concurrent homodimerization, kinetic studies revealed that the amount of Glaser-type coupling product could be reduced using an excess of nucleophile **50**. They could also show that recycling of the catalyst was possible up to four times.<sup>[63]</sup>

Very recently, an access to highly electrophilic alkyne-pyridine conjugates, *N*-alkynylpyridinium salts **52**, by utilizing alkynyl- $\lambda^3$ -iodanes **51** has been reported by UCHIYAMA et al. (Scheme **16**).<sup>[66]</sup>



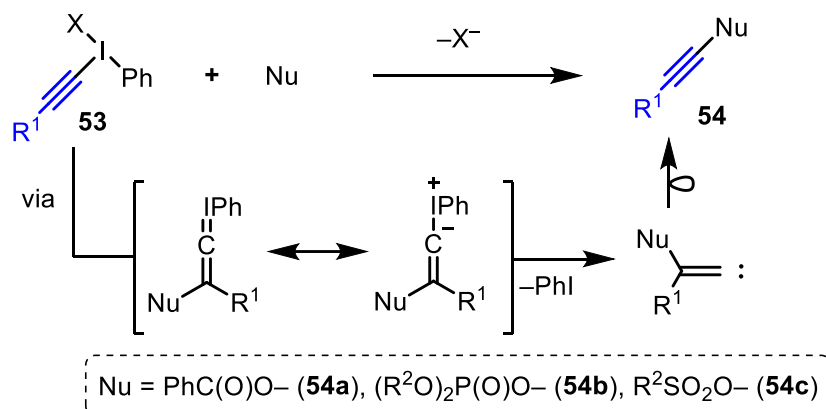
Scheme **16**: Access to *N*-alkynylpyridinium salts **52** by alkynylation with alkynyl- $\lambda^3$ -iodanes **51**.<sup>[66]</sup>

The synthesized alkynylammonium salts **52** exhibit a high electron-accepting character with extended  $\pi$ -conjugation and were remarkable precursors for the synthesis of quinolizinium salts with unique optical and electrochemical properties.

## P-, O-, S-NUCLEOPHILES

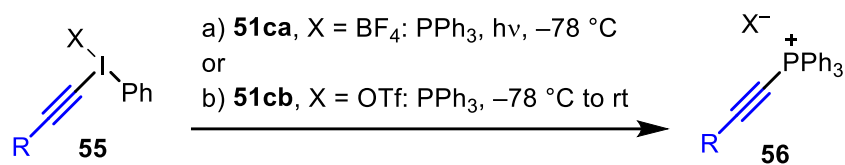
In contrast to *N*-nucleophiles, reports of the transformation of *P*-, *O*- and *S*-nucleophiles with electrophilic alkynes are far less prevalent.

### (I) Stang (1985-1989)

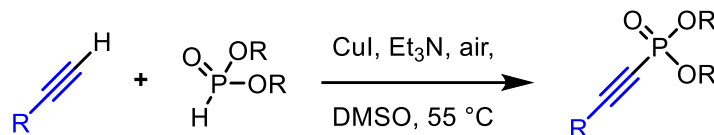


### (II) a) Ochiai (1987)

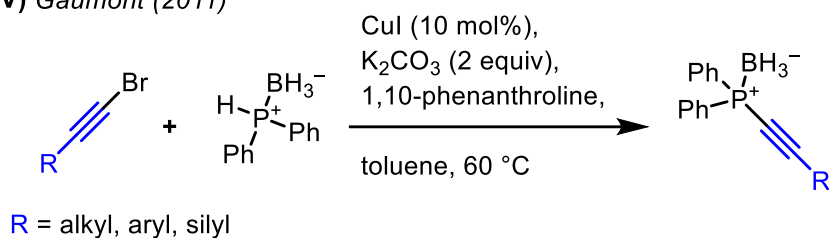
### b) Stang (1992)



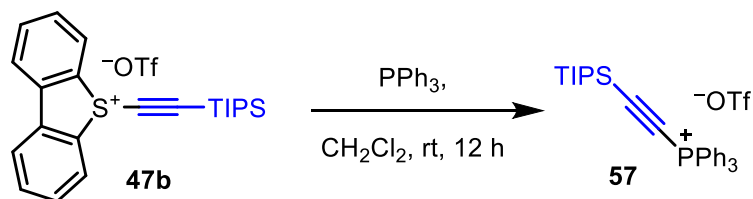
### (III) Zhao, Han (2009)



### (IV) Gaumont (2011)



### (V) Alcarazo (2018)



Scheme 17: Alkynylation of *O*- and *P*-nucleophiles.



In a number of publications, STANG (Scheme 17-I) reported on access to alkynylcarboxylates **54a**, alkynyldialkylphosphates **54b** and alkynylsulfonates **54c** with utilization of alkynyliodonium salts **53** following by a Michael addition/1,2-shift sequence, albeit requiring different reaction conditions: Alkynyl sulfonates **54c** can be obtained from alkynyl(phenyl)iodonium mesylates or tosylates under catalysis with 5–10 mol% CuOTf or AgOTs; alkynyl carboxylates **54a** – by either reaction of  $\text{PhI}(\text{O}_2\text{Ph})_2$  with acetylide ions or, *vice versa*, of alkynyl(phenyl)iodonium triflates with  $\text{C}_6\text{H}_5\text{CO}_2\text{Na}$ . Decomposition of alkynyl(phenyl)iodinium dialkylphosphates gave alkynyl dialkylphosphate esters **54b**.<sup>[67]</sup>

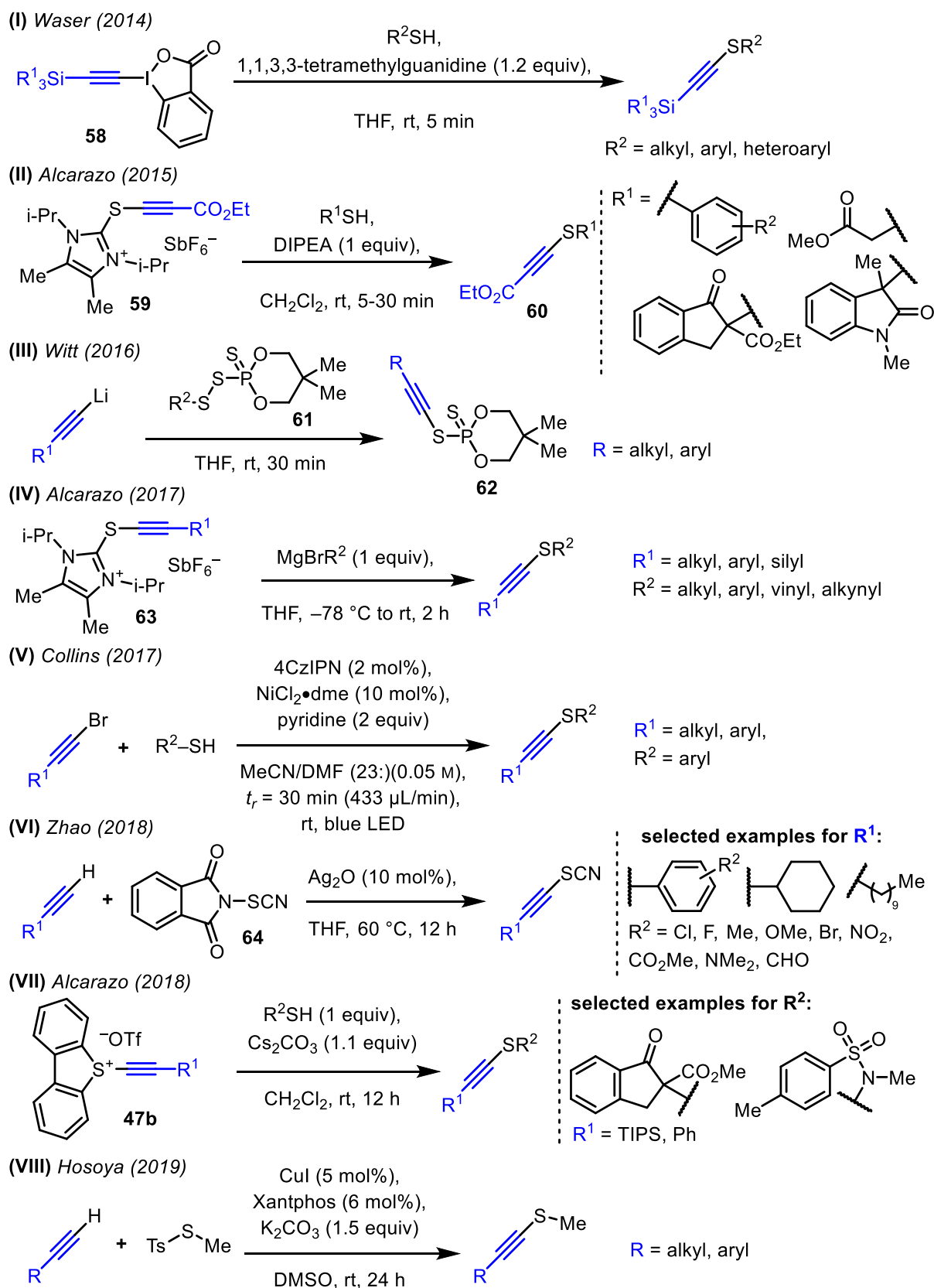
The mechanism proposed by STANG is in agreement with the mechanistic scenarios described for *N*-nucleophiles by FELDMANN and WITULSKI in the last Chapter.

At the same time OCHIAI et al. (Scheme 17-II) reported the synthesis of alkylethynyl triphenylphosphoniums **56**, from alkynyliodonium tetrafluoroborates **55** and triphenylphosphines, in which the presence of light was necessary. Alternatively, the preparation of alkynyliodonium triflate **51cb** reported by STANG et al. (Scheme 17-II) did not require light irradiation.<sup>[68]</sup>

In 2009 ZHAO, HAN et al. (Scheme 17-III) published a protocol for the oxidative coupling of terminal acetylenes and H-phosphonates in analogy to STANG's protocol, featuring a broad scope and large functional group tolerance.<sup>[69]</sup>

Representing the only publication on reactivity of halogenoalkynes within this area, GAUMONT et al. (Scheme 17-IV) utilized phosphine-boranes to couple with bromoalkynes to give access to alkynylphosphines. The use of phosphine-boranes was found to be necessary to circumvent catalyst poisoning by free phosphine.<sup>[70]</sup>

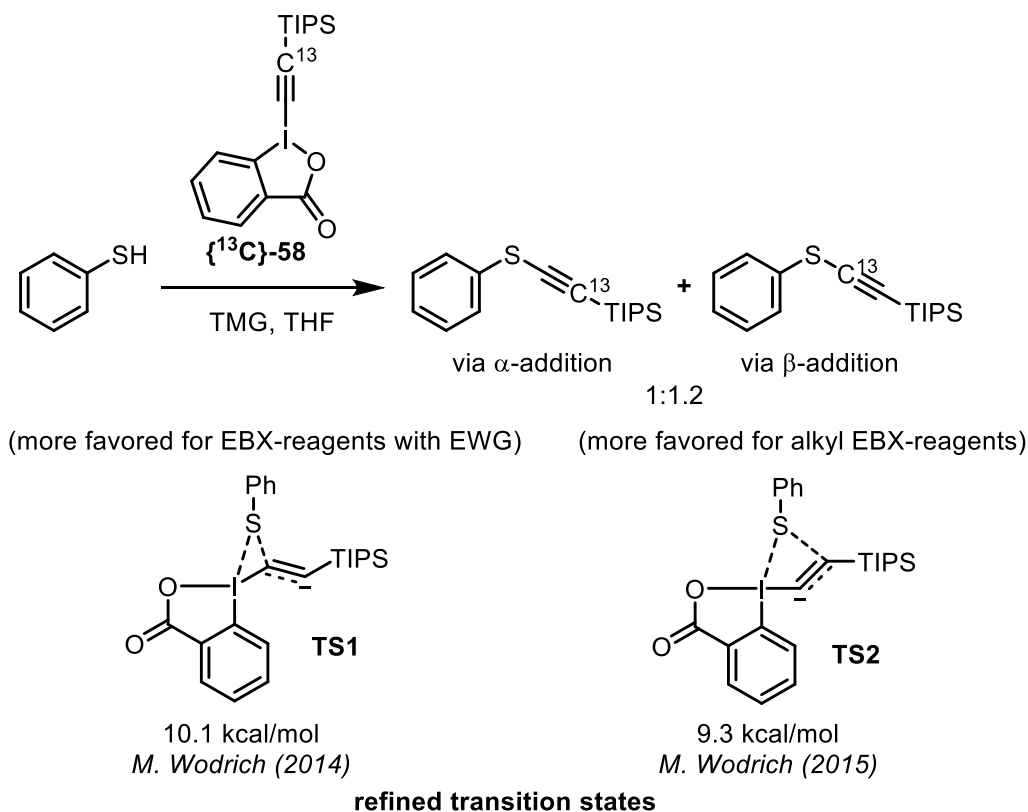
ALCARAZO et al. (Scheme 17-V) have demonstrated their novel dibenzothiophene-based electrophilic alkynylation reagent **47b** to be able to convert triphenylphosphine into the corresponding alkynylphosphonium salt **57** under unprecedented mild conditions, cleanly and in excellent yield.<sup>[54]</sup>



Scheme 18: Synthesis of alkynyl sulfides.

In 2014 J. WASER and RETO (Scheme 18-I) published an unprecedented alkynylation of thiols utilizing [(triisopropylsilyl)-ethynyl]benzodioxolone (TIPS-EBX, **58**) and its other silyl

derivatives, the latter being hypervalent iodine-based alkyne transfer reagents.<sup>[50]</sup> The conversion of thiols takes place within five minutes at room temperature in an open flask using commercially available reagents and could be scaled up to gram levels. They further underlined the use of the thiol-alkynylation by postsynthetic modification of a cysteine-containing peptide via a standard CuAAC reaction introducing a dansyl fluorophore tag.<sup>[71]</sup>



Scheme 19: Mechanistic investigations by J. WASER et al.<sup>[72,73]</sup>

Mechanistic investigations of J. WASER in cooperation with WODRICH revealed, that two scenarios, a three atom concerted transition state **TS1**, in which C-S bond formation takes place on the  $\alpha$ -carbon *versus* a four atom concerted transition state **TS2**, in which attack of the sulfur takes place on the  $\beta$ -carbon, are within a very small energy range for silyl-EBX reagents. This was in agreement with experiments conducted with  $^{13}\text{C}$ -labeled TIPS-EBX **{ $^{13}\text{C}$ }-58**. Furthermore calculations showed that for EBX-reagents with EWGs, **TS1** is favoured, while for alkyl substituted EBX reagents, **TS2** is preferred (Scheme 19).<sup>[72,73]</sup>

In 2015, ALCARAZO et al. revealed that their EWG-substituted thioimidazolium-based acetylene transfer reagent **59** was able to react with thiols in a straightforward fashion to give thioacetylenes **60** (Scheme 18-II).<sup>[41]</sup>

Development of a thiation agent **61**, structurally reminiscent of Lawesson's reagent, was reported by WITT et al. (Scheme 18-III) in 2016.<sup>[74]</sup> Functionalized unsymmetrical alkynyl sulfides **62** including hydroxy-, carboxy- or amino-substituted derivatives were obtained after reaction of the reagent **61** with lithium acetylides.

Two years after their initial publication about sulfur based electrophilic transfer reagents, ALCARAZO et al. could expand the scope of thioacetylenes reported in previously published work.<sup>[41,75]</sup> Synthesis of a wide range of electrophilic acetylenes **63** based on thioimidazolium was reported, and their successful transformation with alkyl-, aryl, vinyl- or alkynylmagnesium Grignards as well as with zinc organyls were described (Scheme **18-IV**).<sup>[75]</sup> Notably, analogous reactivity was observed when imidazolium selenoalkynes were employed in the transformation.

Distinguished by its practical application, the photochemical dual-catalytic cross-coupling to form alkynyl sulfides via C(sp)–S bond formation was described by COLLINS (Scheme **18-V**) in 2017. Combining a soluble organic carbazole-based photocatalyst with continuous flow techniques, the synthesis of alkynyl sulfides bearing electronically or sterically diverse aromatic alkynes and thiols could be achieved. In addition, the continuous flow setup also allows for short reaction times (30 min) and reproducibility on gram scale.<sup>[76]</sup>

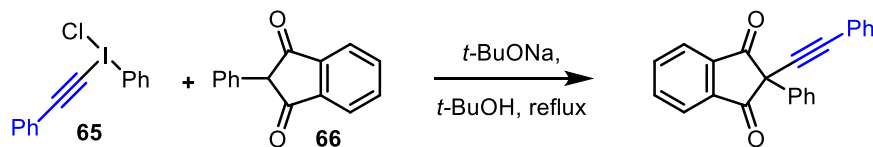
A one-pot protocol for thiocyanation of terminal alkynes with *N*-thiocyanophthalimide (**64**) and employing silver(I) oxide as an oxidant was developed by ZHAO et al. (Scheme **18-VI**).<sup>[77]</sup> Noteworthy, when a silver/gold relay catalysis was used, access to  $\alpha$ -thiocyanoketones was also possible. Derivatization into a variety of valuable sulfur-containing heterocycles and sulfides could be demonstrated as well.

*S*-(Alkynyl)dibenzothiophenium triflate **47b** developed by ALCARAZO et al. also proved to be able to transform a number of *S*-nucleophiles, including aromatic and aliphatic thiols, into the corresponding thioacetylenes (Scheme **18-VII**).<sup>[54]</sup> Functional groups such as esters, carbonyls and nitro moieties were well tolerated.

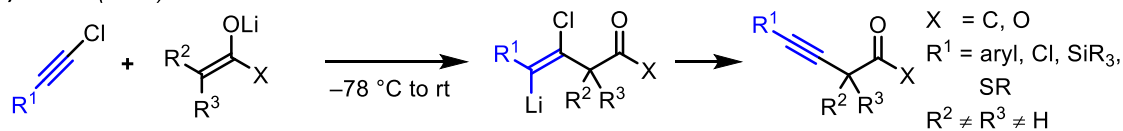
Another example for the oxidation of terminal alkynes with utilization of copper catalysis and thiosulfonates as the source of sulfur was presented by HOSOYA (Scheme **18-VIII**). In addition, subsequent iodocyclization could be used to access benzofuranes, benzothiophenes and indols.<sup>[78]</sup>

## C-NUCLEOPHILES

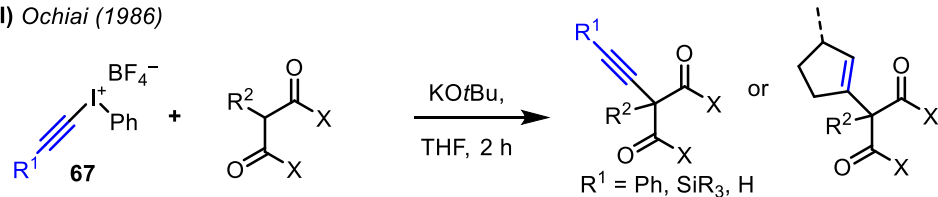
### (I) Beringer (1965)



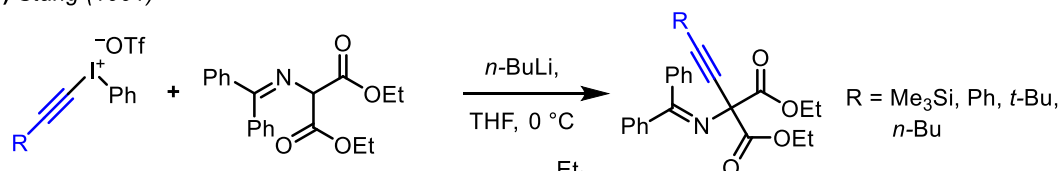
### (II) Kende (1984)



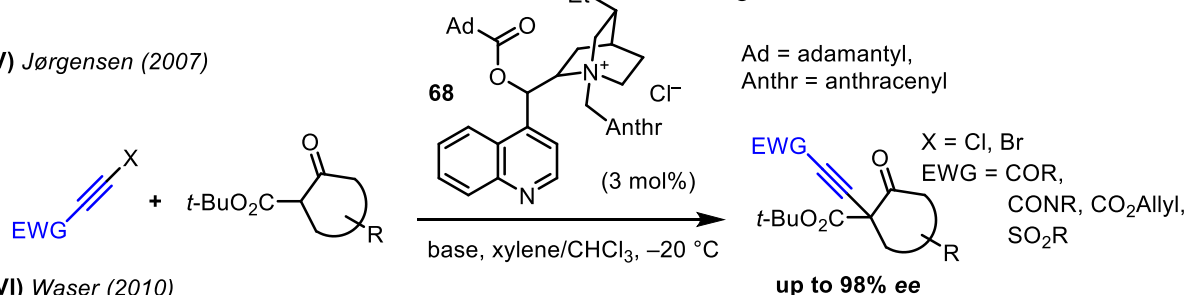
### (III) Ochiai (1986)



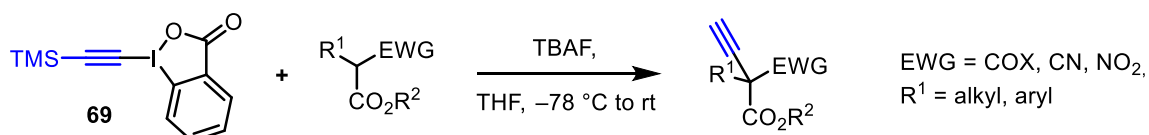
### (IV) Stang (1991)



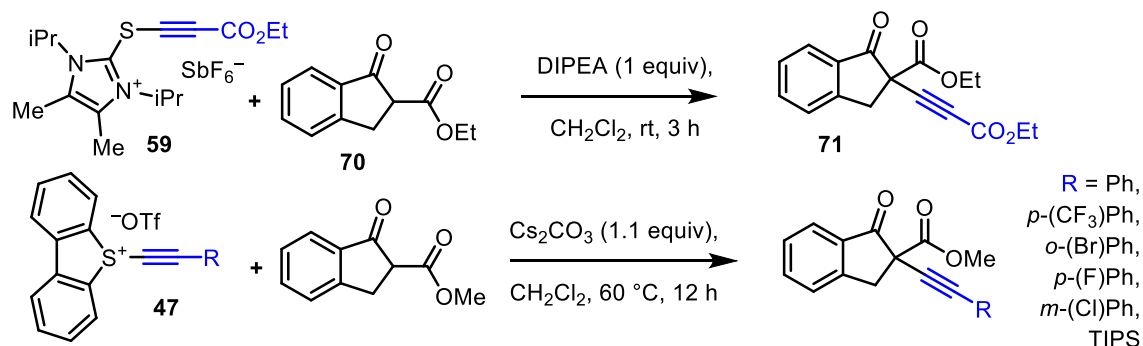
### (V) Jørgensen (2007)



### (VI) Waser (2010)



### (VII) Alcarazo (2015, 2018)

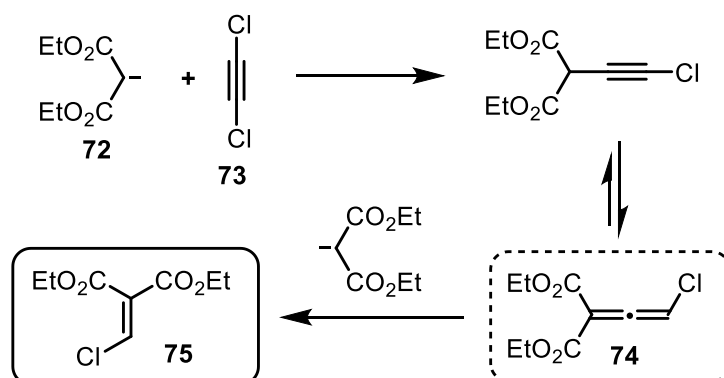


Scheme 20: Alkynylation of C-Nucleophiles.

Laying the foundation for all research towards hypervalent iodonium salts was accomplished by BERINGER Scheme 20-I) in 1965. Successful synthesis of the acyclic chloride **65** form and

investigation of its reactivity towards indandione **66** was performed.<sup>[18]</sup> Even then, weak enolates were identified as good candidates for C-nucleophiles.

It took almost 20 years until KENDE et al. in 1984 reported the reaction of chloroalkynes, with lithiunenolates, generated by addition of LDA, from ketones or esters (Scheme 20-II).<sup>[79]</sup> The reaction proved to tolerate chloro-, silicon-, sulfur- and aryl-substituted alkynes, but the methodology reached its limits when aliphatic alkynes were used. An explanation is given by the mechanism: The addition-elimination mechanism involves a transient  $\beta$ -carbanion which experiences mild stabilization, if the adjacent substituent is of aromatic nature. This mild stabilization is absent in the case of aliphatic substituents. This rationale could be further consolidated, by showing that the use of 1-bromo-1-hexyne results exclusively in the bromination, without formation of the desired product. Furthermore, only tertiary enolates underwent the reaction thus forming quaternary centres. Primary and secondary enolates gave unidentified products with only one exception: Reaction of diethylmalonate **72** with dichloroacetylene **73** in dry ether gave compound **75**, which was characterized by the authors as "Ott diadduct". Most probably, product **75**, resulted from the second Michael addition of another equivalent of diethylmalonate onto the chloroallene intermediate **74** (Scheme 21).<sup>[79]</sup>



Scheme 21: Formation of „Ott diadduct“ **75** via a chloroallene intermediate **74**.

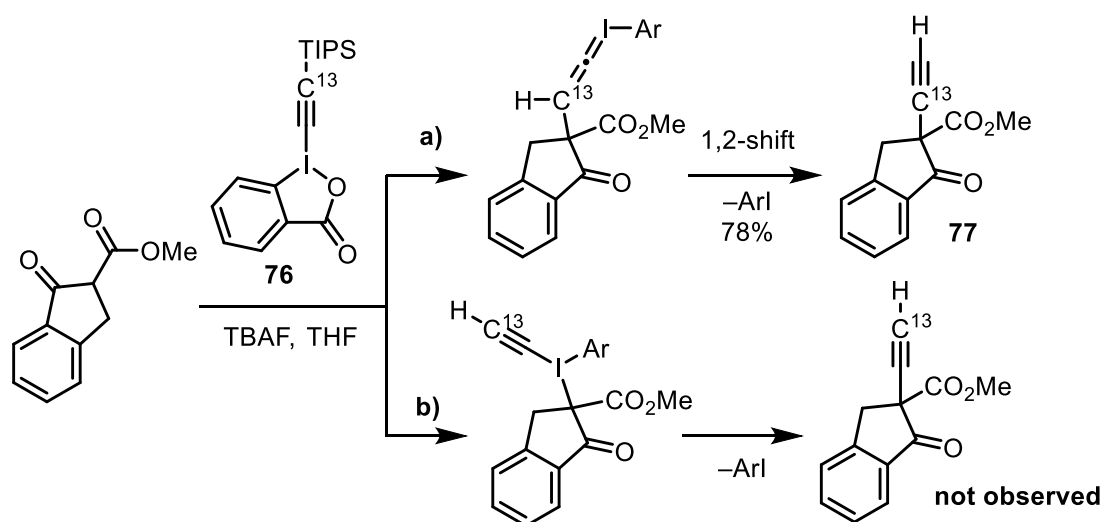
Two years later OCHIAI et al. synthesized an ethynyl(phenyl)iodonium salt **67** and used the weakly coordinating  $\text{BF}_4^-$  as anion. This enabled them to subsequently modify acyclic diketones and realize tandem cyclopenten annulations (Scheme 20-III).<sup>[80]</sup>

A noteworthy variant of malonate functionalization is the alkynylation of diethyl 2-aminomalونات which gives access to propargylic amines and in addition constitutes one of the few examples for which alkylsubstituted acetylenes could be employed (Scheme 20-IV).<sup>[81]</sup>

While successfully applied in several additional publications, the methodology of alkynylations of activated enolates with hypervalent iodonium salts could not be further extended in the following 20 years. It was in 2007 when JØRGENSEN et al. reported the first and unique enantioselective procedure with *ee* values above 90%. They used chloro- and

bromoalkynes, which had to be additionally activated by electron-withdrawing groups such as ketones, esters, sulfones and amides to increase the electrophilicity of the triple bond. By employing the dihydrocinchonine-containing phase transfer catalyst **68**, they were able to achieve an ee of up to 98% (Scheme 20-V).<sup>[82]</sup>

Contributions of WASER et al. from 2010 showed that with TMS-EBX **69** it is also possible to alkynylate both cyclic and acyclic activated carbonyl compounds (Scheme 20-VI).<sup>[50]</sup> Synthesis of a C<sup>13</sup>-labeled TIPS-EBX **76** enabled the authors to gain insight into the mechanism. Of the two possible pathways, on one hand conjugate addition to the alkyne, followed by reductive elimination and 1,2-shift leading to product **77** (pathway a) and, on the other hand, addition-elimination on the iodine atom (pathway b), the former could be indentified as occurring (Scheme 22).



Scheme 22: Experiment with C<sup>13</sup>-labeled reagent **76** by J. WASER et al. to investigate possible mechanistic pathways.

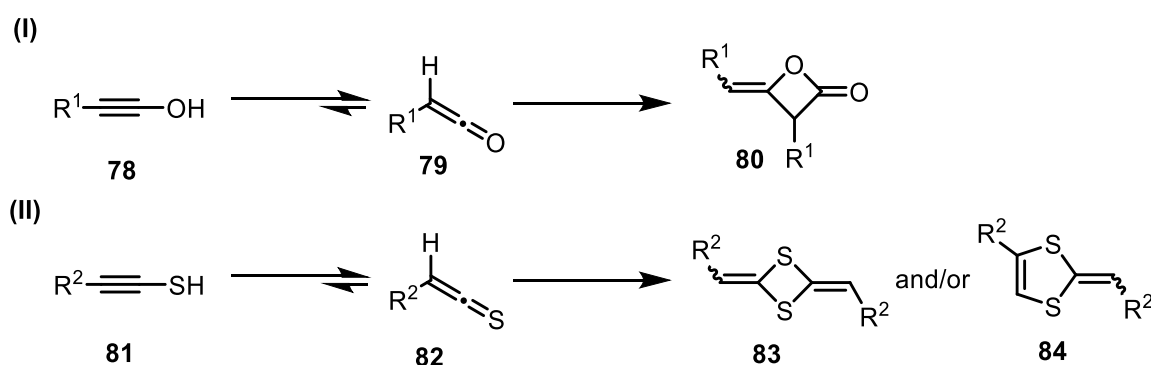
Application of conditions similar to the JØRGENSEN protocol gave them an ee of up to 40%.<sup>[50]</sup>

The activation of acetylenes with electron-withdrawing groups was also exploited by ALCARAZO et al. for the synthesis of imidazolium thioalkyne **59**.  $\beta$ -Ketoester **70** as well as activated amides could be alkynylated (Scheme 20-VII, top).<sup>[41]</sup> Significant extension of the reaction scope could be achieved by replacing the imidazolium backbone with the dibenzothiophene one in **47**. This enabled substitution of the reagents with aromatic and silyl groups on the acetylene moiety (Scheme 20-VII, bottom).<sup>[54]</sup>

As of today, the extension of electrophilic alkynylations for non-activated carbonyl compounds still poses a serious challenge to be overcome. Other frontiers are the successful application of aliphatic acetylenes: the latter, as indicated above, have only found limited application so far. In addition, the modification of non-tertiary propargylic positions also still requires further intensive studies.

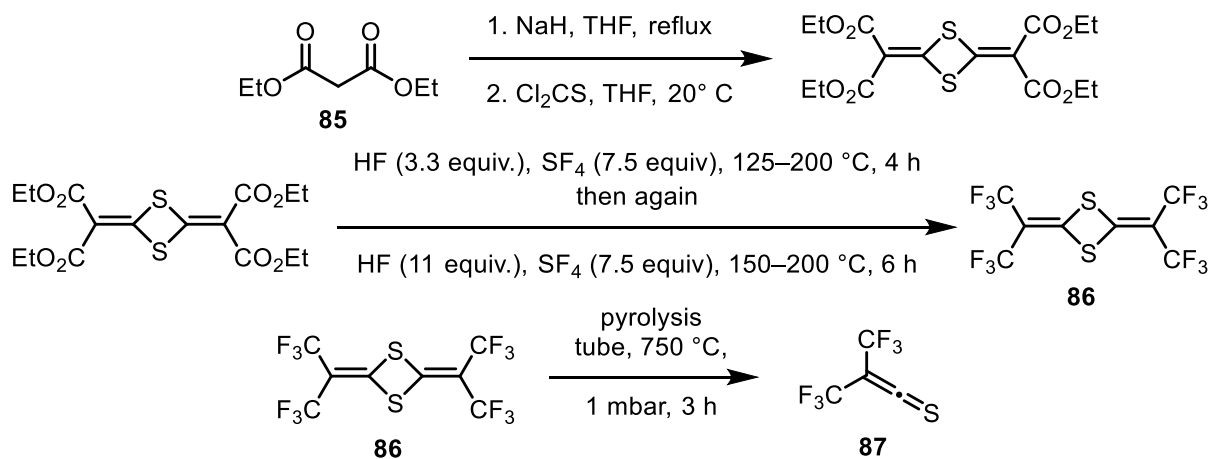
## DITHIOESTER, THIOAMIDES AND THIONOESTERS

The last Chapter covered the synthesis and reactivity of heteroatom substituted alkynes by nucleophilic attack of a heteroatom nucleophile on an electrophilic alkyne. This is a reasonable approach to access a multitude of products. In theory, an alternative approach would be the use of an ynol such as **78** or thioynol **81** (Scheme 23), as a nucleophile and react it with an electrophile. However, this “inverted case” is not feasible due to the fact, that these compounds (protonated or deprotonated) are not stable and equilibrate with their tautomeric form – ketenes **79** and thioketenes **82**, respectively. Moreover, the equilibrium is completely shifted to the side of the carbonyl species.<sup>[67]</sup>



Scheme 23: Ynol-ketene equilibrium and dimerization to diketene **164** (I) and thioynol-thioketene equilibrium and dimerization to dithioketene **167** or dithiafulvenes **168** (II).

Fatefully, both aldoketenes and aldothioketenes are notoriously unstable themselves and dimerize to their corresponding diketene **80**/dithioketene **83** or to dithiafulvenes **84**. On the other hand, for disubstituted (thio)ketenes several stable derivatives exist: RAASCH reported on the successful synthesis of bis(trifluoromethyl)thioketene **87** in 1966 and applications thereof between 1970 and 1977 (Scheme 24).<sup>[83,84]</sup> Alongside diverse cycloadditions, he could show that thioketenes react with alcohols, thiols and amines to form thionoesters, dithioesters and thioamides respectively (see below, Scheme 29).<sup>[85]</sup>

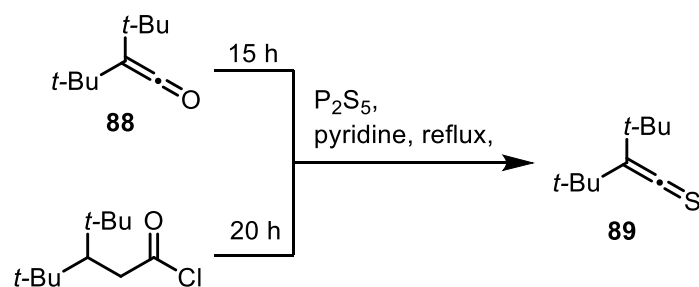


Scheme 24: Synthesis of bis(trifluoromethyl)thioketene **87** by RAASCH.<sup>[83]</sup>



The tedious preparation of monomeric bis(trifluoromethyl)thioketene **87** requires cracking of its dimer **86**, which is synthesized from diethylmalonate **85**, thiophosgene and sulfur tetrafluoride (Scheme **24**). After pyrolysis at 650–750 °C, the monomer can be isolated as a reddish orange liquid, which is then surprisingly stable at 25 °C in glass equipment for several months with only little dimerization.

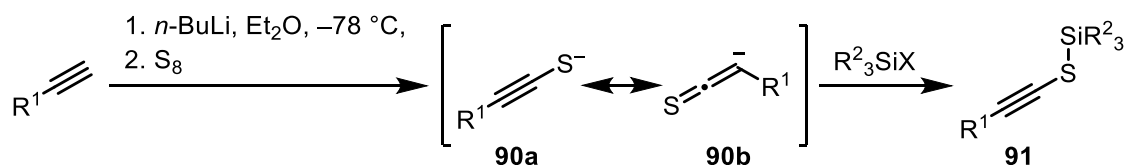
Around the same time BRANNOCK et al.<sup>[86]</sup> successfully synthesized di-*tert*-butylthioketene **89** (Scheme **24**) in analogy to the synthetic route, that provides access to di-*tert*-butylketene **88**, as reported by NEWMAN et al.<sup>[87]</sup>



Scheme **25**: Synthesis of di-*tert*-butylthioketene **89** by BRANNOCK et al..<sup>[86]</sup>

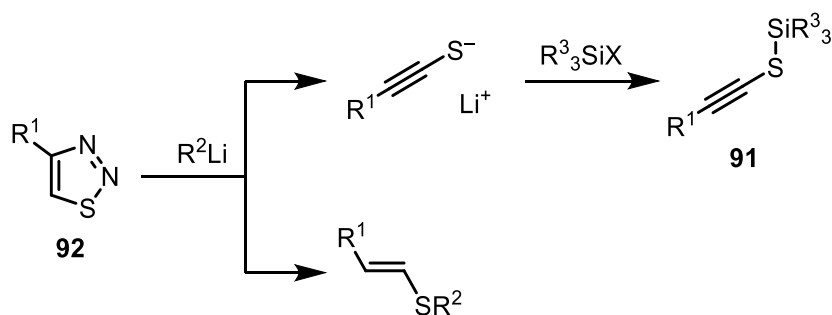
While the sterical shielding of the *tert*-butyl groups, on the one hand, makes the compound stable, on the other hand, its reactivity also decreases for the same reason. Nevertheless, reactions with small nucleophiles were documented and are covered in the following Section. Overall the number of stable thioketenes remains scarce even today.

A viable alternative approach to facilitate transformations with thioketenes is to use thioketene equivalents, from which the reactive species are formed *in situ*. One of the most prominent examples which in fact exploits the aforementioned equilibrium in the described above way (Scheme **23-II**), is presented by SCHAUMANN, who utilized of alkynyl silyl sulfides as thioketene equivalents.<sup>[88]</sup>



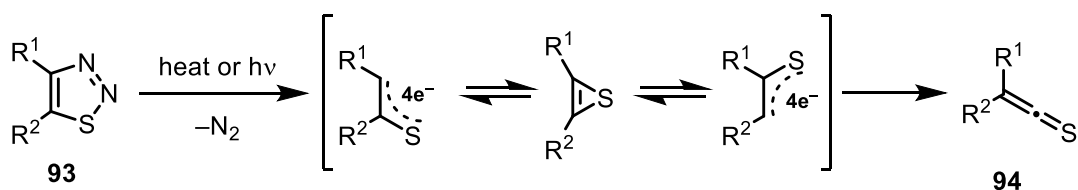
Scheme **26**: Synthesis of silylated alkynylsulfides **91** by Schaumann et al..<sup>[88]</sup>

Starting from terminal alkynes, deprotonation with an alkali metal base was carried out. The formed acetylide was also capable of breaking up the S<sub>8</sub> ring structure, thus affording the intermediate alkynethiolates **90**. Trapping of the latter with the corresponding organosilylhalide via S-silylation gives alkynyl silyl sulfides **91**. These represent a more stable analogon of ynethiols with regard to their reactivity.



Scheme 27: Base-induced cycloreversion of 5-unsubstituted 1,2,3-thiadiazoles **92**.

SCHAUMANN et al. also compared the procedure they developed for the synthesis of silylated alkynylsulfides with the known protocol that utilizes 1,2,3-thiadiazoles **92** (Scheme 27).<sup>[89]</sup> In fact, these compounds are also used as thioketene equivalents. When 1,2,3-thiadiazoles **93** are activated either by heat or light, they give, what can best be described as thioacyl carbene, 1,3-dipole, or 1,3-diradical. Eventually either of these species rearranges to form thioketenes **94** (Scheme 28).

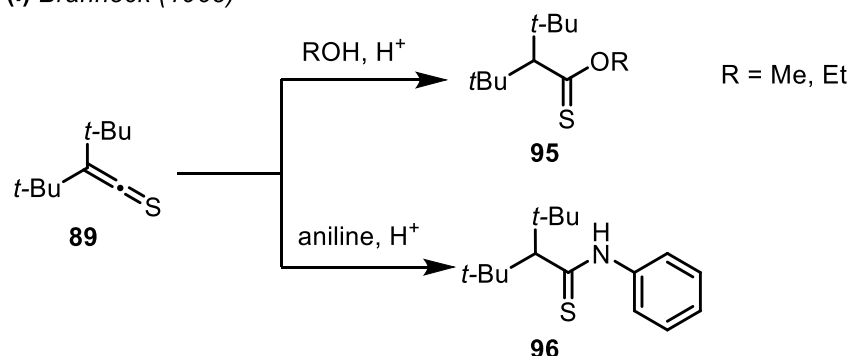


Scheme 28: Formation of thioketene **94** starting from 1,2,3-thiadiazoles **93**.

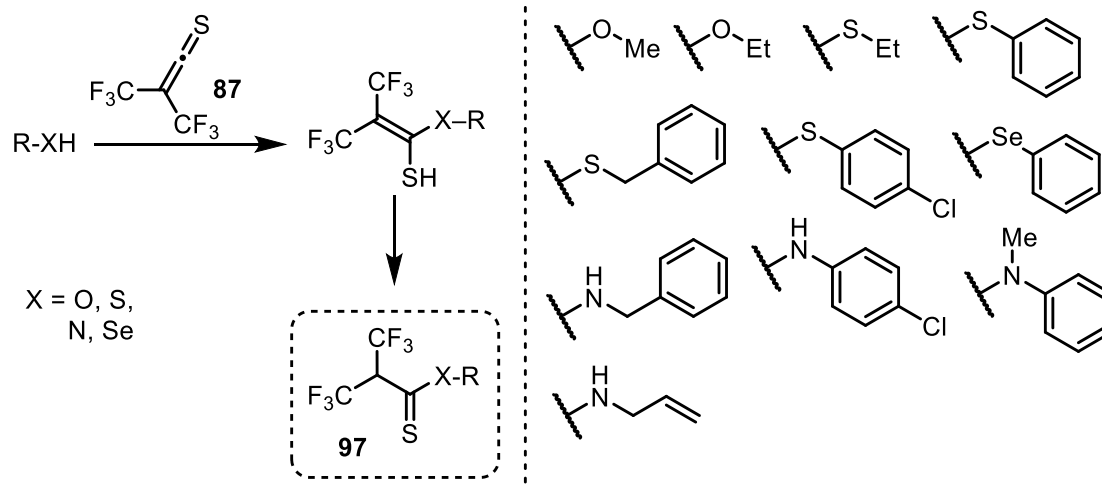
## SYNTHESIS OF DITHIOESTERS, THIOAMIDES AND THIONOESTERS

The in the Section above described thioketenes and thioketene equivalents can serve as materials for the synthesis of thiocarbonyl compounds:

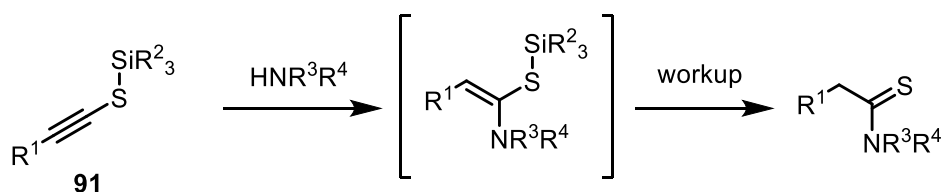
### (I) Brannock (1968)



### (II) Raasch (1972)



### (III) Schaumann (2014)



Scheme 29: Access to thioacylation products by utilization of stable thioketenes or thioketene equivalents.

After successful synthesis of the stable di-*tert*-butylthioketene **89**, BRANNOCK et al. investigated its behavior towards small nucleophiles. Thioacylation took place with methanol and ethanol, giving rise to thionoesters **95**, and reaction with aniline gave the corresponding thioamide **96** (Scheme 29-I). No further reactions were reported, as the authors stated that, similar to the ketene analogon **88**, the reactivity of **89** is severely hindered by the steric shielding, which also increases its stability.<sup>[86]</sup>

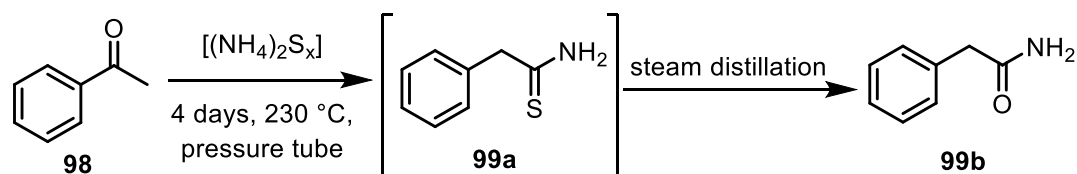
Reaction of bis(trifluoromethyl)thioketene **87** with *N*- *S*- and *O*-nucleophiles gives the corresponding thioacylation products **97**, as reported by RAASCH (Scheme 29-II).<sup>[85]</sup> The

obvious limitation for this procedure, as well as of the aforementioned, is the predefined substitution pattern of either bis(trifluoromethyl)- or di-*tert*-butyl-substitution in  $\alpha$ -position to the thiocarbonyl functionality.

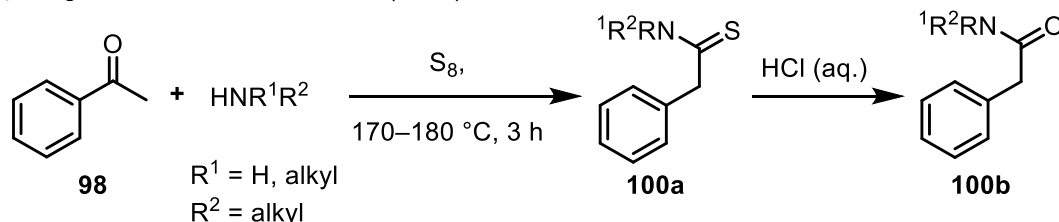
The thioacylation protocol reported by SCHAUMANN which uses silylated alkynylsulfides **91**, is also limited (Scheme 29-III).<sup>[88]</sup> The oxophilic nature of silicon does not permit convenient thioacylation of alcohols, and reports with other simple *N*- or *S*-nucleophiles are also scarce. Its advantages lie in its ability to undergo cyclization reactions with azomethines to give  $\beta$ -thiolactams and, furthermore, cyclizations with (thio)imidates and ynamides.

An alternative for the synthesis of thioamides, which is not relying on the use of thioketene or thioketene-mimetic chemistry, is the Willgerodt-Kindler reaction. Originally discovered as Willgerodt Carbonyl Transposition (Scheme 30-I) in 1887,<sup>[90]</sup> the reaction was further developed by KINDLER (II) in 1923 (Scheme 30-II).<sup>[91]</sup>

(I) Willgerodt Carbonyl Transposition (1887)



(II) Willgerodt-Kindler modification (1923)

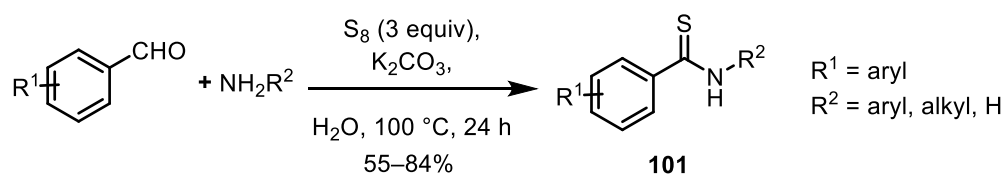


Scheme 30: The original Willgerodt reaction and its Willgerodt-Kindler modification.

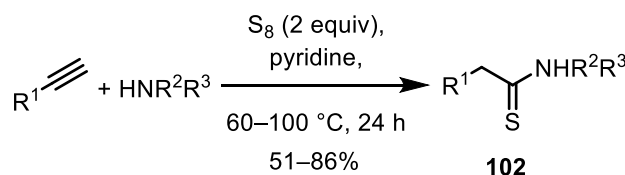
The original protocol was used to synthesize amides **99b** from arylketones **98**; intermediate thioamides **99a** were *in situ* hydrolyzed to amides. The Kindler modification features much milder reaction conditions and easier to handle compounds. This procedure consists in heating of an aryl ketone **98** in the presence of sulfur and an amine and allows to isolate the thioamides **100a**. Subjecting them to hydrolysis conditions again, the corresponding amides **100b** are obtained. While the reaction is historically well utilized, it is limited to aryl ketones, and yields above 60% are mostly only achieved when methyl ketones are employed.

Contemporary literature with resembling conditions of the Willgerodt-Kindler reaction is provided by ZHOU et al. and NGUYEN et al.<sup>[92,93]</sup>

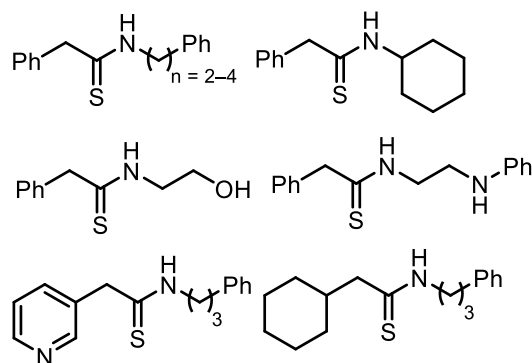
(I) Zhou (2013)



(II) Nguyen (2014)

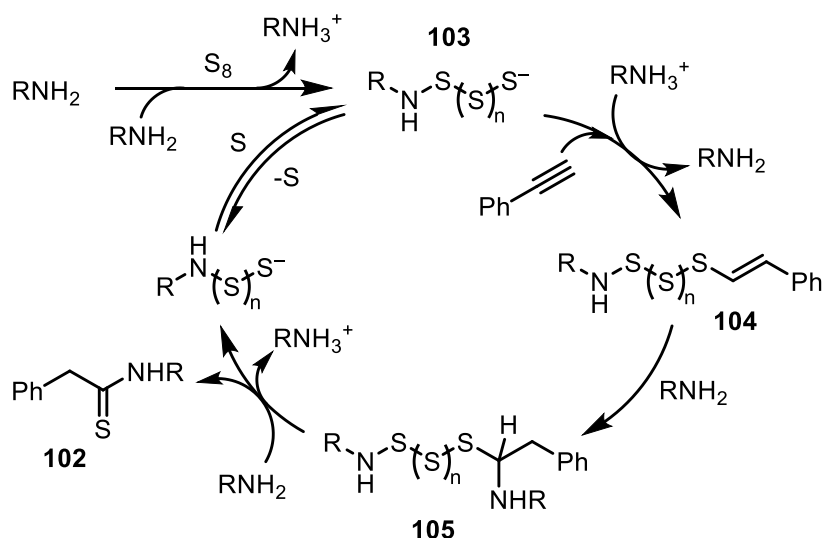


selected examples



Scheme 31: Recent literature on thioamide synthesis, related to Willgerodt-Kindler conditions.

ZHOU et al. proposed that formation of the thioamide **101** takes place either by Willgerodt-Kindler reaction or by thionation. In a model reaction, thionation of *N*-phenylbenzamide under their standard conditions gave thioamide **101** in 12% yield, whereas the reaction of *N*-benzylideneaniline in the presence of sulfur, resembling Willgerodt-Kindler reaction conditions, gave the corresponding thioamide in 82% yield, thus strongly suggesting this mode of reaction to be the actual one. The advantage of the reported methodology clearly is the use of water as a solvent, in which employment of  $\text{K}_2\text{CO}_3$  as a base prevents subsequent hydrolysis to the amide during the reaction (Scheme 31-I).<sup>[92]</sup>

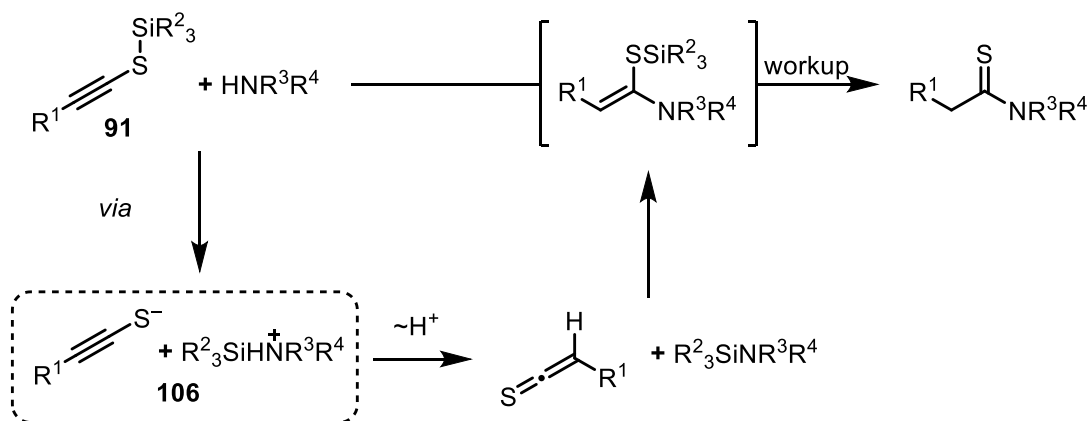


Scheme 32: Mechanism proposed by NGUYEN et al.

Instead of carbonyl compounds also terminal alkynes can be utilized to give access to thioamides **102**, as reported by NGUYEN et al. (Scheme 31-II). The authors propose a mechanism in which the  $\text{S}_8$  ring structure is cleaved by the amine, which gives the

polysulfidic species **103**. The alkyne subsequently adds to the latter, thus resulting in a vinyl polysulfide **104**. The polarized double bond in **104** is then attacked by the amine to give a thioaminal **105**, which experiences stabilization by elimination to the thioamide **102** as final product (Scheme 32).<sup>[93]</sup>

On the other hand, a mechanism more similar to that proposed by SCHAUMANN et al.,<sup>[88]</sup> in which a transiently formed thioynolate ammonium salt **106** is an intermediate of the transformation, might be a viable alternative (Scheme 33).



Scheme 33: Proposed mechanism by SCHAUMANN for the formation of thioamides utilizing alkynyl silyl sulfides.<sup>[88]</sup>

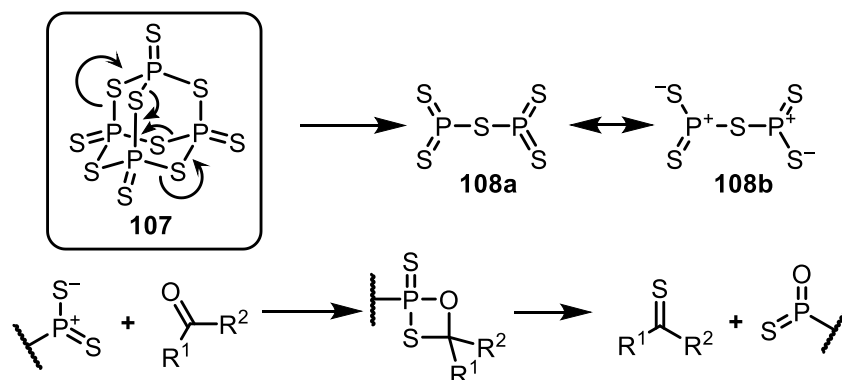
NGUYEN et al. pointed out that product formation could be observed neither for anilines nor for alcoholates, thus demonstrating the limitations of the developed procedure. Transformation with (triisopropylsilyl)acetylene gave the desilylated product under the reported reaction conditions. In summary, the protocol is advantageous in terms of the atom-economy,<sup>[94]</sup> given that this is a three component reaction; however, functional group tolerance is limited. In addition, and similar to the majority of literature procedures that give access to thioamides, reaction temperatures are relatively high.

Other more conventional methods to access thioamides are the straightforward thionation of amides with either Lawesson's Reagent (LR) **125** (Scheme 34) or phosphorus pentasulfide ( $P_4S_{10}$ ) **107** (Scheme 38).<sup>[95]</sup>

Phosphorus pentasulfide can be obtained by reacting liquid white phosphorus ( $P_4$ ) with sulfur at temperatures above 300 °C. The reaction, however, can be quite violent, which is why alternative routes were developed. In one of them white phosphorus was substituted with red one, another employs either elemental sulfur or pyrite ( $FeS_2$ ) to react with ferrophosphorous.

Besides direct thionation,  $P_4S_{10}$  is also commonly used for the synthesis of heterocycles such as thiazines, thiazoles, thiophenes, pyrimidines, imides, dithiins, dithiazoles, thiazolines, imidazolines and thiadiazoles. General reaction conditions are refluxing  $P_4S_{10}$  and the desired

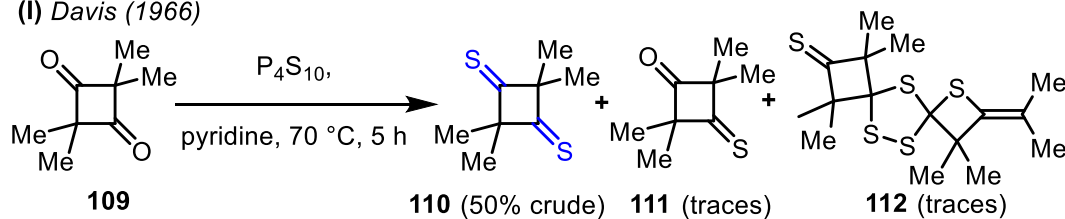
substrate in solvents such as toluene, xylene, THF, acetonitrile or CS<sub>2</sub>, with addition of bases like pyridine, Et<sub>3</sub>N, Na<sub>2</sub>CO<sub>3</sub>, NaHCO<sub>3</sub> or Na<sub>2</sub>SO<sub>3</sub>.



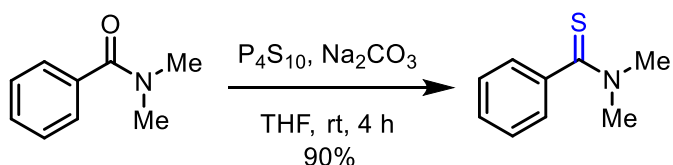
Scheme **34**: Dissociation mechanism of P<sub>4</sub>S<sub>10</sub> and proposed mechanism for the thionation with P<sub>4</sub>S<sub>10</sub>.

While the detailed mechanism of thionation is not fully elucidated, the general rationale is that dissociation of P<sub>4</sub>S<sub>10</sub> to P<sub>2</sub>S<sub>5</sub> **108** plays a crucial role (Scheme **34**). This hypothesis is generally accepted, as isolation of P<sub>2</sub>S<sub>5</sub> from reaction mixtures and its characterization by X-ray diffractometry furnishes the evidence.

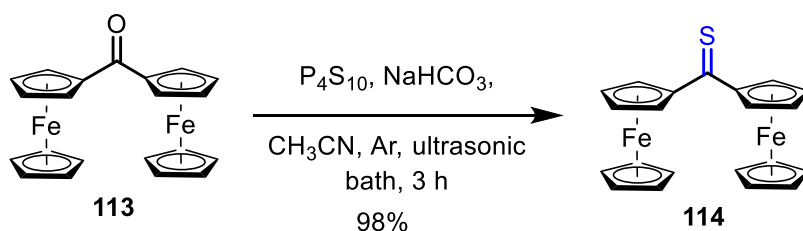
(I) Davis (1966)



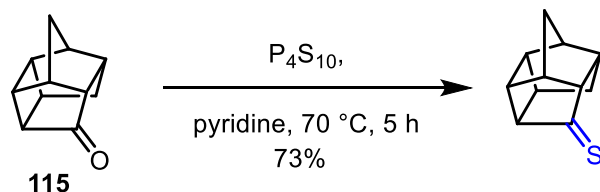
(II) Brillon (1990)



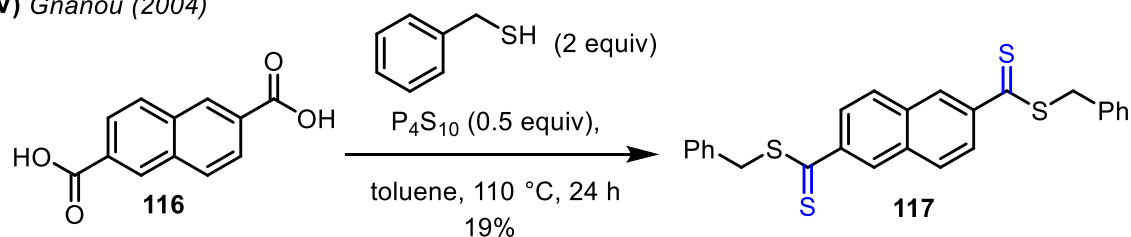
(III) Bildstein (1993)



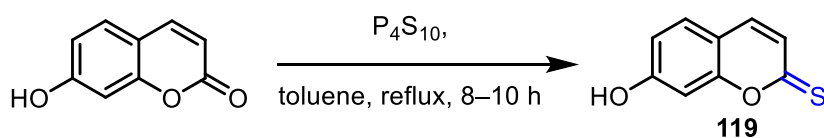
(IV) Mloston (2002)



(V) Gnanou (2004)



(VI) Ibrahim (2006)

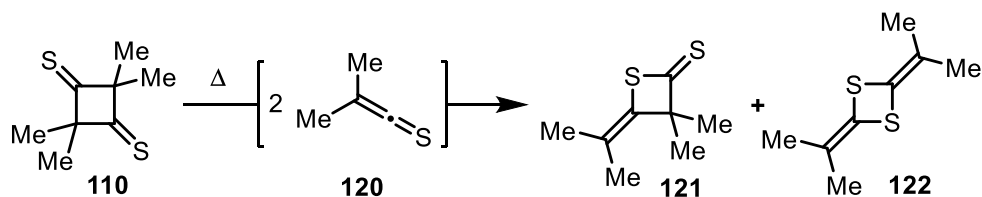


Scheme 35: Selected examples of thionations with  $\text{P}_4\text{S}_{10}$ .<sup>[96–101]</sup>

In an attempt to find new ways to access monomeric thioketenes, DAVIS and ELAM thionated diketone dimer **109** on large scale (2.1 mol) and analyzed the isolable products (Scheme 35-I). Depending on the amount of starting material, they were able to favour either dithionation to thioketene-dimer **110** or monothionation to obtain tetramethyl-3-thio-1,3-cyclobutanedione (**111**). Pioneering in this field, they reported NMR data of the formerly unknown compounds. Although the authors were unsuccessful in obtaining monomeric thioketene **120** by pyrolysis, characteristic formation of thiethanethione **121** and dithiethane



**122** was observed, thus indicating the monomeric form to be a short-lived species (Scheme 36).<sup>[96]</sup>

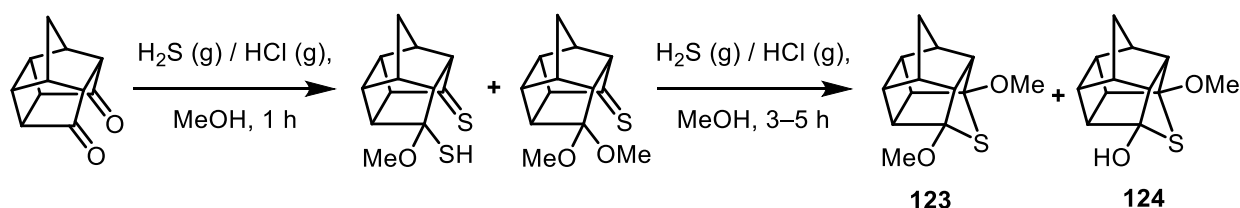


Scheme 36: Pyrolysis of thioketene-dimer.

Investigations towards enhancing the reactivity of  $P_4S_{10}$  were conducted by BRILLON as early as 1990 (Scheme 35-II).<sup>[97]</sup> Pretreatment of  $P_4S_{10}$  with  $Na_2CO_3$  proved to be beneficial when compared to former literature reports. He proposed the compound with the empirical formula  $(P_4S_{10}O)^{2-}Na_2^{2+}$  to be the active agent, with ambiphilic properties.<sup>1</sup> Applying this protocol, the *in situ* preformation of a species that is more reactive than  $P_4S_{10}$  itself, a number of thionations at room temperature could be performed.

The same concept enabled BILDSTEIN and DENIFL to transform diferrocenylketone (**113**) to diferrocenylthioketone (**114**) (Scheme 35-III). ). A combination of  $P_4S_{10}$  and  $NaHCO_3$ , gave access to the corresponding thiocarbonyl compound **114**, which then enabled them to study this compound's ability to coordinate different metal carbonyl complexes with the general formula  $[THF][M(CO)_x](M = Cr, Mo, W)$ .<sup>[98]</sup>

For MŁOSTOŃ and ROMAŃSKI,  $P_4S_{10}$  was the thionating reagent of choice for the first synthesis of thiocarbonyl derivatives of cage ketones **115** (Scheme 35-IV). During their investigations they also employed a thionation protocol with a combination of  $H_2S/HCl$  (gas) which, upon longer reaction times, gave unexpected novel cyclization products **123** and **124** (Scheme 37).<sup>[99]</sup>



Scheme 37: Cyclization of cage thioketones.

One of the major applications for dithioesters is as chain transfer reagents (CTA) for reversible addition-fragmentation chain transfer (RAFT) polymerization. The group of GNANOU synthesized RAFT agent **117** starting from 1,4-naphthalenedicarboxylic acid **116**, which enabled them to control the molar masses and polydispersities of the formed polymers (Scheme 35-V). Thus, they were able to obtain linear poly(*tert*-butylacrylate-*b*-

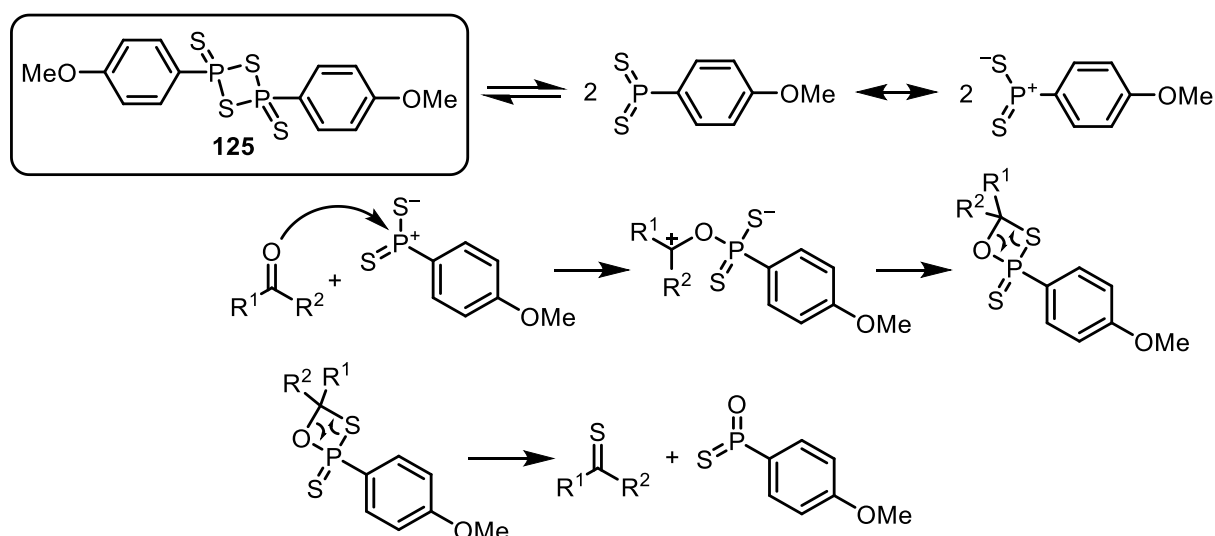
<sup>1</sup> According to the autor, reaction of  $P_4S_{10}$  with  $NaHCO_3$  involves phosphorus-sulfide bond breaking and formation of ionic thiophosphate groups.

styrene-*b*-*tert*-butylacrylate) triblock copolymers as well as three-arm polystyrene stars following an “arm-first” approach.<sup>[100]</sup>

Investigations of the behavior of sulfur reagents towards coumarins were reported by IBRAHIM. Hydroxycoumarin **118** was converted to thionolactones **119** when P<sub>4</sub>S<sub>10</sub> was used, without touching the hydroxyl functionality (Scheme 35-VI). Different sulfur reagents were compared, and it could be shown that LR, too gave the same product for the depicted transformation.<sup>[101]</sup>

A plethora of other reactions resulting from the increased reactivity of thioanaloga compared to their oxygen parent compounds have been reported, most of which being condensation or cyclization reactions as also implied in selected examples discussed above (Scheme 35, Scheme 37).

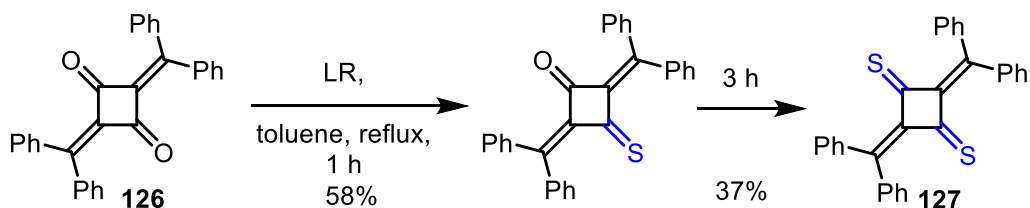
Lawesson’s reagent **125** can be synthesized in laboratory scale by heating P<sub>4</sub>S<sub>10</sub> in the presence of anisole until hydrogen sulfide evolution ceases. Alternatively it can be prepared from elemental sulfur, red phosphorous and anisole. It is commonly purified by recrystallization from xylene or toluene. It decomposes slowly at temperatures above 110 °C in solution.



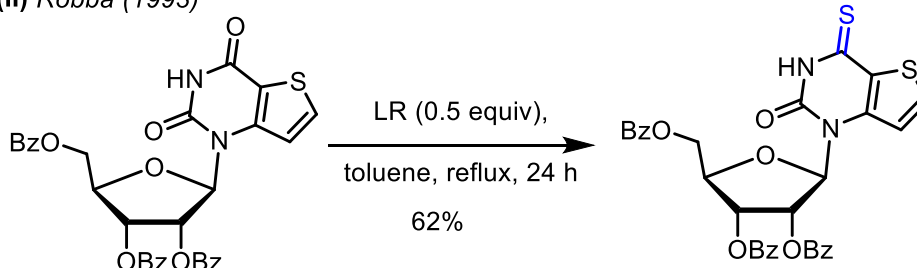
Scheme 38: Lawesson’s reagent (LR) **231** and mechanism of the thionation with LR.

Usual thionations with LR are performed on carbonyl compounds, enones, esters, lactones, amides, lactams, and quinones (Scheme 38). Its diverse application possibilities are highlighted in Scheme 39. They range from modifications of complex structures, such as nucleosides (Scheme 39-II) over peptides (Scheme 39-III) to steroids (Scheme 39-IV).

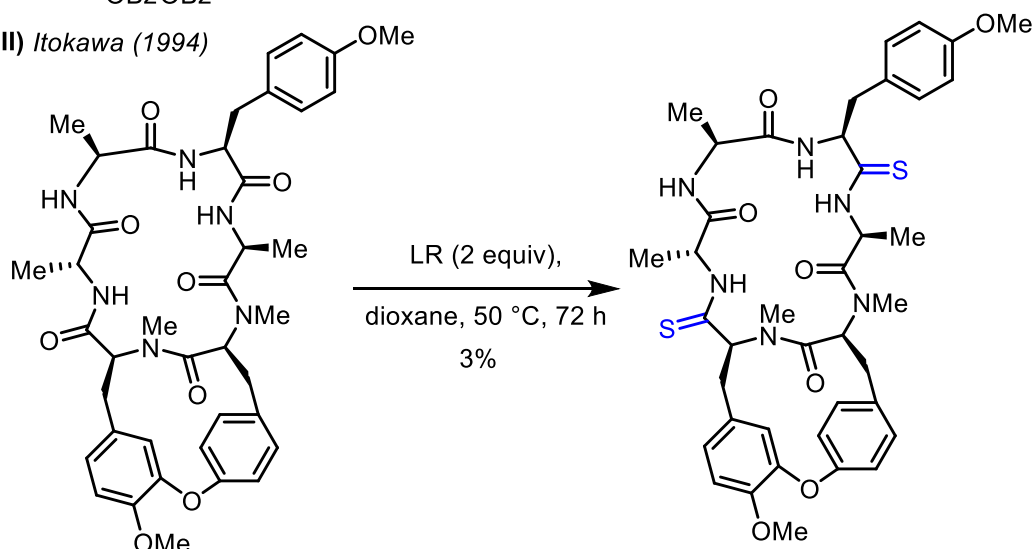
(I) Strehlow (1991)



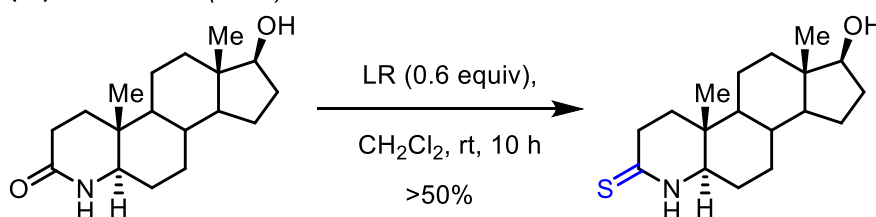
(II) Robba (1993)



(III) Itokawa (1994)



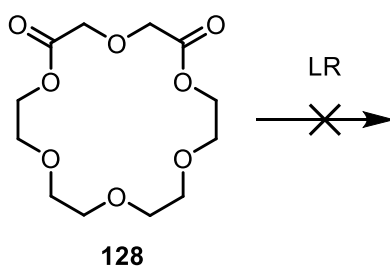
(IV) Ferraboschi (1997)



Scheme 39: Highlighted products obtained by thionation with LR.<sup>[102]</sup>

In order to synthesize novel diradical dianions and to determine their electronic properties, STREHLOW et al. (I) transformed cyclobutandione **126** into their respective thioketone analogue **127**. Similar to DAVIS work with P<sub>4</sub>S<sub>10</sub> (Scheme 35-I), reaction time determined either the onefold or twofold thionation products to occur as the major product.

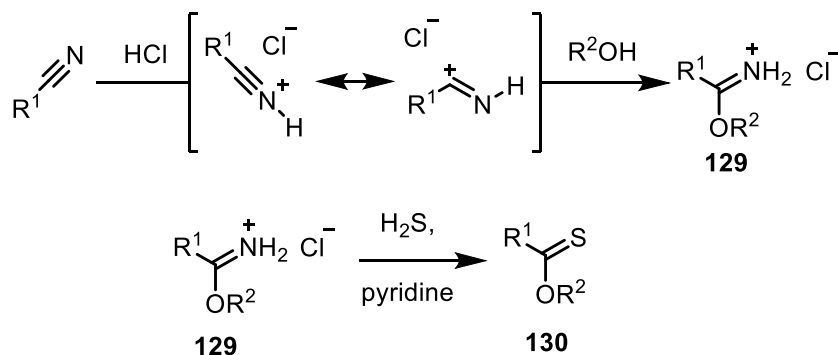
While LR obviously is able to be applied in diverse fields, it reaches its limitations for compounds with ether-containing ester functionalities. For example, crown ether **128** with two ester moieties (Scheme 40) could not be thionated by LR.



Scheme 40: Limitations of LR.<sup>[103]</sup>

While phosphorus pentasulfide, mostly due to the fact that it is one of the historically oldest thionating agents, has found countless applications as well as LR, which is still the most used chemical for thionations, their obvious drawbacks will always remain the same: Harsh reaction conditions, long reaction times, tedious chromatographic purifications, high toxicity of both the reagent, the formation of the by-products and unpleasant odour are major drawbacks of both reagents. This requires the development of novel methodologies and reagents for thionation and discovery of other reaction pathways to access thioamides, dithioesters and thionoesters.

Another possibility to obtain thionoesters is in the context of the Pinner reaction. Pinner salts **129** when reacted with  $\text{H}_2\text{S}$ , give the corresponding thionoesters **130** (Scheme 41). In the same fashion, when thiols are used instead of normal alcohols, access to dithioesters becomes available.

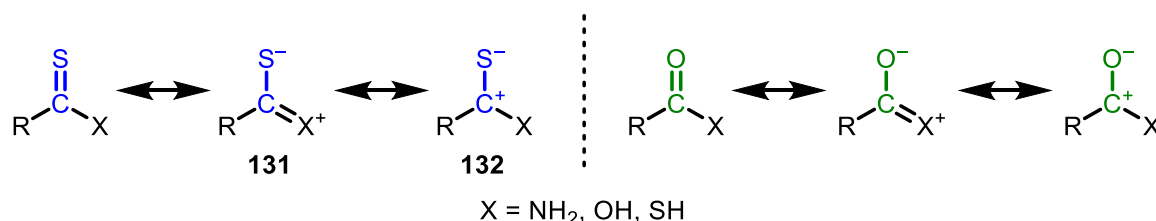


Scheme 41: Pinner salt formation and synthesis of thionoesters **130** utilizing the former.

Numerous further examples from literature, which extensively cover the topic of thioamides and dithioesters in depth, are available.<sup>[104]</sup>

## PROPERTIES OF DITHIOESTERS, THIOAMIDES AND THIONOESTERS

Comparison of dithioesters, thioamides and thionoesters with their corresponding oxyanaloga shows that all three of the former generally exhibit an increased reactivity towards both electrophiles and nucleophiles.



Scheme 42: Comparison of the importance of resonance structures in carbonyl and thiocarbonyl compounds.

A qualitative explanation can be drawn from evaluating the importance of resonance structures for carbonyl and thiocarbonyl compounds. For thiocarbonyls the mesoionic resonance structure **131**, in which  $\pi$ -electron donation into the X=C bond takes place and a negative charge resides on the sulfur (Scheme 42), is more important.<sup>[105]</sup>

Determination of rotational barriers for the C–N bonds in thioamides gives quantitative evidence for the increased importance of the C=X resonance structure and thus the actual electron density distribution. An example is given by the comparison of *N,N*-dimethylformamide (DMF) and *N,N*-dimethylacetamide (DMA) with *N,N*-dimethylthioformamide (DMTF) and *N,N*-dimethylthioacetamide (DMTA) (Table 1).<sup>[105,106]</sup>

Table 1: Comparison of rotational barriers (in kcal·mol<sup>-1</sup>) of DMF, DMTF, DMA and DMTA.<sup>[105,106]</sup>

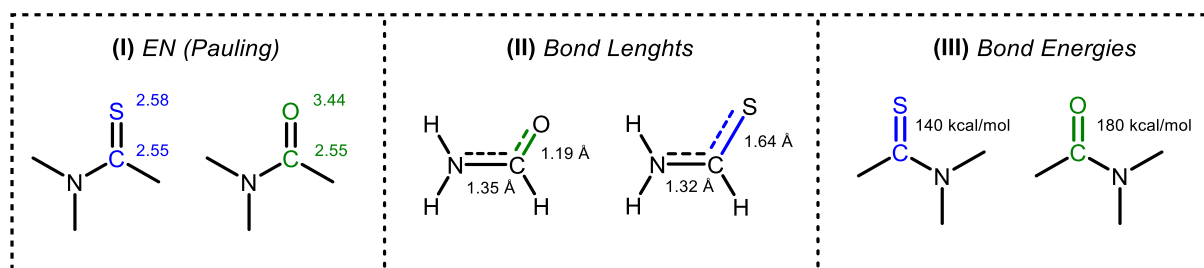
Solvent	$\epsilon$	DMF	DMTF	DMA	DMTA
Gas phase	1	19.25	22.0	15.33	17.7
Cyclohexane	2.02 (1.98)	19.73	23.5	16.36	19.6
Dichloromethane	9.08	-	-	17.95	21.9

As shown in Table 1, rotational barriers for thiocarbonyl compounds are approximately 3 kcal·mol<sup>-1</sup> higher than for their related carbonyl compounds. This fact that can also be visualized by NMR spectroscopy: While for DMA one signal for both methyl groups is observed, for DMTA, two separate signals for each CH<sub>3</sub> groups are detected. The rates of rotation could be obtained by selective inversion-recovery (Sir) NMR experiments.<sup>[107]</sup>

The described  $\pi$ -electron donation into the X=C bond also results in weaker H-bond acceptor and higher H-bond donor abilities for thioamides. LEE, PARK et al. quantitatively proved this statement with a comparative study on amides and thioamides by using near IR spectroscopy.<sup>[108]</sup>

An additional consequence is that protons on the heteroatom are more acidic (in case of unsubstituted thiocarbonyls this accounts for  $\alpha$ -protons): Taken for example that the pKa values of thiobenzoic acid and thioacetic acid are 3.33 and 2.48, respectively, values for benzoic acid and acetic acid are 4.20 and 4.76. This also means that thioacids undergo easier deprotonation by the usual array of inorganic and amine bases.<sup>[109]</sup>

Yet, this does not explain the observed increased electrophilicity of thiocarbonyl carbons. The dipolar thiocarbonyl resonance structure **132** provides an answer for both, the heightened C-electrophilic-, and S-nucleophilic character of thiocarbonyl compounds. Quantitatively it can be explained by comparing the covalent radii for oxygen and sulfur, which determine their respective S–C/O–C bond lengths.<sup>[110]</sup> The longer S–C bond in this case, results in a decrease of electron density directed from the sulfur towards the carbonyl carbon.



Scheme **43**: Exemplary comparison of electronegativity, bond lengths and bond energies between amides and thioamides.<sup>[110,111]</sup>

Finally, an explanation for the increased reactivity of thiocarbonyl compounds compared to their oxygen analoga can be given by examining their bond dissociation energies (Scheme **43-III** and Table 2).<sup>[112]</sup>

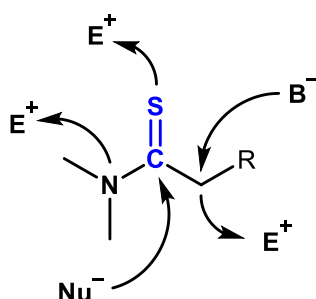
Table 2: Bond dissociation energies ( $D_{298}$ ) in kcal·mol<sup>-1</sup>.<sup>[112]</sup>

Compound	Observed	Calculated (CCSD)
H <sub>2</sub> C=O	179	175
H <sub>2</sub> C=S	137	1273
$\pi$ C=O	(87)	-
$\pi$ C=S	(52)	-

Bond dissociation energy for thiocarbonyl compounds is lower by approximately 40 kcal·mol<sup>-1</sup>, meaning that the former bond is significantly easier to break.

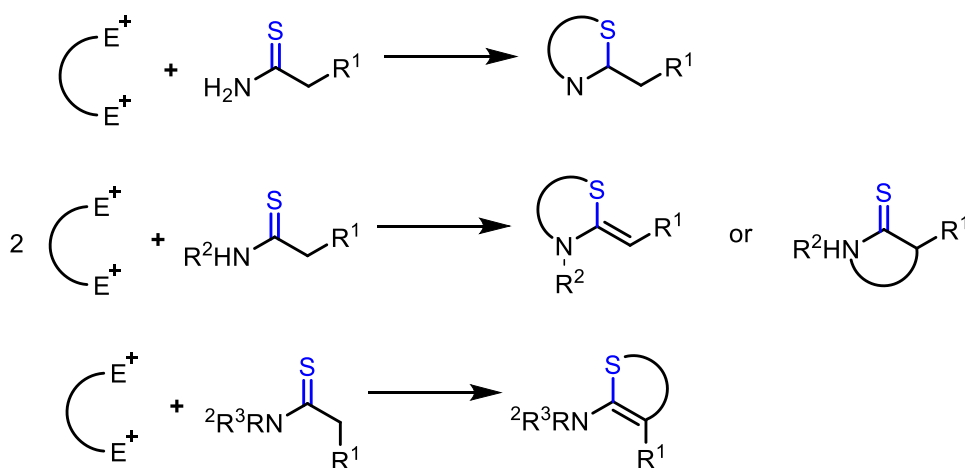
## APPLICATION AND REACTIVITY OF DITHIOESTERS, THIOAMIDES AND THIONOESTERS

As described in the previous Chapter, two properties of the thiocarbonyl group stand out. One is the electrophilic character of the carbonyl carbon, which favors condensation reactions of the thiocarbonyl unit. This also results in thiocarbonyl compounds being more prone to reduction. For example, if reduction of an amide to the amine is not possible in a straightforward manner, transformation to the thioamide and successive reduction to amines is used as a devious route. The second major difference is the increased nucleophilicity on sulfur, which, for example, results in selective S-alkylation for enethiolates, as compared to enolates. Along with that, as mentioned above,  $\alpha$ -protons show increased acidity.



Scheme 44: Representative reactive positions of thioamides.

The described reactivity of thioamides, dithioesters and thionoesters (Scheme 44 and Scheme 45) is used mainly for the synthesis of heterocycles.<sup>[113]</sup>



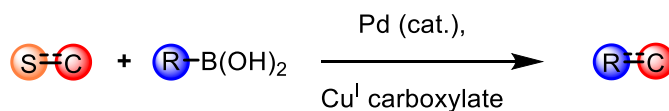
Scheme 45: Reactivity of primary, secondary or tertiary thioamides.

Other applications are thiopeptide antibiotics synthesis, for thioamides and RAFT polymerization for dithioesters respectively, as they can be used as chain transfer agents (CTA) to control the polymerization process.<sup>[114]</sup>

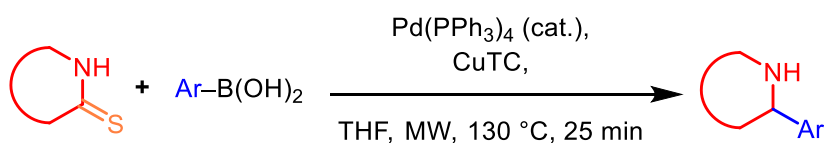
The Liebeskind-Srogl coupling is one of the few transition metal mediated cross couplings which utilizes sulfur containing compounds for the construction of carbon-carbon bonds

(Scheme **46-I**).<sup>[115]</sup> A number of structures have proven to be applicable in the cross coupling, such as thiol esters, diarylsulfides, thiocyanates, (hetero)aryl thioethers, thioalkynes and cyclic thioamides.

(I) *Liebeskind-Srogl coupling* (2000)



(II) *Lengar & Kappe* (2004)



Scheme **46**: Schematic Liebeskind-Srogl coupling<sup>[115]</sup> and exemplary transformation of cyclic thioamides by LENGAR and KAPPE (CuTC = Cu(I) thiophene-2-carboxylate).<sup>[116]</sup>

LENGAR and KAPPE reported a microwave-assisted boronic acid-thioamide Liebeskind-Srogl coupling protocol, which gave them valuable diaryls (Scheme **46-II**). By addition of phenanthroline, they could also favour the selectivity of the reaction towards carbon-sulfur coupling, which gave them diarylthioethers.

The difference in  $n \rightarrow \pi^*$  transition for thiocarbonyl and carbonyl compounds can be used for applications in protein chemistry: By implementation of the thioamide functionality as fluorescence quenching probes, PETERSSON et al were able to track protein folding and their stability.<sup>[117]</sup>

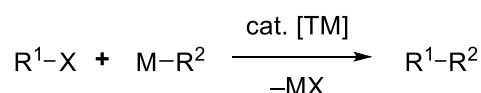


## ELECTROPHILIC ALKYNYLATION WITH TRANSITION METAL GENERATED NUCLEOPHILES

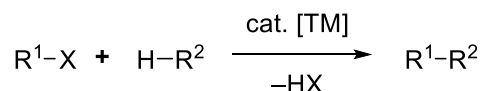
### C–H FUNCTIONALIZATION

Functionalization of otherwise inert carbon hydrogen bonds (C–H functionalization) has been one of the last major frontiers in organic chemistry. With its high dissociation energy (110 kcal·mol<sup>-1</sup> for benzene and 105 kcal·mol<sup>-1</sup> for methane) mediation for the bond breaking step by a metal is often required.<sup>[118]</sup> Roughly 20 years ago the field of transition metal mediated C–H activation, functionalization, reemerged. Since then it has significantly enriched the chemists repertoire of possible C–C bonding reactions and has matured to a viable alternative to classic cross coupling reactions such as, Heck-, Suzuki-Miyaura, Stille-, Sonogashira-Hagihara reactions and others, for many cases.<sup>[6–12,14,15]</sup>

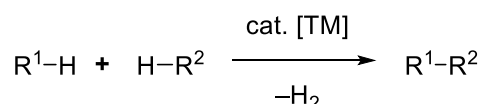
(I) *cross coupling reaction*



(II) *C–H functionalization*



(III) *cross-dehydrogenative coupling*

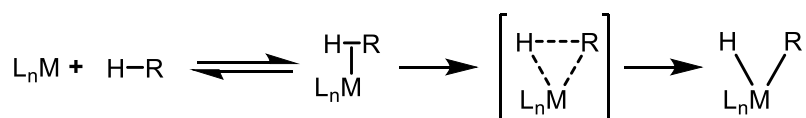


Scheme 47: Comparison of concepts for C–C bond formation.

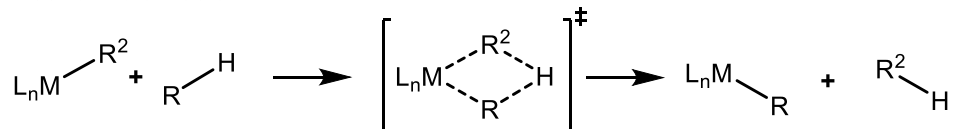
As can be seen from Scheme 47, the major difference between cross-coupling reactions and C–H functionalization is the breaking of either a C–X or a C–H bond and concomitant formation of either a MX or HX species. This in return requires prefunctionalization of the to-be-modified carbon center in an additional foregoing step. The consequence is additional necessity of reagents, solvent, energy and time. In addition, halide containing byproducts are inevitably obtained.

For the key C–H bond breaking step of C–H functionalization, four major pathways have been proposed, depending on the transition metal, its oxidation state and partaking ligands (Scheme 48).

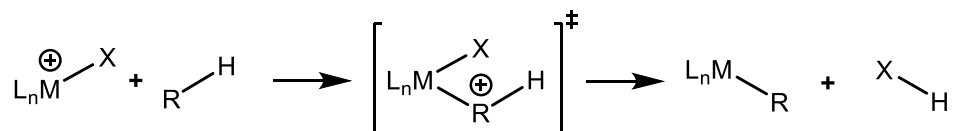
(I) oxidative addition



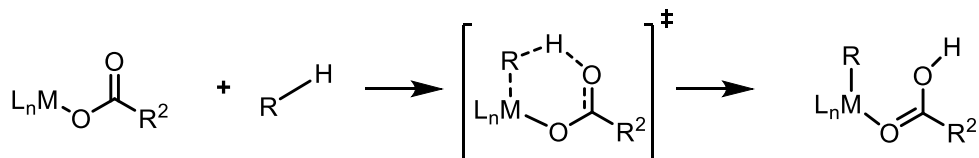
(II)  $\sigma$ -bond metathesis



(III) electrophilic substitution

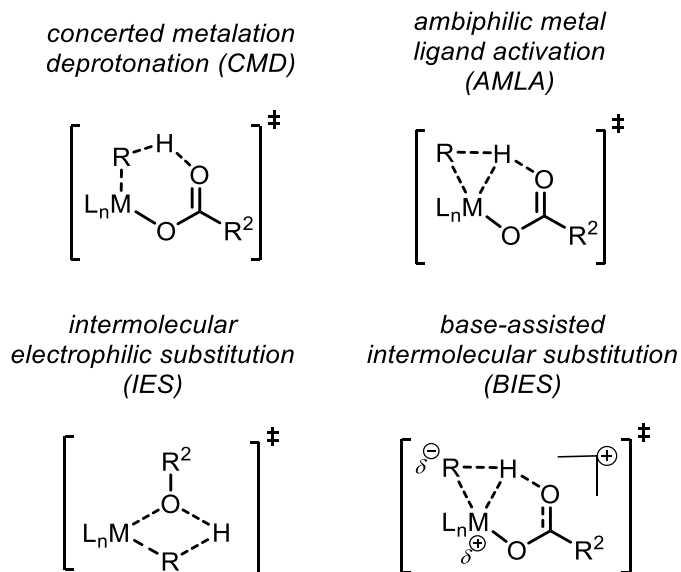


(IV) base-assisted metalation



Scheme 48: Mechanisms of C-H bond metallation.

Oxidative addition (Scheme 47-I) is the operating mechanism for late, electron rich transition metals in low oxidation states, for example rhodium(0), palladium(0), ruthenium(0) and low valent cobalt systems. Early transition metals in high oxidation states are unable to partake in oxidative addition. They favourably react via  $\sigma$ -bond metathesis (SBM or  $\sigma$ BM) (Scheme 47-II). For late transition metals in higher oxidation states, electrophilic substitution (Scheme 47-III) becomes favoured. In this case the Lewis acidity of the catalyst increases and dictates the mode of reaction. The historically most recently discovered (and arguably most investigated) pathway, is the base-assisted metalation (Scheme 47-IV) in which an added base for one ligates the metal centre. Secondly, it facilitates the proximal proton abstraction with an additional Lewis-basic heteroatom it possesses. The most prominent group of bases used therefor are carboxylates.<sup>[119,120]</sup> For this fourth mechanistic pathway, additional investigations have been carried out. Four feasible transition states are discussed here.



Scheme 49: Transition states for base-assisted metalation.<sup>[121–126]</sup>

Independently described by FAGNOU and DAVIES & MACGREGOR are the concerted metalation-deprotonation (CMD) pathway and the ambiphilic metal ligand activation (AMLA) respectively, although the denomination CMD has prevailed. They both describe either a 4- or 6-membered transition state, in which intramolecular deprotonation and metalation occur simultaneously. For CMD mechanisms the C-H bond cleavage step is kinetically significant (Scheme 49).<sup>[121–123]</sup>

A third scenario, an 4-membered transition state, characteristic in case of either alkoxy bases or hydroxide as intramolecular base, is termed internal electrophilic substitution (IES) by OXGAARD.<sup>[124]</sup> Adding on these results, ACKERMANN could extend the concept to carboxylates, coining the term base-assisted internal electrophilic substitution (BIES). BIES mechanisms can be identified by their dependence on the electronic nature of the substrate: The more electron-rich the arene, the lower is the activation energy for the C-H activation step.<sup>[125,126]</sup>

C–H functionalization with guided selectivity requires certain considerations before using it for the modification of a molecule, regarding the choice of the directing group. If introduction, utilization for C–H activation, functionalization and removal of the required directing group takes place in a single reaction it is considered a transient directing group. When only a preceding introduction is necessary and removal of the directing group takes place in the same reaction, the directing group is denoted traceless. When all three steps, introduction of the directing group, reaction and removal of the directing group take place separately, it is called a removable directing group. In any of these cases, evaluation of the feasibility of a C–H functionalization protocol, or classic cross coupling is recommended.<sup>[127]</sup> In general, any functional group with a free electron pair (lone pair) can be considered and by now, has been investigated, as a directing group.<sup>[128]</sup>

Choice of the right directing group is essential, since it must fulfill several roles during the reaction. First it needs to be able to coordinate the active catalyst species and selectively "direct" it to the reaction site, the C–H bond that should be functionalized. It has to further stabilize the transition state during C–H activation as well as partake in the metallacycle. Afterwards de-coordination is necessary to liberate the catalyst, so it can undergo the next catalytic cycle. The alternative, too strong coordination, leads to inactive substrate-catalyst species. One possibility to determine the coordination strength of directing groups is to evaluate their Lewis basicity by measuring their affinity towards Lewis acids such as SbCl<sub>5</sub> or BF<sub>3</sub>.<sup>[129]</sup> Similar rules apply for the choice of transition metal catalyst which can be considered Lewis acids.

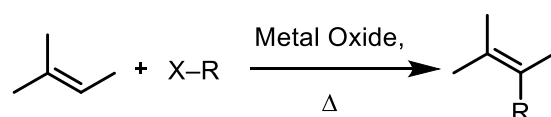
When discussing C–H functionalization, precise definition of which area is necessary, since it has become such a large field of research. Categorization is possible, for example, by employed metal, agent of oxidation, directing group or hybridization of the functionalized C–H bond.

The first precedent for the functionalization of aromatic sp<sup>2</sup>-carbon hydrogen bonds (C–H functionalization) arguably was given by OTTO DIMROTH in 1902, when he reported the reaction of mercury(II) acetate with benzene (Scheme 50-II),<sup>[130]</sup> predeceased only by the Butlerov-Eltekov-Lermontova-reaction for the functionalization of acyclic olefinic carbons from 1874 (Scheme 50-I).<sup>[131]</sup> However, when compared to more contemporary literature on C–H functionalization, these examples lack one crucial component, a directing group (DG), which is able to coordinate a metal center in order to direct the C–H activation step to a particular proximal carbon-hydrogen bond.

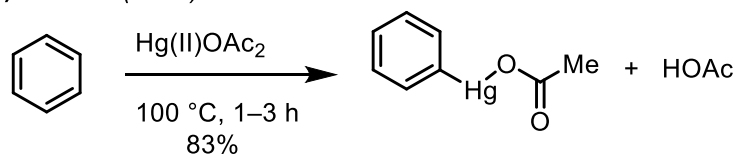
Consequently C–H functionalization with innate selectivity (no influence of directing forces) and guided selectivity (employment of a DG) is differentiated.

The first reported C–H functionalization with guided selectivity was published by SHUNSUKE MURAHASHI in 1955, where Co<sub>2</sub>(CO)<sub>8</sub> was used as a catalyst to transform (*E*)-*N*,1-diphenylmethanimine (**133**) into 2-phenylisoindolin-1-one (**134**) under an atmosphere of CO (100–200 atm) at 220–230 °C (Scheme 50-II).<sup>[132]</sup>

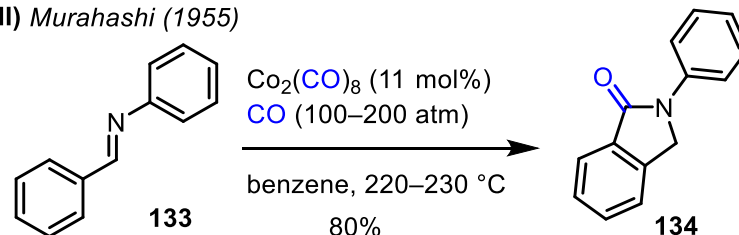
(I) *Lermontova* (1876)



(II) *Dimroth* (1902)

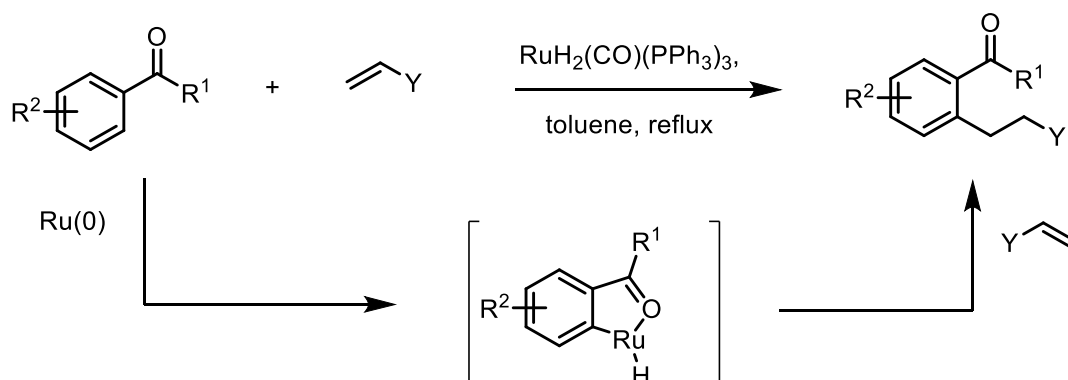


(III) *Murahashi* (1955)



Scheme 50: Butlerov-Eltekov-Lermontova-reaction, C–H activation of benzene with mercury(II) acetate by DIMROTH (I) as an example for innate selectivity and synthesis of indolinones by MURAHASHI by utilization of the imine functionality as a DG using guided selectivity (II).<sup>[130,132,133]</sup>

Another milestone in C–H functionalization worth mentioning is MURAI'S work using weakly coordinating aromatic ketones with alkenes employing a ruthenium species as catalyst, which gave rise to a plethora of subsequent publications on the topic of  $C(sp^2)\text{--}H$  functionalization.<sup>[134,135]</sup>



Scheme 51: MURAI'S milestone in Ru-catalyzed C–H functionalization with weakly coordinating aromatic ketones.

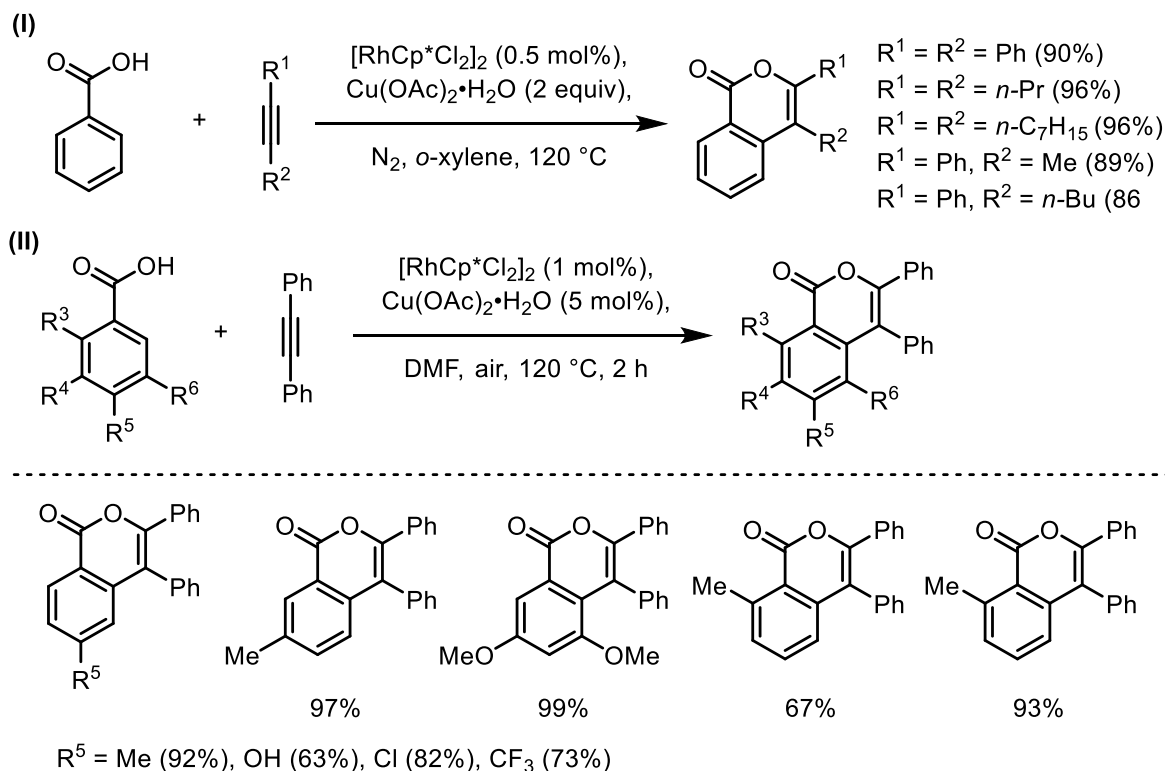
C–H activation has become such an immense field, that covering all literature has become simply impossible. Nevertheless, several reviews and books which thoroughly cover important aspects of the field have been written and give an excellent overview.<sup>[[119,128,135,136,137,138–140]</sup>

While 'classical' C–H functionalization chemistry with precious transition metals as of now seems to slowly plateau, the acquired knowledge enables today's chemists to implement- or

combine it with other fields, such as material science, natural product synthesis, polymer science, electrochemistry, photochemistry or electrophilic transfer reagents.<sup>[141]</sup>

## C–H FUNCTIONALIZATION -ALKYNYLATION

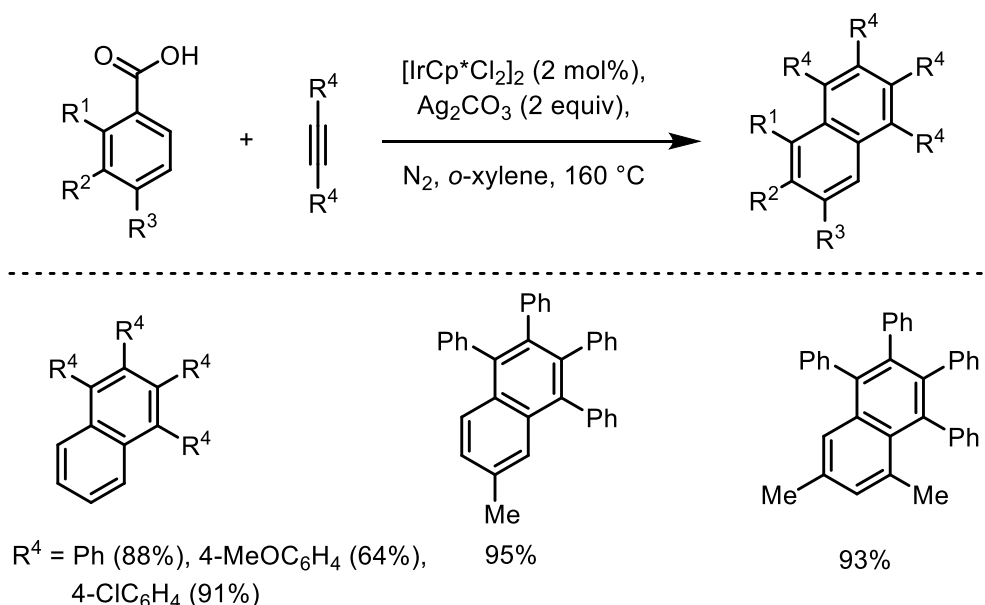
The largest part of C–H activation alkylation research has undoubtedly been done by employing internal alkynes. Upon these, diphenylacetylene (tolan) is commonly used as model substrate and extensively covered in the literature.<sup>[136,139]</sup>



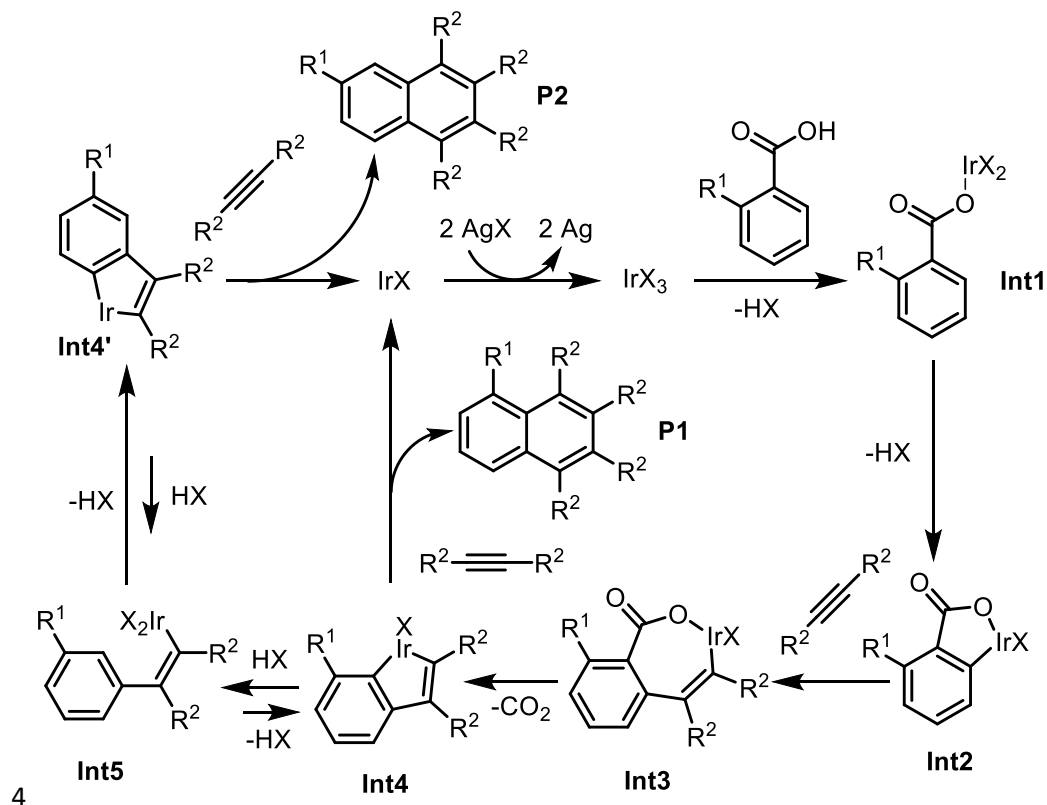
Scheme 52: Coupling of benzoic acids with internal alkynes.<sup>[142,143]</sup>

In 2007 SATOH and MIURA could show that transformation of 1:1 mixture of benzoic acid derivatives and internal alkynes to 3,4-substituted isocoumarins with utilization of  $[\text{RhCp}^*\text{Cl}_2]_2$  (0.5 mol%) and  $\text{Cu(OAc)}_2\cdot\text{H}_2\text{O}$  in *o*-xylene under  $\text{N}_2$  at 120 °C could be achieved (Scheme 52-I).<sup>[142,143]</sup> Later, reaction conditions were further optimized requiring only catalytic amounts of  $\text{Cu(OAc)}_2$ , which could be regenerated by oxygen from air (Scheme 52-II).

A discovered competitive reaction was the decarboxylation with concomitant insertion of the second alkyne equivalent. This is negligible when using  $[\text{RhCp}^*\text{Cl}_2]_2$ , but could selectively be favoured by replacing the catalyst with  $[\text{IrCp}^*\text{Cl}_2]_2$  and the oxidant  $\text{Cu(OAc)}_2\cdot\text{H}_2\text{O}$  by  $\text{Ag}_2\text{CO}_3$  at 160 °C (Scheme 53).



**Plausible Mechanism:**



Scheme 53: Decarboxylative 1:2 coupling of benzoic acids with internal alkynes.<sup>[143]</sup>

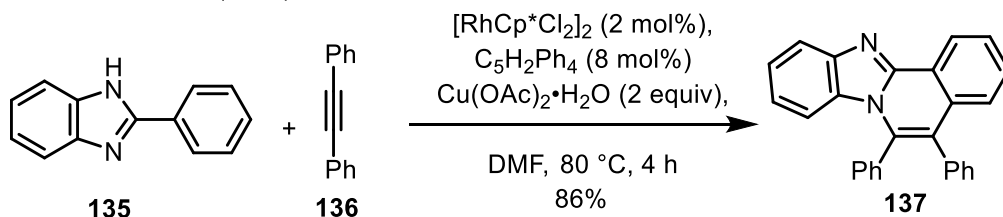
A plausible mechanistic cycle for the decarboxylative coupling starts with coordination of the substrate to an Ir<sup>III</sup>-species by ligand exchange, to give **Int1**. *Ortho*-iridation gives five membered iridium metallacycle **Int2**, which, after insertion of the internal alkyne, results in a seven membered iridium metallacycle **Int3**. This species then favourably undergoes decarboxylation rather than reductive elimination as observed for the aforementioned rhodium catalyzed procedure (Scheme 52), to again, give a five membered iridium



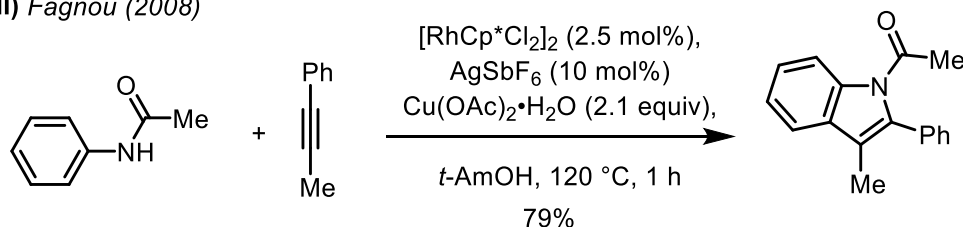
metallacycle **Int4**. The subsequent second alkyne insertion then gives the naphthalene product **P1**, and the catalyst species is regenerated in the presence of a silver salt. For 2-substituted benzoic acids, the key intermediate **Int4** can undergo rearrangement, due to steric hindrance, passing through **Int5**, to give an isomeric iridacycle **Int4'**. This pathway explains the observed isomeric product formation of **P2**.

A multitude of reports followed. In order to keep this chapter in an acceptable extent, only highlights relevant for the results discussed later on, are covered (the up to now most recent comprehensive review and references to foregoing reviews therein are highly recommended).<sup>[140]</sup>

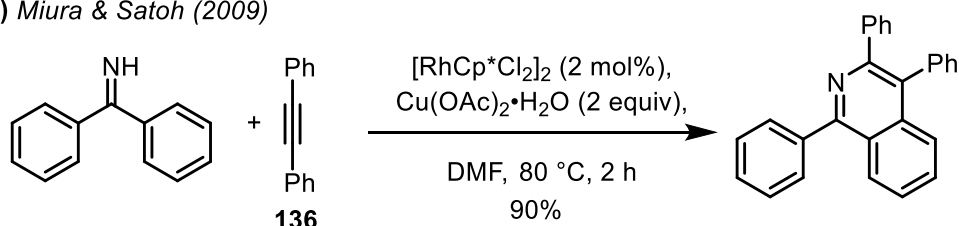
(I) Miura & Satoh (2008)



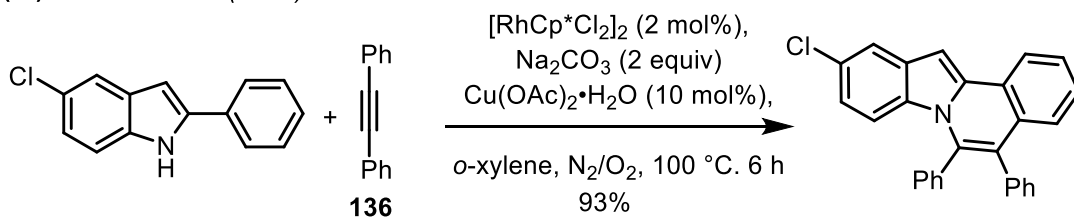
(II) Fagnou (2008)



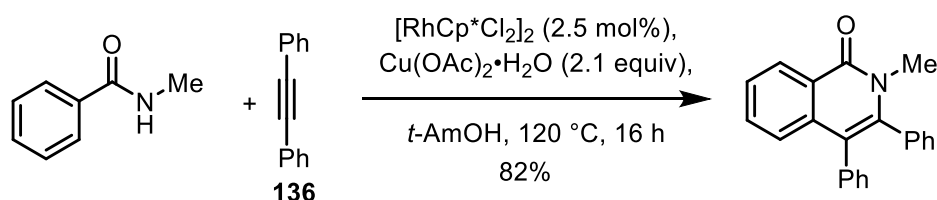
(III) Miura & Satoh (2009)



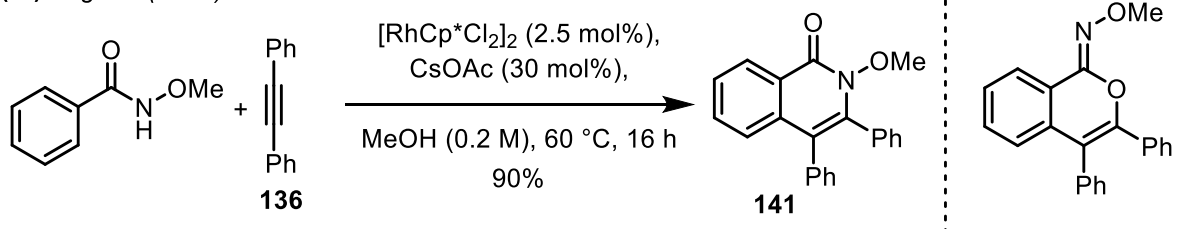
(IV) Miura & Satoh (2010)



(V) Rovis (2010)




(VI) Fagnou (2010)



Scheme 54: Progress in C–H activation-alkynylation.

In addition to their work on annulations of benzoic acids with internal alkynes, SATOH and MIURA could also prove the utility of their methodology by modifying phenylazoles **135** to obtain naphthyl- and anthryl-azoles **137** (Scheme 54-I), which exhibit intense fluorescence in solid state.<sup>[144]</sup>

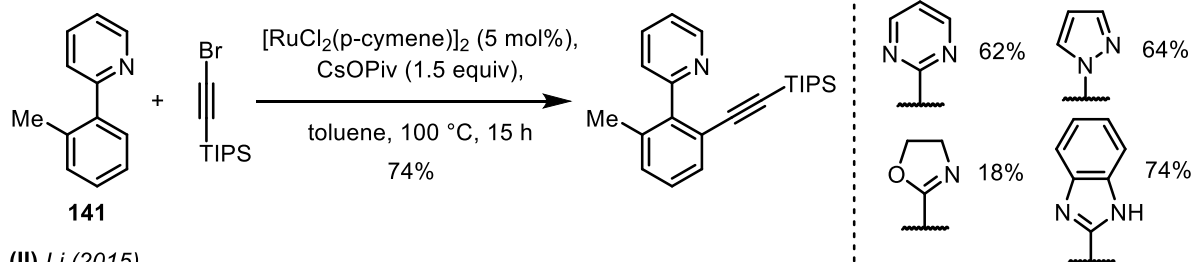
FAGNOU et al. revised their originally postulated structure for the compound **141** (Scheme **54-VI**) after findings by HUANG et al. This group reported a Pd-catalyzed reaction starting from the same substrate to access isoquinolines  which structure was confirmed by X-ray crystallography. Controversially, no corrigendum could be found by ROVIS et al. (Scheme **54-V**).<sup>[145]</sup> It is possible that the reaction protocol developed by ROVIS et al. in fact forms cyclic imidates, taking into account their observations of competitive isocoumarin formation, which can be formed by hydrolysis of this cyclic imidates. A rhodium-catalyzed alkynylation/cyclization of *N*-unsubstituted and *N*-monosubstituted benzamides by MIURA AND SATOH from 2010 also described *N*-cyclization.<sup>[146]</sup>

The regioselectivity for rhodium catalysts is summarized by You et al. and selectivity is also discussed within Yu et al.'s review on C–H functionalizations of *N*-methoxy amides with an emphasis on palladium catalysis.<sup>[138,140]</sup> Additionally, numerous ruthenium-catalyzed examples can be found in literature.<sup>[147]</sup>

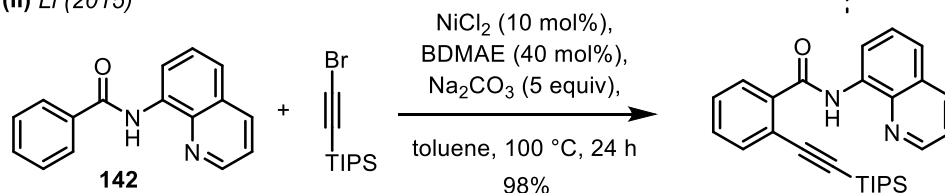
## **C–H FUNCTIONALIZATION UTILIZING ACTIVATED ACETYLENES**

Along with C–H functionalizations employing internal alkynes significant effort to employ terminal alkynes has been made.

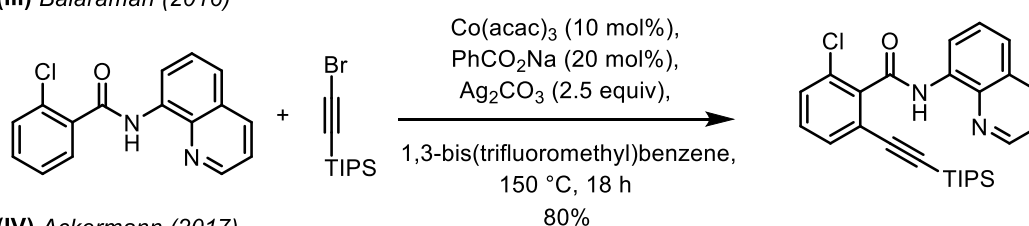
(I) Chatani (2012)



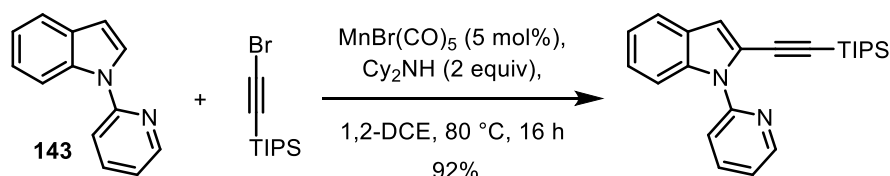
(II) Li (2015)



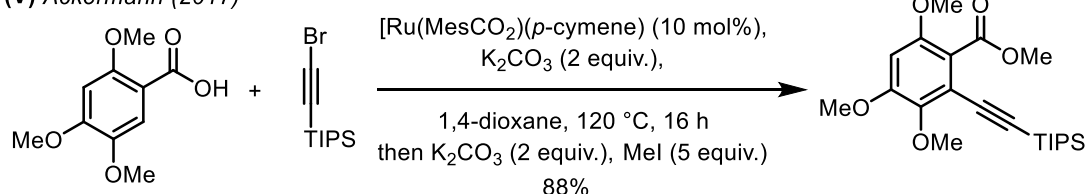
(III) Balaraman (2016)



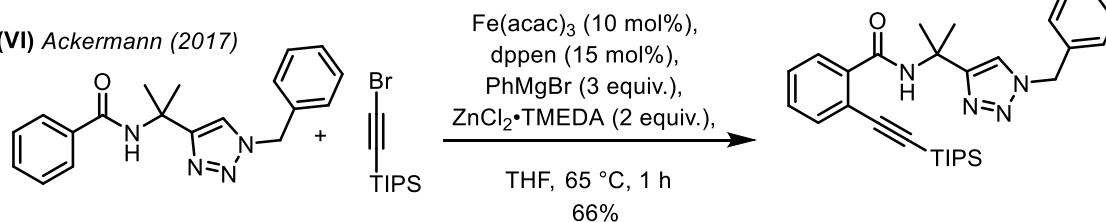
(IV) Ackermann (2017)



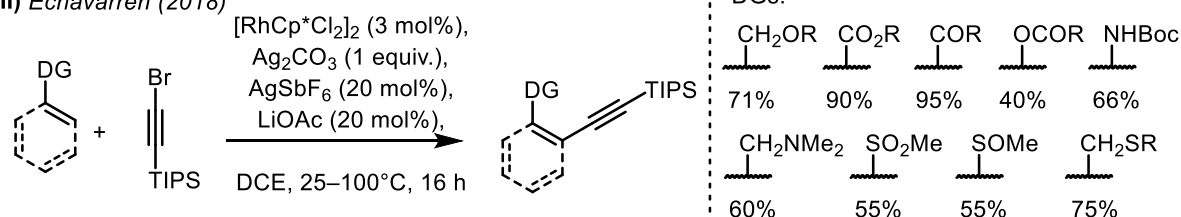
(V) Ackermann (2017)



(VI) Ackermann (2017)



(VII) Echavarren (2018)



Scheme 55: C–H functionalization: alkyne coupling utilizing haloalkynes.

However, their intrinsic electronic properties render them nucleophiles after deprotonation. Hence inversion of their natural electronic state to access the desired reactivity of an

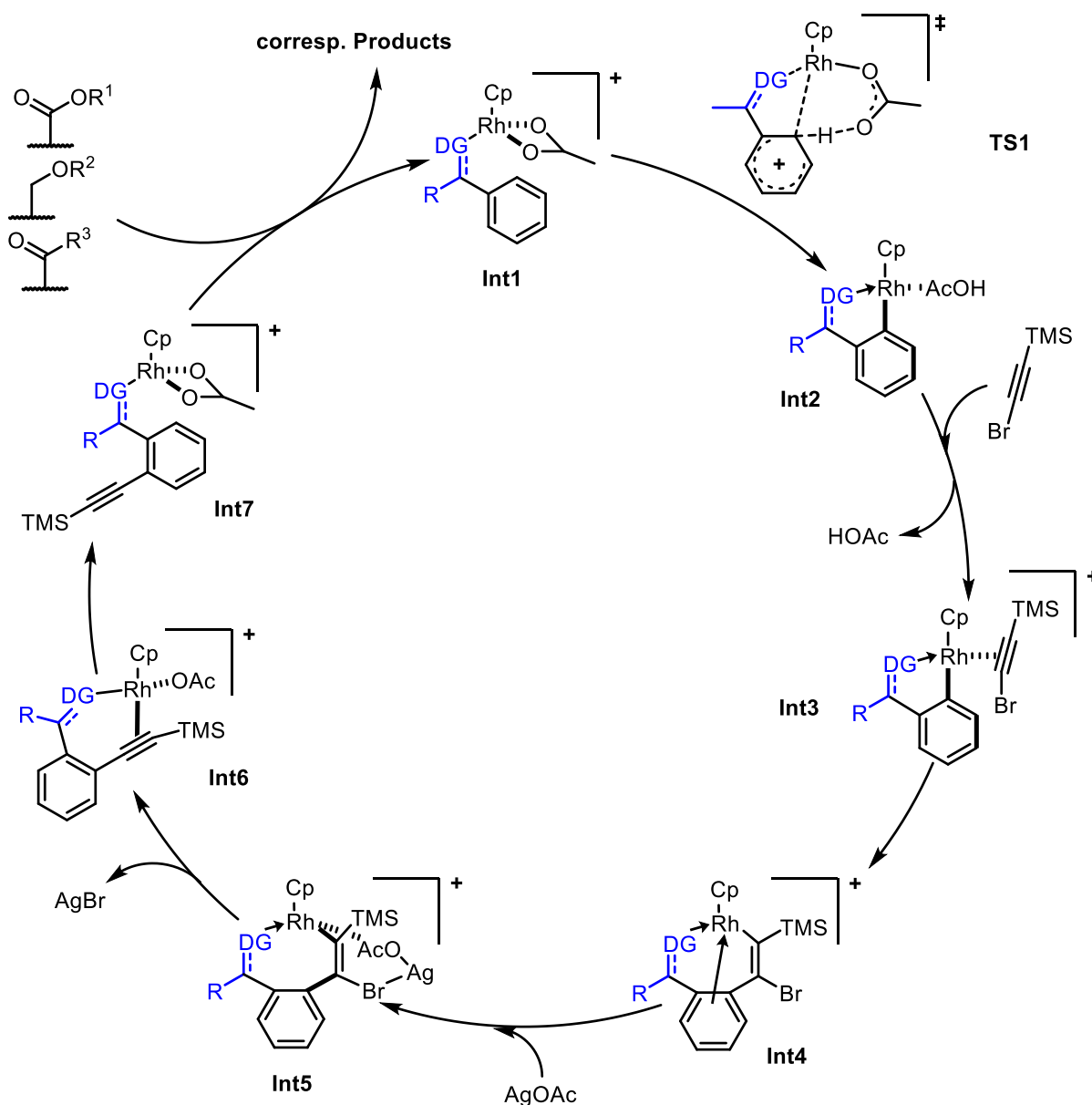
electrophile has been realized in different ways. In general, attachment of an electron-withdrawing substituent to the alkyne is the solution of a problem. The most prevalent examples are employment of halides, sulfones or hypervalent iodonium reagents.

As not only expensive transition metals such as rhodium or palladium but the roughly tenfold cheaper ruthenium as catalysts is able to provide in C–H activation, in 2012 CHATANI et al. were able to show that by utilization of weakly polarizing bromoalkyne, arenes **141** could be directly alkynylated with the chelation assistance of nitrogen-containing heterocycles such as pyridine, pyrimidine, pyrazole, and imidazole (Scheme 55-I).<sup>[148]</sup> Further development was performed by ACKERMANN et al. (Scheme 55-V).<sup>[149]</sup> Extending the list of directing groups and employing one of the most exploited DGs recently, Li et al. reported on a catalytic nickel system for the direct *ortho* C–H alkynylation of amides with the directing assistance of bidentate 8-aminoquinoline **142** as an auxiliary (Scheme 55-II).<sup>[150]</sup>

BALARAMAN et al. successfully demonstrated that cobalt-catalyzed selective bis-alkynylation of amides via double C–H bond activation is possible upon the directing assistance of 8-aminoquinoline as well, and proved the feasibility of this DGs by exemplary subsequent removal of it (Scheme 55-III).<sup>[151]</sup>

Extending the range of viable metals to manganese for C–H alkynylation of indol derivatives **143** carrying a pyridine directing group with bromoalkynes, ACKERMANN et al. could successfully introduce silyl-, aryl-, alkenyl- and alkylalkyne moieties (Scheme 55-IV).<sup>[152]</sup> Furthermore, in the same year they could also show for the first time, that iron-catalyzed C–H activation is possible by using a rather complex reaction protocol and involving another popular directing group, the triazole moiety. Nevertheless, a remarkable extension of the versatility of C–H activation protocols, alkynylation of arenes, heteroarenes and even acyclic alkenes was possible (Scheme 55-VI).<sup>[153]</sup>

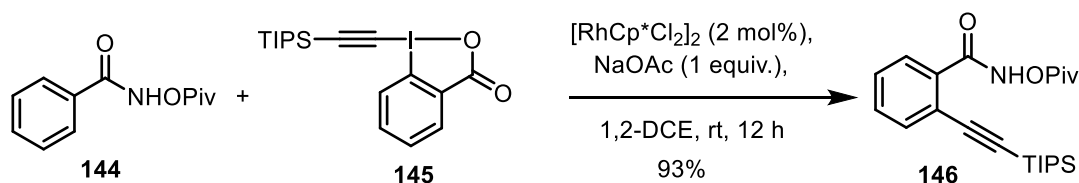
One of the most prominent examples was given by ECHAVARREN et al. (Scheme 55-VII) in 2018: They reported alkynylation with mostly silylsubstituted bromoalkynes and a multitude of different directing groups. In addition to common DGs such as esters, ketones, and ethers also less exploited DGs like thioethers, sulfoxides, sulfones, amines, phenol esters and carbamates proved to be suitable for their protocol. Mechanistic investigations, supported by DFT calculations, suggest an BIES mechanism (Scheme 56).<sup>[154]</sup>



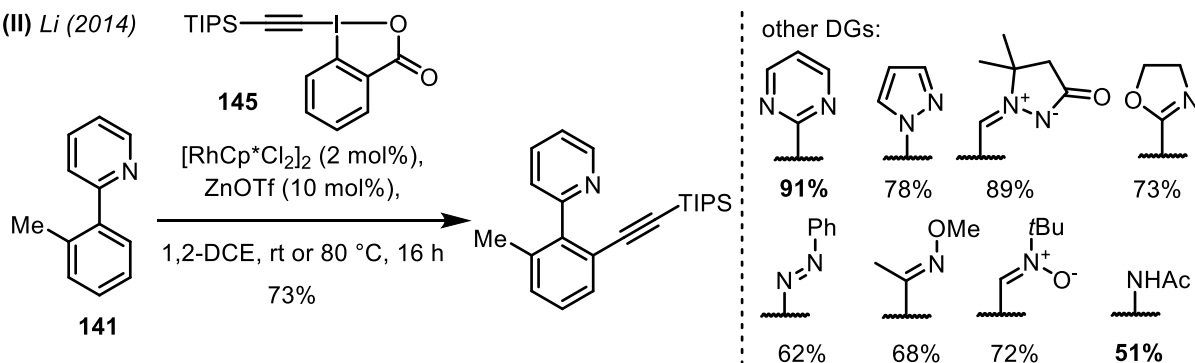
Scheme 56: Proposed mechanism by ECHAVARREN et al., based on DFT calculations.

Calculations for methyl benzoate as substrate suggest, that starting with **Int1**, C-H functionalization is intramolecularly assisted by the acetate ligand, undergoing the cyclic six-membered transition state **TS1**. Calculations for alternative transition states, such as a cyclic four membered scenario or intermolecular acetate assisted C-H activation, gave much higher energy barriers and could thus be ruled out. The resulting **Int2** then undergoes dissociative ligand exchange, to give  $(\eta^2\text{-alkyne})\text{rhodium}$  complex **Int3**. Alkyne insertion to form **Int4**, is followed by AgOAc-assisted bromide elimination, passing through **Int5**, to give **Int6** and afterwards **Int7**. Finally, ligand exchange liberates the alkynylated product and regenerates **Int1**.

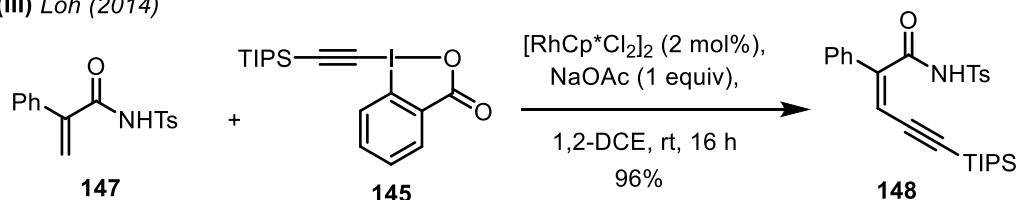
(I) Loh (2014)



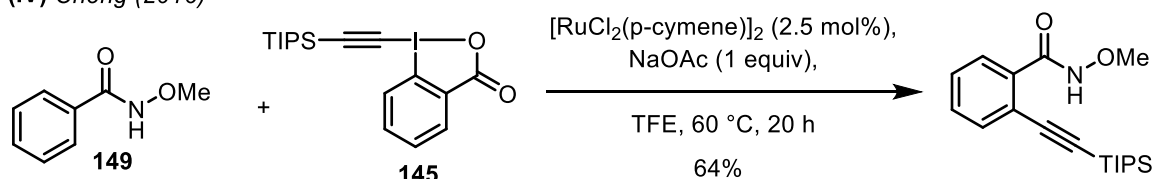
(II) Li (2014)



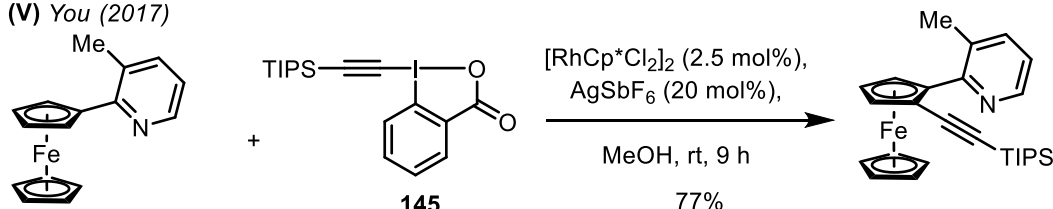
(III) Loh (2014)



(IV) Cheng (2016)



(V) You (2017)



Scheme 57: C–H functionalization: alkylation utilizing hypervalent iodine-alkyne reagents.

In early 2014, the group of LOH (I) published a rhodium(III) catalyzed C–H alkylation procedure of *N*-pivaloyloxyl amides **144** under remarkably mild reaction conditions (room temperature) and with high selectivity towards monoalkynylation products **146** (Scheme 57-I).<sup>[155]</sup>

Only one month later, an extensive report on rhodium(III) catalyzed C–H alkylation utilizing hypervalent iodonium salts **145** was presented by LI et al. (Scheme 57-II). They could prove that iodonium compounds of the BX family are compatible with a number of heterocyclic as well as non-cyclic directing groups such as *O*-methyl oximes, *N*-*tert*-butyl- $\alpha$ -phenylnitrones, azomethine imines, *N*-nitrosoanilines, azobenzene, azoxybenzene and acetanilines. Even more: a scope of rhodium(III)-catalyzed C–H alkylation of *N*-



pivaloyloxybenzamides and iridium(III) catalyzed C–H alkynylation of *N*-methoxycarboxamides was reported, both utilizing TIPS-EBX as alkynylating agent. Mechanistic insights were gained by isolation of an intermediate rhodium vinyl complex formed from substrate, catalyst and reagent, which was characterized by X-ray diffractometry, and through study of kinetic isotope effects (KIE).<sup>[156]</sup>

One of the few examples in C–H alkynylation, which makes use of acyclic substrates, was contributed by the group of LOH. They could show, that the use of TIPS-EBX **145** and a weakly-coordinating tosylimide as a DG were the best combination for the functionalization of acrylamides **147**. A number of  $\beta$ -unsubstituted acrylamides could be transformed into the corresponding 1,3-enynes **148**. By switching solvent from 1,2-DCE to MeOH also  $\alpha,\beta$ -disubstituted acrylamides could be modified (Scheme **57-III**).<sup>[157]</sup>

*N*-methoxyamides **149** are popular substrates in C–H activation due to their N–O redox active bond, which is exploited as an internal oxidant in a number of transformations.<sup>[138]</sup> However, in the reaction reported by CHEN et al. (Scheme **57-IV**) the directing group remains intact. The authors postulate a redox neutral mechanism following an ES pathway. Whereas they were unable to find conditions where dialkynylation was completely excluded, after optimization, formation of the corresponding dialkynylated products were in the range of only 0–7%.

You et al. (Scheme **57-VI**) could functionalize rather exotic substrates, namely ferrocene derivatives, with EBX as an alkynylating agent. They were successful in controlling mono- and dialkynylation by choice of the directing group (pyridine or isoquinoline) and the amount of EBX.

More extensive literature covering the topic of transition metal catalyzed C–H alkynylation with hypervalent iodonium compounds is given by J. WASER in two reviews.<sup>[52,158]</sup>

It could be shown that, depending on reaction conditions, catalyst or electrophilic alkynylation agent, a plethora of either annulation or alkynylation products can be accessed. A large number of directing groups can be used, giving a wide span of possibilities for application. As already mentioned classic C–H activation now already is a mature research area. Amalgamation with other research fields such as material science, for example highly fluorescent polyaromatic compounds, or peptide synthesis proves the relevancy of the established chemistry.

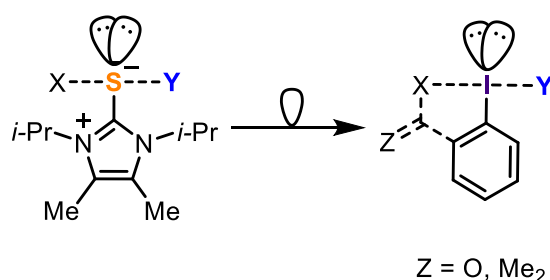
## RESULTS AND DISCUSSION

### SYNTHESIS AND EVALUATION OF NOVEL PYRIDINIUM BASED ELECTROPHILIC TRANSFER REAGENTS

#### PROJECT AIMS

The objective of this project is to create alternative platforms for electrophilic group-transfer reactions in order to expand the field of electrophilic group-transfer reagents.

In this context utilization of scaffolds which are isolobal to hypervalent iodonium salts, yet not based on iodine, our group envisioned sulfur-based reagents isolobal to the former. Such sulfur-based reagents show similar properties as iodine compounds: In contrast to light p-block elements which commonly form interatomic  $\pi$ -bonds, a three-center-four-electron bond (3c-4e) is observed for both compound classes (Scheme 58). The 3c-4e bond is a popular example for a hypervalent bond. It is a weak and highly polarized bond, intrinsic to the reactivity pattern observed for these compounds.



Scheme 58: Isolobality of sulfur- and iodine-based transfer reagents.

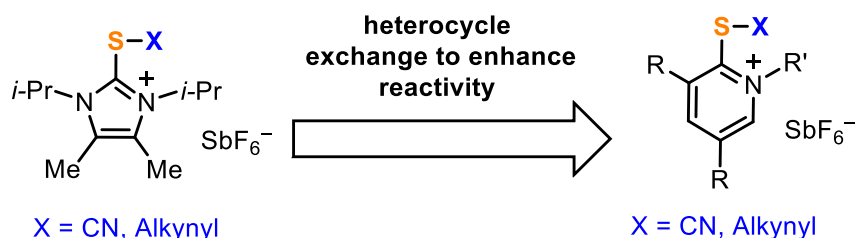
While the research field of hypervalent iodonium salts has been a topic of constantly increasing interest for the last 20 years, their stability has been an issue since their discovery. Even significantly more stable, cyclic hypervalent iodonium salts are showing thermal instability in some cases.

The first sulfur containing transfer reagents, comprising an imidazolium moiety, for the electrophilic transfer of nitriles as well as alkynes were successfully synthesized in 2015 by our group.<sup>[41]</sup> After characterization and evaluation of their reactivity towards different nucleophiles, we contemplated, how the reactivity of sulfur based reagents could be further enhanced.

In this regard in-group knowledge on the research of electron poor cationic phosphines gave the decisive motivation, since the tuning of the phosphine ligands follows a similar rationale:

By exchanging imidazolium to pyridinium in the backbone of the phosphine ligands, which are used for  $\pi$ -acid catalysis, these are rendered more electron deficient.<sup>[159]</sup>

Logically, by exchanging the imidazolium backbone to an even more electron withdrawing moiety, the pyridinium, an electrophilic sulfur based transfer reagent with extended reactivity will be accessible.

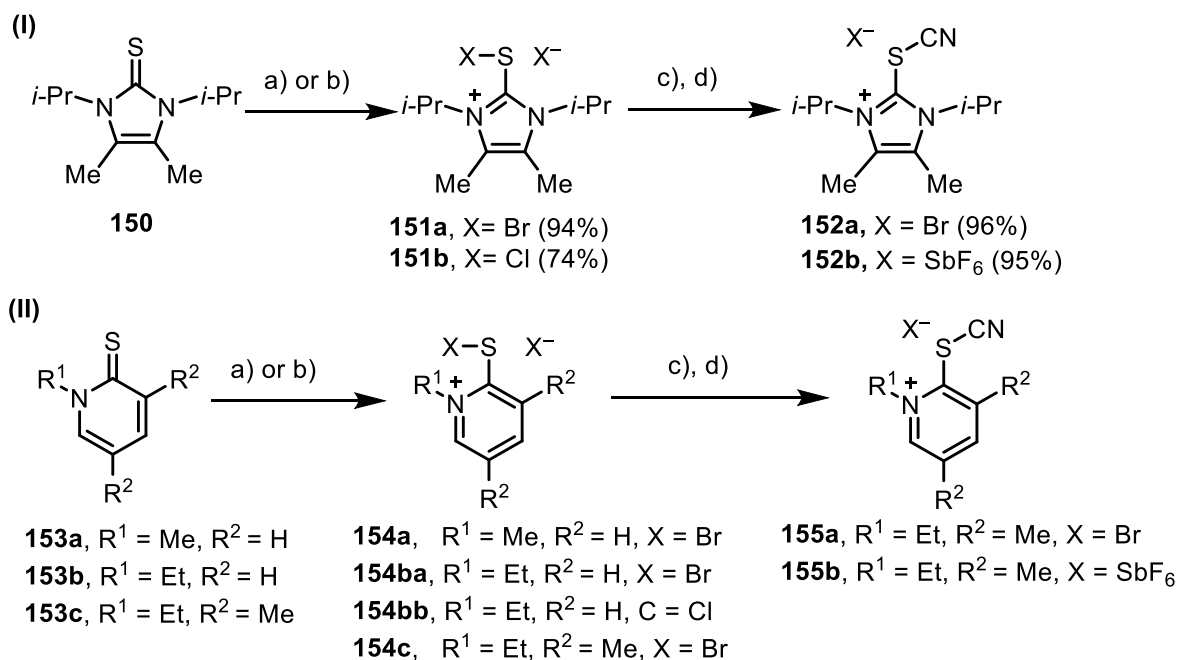


Scheme 59: Extension of reactivity by heterocycle exchange.

Thus the aims of this project can be formulated as follows:

1. A synthesis sequence to access novel sulfur based electrophilic transfer reagents, which contain the pyridinium moiety as key motif, will be developed.
2. Hypervalent dihalo(pyridinium) species **154** will be used as a key intermediates *en route* to electrophilic transfer reagents. They are expected to possess similar properties compared to those of known dihalo(imidazolium)sulfuranes and will be subjected to structural investigations in order to evaluate their electronic nature.
3. From **154**, pyridinium thiocyanates will be synthesized and their behavior towards nucleophiles will be tested, aiming to extend the scope of electrophilic cyanation reactions.
4. Analogously the synthesis of alkynylthiopyridinium salts from **154** will be developed and their reactivity in the presence of nucleophiles will be investigated.

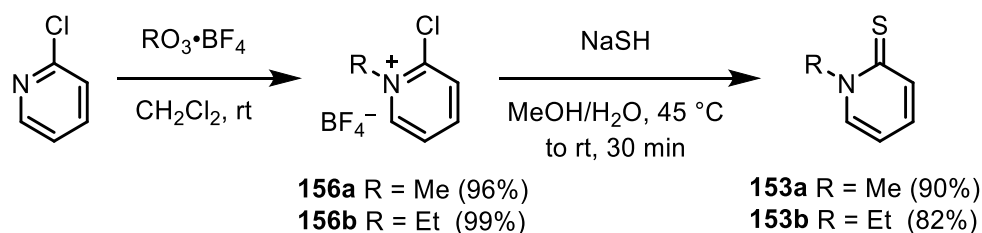
With the established knowledge for the synthesis of the original imidazolium based electrophilic cyanating reagent in hand (Scheme 60-I), a synthetic route for pyridinium based transfer reagents is envisioned (Scheme 60-II).



Scheme 60: (I) Sequence developed by the ALCARAZO group for the synthesis of imidazolium-substituted sulfuranes **152** and (II) tentative analogous synthetic route to access pyridinium thiocyanates **155**. Reaction conditions: a) SO<sub>2</sub>Cl<sub>2</sub>, CH<sub>2</sub>Cl<sub>2</sub>, RT; b) Br<sub>2</sub>, CH<sub>2</sub>Cl<sub>2</sub>, 0°C → rt; c) TMSCN, CH<sub>2</sub>Cl<sub>2</sub>, rt, d) aq. NaSbF<sub>6</sub>.

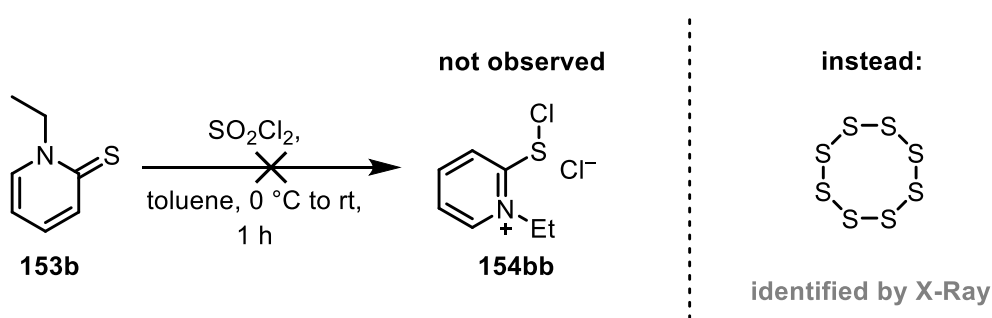
## SYNTHESIS, CHARACTERISTIC PROPERTIES AND APPLICATION OF NOVEL PYRIDINIUM-BASED ELECTROPHILIC TRANSFER REAGENTS

Setting out from 2-chloropyridine, *N*-alkylation was achieved in high yields employing trialkyloxonium tetrafluoroborates as the alkylating reagents. Afterwards introduction of the sulfur atom was achieved by using sodium hydrogen sulfide giving the thiolactams **153a** and **153b** in 90 and 82% yields, respectively (Scheme 61).



Scheme 61: Synthesis sequence towards the thiolactam backbones **153** starting from 2-chloropyridine.

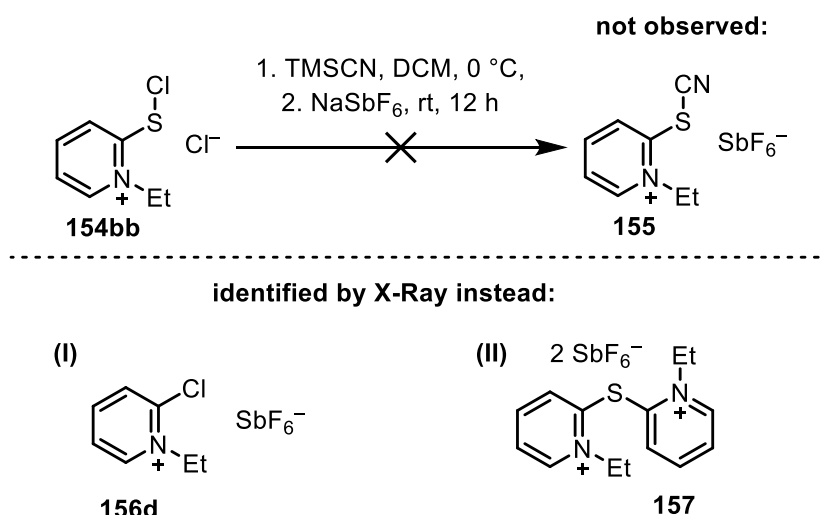
With **153b** in hand, the synthesis of the hypervalent dihalo(pyridinium)sulfuranes was attempted by chlorination with sulfonyl chloride (Scheme 62). <sup>1</sup>H NMR analysis of the formed product showed a deep field shifted doublet for the proton in  $\alpha$ -position to the cationic nitrogen ( $\delta$  = 10.71 ppm, initial shift 7.67 ppm), which is characteristic for highly electronegative pyridinium species. However, poor solubility and instability of the product towards air, moisture and protic solvents made a full characterization by <sup>13</sup>C NMR spectroscopy as well as by high resolution mass spectroscopy impossible. Nevertheless the target mass could be observed in traces, thus encouraging further investigations of this synthetic route. After several crystallization attempts a crystal suitable for analysis by X-Ray diffractometry was obtained and revealed S<sub>8</sub> as the major product of decomposition of this extremely unstable compound (Scheme 62).



Scheme 62: Attempted synthesis of dichloro(pyridinium)sulfurane **154bb**.

In an attempt to generate the dichloro(pyridinium)sulfurane **154bb** *in situ* and directly utilize it in the nucleophilic substitution with TMSCN, more crystals were obtained, comprising another part of the decomposition pathway (Scheme 63 (I)). The analyzed structure gave important insights into the electronic properties and thus the preferential reactivity of this hypervalent pyridinium species. It is assumed that during the reaction a pyridinium species

partly becomes so electron depleted, that the chloride anion is nucleophilic enough to attack the carbon atom in  $\alpha$ -position to the sulfur and thus cleaving out the sulfur. Formally the employed reaction sequence is hence reversed giving, 2-chloro-1-ethyl-pyridinium. By taking the electronegativity of a nitrile group into account, which can be calculated and scaled to be compatible with the Pauling scale, a nitrile group possesses an electronegativity (EN) of 3.3, compared to chlorine with 3.16 and bromine with 2.96. <sup>[160]</sup> Thus the potential electrophilic cyanating reagent **155** is the most electron depleted species of these three compounds formed in the reaction and most prone to undergo nucleophilic aromatic substitution.



Scheme **63**: Attempted syntheses of pyridinium thiocyanates starting from dichloro(pyridinium)sulfurane **154bb**.

Crystals obtained in another attempt to synthesize the electrophilic cyanating reagent **155** revealed to be dicationic species **157** (Scheme **63** (II)). This further underlines that an aromatic substitution at the pyridine is favoured and that the pyridinium moiety preferably acts as a leaving group. Additional attempts to access nitrile transfer reagents, were unsuccessful, neither anion exchange with an aqueous NaSbF<sub>6</sub> solution nor the exchange in acetonitrile gave the desired compound.

It can be concluded, that **154bb** is indeed formed in the reaction sequence, since subsequent reactions gave products which are a direct result of the formation of this highly reactive intermediate. However its instability under the conditions elaborated, prevented any further analysis.

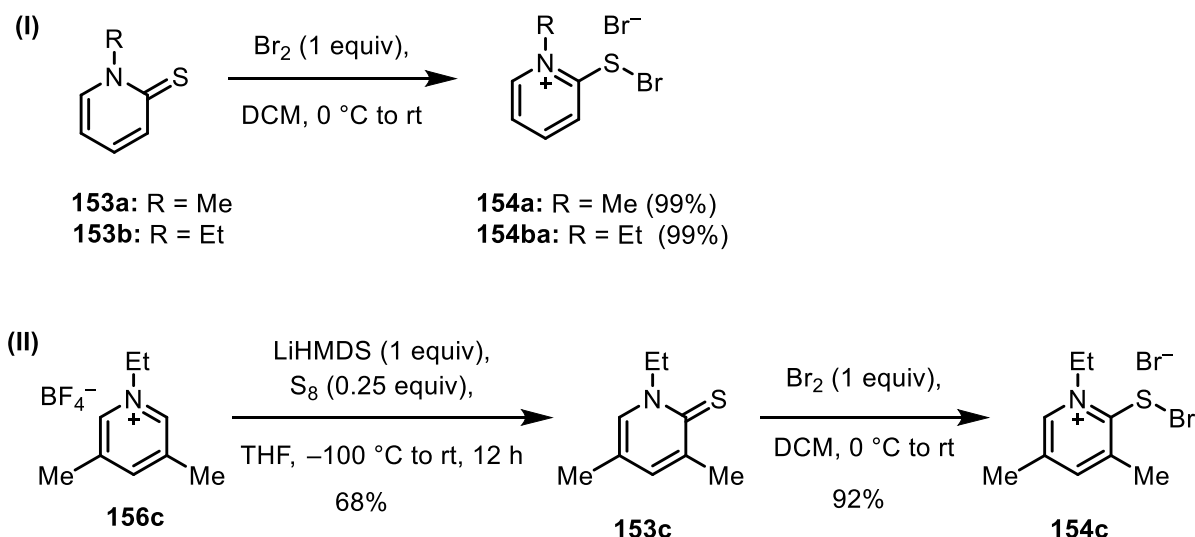
Having identified, that the relatively high electronegativity of the chloride anion is one of the driving factors, which promotes a nucleophilic attack in  $\alpha$ -position to the sulfur, and not in the desired position, the most logical alternative was to attempt bromination instead. The resulting product, a dibromo(pyridinium) sulfurane **154ba**, then holds the less electron withdrawing bromide.

The synthesis of *N*-ethyldibromo(pyridinium) sulfurane (**154ba**) proved to be significantly more gratifying, giving instant precipitation of the desired product at 0 °C. The target

compound could be successfully characterized by NMR spectroscopy, and two additional derivatives, **154a** and **154c**, were synthesized (

**Scheme 64**). For the latter compound, a concise synthesis starting from 3,5-lutidine was designed (

**Scheme 64, (II)**).



Scheme 64: Synthesis of dibromo(pyridinium) sulfuranes **154**.

Deprotonation of the salt **156c** in  $\alpha$ -position to the nitrogen with lithium hexamethyldisilazide followed by treatment with sulfur afforded thiolactam **153c** in 68% yield. Bromination of **153c** proceeded quantitatively at  $0\text{ }^\circ\text{C}$  to give the hypervalent dibromo(thiolutidinium) salt **154c**.

We hypothesized that due to the higher sterical encumberment and the +I stabilizing effect of the methyl groups, disfavoring the aforementioned decomposition pathway, this derivative will possess an increased stability as well as better solubility in organic solvents. Indeed the strategy proved to be successful and crystals of the dibromo(lutidinium) sulfurane (Martin-Arduengo N-X-L designation:<sup>[161]</sup> 10-S-3) **154c** were grown and analyzed by X-ray crystallography (Figure 1).

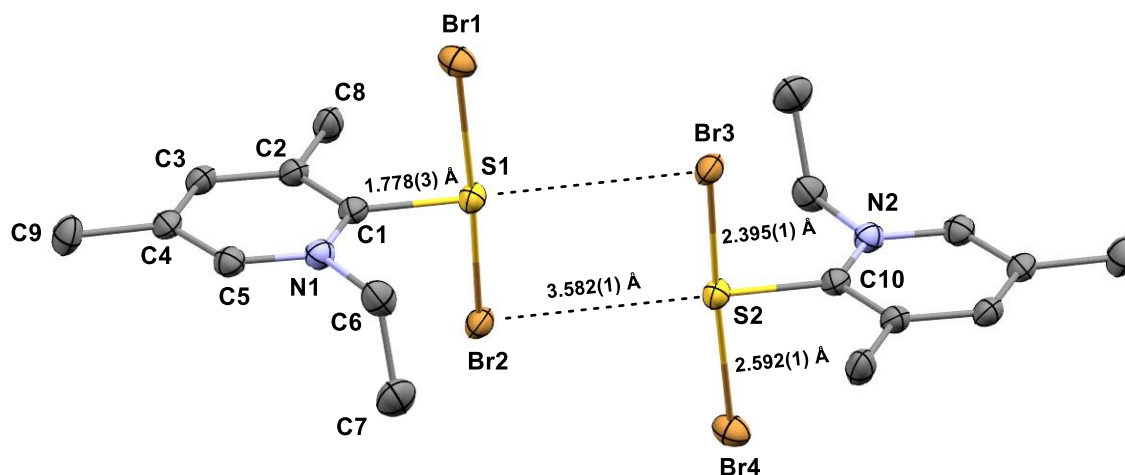


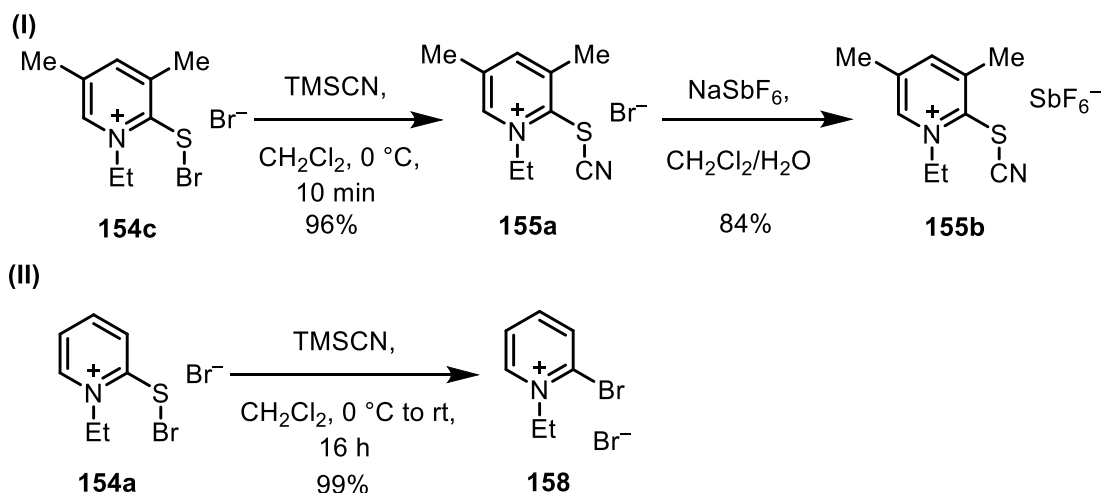
Figure 1: Structure of compound **154c** in the crystal. Anisotropic displacement parameter shown at 50% probability level, hydrogen atoms omitted for clarity. Selected bond lengths [Å] and angles [deg]: S1–Br1, 2.592(1); S1–Br2, 2.395(1); S1–C1, 1.778(3); Br1–S1–Br2, 177.50(3).

The obtained structure showed the typical T-shaped geometry similar to that in hypervalent dihalo(imidazolium) and iodonium salts (Scheme 58). Minor deviation from the ideal 180° does take place [177.5°(3)] for Br1–S1–Br2 angle. However, of much higher interest is the difference in Br1–S [2.592(1) Å] and Br2–S1 [2.395(1) Å] bond lengths, which is in stark contrast to the even distances for Br1–S1–Br2 in a dibromoimidazolium sulfurane. Upon closer investigation and identification of the most proximal contacts, we found that the compound organizes itself as a chalcogen bonding (ChB) complex.<sup>[162]</sup> An angle of 175.7° for C1–S1–Br3 (and Br2–S2–C10, respectively) is observed, and strong positive polarization of the sulfur atom is facilitated by the pyridinium ring. The neighboring bromine atoms serve as Lewis Base (LB), interacting with the sulfur through partial donation of their electron density. This results in a shorter bond length towards the covalent bound sulfur, while for the remaining two bromine atoms elongated bonds to the sulfur centerpiece are observed.

While no further investigations towards the potential existence of charge-shift bonds in this compound have been undertaken, it shares significant similarities with compounds described to possess such.<sup>[163]</sup>

Successive synthesis of the lutidinium thiocyanate was achieved. In a first step the pyridinium thiocyanate **155a** bearing a bromide anion was synthesized by nucleophilic substitution with TMSCN in 96% yield. Anion exchange with SbF<sub>6</sub><sup>−</sup> then gave **155b** in a yield of 84%. Unfortunately, this result was not reproducible in several attempts.





Scheme 65: Synthesis of lutidinium thiocyanate **155** and attempted synthesis of pyridinium thiocyanate.

During the unsuccessful attempts, at least three different pyridine species were formed during reaction progress, as could be observed in  $^1\text{H}$  NMR spectra. Purification was possible neither applying various solvent combinations for crystallization nor by column chromatography. We suspected that all of the formed compounds are salts, due to their behavior on thin layer chromatography. This could partly be verified by stirring a solution of **154a** in the presence of TMSCN for 16 h. Full conversion to 2-bromo-1-ethylpyridinium bromide (**158**) was observed, indicating that the reaction time is a crucial parameter (Scheme 65 (II)). Nevertheless, compound **155b** was successfully crystallized. Notably crystals could also be obtained from less successful reactions in which byproducts had formed, albeit isolation of the pure substance in significant amounts in these cases was possible neither by crystallization nor by column chromatography.

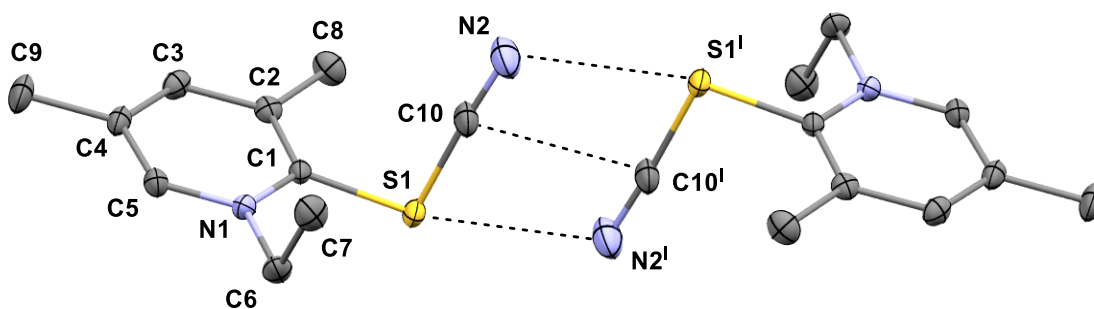
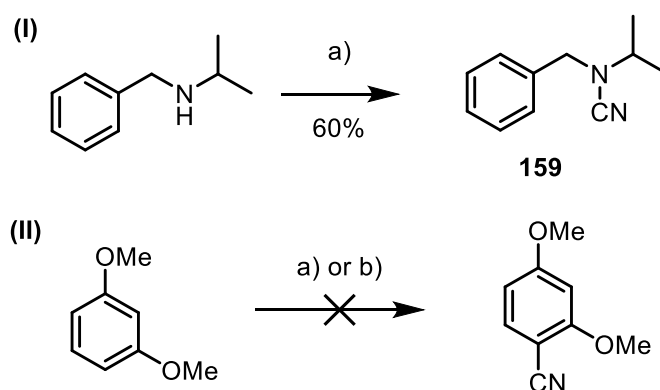


Figure 2: Crystal structure of **155b**, Anisotropic displacement parameter shown at 50% probability level, hydrogen atoms and counterions omitted for clarity (Symcode: I = -x,1-y,1-z).

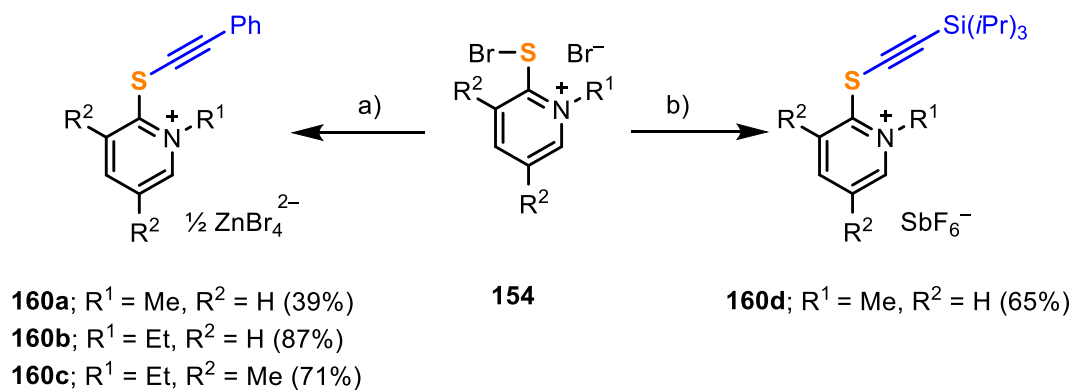
The reactivity of the reagents **155** towards different nucleophiles was tested as well. Reaction conditions similar to those optimized for the analogue imidazolium thiocyanate **152** were chosen. It was found that the reagent **155a** is active in the cyanation of *N*-

isopropylbenzylamine, however, giving product **159** in lower yield of 60%, when compared to the reaction with imidazolium thiocyanate reagent **152a** (92% after 20 min.) (Scheme 66). This is presumably due to the lower stability of the pyridinium thiocyanate. In additional experiments it was demonstrated that compound **155b** decomposes in solution at temperatures above 50 °C. This result was further confirmed by a control experiment in which the reagent was heated in d<sub>3</sub>-acetonitrile to 80 °C to recreate reaction conditions and lead to decomposition of the reagent (Scheme 66).



Scheme 66: Cyanation of *N*-benzyl-*N*-isopropylamine and attempted reactions with dimethoxybenzene. Reagents and conditions: a) lutidinium thiocyanate bromide **155a** (1.2 equiv), DIPEA (1.1 equiv), CH<sub>2</sub>Cl<sub>2</sub>, rt, 20 min; b) lutidinium thiocyanate **155b** (1.2 equiv), BF<sub>3</sub>·Et<sub>2</sub>O (0.2 eq.), 1,2-DCE, 80 °C, 16 h.

Due to these results, further investigations were focused on potential alkynylating reagents with a pyridinium backbone with the purpose to obtain more stable compounds. The electronegativity of a nonsubstituted acetylene group is calculated to be 3.3, *i. e.* the same as of a nitrile group. This means that theoretically any transfer reagent with an unprotected acetylene moiety should be equally unstable. On the other hand, we expected to decrease this value by substituting the triple bond with electron-rich groups and to obtain more practically useful compounds.<sup>[160]</sup> With this rationale in mind, phenylacetylene and (triisopropylsilyl)acetylene were chosen for the synthesis of the corresponding reagents. Applying a modified strategy adapted from the thioimidazolium-based reagent, gratifyingly several promising thiopyridinium-based acetylene transfer reagents were synthesized (Scheme 67).



Scheme 67: Synthesis of alkynylthiopyridinium salts **160**. Reaction conditions: a) phenylacetylene (1.1 equiv), *n*-BuLi (1.1 equiv), THF, -78 °C to rt, then ZnBr<sub>2</sub> (1.1 equiv); b) TIPS-C≡CH (1 equiv), *n*-BuLi (1 equiv), THF, -78 °C to rt, then ZnBr<sub>2</sub> and finally aq. NaSbF<sub>6</sub>. TIPS = triisopropylsilyl.

Thus, compounds **160a–c** were isolated in moderate to good yields of 39, 87 and 71%, respectively. Attempted replacing of the counterion ZnBr<sub>4</sub><sup>2-</sup> with the non-coordinating SbF<sub>6</sub><sup>-</sup> one was unsuccessful for phenylacetylene-substituted reagents **160a–c**, whereas counterion exchange underwent smoothly for the (triisopropylsilyl)acetylene-substituted derivative affording compound **160d** (Scheme 67). The TIPS-reagent **160d** could be synthesized in an overall yield of 65% over two steps.

A possible explanation for the unsuccessful counterion exchange might be the difference in lattice energy, which correlates with the ion size and thus should be smaller for **160d** than for **160a–c**, making the anion exchange easier to proceed.

Crystallization of the alkynyl pyridinium salts unambiguously verified their connectivities (Figure 3).

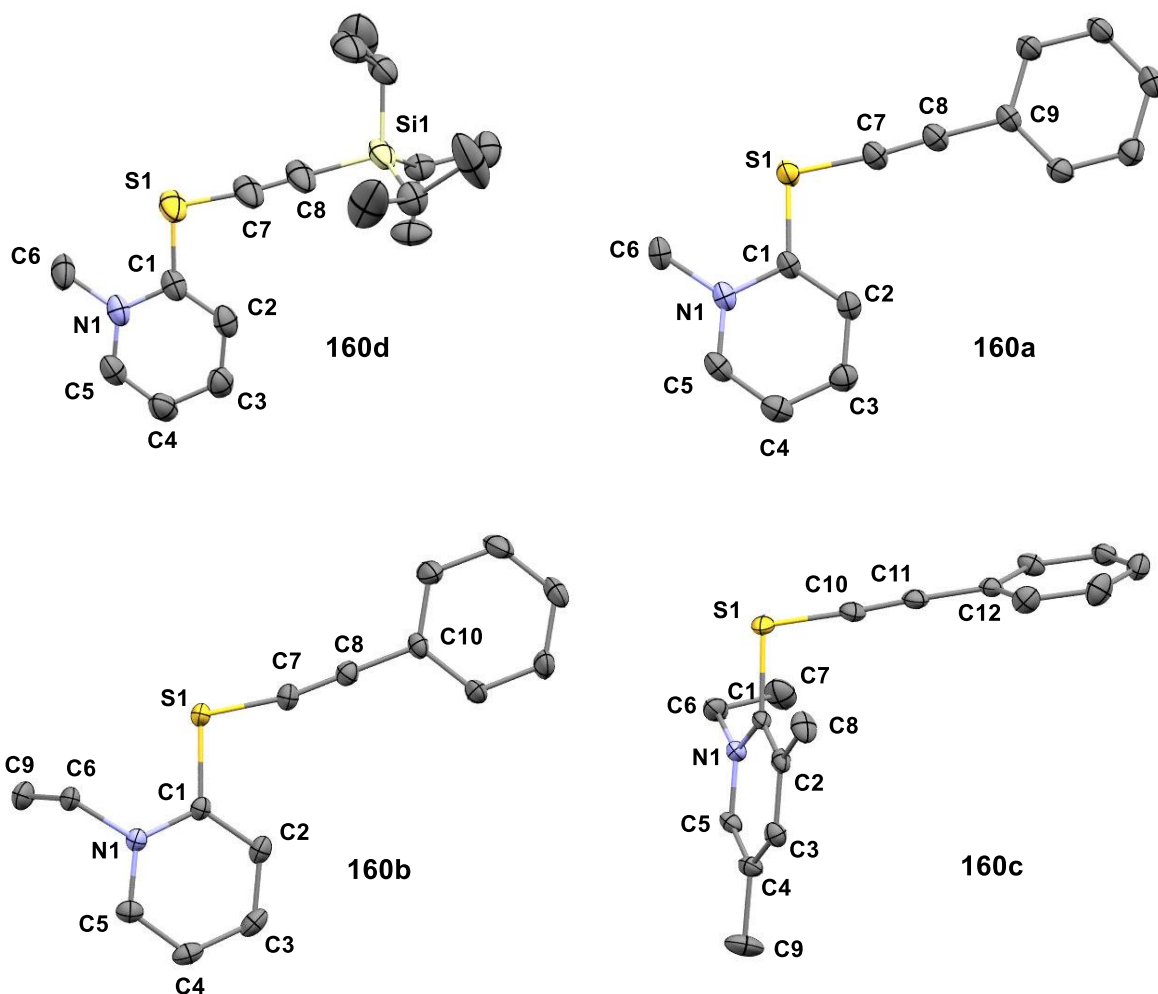
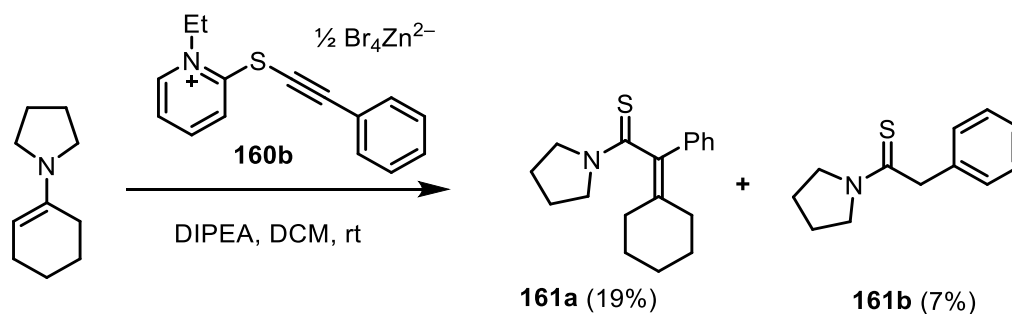


Figure 3: Structures of the salts **160a–d** in the crystal. Anisotropic displacement parameter shown at 50% probability level, hydrogen atoms and anions omitted for clarity.

Once characterization of the alkynylthiopyridinium salts was complete, their chemical behavior towards different kinds of nucleophiles was examined.

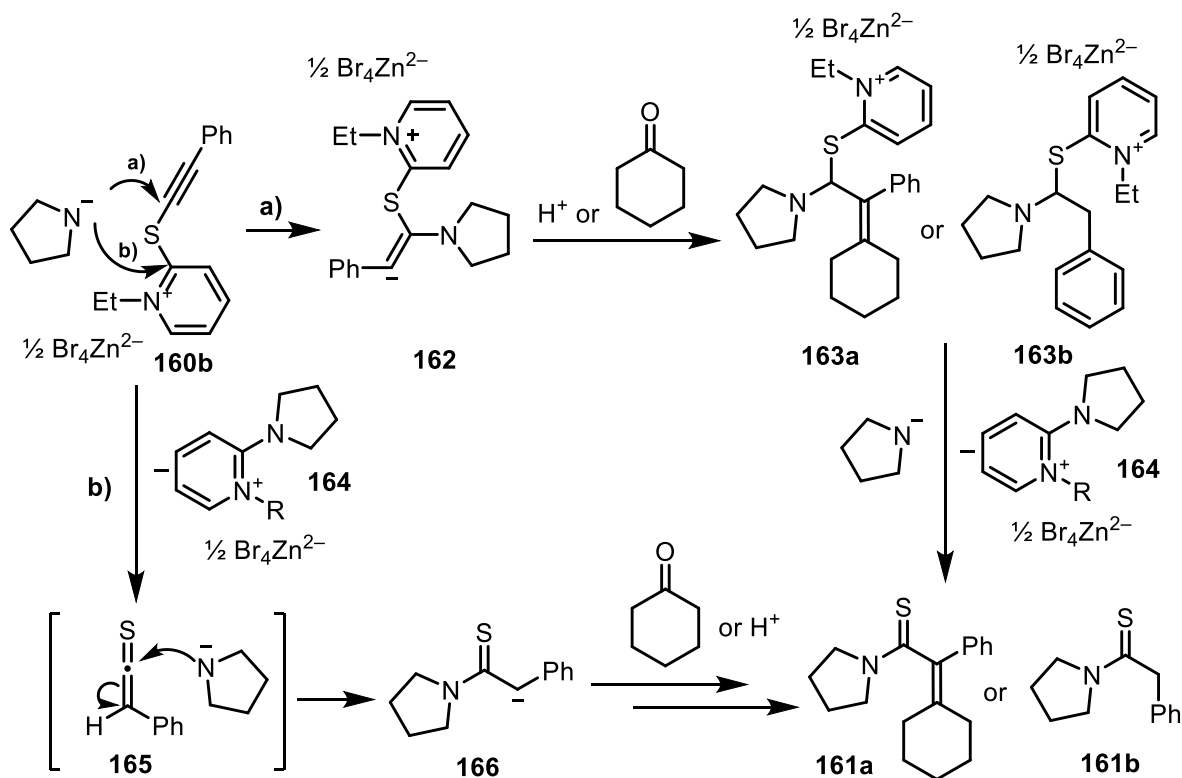
Already preliminary reactions between reagent **160b** and enamines gave intriguing results.



Scheme 68: Reaction of alkynylthiopyridinium salt **160b** with 1-(cyclohex-1-en-1-yl)pyrrolidine.

We presume that upon slow hydrolysis of the substrate during the quenching process after the reaction, cyclohexanone and pyrrolidine formed and then subsequently reacted. This

also explains the low yields, as hydrolysis of the starting material only sluggishly provides the reactants.



Scheme 69: Feasible mechanistic considerations.

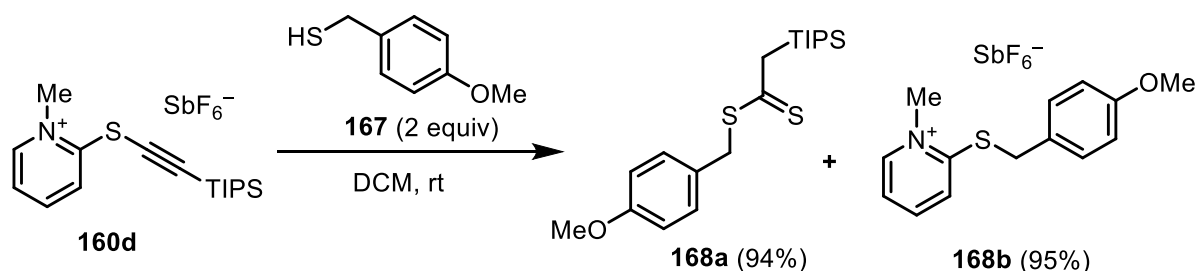
Therefore two possible mechanistic pathways can be considered: After initial deprotonation of the pyrrolidine by Hünig's base, nucleophilic attack of the formed anion to either  $\alpha$ -positioned carbon atoms with respect to the sulfur can take place.

- If the pyrrolidide attacks the acetylenic  $\alpha$ -position first, intermediate **162** is formed. The latter then reacts as nucleophile, either with a proton source or cyclohexanone to give product **163a** or **163b** after elimination of a pyridine moiety **164** by reaction with a second equivalent of pyrrolidide.
- If the nucleophilic attack takes place at the aromatic ring, thioketene **165** is formed. Subsequently, an additional equivalent of pyrrolidide then attacks this species to give intermediate **166**, which, in turn, reacts with either cyclohexanone or a proton source to produce product **161a** or **161b**, respectively.

The results of the reaction illustrate that not only protons but also other compounds can serve as electrophiles in this transformation.

While these results were already quite informative from the viewpoint of the agents reactivity, more information about the behavior of the alkynylthiopyridinium salts **160** could be gathered when thiols were investigated as nucleophiles. Thus, with one equivalent of deprotonated 4-(methoxyphenyl)methanethiol (**167**), the successive reaction of the reagent **160d** gave a 1:1 mixture of dithioester **168a** and pyridinium salt **168b** which presumably is the result of a  $\text{S}_{\text{N}}\text{Ar}$  reaction of the substrate with the carbon of the pyridinium ring in  $\alpha$ -

position to sulfur. We also observed that half an equivalent of the salt **160d** was still intact. For a complete conversion two equivalents of thiol were necessary, as optimization reactions revealed.



Scheme 70: Reaction of reagent **160d** with thiol **167**.

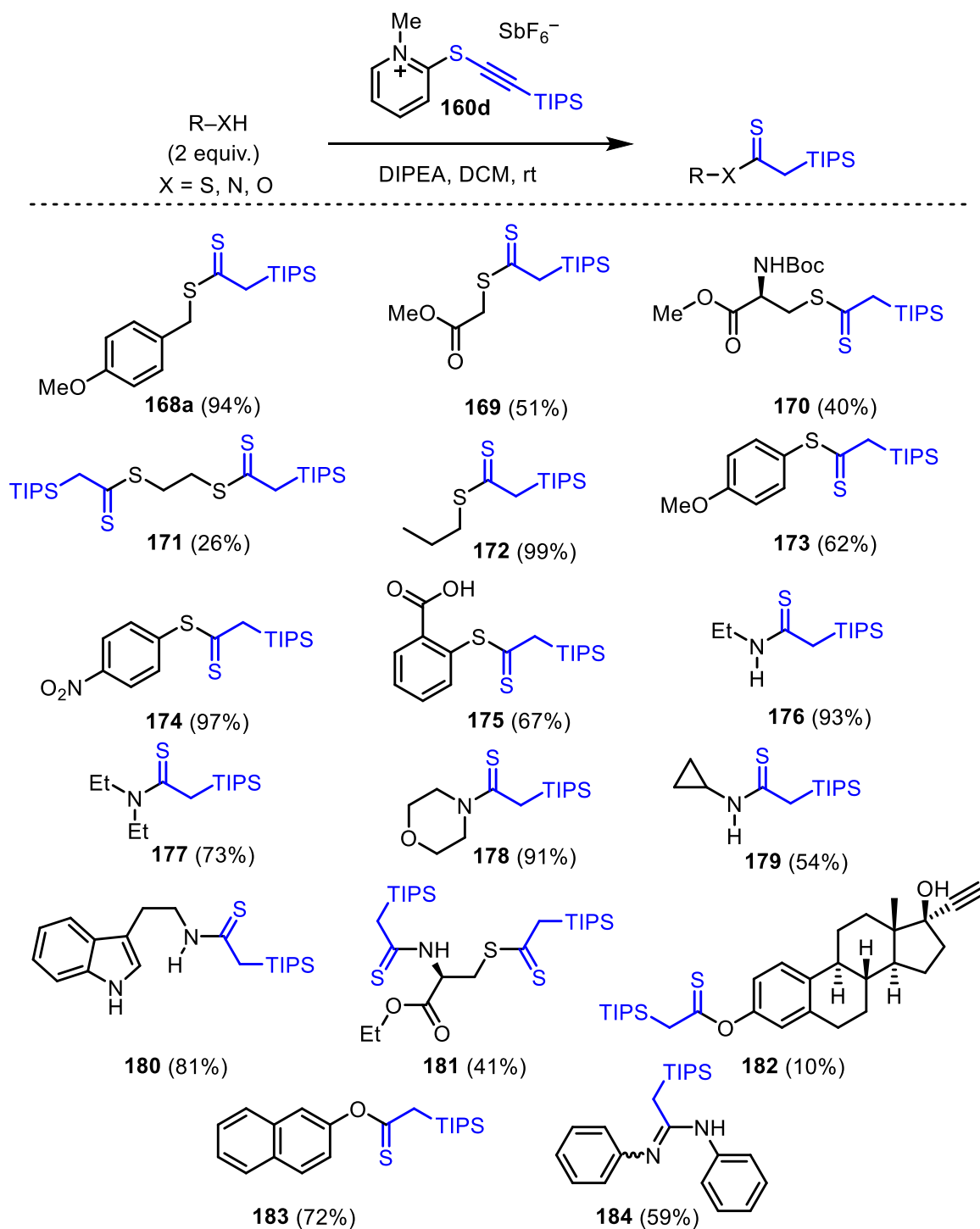
This reactivity could be proven to be general for aliphatic and aromatic thiols **168a–175** (

**Scheme 71**). Furthermore, the reaction scope could be extended to primary and secondary aliphatic amines **176–181**. It is worth mentioning that no additional base is required to start the reaction with amines. However in order to drive the reaction to completion, equimolar amounts of DIPEA were necessary.

Double functionalization of dithiols and of substrates with the amine and thiol functionalities was possible as well. Noteworthy, in the product **181** obtained from cysteine ethyl ester, the original stereochemistry of the latter remained unchanged. It could also be shown that the reaction tolerates carboxylic acids, nitro groups and ethers. Valuable building blocks for prodrugs like morpholine and tryptamine underwent the reaction smoothly as well.

While small alcohols like methanol or *tert*-butanol gave no product, the phenolic constituent of 17 $\alpha$ -ethynylestradiol entered the transformation without observation of competing reactivity on the tertiary alcohol or on the alkyne moieties, despite the low yield of **182**. However, for a more extended aromatic system the reaction went smoothly: The softer alcoholate generated from 2-naphthol gave the corresponding thionoester **183** in good yield of 59%. When aromatic amines were investigated as nucleophiles, rapid characteristic thioamide formation could be observed by TLC. However, due to the presence of two equivalents of aniline in the reaction mixture, subsequent condensation of the second nucleophile takes place and gives the corresponding acetamidine **184**.<sup>2</sup> In addition it should be pointed out, that slow hydrolysis to the amide takes place in the presence of water and base.

<sup>2</sup>To isolate the product on the thioamide stage, reaction progress needs to be monitored accurately and the reaction has to be quenched at the appropriate time.

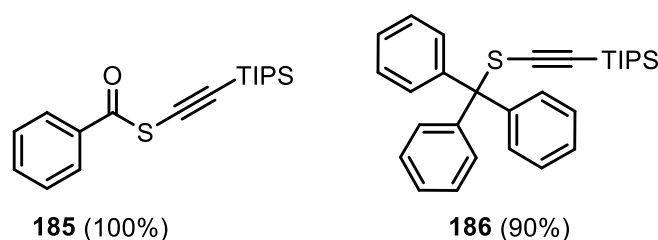


Scheme 71: Scope of *S*-, *N*- and *O*-nucleophiles (isolated yields with respect to the reagent, if not otherwise mentioned<sup>3</sup>).

During the investigation of the general reactivity of the reagent **160d**, a number of unusual results were obtained. When thiobenzoic acid was employed as a substrate, the alkynylation product **185** was isolated exclusively (Scheme 72). We presume that due to the more delocalized negative charge, the preferred target of attack is the softer  $\alpha$ -position of the

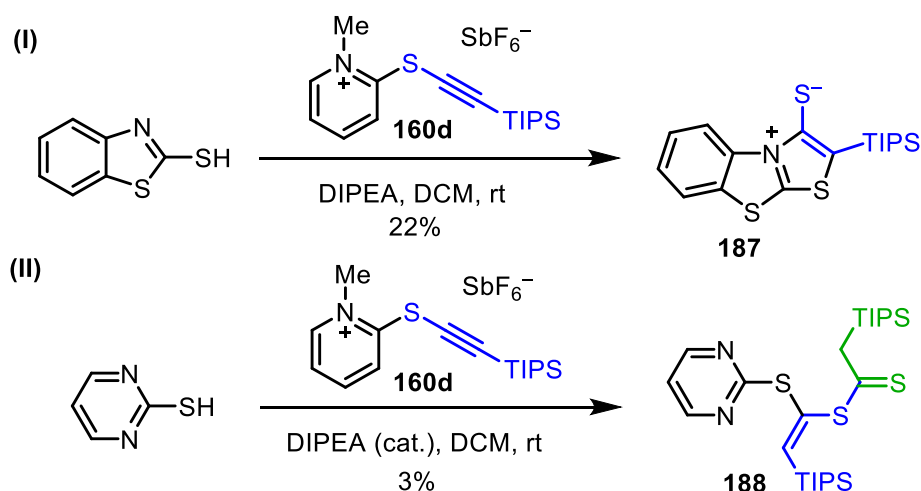
<sup>3</sup> See experimental part TOPIC: "SYNTHESIS AND EVALUATION OF NOVEL PYRIDINIUM-BASED ELECTROPHILIC TRANSFER REAGENTS" for details.

alkyne, which gives product **185** after elimination of the thiopyridone. Similar selectivity was observed with tritylthiol, in which the sterical encumberment plays the decisive role for the formation of alkyne product **186** (Scheme 72).



Scheme 72: S-Alkynylation of thiobenzoic acid and tritylthiol.

As the reagent showed reactivity reminiscent to that of thioketenes, further reactions potentially verifying this parallelism were investigated. Thioketenes and their surrogates are known to undergo cycloadditions with various substrates. In order to test the reagents behavior in this regard, a number of potential candidates for cycloaddition were tested. From examined unpolarized dienes, 2,3-dimethylbutadiene, norbornadiene and 1,3-dipole benzylazide no reactivity was observed. Surprisingly, when benzo[*d*]thiazole-2-thiol was employed as a nucleophile, the zwitterionic product **187** was obtained in 22% yield instead of the expected formation of a dithioester (Scheme 72-I).



Scheme 73: Unexpected cycloaddition and twofold functionalization with catalytic amounts of base.

In order to validate if this reactivity is general, pyrimidine-2-thiol was employed as substrate. However, after an instant colour change of the solution was observed upon addition of the first drop of a base, further addition was stopped, and it was decided to monitor the progress of the reaction in the presence of only catalytic amounts of a base. Surprisingly, only product **188** was isolated in a low yield of 3%. It is feasible to assume that in this case the intermediate aldothioketene is so highly reactive, that a direct subsequent reaction step, which leads to formation of the observed product, takes place. When the same experiment (Scheme 73-II) was conducted with stoichiometric amounts of base, no cycloaddition



products related to **187** were observed. The structure of **188** could be unambiguously confirmed by X-ray diffractometry (Figure 4).

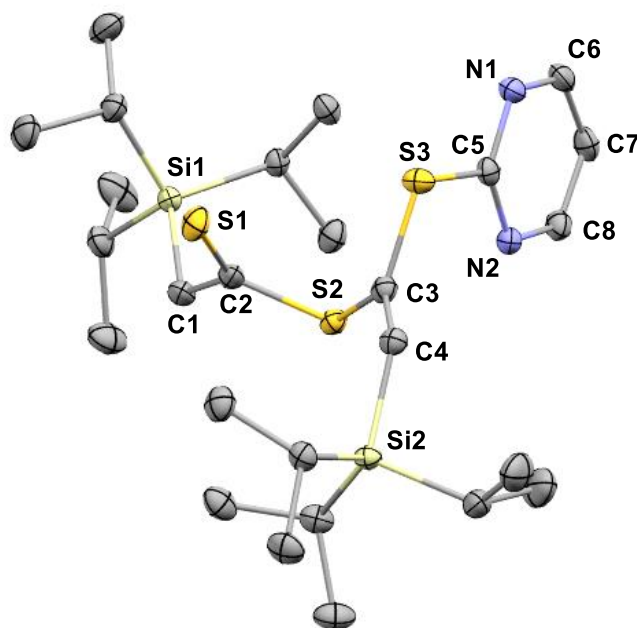
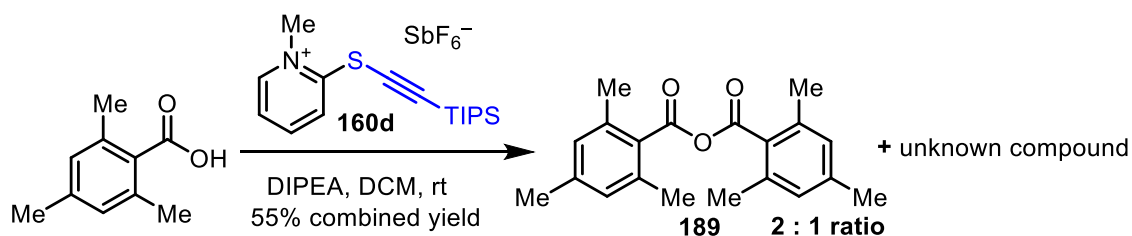


Figure 4: Crystal structure of **188**, Anisotropic displacement parameter shown at 50% probability level, hydrogen atoms omitted for clarity.

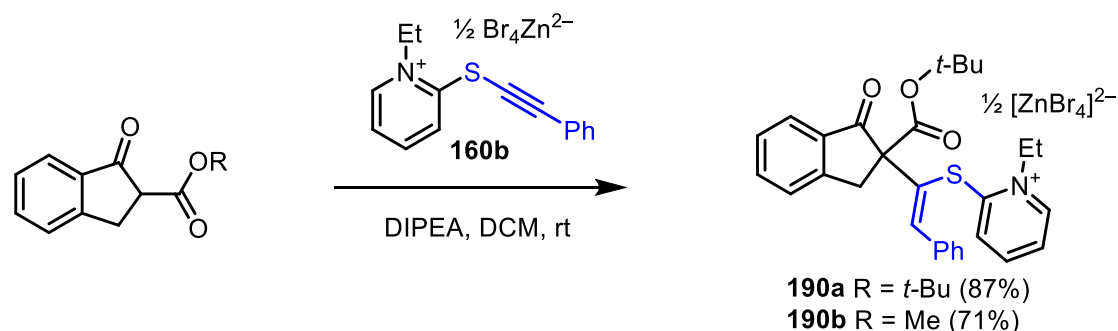
With 2,4,6-trimethylbenzoic acid as a nucleophile, an inseparable mixture of two compounds was obtained (Scheme 74). One of which could be crystallized to obtain its solid state structure, which revealed to be the anhydride **189** of the starting material. We assume that, once thiopyridone is eliminated during the reaction progress, a nucleophilic attack on the carbonyl atom by sulfur takes place. An activated intermediate is formed, which then undergoes acylation by another equivalent of substrate (mercaptopyridines are known for their application as acylating agents).<sup>[164]</sup> In a similar fashion thioanhydrides can be synthesized starting from thioesters and 2-chloroalkylpyridinium salts.<sup>[109,165]</sup>



Scheme 74: Changed reactivity for sterically demanding benzoic acid derivative.

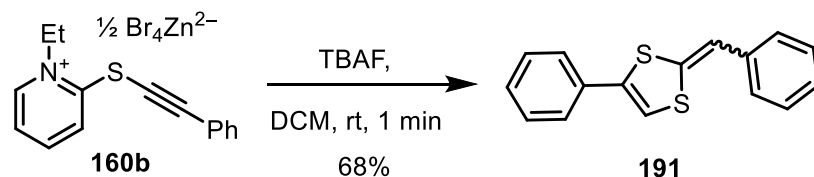
It can be concluded that an aldothioketene or a surrogate thereof is an intermediate in the major product formation pathway of alkynylthiopyridinium salts. Further proof for this hypothesis gave the reaction with a cyclic  $\beta$ -ketoester, in which an adduct of the substrate onto the reagent formed. This “stuck-intermediate” **190** which we assume is too sterically demanding to undergo elimination of the pyridinium moiety, appeared to be quite stable in

our hands, as it even survived purification by column chromatography. Its absolute configuration could be determined *via* NOE and HSQC-NMR experiments.



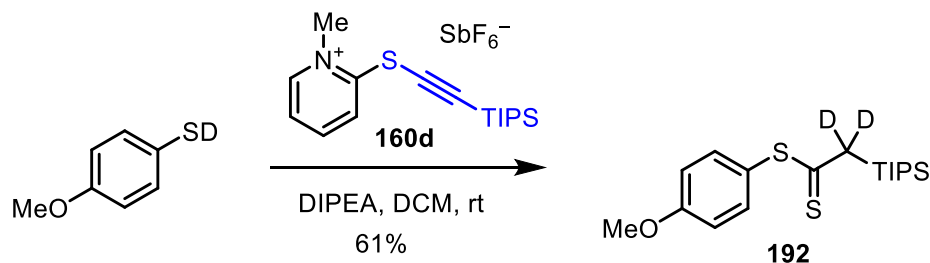
Scheme 75: Product of addition of a cyclic  $\beta$ -ketoesters onto the pyridinium reagent **160b**.

In order to gather an additional mechanistic evidence, we hypothesized that a relatively weak and small nucleophile such as the fluoride anion in  $(\text{Bu})_4\text{NF}$  should be strong enough to provoke a  $\text{S}_{\text{N}}\text{Ar}$ -reaction on the pyridinium ring of alkynylthiopyridinium salts, but not to participate in the reaction with the formed thioketene. Therefore, we made use of the phenylacetylene thiopyridinium salt **160b**, which is not subject to decomposition by a fluoride source (in contrast to **160d**). Indeed, we were able to observe the formation of an isomeric mixture of *cis*- and *trans*-dithiafulvenes **191**, which supports our hypothesis of aldothioketene formation (Scheme 76).



Scheme 76: Formation of dithiafulvenes **191** upon reaction of **160b** with TBAF.

An experiment with the deuterated substrate could prove that in **192** the protons in  $\beta$ -position to the sulfur originate from the nucleophile (Scheme 77).

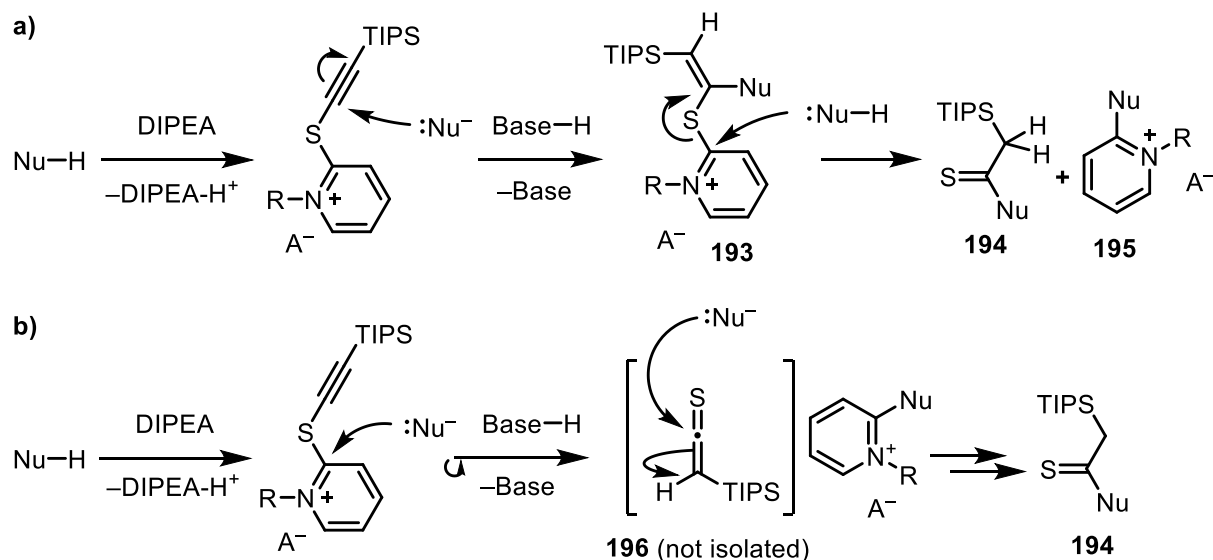


Scheme 77: Experiment with deuterated *p*-methoxythiophenol.

Based on the formerly presented investigations, two plausible mechanistic rationalizations for the reaction are considered (Scheme 78). Initial deprotonation by a base is followed by the nucleophilic attack of the nucleophile.

a) When nucleophilic attack takes place at the acetylenic  $\alpha$ -position of sulfur, an olefinic intermediate **193** is formed. Successive attack of another nucleophile then gives product **194** after elimination of pyridinium species **195**.

b) If the nucleophile attacks the pyridinium carbon in  $\alpha$ -position of sulfur first, an aldothioketene is generated as intermediate **196**. This intermediate is then attacked by a second equivalent of nucleophile to give product **194**.

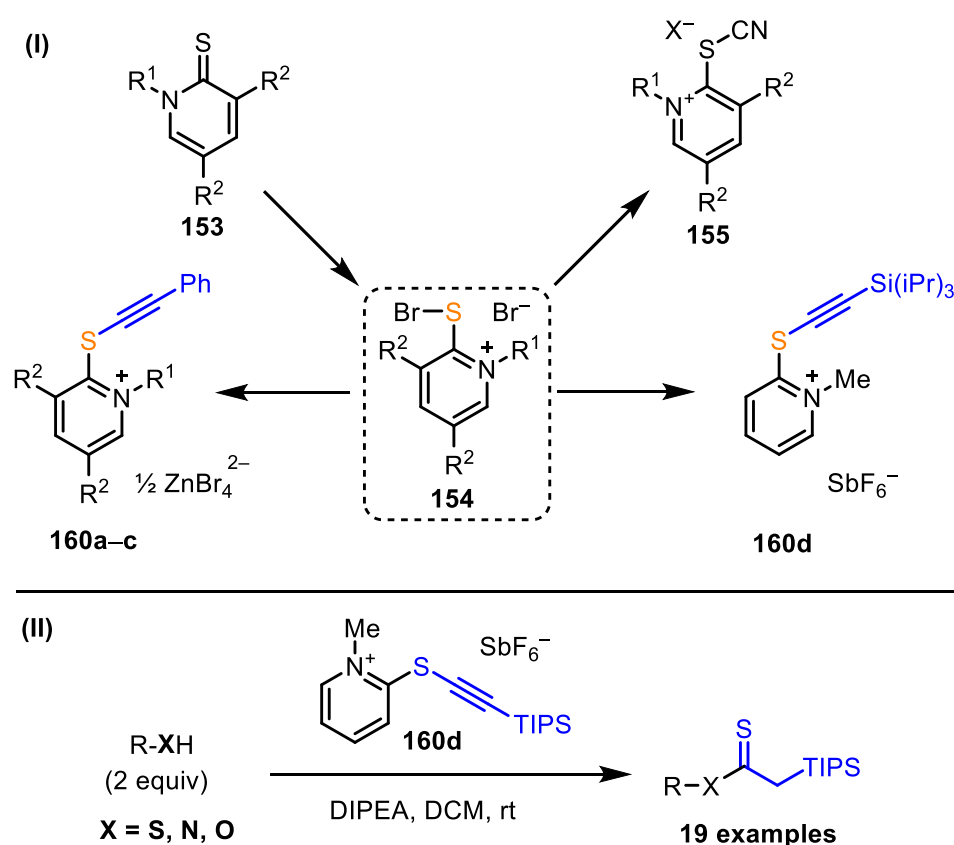


Scheme **78**: Plausible mechanistic rationalizations involving an aldothioketene(-mimetic) species.

Both mechanisms lead to the same product, however whereas the behavior of cyclic  $\beta$ -ketoester **190** is in line with pathway **a)**, the observations made in the experiment of reagent **160b** with TBAF as a nucleophilic source are pointing towards pathway **b)** to be preferred. Furthermore, taking the reactivity of thiobenzoic acid and tritylthiol into account, it can be concluded, that site preference for the nucleophilic attack in either  $\alpha$ -position to sulfur solely depends on the nature of the nucleophile.

## CONCLUSION AND OUTLOOK

A concise synthesis of novel sulfur-based electrophilic transfer reagents was realized (Scheme 79). The initial phase of the project was focused on electrophilic cyanation reagents **155**. Surprisingly, the extreme electron deficiency of the employed pyridinium backbone led to formation of highly unstable intermediates. Isolation of different decomposition products gave insight into the favored pathway thereof. Alternatively, more stable reagents **160**, originally designed for electrophilic alkynylation, were then synthesized. Unexpectedly, the dominating reactivity for the majority of investigated nucleophiles was thioacylation. This gave access to dithioesters, thioamides and thionoesters, which are otherwise accessible only by employing environmentally unfriendly thionating reagents such as Lawesson's reagent or  $P_4S_{10}$ . The disadvantages of the latter are toxicity of not only the reagents themselves, but also of byproducts, harsh reaction conditions and difficulties of product isolations.<sup>4</sup> On the other hand, the use of thioketenes is limited to few available examples with defined substitution patterns.



Scheme 79: **(I)** Synthesis of dibromo(pyridinium)sulfuranes **154**, pyridinium thiocyanates **155** and pyridinium thioalkynes **160**. **(II)** General reactivity of pyridinium thioalkynes **160d** towards S-, N-, O-nucleophiles.

The higher reactivity of the obtained products containing a thione group, as compared to their carbonyl analogs, makes them attractive intermediates for further functionalizations such as the modification of prodrugs in medicinal chemistry or agrochemicals, as was

<sup>4</sup> See Chapter "SYNTHESIS OF DITHIOESTERS, THIOAMIDES AND THIONOESTERS"

demonstrated for selected cases. In addition, several new reactivities were discovered and illustrate that continued research on the project is justified. Exploitation of the reagent as an aldothioketene equivalent has yet to be fully extended to examples in which thioketenes show unique reactivity. These are namely a number of cyclization reactions and most relevant for medicinal chemistry, the synthesis of  $\beta$ -thiolactams as core units for novel antibiotics and their derivatization. Furthermore, the possibility to modify the pyridinium backbone should enable fine tuning, to regulate the reagents reactivity. Only one exemplary approach would be the introduction of an oxy-tether in analogy to hypervalent iodonium salts and the prominent example of EBX.<sup>5</sup>

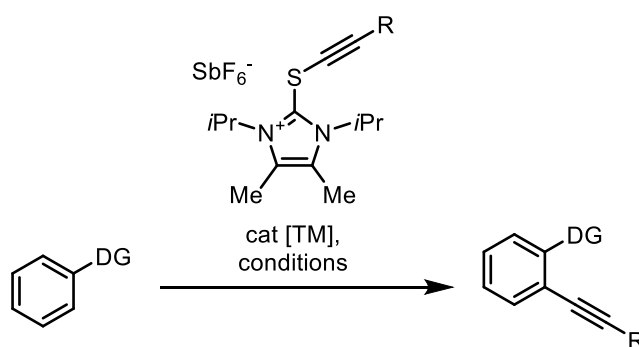
---

<sup>5</sup> See Chapter "ELECTROPHILIC TRANSFER REAGENTS"

## C–H FUNCTIONALIZATION UTILIZING THIOIMIDAZOLONE-BASED ELECTROPHILIC TRANSFER REAGENTS

### PROJECT AIMS

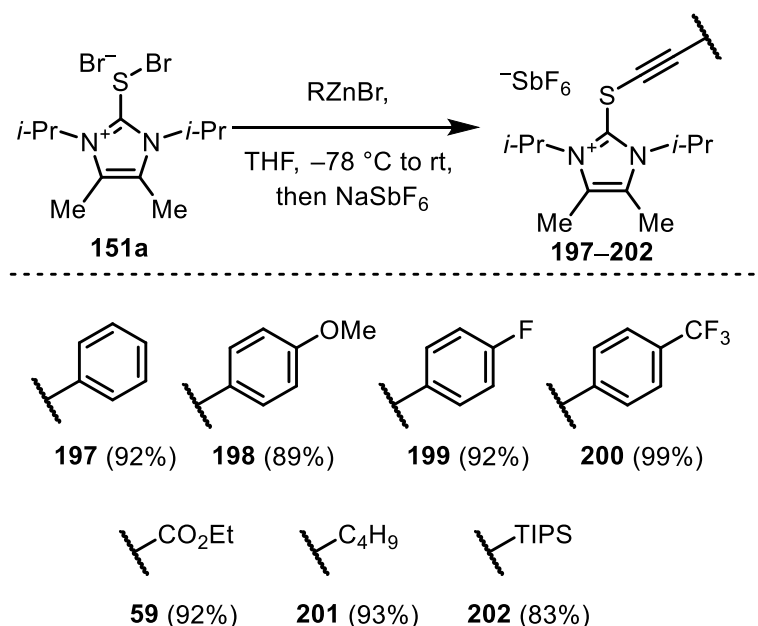
The aim of this project will be to extend the scope of the in group developed imidazolium thioalkynes towards their application in transition metal catalysis. More particular this Chapter will cover the development of a catalytic system in which the mentioned imidazolium thioalkynes will function as terminal electrophilic alkynylation synthons, which are difficult to be developed by other approaches. C–H activation by a transition metal will be used to facilitate the generation of a C-nucleophile from a suitable substrate (Scheme 80). In this context, the choice of an appropriate directing group will be one of the focal points. Once a suitable system is found, investigation of the scope and limitations as well as elucidation of the mechanism will be conducted.



Scheme 80: Proposed C–H activation protocol for the electrophilic alkynylation with imidazolium thioalkynes.

## PRELIMINARY SCREENING

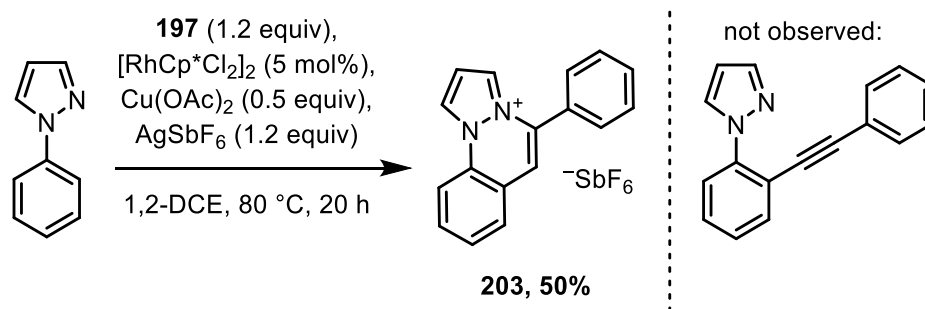
To commence the research in this project, high throughput screenings with a plethora of different reaction parameters were run, after which a selection of promising conditions were further investigated and optimized. Core of these screenings was the variation of transition metals, oxidants, bases, substrates with varying directing groups, solvents and a range of thioimidazolium based electrophilic transfer reagents (Scheme **81**).<sup>6</sup>



Scheme **81**: Alkynylthioimidazolium salts employed during the investigation of C–H functionalization reactions.

1-Phenylpyrazole as a substrate gave one of the most promising initial hits obtained from high throughput screening. The reaction took place in the presence of pentamethylcyclopentadienylrhodium(III) chloride dimer (5 mol%), 0.5 equivalents of copper(II) acetate, silver hexafluoroantimonate(V) and thioimidazolium salt **197**. However, instead of the expected alkynylated product, compound **203** was isolated in 50% yield (Scheme **82**). Salt **203**, which structure was also verified by X-ray diffractometry (Figure **5**), is most probably the result of a *6-endo-dig* cyclization after successful C–H functionalization.

<sup>6</sup> High throughput screenings were conducted in cooperation with Bayer, a NDA was signed.



Scheme **82**: Obtained product for the C–H functionalization of 1-phenylpyrazole with electrophilic thioimidazolium acetylene transfer reagent **197**.

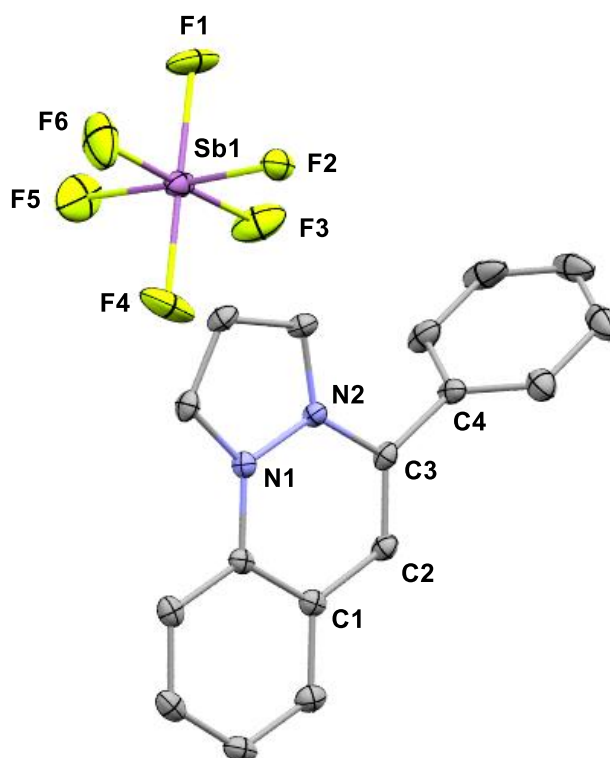


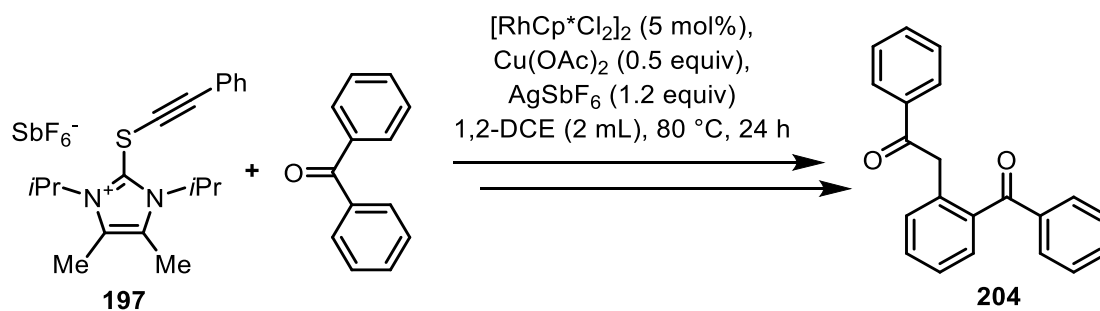
Figure **5**: Structure of compound **203** in the crystal. Anisotropic displacement parameter shown at 50% probability level, hydrogen atoms are omitted for clarity.

Other preliminary results utilizing benzophenone, pivalophenone and acetophenone showed consumption of substrate and reagent as well. While several attempts to isolate a defined product for experiments with benzophenone failed, in one case isolation of a benzophenone derivative was possible. After structural elucidation the latter proved to be the diketone **204** (Scheme **83**). The structure implies, that after successful C–H alkynylation, hydration of the alkyne functionality takes place, either still during the reaction process or during purification by LC-MS. In addition, mass analysis suggested the formation of an adduct of the transfer reagent and the substrate for benzophenone, pivalophenone and acetophenone.<sup>7</sup> Nevertheless, from these preliminary reactions with ketones, it could be concluded, that

<sup>7</sup> Recently isolation of such an adduct starting from azobenzene as a substrate was successful as well (see Chapter: "THE DIAZENYL FUNCTIONALITY AS A DIRECTING GROUP").



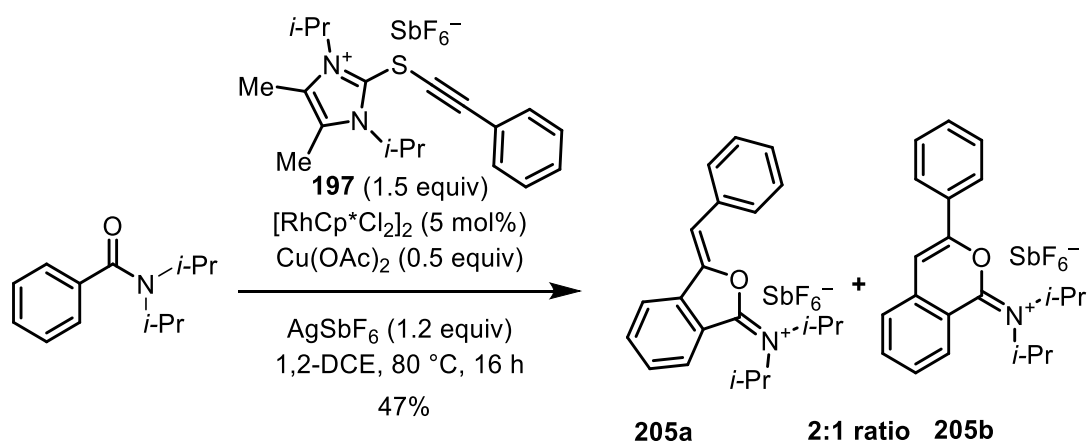
weakly coordinating DGs are promising candidates for C–H functionalization reactions with the designed alkynylthioimidazolium salts.



Scheme **83**: Diketone **204** isolated after applying C–H alkylation protocol with benzophenone as a substrate.

## AMIDES AS WEAKLY COORDINATING DIRECTING GROUPS

The results obtained with ketones as directing groups motivated us to investigate other weakly coordinating directing groups, such as benzamides. When *N,N*-diisopropylbenzamide was employed as a substrate, TLC monitoring of the transfer reaction with alkynylating agent **197** under the elaborated conditions showed the formation of a mixture of salts (Scheme **84**). Purification gave a crystalline solid in a crude yield of 84% with respect to the alkynylation product. NMR analysis revealed that a mixture of two isomers **205a** and **205b** had formed.



Scheme **84**: C–H functionalization of *N,N*-diisopropylbenzamide with alkynylthioimidazolium salt **197**.

Crystals suitable for X-ray analysis were grown by recrystallization from warm acetone on air. X-ray diffractometry unambiguously verified the structure of one of the isomers as the salt **205a** (Figure **6**). Based on the obtained product structure we suggest that *O*-cyclization occurs after C–H activation and alkynylation.

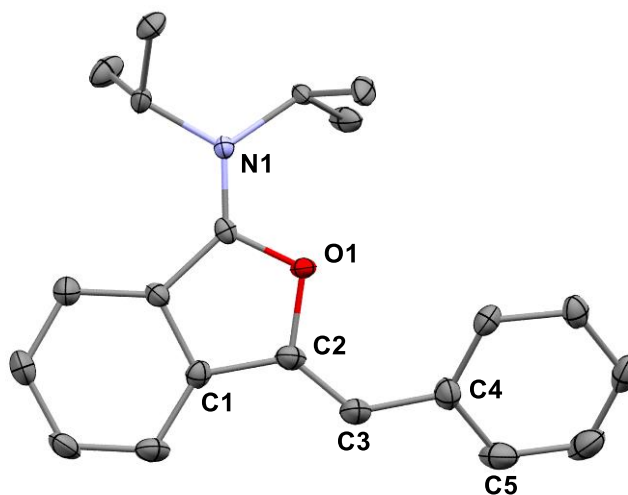
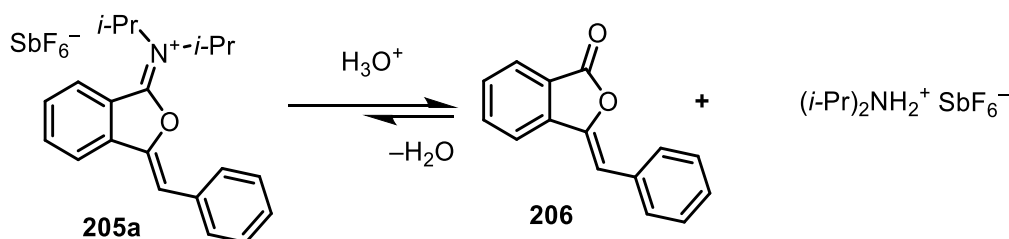


Figure **6**: Structure of compound **205a** in the crystal. Anisotropic displacement parameter shown at 50% probability level, hydrogen atoms and anion are omitted for clarity.

Taking this results into account, a final yield of 47% was determined. In contrast to the reactivity of 1-phenylpyrazole (Scheme **82**), an isomeric mixture of 5-*exo*- and 6-*endo*-dig cyclization products is formed, giving a phthalanylideneammonium salt **205a** and the corresponding isochromene iminium salt **205b**. Attempts to separate these salts failed due to high similarity in their physical properties. It is worth mentioning, that synthesis of this particular class of compounds, in which the nitrogen is a quaternary all-carbon substituted center, and further reactions thereof are described in only two papers by BOYD.<sup>[166,167]</sup>

Much to our delight, it was possible to conduct the hydrolysis of the iminium salts (Scheme **85**). The resulting stable products could be purified by column chromatography.<sup>8</sup> These results are in accordance with the methods formerly described by BOYD.<sup>[167]</sup>



Scheme **85**: Equilibrium of phthalanylideneammonium salt and phthalide.

Optimizational studies were conducted in order to improve overall yield, as well as identify parameters, which influence the selectivity towards either of the constitutional isomers (Table **3**).

Table **3**: Screening of catalyst, base and temperature.

Entry	Catalyst	Base	mmol	Temperature (°C)	Yield of <b>205</b> (%)
1	[RhCp*Cl <sub>2</sub> ] <sub>2</sub>	Cu(OAc) <sub>2</sub>	0.15	80	47
2	[RhCp*Cl <sub>2</sub> ] <sub>2</sub>	Cu(OAc) <sub>2</sub>	0.15	rt	51
3	[RhCp*Cl <sub>2</sub> ] <sub>2</sub>	Na <sub>2</sub> CO <sub>3</sub>	0.3	80	-
4	[RhCp*Cl <sub>2</sub> ] <sub>2</sub>	K <sub>2</sub> CO <sub>3</sub>	0.3	rt	-
5	[RhCp*Cl <sub>2</sub> ] <sub>2</sub>	NaOAc	0.3	80	47
6	[IrCp*Cl <sub>2</sub> ] <sub>2</sub>	NaOAc	0.3	80	-

Reaction conditions: catalyst (0.015 mmol, 5 mol%), AgSbF<sub>6</sub> (125.5 mg, 365 μmol), **197** (247.2 mg, 0.45 mmol), *N,N*-diisopropylbenzamide (61.6 mg, 0.3 mmol), base, 16 h, N<sub>2</sub>.

When *N,N*-diisopropylbenzamide was employed as a substrate at 80 °C and Cu(OAc)<sub>2</sub> as a base, an initial yield of 47% was determined (Table **3**, Entry 1). Under the same conditions at room temperature, the yield slightly increased to 51% (Table **3**, Entry 2). Substitution of Cu(OAc)<sub>2</sub> with NaOAc as the base, gave the same yield of 47% (Table **3**, Entry 5). When

<sup>8</sup> While isolation of the neutral imines obtained as products starting from *N*-methylbenzamides is possible, by quenching the reaction with aqueous K<sub>2</sub>CO<sub>3</sub> solution and subsequent column chromatography, yields are either equal, but more often lower than yields for the hydrolysis products.

carbonates were used as a base or iridium catalyst was used instead of rhodium one, no reaction was observed (Table 3, Entries 3, 4, 6).

With suitable conditions in hand, the selectivity of isomers was still an issue to be addressed. In fact the difference in selectivity for 1-phenylpyrazole (exclusively 6-*endo*). and *N*-substituted benzamide (competitive 5-*exo* and 6-*endo* cyclization), motivated us to investigate the importance of steric bulk of the *N*-substituents of the benzamide, reasoning that 6-*endo-dig* cyclization becomes more favoured with less hindrance. Thus the starting material was changed to *N,N*-dimethylbenzamide (Table 3).

Table 4: Screenings with *N,N*-dimethylbenzamide.

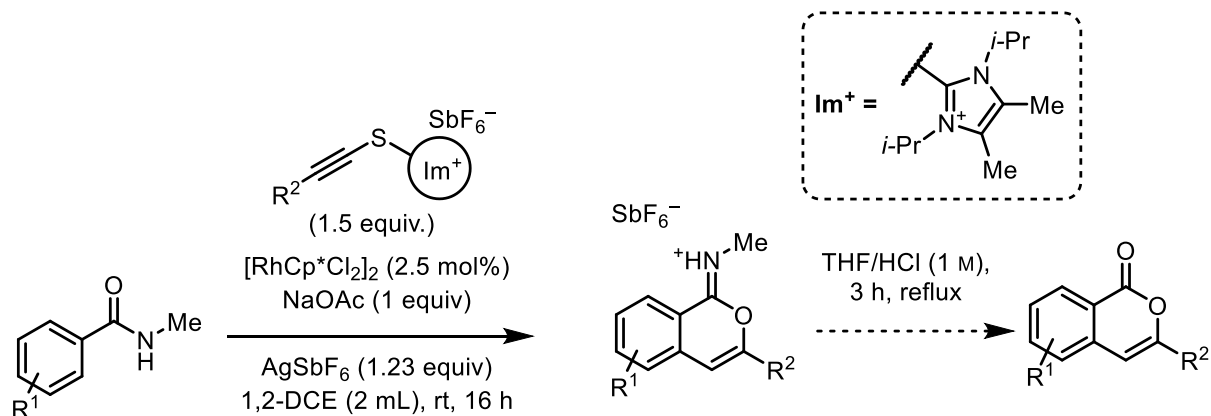
Entry	Solvent	Temperature (°C)	Yield (%)	Isomeric ratio (6- <i>endo</i> :5- <i>exo</i> )
1	DCE	80	48	1.4:1
2	DCE	80	traces <sup>a)</sup>	-
3	DCE <sup>b)</sup>	100	51	1.5:1
4	CH <sub>3</sub> CN	80	-	-
5	CH <sub>2</sub> Cl <sub>2</sub>	60	37	3.6:1
6	CH <sub>2</sub> Cl <sub>2</sub>	rt	-	-
7 <sup>c)</sup>	DCE	rt	60	16:1

Reaction conditions: [RhCp\*Cl<sub>2</sub>]<sub>2</sub> (9.3 mg, 15 μmol, 5 mol%), AgSbF<sub>6</sub> (125.5 mg, 0.37 mmol), **197** (247.2 mg, 0.45 mmol), *N,N*-dimethylbenzamide (44.8 mg, 0.3 mmol), NaOAc (24.6 mg, 0.3 mmol), 16 h, N<sub>2</sub>; a) 0.06 mmol AgSbF<sub>6</sub>, b) 5 mL, c) 2.5 mol% [RhCp\*Cl<sub>2</sub>]<sub>2</sub>, *N*-methylbenzamide was used instead of *N,N*-dimethylbenzamide.

The experiments conducted with *N,N*-dimethylbenzamide verified, that decrease of steric bulk on the imine moiety favors 6-*endo* cyclization, while overall yields remained similar (Table 4, Entry 1). When substoichiometric amounts of silver-salt were used, only traces of product formation were observed (Table 4, Entry 2). Increasing the temperature to 100 °C only marginally increased the overall yield and exerts only little influence on the selectivity (Table 4, Entry 3). Switching to the more polar acetonitrile as a solvent completely suppressed product formation (Table 4, Entry 4). Using dichloromethane as a solvent resulted in a decrease of the yield. On the other hand, an increase in the proportion of 6-*endo* product was observed, which can either be attributed to the nature of solvent or to the decrease in temperature (Table 4, Entry 5). However, no product was formed under essentially the same conditions, but at room temperature (Table 4, Entry 6). Finally, switching to *N*-methylbenzamide as a substrate as further decreasing the size of *N*-substituents, not only gave an 6-*endo*:5-*exo* isomeric mixture in ratio 16:1, but also increased the combined yield to 60%. In addition, lowering the catalyst loading to 2.5 mol% did not give any drop in the yield (Table 4, Entry 7).

Summarizing these results, on going from *N,N*-diisopropylbenzamide to *N*-methylbenzamide and applying the C–H functionalization/hydrolysis sequence, access to isocoumarins was elaborated (Scheme 86). At last, switching from anhydrous 1,2-dichloroethane to technical

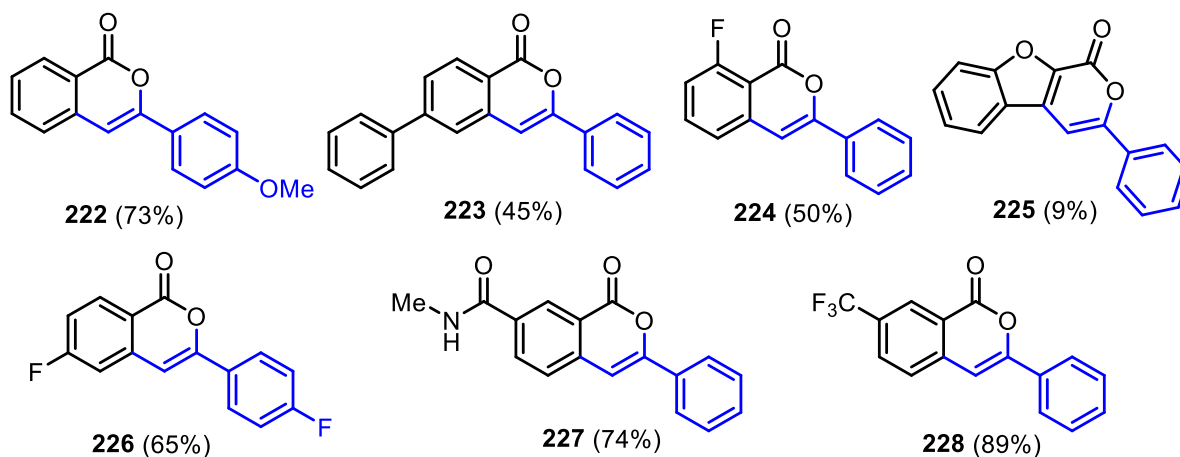
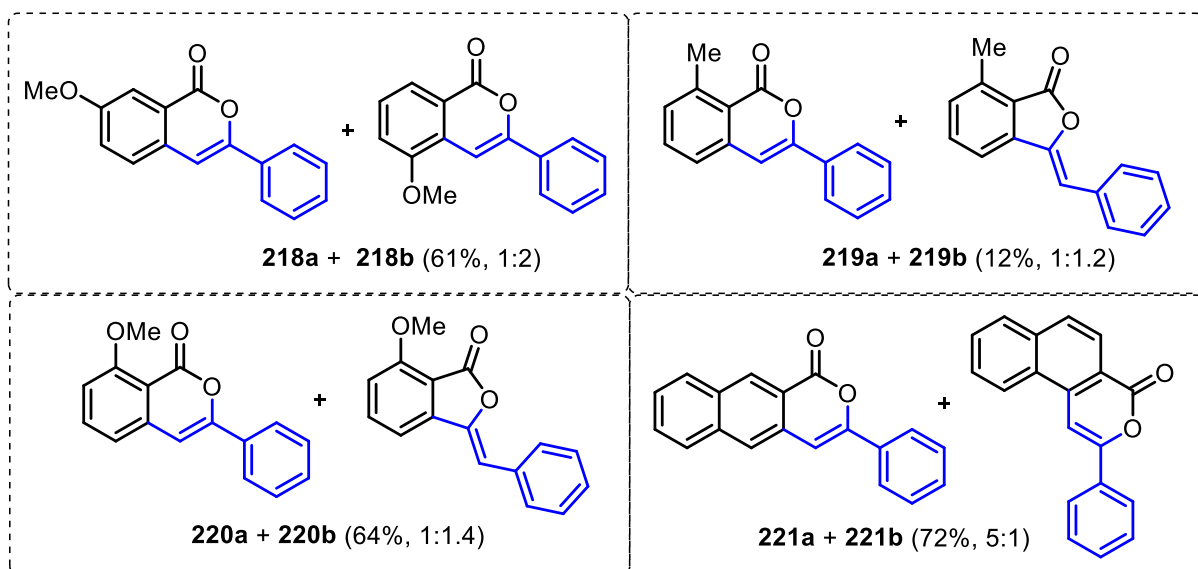
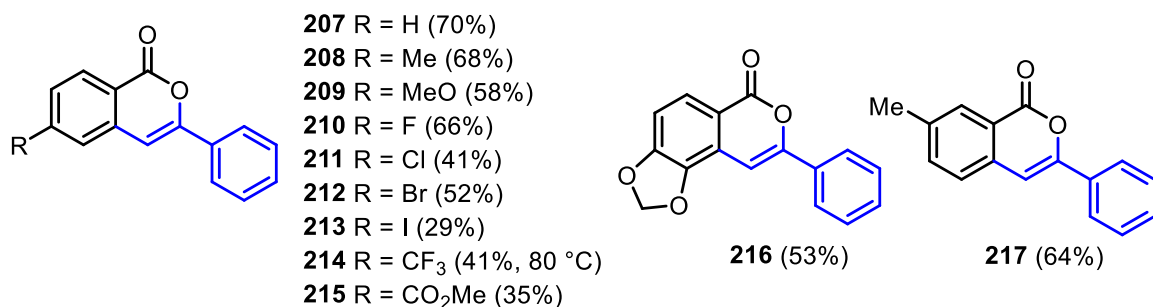
grade solvent increased the efficacy again, affording homalicine **207** from *N*-methylbenzamide in 70% yield (Scheme **87**).



Scheme **86**: Developed catalytic system for the synthesis of 3-substituted isocoumarins from *N*-methylbenzamides and alkynylthioimidazolium salts.

After identification of a suitable directing group, the influence of electron withdrawing as well as of electron donating substituents in the backbone of the starting material was explored (Scheme **87**). During this process, the influence on chemoselectivity by sterically demanding substituents was recognized.

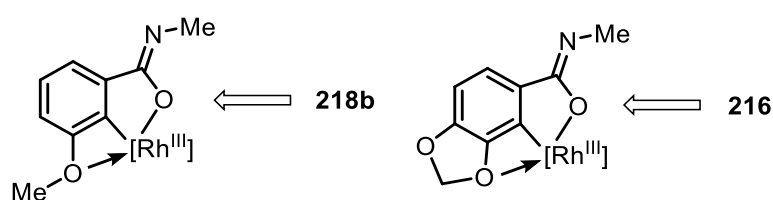
It is worth mentioning, that, since annulation also incorporates the directing group, overfunctionalization through a second C–H-activation step is circumvented.



Scheme **87**: Scope of *N*-methylbenzamides to synthesize 3-substituted isocoumarins.

To investigate the effects of electron donating groups, the tolyl derivative with the methyl group in *para*-position, featuring an additional +I effect, was tested in the reaction. Yet, the observed yield of 68% for **208** was similar to that of **207**. Assuming, that employing an EDG with the stronger +M effect in a starting material would increase the nucleophilicity of the *in situ* formed metallacycle (see below, Scheme **93-II**) and thus enhance the yield, *p*-methoxy-*N*-methylbenzamide was used as a substrate. Selective transformation to the corresponding isocoumarin **209**, however, gave the product in a yield of 58%. Furthermore, when the reactivity of an electron richer substrate containing the dioxolane moiety was tested, the

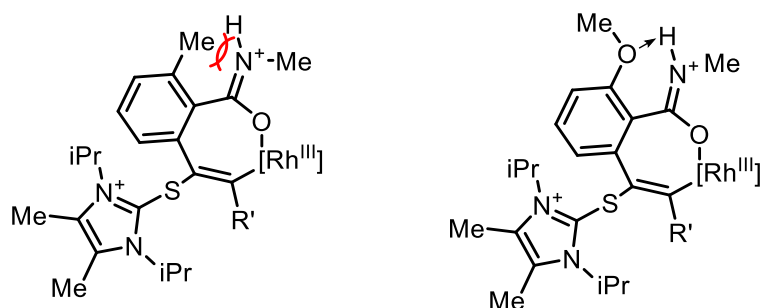
yield remained similar with 53% for **216**. Surprisingly, product analysis revealed that only one of two possible isomers was formed. The structure of the product suggested that a lone pair-containing *meta* substituent might play a decisive mechanistic role in the reaction. To verify this hypothesis, *m*-methoxy-*N*-methyl benzamide was employed in the reaction, giving two regioisomers **218a** and **218b** in an 1:2 ratio and overall yield of 61%. Formation of the latter might be explained by a coordinated chelating effect of the amido group and a secondary chelating effect exerted by the methoxy substituents. This resulted in the initial C–H-activation in *ortho*-position to both the directing and the methoxy groups. Such a secondary stabilizing effect by interaction of the adjacent *O*-containing group with the catalyst during the C–H-activation step can be considered as a general explanation (Scheme **88**). Formation of a chelate with the active rhodium species would also explain the selectivity for the aforementioned dioxolane compound **216**.



Scheme **88**: Directed selectivity observed for *O*-containing *meta* substituents.

To conclude that this hypothesis is true, the reactivity of *N*-methyl-*m*-toluamide was investigated. But in case of aliphatic substituents in *meta* position, no secondary effects play any role, as isochromene **217** was isolated in 64% yield as a single isomer.

For *ortho*-substituted substrates the reaction strongly depends on sterical factors. Thus, from *N*-methyl-*o*-toluamide, an isomeric mixture of isocoumarin **219a** and phthalide **219b** with a respective ratio of 1:1.2 was isolated in 12% yield. We suggest that the initially formed five-membered rhodacycle underwent an insertion of the alkyne moiety affording a seven-membered metallacycle (Scheme **89**, right, and intermediate **III** in Scheme **93**).<sup>[168,169]</sup> For this scenario, *o*-methyl substitution creates a disfavoured transition state due to sterical repulsion of the methyl group and the iminium group (Scheme **89**).



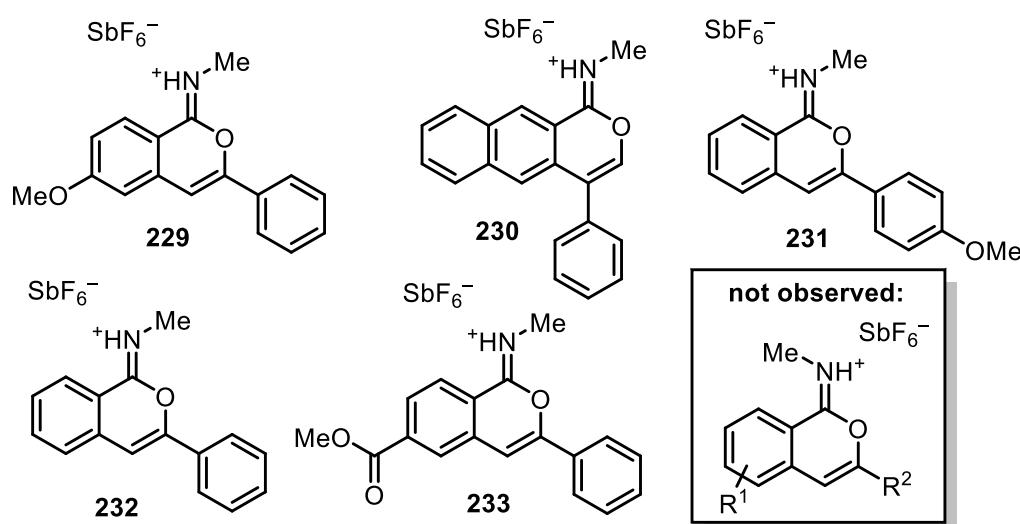
Scheme **89**: Sterical clash created by *o*-alkyl-substituents (left) and H-bonding by the *o*-methoxy group (right).

For the comparison, when *o*-methoxybenzamide was employed as a substrate, an isomeric mixture of isocoumarin **220a** and phthalide **220b** in an overall 64% yield with a ratio of 1:1.4

was isolated. This is an additional evidence for the postulated mechanism: In this case the methoxy group in *ortho* position stabilizes the transition state through hydrogen bonding.

Noteworthy, while potentially competing *N*-cyclization has been reported in literature,<sup>[146]</sup> it was not observed in any reaction conducted within this project. Even more: based on our findings, we suggest that nothing but the oxygen of the amide functionality is exclusively responsible for the coordination of the catalytically active rhodium species during the formation of the metallacycle in the C–H activation step and subsequently for the nucleophilic attack in the ring closing step. Consequently, the nitrogen faces away from the reaction site.

On the other hand, hydrogen bonding (Scheme 89, right) is not the sole factor determining the spatial orientation of *N*-methyl groups, as sterical reasons are of prime importance as well (analogously to Scheme 89, left). Thus, only one singlet for the *N*-methyl group was observed in crude NMR spectra of compounds **229–233** (Scheme 90).<sup>9</sup>



Scheme 90: Structures of compounds **229–233** picked as crystals from reaction crudes and identified by X-ray diffractometry.

According to their crystal structures (Figure 7), the methyl substituents on the nitrogen were found to be *anti* oriented towards the parent aryl ring from the substrate in all cases. This cannot be explained by the packing effects and thus indicates that such an orientation is very probably favored and determined during the C–H activation and insertion steps (See next Chapter, Scheme 93).

<sup>9</sup> All crystals shown in Figure 7 were taken from reaction crudes before hydrolysis to the final isocoumarins presented in Scheme 87.



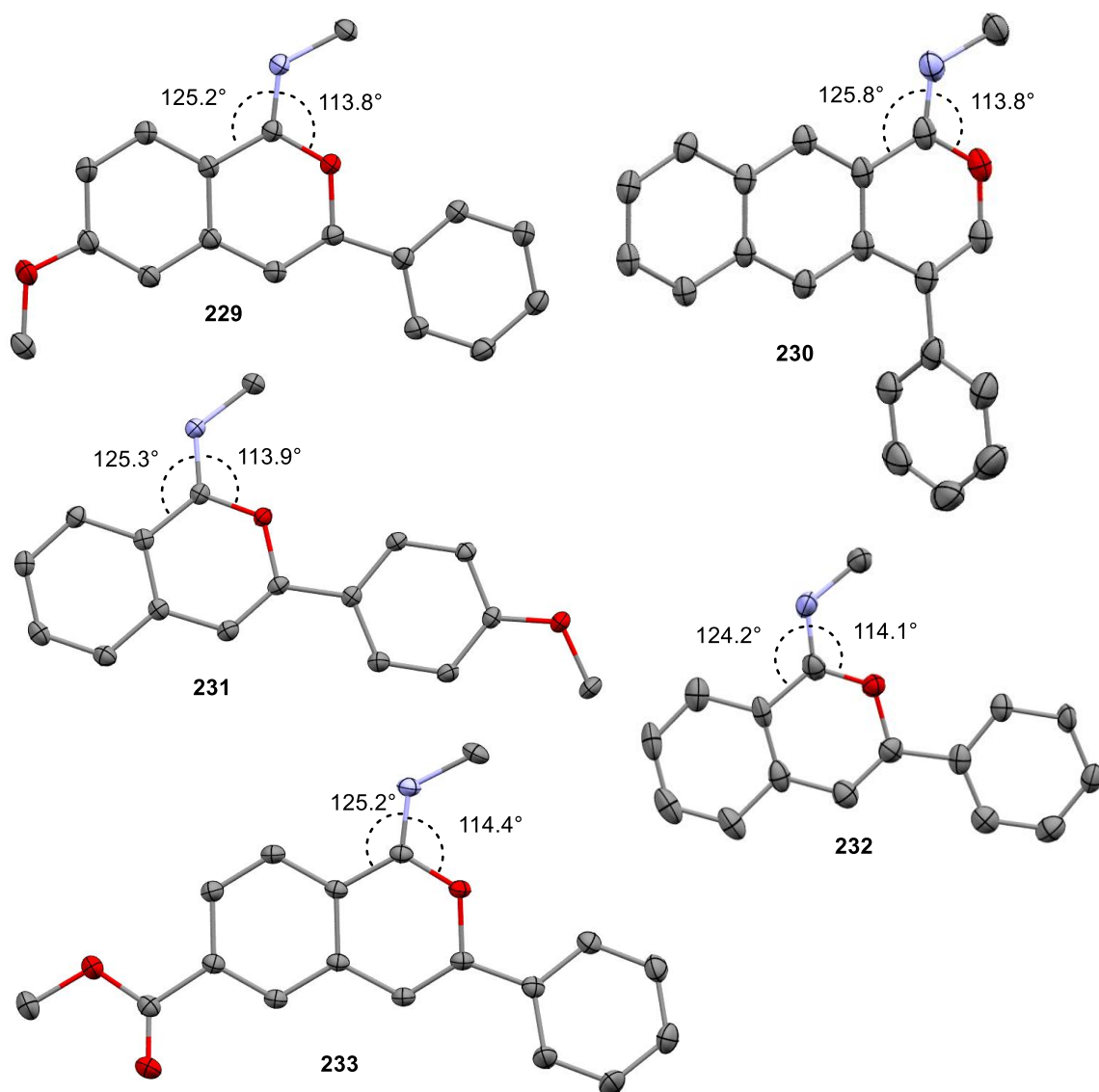
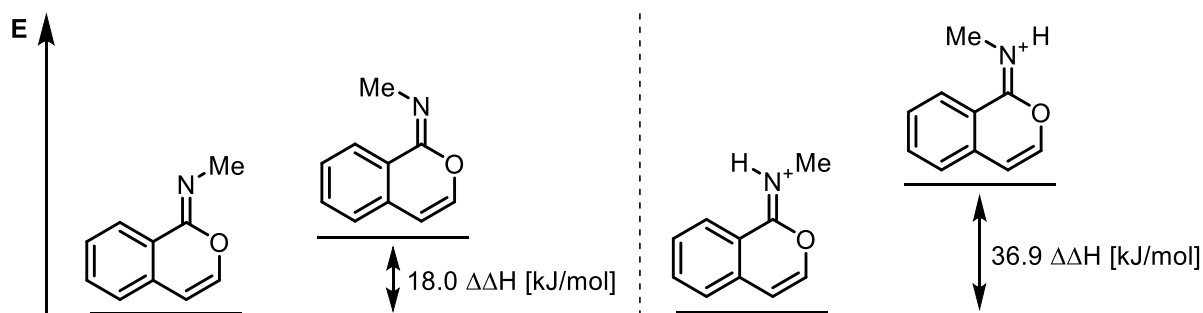


Figure 7: Structures of **229–233** in the crystals. Anisotropic displacement parameter shown at 50% probability level, hydrogen atoms and anions are omitted for clarity.<sup>10</sup>

The deviation from an ideal 120° angle depicted for compounds **229–233** is a result of the shorter C-O bond. Similar angles are also observed for the corresponding isocoumarins, which means that the bending does not originate from steric repulsion.

Finally, the observed conformational preference is in line with the results of *ab initio* calculations to compare relative energies of *E*- and *Z*-isomers for model substrates (Scheme 91).

<sup>10</sup> The unusual regioselectivity for compound **230** is discussed in the next Chapter (Figure 13).



Scheme 91: Calculated energy difference for isochromene imine and iminium isomers as model substrates (B3LYP/6-31G(d) Opt Freq).

Nevertheless it can not be excluded that the observed orientation of the methyl group is the result of the thermodynamically favoured isomer.

It quickly became clear, that electron withdrawing groups in *para*-position to the directing group reduce the product formation. The explanation is the overall reduced electron density: this makes the generated nucleophile weaker after the C–H activation step. Thus, *p*-trifluoromethyl and *p*-methylcarboxylate-substituted substrates afforded the corresponding products **214** and **215** in only moderate yields (41% and 35%, respectively). As expected, in line with their higher electronegativity, halogen substituents *p*-chloro- and *p*-bromo- slightly decrease the yields of the corresponding isochromenes **211** (41%) **212** (52%), when compared with the non-substituted compound **207**. Due to its lowest electronegativity among the other halogens, *p*-iodo-*N*-methylbenzamide was expected to give product **213** in better yield, than compound **212**. Surprisingly, the product yield of 29% was the lowest from all obtained with the halogen-substituted substrates. *p*-Fluorine substitution did not decrease the efficacy essentially, as compared to the model substrate, giving the desired product in 66% yield. In contrast, *p*-nitro-*N*-methylbenzamide as a substrate furnished only traces of product, observed in crude  $^1\text{H}$  NMR spectrum and by TLC. Besides the electron poor character of the compound, in this case we presume the low solubility of the substrate under the reaction conditions to play a major role.

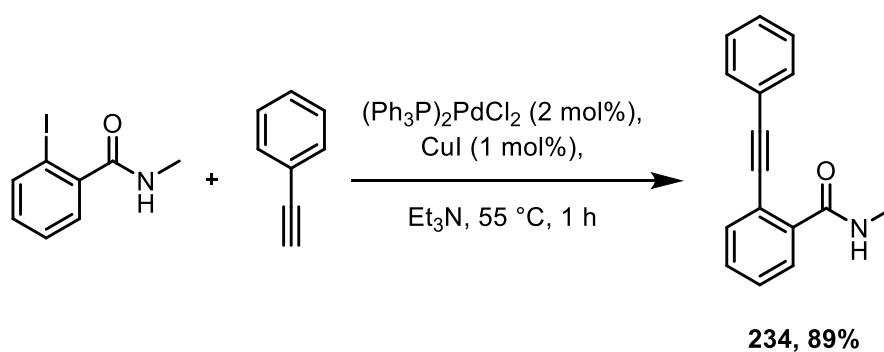
Wondering if the employment of the directing group twice in the same molecule would provoke a twofold transformation and would give an increase in yield,  $N^1,N^3$ -dimethylisophthalamide was synthesized and used as a substrate. In spite of the fact that this substrate can be considered as bearing two *ortho*-DGs, the single C–H activation occurred in *o,p*-position. While purification proved to be difficult, the desired mono-cyclized product **227** was isolated in a good yield of 74%. To further investigate whether the predominating effect for the increase in yield was due to the two DGs or the *ortho*-EWG, *o*-CF<sub>3</sub>-*N*-methylbenzamide was used as a substrate. The product was isolated in excellent 89% yield, thus indicating that an *o*-EWG substitution was indeed benefiting product formation substantially. When a phenyl ring in the substrate was replaced by a heterocyclic moiety, such as thiophene or furane, no product could be obtained under different reaction conditions.

Nevertheless, characteristic strong UV-activity on TLC suggested product formation, at least in traces. Treatment of the benzofurane derivative under standard reaction conditions lead to isolation of the desired product; however, only in 9% yield, thus discouraging any further investigations towards other heterocyclic substrates.

Low reaction temperatures proved to be detrimental for product formation. While *p*-(dimethylamino)-*N*-methylbenzamide only showed traces of product formation under standard conditions, the same reaction at 80 °C resulted in the complete removal of the directing group. These findings supplement the reports by GLORIUS et al.<sup>[169,170]</sup> who observed dehydration and dehydrocarbonylation as common side reactions in the C–H functionalization of aryl ketones and aldehydes, respectively.

## MECHANISTIC INVESTIGATIONS

To gain insight into the mechanism of the cyclization step, model substrate **234** was synthesized from phenylacetylene and *ortho*-iodo-*N*-methylbenzamide via Sonogashira-Hagihara coupling following the modified literature procedure (Scheme 92). Fortunately, a small amount of palladium-coordinated cyclized intermediate **235** was isolated and crystallized during the purification process of **234**. Investigation by X-Ray diffractometry revealed its structure (Figure 8), hinting at the fact that the target cyclization of **234** can also take place under various catalytic conditions.



Scheme 92: Synthesis of cyclization-model substrate **234** via Sonogashira-Hagihara coupling.

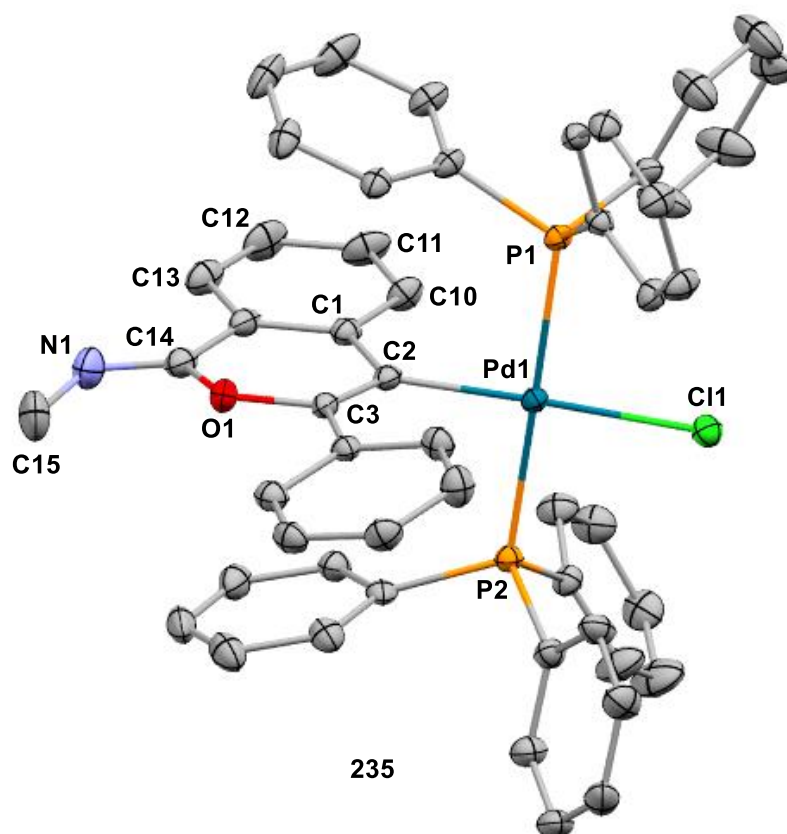


Figure 8: Structure of deactivated Pd-substrate complex **235** in the crystal with the substrate still attached. Anisotropic displacement parameter shown at 50% probability level, hydrogen atoms and anions, minor disorder part (11%) of isochromene imine, are omitted for clarity. The chlorine position is partially occupied with an iodine atom (refined to 22% occupancy).

With model substrate **234** in hand, a set of experiments under different reaction conditions was carried out (Table 5):

Table 5: Investigation of the annulation step.

Entry	Rh-precatalyst	AgSbF <sub>6</sub> (quantity)	Conversion (%)
1	[RhCp*Cl <sub>2</sub> ] <sub>2</sub> (5 mol%)	-	-
2	-	1.5 equiv	100
3	[RhCp*Cl <sub>2</sub> ] <sub>2</sub> (5 mol%)	1.5 equiv	100
4	[RhCp*Cl <sub>2</sub> ] <sub>2</sub> (5 mol%)	5 mol%	traces
5	RhCp*(MeCN) <sub>3</sub> (SbF <sub>6</sub> ) <sub>2</sub> (2.5 mol%)	-	86

After analysis of the experiments summarized in Table 5, it was concluded, that both – the catalytically active rhodium species as well as the silver salt – are responsible for the annulation process. Actually, this type of annulation has been reported to proceed with benzamides and similar substrates under catalysis with a variety of Lewis and Brønsted acids.<sup>[171]</sup> Interestingly, from the attempted cyclization with RhCp\*(MeCN)<sub>3</sub>(SbF<sub>6</sub>)<sub>2</sub> (Table 5, Entry 5) deep red crystals were collected. The latter revealed to be the deactivated catalyst

species **236a** (Figure 9), in which one equivalent of thiourea is coordinated to the rhodium center, hinting at one of the catalysts deactivation pathways.

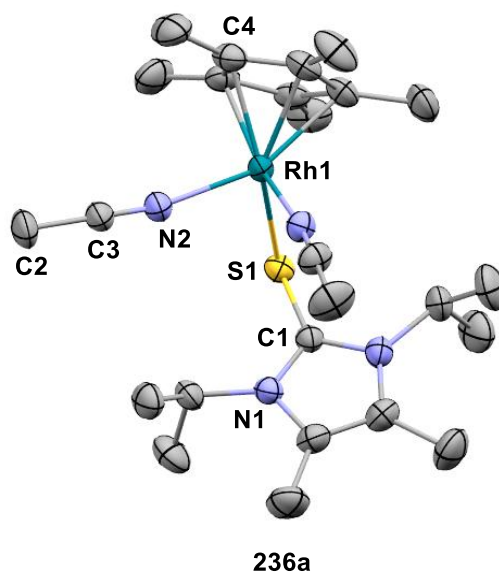
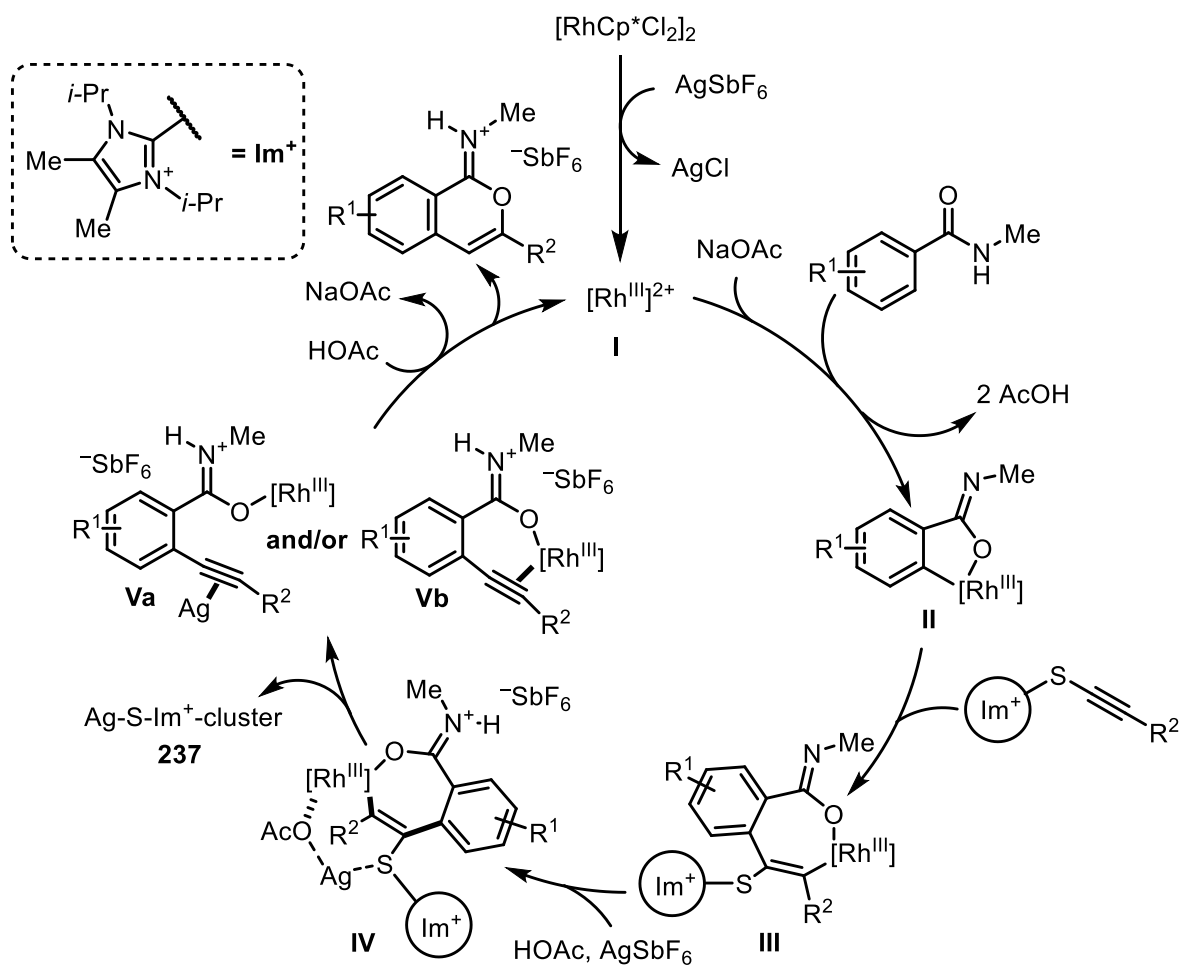


Figure 9: Structure of isolated deactivated rhodium species **236a** in the crystal. Anisotropic displacement parameter shown at 50% probability level, hydrogen atoms and anions are omitted for clarity.

Analyzing the informations gained during the study of the reaction scope with respect to the influence of different substitution patterns, as well as the investigations towards the cyclization step, a tentative catalytic cycle can be postulated (Scheme **93**).



Scheme 93: Postulated catalytic cycle for the C–H functionalization of *N*-methylbenzamides with alkynylthioimidazolium salts.

Generation of the active catalyst species (**I**) is facilitated by abstraction of the chloride ligands by  $\text{AgSbF}_6$ . Then coordination of the amide oxygen to the catalyst followed by acetate-assisted deprotonation affords the five-membered metallacycle (**II**). After alkyne insertion and formation of a seven-membered metallacycle (**III**), silver assisted sulfur elimination gives compound **Va** or **Vb** and **237** (Figure 10). Subsequent annulation gives the isochromene iminium salt as a pre-product and the free catalyst.

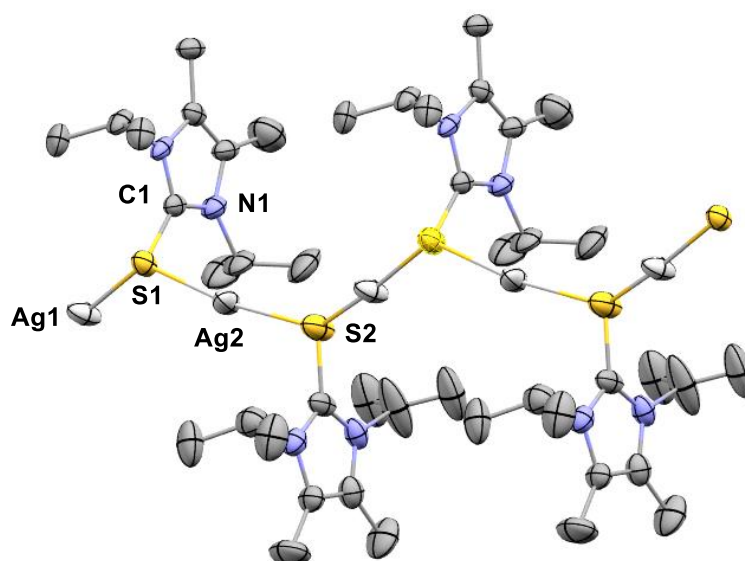
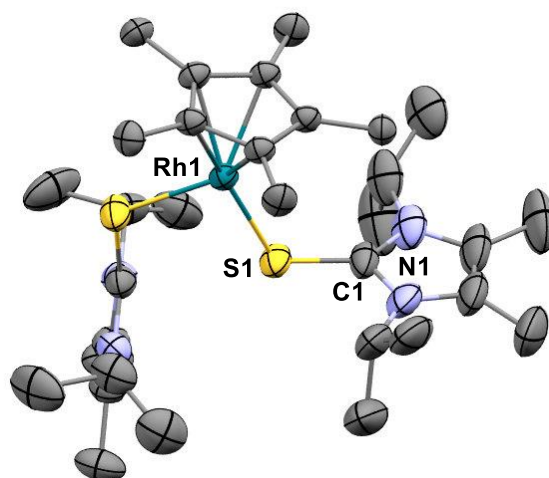


Figure 10: Structure of Ag-S-Im<sup>+</sup>-cluster **237** in the crystal. Anisotropic displacement parameter shown at 50% probability level, hydrogen atoms, solvent and anions are omitted for clarity.

Another compound suggesting a deactivation pathway, which is considered to be in equilibrium with species **237**, is **236b**, justifying the amount of silver-salt used (Figure 11).



**236b**

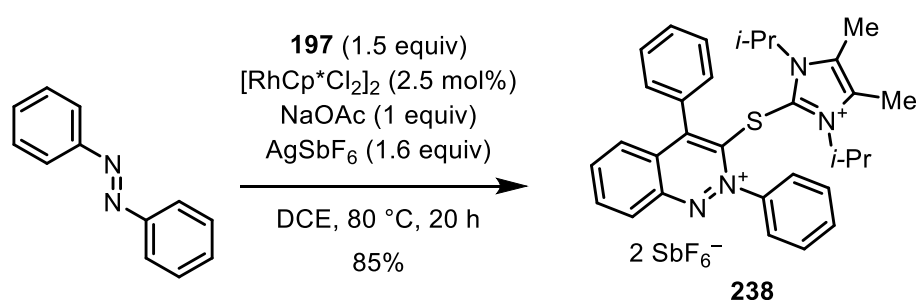
Figure 11: Structure of deactivated catalyst species **236b** in the crystal. Anisotropic displacement parameter shown at 50% probability level, hydrogen atoms, solvent and anions are omitted for clarity.



## THE DIAZENYL FUNCTIONALITY AS A DIRECTING GROUP

After the mode of reactivity of 1-phenylpyrazole was resolved, the structurally similar compounds phenylhydrazine and azobenzene were investigated as substrates. Whereas phenylhydrazine showed no reactivity at all, when employing azobenzene, full consumption of the starting material was observed under slightly modified reactions condition.

The reaction was worked up as described by CHENG et al.<sup>[172]</sup> X-ray crystal structure analysis revealed that an annulation of the former triple bond took place in a similar manner as observed before. However, inverted regioselectivity with respect to the alkyne was observed this time. In addition, the thiourea backbone was still attached (Scheme 94 and Figure 12).



Scheme 94: Reactivity observed for the C–H activation-initiated functionalization of azobenzene with **197**.

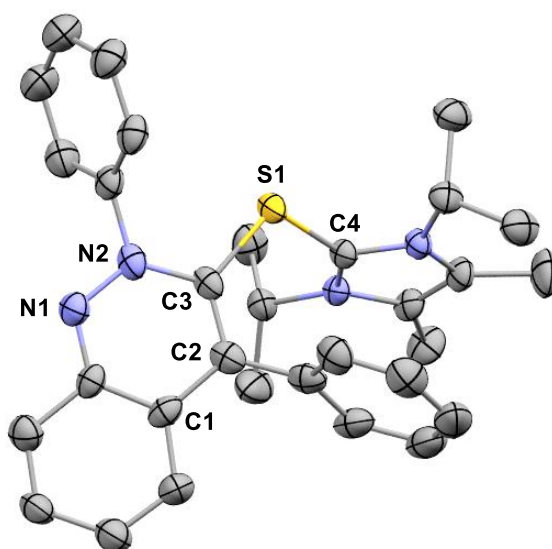


Figure 12: Structure of the adduct obtained after C–H activation of azobenzene followed by cyclization with **197** in the crystal. Anisotropic displacement parameter shown at 50% probability level, hydrogen atoms and anions are omitted for clarity.

This unexpected result along with isochromene iminium **230** (Figure 7, Figure 13), which was obtained in a single case from a crude reaction mixture upon the synthesis of compound **221**<sup>11</sup>, motivated us to further investigate the mode of cyclization by experiments of both *N*-methylbenzamide and azobenzene as substrates with  $^{13}\text{C}$ -labeled reagent **241**.<sup>[54]</sup>

<sup>11</sup> The reaction was run a total of three times.

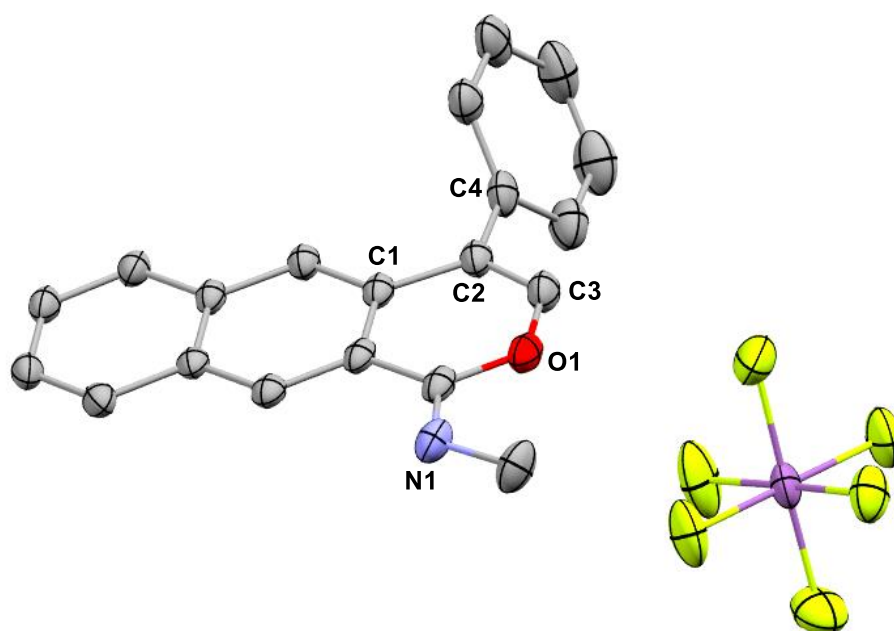
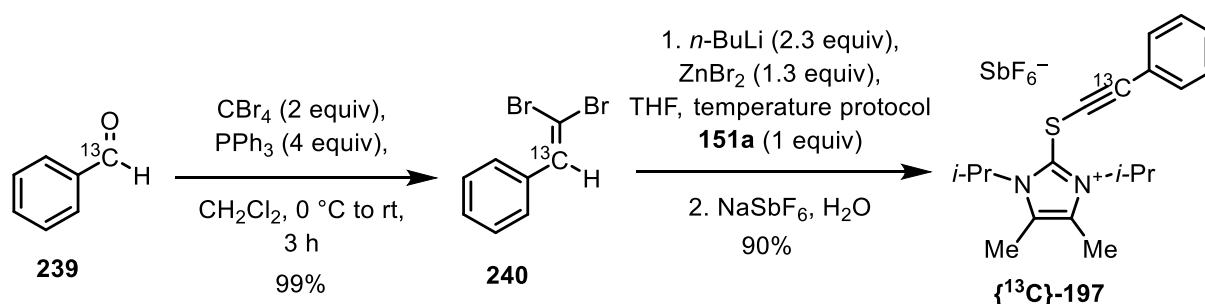


Figure 13: Molecular structure of isochromene iminium **230**, obtained in a single case from a crude reaction mixture upon the synthesis of compound **221**, in the crystal. Anisotropic displacement parameter shown at 50% probability level, hydrogen atoms are omitted for clarity.

Carbon scrambling observed for reactions involving (alkynyl)dibenzothiophenium reagents, as developed by ALCARAZO and WALDECKER,<sup>[54]</sup> gave reason to investigate the observed regioselectivity of the aforementioned reactions.

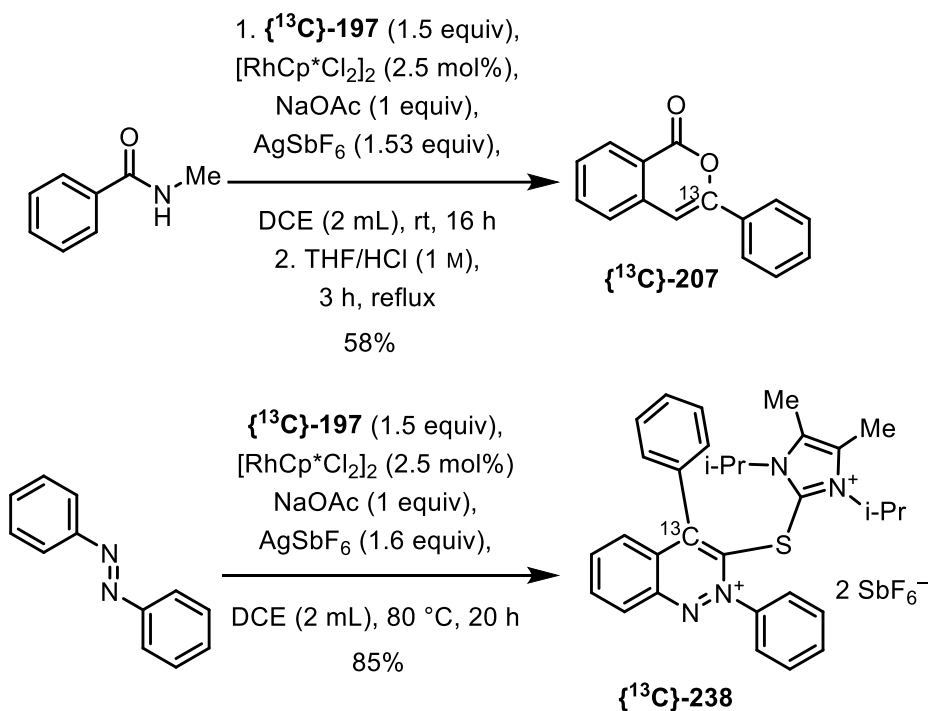
Thus synthesis of a <sup>13</sup>C-enriched imidazolium thioalkyne reagent **241** was conducted as presented in Scheme 93.



Scheme 95: Synthesis of the <sup>13</sup>C-enriched alkynylthioimidazolium salt.<sup>12</sup>

In the first step, <sup>13</sup>C-labeled benzaldehyde **239** was quantitatively transformed to dibromoalkene **240** employing a Corey-Fuchs reaction. Treatment of **240** with *n*-butyllithium caused the Fritsch-Buttenberg-Wiechell rearrangement followed by intermediate formation of alkynyllithium, which was directly transmetalated with a zinc salt. *In situ* reaction of the latter with dibromo(imidazolium)sulfurane **151a** gave the <sup>13</sup>C-labeled alkynylating agent **{<sup>13</sup>C}-197** in 90% yield.

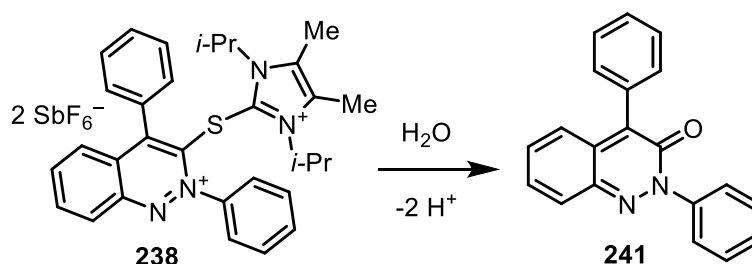
<sup>12</sup> GP C was applied for the last step.



Scheme 96: Reaction of  $^{13}\text{C}$ -enriched alkynylthioimidazolium salt **241** with *N*-methylbenzamide and azobenzene.

While the aforementioned results indicated, that scrambling of the phenyl group during the reagent synthesis or the catalytic reaction itself might occur,<sup>[54]</sup> our experiments suggest that scrambling in the products **242** and **243** (Scheme 96) does not proceed at all in both cases. Accordingly, the regioselectivity of the nucleophilic attack on the alkyne is predefined by the properties of the nucleophile.

Additional information was obtained from experiments carried out with dication **238**. Exposure to air and moisture led to the formation of an apolar species, as was observed by TLC. Successful isolation, crystallization and structural analysis revealed the product to possess the structure of cinnolinone **244** (Scheme 97 and Figure 14).<sup>13</sup>



Scheme 97: Cinnolinone **241** obtained after prolonged exposure to ambient conditions.

<sup>13</sup> Sufficient amounts for characterization were isolated, however no final yield was determined.

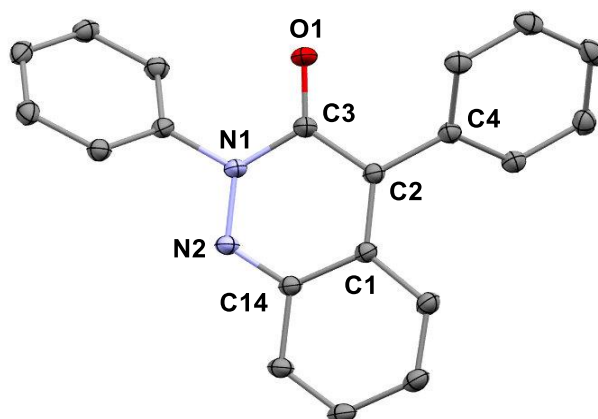
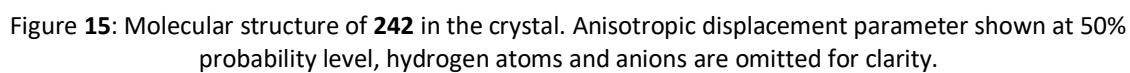


Figure 14: Molecular structure of compound **241** in the crystal. Anisotropic displacement parameter shown at 50% probability level, hydrogen atoms and anions are omitted for clarity.

When cinnolinium salt **238** was heated in presence of a strong base such as NaOH, ring-contracted product **245** was obtained. Presumably, initial nucleophilic attack of hydroxide furnished an acyclic carboxylic acid, followed by ring closure and successive decarboxylation and air oxidation afforded the indazole framework (Scheme 98 and Figure 15).<sup>14[174]</sup>

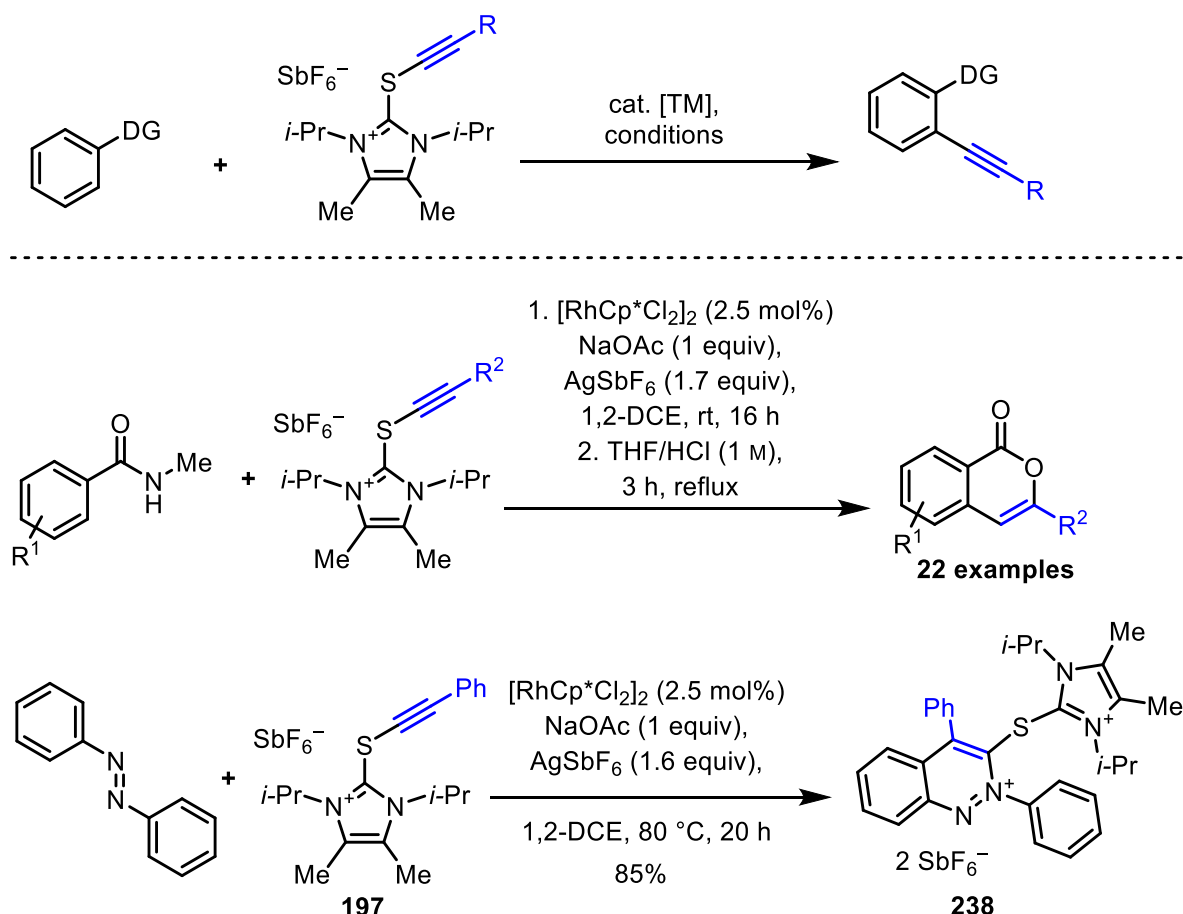
On the other hand, participation of the thiourea to facilitate either decarbonylation or decarboxylation by activation of the carbonyl group in a similar fashion as observed for thiolactam **153a** in Scheme 74, can not be excluded.<sup>[173]</sup>

<sup>14</sup> Sufficient amounts for characterization were isolated, however no final yield was determined.



## CONCLUSION AND OUTLOOK

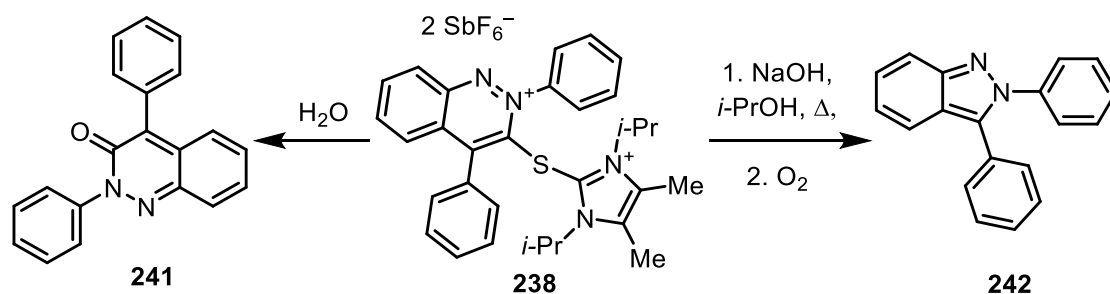
The task to elaborate an appropriate catalytic system to prove the compatibility of cationic sulfur reagents transferring electrophilic groups in a transition metal-mediated C–H activation/functionalization reaction was successfully accomplished. After identification of an appropriate directing group and careful optimization of the reaction conditions, a sequence consisting in electrophilic alkynylation of *N*-methylbenzamides followed by annulation and final hydrolysis gave isocoumarins in moderate to good yields. The substitution pattern on the aromatic framework of the benzamides revealed to be decisive for the selectivity of product formation. The observed selectivities during the establishment of the scope (Scheme 88, Scheme 89), the interpretation of the crystallographic evidence from structures 229–233, 237 and 236 as well as the  $^{13}\text{C}$ -labeling experiments enabled us to formulate a tentative mechanism (Scheme 93). It can be concluded that the substitution pattern on the nitrogen of the amide functionality plays a vital role, but also depending on the decoration of the benzyl ring of the benzamide, secondary effects can favor selectivity or suppress product formation.



Scheme 99: Established catalytic systems utilizing imidazolium thioalkynes.

Furthermore, numerous other directing groups were screened and showed promising compatibility. For azobenzene, inverted selectivity with respect to the nucleophilic attack on

the alkyne was observed. In addition, structure of the product suggests, that elimination of the transfer reagent is also substrate-dependent, as similar behavior was observed in initial experiments with benzophenone and other ketones.<sup>15</sup> The dicationic product **238** was easily purified and proved to open up new exciting opportunities for diversification in preliminary experiments.



Scheme **100**: Diversification of dicationic cinnolinium salt **238**.

<sup>15</sup> The mass of the corresponding adduct was observed in ESI-MS for numerous examples with the keto functionality.

## BIBLIOGRAPHY

- [1] J. McMurry, *Organic chemistry*, Cengage Learning, Boston, MA, USA, **2015**.
- [2] a) E. J. Corey, D. Seebach, *Angew. Chem.* **1965**, *77*, 1134; b) D. Seebach, *Angew. Chem. Int. Ed. Engl.* **1979**, *18*, 239.
- [3] Wöhler, Liebig, *Ann. Pharm.* **1832**, *3*, 249. Catalytic version: b) N. Zinin, *Ann. Pharm.* **1839**, *31*, 329.
- [4] a) C. Djerassi, *Chem. Rev.* **1948**, *43*, 271; b) N. Shibata, A. Matsnev, D. Cahard, *Beilstein J. Org. Chem.* **2010**, *6*.
- [5] T. Umemoto, *Chem. Rev.* **1996**, *96*, 1757.
- [6] R. F. Heck, J. P. Nolley, *J. Org. Chem.* **1972**, *37*, 2320.
- [7] T. Mizoroki, K. Mori, A. Ozaki, *Bull. Chem. Soc. Jpn.* **1971**, *44*, 581.
- [8] D. Milstein, J. K. Stille, *J. Am. Chem. Soc.* **1978**, *100*, 3636.
- [9] D. Milstein, J. K. Stille, *J. Am. Chem. Soc.* **1979**, *101*, 4992.
- [10] J. K. Stille, *Angew. Chem. Int. Ed. Engl.* **1986**, *25*, 508.
- [11] M. Kosugi, Y. Shimizu, T. Migita, *Chem. Lett.* **1977**, *6*, 1423.
- [12] N. Miyaura, K. Yamada, A. Suzuki, *Tetrahedron Lett.* **1979**, *20*, 3437.
- [13] N. Miyaura, A. Suzuki, *J. Chem. Soc., Chem. Commun.* **1979**, 866.
- [14] N. Miyaura, A. Suzuki, *Chem. Rev.* **1995**, *95*, 2457.
- [15] K. Sonogashira, Y. Tohda, N. Hagihara, *Tetrahedron Lett.* **1975**, *16*, 4467.
- [16] C. Zhang, *Org. Biomol. Chem.* **2014**, *12*, 6580.
- [17] W. B. Jensen, *J. Chem. Educ.* **2006**, *83*, 1751.
- [18] F. M. Beringer, S. A. Galton, *J. Org. Chem.* **1965**, *30*, 1930.
- [19] M. Ochiai, T. Sueda, K. Miyamoto, P. Kiprof, V. V. Zhdankin, *Angew. Chem. Int. Ed.* **2006**, *45*, 8203.
- [20] a) T. G. Appleton, H. C. Clark, L. E. Manzer, *Coord. Chem. Rev.* **1973**, *10*, 335; b) A. Pidcock, R. E. Richards, L. M. Venanzi, *J. Chem. Soc. A* **1966**, 1707.
- [21] a) E. M. Shustorovich, Y. A. Buslaev, *Inorg. Chem.* **1976**, *76*, 1142; b) E. Shustorovich, *J. Am. Chem. Soc.* **1978**, *100*, 7513; c) E. M. Shustorovich, Y. A. Buslaev, *Koord. Khim.* **1975**, *1*, 1020.
- [22] a) R. J. Hach, R. E. Rundle, *J. Am. Chem. Soc.* **1951**, *73*, 4321; b) G. C. Pimentel, *J. Chem. Phys.* **1951**, *19*, 446.
- [23] a) V. Zhdankin, *Curr. Org. Synth.* **2005**, *2*, 121; b) T.-Y. Sun, X. Wang, H. Geng, Y. Xie, Y.-D. Wu, X. Zhang, H. F. Schaefer, *Chem. Commun.* **2016**, *52*, 5371.
- [24] a) U. Teruo, I. Sumi, *Tetrahedron Lett.* **1990**, *31*, 3579; b) H. Li, *Synlett* **2012**, *23*, 2289; c) L. M., Yagupolskii, N. V. Kondratenko, G. N. Timofeeva, *J. Org. Chem. USSR* **1984**, *20*, 103.
- [25] T. Umemoto, S. Ishihara, *J. Am. Chem. Soc.* **1993**, *115*, 2156.
- [26] F. Kurzer, *J. Chem. Soc.* **1949**, 1034.
- [27] D. Kahne, D. B. Collum, *Tetrahedron Lett.* **1981**, *22*, 5011.
- [28] a) S. Thambidurai, K. Jeyasubramanian, S. K. Ramalingam, *Polyhedron* **1996**, *15*, 4011; b) S. Kim, C. J. Lim, *Angew. Chem. Int. Ed.* **2002**, *41*, 3265; c) Y. Kita, S. Akai, T. Okuno, M. Egi, T. Takada, H. Tohma, *Heterocycles* **1996**, *42*, 47; d) M. Kasthuri, H. Babu, K. Kumar, C.



- Sudhakar, P. Kumar, *Synlett* **2015**, 26, 897; e) S. V. Bhat, D. Robinson, J. E. Moses, P. Sharma, *Org. Lett.* **2016**, 18, 1100; f) A.-P. Schaffner, V. Darmency, P. Renaud, *Angew. Chem. Int. Ed.* **2006**, 45, 5847; g) G. L. Adams, P. J. Carroll, A. B. Smith, *J. Am. Chem. Soc.* **2012**, 134, 4037; h) O. Loreau, N. Camus, F. Taran, D. Audisio, *Synlett* **2016**, 27, 1798; i) M. V. Vita, P. Caramenti, J. Waser, *Org. Lett.* **2015**, 17, 5832.
- [29] T. V. Hughes, S. D. Hammond, M. P. Cava, *J. Org. Chem.* **1998**, 63, 401.
- [30] V. V. Zhdankin, C. J. Kuehl, A. P. Krasutsky, J. T. Bolz, B. Mishmash, J. K. Woodward, A. J. Simonsen, *Tetrahedron Lett.* **1995**.
- [31] R. Akula, Y. Xiong, H. Ibrahim, *RSC Adv.* **2013**, 3, 10731.
- [32] P. Anbarasan, H. Neumann, M. Beller, *Chem. Eur. J.* **2010**, 16, 4725.
- [33] P. Anbarasan, H. Neumann, M. Beller, *Chem. Eur. J.* **2011**, 17, 4217.
- [34] Y. Yang, Y. Zhang, J. Wang, *Org. Lett.* **2011**, 13, 5608.
- [35] K. Kiyokawa, T. Nagata, S. Minakata, *Angew. Chem. Int. Ed.* **2016**, 55, 10458.
- [36] Alan R. Katritzky, Rufine Akue-Gedu, Anatoliy V. Vakulenko, *Arkivoc* **2006**, 2007, 5.
- [37] Y.-F. Wang, J. Qiu, D. Kong, Y. Gao, F. Lu, P. G. Karmaker, F.-X. Chen, *Org. Biomol. Chem.* **2015**, 13, 365.
- [38] R. Frei, T. Courant, M. D. Wodrich, J. Waser, *Chem. Eur. J.* **2015**, 21, 2662.
- [39] R. Chowdhury, J. Schörghener, J. Novacek, M. Waser, *Tetrahedron Lett.* **2015**, 56, 1911.
- [40] M. Chen, Z.-T. Huang, Q.-Y. Zheng, *Org. Biomol. Chem.* **2015**, 13, 8812.
- [41] G. Talavera, J. Peña, M. Alcarazo, *J. Am. Chem. Soc.* **2015**, 137, 8704.
- [42] X. Li, C. Golz, M. Alcarazo, *Angew. Chem. Int. Ed.* **2019**, 58, 9496.
- [43] Y.-q. Wu, D. C. Limburg, D. E. Wilkinson, G. S. Hamilton, *Org. Lett.* **2000**, 2, 795.
- [44] a) A. Yoshimura, V. V. Zhdankin, *Chem. Rev.* **2016**, 116, 3328; b) M. Ochiai, Y. Masaki, M. Shiro, *J. Org. Chem.* **1991**, 56, 5511. Essentially, the first hypervalent iodine compound,  $\text{PhICl}_2$ , was prepared in 1886: c) Willgerodt, *J. Prakt. Chem.* **1886**, 33, 185; however, a renaissance in the chemistry of polyvalent iodine has occurred only in the past 30 years: d) V. V. Zhdankin, *Hypervalent Iodine Chemistry: Preparation, Structure, and Synthetic Applications of Polyvalent Iodine Compounds*, Wiley, Chichester, **2013**; e) Special Issue *Hypervalent Iodine Chemistry*, T. Wirth (Ed.), *Top. Curr. Chem.* **2016**, 373, 316 pp.
- [45] D. P. Hari, P. Caramenti, J. Waser, *Acc. Chem. Res.* **2018**, 51, 3212.
- [46] V. V. Zhdankin, A. P. Krasutsky, C. J. Kuehl, A. J. Simonsen, J. K. Woodward, B. Mismash, J. T. Bolz, *J. Am. Chem. Soc.* **1996**, 118, 5192.
- [47] M.-X. Sun, Y.-F. Wang, B.-H. Xu, X.-Q. Ma, S.-J. Zhang, *Org. Biomol. Chem.* **2018**, 16, 1971.
- [48] A. J. Arduengo, E. M. Burgess, *J. Am. Chem. Soc.* **1977**, 99, 2376.
- [49] H. W. Roesky, U. N. Nehete, S. Singh, H.-G. Schmidt, Y. G. Shermolovich, *Main Group Chem.* **2005**, 4, 11.
- [50] a) D. Fernández González, J. P. Brand, J. Waser, *Chem. Eur. J.* **2010**, 16, 9457. b) J. P. Brand, J. Charpentier, J.; Waser, *Angew. Chem. Int. Ed.* **2009**, 48, 9346.
- [51] a) J. P. Brand, J. Waser, *Chem. Soc. Rev.* **2012**, 41, 4165; b) J. Waser, *Johnson Matthey Technol. Rev.* **2015**, 59, 284.
- [52] J. Waser, *Synlett* **2016**, 27, 2761.

- [53] A. G. Barrado, A. Zieliński, R. Goddard, M. Alcarazo, *Angew. Chem. Int. Ed.* **2017**, *56*, 13401.
- [54] B. Waldecker, F. Kraft, C. Golz, M. Alcarazo, *Angew. Chem. Int. Ed.* **2018**, *57*, 12538.
- [55] K. F. G. Aversch, H. Pesch, C. Golz, M. Alcarazo, *Chem. Eur. J.* **2019**, *25*, 10472.
- [56] J. Peña, G. Talavera, B. Waldecker, M. Alcarazo *Chem. Eur. J.* **2017**, *23*, 75.
- [57] M. J. Böhm, C. Golz, I. Rüter, M. Alcarazo, *Chem. Eur. J.* **2018**, *24*, 15026.
- [58] P. Murch, B. L. Williamson, P. J. Stang, *Synthesis* **1994**, *1994*, 1255.
- [59] M. O. Frederick, J. A. Mulder, M. R. Tracey, R. P. Hsung, J. Huang, K. C. M. Kurtz, L. Shen, C. J. Douglas, *J. Am. Chem. Soc.* **2003**, *125*, 2368.
- [60] J. R. Dunetz, R. L. Danheiser, *Org. Lett.* **2003**, *5*, 4011.
- [61] T. Hamada, X. Ye, S. S. Stahl, *J. Am. Chem. Soc.* **2008**, *130*, 833.
- [62] Y. Tu, X. Zeng, H. Wang, J. Zhao, *Org. Lett.* **2018**, *20*, 280.
- [63] H. Singh, T. Sahoo, C. Sen, S. M. Galani, S. C. Ghosh, *Catal. Sci. Technol.* **2019**, *9*, 1691.
- [64] K. S. Feldman, M. M. Bruendl, K. Schildknegt, A. C. Bohnstedt, *J. Org. Chem.* **1996**, *61*, 5440.
- [65] B. Witulski, T. Stengel, *Angew. Chem. Int. Ed.* **1998**, *37*, 489.
- [66] N. Toriumi, N. Asano, K. Miyamoto, A. Muranaka, M. Uchiyama, *J. Am. Chem. Soc.* **2018**, *140*, 3858.
- [67] P. J. Stang, *Acc. Chem. Res.* **1991**, *91*, 304.
- [68] a) M. Ochiai, M. Kunishima, Y. Nagao, K. Fuji, E. Fujita, *J. Chem. Soc., Chem. Commun.* **1987**, 1708; b) P. J. Stang, C. M. Crittall, *J. Org. Chem.* **1992**, *57*, 4305.
- [69] Y. Gao, G. Wang, L. Chen, P. Xu, Y. Zhao, Y. Zhou, L.-B. Han, *J. Am. Chem. Soc.* **2009**, *131*, 7956.
- [70] E. Bernoud, C. Alayrac, O. Delacroix, A.-C. Gaumont, *Chem. Commun.* **2011**, *47*, 3239.
- [71] R. Frei, J. Waser, *J. Am. Chem. Soc.* **2013**, *135*, 9620.
- [72] M. D. Wodrich, P. Caramenti, J. Waser, *Org. Lett.* **2016**, *18*, 60.
- [73] R. Frei, M. D. Wodrich, D. P. Hari, P.-A. Borin, C. Chauvier, J. Waser, *J. Am. Chem. Soc.* **2014**, *136*, 16563.
- [74] J. Doroszuk, M. Musiejuk, S. Demkowicz, J. Rachon, D. Witt, *RSC Adv.* **2016**, *6*, 105449.
- [75] J. Peña, G. Talavera, B. Waldecker, M. Alcarazo, *Chem. Eur. J.* **2017**, *23*, 75.
- [76] J. Santandrea, C. Minozzi, C. Cruché, S. K. Collins, *Angew. Chem. Int. Ed.* **2017**, *56*, 12255.
- [77] J. Y. See, Y. Zhao, *Org. Lett.* **2018**, *20*, 7433.
- [78] K. Kanemoto, S. Yoshida, T. Hosoya, *Org. Lett.* **2019**, *21*, 3172.
- [79] A. S. Kende, P. Fludzinski, J. H. Hill, *J. Am. Chem. Soc.* **1984**, *106*, 3551.
- [80] a) M. Ochiai, M. Kunishima, Y. Nagao, K. Fuji, M. Shiro, E. Fujita, *J. Am. Chem. Soc.* **1986**, *108*, 8281; b) M. Ochiai, T. Ito, Y. Takaoka, Y. Masaki, M. Kunishima, S. Tani, Y. Nagao, *J. Chem. Soc., Chem. Commun.* **1990**, 118.
- [81] M. D. Bachi, N. Bar-Ner, C. M. Crittall, P. J. Stang, B. L. Williamson, *J. Org. Chem.* **1991**, *56*, 3912.
- [82] T. B. Poulsen, L. Bernardi, J. Aleman, J. Overgaard, K. A. Jørgensen, *J. Am. Chem. Soc.* **2007**, *129*, 441.
- [83] M. S. Raasch, *Chem. Commun. (London)* **1966**, 577.

- [84] M. S. Raasch, *J. Org. Chem.* **1970**, 35, 3470.
- [85] M. S. Raasch, *J. Org. Chem.* **1972**, 37, 1347.
- [86] E. U. Elam, F. H. Rash, J. T. Dougherty, V. W. Goodlett, K. C. Brannock, *J. Org. Chem.* **1968**, 33, 2738.
- [87] M. S. Newman, A. Arkell, T. Fukunaga, *J. Am. Chem. Soc.* **1960**, 82, 2498.
- [88] C. Spanka, E. Schaumann, *Synlett* **2014**, 25, 2415.
- [89] a) U. Timm, U. Merkle, H. Meier, *Chem. Ber.* **1980**, 113, 2519; b) E. Schaumann, *Tetrahedron* **1988**, 44, 1827.
- [90] C. Willgerodt, *Ber. Dtsch. Chem. Ges.* **1887**, 20, 2467.
- [91] K. Kindler, *Justus Liebigs Ann. Chem.* **1923**, 431, 187.
- [92] H. Xu, H. Deng, Z. Li, H. Xiang, X. Zhou, *Eur. J. Org. Chem.* **2013**, 2013, 7054.
- [93] T. B. Nguyen, M. Q. Tran, L. Ermolenko, A. Al-Mourabit, *Org. Lett.* **2014**, 16, 310.
- [94] For the principles of atom- and step-economy, see a) B. M. Trost, *Acc. Chem. Res.* **2002**, 35, 695; b) P. A. Wender, V. A. Verma, T. J. Paxton, T. H. Pillow, *Acc. Chem. Res.* **2008**, 41, 40.
- [95] a) M. Jesberger, T. P. Davis, L. Barner, *Synthesis* **2003**, 1929; b) T. Ozturk, E. Ertas, O. Mert, *Chem. Rev.* **2010**, 110, 3419.
- [96] E. U. Elam, H. E. Davis, *J. Org. Chem.* **1967**, 32, 1562.
- [97] D. Brillon, *Synth. Commun.* **1990**, 20, 3085.
- [98] P. Denifl, B. Bildstein, *J. Org. Chem.* **1993**, 453, 53.
- [99] J. Romański, G. Mlostoń, *Synthesis* **2002**, 1355.
- [100] A. Duréault, D. Taton, M. Destarac, F. Leising, Y. Gnanou, *Macromolecules* **2004**, 37, 5513.
- [101] N. M. Ibrahim, *Phosphorus, Sulfur, Silicon Relat. Elem.* **2006**, 181, 1773.
- [102] a) T. Strehlow, J. Voß, R. Spohnholz, G. Adiwidjaja, *Chem. Ber.* **1991**, 124, 1397; b) Y. Hitotsuyanagi, J. Suzuki, Y. Matsumoto, K. Takeya, H. Itokawa, *J. Chem. Soc., Perkin Trans. 1* **1994**, 1887; c) P. Grisenti, A. Magni, A. Manzocchi, P. Ferraboschi, *Steroids* **1997**, 62, 504; d) C. Fossey, H. Landelle, D. Ladureey, M. Robba, *Nucleosides Nucleotides* **1993**, 12, 973.
- [103] S. L. Baxter, J. S. Bradshaw, *J. Org. Chem.* **1981**, 46, 831.
- [104] a) K. A. Petrov, L. N. Andreev, *Russ. Chem. Rev.* **1969**, 38, 21; b) Brown, Ellis, V., *Synthesis* **1975**, 1975, 358; c) A. B. Charette, M. Grenon, *J. Org. Chem.* **2003**, 68, 5792; d) J. Houben, *Ber. Dtsch. Chem. Ges.* **1906**, 39, 3219; e) J. Houben, K. M. L. Schultze, *Ber. Dtsch. Chem. Ges.* **1910**, 43, 2481; f) E. J. Hedgley, H. G. Fletcher, *J. Org. Chem.* **1965**, 30, 1282; g) P. J. W. Schuijl, L. Brandsma, J. F. Arens, *Recl. Trav. Chim. Pays-Bas* **1966**, 85, 889; h) J. Meijer, P. Vermeer, L. Brandsma, *Recl. Trav. Chim. Pays-Bas* **1973**, 92, 601; i) H. Westmijze, H. Kleijn, J. Meijer, P. Vermeer, *Synthesis* **1979**, 1979, 432; j) R. Hoffmann, K. Hartke, *Chem. Ber.* **1980**, 113, 919; k) A. C. Worth, C. E. Needham, D. B. Franklin, A. J. Lampkins, *Synth. Commun.* **2012**, 42, 2694.
- [105] K. B. Wiberg, D. J. Rush, *J. Am. Chem. Soc.* **2001**, 123, 2038.
- [106] K. B. Wiberg, P. R. Rablen, D. J. Rush, T. A. Keith, *J. Am. Chem. Soc.* **1995**, 117, 4261.
- [107] T. J. Williams, A. D. Kershaw, V. Li, X. Wu, *J. Chem. Educ.* **2011**, 88, 665.

- [108] B. K. Min, H.-J. Lee, Y. S. Choi, J. Park, C.-J. Yoon, J.-A. Yu, *J. Mol. Struct.* **1998**, 471, 283.
- [109] S. J. Collier, *Science of Synthesis* **2007**.
- [110] K. B. Wiberg, *Acc. Chem. Res.* **1999**, 32, 922.
- [111] L. Pauling, *The Nature of the Chemical Bond*, Cornell University Press, Ithaca, U.S.A., **1960**.
- [112] K. B. Wiberg, Y. Wang, *Arkivoc* **2011**, 2011, 45.
- [113] T. S. Jagodziński, *Chem. Rev.* **2003**, 103, 197.
- [114] a) M. C. Bagley, J. W. Dale, E. A. Merritt, X. Xiong, *Chem. Rev.* **2005**, 105, 685; b) T. Sifferlen, M. Rueping, K. Gademann, B. Jaun, D. Seebach, *Helv. Chim. Acta* **1999**, 82, 2067; c) G. Moad, E. Rizzardo, S. H. Thang, *Aust. J. Chem.* **2012**, 65, 985.
- [115] H.-G. Cheng, H. Chen, Y. Liu, Q. Zhou, *Asian J. Org. Chem.* **2018**, 7, 490.
- [116] A. Lengar, C. O. Kappe, *Org. Lett.* **2004**, 6, 771.
- [117] E. J. Petersson, J. M. Goldberg, R. F. Wissner, *Phys. Chem. Chem. Phys.* **2014**, 16, 6827.
- [118] a) D. R. Lide (Ed.) *CRC handbook of chemistry and physics. A ready-reference book of chemical and physical data*, CRC Press, Boca Raton, Fla., **1990**; b) V. V. Grushin, H. Alper, *Chem. Rev.* **1994**, 94, 1047; c) J. D. Cox, G. Pilcher, *Thermochemistry of organic and organometallic compounds*, Acad. Press, London, **1970**.
- [119] L. Ackermann, *Chem. Rev.* **2011**, 111, 1315.
- [120] a) L. Ackermann (Ed.) *Modern arylation methods*, Wiley-VCH, Weinheim, **2009**; b) N. Chatani, L. Ackermann (Eds.) *Topics in organometallic chemistry, Vol. 24*, Springer, Berlin, Heidelberg, **2007**.
- [121] D. Lapointe, K. Fagnou, *Chem. Lett.* **2010**, 39, 1118.
- [122] Y. Boutadla, D. L. Davies, S. A. Macgregor, A. I. Poblador-Bahamonde, *Dalton Trans.* **2009**, 5887.
- [123] Y. Boutadla, D. L. Davies, S. A. Macgregor, A. I. Poblador-Bahamonde, *Dalton Trans.* **2009**, 5820.
- [124] J. Oxgaard, W. J. Tenn, R. J. Nielsen, R. A. Periana, W. A. Goddard, *Organometallics* **2007**, 26, 1565.
- [125] W. Ma, R. Mei, G. Tenti, L. Ackermann, *Chem. Eur. J.* **2014**, 20, 15248.
- [126] D. Zell, M. Bursch, V. Müller, S. Grimme, L. Ackermann, *Angew. Chem. Int. Ed.* **2017**, 56, 10378.
- [127] F. Zhang, D. R. Spring, *Chem. Soc. Rev.* **2014**, 43, 6906.
- [128] Z. Chen, B. Wang, J. Zhang, W. Yu, Z. Liu, Y. Zhang, *Org. Chem. Front.* **2015**, 2, 1107.
- [129] C. Laurence, J.-F. Gal, *Lewis basicity and affinity scales. Data and measurement*, Wiley, Chichester, **2010**.
- [130] O. Dimroth, *Ber. Dtsch. Chem. Ges.* **1898**, 31, 2154.
- [131] L. Y., *Zh. Russ. Phys-Khim. Obshch.* **1876**, 8, 281.
- [132] S. Murahashi, *J. Am. Chem. Soc.* **1955**, 77, 6403.
- [133] W. C. Baird, R. L. Hartgerink, J. H. Surridge, *J. Org. Chem.* **1985**, 50, 4601.

- [134] a) S. Murai, F. Kakiuchi, S. Sekine, Y. Tanaka, A. Kamatani, M. Sonoda, N. Chatani, *Nature* **1993**, 366, 529; b) D. Alberico, M. E. Scott, M. Lautens, *Chem. Rev.* **2007**, 107, 174; c) E. M. Beccalli, G. Broggini, M. Martinelli, S. Sottocornola, *Chem. Rev.* **2007**, 107, 5318; d) D. A. Colby, R. G. Bergman, J. A. Ellman, *Chem. Rev.* **2010**, 110, 624; e) G. P. McGlacken, L. M. Bateman, *Chem. Soc. Rev.* **2009**, 38, 2447.
- [135] X. Chen, K. M. Engle, D.-H. Wang, J.-Q. Yu, *Angew. Chem. Int. Ed.* **2009**, 48, 5094.
- [136] T. Satoh, M. Miura, *Chem. Eur. J.* **2010**, 16, 11212.
- [137] a) G. Song, F. Wang, X. Li, *Chem. Soc. Rev.* **2012**, 41, 3651; b) K. M. Engle, T.-S. Mei, M. Wasa, J.-Q. Yu, *Acc. Chem. Res.* **2012**, 45, 788; c) R. Shang, L. Ilies, E. Nakamura, *Chem. Rev.* **2017**, 117, 9086; d) M. Moselage, J. Li, L. Ackermann, *ACS Catal.* **2016**, 6, 498; e) R. Das, G. S. Kumar, M. Kapur, *Eur. J. Org. Chem.* **2017**, 2017, 5439; f) A. Peneau, C. Guillou, L. Chabaud, *Eur. J. Org. Chem.* **2018**, 2018, 5777; g) P. G. Chirila, C. J. Whiteoak, *Dalton Trans.* **2017**, 46, 9721; h) L. Ackermann, *Acc. Chem. Res.* **2014**, 47, 281; i) H. M. L. Davies, D. Morton, *J. Org. Chem.* **2016**, 81, 343; j) X.-F. Wu (Ed.) *Transition metal-catalyzed heterocycle synthesis via C-H activation*, Wiley-VCH, Weinheim, **2016**; k) J.-Q. Yu, L. Ackermann (Eds.), *Top. Curr. Chem.*, Vol. 292, Springer, Berlin, **2010**; l) F. W. Patureau, J. Wencel-Delord, F. Glorius, *Aldrichimica Acta* **2012**, 45, 31.
- [138] R.-Y. Zhu, M. E. Farmer, Y.-Q. Chen, J.-Q. Yu, *Angew. Chem. Int. Ed.* **2016**, 55, 10578.
- [139] Z. Huang, H. N. Lim, F. Mo, M. C. Young, G. Dong, *Chem. Soc. Rev.* **2015**, 44, 7764.
- [140] Y. Yang, K. Li, Y. Cheng, D. Wan, M. Li, J. You, *Chem. Commun.* **2016**, 52, 2872.
- [141] D. J. Abrams, P. A. Provencher, E. J. Sorensen, *Chem. Soc. Rev.* **2018**, 47, 8925.
- [142] K. Ueura, T. Satoh, M. Miura, *Org. Lett.* **2007**, 9, 1407.
- [143] K. Ueura, T. Satoh, M. Miura, *J. Org. Chem.* **2007**, 72, 5362.
- [144] N. Umeda, H. Tsurugi, T. Satoh, M. Miura, *Angew. Chem. Int. Ed.* **2008**, 47, 4019.
- [145] a) T. K. Hyster, T. Rovis, *J. Am. Chem. Soc.* **2010**, 132, 10565; b) H. Zhong, D. Yang, S. Wang, J. Huang, *Chem. Commun.* **2012**, 48, 3236.
- [146] S. Mochida, N. Umeda, K. Hirano, T. Satoh, M. Miura, *Chem. Lett.* **2010**, 39, 744.
- [147] M. Deponti, S. I. Kozhushkov, D. S. Yufit, L. Ackermann, *Org. Biomol. Chem.* **2013**, 11, 142.
- [148] Y. Ano, M. Tobisu, N. Chatani, *Synlett* **2012**, 23, 2763.
- [149] R. Mei, S.-K. Zhang, L. Ackermann, *Org. Lett.* **2017**, 19, 3171.
- [150] J. Yi, L. Yang, C. Xia, F. Li, *J. Org. Chem.* **2015**, 80, 6213.
- [151] V. G. Landge, G. Jaiswal, E. Balaraman, *Org. Lett.* **2016**, 18, 812.
- [152] Z. Ruan, N. Sauermann, E. Manoni, L. Ackermann, *Angew. Chem. Int. Ed.* **2017**, 56, 3172.
- [153] G. Cera, T. Haven, L. Ackermann, *Chem. Eur. J.* **2017**, 23, 3577.
- [154] E. Tan, O. Quinonero, M. Elena de Orbe, A. M. Echavarren, *ACS Catal.* **2018**, 8, 2166.
- [155] C. Feng, T.-P. Loh, *Angew. Chem. Int. Ed.* **2014**, 53, 2722.
- [156] F. Xie, Z. Qi, S. Yu, X. Li, *J. Am. Chem. Soc.* **2014**, 136, 4780.
- [157] C. Feng, D. Feng, Y. Luo, T.-P. Loh, *Org. Lett.* **2014**, 16, 5956.
- [158] J. Waser, *Top. Curr. Chem.* **2016**, 373, 187.
- [159] M. Alcarazo, *Acc. Chem. Res.* **2016**, 49, 1797.

- [160] A. Streitwieser, R. W. Taft, *Progress in Physical Organic Chemistry*, John Wiley & Sons, Inc, Hoboken, NJ, USA, **1968**.
- [161] a) C. W. Perkins, J. C. Martin, A. J. Arduengo, W. Lau, A. Alegria, J. K. Kochi, *J. Am. Chem. Soc.* **1980**, *102*, 7753; b) P. J. Stang, V. V. Zhdankin, *Chem. Rev.* **1996**, *96*, 1123.
- [162] L. Vogel, P. Wonner, S. M. Huber, *Angew. Chem. Int. Ed.* **2019**, *58*, 1880, and references cited therein.
- [163] a) S. Shaik, D. Danovich, W. Wu, P. C. Hiberty, *Nat. Chem.* **2009**, *1*, 443; b) B. Braïda, P. C. Hiberty, *Nat. Chem.* **2013**, *5*, 417.
- [164] E. J. Adams, T. Skrydstrup, K. B. Lindsay in *Encyclopedia of Reagents for Organic Synthesis*, John Wiley & Sons, Ltd, Chichester, **2001**.
- [165] H. Masumoto, H. Tsutumi, T. Kanda, M. Komada, T. Murai, S. Kato, *Sulfur Lett.* **1989**, *10*, 103.
- [166] G. V. Boyd, *Tetrahedron Lett.* **1972**, *13*, 2711.
- [167] G. V. Boyd, *J. Chem. Soc., Perkin Trans. 1* **1973**, 1731.
- [168] K. Muralirajan, K. Parthasarathy, C.-H. Cheng, *Angew. Chem. Int. Ed.* **2011**, *50*, 4169.
- [169] F. W. Patureau, T. Besset, N. Kuhl, F. Glorius, *J. Am. Chem. Soc.* **2011**, *133*, 2154.
- [170] S. H. Park, J. Y. Kim, S. Chang, *Org. Lett.* **2011**, *13*, 2372.
- [171] a) G. Liu, Y. Zhou, D. Ye, D. Zhang, X. Ding, H. Jiang, H. Liu, *Adv. Synth. Catal.* **2009**, *351*, 2605; b) M. Bian, W. Yao, H. Ding, C. Ma, *J. Org. Chem.* **2010**, *75*, 269; c) H. Sashida, *Synthesis* **1999**, 1145; d) J. D. Tovar, T. M. Swager, *J. Org. Chem.* **1999**, *64*, 6499; e) T. Wakamatsu, Y. Ogawa, M. Maruno, *Heterocycles* **1995**, *41*, 2587; f) P. Zhao, D. Chen, G. Song, K. Han, X. Li, *J. Org. Chem.* **2012**, *77*, 1579; g) H. Sun, L. Xiao, W. Li, Q. Xie, L. Shao, *Synthesis* **2017**, *49*, 4845; h) X. Zhang, B. Liu, X. Shu, Y. Gao, H. Lv, J. Zhu, *J. Org. Chem.* **2012**, *77*, 501.
- [172] K. Muralirajan, C.-H. Cheng, *Chem. Eur. J.* **2013**, *19*, 6198.
- [173] K. Inomata, H. Kinoshita, H. Fukuda, K. Tanabe, H. Kotake, *BCSJ* **1978**, *51*, 1866.
- [174] J. Chi, C. Hang, Y. Zhu, H. Katayama, *Synth. Commun.* **2010**, *40*, 1123.

## EXPERIMENTAL

**General:** If not otherwise specified, all reactions were carried out in oven-dried glassware under N<sub>2</sub>. All solvents were purified by distillation over the appropriate drying agents and were transferred under N<sub>2</sub>. Alternatively, dry solvents were obtained using an MBraun MB-SPS-800 solvent purification system (tetrahydrofuran, diethyl ether, toluene, pentane, dichloromethane, acetonitrile). IR: Nicolet FT-7199 spectrometer, JASCO FT-4100 spectrometer, wavenumbers in cm<sup>-1</sup>. MS (EI): Finnigan MAT 8200 (70 eV), ESIMS: Finnigan MAT 95, accurate mass determinations: Bruker APEX III FT-MS (7 T magnet). NMR: Spectra were recorded on a Bruker AV 600, AV 500, AV 400 or DPX 300; <sup>1</sup>H and <sup>13</sup>C chemical shifts (δ) are given in ppm relative to TMS, coupling constants (*J*) in Hz. Residual solvent signals were used as references and the chemical shifts converted to the TMS scale. X-ray-diffraction: Single crystal structure determination was performed by Dr. Christopher Golz at the University of Göttingen or by the department of chemical crystallography at the Max-Planck-Institut für Kohlenforschung. Experimental setup in Göttingen: Data collection was done on a *Bruker D8 Venture* four-circle-diffractometer from *Bruker AXS GmbH*; detector: *Photon II* from *Bruker AXS GmbH*; X-ray sources: microfocus *I $\mu$ S* Cu/Mo from *Incoatec GmbH* with mirror optics *HELIOS* and single-hole collimator from *Bruker AXS GmbH*. Used programs: *APEX3 Suite* (v2017.3-0) and therein integrated programs *SAINT* (Integration) und *SADABS* (Absorption correction) from *Bruker AXS GmbH*; structure solution was done with *SHELXT*, refinement with *SHELXS* (Both: G.M. Sheldrick, *Acta Cryst.* **2008**, *A64*, 112-122.); *OLEX<sup>2</sup>* was used for data finalization (O.V. Dolomanov, L.J. Bourhis, R.J. Gildea, J.A.K. Howard, H. Puschmann, *J. Appl. Cryst.* **2009**, *42*, 339-341.). Special Utilities: *SMZ1270* stereomicroscope from *Nikon Metrology GmbH* was used for sample preparation; crystals were mounted on *MicroMounts* or *MicroLoops* from *MiTeGen*; for sensitive samples the *X-TEMP 2* System was used for picking of crystals (T. Kottke, D. Stalke, *J. Appl. Cryst.* **1993**, *26*, 615-619.); crystals were cooled to given temperature with *Cryostream 800* from *Oxford Cryosystems*. Experimental set up at the Max-Planck-Institut für Kohlenforschung: Data collection was done on a Bruker AXS Proteum X8, Bruker AXS KappaCCD and/or Bruker AXS Apex II diffractometers. The crystal structures were solved by direct methods using *SHELXS97* and refined with *SHELXL-2014*. Column chromatography was performed on Merck 60 silica gel (40-63 μm), and for thin-layer chromatography (TLC) analysis, Merck silica gel 60 F254 TLC plates or polygram SIL G/UV254 from Macherey Nagel were used and visualized by UV irradiation and/or phosphomolybdic acid or KMnO<sub>4</sub> dip. All commercially available compounds (ABCR, Acros Organics, Alfa Aesar, Chempur GmbH, J and K Scientific, Sigma Aldrich, Thermo Fisher Scientific, Tokyo Chemical Industry) were used as received. Triethyloxonium tetrafluoroborate<sup>[16]</sup>, *N*-methylbenzamides<sup>17</sup> [RhCp\*Cl<sub>2</sub>]<sub>2</sub><sup>18</sup>,

<sup>16</sup> H. Meerwein, *Org. Synth.* **1966**, *46*, 113 ff.

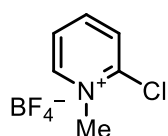
<sup>17</sup> L. Ackermann, A. V. Lygin, N. Hofmann, *Angew. Chem. Int. Ed.* **2011**, *50*, 6379–6382.

<sup>18</sup> J.W. Kang, K. Moseley, P. M. Maitlis, *J. Am. Chem. Soc.* **1969**, *91*, 5970–5977.

RhCp\*(MeCN)<sub>3</sub>[SbF<sub>6</sub>]<sub>2</sub><sup>19</sup>, were prepared according to literature procedures. X-ray structures of **230–233** were obtained by picking suitable crystals from the reaction crude. If not mentioned otherwise, no further characterization for these compounds was conducted.

## TOPIC:” SYNTHESIS AND EVALUATION OF NOVEL PYRIDINIUM-BASED ELECTROPHILIC TRANSFER REAGENTS”

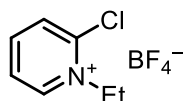
### 2-Chloro-1-methylpyridin-1-ium tetrafluoroborate (**156a**):



Following the literature procedure,<sup>[20]</sup> the salt **156a** was prepared by alkylation of 2-chloropyridine (2.2 g, 19.38 mmol, 1 equiv.) with trimethyloxonium tetrafluoroborate (3.0 g, 20.3 mmol, 1.05 equiv.) in dry CH<sub>2</sub>Cl<sub>2</sub> (15 mL) at 0 °C. The solution was stirred overnight, the CH<sub>2</sub>Cl<sub>2</sub> was filtered off with a filter stick and the residue was washed two more times with CH<sub>2</sub>Cl<sub>2</sub>. Compound **156a** was obtained as a white solid after drying *in vacuo* (4.0 g, 18.57 mmol, 96%).<sup>[21]</sup>

<sup>1</sup>H NMR: (300 MHz, CD<sub>3</sub>CN) δ = 8.74 (d, *J* = 6.0 Hz, 1H), 8.46 (td, *J* = 8.1, 1.7 Hz, 1H), 8.19 – 8.06 (m, 1H), 7.94 (t, *J* = 6.8 Hz, 1H), 4.29 (s, 3H) ppm. <sup>19</sup>F NMR: (282 MHz, CD<sub>3</sub>CN) δ = –151.77 ppm.

### 2-Chloro-1-ethylpyridin-1-ium tetrafluoroborate (**156b**):



Salt **156b** was prepared by alkylation of 2-chloropyridine (1 equiv., 1.135 g, 10 mmol) with triethyloxonium tetrafluoroborate (1 equiv., 1.9 g, 10 mmol) in dry CH<sub>2</sub>Cl<sub>2</sub> (40 mL) at 0 °C. The solution was stirred overnight, the CH<sub>2</sub>Cl<sub>2</sub> was removed *in vacuo* and the residue was washed with Et<sub>2</sub>O (3 × 20 mL) to afford compound **156b** as a white solid (2.3 g, 10 mmol, 99%).<sup>[22]</sup>

<sup>1</sup>H NMR: (300 MHz, CD<sub>3</sub>CN) δ = 8.77 (dd, *J* = 6.3, 1.7 Hz, 1H), 8.46 (td, *J* = 8.0, 1.8 Hz, 1H), 8.11 (dd, *J* = 8.3, 1.4 Hz, 1H), 8.04 – 7.90 (m, 1H), 4.72 (q, *J* = 7.3 Hz, 2H), 1.58 (t, *J* = 7.3 Hz, 3H) ppm. <sup>13</sup>C NMR: (101 MHz, CD<sub>3</sub>CN) δ = 148.2, 147.7, 131.4, 127.8, 57.3, 14.8 ppm.

<sup>19</sup> Y. Du, T. K. Hyster, T. Rovis, *Chem. Commun* **2011**, 47, 12074–12076

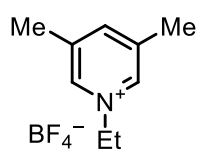
<sup>20</sup> H. Tinnermann, C. Wille, M. Alcarazo, *Angew. Chem. Int. Ed.* **2014**, 53, 8732–8736.

<sup>21</sup> Analytical data are in agreement with the previously published ones: H. Tinnermann, C. Wille, M. Alcarazo., *Angew. Chem. Int. Ed.* **2014**, 53, 8732–8736, **Compound 6**.

<sup>22</sup> Analytical data are in agreement with the previously reported ones: H. Tinnermann, PhD Thesis, University of Göttingen (Germany), **2017**, **Compound 129c**.



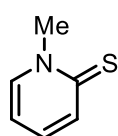
### 1-Ethyl-3,5-dimethylpyridin-1-ium tetrafluoroborate (**156c**):



Salt **156c** was prepared by alkylation of 3,5-lutidine (1 equiv., 5.7 g, 53.2 mmol) with triethyloxonium tetrafluoroborate (0.99 equiv., 10.0 g, 52.6 mmol) in dry  $\text{CH}_2\text{Cl}_2$  (50 mL) at 0 °C. The solution was stirred overnight, then the solvent was removed in vacuo and the residue was washed with  $\text{Et}_2\text{O}$  ( $3 \times 50$  mL). Salt **156c** was obtained as white solid after drying *in vacuo* (10.6 g, 47.53 mmol, 90%).

**$^1\text{H}$  NMR:** (400 MHz,  $\text{CD}_3\text{CN}$ )  $\delta$  = 8.39 (s, 2H), 8.13 (s, 1H), 4.46 (q,  $J$  = 7.4 Hz, 3H), 2.47 (s, 3H), 2.46 (s, 3H), 1.56 (t,  $J$  = 7.4 Hz, 3H) ppm.  **$^{13}\text{C}$  NMR:** (101 MHz,  $\text{CD}_3\text{CN}$ )  $\delta$  = 147.3, 141.9 (t,  $J$  = 8.8 Hz), 139.9, 57.8 (t,  $J$  = 3.8 Hz), 18.2, 16.5 ppm.  **$^{19}\text{F}$  NMR:** (377 MHz,  $\text{CD}_3\text{CN}$ )  $\delta$  = -151.70 ppm. **IR:** (ATR,  $\text{cm}^{-1}$ ) 3082, 2360, 1497, 1458, 1391, 1304, 1189, 1093, 1047, 1033, 887, 811, 691, 521. **HRMS:** *calcd.* for  $\text{C}_9\text{H}_{14}\text{N}^+ [\text{M} - \text{BF}_4^-]$ : 136.112074; found (ESI): 136.112230.

### 1-Methylpyridine-2(1H)-thione (**153a**):

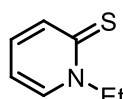


Compound **156a** (4.0 g, 18.57 mmol) was dissolved in methanol (70 mL). A solution of sodium hydrosulfide hydrate (2 equiv, 2.8 g, 37.8 mmol) in water (140 mL) was prepared and subsequently added to the former dropwise at 45 °C. After stirring for 30 min, the reaction mixture was poured into 100 mL of water, the solution extracted with  $\text{CH}_2\text{Cl}_2$  ( $3 \times 70$  mL), and the organic phase was dried over  $\text{Na}_2\text{SO}_4$ . Removal of all solvents *in vacuo* afforded crude **153a**, which was purified by column chromatography (EtOAc) and obtained as a pale yellow crystalline solid (2.1 g, 16.8 mmol, 90%).

Alternatively compound **AVK-AA-429** was prepared following the same procedure but starting from commercially available 2-chloro-1-methylpyridin-1-ium iodide (30.0 g, 117.4 mmol), in methanol (60 mL), sodium hydrosulfide hydrate (1.7 equiv, 14.3 g, 193 mmol) in water (30 mL) after column chromatography (EtOAc) as a pale yellow crystalline solid (13.4 g, 107 mmol, 91%).

**$^1\text{H}$  NMR:** (300 MHz,  $\text{CD}_3\text{CN}$ )  $\delta$  = 7.82 (dd,  $J$  = 6.6, 1.3 Hz, 1H), 7.51 (d,  $J$  = 8.6 Hz, 1H), 7.24 (ddd,  $J$  = 8.6, 6.9, 1.6 Hz, 1H), 6.68 (td,  $J$  = 6.8, 1.4 Hz, 1H), 3.87 (s, 3H) ppm.  **$^1\text{H}$  NMR:** (400 MHz,  $\text{C}_2\text{D}_2\text{Cl}_4$ )  $\delta$  = 7.58 (dd,  $J$  = 6.6, 1.3 Hz, 1H), 7.55 (ddd,  $J$  = 8.7, 1.5, 0.7 Hz, 1H), 7.13 (ddd,  $J$  = 8.6, 7.0, 1.6 Hz, 1H), 6.57 (td,  $J$  = 6.8, 1.5 Hz, 1H), 3.85 (s, 3H) ppm.  **$^{13}\text{C}$  NMR:** (101 MHz,  $\text{C}_2\text{D}_2\text{Cl}_4$ )  $\delta$  = 180.1, 141.3, 136.0, 134.7, 113.9, 46.4 ppm. **IR:** (ATR,  $\text{cm}^{-1}$ ) 3006, 1617, 1536, 1474, 1408, 1310, 1187, 1142, 1108, 1054, 1022, 802, 752, 707. **HRMS:** *calcd.* for  $\text{C}_6\text{H}_8\text{NS}^+ [\text{M} + \text{H}]^+$ : 126.0372; found (ESI): 126.0372.

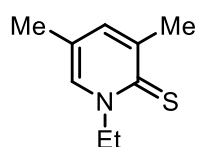
### 1-Ethylpyridine-2(1H)-thione (153b):



Salt **156b** (7.6 g, 33.1 mmol) was dissolved in methanol (120 mL). A solution of sodium hydrosulfide hydrate (2 equiv., 3.7 g, 66.3 mmol) in water (240 mL) was prepared and subsequently added dropwise to the former one at 45 °C. After stirring for 30 min, the reaction mixture was poured into 100 mL of water, the solution extracted with CH<sub>2</sub>Cl<sub>2</sub> (3 × 70 mL) and the combined organic phases dried over Na<sub>2</sub>SO<sub>4</sub>. Removal of the solvents in vacuo afforded **153b** as a yellow crystalline material (3.8 g, 27.3 mmol, 82%).

**<sup>1</sup>H NMR:** (300 MHz, CDCl<sub>3</sub>) δ = 7.67 (ddd, *J* = 8.7, 1.5, 0.7 Hz, 1H), 7.61 (ddd, *J* = 6.6, 1.7, 0.7 Hz, 1H), 7.14 (ddd, *J* = 8.6, 6.8, 1.7 Hz, 1H), 6.64 (td, *J* = 6.7, 1.5 Hz, 1H), 4.58 (q, *J* = 7.2 Hz, 2H), 1.46 (t, *J* = 7.2 Hz, 3H) ppm. **<sup>1</sup>H NMR:** (300 MHz, CD<sub>3</sub>CN) δ = 7.80 (ddd, *J* = 6.7, 1.7, 0.8 Hz, 1H), 7.50 (ddd, *J* = 8.7, 1.5, 0.7 Hz, 1H), 7.21 (ddd, *J* = 8.6, 6.9, 1.7 Hz, 1H), 6.71 (td, *J* = 6.8, 1.5 Hz, 1H), 4.53 (q, *J* = 7.1 Hz, 2H), 1.36 (t, *J* = 7.1 Hz, 3H) ppm. **<sup>1</sup>H NMR:** (400 MHz, DMSO-d<sub>6</sub>) δ = 8.14 (ddd, *J* = 6.6, 1.7, 0.8 Hz, 1H), 7.45 (ddd, *J* = 8.6, 1.6, 0.7 Hz, 1H), 7.31 (ddd, *J* = 8.6, 6.9, 1.7 Hz, 1H), 6.81 (td, *J* = 6.7, 1.6 Hz, 1H), 4.51 (q, *J* = 7.1 Hz, 2H), 1.30 (t, *J* = 7.1 Hz, 3H) ppm. **<sup>13</sup>C NMR:** (101 MHz, CDCl<sub>3</sub>) δ = 179.6, 139.6, 136.7, 133.8, 113.9, 52.2, 14.0 ppm. **<sup>13</sup>C NMR:** (101 MHz, DMSO-d<sub>6</sub>) δ = 178.0, 141.5, 134.8, 134.6, 113.8, 50.8, 13.7 ppm. **IR:** (ATR, cm<sup>-1</sup>) 3060, 3019, 2967, 2927, 1615, 1531, 1471, 1415, 1374, 1260, 1185, 1137, 1106, 1080, 961, 770, 699, 487, 458. **HRMS:** calcd. for C<sub>7</sub>H<sub>9</sub>NNaS<sup>+</sup> [M+Na]<sup>+</sup>: 162.034791; found: 162.034770.

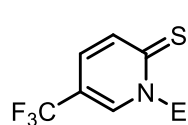
### 1-Ethyl-3,5-dimethylpyridine-2(1H)-thione (153c):



To a stirred suspension of **156c** (1 equiv, 8.0 g, 35.9 mmol) and S<sub>8</sub> (1/4 equiv, 2.3 g, 72 mmol) in THF (10 mL/mmol), a solution of LiHMDS (1 equiv, 5 mL/mmol of a solution in THF) was added at -100 °C. The resulting mixture was stirred overnight, while allowing it to slowly warm up to room temperature. After removal of all solvents, the crude mixture was purified by column chromatography (pentane/EtOAc, 1:1) and dried *in vacuo* to afford thione **153c** as yellow crystals (4.1 g, 24.5 mmol, 68%).

**<sup>1</sup>H NMR:** (400 MHz, CDCl<sub>3</sub>) δ = 7.45 (s, 1H), 7.19 (s, 1H), 4.66 (q, *J* = 7.2 Hz, 2H), 2.45 (s, 3H), 2.15 (s, 3H), 1.47 (t, *J* = 7.2 Hz, 3H) ppm. **<sup>13</sup>C NMR:** (101 MHz, CDCl<sub>3</sub>) δ = 176.6, 142.3, 136.3, 136.0, 122.5, 53.1, 23.9, 17.6, 14.1 ppm. **IR:** (ATR, cm<sup>-1</sup>) 1634, 1544, 1455, 1402, 1375, 1279, 1240, 1180, 1120, 1083, 1019, 980, 861, 717, 658, 539. **HRMS:** calcd. for C<sub>9</sub>H<sub>14</sub>NNaS<sup>+</sup> [M+Na]<sup>+</sup>: 190.066090; found (ESI): 190.066110.

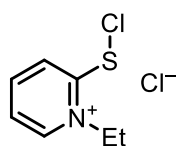
### 1-Ethyl-5-(trifluoromethyl)pyridine-2(1*H*)-thione (**153d**):



2-Chloro-1-ethyl-5-(trifluoromethyl)pyridin-1-ium tetrafluoroborate (537 mg, 1.8 mmol) was dissolved in methanol (10 mL). A solution of sodium hydrosulfide hydrate (202 mg, 3.6 mmol) in water (20 mL) was prepared and added to the former dropwise at 45 °C. After stirring for 30 min, the reaction mixture was poured into 50 mL of water, the solution extracted with CH<sub>2</sub>Cl<sub>2</sub> (3 × 70 mL), and the organic phase was dried over Na<sub>2</sub>SO<sub>4</sub>. Removal of all solvents *in vacuo* afforded compound **153d** as yellow crystals (292 mg, 1.4 mmol, 78% ).

**<sup>1</sup>H NMR:** (300 MHz, CDCl<sub>3</sub>) δ = 7.87 (td, *J* = 2.0, 1.0 Hz, 1H), 7.68 (dt, *J* = 9.2, 0.9 Hz, 1H), 7.20 (dd, *J* = 9.1, 2.2 Hz, 1H), 4.57 (q, *J* = 7.2 Hz, 2H), 1.49 (t, *J* = 7.2 Hz, 3H) ppm.

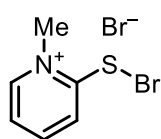
### 2-(Chlorothio)-1-ethylpyridin-1-ium chloride (**154bb**):



Sulfuryl chloride (1.35 equiv, 158 μL, 264 mg, 1.95 mmol) was added to a solution of thiolactam **153a** (1 equiv, 200 mg, 1.44 mmol) in toluene (10 mL) at 0 °C. The reaction mixture was stirred at 0 °C for 15 min and then allowed to warm up to room temperature over 1 h. The supernatant was filtered off, the residue was washed with cold toluene (10 mL) and dried *in vacuo* to afford **154bb** as a bright yellow powder in 78% yield.

**<sup>1</sup>H NMR:** (300 MHz, CDCl<sub>3</sub>) δ = 10.71 (dd, *J* = 6.2, 1.6 Hz, 1H), 8.54 (td, *J* = 7.9, 1.5 Hz, 1H), 8.22 (t, *J* = 6.7 Hz, 1H), 8.03 (dd, *J* = 8.2, 1.3 Hz, 1H), 5.30 (q, *J* = 7.2 Hz, 2H), 1.73 (t, *J* = 7.2 Hz, 3H) ppm.

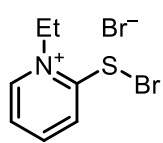
### 2-(Bromothio)-1-methylpyridin-1-ium bromide (**154a**):



To an oven-dried schlenk flask charged with **153a** (893 mg, 7.1 mmol); dry CH<sub>2</sub>Cl<sub>2</sub> (20 mL) was added, and the solution was cooled to 0 °C. Bromine (1 equiv, 365 μL, 1.133g, 7.1 mmol) was added slowly at 0 °C under stirring, and the reaction mixture was then slowly warmed up to room temperature over 2 h. After removal of all volatiles *in vacuo*, **154a** was obtained as a bright orange solid (2.0 g, 7.0 mmol, 99%).

**<sup>1</sup>H NMR:** (500 MHz, C<sub>2</sub>D<sub>2</sub>Cl<sub>4</sub>) δ = 8.39 (d, *J* = 7.9 Hz, 1H), 8.28 (d, *J* = 6.2 Hz, 1H), 8.17 (t, *J* = 7.8 Hz, 1H), 7.69 (ddd, *J* = 7.7, 6.2, 1.6 Hz, 1H), 4.44 (s, 3H) ppm. **<sup>13</sup>C NMR:** (126 MHz, C<sub>2</sub>D<sub>2</sub>Cl<sub>4</sub>) δ = 163.5, 145.5, 144.6, 137.5, 125.8, 48.9 ppm. **HRMS:** *calcd.* for C<sub>6</sub>H<sub>7</sub>BrNS<sup>+</sup> [M-Br]<sup>+</sup>: 203.9477; found (ESI): 203.9475.

## 2-(Bromothio)-1-ethylpyridin-1-ium bromide (**154ba**):



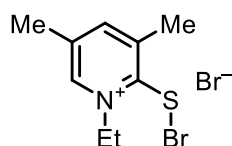
To an oven-dried schlenk flask charged with **153b** (1.5 g, 10.8 mmol); dry  $\text{CH}_2\text{Cl}_2$  (50 mL) was added, and the solution was cooled to 0 °C. Bromine (1 equiv., 554  $\mu\text{L}$ , 1.719 g, 10.8 mmol) was added slowly at 0 °C under stirring, and the reaction mixture was then slowly warmed up to room temperature over 2 h. After removal of all volatiles *in vacuo*, **154ba** was obtained as a bright orange solid (3.2 g, 10.7 mmol, 99%).

**$^1\text{H}$  NMR** (400 MHz,  $\text{CD}_2\text{Cl}_2$ )  $\delta$  = 8.46 (d,  $J$  = 8.0 Hz, 1H), 8.39 (d,  $J$  = 5.7 Hz, 1H), 8.27 – 8.18 (m, 1H), 7.85 – 7.77 (m, 1H), 5.04 (q,  $J$  = 7.4 Hz, 2H), 1.84 (t,  $J$  = 7.4 Hz, 3H) ppm  **$^{13}\text{C}$  NMR**: (101 MHz,  $\text{CD}_2\text{Cl}_2$ )  $\delta$  = 164.2 (only visible by HMBC), 145.3, 143.7, 138.4, 126.4, 57.1, 15.2 ppm.

HRMS measurement of methanol solutions of **154a** revealed the methanol-adduct  $\text{C}_7\text{H}_9\text{NS}\cdot\text{CH}_3\text{O}$  to be the major compound present, in addition the decomposition product  $\text{C}_7\text{H}_9\text{NBr}^+$  was detected.

**HRMS**: *calcd.* for  $\text{C}_8\text{H}_{12}\text{NSO}$  [ $\text{M}-\text{Br}_2+\text{MeOH}$ ]: 170.0630; found (ESI): 170.0634. **HRMS**: *calcd.* for  $\text{C}_7\text{H}_9\text{NBr}^+$  [ $\text{M}-\text{SBr}$ ] $^+$ : 185.9913, found (ESI): 186.0577

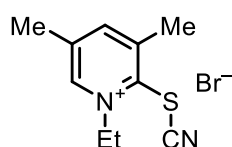
## 2-(Bromothio)-1-ethyl-3,5-dimethylpyridin-1-ium bromide (**154c**):



To an oven-dried schlenk flask charged with **153c** (2.82 g, 16.9 mmol); dry  $\text{CH}_2\text{Cl}_2$  (20 mL) was added, and the solution was cooled to 0 °C. Bromine (1 equiv, 870  $\mu\text{L}$ , 2.700 g, 16.9 mmol) was added slowly at 0 °C, and the reaction mixture was then slowly warmed up to room temperature over 2 h. After removal of all volatiles under vacuum, the residue was washed with dry  $\text{Et}_2\text{O}$  ( $3 \times 20$  mL). Compound **154c** was obtained as a bright orange solid (5.1 g, 15.6 mmol, 92%).

**$^1\text{H}$  NMR**: (300 MHz,  $\text{CD}_3\text{CN}$ )  $\delta$  = 8.46 (s, 1H), 8.15 – 8.07 (m, 1H), 4.98 (q,  $J$  = 6.6 Hz, 2H), 2.66 (s, 3H), 2.41 (s, 3H), 1.77 (t,  $J$  = 7.3 Hz, 3H) ppm.  **$^1\text{H}$  NMR**: (400 MHz,  $\text{CD}_2\text{Cl}_2$ )  $\delta$  = 8.14 (s, 1H), 7.97 (s, 1H), 5.06 (q,  $J$  = 7.4 Hz, 2H), 2.78 (s, 3H), 2.44 (s, 3H), 1.86 (t,  $J$  = 7.4 Hz, 3H) ppm.  **$^{13}\text{C}$  NMR**: (101 MHz,  $\text{CD}_2\text{Cl}_2$ )  $\delta$  = 159.9, 147.4, 145.0, 141.5, 137.6, 57.6, 22.4, 18.8, 15.5 ppm. **HRMS**: *calcd.* for  $\text{C}_9\text{H}_{13}\text{BrNS}^+$  [ $\text{M}-\text{Br}$ ] $^+$ : 245.9947; found: 245.9944.

## 1-Ethyl-3,5-dimethyl-2-thiocyanatopyridin-1-ium bromide (**155a**):

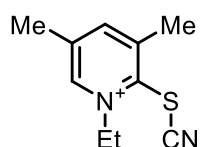


Under stirring, to a solution of compound **154c** (1 equiv, 2.5 g, 7.6 mmol) in dry  $\text{CH}_2\text{Cl}_2$  (40 mL)  $\text{TMSCN}$  (1.18 equiv, 1.13 mL, 893 mg, 9.0 mmol) was slowly added at 0 °C. After addition, the ice bath was removed, and the mixture was stirred for another 10 minutes, before removing all

volatiles *in vacuo*. The residue was washed with dry Et<sub>2</sub>O (3 × 20 mL). Compound **155a** was isolated as a pale yellow-orange solid (2.0 g, 7.3 mmol, 96%).

**<sup>1</sup>H NMR:** (400 MHz, CD<sub>3</sub>CN) δ = 8.85 (s, 1H), 8.31 (s, 1H), 4.96 (q, *J* = 7.3 Hz, 2H), 2.75 (s, 3H), 2.51 (s, 3H), 1.68 (t, *J* = 7.3 Hz, 3H) ppm.

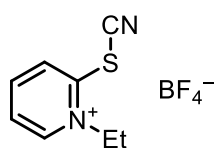
### 1-Ethyl-3,5-dimethyl-2-thiocyanatopyridin-1-ium hexafluoroantimonate (**155b**):



Compound **155a** (1 equiv, 700 mg, 2.56 mmol) was dissolved in CH<sub>2</sub>Cl<sub>2</sub> (70 mL), and an aqueous solution of NaSbF<sub>6</sub> (2.7 equiv, 1.8 g, 6.96 mmol in 70 mL H<sub>2</sub>O) was added. The mixture was stirred for 5 min at room temperature, transferred to a separation funnel, and the aqueous phase was extracted with CH<sub>2</sub>Cl<sub>2</sub> (3 × 20 mL). The combined organic phases were dried over Na<sub>2</sub>SO<sub>4</sub>, filtered, and all volatiles were removed *in vacuo*. The product **155b** (927.4 mg, 2.16 mmol, 84%) was isolated as colourless crystals. It is highly recommended to store this salt under inert atmosphere.

**<sup>1</sup>H NMR:** (400 MHz, CD<sub>3</sub>CN) δ = 8.71 (d, *J* = 1.5 Hz, 1H), 8.34 (s, 1H), 4.86 (q, *J* = 7.3 Hz, 2H), 2.76 (s, 3H), 2.53 (s, 3H), 1.63 (t, *J* = 7.3 Hz, 3H) ppm. **<sup>13</sup>C NMR:** (101 MHz, CD<sub>3</sub>CN) δ = 149.7, 148.2, 147.1, 142.9, 106.9, 59.4, 21.6, 18.4, 16.2 ppm.<sup>23</sup> **<sup>19</sup>F NMR:** (282 MHz, CD<sub>3</sub>CN) δ = −123.98 (sext, *J*<sub>F-121Sb</sub> = 1938.3 Hz), −123.98 (oct, *J*<sub>F-123Sb</sub> = 1052.1 Hz) ppm. **IR:** (ATR, cm<sup>−1</sup>) 2359, 2342, 1602, 1508, 1457, 1253, 1174, 1109, 1031, 657, 630, 540. **HRMS:** *calcd.* for C<sub>10</sub>H<sub>13</sub>N<sub>2</sub>S<sup>+</sup> [M−SbF<sub>6</sub><sup>−</sup>]: 193.079395; found (ESI): 193.079640.

### 1-Ethyl-2-thiocyanatopyridin-1-ium tetrafluoroborate (**155c**):



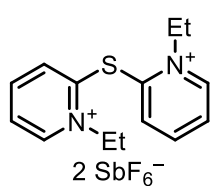
Compound **154bb** was dissolved in cold DCM (10 mL) and stirred in an ice bath. TMSCN (1.0 equiv, ) was added slowly to the solution and after addition, the mixture was stirred for 20 more minutes. Dry NaBF<sub>4</sub> was added, and the reaction mixture was stirred overnight. The supernatant was filtered off, and the solvent was removed under vacuum. Et<sub>2</sub>O (10 mL) was added, and the reaction mixture was ultrasonicated for 5 min. The ether was then filtered off, and the residue was dried *in vacuo*.

**<sup>1</sup>H NMR:** (300 MHz, CD<sub>3</sub>CN) δ = 8.96 (dd, *J* = 6.2, 1.6 Hz, 1H), 8.45 (td, *J* = 8.0, 1.6 Hz, 1H), 8.10 (ddd, *J* = 7.7, 6.2, 1.4 Hz, 1H), 7.92 (dd, *J* = 8.3, 1.4 Hz, 1H), 4.80 (q, *J* = 7.3 Hz, 2H), 1.65 (t, *J* = 7.3 Hz, 3H) ppm.

**<sup>19</sup>F NMR:** (282 MHz, CD<sub>3</sub>CN) δ = −152.98, −153.03 ppm.

<sup>23</sup>The quarternary carbon in α-position to sulfur was not visible in a routine <sup>13</sup>C measurement, similar behaviour is observed for derivatives **154a–c**.

### 2,2'-Thiobis(1-ethylpyridin-1-ium) bishexafluoroantimonate (**157**):



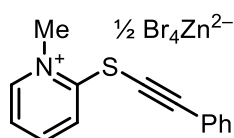
Compound **154bb** (255.4 mg, 1.22 mmol) was dissolved in cold DCM (20 mL) and stirred in an ice bath. TMSCN (1.0 equiv, 151  $\mu$ L, 119 mg, 1.22 mmol) was added slowly to the solution. The mixture was stirred for 10 minutes before NaSbF<sub>6</sub> (1 equiv, 314.4 mg 1.22 mmol) was added. The reaction mixture was stirred overnight, and the supernatant was filtered off. and the solvent was removed *in vacuo*. Et<sub>2</sub>O (10 mL) was added, and the reaction mixture was ultrasonicated for 5 min. The ether was then filtered off. After filtration, the residue was taken off with CH<sub>2</sub>Cl<sub>2</sub>, forming colorless crystals of **157**.

**<sup>1</sup>H NMR:** (400 MHz, DMSO-d<sub>6</sub>)  $\delta$  = 9.34 (dd, *J* = 6.2, 1.5 Hz, 1H), 8.55 (td, *J* = 8.0, 1.6 Hz, 1H), 8.23 (ddd, *J* = 7.7, 6.1, 1.4 Hz, 1H), 8.16 (dd, *J* = 8.2, 1.4 Hz, 1H), 4.83 (q, *J* = 7.3 Hz, 2H), 1.60 (t, *J* = 7.3 Hz, 3H). **<sup>13</sup>C NMR:** (101 MHz, DMSO-d<sub>6</sub>)  $\delta$  = 149.25, 148.23, 146.23, 133.06, 128.21, 55.97, 15.23 ppm. **<sup>19</sup>F NMR:** (282 MHz, DMSO-d<sub>6</sub>)  $\delta$  = -102.28 to -137.00 (m) ppm. **IR:** (ATR, cm<sup>-1</sup>) 3141, 3108, 1605, 1567, 1489, 1467, 1434, 1284, 1225, 1554, 778, 651. **HRMS:** calcd. for C<sub>14</sub>H<sub>18</sub>F<sub>6</sub>N<sub>2</sub>SSb [M-SbF<sub>6</sub><sup>-</sup>]: 481.012689; found: 481.012570.

### General Procedure for the synthesis of alkynylthiopyridinium salts (GP A):

*n*-BuLi (1.6 M/2.5 M in hexanes, 1.1 equiv.) was added dropwise to a solution of the corresponding acetylene (1.1 equiv.) in THF (10 mL) at -78 °C. The reaction mixture was allowed to warm up to room temperature over 2 h, then cooled down to -78°C again. Then a solution of ZnBr<sub>2</sub> (1.1 equiv.) in THF (1 M) was added dropwise, to the former one and the reaction mixture was stirred for an additional 1 h before allowing it to reach rt. The solution thus obtained was then added dropwise to a solution of **154** (1 equiv.) in THF (0.5 M) at -78 °C. Once the addition finished, the reaction mixture was removed from the cooling bath and allowed to warm to rt. After **154** was completely consumed, the solvents were removed in vacuum and the solid obtained washed three times with Et<sub>2</sub>O (ultrasonication for 5 minutes each time) and dried.

### 1-Methyl-2-[(phenylethynyl)thio]pyridin-1-ium tetrabromozincate (**160a**):

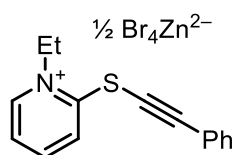


Following GP A, **160a** was prepared from **154a** (1 equiv, 1.3 g, 4.56 mmol), phenylacetylene (1.1 equiv, 549  $\mu$ L, 511 mg, 5.0 mmol), *n*-BuLi (1.1 equiv, 2.5 M, 2.0 mL, 5.0 mmol) and ZnBr<sub>2</sub> (1.16 equiv, 1.2 g, 5.3 mmol) in THF as a pale yellow powder (747 mg 1.78 mmol, 39%).

**<sup>1</sup>H NMR:** (400 MHz, CD<sub>3</sub>CN)  $\delta$  = 8.68 – 8.64 (m, 1H), 8.47 (dd, *J* = 8.4, 1.3 Hz, 1H), 8.44 – 8.39 (m, 1H), 7.81 (ddd, *J* = 7.7, 6.3, 1.5 Hz, 1H), 7.73 – 7.67 (m, 2H), 7.59 – 7.53 (m, 1H), 7.52 – 7.46 (m, 2H), 4.17 (s, 3H) ppm. **<sup>13</sup>C NMR:** (101 MHz, CD<sub>3</sub>CN)  $\delta$  = 157.4, 148.4, 145.9, 133.4,

131.8, 129.9, 127.5, 125.5, 121.3, 105.4, 67.2, 47.1 ppm. **IR:** (ATR,  $\text{cm}^{-1}$ ) 1614, 1563, 1481, 1440, 1281, 1187, 1161, 1108, 759, 693, 563, 520. **HRMS:** *calcd.* for  $\text{C}_{14}\text{H}_{12}\text{NS}^+ [\text{M}-\frac{1}{2} \text{ZnBr}_4]$ : 226.0685; found (ESI): 226.0693

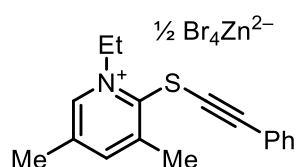
### 1-Ethyl-2-[(phenylethynyl)thio]pyridin-1-ium tetrabromozincate (**160b**):



Following the modified GP **A**, **160b** (2.5g, 5.8 mmol, 87%) was prepared as a pale, off white solid from **154ba** (1 equiv., 2.0 g, 6.7 mmol), phenylacetylene (1.1 equiv., 813  $\mu\text{L}$ , 756 mg, 7.4 mmol), *n*-BuLi (1.6 M, 4.6 mL, 7.4 mmol, 1.1 equiv.) and  $\text{ZnBr}_2$  (1.1 equiv, 1.67 g, 7.4 mmol) in THF. However, in order to obtain pure material, crude **160b** was washed with THF ( $2 \times 10$  mL).

**$^1\text{H}$  NMR:** (400 MHz,  $\text{CD}_3\text{CN}$ )  $\delta$  = 8.79 (dd,  $J$  = 6.3, 1.7 Hz, 1H), 8.49 (ddd,  $J$  = 8.5, 1.6, 0.6 Hz, 1H), 8.42 (ddd,  $J$  = 8.6, 7.5, 1.5 Hz, 1H), 7.89 (ddd,  $J$  = 7.5, 6.2, 1.4 Hz, 1H), 7.74 – 7.64 (m, 2H), 7.59 – 7.44 (m, 3H), 4.56 (q,  $J$  = 7.3 Hz, 3H), 1.59 (t,  $J$  = 7.3 Hz, 3H) ppm.  **$^{13}\text{C}$  NMR:** (101 MHz,  $\text{CD}_3\text{CN}$ )  $\delta$  = 156.1, 147.3, 145.9, 133.3, 131.7, 129.8, 128.0, 126.2, 121.3, 105.77, 55.9, 14.6 ppm. **IR:** (ATR,  $\text{cm}^{-1}$ ) 3052, 2159, 2007, 1607, 1564, 1488, 1461, 1431, 1325, 1177, 1148, 1113, 771, 753, 716, 689, 569, 516. **HRMS:** *calcd.* for  $\text{C}_{15}\text{H}_{14}\text{NS}^+ [\text{M}-\frac{1}{2} \text{ZnBr}_4]$ : 240.084146, found (ESI): 240.084210.

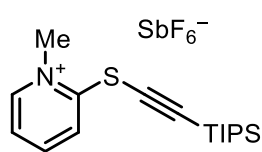
### 1-Ethyl-3,5-dimethyl-2-[(phenylethynyl)thio]pyridin-1-ium tetrabromozincate (**160c**):



Following the modified GP **A**, **160c** (689 mg, 1.50 mmol, 71%) was prepared as a pale, off white solid from **154c** (1 equiv, 684 mg, 2.1 mmol), phenylacetylene (1.1 equiv, 252  $\mu\text{L}$ , 234 mg, 2.3 mmol), *n*-BuLi (1.1 equiv, 2.5 M, 920  $\mu\text{L}$ , 2.3 mmol),  $\text{ZnBr}_2$  (1.1 equiv, 528 mg, 2.34 mmol) in THF. However, in order to obtain pure material, crude **160c** was washed with THF ( $2 \times 5$  mL).

**$^1\text{H}$  NMR:** (400 MHz,  $\text{CDCl}_3$ )  $\delta$  = 9.58 (d,  $J$  = 2.0 Hz, 1H), 8.04 (s, 1H), 7.47 – 7.29 (m, 5H), 5.33 (q,  $J$  = 7.2 Hz, 2H), 2.83 (s, 3H), 2.71 (s, 3H), 1.79 (t,  $J$  = 7.3 Hz, 3H) ppm.  **$^1\text{H}$  NMR:** (400 MHz,  $\text{CD}_3\text{CN}$ )  $\delta$  = 8.88 (d,  $J$  = 5.0 Hz, 1H), 8.32 – 8.25 (m, 1H), 7.46 (d,  $J$  = 1.3 Hz, 3H), 7.44 – 7.35 (m, 6H), 5.06 – 4.97 (m, 4H), 2.79 (s, 3H), 2.53 (d,  $J$  = 0.9 Hz, 4H), 1.67 (t,  $J$  = 7.2 Hz, 4H) ppm.  **$^{13}\text{C}$  NMR:** (101 MHz,  $\text{CD}_3\text{CN}$ )  $\delta$  = 149.1, 147.0, 145.6, 140.9, 133.0, 130.9, 129.7, 122.1, 96.1, 58.8, 21.5, 18.5, 16.8 ppm. **IR:** (ATR,  $\text{cm}^{-1}$ ) 2360, 2341, 1602, 1585, 1486, 1464, 1443, 1381, 1304, 1250, 1092, 1029, 876, 864, 766, 753, 720, 689, 539. **HRMS:** *calcd.* for  $\text{C}_{17}\text{H}_{18}\text{NS}^+ [\text{M}-\frac{1}{2} \text{ZnBr}_4]$ : 268.1154; found (ESI): 268.1156.

**1-Methyl-2-[[[(triisopropylsilyl)ethynyl]thio]pyridin-1-ium hexafluoroantimonate (160d):**



Following the modified GP A, **160d** was prepared from **154a** (13.3 g, 46.7 mmol), (triisopropylsilyl)acetylene (1.1 equiv, 11.5 mL, 9.36 g, 51.3 mmol), *n*-BuLi (1.1 equiv, 2.5 M, 20.5 mL, 51.3 mmol) and ZnBr<sub>2</sub> (1.1 equiv, 11.55 g, 51.3 mmol). Instead of removing the solvents after consumption of **154a**, an aqueous solution of NaSbF<sub>6</sub> (3.0 equiv., 36.2 g, 139.9 mmol) was added while stirring vigorously, and successively the reaction mixture was transferred to a separatory funnel. The aqueous phase was extracted with EtOAc (3 × 100 mL), the combined organic phases were dried with Na<sub>2</sub>SO<sub>4</sub>, filtered, and the solvent was removed *in vacuo* to afford **160d** as a beige solid (16.3 g, 30.0 mmol, 64%).

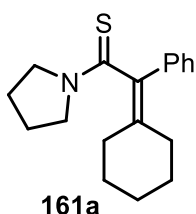
**<sup>1</sup>H NMR:** (300 MHz, CDCl<sub>3</sub>) δ = 8.73 (d, *J* = 6.2 Hz, 1H), 8.42 – 8.26 (m, 2H), 7.83 (ddd, *J* = 7.8, 6.3, 1.7 Hz, 1H), 4.22 (s, 3H), 1.29 – 1.03 (m, 21H) ppm. **<sup>1</sup>H NMR:** (300 MHz, CD<sub>3</sub>CN) δ = 8.64 – 8.56 (m, 1H), 8.44 (td, *J* = 8.0, 7.6, 1.5 Hz, 1H), 8.31 (dd, *J* = 8.5, 1.4 Hz, 1H), 7.78 (ddd, *J* = 7.6, 6.2, 1.5 Hz, 1H), 4.09 (s, 3H), 1.32 – 1.07 (m, 21H) ppm. **<sup>13</sup>C NMR:** (75 MHz, CD<sub>3</sub>CN) δ = 157.3, 148.4, 146.0, 127.0, 125.5, 113.6, 82.7, 46.9, 18.8, 11.9 ppm. **IR:** (ATR, cm<sup>-1</sup>) 3516, 3140, 2943, 2867, 2104, 1617, 1571, 1489, 1456, 1282, 1168, 1110, 993, 878, 851, 767, 656, 625, 595. **HRMS:** *calcd.* for C<sub>17</sub>H<sub>28</sub>NSSi<sup>+</sup> [M]<sup>+</sup>: 306.1706; found (ESI): 306.1707.



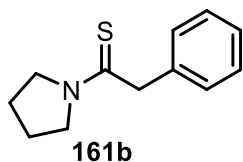
### General Procedure for the synthesis of dithioesters and thioamides (GP B):

An oven dried schlenk flask was charged with solid **160** (1 equiv.), CH<sub>2</sub>Cl<sub>2</sub> (2 mL) and the desired substrate. Subsequently DIPEA (1–2 equiv.) was added, and the progress of reaction was monitored by TLC. Once the starting materials were consumed, the solvent was removed *in vacuo*, and the product purified by column chromatography.

### 2-Cyclohexylidene-2-phenyl-1-(pyrrolidin-1-yl)ethane-1-thione (**161a**) and 2-phenyl-1-(pyrrolidin-1-yl)ethane-1-thione (**161b**):



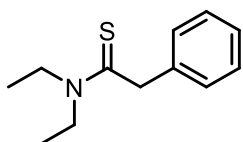
Column chromatography (petrol ether/EtOAc, 10:1) of the reaction mixture obtained from 1-(cyclohex-1-en-1-yl)pyrrolidine (1 equiv, 48.4 mg, 51.5  $\mu$ L, 0.32 mmol) and **160b** (1.1 equiv, 151.3 mg, 0.35 mmol) in CH<sub>2</sub>Cl<sub>2</sub> (2 mL) following GP B<sup>24</sup> afforded products **161a** (17.5 mg, 61.3  $\mu$ mol, 19%) as a pale yellow solid and **161b** (4.6 mg, 22.4  $\mu$ mol, 7%) as a crystalline off-white solid.



Compound **161a**: <sup>1</sup>H NMR: (500 MHz CD<sub>2</sub>Cl<sub>2</sub>)  $\delta$  = 7.47 – 7.43 (m, 2H), 7.35 – 7.30 (m, 2H), 7.28 – 7.24 (m, 1H), 3.88 – 3.80 (m, 1H), 3.73 – 3.64 (m, 2H), 3.51 – 3.43 (m, 1H), 2.29 (m, 1H), 2.21 – 2.09 (m, 2H), 2.05 – 1.87 (m, 4H), 1.76 – 1.67 (m, 1H), 1.64 – 1.53 (m, 5H). <sup>13</sup>C NMR: (126 MHz, , CD<sub>2</sub>Cl<sub>2</sub>)  $\delta$  = 197.8, 137.5, 137.1, 136.3, 130.2, 128.5, 127.5, 52.8, 52.2, 33.2, 31.2, 28.6, 28.0, 27.1, 26.8, 25.0 ppm. IR: (ATR, cm<sup>-1</sup>) 2925, 2851, 1732, 1598, 1469, 1444, 1327, 1257, 1191, 1088, 952, 851, 752, 703, 675. HRMS: calcd. for C<sub>18</sub>H<sub>24</sub>NS<sup>+</sup> [M+H]<sup>+</sup>: 286.1624; found: 286.1626.

Compound **161b**:<sup>25</sup> <sup>1</sup>H NMR: (400 MHz, CD<sub>2</sub>Cl<sub>2</sub>)  $\delta$  = 7.37 – 7.20 (m, 5H), 4.15 (d, *J* = 0.6 Hz, 2H), 3.82 (dddt, *J* = 7.2, 6.1, 1.1, 0.6 Hz, 2H), 3.54 (ddt, *J* = 8.0, 6.9, 1.1 Hz, 2H), 2.04 – 1.88 (m, 4H) ppm. <sup>13</sup>C NMR: (126 MHz, CD<sub>2</sub>Cl<sub>2</sub>)  $\delta$  = 197.4, 136.6, 129.1, 129.1, 127.3, 51.5, 51.5, 30.2, 27.0, 24.9 ppm.

### *N,N*-Diethyl-2-phenylethanethioamide (**161c**):



Following GP B, compound **161c** was obtained from diethylamine (1 equiv, 17.4  $\mu$ L, 0.17 mmol) and **160a** (1 equiv, 73.0 mg, 0.17 mmol) in

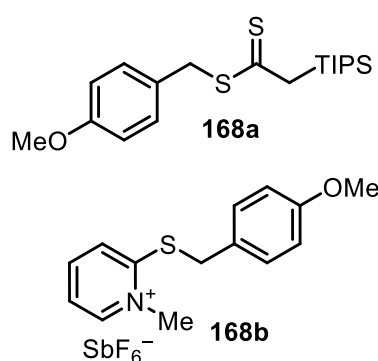
<sup>24</sup> No additional base was added.

<sup>25</sup> Analytical data are in agreement with the previously published ones: T. Guntreddi, R. Vanjari, K. N. Singh, *Org. Lett.* **2014**, *16*, 3624–3627.

CH<sub>2</sub>Cl<sub>2</sub> (2 mL) as a pale brown solid (8.4 mg, 41 μmol, 24%) after column chromatography (petrol ether/EtOAc, 10:1).<sup>26</sup>

**<sup>1</sup>H NMR:** (600 MHz, CD<sub>2</sub>Cl<sub>2</sub>) δ = 7.34 – 7.29 (m, 3H), 7.26 – 7.22 (m, 1H), 4.25 (s, 2H), 3.98 (q, *J* = 7.1 Hz, 2H), 3.48 (q, *J* = 7.2 Hz, 2H), 1.26 (t, *J* = 7.1 Hz, 3H), 1.11 (t, *J* = 7.2 Hz, 3H) ppm. **<sup>13</sup>C NMR:** (126 MHz, CD<sub>2</sub>Cl<sub>2</sub>) δ = 199.3, 137.3, 129.1, 128.4, 127.2, 50.8, 48.1, 47.1, 13.7, 11.3 ppm.

**4-Methoxybenzyl 2-(triisopropylsilyl)ethanedithioate (168a) and 2-[(4-methoxybenzyl)thio]-1-methylpyridin-1-ium hexafluoroantimonate (168b):**



The reaction mixture obtained from (4-methoxyphenyl)-methanethiol (2 equiv, 92.5 mg, 83.6 μL, 0.6 mmol), **160d** (1 equiv, 162.7 mg, 0.3 mmol) and DIPEA (2 equiv, 77.6 mg, 104.5 μL, 0.6 mmol) in CH<sub>2</sub>Cl<sub>2</sub> (2 mL) following GP **B**<sup>27</sup> was filtered. The precipitate was washed with CH<sub>2</sub>Cl<sub>2</sub> (3 × 2 mL) affording a white solid, which was identified as **168b** (136.9 mg, 28.4 μmol, 95%). The combined filtrates were concentrated and purified by column chromatography (hexanes/ethyl acetate, 20:1) to give compound **168a** as an

orange oil in 94 % yield.

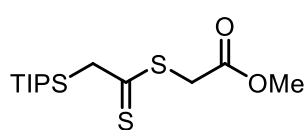
Compound **168a**: **<sup>1</sup>H NMR:** (300 MHz, CDCl<sub>3</sub>) δ = 7.25 – 7.20 (m, 2H), 6.87 – 6.80 (m, 2H), 4.39 (s, 2H), 3.79 (s, 3H), 3.16 (s, 2H), 1.32 – 1.17 (m, 3H), 1.16 – 1.05 (m, 18H) ppm. **<sup>13</sup>C NMR:** (126 MHz, CDCl<sub>3</sub>) δ = 236.1, 159.2, 130.5, 127.5, 114.2, 55.4, 42.5, 41.8, 18.7, 11.6 ppm. **IR:** (ATR, cm<sup>-1</sup>) 2940, 2864, 1610, 1510, 1462, 1301, 1248, 1174, 1102, 1036, 911, 880, 830, 658, 510. **HRMS:** calcd. for C<sub>19</sub>H<sub>33</sub>OS<sub>2</sub>Si<sup>+</sup> [*M*+H]<sup>+</sup>: 369.1737; found: 369.1736.

Compound **168b**: **<sup>1</sup>H NMR:** (600 MHz, CD<sub>3</sub>CN) δ = 8.50 (ddt, *J* = 6.3, 1.3, 0.6 Hz, 1H), 8.23 (ddd, *J* = 8.9, 7.5, 1.6 Hz, 1H), 7.89 (dt, *J* = 8.5, 0.8 Hz, 1H), 7.61 (ddd, *J* = 7.7, 6.3, 1.4 Hz, 1H), 7.44 – 7.40 (m, 2H), 6.97 – 6.94 (m, 2H), 4.55 (s, 2H), 4.07 (s, 3H), 3.79 (s, 3H) ppm. **<sup>13</sup>C NMR:** (126 MHz, CD<sub>3</sub>CN) δ = 160.9, 160.8, 147.5, 144.3, 131.6, 126.4, 125.6, 123.4, 115.5, 56.1, 47.1, 37.9 ppm. **<sup>19</sup>F NMR:** (282 MHz, CD<sub>3</sub>CN) δ = –104.38 to –144.00 (m) ppm. **IR:** (ATR, cm<sup>-1</sup>) 2918, 2849, 2359, 1611, 1566, 1513, 1492, 1456, 1438, 1250, 1178, 1117, 1228, 845, 766, 658, 641. **HRMS:** calcd. for C<sub>14</sub>H<sub>16</sub>NOS<sup>+</sup> [*M*–SbF<sub>6</sub>]<sup>+</sup>: 246.0947; found: 246.0947.

<sup>26</sup> Analytical data are in agreement with the previously published ones: Y. Sun, H. Jiang, W. Wu, W. Zeng, J. Li, *Org. Biomol. Chem.* **2014**, *12*, 700–707.

<sup>27</sup> Experiment was run on air.

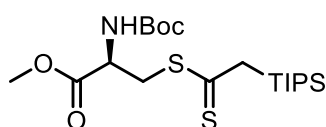
### Methyl 2-[[2-(triisopropylsilyl)ethanethioyl]thio]acetate (**169**):



Following GP **B**, compound **169** (49.0 mg, 0.153 mmol, 51%) was obtained as a yellow oil from methyl thioglycolate (1 equiv, 31.8 mg, 26.8  $\mu$ L, 0.3 mmol), **160d**, (1 equiv, 162.7 mg, 0.3 mmol) and DIPEA (1 equiv, 77.6 mg, 104.5  $\mu$ L, 0.6 mmol) in  $\text{CH}_2\text{Cl}_2$  (2 mL) after column chromatography (hexanes/EtOAc, 80:1).

**$^1\text{H}$  NMR:** (300 MHz,  $\text{CDCl}_3$ )  $\delta$  = 4.07 (s, 2H), 3.72 (s, 3H), 3.20 (s, 2H), 1.34 – 1.18 (m, 3H), 1.14 – 1.07 (m, 18H) ppm.  **$^{13}\text{C}$  NMR:** (126 MHz,  $\text{CDCl}_3$ )  $\delta$  = 234.12, 168.40, 52.82, 42.44, 39.17, 18.72, 11.57 ppm. **IR:** (ATR,  $\text{cm}^{-1}$ ) 2942, 2865, 1741, 1461, 1435, 1294, 1231, 1155, 1138, 1102, 999, 913, 879, 660, 510. **HRMS:** calcd. for  $\text{C}_{14}\text{H}_{29}\text{O}_2\text{S}_2\text{Si}^+$   $[\text{M}+\text{H}]^+$ : 321.1373; found (ESI): 321.1375.

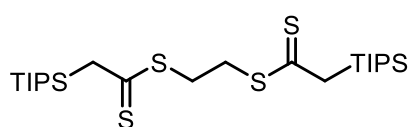
### Methyl *N*-(*tert*-butoxycarbonyl)-*S*-[2-(triisopropylsilyl)ethanethioyl]-*L*-cysteinate (**170**):



Following GP **B**, compound **170** (54.6 mg, 0.12 mmol, 40%, 59% RSM) was obtained from *N*-(*tert*-butoxycarbonyl)-*L*-cysteine methyl ester (1 equiv, 70.6 mg, 61.8  $\mu$ L, 0.3 mmol), **160d**, (1 equiv, 162.7 mg, 0.3 mmol) and DIPEA (1 equiv, 77.6 mg, 54  $\mu$ L, 0.31 mmol) in  $\text{CH}_2\text{Cl}_2$  (2 mL) after column chromatography (hexanes/EtOAc, 80:1 to 5:1) as bright yellow crystals.

**$^1\text{H}$  NMR:** (300 MHz,  $\text{CDCl}_3$ )  $\delta$  = 5.21 (d,  $J$  = 7.6 Hz, 1H), 4.65 – 4.54 (m, 1H), 3.81 (dd,  $J$  = 13.9, 4.5 Hz, 1H), 3.76 (s, 3H), 3.63 (dd,  $J$  = 13.7, 7.2 Hz, 1H), 3.18 (s, 2H), 1.43 (s, 9H), 1.30 – 1.17 (m, 3H), 1.09 (d,  $J$  = 6.7 Hz, 18H).  **$^{13}\text{C}$  NMR:** (126 MHz,  $\text{CDCl}_3$ )  $\delta$  = 235.6, 171.3, 155.2, 80.4, 52.9, 52.66, 43.2, 38.9, 28.4, 18.8, 11.6 ppm. **IR:** (ATR,  $\text{cm}^{-1}$ ) 3369, 2943, 2866, 1747, 1719, 1500, 1366, 1220, 1166, 1105, 913, 881, 661. **HRMS:** calcd. for  $\text{C}_{20}\text{H}_{40}\text{NO}_4\text{S}_2\text{Si}^+$   $[\text{M}+\text{H}]^+$ : 450.2163; found (ESI): 450.2167.

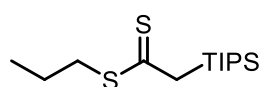
### Ethane-1,2-diyl bis[2-(triisopropylsilyl)ethanedithioate] (**171**):



Following GP **B**, compound **171** (40.2 mg, 76.8  $\mu$ mol, 26%) was obtained from ethane-1,2-dithiol (1 equiv, 28.3 mg, 25.2  $\mu$ L, 0.3 mmol), **160d**, (1 equiv, 162.7 mg, 0.3 mmol) and DIPEA (1 equiv, 77.6 mg, 54  $\mu$ L, 0.31 mmol) in  $\text{CH}_2\text{Cl}_2$  (2 mL) after column chromatography (hexanes/EtOAc, 200:1) as bright yellow crystals.

**$^1\text{H}$  NMR:** (400 MHz,  $\text{CDCl}_3$ )  $\delta$  = 3.49 (s, 4H), 3.17 (s, 4H), 1.29 – 1.20 (m, 6H), 1.10 (d,  $J$  = 7.3 Hz, 36H) ppm.  **$^{13}\text{C}$  NMR:** (101 MHz,  $\text{CDCl}_3$ )  $\delta$  = 235.9, 43.0, 34.6, 27.1, 18.8, 11.6 ppm. **IR:** (ATR,  $\text{cm}^{-1}$ ) 2941, 2875, 1463, 1388, 1226, 1103, 912, 882, 658. **HRMS:** calcd. for  $\text{C}_{24}\text{H}_{51}\text{S}_4\text{Si}_2^+$   $[\text{M}+\text{H}]^+$ : 523.2407; found (ESI): 523.2410

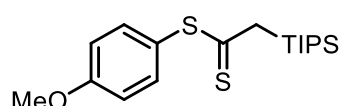
#### Propyl 2-(triisopropylsilyl)ethanedithioate (**172**):



Following GP **B**, compound **172** (87.1 mg, 0.3 mmol, 99%) was obtained from 1-propanethiol (2 equiv, 45.7 mg, 54.4  $\mu$ L, 0.6 mmol), **160d**, (1 equiv, 162.7 mg, 0.3 mmol) and DIPEA (1 equiv, 77.6 mg, 54  $\mu$ L, 0.31 mmol) in  $\text{CH}_2\text{Cl}_2$  (2 mL) after column chromatography (hexanes/EtOAc, 50:1) as a yellow solid.

**$^1\text{H}$  NMR:** (300 MHz,  $\text{CDCl}_3$ )  $\delta$  = 3.21 – 3.13 (m, 4H), 1.69 (h,  $J$  = 7.3 Hz, 2H), 1.33 – 1.17 (m, 3H), 1.10 (d,  $J$  = 6.8 Hz, 18H), 1.01 (t,  $J$  = 7.3 Hz, 3H) ppm.  **$^{13}\text{C}$  NMR:** (126 MHz,  $\text{CDCl}_3$ )  $\delta$  = 237.0, 42.9, 39.2, 21.1, 18.8, 13.8, 11.6 ppm. **IR:** (ATR,  $\text{cm}^{-1}$ ) 2961, 2941, 2866, 1715, 1634, 1551, 1462, 1224, 1109, 915, 881, 662. **HRMS:** calcd. for  $\text{C}_{14}\text{H}_{31}\text{S}_2\text{Si}^+$  [ $\text{M}+\text{H}$ ] $^+$ : 291.1631; found (ESI): 291.1629.

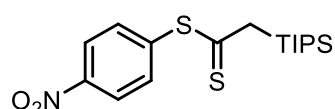
#### 4-Methoxyphenyl 2-(triisopropylsilyl)ethanedithioate (**173**):



Following GP **B**, compound **173** (66.2 mg, 0.19 mmol, 62%) was obtained from 4-methoxythiophenol (1 equiv, 42.1 mg, 36.9  $\mu$ L, 0.3 mmol), **160d** (1 equiv, 162.7 mg, 0.3 mmol) and DIPEA (1 equiv, 77.6 mg, 54  $\mu$ L, 0.31 mmol) in  $\text{CH}_2\text{Cl}_2$  (2 mL) after column chromatography (hexanes/EtOAc, 80:1 to 60:1) as a yellow oil.

**$^1\text{H}$  NMR:** (300 MHz,  $\text{CDCl}_3$ )  $\delta$  = 7.31 – 7.25 (m, 2H), 7.02 – 6.95 (m, 2H), 3.85 (s, 3H), 3.24 (s, 2H), 1.43 – 1.21 (m, 3H), 1.21 – 1.09 (m, 18H) ppm.  **$^{13}\text{C}$  NMR:** (126 MHz,  $\text{CDCl}_3$ )  $\delta$  = 237.9, 161.2, 136.7, 123.5, 115.1, 55.5, 41.9, 18.8, 11.6 ppm. **IR:** (ATR,  $\text{cm}^{-1}$ ) 2941, 2864, 1591, 1494, 1462, 1291, 1250, 1173, 1103, 1032, 904, 882, 824, 799, 664, 645. **HRMS:** calcd. for  $\text{C}_{18}\text{H}_{31}\text{OS}_2\text{Si}^+$  [ $\text{M}+\text{H}$ ] $^+$ : 355.1580; found: 355.1570.

#### Compound **174**, 4-Nitrophenyl 2-(triisopropylsilyl)ethanedithioate (**174**)

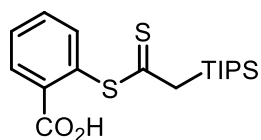


Following GP **B**, compound **174** (108.0 mg, 0.29 mmol, 97%) was obtained from 4-nitrothiophenol (2 equiv, 93.1 mg, 0.6 mmol), **160d** (1 equiv, 162.7 mg, 0.3 mmol) and DIPEA (1 equiv, 77.6 mg, 54  $\mu$ L, 0.31 mmol) in  $\text{CH}_2\text{Cl}_2$  (2 mL) after column chromatography (hexanes/EtOAc, 50:1) as a bright yellow oil.

**$^1\text{H}$  NMR:** (300 MHz,  $\text{CDCl}_3$ )  $\delta$  = 8.29 (d,  $J$  = 8.9 Hz, 2H), 7.55 (d,  $J$  = 8.9 Hz, 2H), 3.28 (s, 2H), 1.39 – 1.24 (m, 3H), 1.15 (d,  $J$  = 7.1 Hz, 18H) ppm.  **$^{13}\text{C}$  NMR:** (126 MHz,  $\text{CDCl}_3$ )  $\delta$  = 233.4, 148.8, 139.8, 136.3, 124.4, 43.0, 18.8, 11.6 ppm. **IR:** (ATR,  $\text{cm}^{-1}$ ) 2942, 2866, 1600, 1522,

1463, 1343, 1229, 1101, 902, 882, 851, 743. **HRMS:** calcd. for  $C_{17}H_{28}NO_2S_2Si^+$   $[M+H]^+$ : 370.1325; found (ESI): 370.1320.

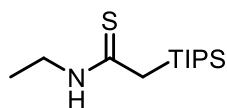
#### 2-([2-(Triisopropylsilyl)ethanethioyl]thio)benzoic acid (**175**):



Following GP **B**, compound **175** (73.6 mg, 0.2 mmol, 67%) was obtained from thiosalicylic acid (2 equiv, 92.5 mg, 62.1  $\mu$ L, 0.6 mmol), **160d** (1 equiv, 162.7 mg, 0.3 mmol) and DIPEA (1 equiv, 77.6 mg, 54  $\mu$ L, 0.31 mmol) in  $CH_2Cl_2$  (2 mL) after column chromatography (cyclohexane/EtOAc, 10:1 to 5:1) as a yellow solid.

**$^1H$  NMR:** (400 MHz,  $CDCl_3$ )  $\delta$  = 8.11 (ddd,  $J$  = 7.6, 1.7, 0.4 Hz, 1H), 7.63 (td,  $J$  = 7.5, 1.7 Hz, 1H), 7.57 (td,  $J$  = 7.6, 1.5 Hz, 1H), 7.52 (ddd,  $J$  = 7.7, 1.5, 0.4 Hz, 1H), 3.26 (s, 2H), 1.37 – 1.24 (m, 3H), 1.14 (d,  $J$  = 7.2 Hz, 18H) ppm.  **$^{13}C$  NMR:** (101 MHz,  $CDCl_3$ )  $\delta$  = 234.7, 171.0, 138.0, 134.1, 133.2, 133.06, 131.8, 130.4, 42.3, 18.9, 11.7 ppm. **IR:** (ATR,  $cm^{-1}$ ) 2942, 2866, 2363, 2342, 1698, 1465, 1406, 1296, 1272, 1228, 1136, 1106, 906, 882, 748, 699, 658. **HRMS:** calcd. for  $C_{18}H_{29}O_2S_2Si^+$   $[M+H]^+$ : 369.1373; found (ESI): 369.1372.

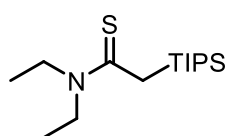
#### N-Ethyl-2-(triisopropylsilyl)ethanethioamide (**176**):



Following the GP **B**, compound **176** (72.7 mg, 0.28 mmol, 93%) was obtained from ethylamine (12 M in  $H_2O$ , 2 equiv, 50  $\mu$ L, 0.6 mmol), **160d** (1 equiv, 162.7 mg, 0.3 mmol) and DIPEA (1 equiv, 77.6 mg, 54  $\mu$ L, 0.31 mmol) in  $CH_2Cl_2$  (2 mL) after separation by column chromatography (cyclohexane/EtOAc, 50:1 to 10:1) as an off-white crystalline solid.

**$^1H$  NMR:** (300 MHz,  $CDCl_3$ )  $\delta$  = 6.86 (bs, 1H), 3.65 (qd,  $J$  = 7.3, 5.2 Hz, 2H), 2.53 (s, 2H), 1.30 – 1.15 (m, 6H), 1.09 (d,  $J$  = 6.8 Hz, 18H) ppm.  **$^{13}C$  NMR:** (75 MHz,  $CDCl_3$ )  $\delta$  = 204.1, 41.1, 34.2, 18.8, 13.5, 11.5 ppm. **IR:** (ATR,  $cm^{-1}$ ) 3238, 2940, 2875, 1527, 1459, 1383, 1328, 1203, 1103, 1036, 881, 799, 735, 642, 605, 559. **HRMS:** calcd. for  $C_{13}H_{30}NSSi^+$   $[M+H]^+$ : 260.1863; found (ESI): 260.1866.

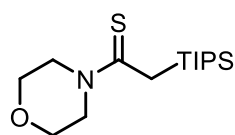
#### N,N-Diethyl-2-(triisopropylsilyl)ethanethioamide (**177**):



Following the GP **B**, compound **177** (76.0 mg, 0.264 mmol, 73%) was obtained from diethylamine (1 equiv, 26.3 mg, 37.2  $\mu$ L, 0.36 mmol), **160d** (1 equiv, 195.2 mg, 0.36 mmol) and DIPEA (1 equiv, 46.5 mg, 62.7  $\mu$ L, 0.36 mmol) in  $CH_2Cl_2$  (2 mL) after column chromatography (hexanes/EtOAc, 20:1) as an off-white solid.

**<sup>1</sup>H NMR:** (400 MHz, CDCl<sub>3</sub>) δ = 4.02 (q, *J* = 7.1 Hz, 2H), 3.57 (q, *J* = 7.1 Hz, 2H), 2.69 (s, 2H), 1.34 – 1.21 (m, 9H), 1.10 (d, *J* = 7.3 Hz, 18H) ppm. **<sup>13</sup>C NMR:** (101 MHz, CDCl<sub>3</sub>) δ = 201.8, 47.7, 46.5, 30.1, 18.9, 13.2, 11.8, 11.5 ppm. **IR:** (ATR, cm<sup>-1</sup>) 3321, 2971, 2873, 2360, 1454, 1381, 1087, 1045, 879, 637. **HRMS:** calcd. for C<sub>15</sub>H<sub>34</sub>NSSi<sup>+</sup> [M+H]<sup>+</sup>: 288.2176; found (ESI): 288.2173.

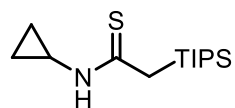
### 1-Morpholino-2-(triisopropylsilyl)ethane-1-thione (178):



Following GP **B**, compound **178** (82.0 mg, 0.272 mmol, 91%) was obtained from morpholine (2 equiv, 52.3 mg, 51.7 μL, 0.6 mmol), **160d** (1 equiv, 162.7 mg, 0.3 mmol) and DIPEA (1 equiv, 77.6 mg, 54 μL, 0.31 mmol) in CH<sub>2</sub>Cl<sub>2</sub> (2 mL) after column chromatography (hexanes/EtOAc, 20:1 to 10:1) as a white crystalline solid.

**<sup>1</sup>H NMR:** (300 MHz, CDCl<sub>3</sub>) δ = 4.44 – 4.34 (m, 2H), 3.83 – 3.70 (m, 6H), 2.79 (s, 2H), 1.37 – 1.18 (m, 3H), 1.18 – 1.05 (m, 18H) ppm. **<sup>13</sup>C NMR:** (126 MHz, CDCl<sub>3</sub>) δ = 203.5, 66.7, 66.3, 50.6, 49.7, 30.1, 18.8, 11.8 ppm. **IR:** (ATR, cm<sup>-1</sup>) 2941, 2865, 1477, 1412, 1276, 1248, 1114, 1024, 1007, 881, 707, 658. **HRMS:** calcd. for C<sub>15</sub>H<sub>32</sub>NOSSi<sup>+</sup> [M+H]<sup>+</sup>: 302.1968; found (ESI): 302.1970.

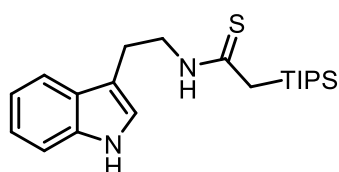
### N-Cyclopropyl-2-(triisopropylsilyl)ethanethioamide (179):



Following GP **B**, compound **179** (43.9 mg, 0.162 mmol, 54%) was obtained from cyclopropanamine (2 equiv, 34.3 mg, 41.6 μL, 0.6 mmol), **160d** (1 equiv, 162.7 mg, 0.3 mmol) and DIPEA (1 equiv, 77.6 mg, 54 μL, 0.31 mmol) in CH<sub>2</sub>Cl<sub>2</sub> (2 mL) after column chromatography (cyclohexane/EtOAc, 20:1) as an off-white crystalline solid.

**<sup>1</sup>H NMR:** (300 MHz, CDCl<sub>3</sub>) δ = 6.89 (s, 1H), 3.17 (tt, *J* = 7.7, 3.9 Hz, 1H), 2.52 (s, 2H), 1.32 – 1.12 (m, 3H), 1.09 (d, *J* = 6.5 Hz, 18H), 0.97 – 0.86 (m, 2H), 0.67 – 0.60 (m, 2H) ppm. **<sup>13</sup>C NMR:** (101 MHz, CDCl<sub>3</sub>) δ = 206.3, 34.1, 29.0, 18.8, 11.5, 7.3 ppm. **IR:** (ATR, cm<sup>-1</sup>) 3330, 3244, 2969, 2942, 2866, 1459, 1382, 1089, 1052, 883, 783, 732, 647, 612. **HRMS:** calcd. for C<sub>14</sub>H<sub>30</sub>NSSi<sup>+</sup> [M+H]<sup>+</sup>: 272.1863 found (ESI): 272.1864.

### N-[2-(1H-Indol-3-yl)ethyl]-2-(triisopropylsilyl)ethanethioamide (180):

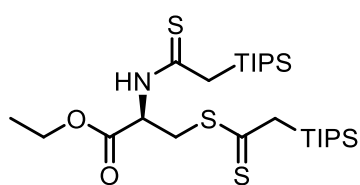


Following GP **B**, **180** (90.6 mg, 0.242 mmol, 81%) was obtained from tryptamine (2 equiv, 96.1 mg, 0.6 mmol), **160d** (1 equiv, 162.7 mg, 0.3 mmol) and DIPEA (1 equiv, 77.6 mg, 54 μL, 0.31 mmol) in CH<sub>2</sub>Cl<sub>2</sub> (2 mL) after column chromatography

(cyclohexane/EtOAc, 10:1) as a colorless oil.

**<sup>1</sup>H NMR:** (500 MHz, CDCl<sub>3</sub>)  $\delta$  = 8.12 (s, 1H), 7.63 (dd,  $J$  = 7.9, 1.0 Hz, 1H), 7.39 (dt,  $J$  = 8.2, 0.9 Hz, 1H), 7.23 (ddd,  $J$  = 8.2, 7.0, 1.2 Hz, 1H), 7.14 (ddd,  $J$  = 8.0, 7.0, 1.0 Hz, 1H), 7.07 (d,  $J$  = 2.4 Hz, 1H), 6.89 (s, 1H), 3.98 (td,  $J$  = 6.7, 5.0 Hz, 2H), 3.12 (td,  $J$  = 6.6, 0.9 Hz, 2H), 2.45 (s, 2H), 1.08 – 0.99 (m, 3H), 0.96 (d,  $J$  = 6.5 Hz, 17H) ppm. **<sup>13</sup>C NMR:** (126 MHz, CDCl<sub>3</sub>)  $\delta$  = 204.2, 136.7, 127.2, 122.7, 122.2, 119.9, 118.8, 112.4, 111.4, 46.2, 34.0, 23.9, 18.6, 11.3 ppm. **IR:** (ATR, cm<sup>-1</sup>) 3408, 3353, 3262, 2939, 2864, 1512, 1456, 1390, 1338, 1228, 1128, 1104, 1011, 999, 880, 739, 647. **HRMS:** calcd. for C<sub>21</sub>H<sub>35</sub>N<sub>2</sub>SSi<sup>+</sup> [M+H]<sup>+</sup>: 375.2285; found (ESI): 375.2271.

**Ethyl *N,S*-bis[2-(triisopropylsilyl)ethanethioyl]-*L*-cysteinate (**181**):**

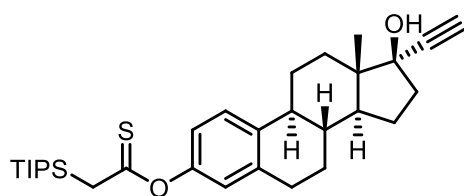


Following GP **B**, compound **181** (72 mg, 0.13 mmol, 43%) was prepared from *L*-cysteine ethyl ester hydrochloride (1 equiv, 55.7 mg, 0.3 mmol), **160d** (1 equiv, 162.7 mg, 0.3 mmol) and DIPEA (2 equiv, 78.8 mg, 106.3  $\mu$ L, 0.61 mmol) in CH<sub>2</sub>Cl<sub>2</sub> (2 mL) after column chromatography (hexanes/EtOAc, 95:5) as a

yellow oil.

**<sup>1</sup>H NMR:** (600 MHz, CDCl<sub>3</sub>)  $\delta$  = 7.70 (d,  $J$  = 7.0 Hz, 1H), 5.43 (td,  $J$  = 6.5, 4.6 Hz, 1H), 4.28 – 4.15 (m, 2H), 4.01 – 3.88 (m, 2H), 3.18 (s, 2H), 2.67 – 2.46 (m, 2H), 1.29 (t,  $J$  = 7.2 Hz, 3H), 1.27 – 1.19 (m, 6H), 1.09 (ddd,  $J$  = 7.3, 4.8, 2.2 Hz, 36H) ppm. **<sup>13</sup>C NMR:** (126 MHz, CDCl<sub>3</sub>)  $\delta$  = 236.2, 205.6, 169.7, 62.4, 57.6, 43.4, 37.6, 34.4, 18.9, 18.8, 14.3, 11.7, 11.5 ppm. **IR:** (ATR, cm<sup>-1</sup>) 3369, 2941, 2866, 1734, 1499, 1464, 1370, 1222, 1193, 1135, 1105, 912, 881, 660. **HRMS:** calcd. for C<sub>27</sub>H<sub>56</sub>NO<sub>2</sub>S<sub>3</sub>Si<sub>2</sub><sup>+</sup> [M+H]<sup>+</sup>: 578.3006; found (ESI): 578.2994.

***O*-[(8*R*,9*S*,13*S*,14*S*,17*R*)-17-Ethynyl-17-hydroxy-13-methyl-7,8,9,11,12,13,14,15,16,17-decahydro-6*H*-cyclopenta[*a*]phenanthren-3-yl] 2-(triisopropylsilyl)ethanethioate (**182**):**



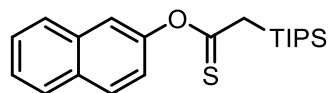
Following GP **B**, compound **182** (15.5 mg, 30.3  $\mu$ mol, 10%) was obtained from 17 $\alpha$ -ethynylestradiol (2 equiv, 177.8 mg, 0.06 mmol), **160d** (1 equiv, 162.7 mg, 0.3 mmol) and DIPEA (1 equiv, 77.6 mg, 54  $\mu$ L, 0.31 mmol) in CH<sub>2</sub>Cl<sub>2</sub> (2 mL) after column chromatography

(cyclohexane/EtOAc, 20:1) as a colorless oil.

**<sup>1</sup>H NMR:** (300 MHz, CDCl<sub>3</sub>)  $\delta$  = 7.33 (d,  $J$  = 8.3 Hz, 1H), 6.81 (dd,  $J$  = 8.5, 2.6 Hz, 1H), 6.73 (d,  $J$  = 2.4 Hz, 1H), 3.00 (s, 2H), 2.90 – 2.87 (m, 2H), 2.61 (s, 1H), 2.36 (m, 2H), 2.28 (m, 1H), 2.03 (ddd,  $J$  = 13.6, 11.9, 3.9 Hz, 1H), 1.95 – 1.87 (m, 3H), 1.80 (dddd,  $J$  = 12.0, 9.6, 7.6, 4.0 Hz, 1H), 1.76 – 1.68 (m, 2H), 1.58 – 1.37 (m, 4H), 1.31 – 1.25 (m, 3H), 1.17 (d,  $J$  = 7.3 Hz, 18H), 0.89 (d,  $J$  = 0.7 Hz, 3H) ppm. **<sup>13</sup>C NMR:** (126 MHz, CDCl<sub>3</sub>)  $\delta$  = 223.3, 152.5, 138.4, 138.3, 126.5, 121.9,

119.2, 87.6, 80.0, 74.3, 49.7, 47.3, 43.9, 39.2, 39.2, 36.3, 32.9, 29.8, 27.2, 26.4, 23.0, 18.8, 12.8, 11.7 ppm. **IR:** (ATR,  $\text{cm}^{-1}$ ) 3305, 2936, 2865, 1493, 1459, 1268, 1192, 1120, 1058, 1048, 880, 651. **HRMS:** calcd. for  $\text{C}_{31}\text{H}_{47}\text{O}_2\text{SSi}^+$   $[\text{M}+\text{H}]^+$ : 511.3061; found (ESI): 511.3053.

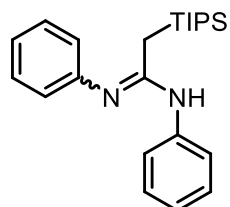
#### **O-(Naphthalen-2-yl) 2-(triisopropylsilyl)ethanethioate (183):**



Following GP **B**, compound **183** (64.0 mg, 0.18 mmol, 60%) was obtained from 2-naphthol (2 equiv, 86.5 mg, 0.6 mmol), **160d** (1 equiv, 162.7 mg, 0.3 mmol) and DIPEA (1 equiv, 77.6 mg, 54  $\mu\text{L}$ , 0.31 mmol) in  $\text{CH}_2\text{Cl}_2$  (2 mL) after column chromatography (cyclohexane/EtOAc, 50/1) as a brown crystalline solid.

**$^1\text{H}$  NMR:** (300 MHz,  $\text{CDCl}_3$ )  $\delta$  = 7.93 – 7.79 (m, 3H), 7.55 – 7.43 (m, 3H), 7.21 (dd,  $J$  = 8.9, 2.3 Hz, 1H), 3.08 (s, 2H), 1.46 – 1.26 (m, 3H), 1.21 (d,  $J$  = 6.6 Hz, 18H) ppm.  **$^{13}\text{C}$  NMR:** (126 MHz,  $\text{CDCl}_3$ )  $\delta$  = 223.4, 152.4, 133.9, 131.8, 129.4, 128.0, 127.9, 126.7, 126.0, 121.9, 119.1, 36.3, 18.8, 11.7 ppm. **IR:** (ATR,  $\text{cm}^{-1}$ ) 3369, 2943, 2866, 1747, 1719, 1500, 1366, 1220, 1166, 1105, 913, 881, 661. **HRMS:** calcd. for  $\text{C}_{21}\text{H}_{31}\text{OSSi}^+$   $[\text{M}+\text{H}]^+$ : 359.1859; found (ESI): 359.1863.

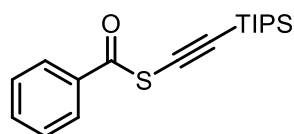
#### **N,N'-Diphenyl-2-(triisopropylsilyl)acetimidamide (184):**



Following GP **B**, compound **184** (79.6 mg, 0.217 mmol, 72%) was obtained from aniline (2 equiv, 55.9 mg, 54.8  $\mu\text{L}$ , 0.6 mmol), **160d** (1 equiv, 162.7 mg, 0.3 mmol) and DIPEA (1 equiv, 77.6 mg, 54  $\mu\text{L}$ , 0.31 mmol) in  $\text{CH}_2\text{Cl}_2$  (2 mL) after column chromatography (hexanes/EtOAc, 10:1 to pure EtOAc) as brownish crystals.

**$^1\text{H}$  NMR:** (400 MHz,  $\text{CDCl}_3$ )  $\delta$  = 7.38 – 6.94 (m, 11H), 1.99 (s, 2H), 1.20 – 1.05 (m, 5H), 1.00 (d,  $J$  = 6.9 Hz, 16H).  **$^{13}\text{C}$  NMR:** (101 MHz,  $\text{CDCl}_3$ )  $\delta$  = 155.4, 129.0, 122.4, 121.8 – 120.3 (s, br), 18.6, 14.4, 11.6 ppm. **IR:** (ATR,  $\text{cm}^{-1}$ ) 3452, 2940, 2865, 1640, 1589, 1521, 1497, 1486, 1435, 1318, 1207, 1155, 881, 750, 698, 653, 639. 505. **HRMS:** calcd. for  $\text{C}_{23}\text{H}_{35}\text{N}_2\text{Si}^+$   $[\text{M}+\text{H}]^+$ : 367.2564; found: 367.2566.

#### **S-(Triisopropylsilyl)ethynyl benzothioate (185):**

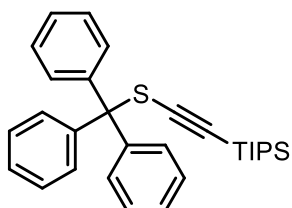


Following GP **B**, compound **185** (95.7 mg, 0.3 mmol, 100%) was obtained from thiobenzoic acid (1 equiv, 41.5 mg, 35.2  $\mu\text{L}$ , 0.3 mmol), **160d** (1 equiv, 162.7 mg, 0.3 mmol) and DIPEA (1 equiv, 77.6 mg, 54  $\mu\text{L}$ , 0.31 mmol) in  $\text{CH}_2\text{Cl}_2$  (2 mL) after column chromatography (hexanes/EtOAc, 95:5) as a yellow oil.



**<sup>1</sup>H NMR:** (400 MHz, CDCl<sub>3</sub>) δ = 7.88 (dd, *J* = 8.5, 1.3 Hz, 2H), 7.67 – 7.57 (m, 1H), 7.51 – 7.45 (m, 2H), 1.15 (d, *J* = 1.8 Hz, 21H) ppm. **<sup>13</sup>C NMR:** (101 MHz, CDCl<sub>3</sub>) δ = 187.6, 135.6, 134.4, 129.1, 127.6, 109.6, 86.0, 18.7, 11.5 ppm. **IR:** (ATR, cm<sup>-1</sup>) 2942, 2834, 2105, 1703, 1462, 1448, 1257, 1202, 1177, 1072, 998, 881, 857, 769, 675, 637, 597, 516. **HRMS:** calcd. for C<sub>18</sub>H<sub>27</sub>OSSi<sup>+</sup> [M+H]<sup>+</sup>: 319.1546; found (ESI): 319.1545.

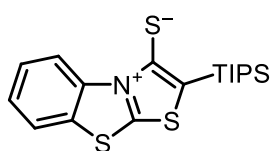
#### Triisopropyl[(tritylthio)ethynyl]silane (**186**):



Following GP **B**, compound **186** (123.7 mg, 0.271 mmol, 90%) was obtained from triphenylmethanethiol (2 equiv, 165.8 mg, 0.6 mmol), **160d** (1 equiv, 162.7 mg, 0.3 mmol) and DIPEA (1 equiv, 77.6 mg, 54 μL, 0.31 mmol) in CH<sub>2</sub>Cl<sub>2</sub> (2 mL). Isolated as colorless crystals after column chromatography (cyclohexane/EtOAc, 50:1).

**<sup>1</sup>H NMR** (300 MHz, CD<sub>2</sub>Cl<sub>2</sub>) δ = 7.37 – 7.23 (m, 15H), 0.91 (d, *J* = 1.5 Hz, 21H) ppm. **<sup>13</sup>C NMR:** (126 MHz, CD<sub>2</sub>Cl<sub>2</sub>) δ = 144.4, 130.3, 128.3, 127.8, 102.8, 97.0, 71.8, 18.9, 11.9 ppm. **IR:** (ATR, cm<sup>-1</sup>) 3059, 2940, 2863, 2083, 1596, 1492, 1461, 1443, 995, 881, 854, 755, 735, 695, 671, 659, 631, 590. **HRMS:** calcd. for C<sub>30</sub>H<sub>36</sub>NaSSi<sup>+</sup> [M+Na]<sup>+</sup>: 479.2199; found (ESI): 479.2198.

#### 2-(Triisopropylsilyl)benzo[d]thiazolo[2,3-*b*]thiazol-4-ium-3-thiolate (**187**):

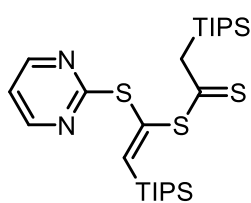


Following GP **B**, compound **187** (24.7 mg, 65 μmol, 22%) was obtained from benzo[d]thiazole-2-thiol (2 equiv, 100.4 mg, 0.6 mmol), **160d** (1 equiv, 162.7 mg, 0.3 mmol) and DIPEA (2 equiv, 78.8 mg, 106.3 μL, 0.61 mmol) in CH<sub>2</sub>Cl<sub>2</sub> (2 mL) after column chromatography (hexanes/EtOAc, 20:1) as colorless crystals.

**<sup>1</sup>H NMR:** (600 MHz, CDCl<sub>3</sub>) δ = 10.99 (dd, *J* = 8.6, 1.3 Hz, 1H), 7.82 – 7.78 (m, 1H), 7.62 (ddd, *J* = 8.5, 7.3, 1.6 Hz, 1H), 7.61 – 7.56 (m, 1H), 1.82 (h, *J* = 7.5 Hz, 3H), 1.23 (d, *J* = 7.5 Hz, 18H) ppm. **<sup>13</sup>C NMR:** (126 MHz, CDCl<sub>3</sub>) δ = 166.5, 160.3, 138.4, 133.0, 127.5, 126.5, 122.5, 119.8 (d, *J* = 15.8 Hz), 115.7, 19.3, 12.7 ppm. **IR:** (ATR, cm<sup>-1</sup>) 3076, 2944, 2865, 1676, 1568, 1462, 1426, 1310, 1234, 1187, 1043, 999, 853, 757, 660, 574. **HRMS:** calcd. for C<sub>18</sub>H<sub>26</sub>NS<sub>3</sub>Si<sup>+</sup> [M+H]<sup>+</sup>: 380.0991; found: 380.0995.

**(Z)-1-(Pyrimidin-2-ylthio)-2-(triisopropylsilyl)vinyl (188):**

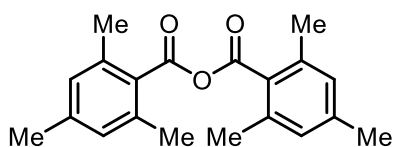
**2-(triisopropylsilyl)ethanedithioate**



Following the GP **B**<sup>28</sup>, compound **188** (4.6 mg, 8.5  $\mu$ mol, 3%) was obtained from pyrimidine-2-thiol (1 equiv, 33.65 mg, 0.3 mmol), **160d** (1 equiv, 162.7 mg, 0.3 mmol) and DIPEA (0.095 equiv, 3.6 mg, 4.9  $\mu$ L, 28  $\mu$ mol) in  $\text{CH}_2\text{Cl}_2$  (2 mL) after column chromatography (cyclohexane/EtOAc, 20:1) as brown crystals.

<sup>1</sup>H NMR: (600 MHz,  $\text{CDCl}_3$ )  $\delta$  = 8.47 (d,  $J$  = 4.8 Hz, 2H), 7.13 (s, 1H), 6.93 (t,  $J$  = 4.8 Hz, 1H), 3.04 (s, 2H), 1.34 – 1.24 (m, 3H), 1.18 – 1.12 (m, 4H), 1.10 (d,  $J$  = 7.5 Hz, 20H), 1.02 (d,  $J$  = 7.3 Hz, 18H) ppm. <sup>13</sup>C NMR: (126 MHz,  $\text{CDCl}_3$ )  $\delta$  = 232.4, 173.6, 159.6, 157.3, 139.1, 116.7, 41.4, 19.0, 18.8, 12.5, 11.6 ppm. IR: (ATR,  $\text{cm}^{-1}$ ) 2942, 2865, 1561, 1548, 1463, 1380, 1188, 912, 882, 671. HRMS: calcd. for  $\text{C}_{26}\text{H}_{49}\text{N}_2\text{S}_3\text{Si}_2^+$   $[\text{M}+\text{H}]^+$ : 541.2591; found: 541.2593.

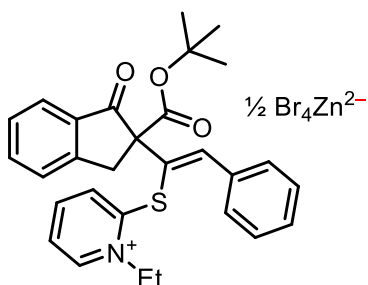
**2,4,6-Trimethylbenzoic anhydride (189):**



Following GP **B**, anhydride **189** was obtained in ca. 36% yield from 2,4,6-trimethylbenzoic acid (2 equiv, 98.5 mg, 0.6 mmol), **160d** (1 equiv, 162.7 mg, 0.3 mmol) and DIPEA (2 equiv, 78.8 mg, 106.3  $\mu$ L, 0.61 mmol) in  $\text{CH}_2\text{Cl}_2$  (2 mL) after column chromatography (pure cyclohexane, then cyclohexane/EtOAc, 200:1) as brown crystals.

<sup>1</sup>H NMR (300 MHz,  $\text{CDCl}_3$ )  $\delta$  = 6.88 (s, 4H), 2.40 (s, 12H), 2.29 (s, 6H) ppm.<sup>29</sup>

**(Z)-2-[[1-[2-(tert-Butoxycarbonyl)-1-oxo-2,3-dihydro-1H-inden-2-yl]-2-phenylvinyl]thio]-1-ethylpyridin-1-ium tetrabromozincate (190a):**



To a solution of *tert*-butyl 1-oxo-2,3-dihydro-1H-indene-2-carboxylate (1 equiv, 69.7 mg, 0.3 mmol) in dry  $\text{CH}_2\text{Cl}_2$  (2 mL), DIPEA (1 equiv, 77.6 mg, 54  $\mu$ L, 0.31 mmol) was added, and the solution was stirred for 5 min. Afterwards **160b** (0.8 equiv, 103.5 mg, 239  $\mu$ mol) was added. The reaction takes place instantly, and was quenched with sat. aqueous  $\text{NH}_4\text{Cl}$  solution and extracted with  $\text{CH}_2\text{Cl}_2$ . The organic layers were dried over

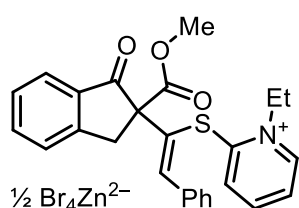
<sup>28</sup> Only catalytic amounts of the base were added.

<sup>29</sup> Analytical data are in agreement with the previously published ones: F. Kazemi, H. Shargi, M. A. Nasseri, *Synthesis* **2004**, 2, 205–207.

anhydrous Na<sub>2</sub>SO<sub>4</sub>, filtered, and all volatiles were removed *in vacuo*. The residue was carefully washed with EtOAc and purified by column chromatography (CH<sub>2</sub>Cl<sub>2</sub>/MeOH, 95:5). Compound **190** (137.9 mg, 207 μmol, 87%) was obtained as a pale beige oil.<sup>30</sup>

**<sup>1</sup>H NMR:** (400 MHz, CD<sub>2</sub>Cl<sub>2</sub>) δ = 9.91 – 9.83 (m, 1H), 7.99 (t, *J* = 7.8 Hz, 1H), 7.90 (dd, *J* = 8.5, 1.2 Hz, 1H), 7.79 (d, *J* = 7.7 Hz, 1H), 7.75 – 7.65 (m, 2H), 7.63 (s, 1H), 7.57 (d, *J* = 7.7 Hz, 1H), 7.48 (t, *J* = 7.5 Hz, 1H), 7.41 – 7.37 (m, 2H), 7.24 (d, *J* = 7.1 Hz, 3H), 4.89 (q, *J* = 7.0 Hz, 2H), 3.94 (d, *J* = 17.5 Hz, 1H), 3.57 (d, *J* = 17.5 Hz, 1H), 1.54 (t, *J* = 7.2 Hz, 3H), 1.39 (s, 9H) ppm. **<sup>13</sup>C NMR:** (126 MHz, CD<sub>2</sub>Cl<sub>2</sub>) δ = 198.6, 168.9, 156.7, 152.1, 147.9, 145.8, 143.3, 136.7, 135.2, 134.6, 130.2, 129.2, 129.0, 129.0, 127.5, 127.0, 125.9, 125.5, 124.6, 84.7, 69.3, 55.1, 39.7, 28.0, 15.4 ppm. **IR:** (ATR, cm<sup>-1</sup>) 1708, 1605, 1463, 1368, 1251, 1147, 839, 754, 695. **HRMS:** *calcd.* for C<sub>29</sub>H<sub>30</sub>NO<sub>3</sub>S<sup>+</sup> [M – ½ZnBr<sub>4</sub>]<sup>+</sup>: 472.1941; found (ESI): 472.1942.

**(Z)-1-Ethyl-2-[[1-[2-(methoxycarbonyl)-1-oxo-2,3-dihydro-1H-inden-2-yl]-2-phenylvinyl]-thio]pyridin-1-ium tetrabromozincate (**190b**):**



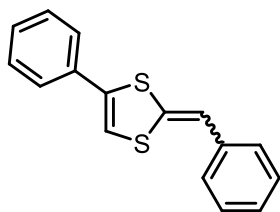
To a solution of methyl 1-oxo-2,3-dihydro-1H-indene-2-carboxylate (1 equiv, 65.5 mg, 0.35 mmol) in dry CH<sub>2</sub>Cl<sub>2</sub> (2 mL) was added DIPEA (1 equiv, 44.5 mg, 60 μl, 0.35 mmol), and the solution was stirred for 5 min to assure complete deprotonation. Afterwards **160b** (1.1 equiv, 167.9 mg, 0.39 mmol) was added. The reaction takes place instantly, and was quenched with sat. aqueous NH<sub>4</sub>Cl solution and extracted with CH<sub>2</sub>Cl<sub>2</sub>. The organic layers were dried over anhydrous Na<sub>2</sub>SO<sub>4</sub>, filtered, and all volatiles were removed *in vacuo*. The residue was carefully washed with EtOAc, leaving the pure product **190b** as a brown oil (155.4 mg, 0.25 mmol, 71%).<sup>31</sup>

**<sup>1</sup>H NMR:** (500 MHz, CDCl<sub>3</sub>) δ = 9.65 (d, *J* = 5.8 Hz, 1H), 8.00 (t, *J* = 7.6 Hz, 1H), 7.84 (d, *J* = 8.2 Hz, 2H), 7.80 (d, *J* = 7.7 Hz, 1H), 7.69 (t, *J* = 7.1 Hz, 1H), 7.63 (s, 1H), 7.60 (d, *J* = 7.7 Hz, 1H), 7.45 (t, *J* = 7.5 Hz, 1H), 7.38 (d, *J* = 6.6 Hz, 2H), 7.24 – 7.20 (m, 3H), 4.88 (q, *J* = 7.2 Hz, 2H), 4.01 (d, *J* = 17.6 Hz, 1H), 3.72 (s, 3H), 3.60 (d, *J* = 17.6 Hz, 1H), 1.54 (t, *J* = 7.1 Hz, 3H) ppm. **<sup>13</sup>C NMR:** (126 MHz, CDCl<sub>3</sub>) δ = 198.1, 170.1, 154.9, 151.9, 148.5, 146.0, 143.1, 136.8, 134.4, 133.8, 130.0, 128.9, 128.7 (2C), 127.0, 126.5, 125.4, 125.2, 124.5, 68.1, 55.2, 53.9, 39.3, 15.3 ppm. **IR:** (ATR, cm<sup>-1</sup>) 3053, 2360, 1607, 1564, 1488, 1461, 1431, 1149, 1113, 770, 753, 689, 517 **MS:** *calcd.* for C<sub>26</sub>H<sub>24</sub>NO<sub>3</sub>S<sup>+</sup> [M – ½ZnBr<sub>4</sub>]<sup>+</sup> 430.1471; found: 430.1.

<sup>30</sup> 2D-NMR experiments gave the absolute configuration of the product.

<sup>31</sup> 2D-NMR Experiments gave the absolute configuration of the product.

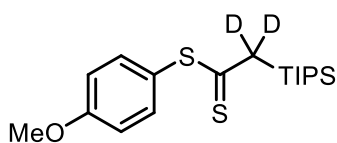
#### (*E/Z*)-2-Benzylidene-4-phenyl-1,3-dithiole (**191**):



TBAF (1 equiv., 400  $\mu$ L of a 1 N solution in THF, 0.4 mmol) was added to a solution of **160b** (1 equiv., 174.0 mg, 0.4 mmol) in  $\text{CH}_2\text{Cl}_2$  (2.5 mL). An instant color change to orange-red was observed. After stirring for 10 min, the reaction was quenched with saturated aqueous  $\text{NH}_4\text{Cl}$  solution (2.5 mL), and the aqueous phase was extracted three times with  $\text{CH}_2\text{Cl}_2$ . The combined organic phases were dried with  $\text{Na}_2\text{SO}_4$ , filtered, and the solvent was removed *in vacuo*. After purification by column chromatography (petrol ether/EtOAc, 50:1 to 20:1), compound **191** (73 mg, 0.27 mmol, 68%) was isolated as a colorless solid, approximately 1:1 (*E/Z*)-isomeric mixture.<sup>32</sup>

**$^1\text{H}$  NMR:** (300 MHz,  $\text{CDCl}_3$ )  $\delta$  = 7.49 – 7.26 (m, 20H), 7.21 – 7.13 (m, 2H), 6.61 (d,  $J$  = 1.4 Hz, 1H), 6.54 (s, 1H), 6.52 (s, 1H), 6.45 (d,  $J$  = 1.5 Hz, 1H) ppm.  **$^{13}\text{C}$  NMR:** (126 MHz,  $\text{CDCl}_3$ )  $\delta$  = 136.8, 135.5, 135.2, 134.3/134.1, 132.7/132.2, 130.6, 128.9, 128.6, 128.5, 128.4, 126.7, 126.3, 126.3, 125.7, 125.6, 113.7/113.3, 111.9/111.8 ppm. **HRMS:** *calcd.* for  $\text{C}_{16}\text{H}_{12}\text{S}_2^+$   $[\text{M}]^+$ : 268.0375; found (ESI): 268.0375.

#### 4-Methoxyphenyl 2,2-dideuterio-2-(triisopropylsilyl)ethanedithioate (**192**):



To an oven dried schlenk flask the transfer reagent **160d** (1 equiv, 162.7 mg, 0.3 mmol) was added, and the schlenk flask was evacuated and flushed with  $\text{N}_2$  three times. Dry acetonitrile (2 mL) was added followed by *S*-deuterio-*p*-methoxythiophenol (2 equiv, 84.7 mg, 74.9  $\mu$ L, 0.6 mmol) under stirring. After this, DIPEA (1 equiv, 77.6 mg, 54  $\mu$ L, 0.31 mmol) was added and the reaction mixture was stirred at ambient temperature under progress monitoring by TLC. After completion of the reaction, the solvent was removed *in vacuo* and the product **192** (64.9 mg, 0.182 mmol, 61%) was isolated as a yellow oil after separation by column chromatography (cyclohexane/EtOAc, 100:1).

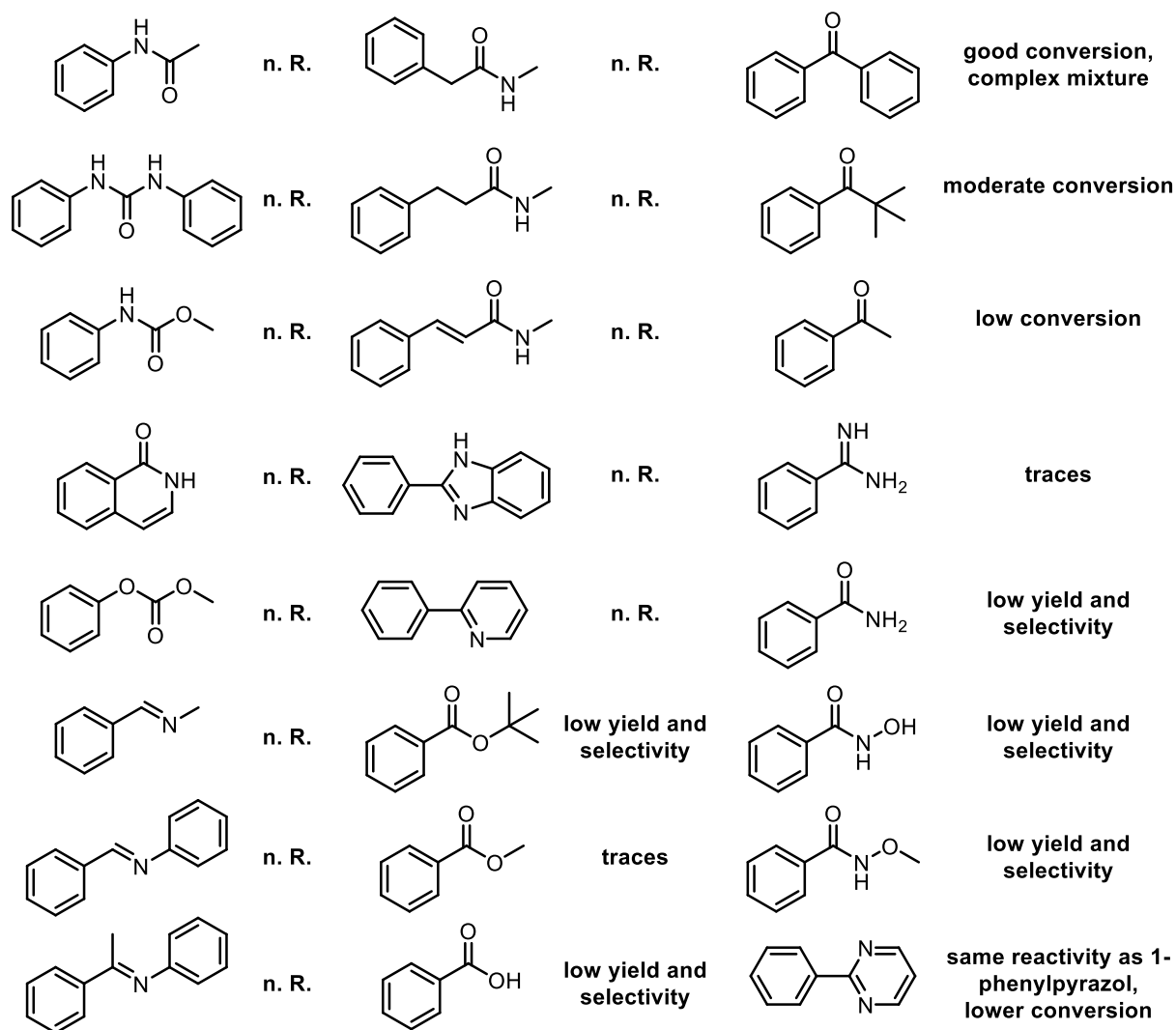
**$^1\text{H}$  NMR:** (300 MHz,  $\text{CDCl}_3$ )  $\delta$  = 7.28 (d,  $J$  = 8.6 Hz, 2H), 6.98 (d,  $J$  = 8.7 Hz, 2H), 3.85 (s, 3H), 3.25 (s, 0.1H), 3.22 (s, 0.27H), 1.40 – 1.24 (m, 3H), 1.15 (d,  $J$  = 7.1 Hz, 18H) ppm.  **$^{13}\text{C}$  NMR:** (101 MHz,  $\text{CDCl}_3$ )  $\delta$  = 237.9, 161.2, 136.7, 123.4 (d,  $J$  = 2.6 Hz), 115.1, 55.5, 18.8, 11.6 (d,  $J$  = 1.4 Hz) ppm. **IR:** (ATR,  $\text{cm}^{-1}$ ) 2940, 2864, 1591, 1494, 1461, 1293, 1250, 1183, 1173, 1068, 1032, 964, 882, 824, 770, 670, 638, 527. **HRMS:** *calcd.* for  $\text{C}_{18}\text{H}_{29}\text{D}_2\text{OS}_2\text{Si}^+$   $[\text{M}+\text{H}]^+$ : 357.1706; found (ESI): 357.1703.

<sup>32</sup> Analytical data are in agreement with the previously published ones: (a) U. Timm, U. Merkle, H. Meier, *Chem. Ber.* **1980**, *113*, 2519–2529; (b) K. Naka, A. Gelover-Santiago, Y. Chujo, *J. Polym. Sci. A* **2004**, *42*, 5872–5876.

## TOPIC: “C–H ACTIVATION UTILIZING THIOIMIDAZOLONE-BASED ELECTROPHILIC TRANSFER REAGENTS”

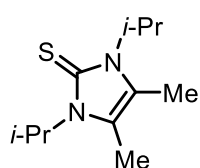
### NON- AND LOW REACTIVE SUBSTRATES

Substrates containing various directing groups were investigated; the ones performing below our expectations are shown in Scheme **101** with short remarks.



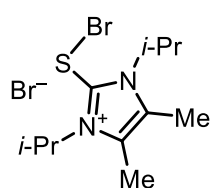
Scheme **101**: Investigated non-reactive substrates and substrates with low reactivity (n. R. = no reaction).

### 1,3-Diisopropyl-4,5-dimethyl-1,3-dihydro-2H-imidazole-2-thione (**150**):



Following literature procedure,<sup>33</sup> acetoin (20.89 g, 20.68 mL, 237.1 mmol) was added to a stirred solution of diisopropylthiourea (38.00 g, 237.1 mmol) in 1-hexanol (225 mL), and the reaction mixture was stirred at 158 °C for 12 h. Subsequently, the solution was cooled down to room temperature, and the solid formed was filtered off and washed with cold ethanol to afford compound **150** (37.20 g, 175.2 mmol, 73%) as a white solid.<sup>33</sup>

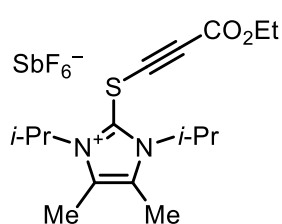
### 2-(Bromothio)-1,3-diisopropyl-4,5-dimethyl-1H-imidazol-3-ium bromide (**151a**):



Following literature procedure, to a stirred solution of compound **150** (20.13 g, 94.79 mmol) in dry CH<sub>2</sub>Cl<sub>2</sub> (100 mL), bromine (15.15 g, 4.9 mL, 94.79 mmol) was added at 0 °C, and the reaction mixture was allowed to warm up to rt over a period of 3 h. After removal of all volatiles under vacuum, compound **151a** (33.05 g, 88.8 mmol, 94%) was obtained as an orange crystalline solid.<sup>33</sup>

<sup>1</sup>H NMR: (400 MHz, CDCl<sub>3</sub>) δ = 5.64 (hept, *J* = 7.1 Hz, 2H), 2.36 (s, 6H), 1.66 (d, *J* = 7.1 Hz, 12H) ppm. <sup>13</sup>C NMR: (101 MHz, CDCl<sub>3</sub>) δ = 145.7, 128.3, 53.6, 20.5, 10.7 ppm.

### 2-[(3-Ethoxy-3-oxoprop-1-yn-1-yl)thio]-1,3-diisopropyl-4,5-dimethyl-1H-imidazol-3-ium hexafluoroantimonate (**59**):



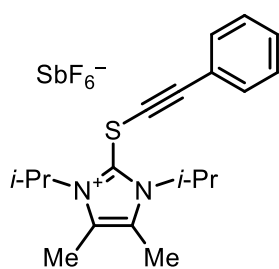
Following a literature procedure,<sup>33</sup> compound **59** was prepared from dibromide **151a** (1.67 g, 4.49 mmol), silver acetylide of ethyl propiolate (0.92 g, 4.49 mmol) in dry DCM (20 mL) maintaining rt with a water bath (note: the reaction is slightly exothermic and may cause DCM to boil). After 5 min, NaSbF<sub>6</sub> (2.32 g, 8.97 mmol) was added, and the reaction mixture stirred vigorously for another 5 min. Silver salts were then filtered off and the solvent removed under vacuum. The remaining solid was washed twice with diethyl ether to afford compound **59** as a pale yellow solid (2.25 g, 4.13 mmol, 92%).<sup>33</sup>

<sup>33</sup> Analytical data were identical to the previously published ones: G. Talavera, J. Peña, M. Alcarazo, *J. Am. Chem. Soc.*, **2015**, *137*, 8704–8707.

### General Procedure C (GP C) for the synthesis of alkynylthioimidazolium transfer reagents:

In a Schlenk flask, *n*-BuLi (1.6 M/2.5 M in hexanes, 1.1 equiv.) was added to a stirred solution of the corresponding terminal alkyne (1.1 equiv.) in THF (10 mL) at  $-78^{\circ}\text{C}$ . After letting the reaction mixture to warm up to room temperature over 2 h, the formed lithium acetylide solution was re-cooled to  $-78^{\circ}\text{C}$  and treated with an ice-cold solution of  $\text{ZnBr}_2$  (1.1 equiv.) in THF (1 M). The reaction mixture was stirred for an additional 1 h at this temperature to ensure the formation of the organozinc derivative, then slowly added to a solution of **151** (1 equiv.) in THF at  $-78^{\circ}\text{C}$ . After 30 minutes at this temperature, the reaction was allowed to warm up to room temperature by removing the cool bath. Upon this, **151** was slowly consumed. Successively an aqueous solution of  $\text{NaSbF}_6$  (3 equiv.) was added, and the reaction mixture was transferred to a separation funnel. The organic phase was separated, and the aqueous phase was extracted two more times with either EtOAc or DCM. The combined organic phases were dried, and the solvent was removed in vacuo. DCM was added, the solution was filtered through a plug of celite and washed two more times with DCM. The solvent was removed again, and the final product was obtained as a white to off-white solid, either directly or after crystallizing with  $\text{Et}_2\text{O}$ . In several cases, a final washing with *n*-pentane is necessary to solidify the product. If the anion exchange did not proceed completely, as detected by ESI-MS, it has to be repeated. Further purification is possible by column chromatography ( $\text{CH}_2\text{Cl}_2$  to  $\text{CH}_2\text{Cl}_2/\text{acetone}$ , 20:1); however, in this case yields dropped.

### 1,3-Diisopropyl-4,5-dimethyl-2-[(phenylethynyl)thio]-1*H*-imidazol-3-ium hexafluoroantimonate (**197**):

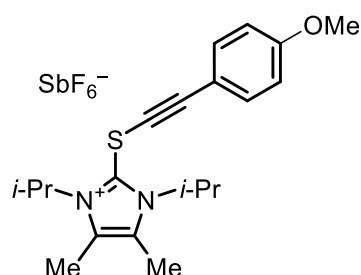


Following GP C, from phenylacetylene (3.27 g, 3.5 mL, 32 mmol), *n*-BuLi (1 equiv, 2.5 M, 12.8 mL, 32 mmol),  $\text{ZnBr}_2$  (7.1 g, 31.5 mmol), **151a** (11.1 g, 30 mmol) and  $\text{NaSbF}_6$  (24.84 g, 96 mmol), compound **197** (15.1 g, 27.5 mmol, 92%) was obtained as a pale white solid.<sup>34</sup>

**$^1\text{H}$  NMR:** (300 MHz,  $\text{CDCl}_3$ )  $\delta$  = 7.45 – 7.29 (m, 5H), 5.26 (hept,  $J$  = 6.8 Hz, 3H), 2.40 (s, 6H), 1.71 (d,  $J$  = 7.1 Hz, 12H) ppm.

<sup>34</sup> Analytical data are in agreement with the previously published ones: J. Peña, G. Talavera, B. Waldecker, M. Alcarazo, *Chem. Eur. J.* **2017**, 23, 75–78

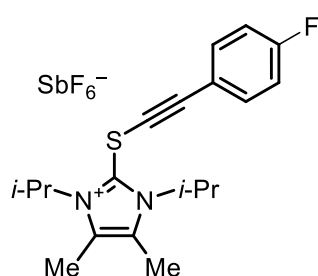
**1,3-Diisopropyl-2-[[4-methoxyphenyl]ethynyl]thio}-4,5-dimethyl-1*H*-imidazol-3-ium hexafluoroantimonate (**198**):**



Following GP **C**, from 1-ethynyl-4-methoxybenzene (519  $\mu$ L, 4 mmol), *n*-BuLi (2.5 M, 1.7 mL, 4.2 mmol), ZnBr<sub>2</sub> (945 mg, 4.2 mmol), **151a** (1.5 g, 4 mmol) and NaSbF<sub>6</sub> (3.1 g, 12 mmol), compound **198** (2.1 g, 3.6 mmol, 89%) was obtained as a pale grey powder.<sup>35</sup>

**<sup>1</sup>H NMR:** (300 MHz CDCl<sub>3</sub>)  $\delta$  = 7.37 (d, *J* = 9.0 Hz, 2H), 6.85 (d, *J* = 8.9 Hz, 2H), 5.27 (hept, *J* = 7.6, 7.1 Hz, 2H), 3.81 (s, 3H), 2.41 (s, 6H), 1.72 (d, *J* = 7.0 Hz, 12H) ppm. **<sup>13</sup>C NMR:** (75 MHz, CDCl<sub>3</sub>)  $\delta$  = 161.4, 134.4, 131.1, 114.5, 112.6, 96.1, 68.0, 55.6, 54.0, 21.3, 10.5 ppm.

**2-[[4-Fluorophenyl]ethynyl]thio}-1,3-diisopropyl-4,5-dimethyl-1*H*-imidazol-3-ium hexafluoroantimonate (**199**):**



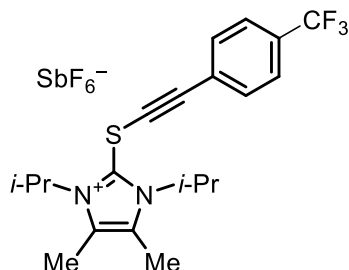
Following GP **C**, from 1-ethynyl-4-fluorobenzene (956.2 mg, 912.4  $\mu$ L, 7.96 mmol), *n*-BuLi (1.6 M, 5.2 mL, 8.32 mmol), ZnBr<sub>2</sub> (1.88 g, 8.36 mmol), **151a** (2.6676 g, 7.168 mmol) and NaSbF<sub>6</sub> (5.5639 g, 21.50 mmol), compound **199** (3.741 g, 6.60 mmol, 92%) was obtained as an orange solid.

**<sup>1</sup>H NMR:** (300 MHz, CDCl<sub>3</sub>)  $\delta$  = 7.42 (dd, *J* = 8.9, 5.2 Hz, 2H), 7.03 (t, *J* = 8.7 Hz, 2H), 5.37 – 5.18 (m, 2H), 2.42 (s, 6H), 1.72 (d, *J* = 7.0 Hz, 12H) ppm. **<sup>1</sup>H NMR:** (300 MHz, CD<sub>3</sub>CN)  $\delta$  = 7.51 (dd, *J* = 9.0, 5.4 Hz, 2H), 7.14 (t, *J* = 8.9 Hz, 2H), 5.26 (dt, *J* = 13.8, 6.8 Hz, 2H), 2.37 (s, 6H), 1.65 (d, *J* = 7.1 Hz, 12H) ppm. **<sup>13</sup>C NMR:** (75 MHz, CDCl<sub>3</sub>)  $\delta$  = 165.33, 161.98, 134.62 (d, *J* = 8.7 Hz), 131.39, 116.92 (d, *J* = 3.5 Hz), 116.29 (d, *J* = 22.3 Hz), 94.42, 69.87, 54.04, 21.38, 10.72 ppm. **<sup>19</sup>F NMR:** (300 MHz, CDCl<sub>3</sub>)  $\delta$  = –107.14 ppm. **IR:** (ATR, cm<sup>–1</sup>) 2987, 2941, 2172, 1614, 1598, 1502, 1456, 1410, 1374, 1219, 1159, 1113, 843, 795, 639, 535. **HRMS:** calcd. for C<sub>19</sub>H<sub>24</sub>FN<sub>2</sub>S<sup>+</sup> [M–SbF<sub>6</sub>]<sup>+</sup> = 331.1636; found: 331.1639.

<sup>35</sup> Analytical data are in agreement with the previously published ones: J. Peña, G. Talavera, B. Waldecker, M. Alcarazo, *Chem. Eur. J.* **2017**, *23*, 75–78

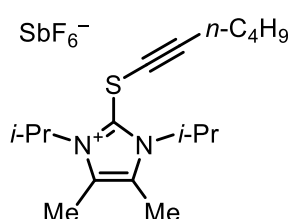


**1,3-Diisopropyl-4,5-dimethyl-2-[[4-(trifluoromethyl)phenyl]ethynyl]thio]-1H-imidazol-3-ium hexafluoroantimonate (**200**):**



Following GP C, from 1-ethynyl-4-(trifluoromethyl)benzene (2.04 g, 1.96 mL, 12 mmol), *n*-BuLi (2.5 M, 4.8 mL, 12 mmol), ZnBr<sub>2</sub> (2.75 g, 12 mmol), **151a** (3.8 g, 10 mmol) and NaSbF<sub>6</sub> (7.06 g, 27 mmol), compound **200** (6.16 g, 10 mmol, 99%) was obtained as a pale orange solid.<sup>35</sup>

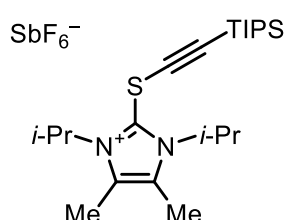
**2-(Hex-1-yn-1-ylthio)-1,3-diisopropyl-4,5-dimethyl-1H-imidazol-3-ium hexafluoroantimonate (**201**):**



Following GP C, from hex-1-yne (1.2 equiv, 985.7 mg, 1.38 mL, 12 mmol), *n*-BuLi (1.2 equiv, 2.5 M, 4.8 mL, 12 mmol), ZnBr<sub>2</sub> (1.2 equiv, 2.70 g, 12 mmol), **151a** (1 equiv, 3.72 g, 10 mmol) and NaSbF<sub>6</sub> (3 equiv, 7.76 g, 30 mmol), compound **201** (4.9 g, 9.3 mmol, 93%) was obtained as a pale, off-white solid.

**<sup>1</sup>H NMR:** (400 MHz, CDCl<sub>3</sub>) δ = 5.27 – 5.12 (m, 2H), 2.39 (s, 6H), 2.29 (t, *J* = 7.1 Hz, 2H), 1.67 (d, *J* = 7.1 Hz, 12H), 1.53 – 1.42 (m, 2H), 1.41 – 1.30 (m, 2H), 0.88 (t, *J* = 7.3 Hz, 3H) ppm. **<sup>13</sup>C NMR:** (101 MHz, CDCl<sub>3</sub>) δ = 131.0, 98.6, 59.6, 53.8, 30.0, 22.0, 21.2, 19.6, 13.5, 10.4 ppm. **<sup>19</sup>F NMR:** (376 MHz, CDCl<sub>3</sub>) δ = –106.97 to –147.46 (m) ppm. **IR:** (ATR, cm<sup>–1</sup>) 2959, 2935, 2873, 1617, 1456, 1380, 1219, 1140, 1116, 908, 750, 653. **HRMS:** calcd. for C<sub>17</sub>H<sub>29</sub>N<sub>2</sub>S<sup>+</sup> [M–SbF<sub>6</sub>]<sup>+</sup>: 293.2046; found: 293.2049.

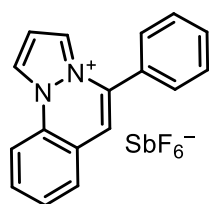
**1,3-Diisopropyl-4,5-dimethyl-2-[[triisopropylsilyl]ethynyl]thio]-1H-imidazol-3-ium hexafluoroantimonate (**202**):**



Following GP C, from ethynyltriisopropylsilane (1.2 equiv, 2.19 g, 2.7 mL, 12 mmol), *n*-BuLi (1.2 equiv, 2.5 M, 4.8 mL, 12 mmol), ZnBr<sub>2</sub> (1.1 equiv, 2.5 g, 11.1 mmol), **151a** (3.72 g, 10 mmol) and NaSbF<sub>6</sub> (3 equiv, 7.762 g, 30 mmol), compound **202** (5.212 g, 8.28 mmol, 83%) was obtained as a white solid.

**<sup>1</sup>H NMR:** (500 MHz, CDCl<sub>3</sub>) δ = 5.21 (brs, 2H), 2.41 (s, 6H), 1.69 (d, *J* = 7.1 Hz, 12H), 1.09 – 0.99 (m, 21H) ppm. **<sup>13</sup>C NMR:** (126 MHz, CDCl<sub>3</sub>) δ = 131.3, 130.2, 102.4, 84.7, 77.2, 54.0, 21.2, 18.5, 11.2, 10.5 ppm. **IR:** (ATR, cm<sup>–1</sup>) 2946, 2870, 1459, 1377, 1216, 1113, 881, 838, 653, 590. **HRMS:** calcd. for C<sub>22</sub>H<sub>41</sub>N<sub>2</sub>SSi<sup>+</sup> [M–SbF<sub>6</sub>]<sup>+</sup>: = 393.2754; found: 393.2750.

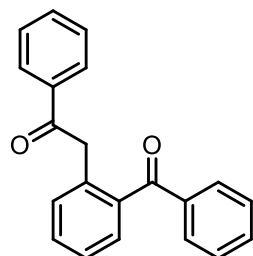
### 5-Phenylpyrazolo[1,2-*a*]cinnolin-4-ium hexafluoroantimonate (**203**):



A pressure vial was charged with  $[\text{RhCp}^*\text{Cl}_2]_2$  (5 mol%, 6.2 mg, 10  $\mu\text{mol}$ ),  $\text{Cu}(\text{OAc})_2$  (0.5 equiv., 18.1 mg, 0.1 mmol), 1-phenylpyrazol (1 equiv, 28.8 mg, 26.4  $\mu\text{L}$ , 0.2 mmol), **197** (1.1 equiv, 120.6 mg, 219.5  $\mu\text{mol}$ ), and finally  $\text{AgSbF}_6$  (1.1 equiv., 75.6 mg, 2.2 mmol). The vial was sealed and flushed with 3  $\text{N}_2$ /Vacuum-Cycles. 1,2-Dichloroethane (2 mL) was added via syringe, and the reaction was stirred for 20 h at 80  $^\circ\text{C}$ . After letting the reaction mixture cool down to room temperature, the solution was diluted with acetonitrile (6 mL), and supernatant phase was filtered through a pad of celite. The operation was repeated twice. Subsequently the organic solvents were removed *in vacuo*. Separation by column chromatography ( $\text{CH}_2\text{Cl}_2$ /acetone, 100:1 to 20:1) gave the salt **203** as pale yellow crystals (50 mg, 103.9  $\mu\text{mol}$ , 52%).

**$^1\text{H}$  NMR:** (400 MHz,  $\text{CD}_3\text{CN}$ )  $\delta$  = 9.25 (d,  $J$  = 3.2 Hz, 1H), 8.43 (d,  $J$  = 3.2 Hz, 1H), 8.26 (d,  $J$  = 8.4 Hz, 1H), 7.94 (dd,  $J$  = 7.9, 1.4 Hz, 1H), 7.90 (ddd,  $J$  = 8.7, 7.4, 1.5 Hz, 1H), 7.78 (td,  $J$  = 7.6, 1.1 Hz, 1H), 7.71 (d,  $J$  = 2.7 Hz, 5H), 7.39 – 7.34 (m, 2H) ppm.  **$^{13}\text{C}$  NMR:** (151 MHz,  $\text{DMSO}-d_6$ )  $\delta$  = 134.0, 131.3, 131.1, 130.1, 129.5, 129.5, 129.4, 129.2, 129.0, 128.7, 128.5, 120.6, 115.6, 114.6, 110.5 ppm. **IR:** (ATR,  $\text{cm}^{-1}$ ) 3150, 2359, 1507, 1465, 1437, 1353, 1296, 1118, 860, 768, 648. **HRMS:** calcd. for  $\text{C}_{17}\text{H}_{13}\text{N}_2^+$  [ $\text{M}-\text{SbF}_6$ ] $^+$  = 245.1073; found: 245.1079.

### 2-(2-Benzoylphenyl)-1-phenylethan-1-one (**204**):



A pressure vial was charged with  $[\text{RhCp}^*\text{Cl}_2]_2$  (10 mol%, 6.2 mg, 10  $\mu\text{mol}$ ),  $\text{Cu}(\text{OAc})_2$  (0.5 equiv., 10 mg, 50  $\mu\text{mol}$ ), benzophenone (1 equiv, 18.2 mg, 100  $\mu\text{mol}$ ), **197** (1.2 equiv, 65.9 mg, 120  $\mu\text{mol}$ ), and finally  $\text{AgSbF}_6$  (1.2 equiv, 41.2 mg, 120  $\mu\text{mol}$ ). The vial was sealed and flushed with 3  $\text{N}_2$ /Vacuum-Cycles. 1,2-Dichloroethane (2 mL) was added via syringe, and the reaction was stirred for 24 h at 80  $^\circ\text{C}$ . After letting the reaction mixture cool down to room temperature, the solution was diluted with acetonitrile (6 mL), and supernatant phase was filtered through a pad of celite. The operation was repeated twice. Subsequently the organic solvents were removed *in vacuo*.<sup>36</sup>

**$^1\text{H}$  NMR:** (400 MHz,  $\text{DMSO}-d_6$ )  $\delta$  = 7.94 (dd,  $J$  = 8.2, 1.1 Hz, 2H), 7.69 (dd,  $J$  = 8.2, 1.3 Hz, 2H), 7.67 – 7.36 (m, 10H), 4.65 (s, 2H) ppm.  **$^{13}\text{C}$  NMR:** (126 MHz,  $\text{DMSO}-d_6$ )  $\delta$  = 197.4, 196.8, 137.9, 137.4, 136.4, 134.9, 133.2, 133.0, 132.5, 130.9, 129.9, 129.7, 128.7, 128.4, 128.0, 126.3, 42.8 ppm.

<sup>36</sup>Analytical data are in agreement with the previously published ones H. Yoshida, M. Watanabe, J. Ohshita, A. Kunai, *Chem. Commun.* **2005**, 3292–3294.

### General Procedure D (GP D) for the alkynylation, cyclization of *N*-methylbenzamides

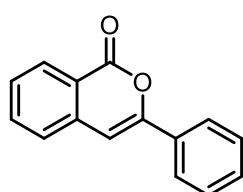
A pressure vial was charged with [RhCp\*Cl<sub>2</sub>]<sub>2</sub> (2.5 mol%, 4.6 mg, 7.44 μmol), NaOAc (1 equiv, 24.3 mg, 0.3 mmol), substrate, (1 equiv, 0.3 mmol), reagent **197**, **198** or **199** (1.5 equiv, 0.45 mmol) and finally AgSbF<sub>6</sub> (1.7 equiv, 175.2 mg, 0.51 mmol). The vial was sealed and flushed three times using N<sub>2</sub>/Vacuum-Cycles. 1,2-Dichloroethane (2 mL) was added via syringe, and the reaction mixture was stirred at room temperature for 20 h, unless otherwise stated.

For work-up, the reaction mixture was diluted with acetonitrile (6 mL), and supernatant phase was filtered through a pad of celite. The operation was repeated twice. Subsequently the organic solvents were removed *in vacuo*.

For hydrolysis, THF (15 mL) and HCl (1 M, 3 mL) were added to the crude residue, and the reaction mixture was stirred under reflux (69 °C) for 3 h, unless otherwise specified.

Afterwards a solution of saturated aqueous NaHCO<sub>3</sub> was added until the aqueous phase showed neutral pH. The aqueous phase was then extracted with EtOAc (3 × 20 mL), and the combined organic phases were dried over Na<sub>2</sub>SO<sub>4</sub>. The solvent was removed *in vacuo* and the final product was obtained after separation by column chromatography (pure DCM, unless otherwise mentioned).

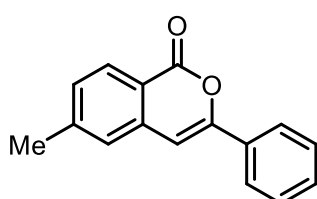
### 3-Phenyl-1*H*-isochromen-1-one (Homalicine, **207**):



Following GP **D**, from *N*-methylbenzamide (1 equiv, 40.6 mg, 0.3 mmol), **197** (1.5 equiv, 247.2 mg, 0.45 mmol), [RhCp\*Cl<sub>2</sub>]<sub>2</sub> (2.5 mol%, 4.6 mg, 7.44 μmol), NaOAc (1 equiv, 24.3 mg, 0.3 mmol), and AgSbF<sub>6</sub> (1.7 equiv, 175.2 mg, 0.51 mmol), compound **207** (46.7 mg, 210 μmol, 70%) was obtained as a white solid.

**<sup>1</sup>H NMR:** (300 MHz, CDCl<sub>3</sub>) δ = 8.32 (dd, *J* = 8.2, 0.9 Hz, 1H), 7.90 (dd, *J* = 8.0, 1.7 Hz, 2H), 7.77 – 7.69 (m, 1H), 7.55 – 7.42 (m, 6H), 6.97 (s, 1H) ppm. **<sup>13</sup>C NMR:** (126 MHz, CDCl<sub>3</sub>) δ = 162.3, 153.7, 137.6, 134.9, 132.1, 130.0, 129.7, 128.9, 128.2, 126.0, 125.3, 120.7, 101.9 ppm. **IR:** (ATR, cm<sup>-1</sup>) 2972, 1734, 1635, 1344, 1086, 1045, 878, 769, 693. **HRMS:** calcd. for C<sub>15</sub>H<sub>11</sub>O<sub>2</sub><sup>+</sup> [M+H]<sup>+</sup>: 223.0757; found: 223.0754.

### 6-Methyl-3-phenyl-1*H*-isochromen-1-one (**208**):

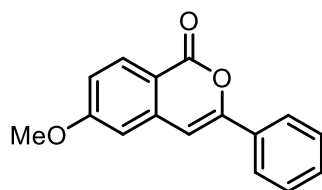


Following GP **D**, from *N*-methyl-*p*-toluamide (1 equiv, 44.8 mg, 0.3 mmol), **197** (1.5 equiv, 247.2 mg, 0.45 mmol), [RhCp\*Cl<sub>2</sub>]<sub>2</sub> (2.5 mol%, 4.6 mg, 0.0075 mmol), NaOAc (1 equiv, 24.3 mg, 0.3 mmol), and AgSbF<sub>6</sub> (1.7 equiv, 175.2 mg, 0.51 mmol), compound **208** (48.0

mg, 203  $\mu\text{mol}$ , 68%) was obtained as a white crystalline solid.

**$^1\text{H}$  NMR:** (400 MHz,  $\text{CDCl}_3$ )  $\delta$  = 8.19 (d,  $J$  = 8.0 Hz, 1H), 7.87 (d,  $J$  = 7.3 Hz, 2H), 7.45 (q,  $J$  = 8.9, 7.8 Hz, 3H), 7.34 – 7.27 (m, 2H), 6.89 (s, 1H), 2.48 (s, 3H) ppm.  **$^{13}\text{C}$  NMR:** (101 MHz,  $\text{CDCl}_3$ )  $\delta$  = 162.5, 153.8, 146.1, 137.8, 132.2, 130.0, 129.8, 129.7, 128.9, 126.1, 125.4, 118.3, 101.9, 22.1 ppm. **IR:** (ATR,  $\text{cm}^{-1}$ ): 2360, 2340, 1710, 1063, 1032, 897, 771, 756, 681, 641. **HRMS:** calcd. for  $\text{C}_{16}\text{H}_{13}\text{O}_2^+$   $[\text{M}+\text{H}]^+$ : 237.0910; found: 237.0914.

#### 6-Methoxy-3-phenyl-1*H*-isochromen-1-one (209):

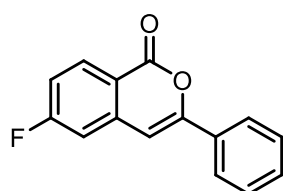


Following GP **D**, from 4-methoxy-*N*-methylbenzamide (1 equiv, 49.6 mg, 0.3 mmol), **197** (1.5 equiv, 247.2 mg, 0.45 mmol),  $[\text{RhCp}^*\text{Cl}_2]_2$  (2.5 mol%, 4.6 mg, 0.0075 mmol), NaOAc (0.5 equiv, 12.3 mg, 0.15 mmol), and  $\text{AgSbF}_6$  (1.7 equiv, 175.2 mg, 0.51 mmol), compound **209** (44.0 mg, 174.4  $\mu\text{mol}$ , 58%) was obtained

as a white solid.

**$^1\text{H}$  NMR:** (400 MHz,  $\text{CDCl}_3$ )  $\delta$  = 8.24 (d,  $J$  = 8.8 Hz, 1H), 7.89 (d,  $J$  = 7.4 Hz, 2H), 7.46 (q,  $J$  = 7.4 Hz, 3H), 7.04 (d,  $J$  = 8.8 Hz, 1H), 6.89 (d,  $J$  = 6.5 Hz, 2H), 3.94 (s, 3H) ppm.  **$^{13}\text{C}$  NMR:** (101 MHz,  $\text{CDCl}_3$ )  $\delta$  = 164.9, 162.2, 154.4, 140.0, 132.2, 132.1, 130.1, 129.0, 125.5, 116.7, 113.9, 108.1, 102.0, 77.2, 55.8 ppm. **IR:** (ATR,  $\text{cm}^{-1}$ ) 2926, 1717, 1601, 1489, 1260, 1029, 859, 769, 690, 611. **HRMS:** calcd. for  $\text{C}_{16}\text{H}_{13}\text{O}_3^+$   $[\text{M}+\text{H}]^+$ : 253.0859; found: 253.0859.

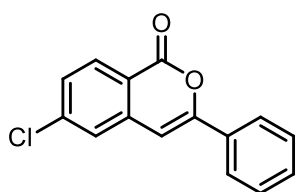
#### 6-Fluoro-3-phenyl-1*H*-isochromen-1-one (210):



Following GP **D**, from 4-fluoro-*N*-methylbenzamide (1 equiv, 45.9 mg, 0.3 mmol), **197** (1.5 equiv, 247.2 mg, 0.45 mmol),  $[\text{RhCp}^*\text{Cl}_2]_2$  (2.5 mol%, 4.6 mg, 0.0075 mmol), NaOAc (1 equiv, 24.3 mg, 0.3 mmol), and  $\text{AgSbF}_6$  (1.7 equiv, 175.2 mg, 0.51 mmol), compound **210** (47.4 mg, 197  $\mu\text{mol}$ , 66%) was obtained as a white solid.

**$^1\text{H}$  NMR:** (300 MHz,  $\text{CDCl}_3$ , 25  $^\circ\text{C}$ )  $\delta$  = 8.33 (dd,  $J$  = 8.7, 5.6 Hz, 1H), 7.93 – 7.84 (m, 2H), 7.54 – 7.41 (m, 3H), 7.23 – 7.12 (m, 2H), 6.91 (s, 1H). ppm.  **$^{13}\text{C}$  NMR:** (126 MHz,  $\text{CDCl}_3$ )  $\delta$  = 166.77 (d,  $J$  = 256.2 Hz), 161.36, 154.99, 140.29 (d,  $J$  = 10.8 Hz), 133.09 (d,  $J$  = 10.4 Hz), 131.67, 130.44, 128.97, 125.51, 117.11 (d,  $J$  = 2.2 Hz), 116.52 (d,  $J$  = 23.4 Hz), 111.59 (d,  $J$  = 22.6 Hz), 101.31 (d,  $J$  = 2.9 Hz) ppm.  **$^{19}\text{F}$  NMR:** (376 MHz,  $\text{CD}_3\text{Cl}$ , 25  $^\circ\text{C}$ )  $\delta$  = -101.85 (td,  $J$  = 8.6, 5.7 Hz) ppm. **IR:** (ATR,  $\text{cm}^{-1}$ ) 2925, 1717, 1617, 1483, 1453, 1257, 1063, 765, 686. **HRMS:** calcd. for  $\text{C}_{15}\text{H}_{10}\text{FO}_2^+$   $[\text{M}+\text{H}]^+$ : 241.0659; found: 241.0659.

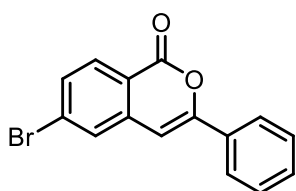
### 6-Chloro-3-phenyl-1*H*-isochromen-1-one (**211**):



Following GP **D**, from 4-chloro-*N*-methylbenzamide (1 equiv, 50.9 mg, 0.3 mmol), **197** (1.5 equiv, 247.2 mg, 0.45 mmol), [RhCp\*Cl<sub>2</sub>]<sub>2</sub> (2.5 mol%, 4.6 mg, 0.0075 mmol), NaOAc (1 equiv, 24.3 mg, 0.3 mmol), and AgSbF<sub>6</sub> (1.7 equiv, 175.2 mg, 0.51 mmol), compound **211** (31.2 mg, 122 μmol, 41%) was obtained as a white solid.

**<sup>1</sup>H NMR:** (300 MHz, CDCl<sub>3</sub>) δ= 8.24 (d, *J* = 8.4 Hz, 1H), 7.90 – 7.85 (m, 2H), 7.46 (m, 5H), 6.88 (s, 1H) ppm. **<sup>13</sup>C NMR:** (126 MHz, CDCl<sub>3</sub>) δ= 161.5, 155.0, 141.6, 139.0, 131.7, 131.4, 130.5, 129.0, 128.7, 125.5, 118.9, 100.9 ppm. **IR:** (ATR, cm<sup>-1</sup>) 3106, 3033, 2921, 1710, 1633, 1595, 1446, 1321, 1237, 1059, 893, 771, 755, 679, 641, 559, 532. **HRMS:** calcd. for C<sub>15</sub>H<sub>9</sub>ClO<sub>2</sub><sup>+</sup> [M]<sup>+</sup>: 256.0291; found (EI): =256.0293.

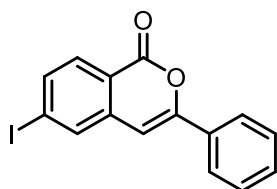
### 6-Bromo-3-phenyl-1*H*-isochromen-1-one (**212**):



Following GP **D**, from 4-bromo-*N*-methylbenzamide (0.97 equiv, 64.2 mg, 0.29 mmol), **197** (1.5 equiv, 247.2 mg, 0.45 mmol), [RhCp\*Cl<sub>2</sub>]<sub>2</sub> (2.5 mol%, 4.6 mg, 0.0075 mmol), NaOAc (1 equiv, 24.3 mg, 0.3 mmol), and AgSbF<sub>6</sub> (1.7 equiv, 175.2 mg, 0.51 mmol), compound **212** (45.2 mg, 150 μmol, 52%) was obtained as a white solid.

**<sup>1</sup>H NMR:** (400 MHz, CDCl<sub>3</sub>) δ= 8.16 (dt, *J* = 8.5, 0.6 Hz, 1H), 7.87 (dd, *J* = 7.9, 1.8 Hz, 2H), 7.67 (dd, *J* = 1.9, 0.5 Hz, 1H), 7.61 (dd, *J* = 8.5, 1.9 Hz, 1H), 7.52 – 7.44 (m, 3H), 6.87 (d, *J* = 0.7 Hz, 1H) ppm. **<sup>13</sup>C NMR:** (101 MHz, CDCl<sub>3</sub>) δ= 161.8, 155.1, 139.2, 131.8, 131.6, 131.5, 130.6, 130.5, 129.1, 128.7, 125.6, 119.3, 100.8 ppm. **IR:** (ATR, cm<sup>-1</sup>) 2956, 1772, 1720, 1181, 1064, 1037, 955, 925, 849, 563. **HRMS:** calcd. for C<sub>15</sub>H<sub>9</sub>BrO<sub>2</sub><sup>+</sup> [M]<sup>+</sup>: 299.9786; found (EI): 299.9786.

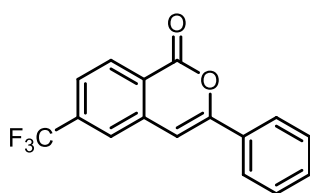
### 6-Iodo-3-phenyl-1*H*-isochromen-1-one (**213**):



Following GP **D**, from 4-iodo-*N*-methylbenzamide (1 equiv, 78.3 mg, 0.3 mmol), **197** (1.5 equiv, 247.2 mg, 0.45 mmol), [RhCp\*Cl<sub>2</sub>]<sub>2</sub> (2.5 mol%, 4.6 mg, 0.0075 mmol), NaOAc (1 equiv, 24.3 mg, 0.3 mmol), and AgSbF<sub>6</sub> (1.7 equiv, 175.2 mg, 0.51 mmol), compound **213** (29.8 mg, 85.5 μmol, 29%) was obtained as pale yellow crystals.

**<sup>1</sup>H NMR:** (300 MHz, CDCl<sub>3</sub>) δ= 7.99 (d, *J* = 8.3 Hz, 1H), 7.93 – 7.79 (m, 4H), 7.53 – 7.43 (m, 3H), 6.85 (s, 1H) ppm. **<sup>13</sup>C NMR:** (126 MHz, CDCl<sub>3</sub>) δ= 161.91, 154.84, 138.91, 137.29, 134.86, 131.71, 130.98, 130.45, 129.00, 125.47, 119.76, 103.35, 100.48 ppm. **IR:** (ATR, cm<sup>-1</sup>) 3417, 3106, 3030, 1698, 1552, 1449, 1313, 1235, 1053, 893, 769, 755, 679, 638, 541, 511. **HRMS:** calcd. for C<sub>15</sub>H<sub>10</sub>IO<sub>2</sub><sup>+</sup> [M+H]<sup>+</sup>: 348.9720; found: 348.9727.

### 3-Phenyl-6-(trifluoromethyl)-1*H*-isochromen-1-one (**214**):

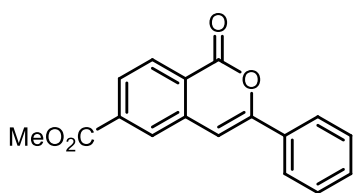


Following GP **D**<sup>37</sup>, from *N*-methyl-4-(trifluoromethyl)benzamide (1 equiv, 61.1 mg, 0.3 mmol), **197** (1.5 equiv, 247.2 mg, 0.45 mmol), [RhCp\*Cl<sub>2</sub>]<sub>2</sub> (2.5 mol%, 4.6 mg, 0.0075 mmol), NaOAc (1 equiv, 24.3 mg, 0.3 mmol), and AgSbF<sub>6</sub> (1.7 equiv, 175.2 mg, 0.51 mmol), compound **214** (36.1 mg, 124.3 μmol, 41%) was obtained as

colorless crystals.

**<sup>1</sup>H NMR:** (300 MHz, CDCl<sub>3</sub>) δ = 8.43 (dq, *J* = 8.3, 0.8 Hz, 1H), 7.93 – 7.87 (m, 2H), 7.78 (s, 1H), 7.71 (ddd, *J* = 8.2, 1.8, 0.7 Hz, 1H), 7.55 – 7.45 (m, 3H), 7.01 (s, 1H) ppm. **<sup>13</sup>C NMR:** (101 MHz, CDCl<sub>3</sub>) δ = 161.3, 155.3, 138.0, 136.5 (q, *J*<sub>C-F</sub> = 32.8 Hz), 131.5, 130.8, 130.7, 129.2, 125.6, 124.4 (q, *J*<sub>C-F</sub> = 3.4 Hz), 123.4 (q, *J*<sub>C-F</sub> = 273.2 Hz), 123.3 (q, *J*<sub>C-F</sub> = 3.9 Hz), 123.0, 101.2 ppm. **<sup>19</sup>F NMR:** (282 MHz, CDCl<sub>3</sub>) δ = -63.47 ppm. **IR:** (ATR, cm<sup>-1</sup>) 2954, 2925, 2853, 2162, 2020, 1714, 1341, 1170, 1121, 1060, 908, 762, 686. **HRMS:** calcd. for C<sub>16</sub>H<sub>10</sub>F<sub>3</sub>O<sub>2</sub> [M+H]<sup>+</sup>: 291.0627; found: 291.0627.

### Methyl 1-oxo-3-phenyl-1*H*-isochromene-6-carboxylate (**215**):

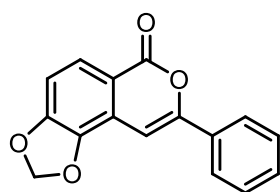


Following GP **D**, from methyl 4-(methylcarbamoyl)benzoate (1 equiv, 58.0 mg, 0.3 mmol), **197** (1.5 equiv, 247.2 mg, 0.45 mmol), [RhCp\*Cl<sub>2</sub>]<sub>2</sub> (2.5 mol%, 4.6 mg, 0.0075 mmol), NaOAc (0.5 equiv, 24.3 mg, 0.3 mmol), and AgSbF<sub>6</sub> (1.7 equiv, 175.2 mg, 0.51 mmol), compound **215** (29.1 mg, 103.8 μmol, 35%)

was obtained as bright yellow crystals.

**<sup>1</sup>H NMR:** (400 MHz, CDCl<sub>3</sub>) δ = 8.37 (dt, *J* = 8.2, 0.7 Hz, 1H), 8.19 (dd, *J* = 1.6, 0.5 Hz, 1H), 8.10 (dd, *J* = 8.3, 1.6 Hz, 1H), 7.91 – 7.86 (m, 2H), 7.52 – 7.43 (m, 3H), 7.01 (s, 1H), 3.99 (s, 3H) ppm. **<sup>13</sup>C NMR:** (101 MHz, CDCl<sub>3</sub>) δ = 166.0, 161.7, 154.6, 137.7, 135.9, 131.8, 130.5, 130.1, 129.1, 128.4, 127.7, 125.5, 123.5, 101.7, 52.9 ppm. **IR:** (ATR, cm<sup>-1</sup>) 3101, 1710, 1633, 1432, 1304, 1235, 1186, 1064, 963, 905, 748, 677, 641, 552, 527. **HRMS:** calcd. for C<sub>17</sub>H<sub>13</sub>O<sub>4</sub><sup>+</sup> [M+H]<sup>+</sup>: 281.0808; found: 281.0807.

### 8-Phenyl-6*H*-[1,3]dioxolo[4,5-*f*]isochromen-6-one (**216**):



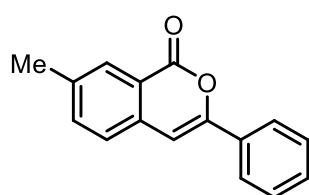
Following GP **D**, from *N*-Methyl-1,3-benzodioxole-5-carboxamide (1 equiv, 53.8 mg, 0.3 mmol), **197** (1.5 equiv, 247.2 mg, 0.45 mmol), [RhCp\*Cl<sub>2</sub>]<sub>2</sub> (2.5 mol%, 4.6 mg, 0.0075 mmol), NaOAc (1 equiv, 24.3 mg, 0.3 mmol), and AgSbF<sub>6</sub> (1.7 equiv, 175.2 mg, 0.51 mmol), compound **216** (42.6 mg, 160 μmol, 53%) was obtained as a white

<sup>37</sup> Reaction was run at 80 °C

amorphous solid after separation by column chromatography (pure CH<sub>2</sub>Cl<sub>2</sub> then CH<sub>2</sub>Cl<sub>2</sub>/EtOAc, 1:1).

**<sup>1</sup>H NMR:** (300 MHz, CDCl<sub>3</sub>) δ = 7.93 (dd, *J* = 8.4, 0.7 Hz, 1H), 7.90 – 7.83 (m, 2H), 7.50 – 7.41 (m, 3H), 7.01 – 6.92 (m, 2H), 6.18 (s, 2H) ppm. **<sup>13</sup>C NMR:** (101 MHz, CDCl<sub>3</sub>) δ = 161.5, 154.0, 152.3, 141.9, 132.1, 130.2, 128.9, 125.9, 125.4, 120.8, 114.8, 109.3, 102.9, 95.0 ppm. **IR:** (ATR, cm<sup>-1</sup>) 2956, 2883, 1726, 1465, 1287, 1186, 1064, 1037, 955, 928, 851. **HRMS:** calcd. for C<sub>16</sub>H<sub>10</sub>O<sub>4</sub> [M]<sup>+</sup>: 266.0579; found (EI): 266.0579.

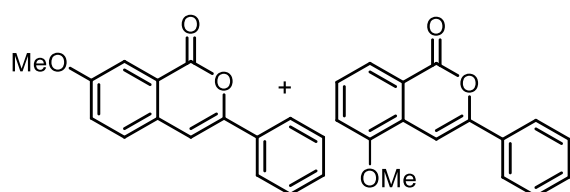
### 7-Methyl-3-phenyl-1*H*-isochromen-1-one (217):



Following GP **D**, from *N*-methyl-*m*-toluamide (1 equiv, 44.8 mg, 0.3 mmol), **197** (1.5 equiv, 247.2 mg, 0.45 mmol), [RhCp\*Cl<sub>2</sub>]<sub>2</sub> (2.5 mol%, 4.6 mg, 0.0075 mmol), NaOAc (1 equiv, 24.3 mg, 0.3 mmol), and AgSbF<sub>6</sub> (1.7 equiv, 175.2 mg, 0.51 mmol), compound **217** was prepared as a white crystalline solid (45.6 mg, 193 μmol, 64%).

**<sup>1</sup>H NMR:** (300 MHz, CDCl<sub>3</sub>) δ = 8.11 (s, 1H), 7.86 (dd, *J* = 8.0, 1.6 Hz, 2H), 7.53 (dd, *J* = 8.0, 1.7 Hz, 1H), 7.50 – 7.36 (m, 4H), 6.92 (s, 1H) 2.47 (s, 3H) ppm. **<sup>13</sup>C NMR:** (126 MHz, CDCl<sub>3</sub>) δ = 162.5, 152.8, 138.5, 136.2, 135.1, 132.1, 129.8, 129.4, 128.8, 126.0, 125.2, 120.5, 101.8, 21.6 ppm. **IR:** (ATR, cm<sup>-1</sup>) 2925, 1731, 1633, 1499, 1072, 767, 699, 538. **HRMS:** calcd. for C<sub>16</sub>H<sub>12</sub>O<sub>2</sub> [M]<sup>+</sup>: 236.0837; found: 236.0840.

### 7-Methoxy-3-phenyl-1*H*-isochromen-1-one (218a) and 5-methoxy-3-phenyl-1*H*-isochromen-1-one (218b):



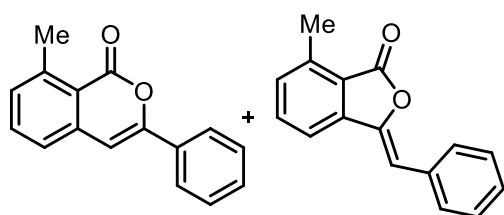
Following GP **D**, from 3-methoxy-*N*-methylbenzamide (1 equiv, 49.6 mg, 0.3 mmol), **197** (1.5 equiv, 247.2 mg, 0.45 mmol), [RhCp\*Cl<sub>2</sub>]<sub>2</sub> (2.5 mol%, 4.6 mg, 0.0075 mmol), NaOAc (1 equiv, 24.3 mg, 0.3 mmol), and AgSbF<sub>6</sub> (1.7 equiv, 175.2 mg, 0.51 mmol), compounds **218a** and **218b** (46.0 mg, 182.3 μmol, 61%, ratio **218a**:**218b** = 1:2) were obtained as a white amorphous solid. The isomers were further separated by preparative HPLC. Separation conditions: 4.6 × 250 mm Zorbax SB-C18 3.5 μm, 30 min isocratic, 1.0 mL/min, CH<sub>3</sub>CN/H<sub>2</sub>O = (50/50), 295 K.<sup>38</sup>

<sup>38</sup> The analytical data correspond to the previously published ones: R. G. Chary, G. R. Reddy, Y. S. S. Ganesh, K. V. Prasad, S. K. P. Chandra, S. Mukherjee, M Pal, *RSC Adv.* **2013**, 3, 9641–9644.

Compound **218a**:  $^1\text{H NMR}$ : (500 MHz,  $\text{CDCl}_3$ )  $\delta$  = 7.90 – 7.85 (m, 2H), 7.74 (d,  $J$  = 2.7 Hz, 1H), 7.46 (td,  $J$  = 8.5, 2.0 Hz, 3H), 7.43 – 7.39 (m, 1H), 7.33 (dd,  $J$  = 8.6, 2.7 Hz, 1H), 6.94 (s, 1H), 3.93 (s, 3H) ppm.  $^{13}\text{C NMR}$ : (126 MHz,  $\text{CDCl}_3$ )  $\delta$  = 162.7, 159.7, 151.9, 132.3, 131.4, 129.7, 129.0, 127.7, 125.1, 125.0, 121.8, 110.2, 101.8, 56.0 ppm. **IR**: (ATR,  $\text{cm}^{-1}$ ) 2924, 1693, 1600, 1501, 1450, 1284, 1245, 1070, 1028, 715. **HRMS**: calcd. for  $\text{C}_{16}\text{H}_{12}\text{O}_3^+$   $[\text{M}]^+$ : = 252.0786; found: 252.0778.

Compound **218b**:  $^1\text{H NMR}$ : (500 MHz,  $\text{CDCl}_3$ )  $\delta$  = 7.93 – 7.89 (m, 3H), 7.47 – 7.40 (m, 4H), 7.36 (s, 1H), 7.16 (dd,  $J$  = 8.1, 1.0 Hz, 1H), 3.98 (s, 3H) ppm.  $^{13}\text{C NMR}$ : (126 MHz,  $\text{CDCl}_3$ )  $\delta$  = 162.5, 154.5, 153.0, 132.4, 129.9, 128.9, 128.6, 128.3, 125.4, 121.5, 121.2, 114.5, 96.4, 56.1 ppm. **IR**: (ATR,  $\text{cm}^{-1}$ ) 2926, 1698, 1596, 1493, 1468, 1266, 1054, 752, 716, 689. **HRMS**: calcd. for  $\text{C}_{16}\text{H}_{12}\text{O}_3^+$   $[\text{M}]^+$ : 252.0786; found: 252.0785.

**8-Methyl-3-phenyl-1H-isochromen-1-one (219a) and (Z)-3-benzylidene-7-methyl-isobenzofuran-1(3H)-one (219b):**

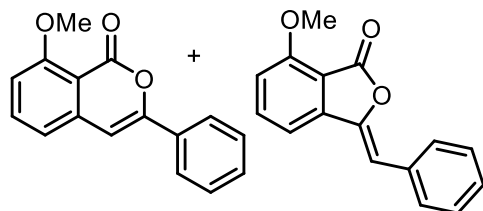


Following GP **D**, from *N*-methyl-*o*-toluamide (1 equiv, 44.8 mg, 0.3 mmol), **197** (1.5 equiv, 247.2 mg, 0.45 mmol),  $[\text{RhCp}^*\text{Cl}_2]_2$  (2.5 mol%, 4.6 mg, 0.0075 mmol), NaOAc (1 equiv, 24.3 mg, 0.3 mmol), and  $\text{AgSbF}_6$  (1.7 equiv, 175.2 mg, 0.51 mmol), compounds **219a**<sup>39</sup> and **219b**<sup>40</sup> (8.6 mg, 36.3  $\mu\text{mol}$ ,

12%; isomeric mixture, 1:1.2) were obtained as a white solid. No further separation was performed.

$^1\text{H NMR}$ : (300 MHz,  $\text{CDCl}_3$ )  $\delta$  = 7.87 (tt,  $J$  = 8.2, 1.5 Hz, 4H), 7.62 – 7.27 (m, 12H), 6.90 (s, 1H) (**219a**), 6.39 (s, 1H) (**219b**), 2.86 (s, 3H) (**219a**), 2.72 (s, 3H) (**219b**) ppm.

**8-Methoxy-3-phenyl-1H-isochromen-1-one (220a) and (Z)-3-benzylidene-7-methoxyisobenzofuran-1(3H)-one (220b):**



Column chromatography ( $\text{CH}_2\text{Cl}_2$ , then toluene:ethyl acetate, 100:0 to 20:1) of the residue obtained from 2-methoxy-*N*-methylbenzamide (1 equiv, 49.5 mg, 0.3 mmol), **197** (1.5 equiv, 247.2 mg, 0.45 mmol),  $[\text{RhCp}^*\text{Cl}_2]_2$  (2.5 mol%, 4.6 mg, 0.0075 mmol), NaOAc (1 equiv, 24.3 mg, 0.3 mmol), and  $\text{AgSbF}_6$  (1.7 equiv, 175.2 mg, 0.51 mmol) following GP **D**,

<sup>39</sup> Analytical data are in agreement with the previously published ones: Y.-F. Liang, L. Yang, T. Rogge, L. Ackermann, *Chem.Eur.J.* **2018**, *24*, 16548–16552.

<sup>40</sup> Analytical data are in agreement with the previously published ones: Y. Liu, Y. Yang, Y. Shi, X. Wang, L. Zhang, Y. Cheng, J. You, *Organometallics* **2016**, *35*, 1350–1353

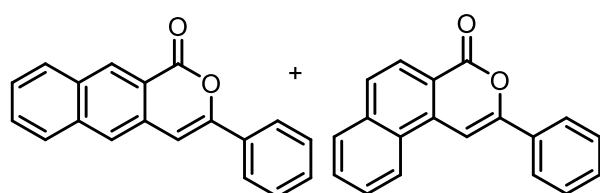


afforded compounds **220a** (28.1 mg, 111  $\mu$ mol, 37%) and **220b** (20.0 mg, 79  $\mu$ mol, 26%) as white crystalline solids.

Compound **220a**:  $^1\text{H NMR}$ : (600 MHz,  $\text{CDCl}_3$ )  $\delta$  = 7.89 – 7.87 (m, 2H), 7.62 (dd,  $J$  = 8.3, 7.7 Hz, 1H), 7.47 – 7.40 (m, 3H), 7.03 (dd,  $J$  = 7.8, 0.9 Hz, 1H), 6.94 (dd,  $J$  = 8.4, 1.0 Hz, 1H), 6.85 (s, 1H), 4.02 (s, 3H) ppm.  $^{13}\text{C NMR}$ : (126 MHz,  $\text{CDCl}_3$ )  $\delta$  = 161.7, 159.0, 154.0, 140.5, 135.8, 132.0, 130.0, 128.8, 125.4, 118.2, 110.0, 109.4, 101.9, 56.5 ppm. **IR**: (ATR,  $\text{cm}^{-1}$ ): 2925, 1734, 1568, 1478, 1277, 1109, 996, 769, 690. **HRMS**: calcd. for  $\text{C}_{16}\text{H}_{13}\text{O}_3^+$   $[\text{M}+\text{H}]^+$ : 253.0859; found: 253.0854.

Compound **220b**:  $^1\text{H NMR}$ : (600 MHz,  $\text{CDCl}_3$ )  $\delta$  = 7.85 – 7.84 (m, 2H), 7.65 (t,  $J$  = 7.9 Hz, 1H), 7.40 (dd,  $J$  = 8.4, 7.1 Hz, 2H), 7.33 – 7.29 (m, 2H), 6.95 (d,  $J$  = 8.2 Hz, 1H), 6.39 (s, 1H), 4.03 (s, 3H) ppm.  $^{13}\text{C NMR}$ : (126 MHz,  $\text{CDCl}_3$ )  $\delta$  = 165.1, 158.6, 144.4, 143.1, 136.6, 133.3, 130.2, 128.8, 128.4, 111.7, 111.3, 111.1, 107.1, 56.3 ppm. **IR**: (ATR,  $\text{cm}^{-1}$ ) 2363, 2338, 1775, 1605, 1489, 1271, 1042, 977, 805, 690. **HRMS**: calcd. for  $\text{C}_{16}\text{H}_{12}\text{O}_3^+$   $[\text{M}+\text{H}]^+$ : 253.0859; found: 253.0859.

### 3-Phenyl-1H-benzo[*g*]isochromen-1-one (**221a**) and 2-phenyl-4H-benzo[*f*]isochromen-4-one (**221b**):



The residue obtained from *N*-methyl-2-naphthamide, (1 equiv, 55.6 mg, 0.3 mmol), **197** (1.5 equiv, 247.2 mg, 0.45 mmol),  $[\text{RhCp}^*\text{Cl}_2]_2$  (2.5 mol%, 4.6 mg, 0.0075 mmol), NaOAc (1 equiv, 24.3 mg, 0.3 mmol),

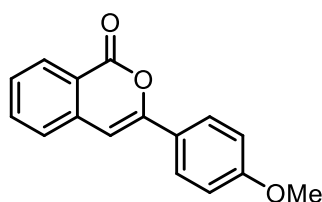
and  $\text{AgSbF}_6$  (1.7 equiv, 175.2 mg, 0.51 mmol) according to GP **D**, was stirred with 3 mL of methanol and filtered off, affording analytically pure compound **221a** (44.1 mg, 162  $\mu$ mol, 54%) as orange crystals. The mother liquor was evaporated *in vacuo* and purified by column chromatography ( $\text{CH}_2\text{Cl}_2$ ) furnishing enriched compounds **221a** (4.1 mg, 5%; 4.5:1 isomeric mixture of **221a**:**221b**) and **221b** (10.3 mg, 38  $\mu$ mol, 13%; 1:4.5 isomeric mixture of **221a**:**221b**), the latter as a white crystalline solid.<sup>41</sup>

Compound **221a**:  $^1\text{H NMR}$ : (300 MHz,  $\text{CDCl}_3$ )  $\delta$  = 8.93 (s, 1H), 8.02 (d,  $J$  = 8.3 Hz, 1H), 7.91 (d,  $J$  = 5.8 Hz, 4H), 7.64 (t,  $J$  = 7.5 Hz, 1H), 7.59 – 7.37 (m, 4H), 7.07 (s, 1H) ppm.  $^{13}\text{C NMR}$ : (126 MHz,  $\text{CDCl}_3$ )  $\delta$  = 162.6, 152.1, 136.7, 132.5, 132.4, 132.3, 132.1, 129.9, 129.5, 128.9, 127.8, 126.8, 125.3, 124.4, 119.1, 102.1 ppm. **IR**: (ATR,  $\text{cm}^{-1}$ ) 2921, 1717, 1628, 1446, 1256, 1183, 1056, 896, 755, 736, 682, 622. **HRMS**: calcd. for  $\text{C}_{19}\text{H}_{12}\text{O}_2^+$   $[\text{M}]^+$ : 272.0837; found: 272.0827.

<sup>41</sup> The analytical data were identical to the previously reported ones: Z.-Y. Ge, X.-D. Fei, T. Tang, Y.-M. Zhu, J.-K. Shen, *J. Org. Chem.* **2012**, 77, 5736–5743.

Compound **221b**:  $^1\text{H NMR}$ : (300 MHz,  $\text{CDCl}_3$ )  $\delta$  = 8.48 – 8.43 (m, 1H), 8.27 (dd,  $J$  = 8.7, 0.7 Hz, 1H), 8.05 – 7.93 (m, 3H), 7.90 (dq,  $J$  = 8.7, 0.4 Hz, 1H), 7.79 – 7.68 (m, 3H), 7.58 – 7.45 (m, 3H) ppm.  $^{13}\text{C NMR}$ : (126 MHz,  $\text{CDCl}_3$ )  $\delta$  = 162.7, 155.1, 136.9, 136.2, 132.3, 130.3, 129.5, 129.1, 129.0, 128.6, 128.0, 127.4, 125.6, 124.5, 124.1, 117.8, 97.7 ppm. **IR**: (ATR,  $\text{cm}^{-1}$ ) 2925, 1732, 1632, 1217, 1059, 763, 688, 594. **HRMS**: calcd. for  $\text{C}_{19}\text{H}_{12}\text{O}_3^+$   $[\text{M}]^+$ : 272.0837; found: 272.0828.

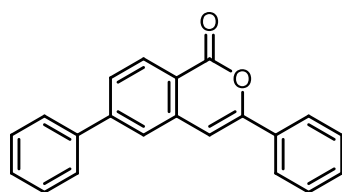
### 3-(4-Methoxyphenyl)-1*H*-isochromen-1-one (**222**):



Following GP **D**, from *N*-methylbenzamide (1 equiv, 40.6 mg, 0.3 mmol), **198** (1.5 equiv, 260.7 mg, 0.45 mmol),  $[\text{RhCp}^*\text{Cl}_2]_2$  (2.5 mol%, 4.6 mg, 0.0075 mmol), NaOAc (0.5 equiv, 12.3 mg, 0.15 mmol), and  $\text{AgSbF}_6$  (1.7 equiv, 175.2 mg, 0.51 mmol), compound **222** (55.3 mg, 219  $\mu\text{mol}$ , 73%) was obtained as white crystals.

$^1\text{H NMR}$ : (600 MHz,  $\text{CDCl}_3$ )  $\delta$  = 8.27 (dd,  $J$  = 8.4, 1.2 Hz, 1H), 7.83 – 7.79 (m, 2H), 7.68 (td,  $J$  = 7.5, 1.3 Hz, 1H), 7.47 – 7.42 (m, 2H), 6.98 – 6.94 (m, 2H), 6.81 (s, 1H), 3.85 (s, 3H) ppm.  $^{13}\text{C NMR}$ : (126 MHz,  $\text{CDCl}_3$ )  $\delta$  = 162.4, 161.1, 153.7, 137.9, 134.8, 129.6, 127.7, 126.9, 125.7, 124.6, 120.2, 114.3, 100.3, 55.6 ppm. **IR**: (ATR,  $\text{cm}^{-1}$ ) 2932, 1731, 1633, 1602, 1513, 1257, 1178, 1029, 825, 689, 533. **HRMS**: calcd. for  $\text{C}_{16}\text{H}_{13}\text{O}_3^+$ ,  $[\text{M}+\text{H}]^+$ : = 253.0859; found: 253.0860.

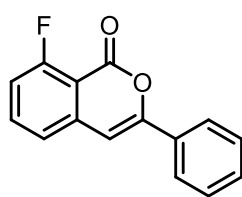
### 3,6-Diphenyl-1*H*-isochromen-1-one (**223**):



Following GP **D**, from *N*-methyl-4-phenylbenzamide (1 equiv, 63.4 mg, 0.3 mmol), **197** (1.5 equiv, 247.2 mg, 0.45 mmol),  $[\text{RhCp}^*\text{Cl}_2]_2$  (2.5 mol%, 4.6 mg, 0.0075 mmol), NaOAc (1 equiv, 24.3 mg, 0.3 mmol), and  $\text{AgSbF}_6$  (1.7 equiv, 175.2 mg, 0.51 mmol) compound **223** (40.6 mg, 136  $\mu\text{mol}$ , 45%) was obtained after column chromatography as bright green crystals.

$^1\text{H NMR}$ : (300 MHz,  $\text{CDCl}_3$ )  $\delta$  = 8.37 (dt,  $J$  = 8.2, 0.7 Hz, 1H), 7.98 – 7.88 (m, 2H), 7.77 – 7.65 (m, 5H), 7.57 – 7.40 (m, 7H), 7.02 (s, 1H) ppm.  $^{13}\text{C NMR}$ : (126 MHz,  $\text{CDCl}_3$ )  $\delta$  = 162.3, 154.1, 147.8, 139.5, 138.1, 132.1, 130.4, 130.1, 129.2, 128.9, 128.8, 127.5, 127.3, 125.4, 124.2, 119.4, 102.1 ppm. **IR**: (ATR,  $\text{cm}^{-1}$ ) 3057, 2919, 2847, 1707, 1606, 1446, 1066, 1026, 890, 752, 688, 516. **HRMS**: calcd. for  $\text{C}_{21}\text{H}_{15}\text{O}_2^+$   $[\text{M}+\text{H}]^+$ : 299.1067; found: 299.1070.

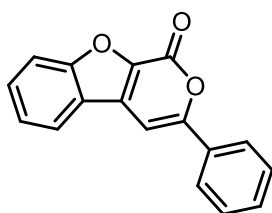
### 8-Fluoro-3-phenyl-1*H*-isochromen-1-one (**224**):



Following GP **D**, from 2-fluoro-*N*-methylbenzamide (1 equiv, 45.9 mg, 0.3 mmol), **197** (1.5 equiv, 247.2 mg, 0.45 mmol), [RhCp\*Cl<sub>2</sub>]<sub>2</sub> (2.5 mol%, 4.6 mg, 0.0075 mmol), NaOAc (1 equiv, 24.3 mg, 0.3 mmol), and AgSbF<sub>6</sub> (1.7 equiv, 175.2 mg, 0.51 mmol) compound **224** (36.2 mg, 151 μmol, 50%) was obtained as a white solid.

**<sup>1</sup>H NMR:** (400 MHz, CDCl<sub>3</sub>) δ= 7.90 – 7.84 (m, 2H), 7.67 (td, *J* = 8.1, 4.9 Hz, 1H), 7.51 – 7.42 (m, 3H), 7.29 – 7.26 (m, 1H), 7.14 (ddd, *J* = 10.6, 8.2, 1.0 Hz, 1H), 6.92 (d, *J* = 2.3 Hz, 1H) ppm. **<sup>13</sup>C NMR:** (101 MHz, CDCl<sub>3</sub>) δ= 163.0 (d, *J* = 266.9 Hz), 157.89 (d, *J* = 5.5 Hz), 154.72, 140.23, 136.32 (d, *J* = 10.1 Hz), 131.60, 130.48, 129.01, 125.52, 121.92 (d, *J* = 4.4 Hz), 115.35 (d, *J* = 21.2 Hz), 109.50 (d, *J* = 7.3 Hz), 101.25 (d, *J* = 3.1 Hz) ppm. **<sup>19</sup>F NMR:** (376 MHz, CDCl<sub>3</sub>) δ = – 107.16 (ddd, *J* = 10.7, 5.0, 2.3 Hz). **IR:** (ATR, cm<sup>-1</sup>) 3107, 3028, 2922, 1714, 1638, 1568, 1472, 1325, 1228, 1072, 1053, 998, 904, 857, 799, 756, 683, 650, 549. **HRMS:** calcd. for C<sub>15</sub>H<sub>10</sub>FO<sub>2</sub><sup>+</sup> [M+H]<sup>+</sup>: 241.0659; found: =241.0662.

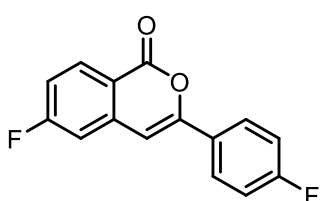
### 3-Phenyl-1*H*-pyrano[3,4-*b*]benzofuran-1-one (**225**):



Following GP **D**, from *N*-methylbenzofuran-2-carboxamide (1 equiv, 52.4 mg, 299.1 μmol), **197** (1.5 equiv, 247.2 mg, 0.45 mmol), [RhCp\*Cl<sub>2</sub>]<sub>2</sub> (2.5 mol%, 4.6 mg, 0.0075 mmol), NaOAc (1 equiv, 24.3 mg, 0.3 mmol), and AgSbF<sub>6</sub> (1.7 equiv, 175.2 mg, 0.51 mmol), compound **225** (7.4 mg, 28.2 μmol, 9%) was obtained as off white crystals.

**<sup>1</sup>H NMR:** (300 MHz, CDCl<sub>3</sub>) δ = 7.97 – 7.88 (m, 3H), 7.71 (dt, *J* = 8.5, 1.0 Hz, 1H), 7.64 (ddd, *J* = 8.5, 7.0, 1.3 Hz, 1H), 7.56 – 7.43 (m, 4H), 7.29 (s, 1H) ppm. **<sup>13</sup>C NMR:** (101 MHz, CDCl<sub>3</sub>) δ = 157.8, 157.2, 154.4, 138.6, 132.0, 131.9, 130.4, 130.4, 129.1, 125.7, 124.5, 122.7, 122.3, 113.4, 95.9 ppm. **IR:** (ATR, cm<sup>-1</sup>) 2926, 1795, 1744, 1682, 1617, 1462, 1448, 1291, 1231, 1069, 755, 695. **HRMS:** calcd. for C<sub>17</sub>H<sub>10</sub>O<sub>3</sub><sup>+</sup> [M]<sup>+</sup>: 262.06299; found: 262.0626.

### 6-Fluoro-3-(4-fluorophenyl)-1*H*-isochromen-1-one (**226**):

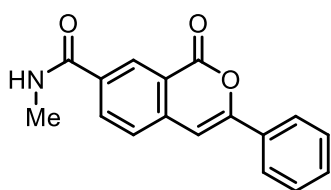


Following GP **D**, from 4-fluoro-*N*-methylbenzamide (1 equiv, 46.0 mg, 0.3 mmol), **199** (1.5 equiv, 255.3 mg, 0.45 mmol), [RhCp\*Cl<sub>2</sub>]<sub>2</sub> (2.5 mol%, 4.6 mg, 0.0075 mmol), NaOAc (1 equiv, 24.3 mg, 0.3 mmol), and AgSbF<sub>6</sub> (1.7 equiv, 175.2 mg, 0.51 mmol), compound **226** (50.0 mg, 194 μmol, 65%) was obtained as a white solid.

**<sup>1</sup>H NMR:** (300 MHz, CDCl<sub>3</sub>) δ= 8.32 (ddt, *J* = 8.8, 5.6, 0.6 Hz, 1H), 7.90 – 7.83 (m, 2H), 7.25 – 7.08 (m, 4H), 6.84 (q, *J* = 0.5 Hz, 1H) ppm. **<sup>13</sup>C NMR:** (126 MHz, CDCl<sub>3</sub>) δ= 166.42 (d, *J* = 352.8

Hz), 164.40 (d,  $J = 347.8$  Hz), 161.2, 154.1, 140.2 (d,  $J = 10.8$  Hz), 133.1 (d,  $J = 10.4$  Hz), 127.9 (d,  $J = 3.3$  Hz), 127.6 (d,  $J = 8.5$  Hz), 117.0 (d,  $J = 2.2$  Hz), 116.6 (d,  $J = 23.2$  Hz), 116.2 (d,  $J = 22.1$  Hz), 111.6 (d,  $J = 22.6$  Hz), 101.1 ppm.  **$^{19}\text{F}$  NMR:** (282 MHz,  $\text{CDCl}_3$ )  $\delta = -101.66$  (td,  $J = 8.5, 5.5$  Hz),  $-109.51$  (tt,  $J = 8.2, 5.1$  Hz) ppm. **IR:** (ATR,  $\text{cm}^{-1}$ ) 2954, 2926, 2853, 1720, 1603, 1511, 1238, 1060, 960, 849, 772. **HRMS:** calcd. for  $\text{C}_{15}\text{H}_9\text{F}_2\text{O}_2$   $[\text{M}+\text{H}]^+$ : 259.0565; found: 259.0570.

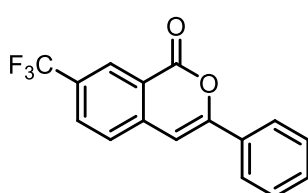
### ***N*-Methyl-1-oxo-3-phenyl-1*H*-isochromene-7-carboxamide (**227**):**



Following GP **D**<sup>42</sup>, from *N*<sup>1</sup>,*N*<sup>3</sup>-dimethylisophthalamide (1 equiv, 57.7 mg, 0.3 mmol), **197** (1 equiv, 164.8 mg, 0.3 mmol),  $[\text{RhCp}^*\text{Cl}_2]_2$  (2.5 mol%, 4.6 mg, 0.0075 mmol), NaOAc (1 equiv, 24.3 mg, 0.3 mmol), and  $\text{AgSbF}_6$  (1.1 equiv, 113.4 mg, 0.33 mmol), compound **227** (61.7 mg, 221  $\mu\text{mol}$ , 74%) was obtained as colorless crystals after separation by column chromatography (toluene/EtOAc, 1/1).

**$^1\text{H}$  NMR:** (300 MHz,  $\text{CDCl}_3$ )  $\delta = 8.57$  (d,  $J = 1.7$  Hz, 1H), 8.29 (dd,  $J = 8.2, 1.9$  Hz, 1H), 7.93 – 7.87 (m, 2H), 7.59 (d,  $J = 8.2$  Hz, 1H), 7.48 (m, 3H), 7.01 (s, 1H), 6.40 (br s, 1H), 3.07 (d,  $J = 4.9$  Hz, 3H) ppm.  **$^{13}\text{C}$  NMR:** (126 MHz,  $\text{CDCl}_3$ )  $\delta = 167.2, 162.5, 155.5, 140.9, 134.5, 132.9, 131.3, 130.0, 129.5, 128.6, 127.7, 126.2, 121.3, 102.6, 26.9$  ppm. **IR:** (ATR,  $\text{cm}^{-1}$ ) 3292, 1715, 1634, 1551, 1497, 1315, 1229, 1125, 1065, 875, 761, 679, 642, 566. **HRMS:** calcd. for  $\text{C}_{17}\text{H}_{14}\text{NO}_3^+$   $[\text{M}+\text{H}]^+$ : 280.0968; found: 280.0970.

### **3-Phenyl-7-(trifluoromethyl)-1*H*-isochromen-1-one (**228**):**

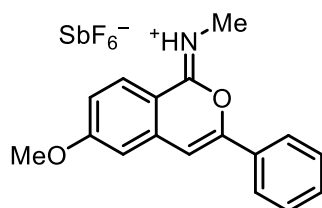


Following GP **D**, from *N*-methyl-3-(trifluoromethyl)benzamide (1 equiv, 60.9 mg, 0.3 mmol), **197** (1.5 equiv, 247.2 mg, 0.45 mmol),  $[\text{RhCp}^*\text{Cl}_2]_2$  (2.5 mol%, 4.6 mg, 0.0075 mmol), NaOAc (1 equiv, 24.3 mg, 0.3 mmol), and  $\text{AgSbF}_6$  (1.7 equiv, 175.2 mg, 0.51 mmol), compound **228** was obtained as a white amorphous solid (77.8 mg, 268  $\mu\text{mol}$ , 89%).

**$^1\text{H}$  NMR:** (300 MHz,  $\text{CDCl}_3$ )  $\delta = 8.59$  (s, 1H), 7.98 – 7.87 (m, 3H), 7.63 (d,  $J = 8.3$  Hz, 1H), 7.49 (dd,  $J = 5.1, 2.0$  Hz, 3H), 7.01 (s, 1H) ppm.  **$^{13}\text{C}$  NMR:** (101 MHz,  $\text{CDCl}_3$ )  $\delta = 161.3, 155.9, 140.5, 131.5, 131.3$  (q,  $J_{\text{C-F}} = 3.4$  Hz), 130.9, 130.3 (d,  $J_{\text{C-F}} = 33.6$  Hz), 129.2, 127.4 (q,  $J_{\text{C-F}} = 4.1$  Hz), 126.9, 125.7, 123.6 (d,  $J_{\text{C-F}} = 272.2$  Hz), 120.7, 101.0 ppm.  **$^{19}\text{F}$  NMR:** (282 MHz,  $\text{CDCl}_3$ )  $\delta = -62.71$  ppm. **IR:** (ATR,  $\text{cm}^{-1}$ ) 2926, 1740, 1625, 1316, 1174, 1129, 1071, 846, 765, 698. **HRMS:** calcd. for  $\text{C}_{16}\text{H}_{10}\text{F}_3\text{O}_2^+$   $[\text{M}+\text{H}]^+ = 291.0627$ ; found = 291.0625.

<sup>42</sup> 1 equiv of reagent **197** was used instead of 1.5.

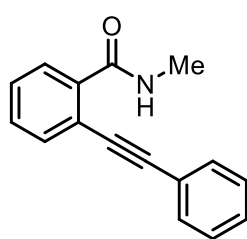
**(Z)-N-(6-Methoxy-3-phenyl-1H-isochromen-1-ylidene)methanaminium hexafluoroantimonate (229):**



A schlenk flask was charged with  $[\text{RhCp}^*\text{Cl}_2]_2$  (1 equiv, 20 mg, 32.3  $\mu\text{mol}$ ), NaOAc (1 equiv, 5.3 mg, 64.6  $\mu\text{mol}$ ), 4-methoxy-*N*-methylbenzamide (1 equiv, 10.69 mg, 64.7  $\mu\text{mol}$ ), **197** (1 equiv, 35.7 mg, 65  $\mu\text{mol}$ ) and  $\text{AgSbF}_6$  (1 equiv, 22.2 mg, 64.6  $\mu\text{mol}$ ). The flask was flushed three times with  $\text{N}_2$ /Vacuum-Cycles. Then 1,2-dichloroethane (2 mL) was slowly added via syringe, and the solution was allowed to stay for 24 h at ambient temperature. Afterwards, dry  $\text{Et}_2\text{O}$  (3 mL) was carefully layered over the reaction mixture, and the solution was left for an additional 24 h. Colorless crystals of compound **229** formed at the interphase between 1,2-DCE and  $\text{Et}_2\text{O}$  and were collected for characterization.

**$^1\text{H}$  NMR:** (500 MHz,  $\text{CD}_3\text{CN}$ )  $\delta$  = 9.18 (s, 1H), 8.10 (d,  $J$  = 9.1 Hz, 1H), 8.00 – 7.93 (m, 2H), 7.63 – 7.58 (m, 3H), 7.57 (s, 1H), 7.35 (dd,  $J$  = 9.1, 2.5 Hz, 1H), 7.29 (d,  $J$  = 2.5 Hz, 1H), 4.02 (s, 3H), 3.38 (s, 3H) ppm.  **$^{13}\text{C}$  NMR:** (126 MHz,  $\text{CD}_3\text{CN}$ )  $\delta$  = 167.9, 165.1, 153.2, 139.9, 132.3, 130.8, 130.4, 129.0, 126.4, 120.9, 110.2, 108.6, 106.0, 57.3, 29.7 ppm.  **$^{19}\text{F}$  NMR:** (471 MHz,  $\text{CD}_3\text{CN}$ )  $\delta$  = –124.0 (sext,  $J_{\text{F-}^{121}\text{Sb}}$  = 1932.5 Hz), –124.8 (oct,  $J_{\text{F-}^{123}\text{Sb}}$  = 1049.6 Hz) ppm. **IR:** (ATR,  $\text{cm}^{-1}$ ) 3360, 1663, 1604, 1565, 1492, 1445, 1377, 1257, 1201, 1129, 1020, 878, 824, 772, 761, 650, 623, 565. **HRMS:** calcd. for  $\text{C}_{17}\text{H}_{16}\text{NO}_2^+ [\text{M}]^+$ : 266.1176; found: 266.1180.

***N*-Methyl-2-(phenylethynyl)benzamide (234):**

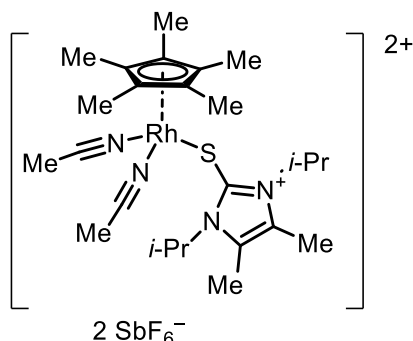


Following a modified literature procedure<sup>43</sup>, **234** was prepared from 2-iodo-*N*-methylbenzamide (783 mg, 3 mmol), phenylacetylene (395  $\mu\text{L}$ , 368 mg, 3.6 mmol) in  $\text{Et}_3\text{N}$  (12 mL),  $\text{PdCl}_2(\text{PPh}_3)_2$  (42 mg, 0.06 mmol, 2 mol%) and  $\text{CuI}$  (5.7 mg, 0.03 mmol, 1 mol%). The reaction mixture was stirred at 55  $^\circ\text{C}$ , and full consumption of the starting material was observed after 30 min by TLC. The reaction was allowed to cool to room temperature. Water (30 mL) and ethyl acetate (40 mL) were added, the aqueous phase was extracted  $\text{EtOAc}$  (3  $\times$  20 mL), the combined organic phases were washed with brine (50 mL), the organic phase was dried over  $\text{Na}_2\text{SO}_4$  and all volatiles were removed *in vacuo*. Separation by column chromatography (cyclohexane/ethyl acetate, 2:1 to 1:1) gave the product **234** (629 mg, 2.67 mmol, 89%) as a white crystalline solid.

**$^1\text{H}$  NMR:** (300 MHz,  $\text{CDCl}_3$ )  $\delta$  = 8.09 – 8.01 (m, 1H), 7.63 – 7.56 (m, 1H), 7.55 – 7.49 (m, 2H), 7.47 – 7.36 (m, 5H), 7.31 (br s, 1H), 3.08 (d,  $J$  = 4.9 Hz, 3H) ppm.  **$^{13}\text{C}$  NMR:** (126 MHz,  $\text{CDCl}_3$ )  $\delta$  = 167.2 (enriched), 136.0, 133.3, 131.6, 130.5, 130.0, 129.2, 129.0, 128.7, 122.3, 119.6, 95.5, 87.8, 27.0 ppm.

<sup>43</sup>Analytical data are in agreement with the previously published ones: C. Schlemmer, L. Andernach, D. Schollmeyer, B. F. Straub, T. Opatz, *J. Org. Chem.* **2012**, 77, 10118–10124.

**Bis(acetonitrile){[(1,3-diisopropyl-4,5-dimethyl-1*H*-imidazol-3-ium-2-yl)thio]}(pentamethylcyclopentadienyl)rhodium(I) bis(hexafluoroantimonate) (**236a**):**

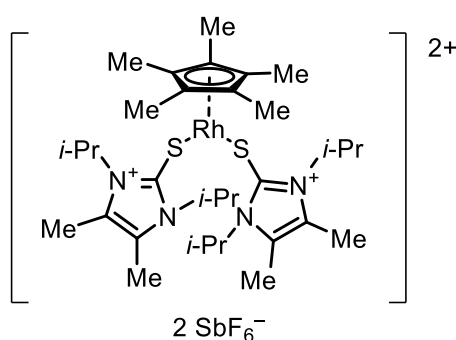


A Schlenk flask was charged with *N*-methyl-*p*-toluamide (1 equiv, 14.9 mg, 0.1 mmol), NaOAc (1 equiv, 8.2 mg, 0.1 mmol) and RhCp\*(MeCN)<sub>3</sub>(SbF<sub>6</sub>)<sub>2</sub> (1 equiv, 83.3 mg, 0.1 mmol) in 1,2-DCE (2 mL), and the reaction mixture was stirred for 1 h. Afterwards stirring was stopped and subsequently a solution of **197** (1 equiv, 54.9 mg, 0.1 mmol) in 1,2-DCE (1 mL) was slowly layered over the reaction mixture. After 24 h, dry Et<sub>2</sub>O (3 mL) was carefully

layered over the reaction mixture and the solution was let stand for an additional 24 h. Red crystals of the product **236a** formed and were collected for analysis.<sup>44</sup>

**<sup>1</sup>H NMR:** (500 MHz, CD<sub>3</sub>CN)  $\delta$  = 5.29 (p, *J* = 7.1 Hz, 1H), 3.81 (s, 1H), 2.31 (s, 3H), 1.96 (s, 4H), 1.71 (s, 8H), 1.45 (d, *J* = 7.2 Hz, 6H) ppm. **<sup>13</sup>C NMR:** (126 MHz, CD<sub>3</sub>CN)  $\delta$  = 147.9, 128.4, 101.2, 101.1, 52.86, 45.51, 21.06, 10.77, 9.48 ppm. **<sup>19</sup>F NMR:** (471 MHz, CD<sub>3</sub>CN)  $\delta$  = -123.93 (h, *J*<sub>F-Sb</sub> = 1609.8 Hz), -123.9 (oct, *J*<sub>F-Sb123</sub> = 1050.7 Hz) ppm. **IR:** (ATR, cm<sup>-1</sup>) 1402, 1020, 655. **HRMS:** calcd. for C<sub>25</sub>H<sub>41</sub>N<sub>4</sub>RhS<sup>2+</sup> [M-2SbF<sub>6</sub>]<sup>2+</sup>: 266.1; found: 263.2.

**Bis{[(1,3-diisopropyl-4,5-dimethyl-1*H*-imidazol-3-ium-2-yl)thio]}(pentamethylcyclopentadienyl)rhodium(I) bis(hexafluoroantimonate) (**236b**):**



A schlenk flask was charged with [RhCp\*Cl<sub>2</sub>]<sub>2</sub> (1 equiv, 20 mg, 32.3  $\mu$ mol), NaOAc (1 equiv, 5.3 mg, 6.46  $\mu$ mol), 4-methoxy-*N*-methylbenzamide (1 equiv, 10.69 mg, 6.47  $\mu$ mol), **197** (1 equiv, 35.7 mg, 6.5  $\mu$ mol), and AgSbF<sub>6</sub> (1 equiv, 22.2 mg, 6.46  $\mu$ mol). The flask was flushed three times with N<sub>2</sub>/Vaccuum-Cycles. Then 1,2-Dichloroethane (2 mL) was slowly added via syringe, and the solution was allowed to stay for 24 h.

Afterwards, dry Et<sub>2</sub>O (3 mL) was carefully layered over the reaction mixture, and the solution was stayed for another 24 h. Black crystals of **236b** formed at the bottom of the flask and were-collected for analysis.<sup>45</sup>

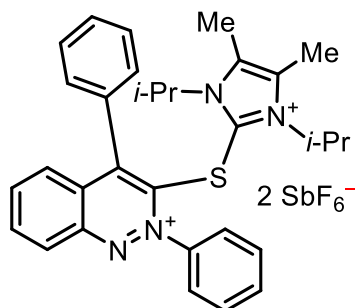
**<sup>1</sup>H NMR:** (500 MHz, CD<sub>3</sub>CN)  $\delta$  = 2.31 (s, 6H), 1.71 (s, 15H), 1.45 (d, *J* = 7.2 Hz, 12H) ppm.

**HRMS:** calcd. for C<sub>32</sub>H<sub>55</sub>N<sub>4</sub>RhS<sub>2</sub> [M-2SbF<sub>6</sub>]<sup>+</sup>: 622.2912 ; found: 622.2996.

<sup>44</sup>No final yield was determined.

<sup>45</sup>No final yield was determined.

**3-[(1,3-Diisopropyl-4,5-dimethyl-1*H*-imidazol-3-ium-2-yl)thio]-2,4-diphenylcinnolin-2-ium hexafluoroantimonate (**238**):**



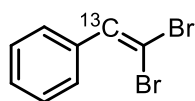
A pressure vial was charged with  $[\text{RhCp}^*\text{Cl}_2]_2$  (2.5 mol%, 26.4 mg, 4.27  $\mu\text{mol}$ ), NaOAc (1 eq, 139.9 mg, 1.71 mmol), azobenzene (1 equiv, 311.6 mg, 1.71 mmol), **197** (1.5 equiv, 1.4 g, 2.55 mmol), and finally  $\text{AgSbF}_6$  (1.6 equiv, 937.4 mg, 2.73 mmol). The vial was sealed and flushed three times with  $\text{N}_2$ /Vacuum-Cycles. 1,2-Dichloroethane (2 mL) was added via syringe, and the reaction mixture was stirred at 80 °C for 20 h. After cooling down to room temperature, the reaction

mixture was diluted with acetonitrile (6 mL), and supernatant phase was filtered through a pad of celite. The operation was repeated twice. Subsequently the organic solvents were removed *in vacuo*. The residue was carefully washed with  $\text{CHCl}_3$  ( $5 \times 2$  mL) to give the pure product as a dark yellow solid (1.4 g, 1.45 mmol, 85%).

**$^1\text{H}$  NMR:** (300 MHz,  $\text{CD}_3\text{CN}$ )  $\delta$  = 8.76 – 8.68 (m, 1H), 8.45 (ddd,  $J$  = 8.6, 6.9, 1.2 Hz, 1H), 8.36 (ddd,  $J$  = 8.2, 6.9, 1.3 Hz, 1H), 7.98 – 7.85 (m, 5H), 7.82 – 7.66 (m, 3H), 7.62 (d,  $J$  = 8.7 Hz, 1H), 7.42 – 7.33 (m, 2H), 4.32 (hept,  $J$  = 6.9 Hz, 2H), 2.21 (s, 6H), 1.19 (d,  $J$  = 6.9 Hz, 12H) ppm.

**$^{13}\text{C}$  NMR:** (101 MHz,  $\text{CD}_3\text{CN}$ )  $\delta$  = 150.9, 148.7, 145.9, 144.8, 143.0, 139.0, 134.5, 133.8, 132.7, 132.3, 132.1, 131.9, 131.1, 130.8, 129.6, 129.9, 129.2, 127.0, 126.4, 55.9, 21.6, 11.2 ppm. **IR:** (ATR,  $\text{cm}^{-1}$ ) 2363, 2161, 1698, 1558, 1507, 1048, 659. **HRMS:** calcd. for  $\text{C}_{31}\text{H}_{34}\text{N}_4\text{S}^{2+}$  [ $\text{M} - 2\text{SbF}_6$ ] $^{2+}$ : 494.2493; found: 494.2499.

**(1- $^{13}\text{C}$ )-2,2-Dibromovinyl)benzene (**240**):**



To a solution of  $\text{CBr}_4$  (2 equiv, 9.0 g, 27.1 mmol) and  $\text{PPh}_3$  (4 equiv, 14.2 g, 54.3 mmol) in dry  $\text{CH}_2\text{Cl}_2$  (40 mL), benzaldehyde (20%  $^{13}\text{C}$ -enriched) (1 equiv, 1.5 mL, 13.6 mmol) in  $\text{CH}_2\text{Cl}_2$  (10 mL) was added at 0 °C. The cooling bath was removed and the reaction was stirred at rt for 3 h. Afterwards the reaction solution was filtered, and the solvents removed *in vacuo*. Purification by column chromatography (hexanes) gave **240** as colourless oil (3.5 g, 13.4 mmol, 99%).

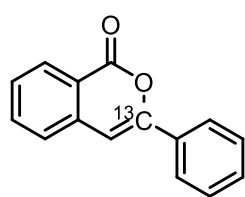
**$^1\text{H}$  NMR:** (300 MHz,  $\text{CDCl}_3$ )  $\delta$  = 7.58 – 7.51 (m, 2H), 7.49( $^{12}\text{C}$ ) (s, 0.8H), 7.49( $^{13}\text{C}$ ) (d,  $J$  = 159.9 Hz, 0.2H), 7.42 – 7.30 (m, 2H) ppm.  **$^{13}\text{C}$  NMR:** (101 MHz,  $\text{CDCl}_3$ )  $\delta$  = 137.0 ( $^{13}\text{C}$ -enriched), 135.5, 128.7, 128.6, 128.5, 89.8 ppm.

**1,3-Diisopropyl-4,5-dimethyl-2-[(phenylethynyl-2-<sup>13</sup>C)thio]-1*H*-imidazol-3-ium hexafluoroantimonate (<sup>13</sup>C)-197):**

Following a modification of GP C, from (2,2-dibromovinyl-1-<sup>13</sup>C)benzene (**240**) (1.17 equiv, 3.8 g, 14.5 mmol), *n*-BuLi (12.5 M, 2.3 equiv, 11.4 mL, 28.5 mmol), ZnBr<sub>2</sub> (1.26 equiv, 3.52 g, 15.6 mmol), **151a** (1 equiv, 4.6 g, 12.4 mmol) and NaSbF<sub>6</sub> (3.8 equiv, 12.1 g, 46.8 mmol), compound **241** (6.1 g, 11.1 mmol, 90%) was obtained after column chromatography (CH<sub>2</sub>Cl<sub>2</sub>/acetone, 50:1) as a white solid.

<sup>1</sup>H NMR: (600 MHz, CDCl<sub>3</sub>) δ = 7.41 (dt, *J* = 7.0, 1.3 Hz, 2H), 7.40 – 7.37 (m, 1H), 7.33 (t, *J* = 7.7 Hz, 2H), 2.40 (s, 6H), 1.71 (d, *J* = 7.1 Hz, 12H) ppm. <sup>13</sup>C NMR: (126 MHz, CDCl<sub>3</sub>) δ = 135.8, 132.2, 131.3, 130.2, 128.7, 120.6, 95.7 (<sup>13</sup>C-enriched), 69.4, 54.1, 21.3, 10.5 ppm. IR: (ATR, cm<sup>-1</sup>) 2998, 2943, 1617, 1486, 1462, 1443, 1380, 1222, 1113, 756, 690, 653. HRMS: calcd. for C<sub>18</sub><sup>13</sup>CH<sub>24</sub>N<sub>2</sub>S<sup>+</sup> [M–H–SbF<sub>6</sub>]<sup>+</sup>: =313.1688; found: 313.1744.

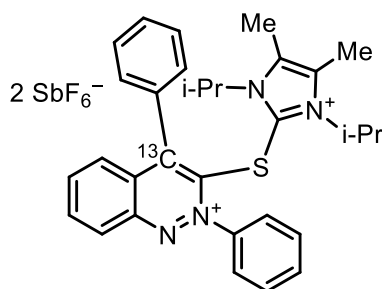
**3-{<sup>13</sup>C}-3-Phenyl-1*H*-isochromen-1-one (3-{<sup>13</sup>C}-Homalicine) (<sup>13</sup>C)-207):**



Following GP D, from *N*-methylbenzamide (1 equiv, 40.6 mg, 0.3 mmol), **241** (1.5 equiv, 247.2 mg, 0.45 mmol), [RhCp\*Cl<sub>2</sub>]<sub>2</sub> (2.5 mol%, 4.6 mg, 0.0075 mmol), NaOAc (1 equiv, 24.3 mg, 0.3 mmol), and AgSbF<sub>6</sub> (1.7 equiv, 175.2 mg, 0.51 mmol), compound <sup>13</sup>C-**207** was obtained as a white solid (38.6 mg, 173 μmol, 58%).

<sup>1</sup>H NMR: (300 MHz, CDCl<sub>3</sub>) δ = 8.32 (dt, *J* = 8.0, 0.9 Hz, 1H), 7.89 (dd, *J* = 7.9, 1.8 Hz, 2H), 7.76 – 7.69 (m, 1H), 7.55 – 7.40 (m, 5H), 6.98 – 6.94 (m, 1H) ppm. <sup>13</sup>C NMR: (75 MHz, CDCl<sub>3</sub>) δ = 162.5, 153.8 (<sup>13</sup>C-enriched), 137.7, 135.0, 132.1, 130.1, 129.8, 129.0, 128.3, 126.1, 125.4, 120.7, 102.0 ppm.

**4-{<sup>13</sup>C}-3-[(1,3-Diisopropyl-4,5-dimethyl-1*H*-imidazol-3-ium-2-yl)thio]-2,4-diphenylcinnolin-2-ium hexafluoroantimonate (<sup>13</sup>C)-238):**



A pressure vial was charged with [RhCp\*Cl<sub>2</sub>]<sub>2</sub> (2.5 mol%, 4.6 mg, 7.5 μmol), NaOAc (1 eq, 24.3 mg, 0.3 mmol), azobenzene (1 eq, 54.7 mg, 0.3 mmol), **241** (1.5 equiv, 247.2 mg, 0.45 mmol), and finally AgSbF<sub>6</sub> (175.2 mg, 0.51 mmol). The vial was sealed and flushed three times with N<sub>2</sub>/Vacuum-Cycles. 1,2-Dichloroethane (2 mL) was added via syringe, and the reaction mixture was stirred at 80 °C for 20 h. After cooling

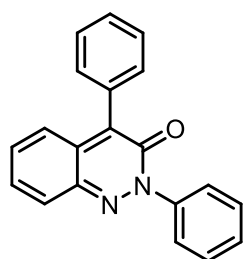
down to room temperature, the reaction solution was diluted with acetonitrile and filtered through a pad of celite. Subsequently the organic solvents were removed *in vacuo*. The



residue was carefully washed with  $\text{CHCl}_3$  ( $5 \times 2$  mL) to give the pure product **243** as a dark yellow solid (301.7 mg, 312.4  $\mu\text{mol}$ , 96%).

**$^1\text{H}$  NMR:** (500 MHz,  $\text{CD}_3\text{CN}$ )  $\delta$  = 8.72 (ddd,  $J$  = 8.7, 1.2, 0.7 Hz, 1H), 8.45 (ddd,  $J$  = 8.7, 6.9, 1.2 Hz, 1H), 8.36 (ddd,  $J$  = 8.7, 6.9, 1.3 Hz, 1H), 7.97 – 7.93 (m, 1H), 7.92 – 7.86 (m, 4H), 7.80 – 7.75 (m, 1H), 7.73 – 7.68 (m, 2H), 7.65 – 7.61 (m, 1H), 7.40 – 7.36 (m, 2H), 4.33 (hept,  $J$  = 6.9 Hz, 2H), 2.21 (s, 6H), 1.19 (d,  $J$  = 6.9 Hz, 12H) ppm.  **$^{13}\text{C}$  NMR:** (126 MHz,  $\text{CD}_3\text{CN}$ )  $\delta$  = 150.9, 148.7, 145.9, 144.8, 143.0, 139.0, 134.5, 133.8, 132.7, 132.3, 132.1, 131.9, 131.1, 130.8, 129.6, 129.1, 127.0, 126.5, 55.9, 21.6, 11.2 ppm.  **$^{19}\text{F}$  NMR:** (471 MHz,  $\text{CD}_3\text{CN}$ )  $\delta$  = -124.0 (sext,  $J_{\text{F-121Sb}}$  = 1942.5 Hz), -124.0 (oct,  $J_{\text{F-123Sb}}$  = 1053.6 Hz) ppm. **IR:** (ATR,  $\text{cm}^{-1}$ ) 2922, 2151, 2037, 2027, 1708, 1620, 1488, 1447, 1291, 1191, 750, 697, 614, 519. **HRMS:** calcd. for  $\text{C}_{30}^{13}\text{CH}_{34}\text{N}_4\text{S}^{2+} [\text{M}-2\text{SbF}_6]^+$ : =495.2526; found = 495.2531.

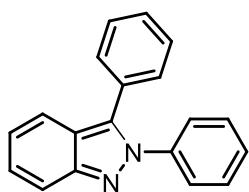
### 2,4-Diphenylcinnolin-3(2H)-one (241):



Salt **238** was stored under ambient conditions for one month. Afterwards an aliquot, purified by column chromatography (pure  $\text{CH}_2\text{Cl}_2$  to  $\text{CH}_2\text{Cl}_2/\text{EtOAc}$ , 95:5) gave **244** as bright orange crystals.<sup>46</sup>

**$^1\text{H}$  NMR:** (300 MHz,  $\text{CDCl}_3$ )  $\delta$  = 7.82 – 7.74 (m, 2H), 7.67 – 7.33 (m, 10H), 7.24 – 7.12 (m, 2H) ppm.  **$^{13}\text{C}$  NMR:** (101 MHz,  $\text{CDCl}_3$ )  $\delta$  = 159.56, 142.74, 142.09, 134.52, 132.50, 131.43, 130.99, 130.80, 129.04, 128.86, 128.81, 128.53, 128.36, 127.63, 126.00, 124.6 ppm.

### 2,3-Diphenyl-2H-indazole (242):



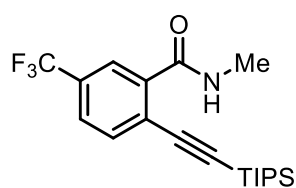
To a solution of salt **238** in *i*-PrOH (1 mL), NaOH (2 equiv) was added and the reaction mixture was slowly heated to reflux. After 1 h the solution was cooled to rt, quenched with aqueous saturated  $\text{NH}_4\text{Cl}$  solution and extracted with  $\text{CH}_2\text{Cl}_2$  ( $3 \times 5$  mL). The combined organic phases were dried over  $\text{Na}_2\text{SO}_4$ . The solvent was removed *in vacuo* and an analytic sample of **242** was obtained after separation by column chromatography (cyclohexane/EtOAc, 10/1).<sup>47</sup>

**$^1\text{H}$  NMR:** (400 MHz,  $\text{CDCl}_3$ )  $\delta$  = 7.81 (d,  $J$  = 8.7 Hz, 1H), 7.72 (d,  $J$  = 8.5 Hz, 1H), 7.48 – 7.33 (m, 11H), 7.15 (dd,  $J$  = 8.5, 6.6 Hz, 1H) ppm.  **$^{13}\text{C}$  NMR:** (101 MHz,  $\text{CDCl}_3$ )  $\delta$  = 149.2, 140.4, 135.6, 130.1, 129.8, 129.1, 128.9, 128.5, 128.4, 127.1, 126.2, 122.7, 121.9, 120.7, 117.9 ppm.

<sup>46</sup>No final yield was determined.

<sup>47</sup>No final yield was determined.

***N*-Methyl-5-(trifluoromethyl)-2-[(triisopropylsilyl)ethynyl]benzamide (**243**):**



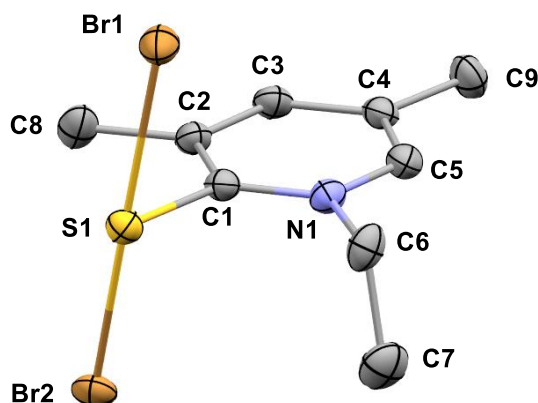
Following a modification of GP **D**, from *N*-methyl-3-(trifluoromethyl)benzamide (1 equiv, 60.9 mg, 0.3 mmol), **160d** (1.5 equiv, 244.0 mg, 0.45 mmol), [RhCp\*Cl<sub>2</sub>]<sub>2</sub> (2.5 mol%, 4.6 mg, 0.0075 mmol), NaOAc (1 equiv, 24.3 mg, 0.3 mmol), and AgSbF<sub>6</sub> (1.7 equiv, 175.2 mg, 0.51 mmol), compound **243** was obtained as a colorless crystalline solid (14.9 mg, 38.8 μmol, 13%).

**<sup>1</sup>H NMR:** (400 MHz, CDCl<sub>3</sub>) δ = 8.42 (dt, *J* = 1.8, 0.9 Hz, 1H), 7.75 (s, 1H), 7.68 – 7.60 (m, 2H), 3.02 (d, *J* = 4.8 Hz, 3H), 1.21 – 1.12 (m, 21H) ppm. **<sup>13</sup>C NMR:** (101 MHz, CDCl<sub>3</sub>) δ = 165.3, 136.1, 134.9, 131.1 (q, *J* = 33.5 Hz), 127.3 (dq, *J* = 59.3, 3.7 Hz), 125.0, 123.1, 122.2, 104.4, 101.9, 27.0, 18.8, 11.3 ppm. **IR:** (ATR, cm<sup>-1</sup>) 3282, 2943, 2864, 1657, 1637, 1558, 1463, 1336, 1301, 1258, 1170, 1131, 882, 674, 650. **HRMS:** calcd. for C<sub>20</sub>H<sub>29</sub>F<sub>3</sub>NOSi<sup>+</sup> [M+H]<sup>+</sup>: 384.1965, found: 384.1964.

## APPENDIX

## X-RAY STRUCTURES

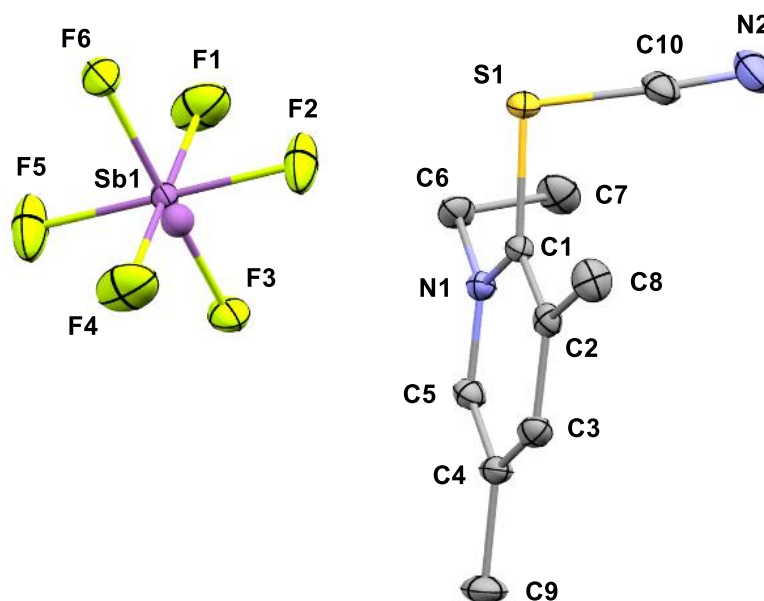
### 2-(Bromothio)-1-ethyl-3,5-dimethylpyridin-1-ium bromide (154c):



Empirical formula	C <sub>9</sub> H <sub>13</sub> Br <sub>2</sub> N S
Color	orange
Formula weight	327.08 g·mol <sup>-1</sup>
Temperature	100 K
Wavelength	1.54178 Å
Crystal system	monoclinic
Space group	C 1 2/c 1, (no. 15)
Unit cell dimensions	a = 23.752(2) Å      α = 90°. b = 7.7745(8) Å      β = 117.597(2)°. c = 14.5136(14) Å    γ = 90°.
Volume	2375.2(4) Å <sup>3</sup>
Z	8
Density (calculated)	1.829 Mg·m <sup>-3</sup>
Absorption coefficient μ	9.956 mm <sup>-1</sup>
F(000)	1280 e
Crystal size	0.21 × 0.20 × 0.08 mm <sup>3</sup>
θ range for data collection	4.200 to 65.082°.
Index ranges	-27 ≤ h ≤ 27, -9 ≤ k ≤ 8, -17 ≤ l ≤ 17
Reflections collected	25385
Independent reflections	2016 [R <sub>int</sub> = 0.0436]
Reflections with I > 2σ(I)	2003
Completeness to θ = 65.082°	100.0 %
Absorption correction	Gaussian
Max. and min. transmission	0.38153 and 0.19076
Refinement method	Full-matrix least-squares on F <sup>2</sup>

Data / restraints / parameters	2016 / 0 / 121	
Goodness-of-fit on $F^2$	1.162	
Final R indices [ $I > 2\sigma(I)$ ]	$R_1 = 0.0232$	$wR^2 = 0.0557$
R indices (all data)	$R_1 = 0.0235$	$wR^2 = 0.0559$
Extinction coefficient	0	
Largest diff. peak and hole	0.410 and -0.478 e $\cdot$ Å $^{-3}$	

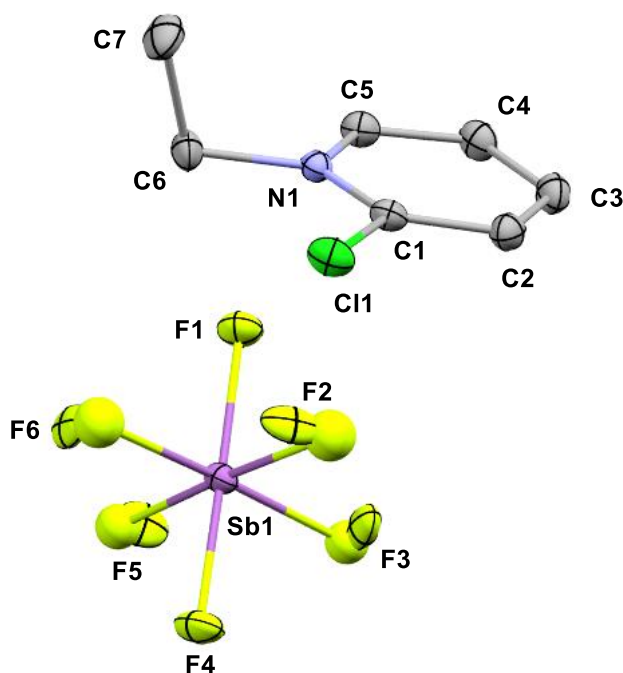
**1-Ethyl-3,5-dimethyl-2-thiocyanatopyridin-1-ium hexafluoroantimonate (155b):**



Empirical formula	$C_{10}H_{13}F_6N_2S Sb$	
Color	colorless	
Formula weight	429.03 $g \cdot mol^{-1}$	
Temperature	100 K	
Wavelength	0.71073 Å	
Crystal system	Monoclinic	
Space group	p 21/n, (no. 14)	
Unit cell dimensions	$a = 7.272(8)$ Å	$\alpha = 90^\circ$ .
	$b = 13.130(13)$ Å	$\beta = 90.92(2)^\circ$ .
	$c = 15.688(17)$ Å	$\gamma = 90^\circ$ .
Volume	$1498(3)$ Å <sup>3</sup>	
Z	4	
Density (calculated)	$1.903$ Mg·m <sup>-3</sup>	
Absorption coefficient $\mu$	$2.036$ mm <sup>-1</sup>	
$F(000)$	832 e	
Crystal size	$0.15 \times 0.15 \times 0.04$ mm <sup>3</sup>	
$\theta$ range for data collection	$2.597$ to $33.700^\circ$ .	
Index ranges	$-10 \leq h \leq 11, -20 \leq k \leq 19, -24 \leq l \leq 23$	
Reflections collected	26606	
Independent reflections	5757 [ $R_{int} = 0.0257$ ]	
Reflections with $I > 2\sigma(I)$	5187	
Completeness to $\theta = 25.242^\circ$	100.0%	
Absorption correction	Gaussian	

Max. and min. transmission	0.91378 and 0.75472	
Refinement method	Full-matrix least-squares on $F^2$	
Data / restraints / parameters	5757 / 0 / 188	
Goodness-of-fit on $F^2$	1.045	
Final R indices [ $I > 2\sigma(I)$ ]	$R_1 = 0.0225$	$wR^2 = 0.0550$
R indices (all data)	$R_1 = 0.0260$	$wR^2 = 0.0562$
Extinction coefficient	n/a	
Largest diff. peak and hole	0.838 and -0.847 e·Å <sup>-3</sup>	

**2-Chloro-1-ethylpyridin-1-ium hexafluoroantimonate (156d):**

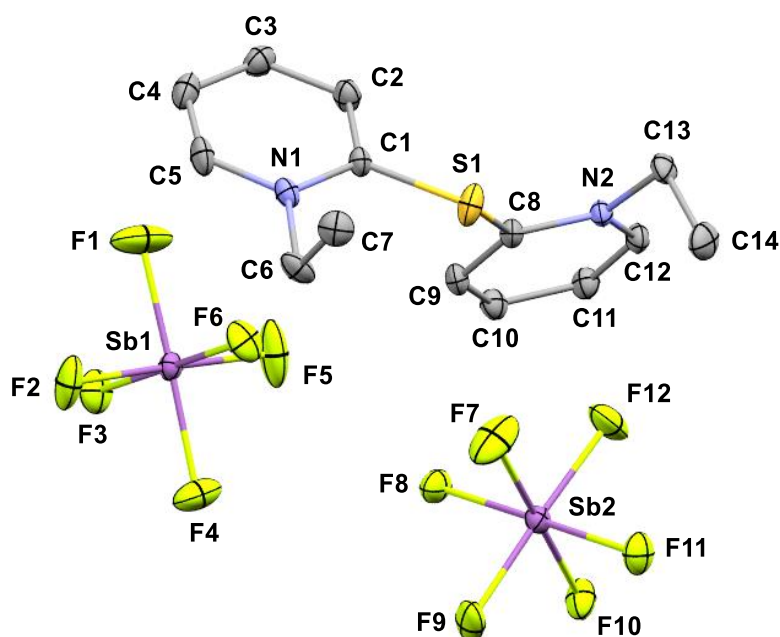


Empirical formula	$C_7H_9ClF_6NSb$	
Color	colorless	
Formula weight	$378.35 \text{ g}\cdot\text{mol}^{-1}$	
Temperature	100 K	
Wavelength	$0.71073 \text{ \AA}$	
Crystal system	monoclinic	
Space group	$P 2_1/n$ , (no. 14)	
Unit cell dimensions	$a = 8.6285(17) \text{ \AA}$	$\alpha = 90^\circ$ .
	$b = 10.996(2) \text{ \AA}$	$\beta = 101.549(3)^\circ$ .
	$c = 12.597(3) \text{ \AA}$	$\gamma = 90^\circ$ .
Volume	$1171.1(4) \text{ \AA}^3$	
Z	4	
Density (calculated)	$2.146 \text{ Mg}\cdot\text{m}^{-3}$	
Absorption coefficient $\mu$	$2.634 \text{ mm}^{-1}$	
$F(000)$	720 e	
Crystal size	$0.18 \times 0.13 \times 0.05 \text{ mm}^3$	
$\theta$ range for data collection	$3.182$ to $35.629^\circ$ .	
Index ranges	$-14 \leq h \leq 14$ , $-18 \leq k \leq 18$ , $-20 \leq l \leq 20$	
Reflections collected	43856	
Independent reflections	5397 [ $R_{\text{int}} = 0.0278$ ]	
Reflections with $I > 2\sigma(I)$	4889	
Completeness to $\square = 25.242^\circ$	99.8%	



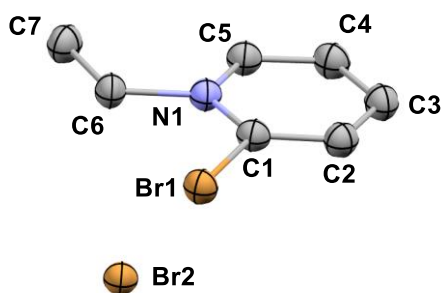
Absorption correction	Gaussian	
Max. and min. transmission	0.91577 and 0.78357	
Refinement method	Full-matrix least-squares on $F^2$	
Data / restraints / parameters	5397 / 0 / 162	
Goodness-of-fit on $F^2$	1.045	
Final $R$ indices [ $I > 2\sigma(I)$ ]	$R_1 = 0.0202$	$wR^2 = 0.0463$
$R$ indices (all data)	$R_1 = 0.0238$	$wR^2 = 0.0480$
Extinction coefficient	n/a	
Largest diff. peak and hole	1.518 and $-0.790 \text{ e} \cdot \text{\AA}^{-3}$	

**2,2'-Thiobis(1-ethylpyridin-1-ium) bishexafluoroantimonate (157):**



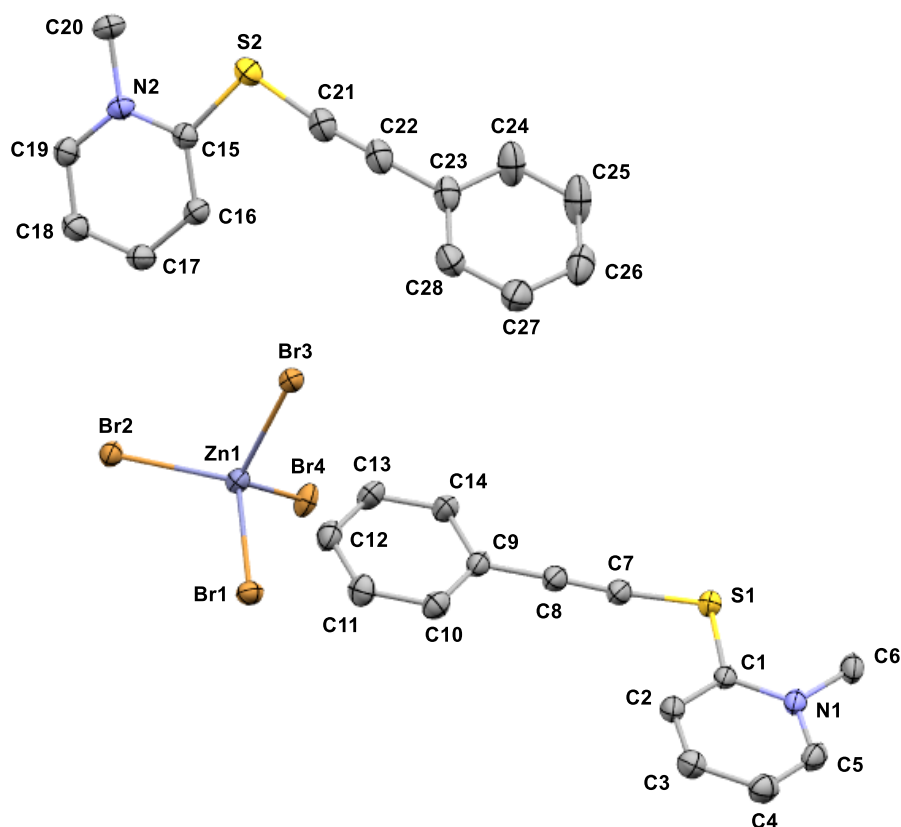
Empirical formula	$C_{14}H_{18}F_{12}N_2SSb_2$	
Color	colorless	
Formula weight	717.86 $g \cdot mol^{-1}$	
Temperature	100 K	
Wavelength	0.71073 Å	
Crystal system	MONOCLINIC	
Space group	$p 2_1/n$ , (no. 14)	
Unit cell dimensions	$a = 16.655(2)$ Å	$\alpha = 90^\circ$ .
	$b = 23.302(3)$ Å	$\beta = 101.886(2)^\circ$ .
	$c = 17.413(2)$ Å	$\gamma = 90^\circ$ .
	$V = 6613.1(14)$ Å <sup>3</sup>	
Volume	6613.1(14) Å <sup>3</sup>	
Z	12	
Density (calculated)	2.163 $Mg \cdot m^{-3}$	
Absorption coefficient	2.650 $mm^{-1}$	
F(000)	4104 e	
Crystal size	0.24 x 0.18 x 0.06 mm <sup>3</sup>	
$\theta$ range for data collection	1.480 to 36.319°.	
Index ranges	$-27 \leq h \leq 27$ , $-38 \leq k \leq 38$ , $-29 \leq l \leq 29$	
Reflections collected	258729	
Independent reflections	32018 [ $R_{int} = 0.0308$ ]	
Reflections with $I > 2\sigma(I)$	26780	
Completeness to $\theta = 25.242^\circ$	99.9 %	
Absorption correction	Gaussian	

Max. and min. transmission	0.7473 and 0.5745	
Refinement method	Full-matrix least-squares on $F^2$	
Data / restraints / parameters	32018 / 0 / 844	
Goodness-of-fit on $F^2$	1.029	
Final R indices [ $I > 2\sigma(I)$ ]	$R_1 = 0.0208$	$wR^2 = 0.0435$
R indices (all data)	$R_1 = 0.0306$	$wR^2 = 0.0473$
Extinction coefficient	n/a	
Largest diff. peak and hole	1.349 and -0.746 e·Å <sup>-3</sup>	

**2-Bromo-1-ethylpyridin-1-ium bromide (158):**

Empirical formula	C <sub>7</sub> H <sub>9</sub> Br <sub>2</sub> N
Formula weight	266.97
Temperature/K	100.02
Crystal system	orthorhombic
Space group	Pnma
a/Å	15.2828(6)
b/Å	6.7822(2)
c/Å	8.4389(4)
α/°	90
β/°	90
γ/°	90
Volume/Å <sup>3</sup>	874.70(6)
Z	4
ρ <sub>calc</sub> /cm <sup>3</sup>	2.027
μ/mm <sup>-1</sup>	9.194
F(000)	512.0
Crystal size/mm <sup>3</sup>	0.596 × 0.064 × 0.034
Radiation	MoKα (λ = 0.71073)
2θ range for data collection/°	5.332 to 59.232
Index ranges	-20 ≤ h ≤ 21, -9 ≤ k ≤ 9, -11 ≤ l ≤ 11
Reflections collected	13108
Independent reflections	1319 [R <sub>int</sub> = 0.0199, R <sub>sigma</sub> = 0.0111]
Data/restraints/parameters	1319/0/61
Goodness-of-fit on F <sup>2</sup>	1.117
Final R indexes [I ≥ 2σ (I)]	R <sub>1</sub> = 0.0226, wR <sub>2</sub> = 0.0573
Final R indexes [all data]	R <sub>1</sub> = 0.0232, wR <sub>2</sub> = 0.0576
Largest diff. peak/hole / e Å <sup>-3</sup>	0.60/-0.36

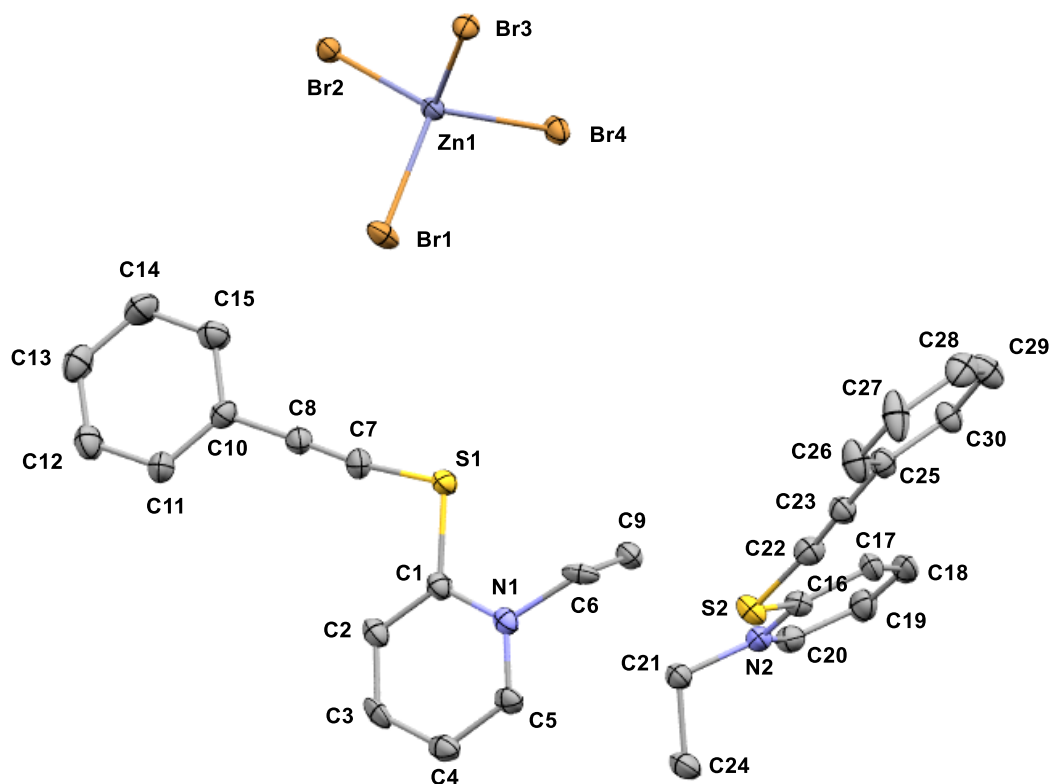
**1-Methyl-2-[(phenylethynyl)thio]pyridin-1-ium tetrabromozincate (160a):**



Empirical formula	C <sub>28</sub> H <sub>24</sub> Br <sub>4</sub> N <sub>2</sub> S <sub>2</sub> Zn
Formula weight	837.62
Temperature/K	99.99
Crystal system	triclinic
Space group	P-1
a/Å	8.5908(4)
b/Å	11.4010(5)
c/Å	16.9074(6)
α/°	101.210(2)
β/°	102.3600(10)
γ/°	100.535(2)
Volume/Å <sup>3</sup>	1542.58(11)
Z	2
ρ <sub>calc</sub> /cm <sup>3</sup>	1.803
μ/mm <sup>-1</sup>	6.133
F(000)	816.0
Crystal size/mm <sup>3</sup>	0.429 × 0.3 × 0.122
Radiation	MoKα (λ = 0.71073)
2θ range for data collection/°	5.496 to 63.134
Index ranges	-12 ≤ h ≤ 12, -16 ≤ k ≤ 16, -24 ≤ l ≤ 24
Reflections collected	70984
Independent reflections	10325 [R <sub>int</sub> = 0.0314, R <sub>sigma</sub> = 0.0208]
Data/restraints/parameters	10325/0/336

Goodness-of-fit on  $F^2$  1.023  
 Final R indexes [ $I \geq 2\sigma(I)$ ]  $R_1 = 0.0182$ ,  $wR_2 = 0.0453$   
 Final R indexes [all data]  $R_1 = 0.0211$ ,  $wR_2 = 0.0463$   
 Largest diff. peak/hole /  $e \text{ \AA}^{-3}$  0.65/-0.38

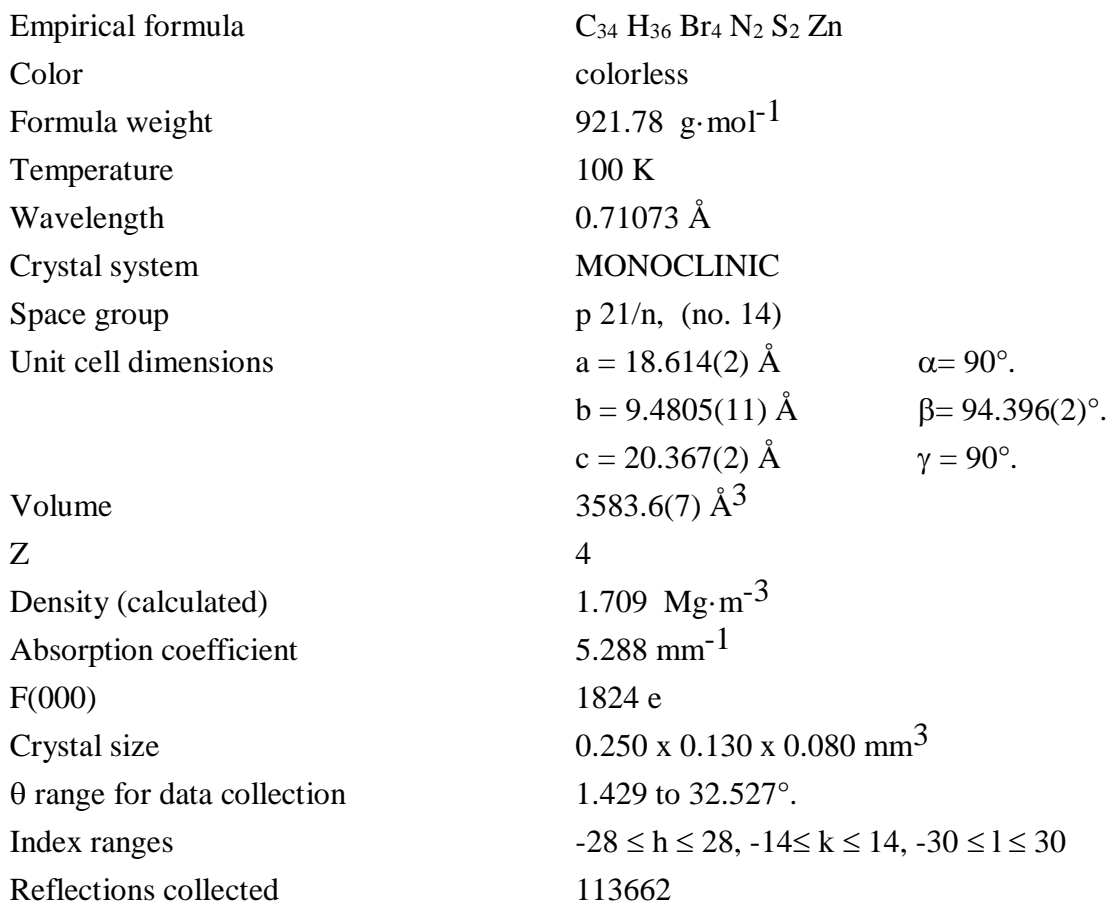
**1-Ethyl-2-[(phenylethynyl)thio]pyridin-1-ium tetrabromozincate (160b):**



Empirical formula	$C_{30}H_{28}Br_4N_2S_2Zn$	
Color	colorless	
Formula weight	$865.67 \text{ g}\cdot\text{mol}^{-1}$	
Temperature	100.15 K	
Wavelength	$0.71073 \text{ \AA}$	
Crystal system	Triclinic	
Space group	$P\bar{1}$ , (no. 2)	
Unit cell dimensions	$a = 9.3174(5) \text{ \AA}$	$\alpha = 104.414(5)^\circ$
	$b = 9.6047(3) \text{ \AA}$	$\beta = 96.515(7)^\circ$
	$c = 18.8633(18) \text{ \AA}$	$\gamma = 91.289(4)^\circ$
Volume	$1622.14(19) \text{ \AA}^3$	
Z	2	
Density (calculated)	$1.772 \text{ Mg}\cdot\text{m}^{-3}$	
Absorption coefficient	$5.835 \text{ mm}^{-1}$	
F(000)	848 e	
Crystal size	$0.08 \times 0.07 \times 0.04 \text{ mm}^3$	
$\theta$ range for data collection	$2.705$ to $33.128^\circ$	
Index ranges	$-14 \leq h \leq 14$ , $-14 \leq k \leq 14$ , $-28 \leq l \leq 28$	
Reflections collected	43143	

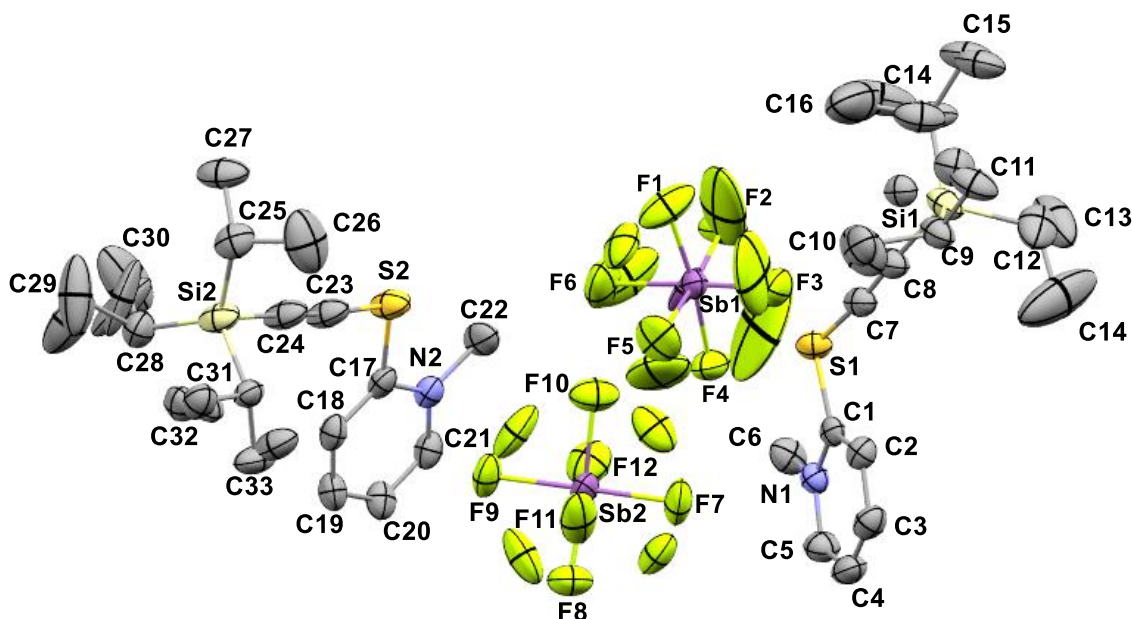
Independent reflections	12306 [ $R_{\text{int}} = 0.0583$ ]	
Reflections with $I > 2\sigma(I)$	10442	
Completeness to $\theta = 25.242^\circ$	99.8 %	
Absorption correction	Gaussian	
Max. and min. transmission	0.72323 and 0.52922	
Refinement method	Full-matrix least-squares on $F^2$	
Data / restraints / parameters	12306 / 0 / 355	
Goodness-of-fit on $F^2$	1.080	
Final R indices [ $I > 2\sigma(I)$ ]	$R_1 = 0.0846$	$wR^2 = 0.2618$
R indices (all data)	$R_1 = 0.0981$	$wR^2 = 0.2750$
Extinction coefficient	n/a	
Largest diff. peak and hole	2.824 and -3.220 e $\cdot\text{\AA}^{-3}$	





Independent reflections	12967 [ $R_{\text{int}} = 0.0420$ ]	
Reflections with $I > 2\sigma(I)$	10698	
Completeness to $\theta = 25.242^\circ$	100.0 %	
Absorption correction	Gaussian	
Max. and min. transmission	0.71051 and 0.44092	
Refinement method	Full-matrix least-squares on $F^2$	
Data / restraints / parameters	12967 / 0 / 394	
Goodness-of-fit on $F^2$	1.142	
Final R indices [ $I > 2\sigma(I)$ ]	$R_1 = 0.0236$	$wR^2 = 0.0601$
R indices (all data)	$R_1 = 0.0366$	$wR^2 = 0.0769$
Extinction coefficient	n/a	
Largest diff. peak and hole	0.925 and -0.551 e·Å <sup>-3</sup>	

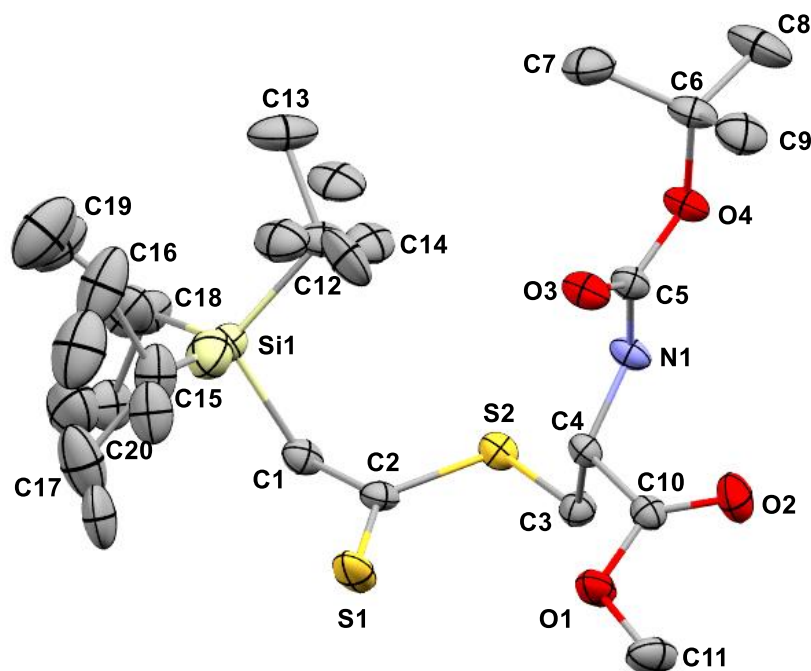
**1-Methyl-2-[[[(triisopropylsilyl)ethynyl]thio]pyridin-1-ium hexafluoroantimonate (160d):**



Empirical formula	C <sub>17</sub> H <sub>28</sub> F <sub>6</sub> NSSbSi
Formula weight	542.30
Temperature/K	100.01
Crystal system	monoclinic
Space group	P2/c
a/Å	22.674(2)
b/Å	13.0853(8)
c/Å	15.9485(10)
α/°	90
β/°	103.430(3)
γ/°	90
Volume/Å <sup>3</sup>	4602.4(6)
Z	8
ρ <sub>calc</sub> /cm <sup>3</sup>	1.565
μ/mm <sup>-1</sup>	1.391
F(000)	2176.0
Crystal size/mm <sup>3</sup>	0.361 × 0.203 × 0.082
Radiation	MoKα (λ = 0.71073)
2θ range for data collection/°	4.83 to 57.498
Index ranges	-30 ≤ h ≤ 30, -17 ≤ k ≤ 17, -21 ≤ l ≤ 20
Reflections collected	78514
Independent reflections	11931 [R <sub>int</sub> = 0.0275, R <sub>sigma</sub> = 0.0183]
Data/restraints/parameters	11931/183/722
Goodness-of-fit on F <sup>2</sup>	1.035
Final R indexes [I ≥ 2σ (I)]	R <sub>1</sub> = 0.0420, wR <sub>2</sub> = 0.0962

Final R indexes [all data]  $R_1 = 0.0515$ ,  $wR_2 = 0.1032$   
Largest diff. peak/hole / e  $\text{\AA}^{-3}$  1.66/-2.01

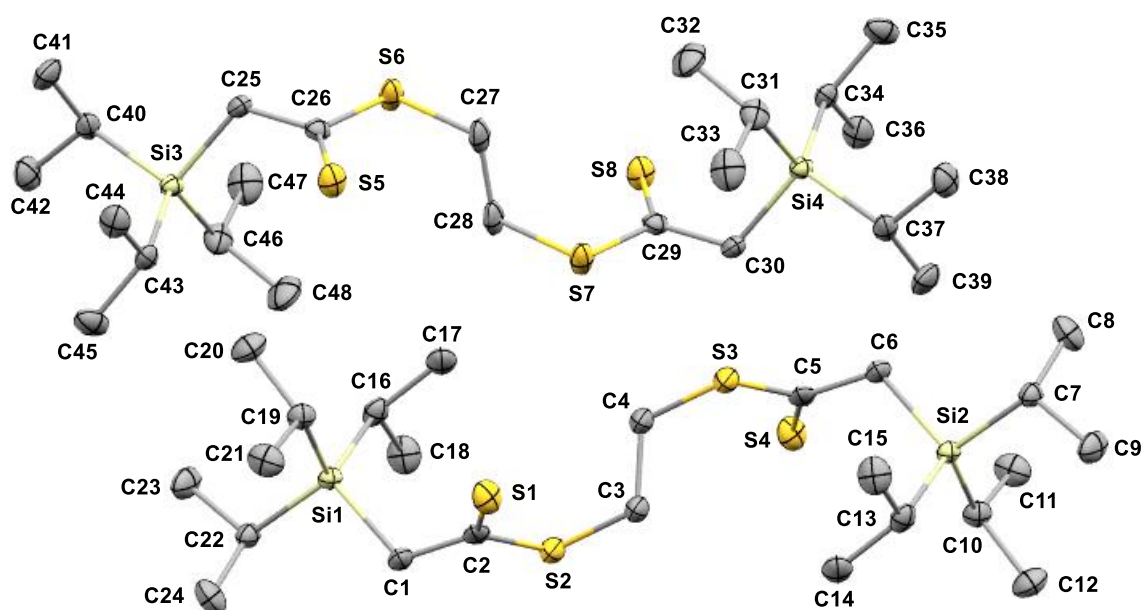
**Methyl *N*-(*tert*-butoxycarbonyl)-*S*-[2-(triisopropylsilyl)ethanethioyl]-*L*-cysteinate (170):**



Empirical formula	C <sub>15</sub> H <sub>31</sub> NOSSi
Formula weight	301.56
Temperature/K	99.98
Crystal system	monoclinic
Space group	P2 <sub>1</sub> /c
<i>a</i> /Å	15.394(2)
<i>b</i> /Å	8.5880(10)
<i>c</i> /Å	14.610(2)
$\alpha$ /°	90
$\beta$ /°	115.589(4)
$\gamma$ /°	90
Volume/Å <sup>3</sup>	1742.0(4)
<i>Z</i>	4
$\rho_{\text{calc}}/\text{cm}^3$	1.150
$\mu/\text{mm}^{-1}$	0.249
<i>F</i> (000)	664.0
Crystal size/mm <sup>3</sup>	0.404 × 0.261 × 0.038
Radiation	MoK $\alpha$ ( $\lambda$ = 0.71073)
2 $\theta$ range for data collection/°	5.578 to 57.552
Index ranges	-20 ≤ <i>h</i> ≤ 20, -11 ≤ <i>k</i> ≤ 11, -19 ≤ <i>l</i> ≤ 19
Reflections collected	29735
Independent reflections	4510 [ <i>R</i> <sub>int</sub> = 0.0270, <i>R</i> <sub>sigma</sub> = 0.0190]
Data/restraints/parameters	4510/0/190
Goodness-of-fit on <i>F</i> <sup>2</sup>	1.102
Final <i>R</i> indexes [ <i>I</i> ≥ 2 $\sigma$ ( <i>I</i> )]	<i>R</i> <sub>1</sub> = 0.0298, <i>wR</i> <sub>2</sub> = 0.0771
Final <i>R</i> indexes [all data]	<i>R</i> <sub>1</sub> = 0.0326, <i>wR</i> <sub>2</sub> = 0.0790

Largest diff. peak/hole / e Å<sup>-3</sup> 0.44/-0.24

**Ethane-1,2-diyl bis[2-(triisopropylsilyl)ethanedithioate] (171):**

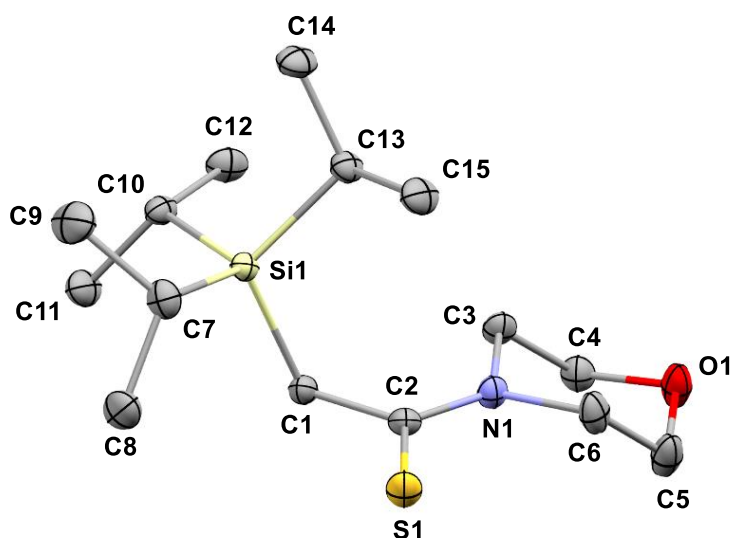


Empirical formula	C <sub>24</sub> H <sub>50</sub> S <sub>4</sub> Si <sub>2</sub>
Formula weight	523.06
Temperature/K	100
Crystal system	triclinic
Space group	P-1
a/Å	8.937(2)
b/Å	10.679(3)
c/Å	15.934(5)
α/°	87.869(9)
β/°	87.665(9)
γ/°	89.140(7)
Volume/Å <sup>3</sup>	1518.3(8)
Z	2
ρ <sub>calc</sub> /cm <sup>3</sup>	1.144
μ/mm <sup>-1</sup>	0.402
F(000)	572.0
Crystal size/mm <sup>3</sup>	0.318 × 0.256 × 0.018
Radiation	MoKα (λ = 0.71073)
2θ range for data collection/°	4.518 to 52.532
Index ranges	-11 ≤ h ≤ 11, -13 ≤ k ≤ 13, 0 ≤ l ≤ 19
Reflections collected	6001
Independent reflections	6001 [R <sub>int</sub> = ?, R <sub>sigma</sub> = 0.0453]

Data/restraints/parameters	6001/172/284
Goodness-of-fit on $F^2$	1.060
Final R indexes [ $I \geq 2\sigma(I)$ ]	$R_1 = 0.0525$ , $wR_2 = 0.1082$
Final R indexes [all data]	$R_1 = 0.0634$ , $wR_2 = 0.1128$
Largest diff. peak/hole / $e \text{ \AA}^{-3}$	0.43/-0.46

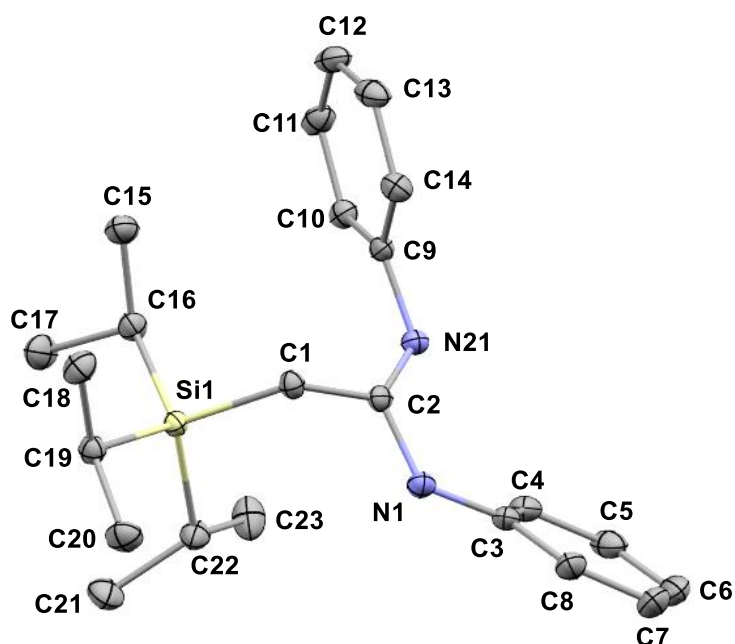


**1-Morpholino-2-(triisopropylsilyl)ethane-1-thione (178):**



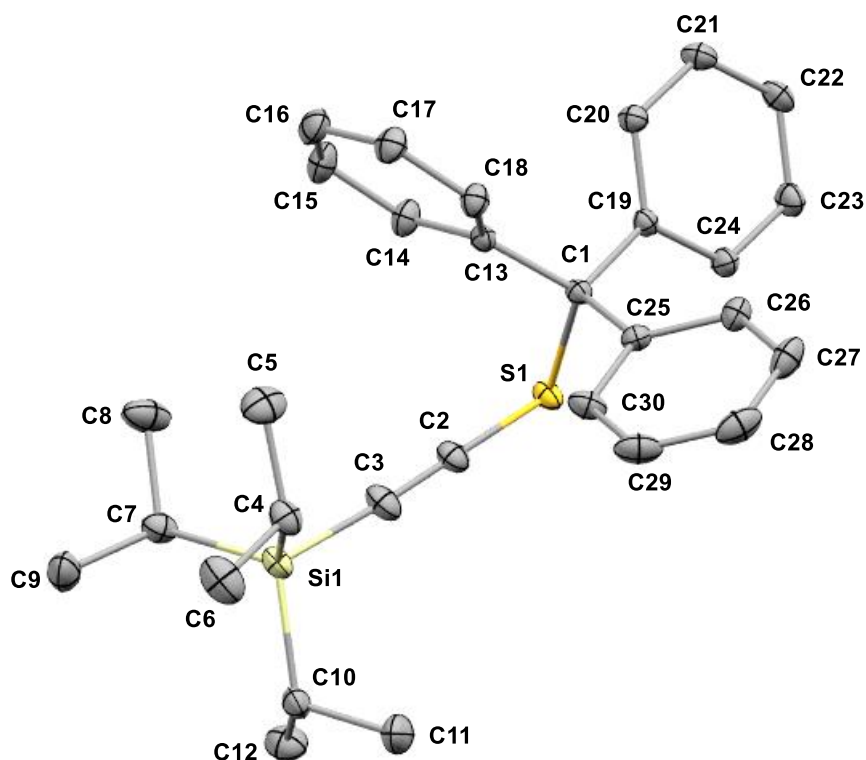
Empirical formula	C <sub>20</sub> H <sub>39</sub> NO <sub>4</sub> S <sub>2</sub> Si
Formula weight	449.73
Temperature/K	99.98
Crystal system	orthorhombic
Space group	P2 <sub>1</sub> 2 <sub>1</sub> 2 <sub>1</sub>
a/Å	7.7423(8)
b/Å	10.4197(8)
c/Å	32.414(3)
α/°	90
β/°	90
γ/°	90
Volume/Å <sup>3</sup>	2614.9(4)
Z	4
ρ <sub>calc</sub> /cm <sup>3</sup>	1.142
μ/mm <sup>-1</sup>	0.272
F(000)	976.0
Crystal size/mm <sup>3</sup>	0.212 × 0.164 × 0.06
Radiation	MoKα (λ = 0.71073)
2θ range for data collection/°	5.026 to 57.462
Index ranges	-8 ≤ h ≤ 10, -12 ≤ k ≤ 14, -30 ≤ l ≤ 43
Reflections collected	21251
Independent reflections	6635 [R <sub>int</sub> = 0.0225, R <sub>sigma</sub> = 0.0250]
Data/restraints/parameters	6635/88/359
Goodness-of-fit on F <sup>2</sup>	1.107
Final R indexes [I ≥ 2σ (I)]	R <sub>1</sub> = 0.0316, wR <sub>2</sub> = 0.0721
Final R indexes [all data]	R <sub>1</sub> = 0.0347, wR <sub>2</sub> = 0.0738
Largest diff. peak/hole / e Å <sup>-3</sup>	0.20/-0.24
Flack parameter	0.006(19)

***N,N'*-Diphenyl-2-(triisopropylsilyl)acetimidamide (184):**



Empirical formula	C <sub>23</sub> H <sub>34</sub> N <sub>2</sub> Si
Formula weight	366.61
Temperature/K	99.98
Crystal system	monoclinic
Space group	P2 <sub>1</sub> /c
a/Å	9.7796(8)
b/Å	22.9294(18)
c/Å	9.9481(8)
α/°	90
β/°	103.240(3)
γ/°	90
Volume/Å <sup>3</sup>	2171.5(3)
Z	4
ρ <sub>calc</sub> /cm <sup>3</sup>	1.121
amiduμ/mm <sup>-1</sup>	0.117
F(000)	800.0
Crystal size/mm <sup>3</sup>	0.452 × 0.168 × 0.092
Radiation	MoKα (λ = 0.71073)
2θ range for data collection/°	5.562 to 59.212
Index ranges	-13 ≤ h ≤ 13, -31 ≤ k ≤ 31, -13 ≤ l ≤ 13
Reflections collected	45001
Independent reflections	6081 [R <sub>int</sub> = 0.0230, R <sub>sigma</sub> = 0.0151]
Data/restraints/parameters	6081/0/245
Goodness-of-fit on F <sup>2</sup>	1.072
Final R indexes [I ≥ 2σ (I)]	R <sub>1</sub> = 0.0328, wR <sub>2</sub> = 0.0850
Final R indexes [all data]	R <sub>1</sub> = 0.0346, wR <sub>2</sub> = 0.0865
Largest diff. peak/hole / e Å <sup>-3</sup>	0.42/-0.25

**Triisopropyl[(tritylthio)ethynyl]silane (186):**

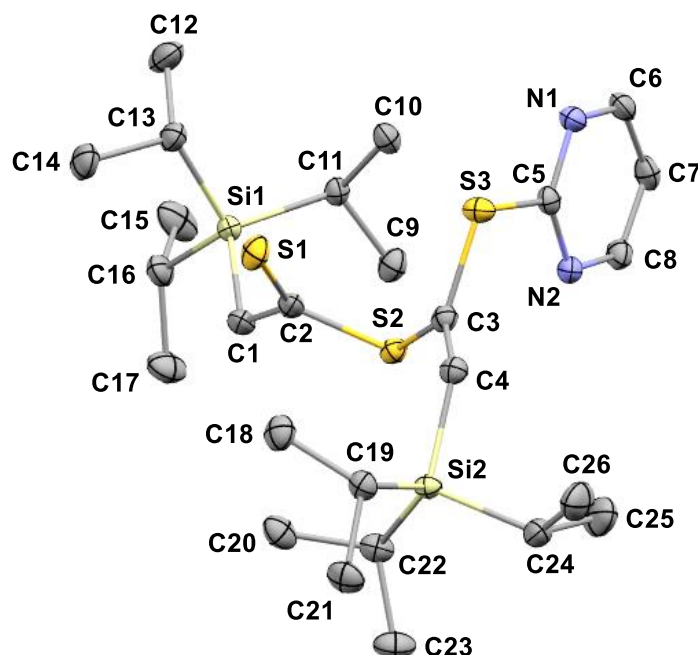


Empirical formula	C <sub>30</sub> H <sub>36</sub> SSi
Formula weight	456.74
Temperature/K	100.02
Crystal system	triclinic
Space group	P-1
a/Å	9.7652(12)
b/Å	10.8607(11)
c/Å	13.3088(15)
α/°	98.629(4)
β/°	92.583(4)
γ/°	108.012(4)
Volume/Å <sup>3</sup>	1320.8(3)
Z	2
ρ <sub>calc</sub> /g/cm <sup>3</sup>	1.148
μ/mm <sup>-1</sup>	0.183
F(000)	492.0
Crystal size/mm <sup>3</sup>	0.273 × 0.241 × 0.198
Radiation	MoKα (λ = 0.71073)
2θ range for data collection/°	4.406 to 61.074
Index ranges	-13 ≤ h ≤ 13, -15 ≤ k ≤ 15, -19 ≤ l ≤ 19
Reflections collected	109718
Independent reflections	8053 [R <sub>int</sub> = 0.0235, R <sub>sigma</sub> = 0.0117]

Data/restraints/parameters	8053/0/295
Goodness-of-fit on $F^2$	1.036
Final R indexes [ $I \geq 2\sigma(I)$ ]	$R_1 = 0.0294$ , $wR_2 = 0.0809$
Final R indexes [all data]	$R_1 = 0.0313$ , $wR_2 = 0.0827$
Largest diff. peak/hole / $e \text{ \AA}^{-3}$	0.43/-0.27

**(Z)-1-(Pyrimidin-2-ylthio)-2-(triisopropylsilyl)vinyl  
(188):**

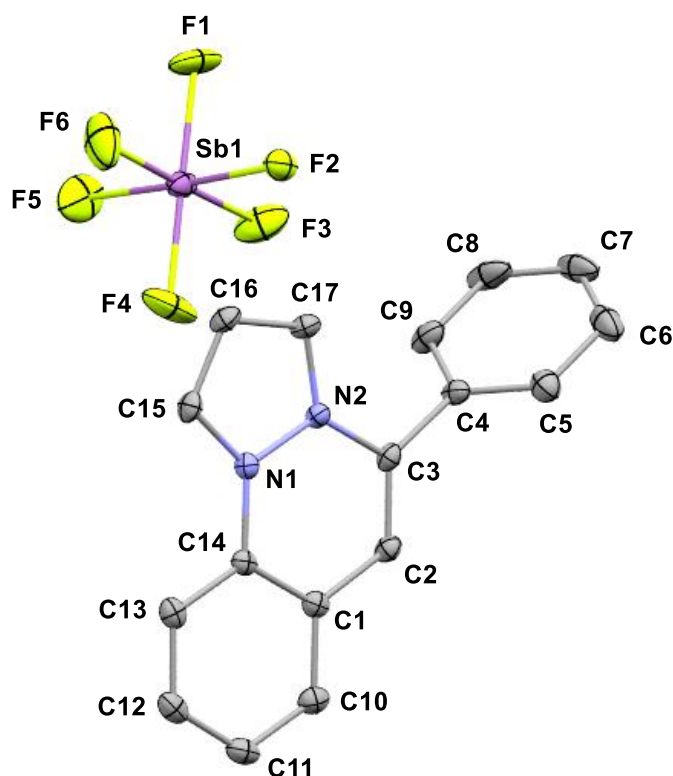
**2-(triisopropylsilyl)ethanedithioate**



Empirical formula	C <sub>26</sub> H <sub>48</sub> N <sub>2</sub> S <sub>3</sub> Si <sub>2</sub>
Formula weight	541.02
Temperature/K	100.02
Crystal system	monoclinic
Space group	P2 <sub>1</sub> /n
a/Å	13.2581(12)
b/Å	9.8280(12)
c/Å	24.350(3)
α/°	90
β/°	103.907(3)
γ/°	90
Volume/Å <sup>3</sup>	3079.9(6)
Z	4
ρ <sub>calc</sub> /g/cm <sup>3</sup>	1.167
μ/mm <sup>-1</sup>	0.336
F(000)	1176.0
Crystal size/mm <sup>3</sup>	0.429 × 0.425 × 0.05
Radiation	MoKα (λ = 0.71073)
2θ range for data collection/°	5.216 to 54.262
Index ranges	-17 ≤ h ≤ 16, 0 ≤ k ≤ 12, 0 ≤ l ≤ 31
Reflections collected	7023
Independent reflections	7023 [R <sub>int</sub> = ?, R <sub>sigma</sub> = 0.0255]
Data/restraints/parameters	7023/0/311
Goodness-of-fit on F <sup>2</sup>	1.052
Final R indexes [I ≥ 2σ (I)]	R <sub>1</sub> = 0.0328, wR <sub>2</sub> = 0.0787

Final R indexes [all data]  $R_1 = 0.0396$ ,  $wR_2 = 0.0832$   
Largest diff. peak/hole / e  $\text{\AA}^{-3}$  0.51/-0.21

**5-Phenylpyrazolo[1,2-*a*]cinnolin-4-ium hexafluoroantimonate (203):**



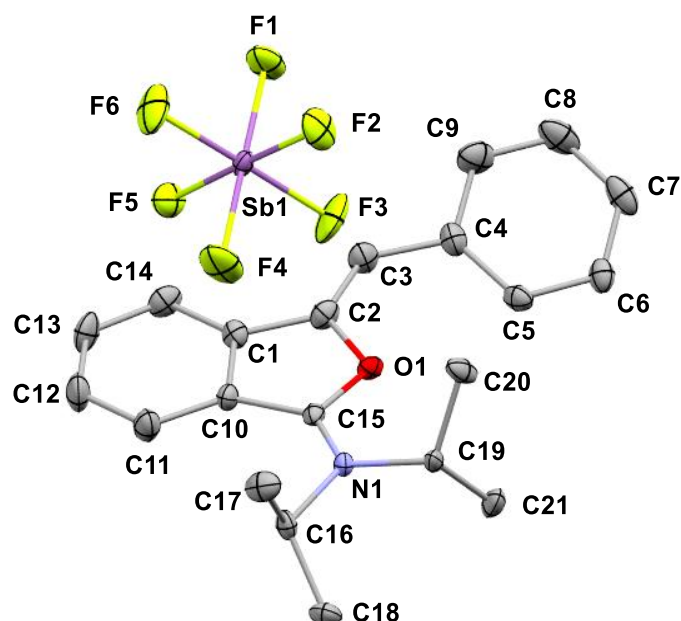
Empirical formula	C <sub>17</sub> H <sub>13</sub> N <sub>2</sub> x SbF <sub>6</sub>
Formula weight	481.04
Temperature/K	120.0
Crystal system	monoclinic
Space group	P2 <sub>1</sub> /c
a/Å	6.8581(4)
b/Å	16.6089(10)
c/Å	14.7649(9)
α/°	90
β/°	93.231(2)
γ/°	90
Volume/Å <sup>3</sup>	1679.13(17)
Z	4
ρ <sub>calc</sub> /g/cm <sup>3</sup>	1.903
μ/mm <sup>-1</sup>	1.708
F(000)	936.0
Crystal size/mm <sup>3</sup>	0.24 × 0.15 × 0.14
Radiation	MoKα (λ = 0.71073)
2θ range for data collection/°	4.906 to 59.998
Index ranges	-9 ≤ h ≤ 9, -23 ≤ k ≤ 23, -20 ≤ l ≤ 20
Reflections collected	36038
Independent reflections	4906 [R <sub>int</sub> = 0.0297, R <sub>sigma</sub> = 0.0164]
Data/restraints/parameters	4906/0/235
Goodness-of-fit on F <sup>2</sup>	1.066
Final R indexes [I ≥ 2σ (I)]	R <sub>1</sub> = 0.0214, wR <sub>2</sub> = 0.0505
Final R indexes [all data]	R <sub>1</sub> = 0.0259, wR <sub>2</sub> = 0.0527

Largest diff. peak/hole / e Å<sup>-3</sup>

0.67/-0.90



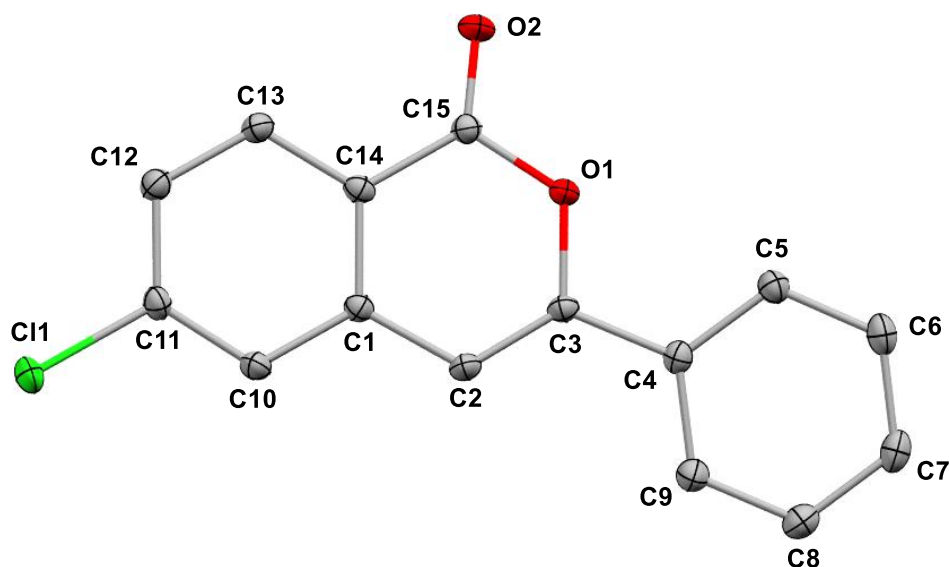
**(Z)-N-(3-benzylideneisobenzofuran-1(3H)-ylidene)-N-isopropylpropan-2-aminium hexafluoroantimonate (205a)**



Empirical formula	C <sub>21</sub> H <sub>24</sub> F <sub>6</sub> NOSb
Formula weight	542.16
Temperature/K	100.0
Crystal system	monoclinic
Space group	P2 <sub>1</sub> /c
a/Å	8.2054(3)
b/Å	17.6617(6)
c/Å	15.2985(5)
α/°	90
β/°	103.954(2)
γ/°	90
Volume/Å <sup>3</sup>	2151.65(13)
Z	4
ρ <sub>calc</sub> /cm <sup>3</sup>	1.674
μ/mm <sup>-1</sup>	1.345
F(000)	1080.0
Crystal size/mm <sup>3</sup>	0.177 × 0.136 × 0.054
Radiation	MoKα (λ = 0.71073)
2θ range for data collection/°	4.612 to 61.166
Index ranges	-11 ≤ h ≤ 11, -24 ≤ k ≤ 24, -21 ≤ l ≤ 21
Reflections collected	69350
Independent reflections	6568 [R <sub>int</sub> = 0.0449, R <sub>sigma</sub> = 0.0248]
Data/restraints/parameters	6568/0/275
Goodness-of-fit on F <sup>2</sup>	1.034
Final R indexes [I ≥ 2σ (I)]	R <sub>1</sub> = 0.0316, wR <sub>2</sub> = 0.0665
Final R indexes [all data]	R <sub>1</sub> = 0.0439, wR <sub>2</sub> = 0.0719

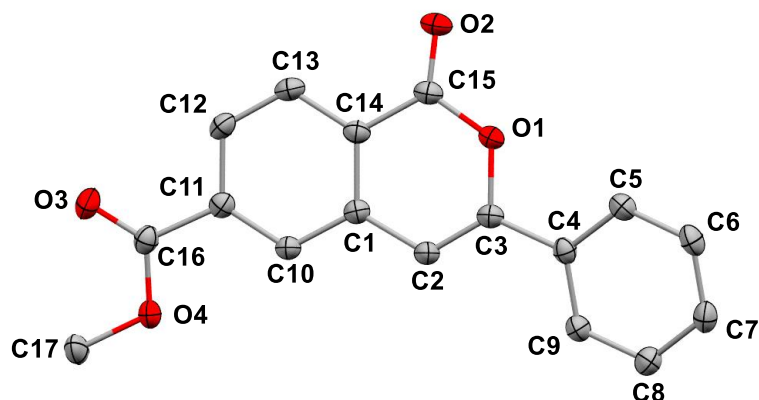
Largest diff. peak/hole / e Å<sup>-3</sup> 1.27/-1.02

**6-Chloro-3-phenyl-1*H*-isochromen-1-one (211):**



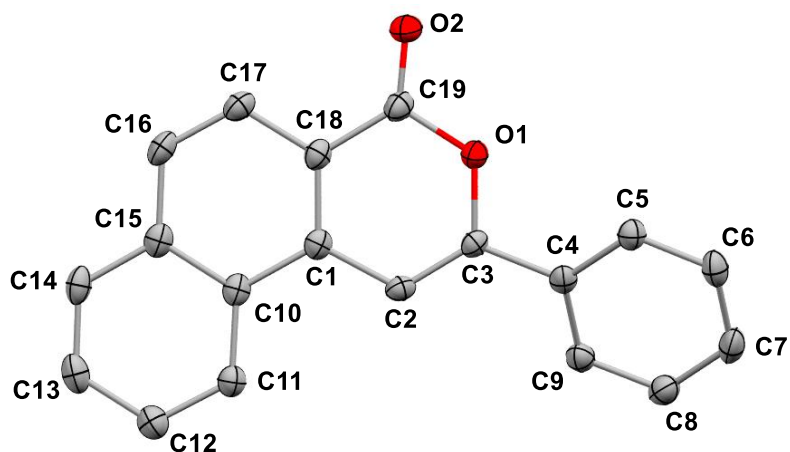
Empirical formula	C <sub>15</sub> H <sub>9</sub> ClO <sub>2</sub>
Formula weight	256.67
Temperature/K	99.98
Crystal system	monoclinic
Space group	P2 <sub>1</sub> /n
a/Å	5.9730(8)
b/Å	3.8086(5)
c/Å	49.432(7)
α/°	90
β/°	90.944(3)
γ/°	90
Volume/Å <sup>3</sup>	1124.4(3)
Z	4
ρ <sub>calc</sub> /cm <sup>3</sup>	1.516
μ/mm <sup>-1</sup>	0.328
F(000)	528.0
Crystal size/mm <sup>3</sup>	0.971 × 0.218 × 0.05
Radiation	MoKα (λ = 0.71073)
2θ range for data collection/°	4.944 to 57.44
Index ranges	-8 ≤ h ≤ 8, -4 ≤ k ≤ 5, -66 ≤ l ≤ 66
Reflections collected	22133
Independent reflections	2857 [R <sub>int</sub> = 0.0241, R <sub>sigma</sub> = 0.0143]
Data/restraints/parameters	2857/0/163
Goodness-of-fit on F <sup>2</sup>	1.172
Final R indexes [I ≥ 2σ (I)]	R <sub>1</sub> = 0.0440, wR <sub>2</sub> = 0.1276
Final R indexes [all data]	R <sub>1</sub> = 0.0453, wR <sub>2</sub> = 0.1286
Largest diff. peak/hole / e Å <sup>-3</sup>	0.51/-0.28

**Methyl 1-oxo-3-phenyl-1*H*-isochromene-6-carboxylate (215)**



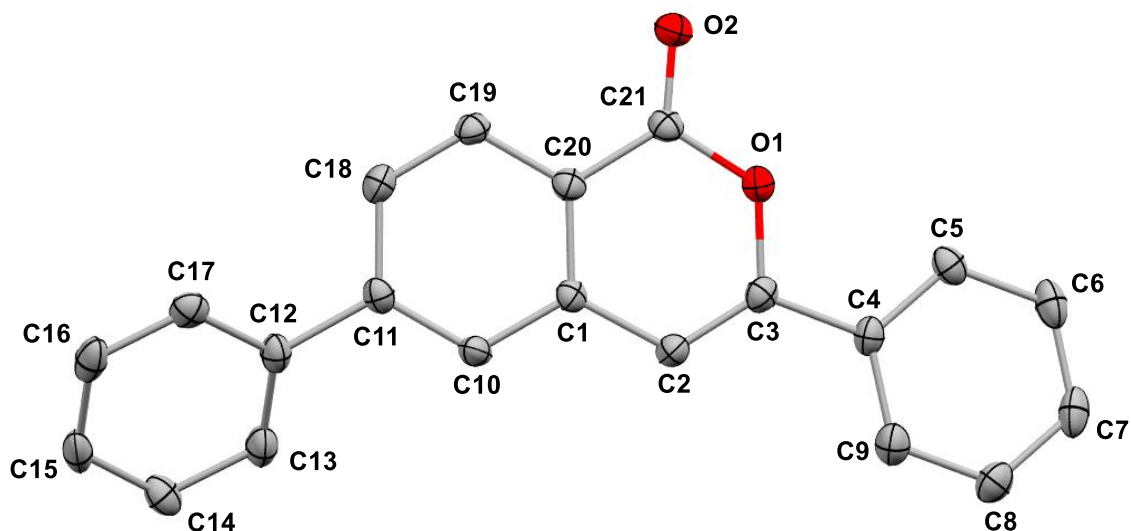
Empirical formula	C <sub>17</sub> H <sub>12</sub> O <sub>4</sub>
Formula weight	280.27
Temperature/K	100.0
Crystal system	orthorhombic
Space group	P2 <sub>1</sub> 2 <sub>1</sub> 2 <sub>1</sub>
a/Å	3.8298(8)
b/Å	6.1007(12)
c/Å	54.735(11)
α/°	90
β/°	90
γ/°	90
Volume/Å <sup>3</sup>	1278.8(4)
Z	4
ρ <sub>calc</sub> /cm <sup>3</sup>	1.456
μ/mm <sup>-1</sup>	0.861
F(000)	584.0
Crystal size/mm <sup>3</sup>	0.322 × 0.081 × 0.042
Radiation	CuKα (λ = 1.54178)
2θ range for data collection/°	9.696 to 159.788
Index ranges	-4 ≤ h ≤ 4, -7 ≤ k ≤ 7, -69 ≤ l ≤ 49
Reflections collected	19765
Independent reflections	2713 [R <sub>int</sub> = 0.0345, R <sub>sigma</sub> = 0.0211]
Data/restraints/parameters	2713/0/191
Goodness-of-fit on F <sup>2</sup>	1.096
Final R indexes [I >= 2σ (I)]	R <sub>1</sub> = 0.0317, wR <sub>2</sub> = 0.0833
Final R indexes [all data]	R <sub>1</sub> = 0.0319, wR <sub>2</sub> = 0.0834
Largest diff. peak/hole / e Å <sup>-3</sup>	0.27/-0.17
Flack parameter	-0.09(8)

**2-Phenyl-4*H*-benzo[*f*]isochromen-4-one (221b):**



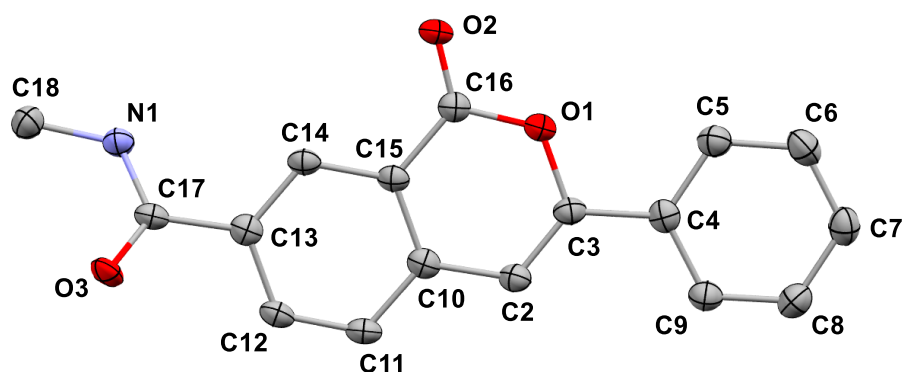
Empirical formula	C <sub>19</sub> H <sub>12</sub> O <sub>2</sub>
Formula weight	272.29
Temperature/K	100.02
Crystal system	orthorhombic
Space group	P2 <sub>1</sub> 2 <sub>1</sub> 2 <sub>1</sub>
<i>a</i> /Å	3.9872(6)
<i>b</i> /Å	14.224(3)
<i>c</i> /Å	22.401(4)
$\alpha$ /°	90
$\beta$ /°	90
$\gamma$ /°	90
Volume/Å <sup>3</sup>	1270.4(4)
<i>Z</i>	4
$\rho_{\text{calc}}$ /cm <sup>3</sup>	1.424
$\mu$ /mm <sup>-1</sup>	0.092
<i>F</i> (000)	568.0
Crystal size/mm <sup>3</sup>	0.948 × 0.104 × 0.038
Radiation	MoK $\alpha$ ( $\lambda$ = 0.71073)
2 $\theta$ range for data collection/°	5.728 to 55.804
Index ranges	-5 ≤ <i>h</i> ≤ 5, -16 ≤ <i>k</i> ≤ 18, -29 ≤ <i>l</i> ≤ 23
Reflections collected	12819
Independent reflections	3045 [ <i>R</i> <sub>int</sub> = 0.0308, <i>R</i> <sub>sigma</sub> = 0.0279]
Data/restraints/parameters	3045/0/190
Goodness-of-fit on <i>F</i> <sup>2</sup>	1.058
Final <i>R</i> indexes [ <i>I</i> ≥ 2 $\sigma$ ( <i>I</i> )]	<i>R</i> <sub>1</sub> = 0.0365, <i>wR</i> <sub>2</sub> = 0.0843
Final <i>R</i> indexes [all data]	<i>R</i> <sub>1</sub> = 0.0431, <i>wR</i> <sub>2</sub> = 0.0880
Largest diff. peak/hole / e Å <sup>-3</sup>	0.22/-0.23
Flack parameter	-0.2(5)

**3,6-Diphenyl-1*H*-isochromen-1-one (223):**



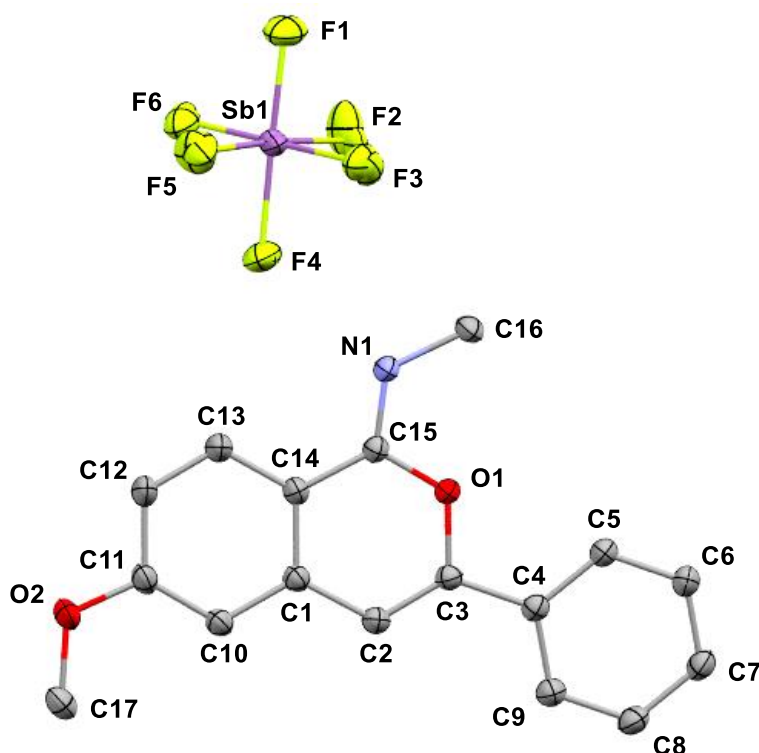
Empirical formula	C <sub>21</sub> H <sub>14</sub> O <sub>2</sub>
Formula weight	298.32
Temperature/K	100.0
Crystal system	triclinic
Space group	P-1
a/Å	13.7646(17)
b/Å	13.8232(16)
c/Å	30.538(4)
$\alpha$ /°	89.363(3)
$\beta$ /°	89.900(4)
$\gamma$ /°	89.945(4)
Volume/Å <sup>3</sup>	5810.0(12)
Z	16
$\rho_{\text{calc}}/\text{cm}^3$	1.364
$\mu/\text{mm}^{-1}$	0.087
F(000)	2496.0
Crystal size/mm <sup>3</sup>	0.204 × 0.187 × 0.121
Radiation	MoK $\alpha$ ( $\lambda$ = 0.71073)
2 $\theta$ range for data collection/°	4.37 to 57.518
Index ranges	-18 ≤ h ≤ 18, -18 ≤ k ≤ 18, -41 ≤ l ≤ 41
Reflections collected	83632
Independent reflections	29981 [ $R_{\text{int}}$ = 0.0491, $R_{\text{sigma}}$ = 0.0663]
Data/restraints/parameters	29981/0/1658
Goodness-of-fit on F <sup>2</sup>	1.041
Final R indexes [ $I \geq 2\sigma(I)$ ]	$R_1$ = 0.0580, $wR_2$ = 0.1474
Final R indexes [all data]	$R_1$ = 0.0979, $wR_2$ = 0.1678
Largest diff. peak/hole / e Å <sup>-3</sup>	0.44/-0.30

***N*-Methyl-1-oxo-3-phenyl-1*H*-isochromene-7-carboxamide (227):**



Empirical formula	C <sub>17</sub> H <sub>13</sub> NO <sub>3</sub>
Formula weight	279.28
Temperature/K	99.98
Crystal system	monoclinic
Space group	P2 <sub>1</sub>
a/Å	5.0291(4)
b/Å	5.1512(4)
c/Å	25.4093(19)
α/°	90
β/°	93.484(2)
γ/°	90
Volume/Å <sup>3</sup>	657.03(9)
Z	2
ρ <sub>calc</sub> /cm <sup>3</sup>	1.412
μ/mm <sup>-1</sup>	0.798
F(000)	292.0
Crystal size/mm <sup>3</sup>	0.516 × 0.089 × 0.051
Radiation	CuKα (λ = 1.54178)
2θ range for data collection/°	10.464 to 149.092
Index ranges	-6 ≤ h ≤ 6, -6 ≤ k ≤ 6, -31 ≤ l ≤ 31
Reflections collected	2709
Independent reflections	2709 [R <sub>int</sub> = ?, R <sub>sigma</sub> = 0.0298]
Data/restraints/parameters	2709/1/195
Goodness-of-fit on F <sup>2</sup>	1.097
Final R indexes [I ≥ 2σ (I)]	R <sub>1</sub> = 0.0371, wR <sub>2</sub> = 0.1062
Final R indexes [all data]	R <sub>1</sub> = 0.0372, wR <sub>2</sub> = 0.1068
Largest diff. peak/hole / e Å <sup>-3</sup>	0.17/-0.18
Flack parameter	-0.23(19)

**(Z)-N-(6-Methoxy-3-phenyl-1*H*-isochromen-1-ylidene)methanaminium hexafluoroantimonate (229):**



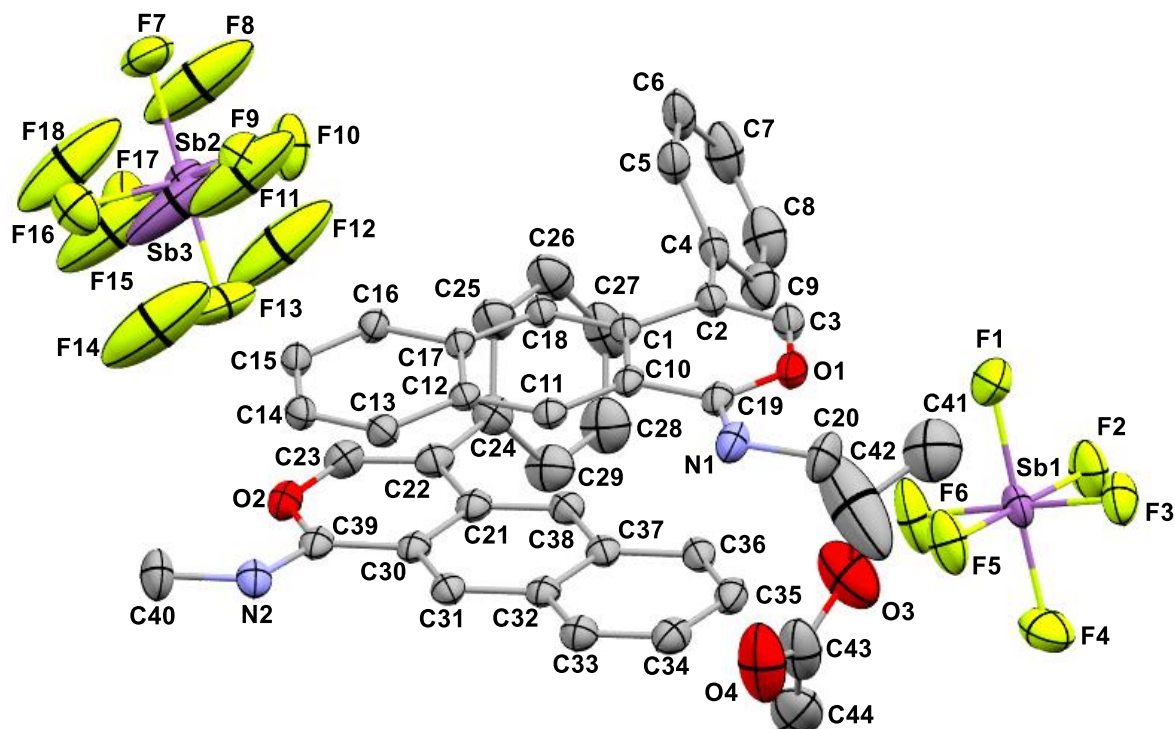
Empirical formula	C <sub>17</sub> H <sub>16</sub> F <sub>6</sub> NO <sub>2</sub> Sb
Formula weight	502.06
Temperature/K	100.0
Crystal system	triclinic
Space group	P-1
a/Å	9.1398(5)
b/Å	10.6685(7)
c/Å	10.9432(6)
α/°	68.724(2)
β/°	68.283(2)
γ/°	66.756(2)
Volume/Å <sup>3</sup>	880.98(9)
Z	2
ρ <sub>calc</sub> /cm <sup>3</sup>	1.893
μ/mm <sup>-1</sup>	1.639
F(000)	492.0
Crystal size/mm <sup>3</sup>	0.56 × 0.35 × 0.114
Radiation	MoKα (λ = 0.71073)
2θ range for data collection/°	5.276 to 61.082
Index ranges	-13 ≤ h ≤ 13, -15 ≤ k ≤ 15, -15 ≤ l ≤ 15
Reflections collected	26295
Independent reflections	5376 [R <sub>int</sub> = 0.0210, R <sub>sigma</sub> = 0.0158]
Data/restraints/parameters	5376/84/313



Goodness-of-fit on  $F^2$  1.124  
 Final R indexes [ $I \geq 2\sigma(I)$ ]  $R_1 = 0.0144$ ,  $wR_2 = 0.0384$   
 Final R indexes [all data]  $R_1 = 0.0148$ ,  $wR_2 = 0.0386$   
 Largest diff. peak/hole /  $e \text{ \AA}^{-3}$  0.44/-0.27

213

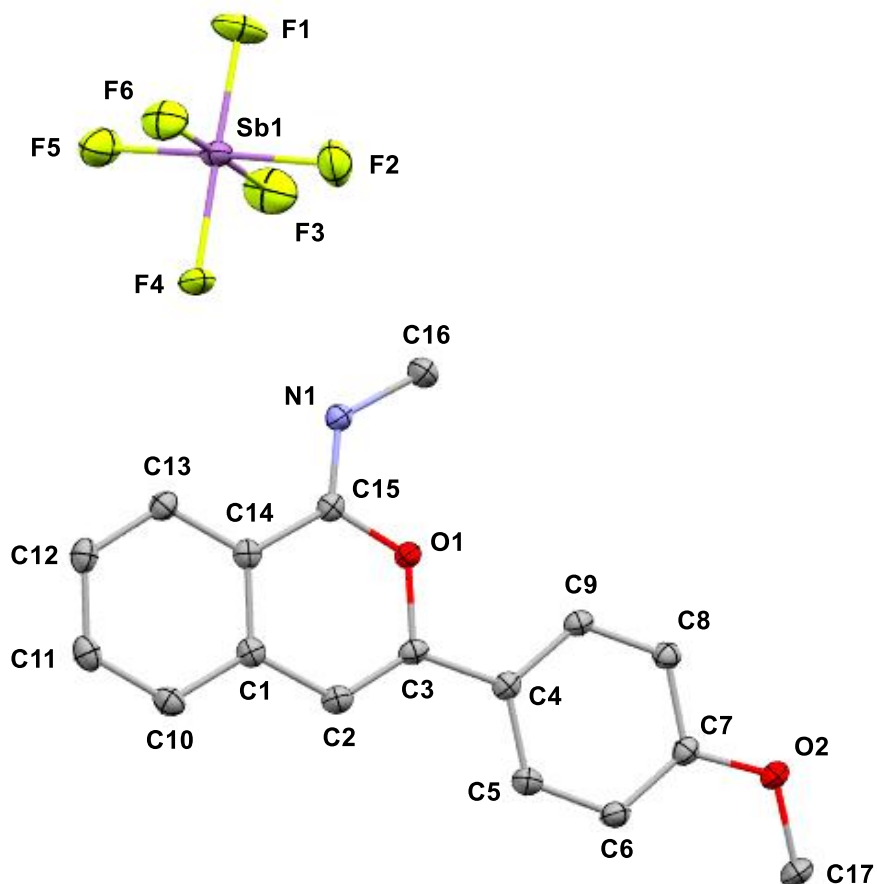
**(Z)-N-(4-phenyl-1*H*-benzo[*g*]isochromen-1-ylidene)methanaminium hexafluoroantimonate (230):**



Empirical formula	C <sub>44</sub> H <sub>38</sub> F <sub>12</sub> N <sub>2</sub> O <sub>4</sub> Sb <sub>2</sub>
Formula weight	1130.26
Temperature/K	100.22
Crystal system	triclinic
Space group	P-1
<i>a</i> /Å	11.6886(15)
<i>b</i> /Å	13.4251(17)
<i>c</i> /Å	15.0768(18)
$\alpha$ /°	76.864(3)
$\beta$ /°	71.293(3)
$\gamma$ /°	86.870(4)
Volume/Å <sup>3</sup>	2181.8(5)
<i>Z</i>	2
$\rho_{\text{calc}}/\text{cm}^3$	1.720
$\mu/\text{mm}^{-1}$	1.334
<i>F</i> (000)	1116.0
Crystal size/mm <sup>3</sup>	0.395 × 0.155 × 0.022
Radiation	MoK $\alpha$ ( $\lambda$ = 0.71073)
2 $\theta$ range for data collection/°	4.626 to 61.148
Index ranges	-16 ≤ <i>h</i> ≤ 16, -19 ≤ <i>k</i> ≤ 19, -21 ≤ <i>l</i> ≤ 21
Reflections collected	76807
Independent reflections	13348 [ <i>R</i> <sub>int</sub> = 0.0367, <i>R</i> <sub>sigma</sub> = 0.0274]
Data/restraints/parameters	13348/76/651

Goodness-of-fit on  $F^2$  1.035  
 Final R indexes [ $I \geq 2\sigma(I)$ ]  $R_1 = 0.0376$ ,  $wR_2 = 0.0928$   
 Final R indexes [all data]  $R_1 = 0.0526$ ,  $wR_2 = 0.1012$   
 Largest diff. peak/hole /  $e \text{ \AA}^{-3}$  1.46/-0.57

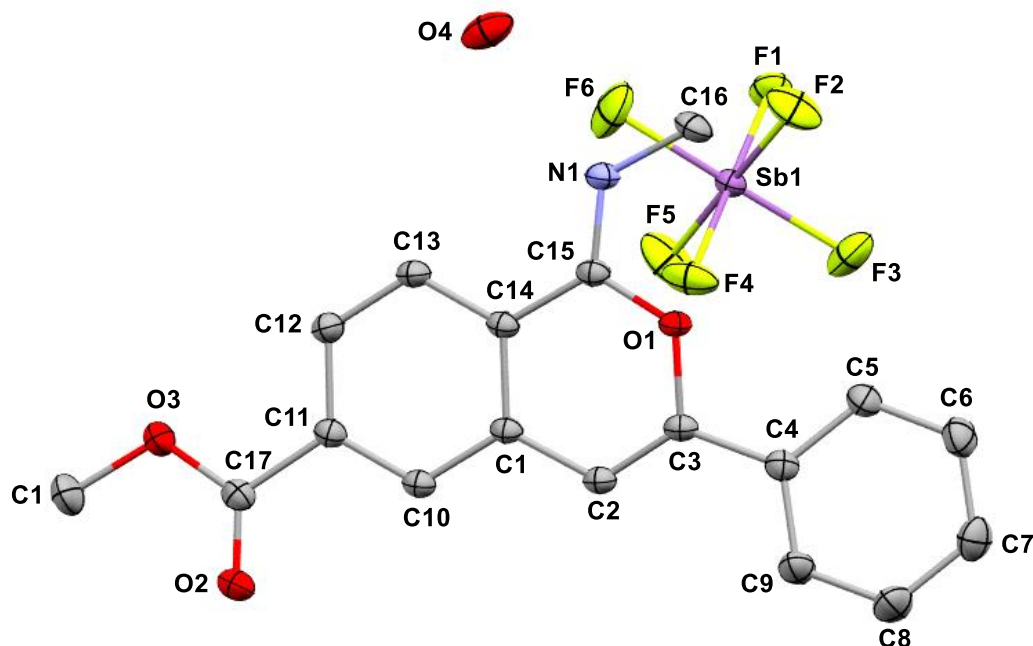
**(Z)-N-[3-(*p*-Methoxyphenyl)-1*H*-isochromen-1-ylidene]methanaminium hexafluoroantimonate (231):**



Empirical formula	C <sub>17</sub> H <sub>16</sub> F <sub>6</sub> NO <sub>2</sub> Sb
Formula weight	502.06
Temperature/K	100.01
Crystal system	monoclinic
Space group	C2/c
<i>a</i> /Å	21.3857(13)
<i>b</i> /Å	7.0061(4)
<i>c</i> /Å	23.513(2)
$\alpha$ /°	90
$\beta$ /°	92.779(4)
$\gamma$ /°	90
Volume/Å <sup>3</sup>	3518.8(4)
<i>Z</i>	8
$\rho_{\text{calc}}/\text{cm}^3$	1.895
$\mu/\text{mm}^{-1}$	1.641
<i>F</i> (000)	1968.0
Crystal size/mm <sup>3</sup>	0.182 × 0.137 × 0.043
Radiation	MoK $\alpha$ ( $\lambda$ = 0.71073)
2 $\theta$ range for data collection/°	5.03 to 59.998

Index ranges	$-30 \leq h \leq 23, -9 \leq k \leq 9, -33 \leq l \leq 33$
Reflections collected	27525
Independent reflections	5124 [ $R_{\text{int}} = 0.0199, R_{\text{sigma}} = 0.0153$ ]
Data/restraints/parameters	5124/0/249
Goodness-of-fit on $F^2$	1.093
Final R indexes [ $I \geq 2\sigma(I)$ ]	$R_1 = 0.0199, wR_2 = 0.0492$
Final R indexes [all data]	$R_1 = 0.0215, wR_2 = 0.0501$
Largest diff. peak/hole / $e \text{ \AA}^{-3}$	0.53/-0.45

**(Z)-N-(6-(methoxycarbonyl)-3-phenyl-1*H*-isochromen-1-ylidene)methanaminium hexafluoroantimonate (233):**

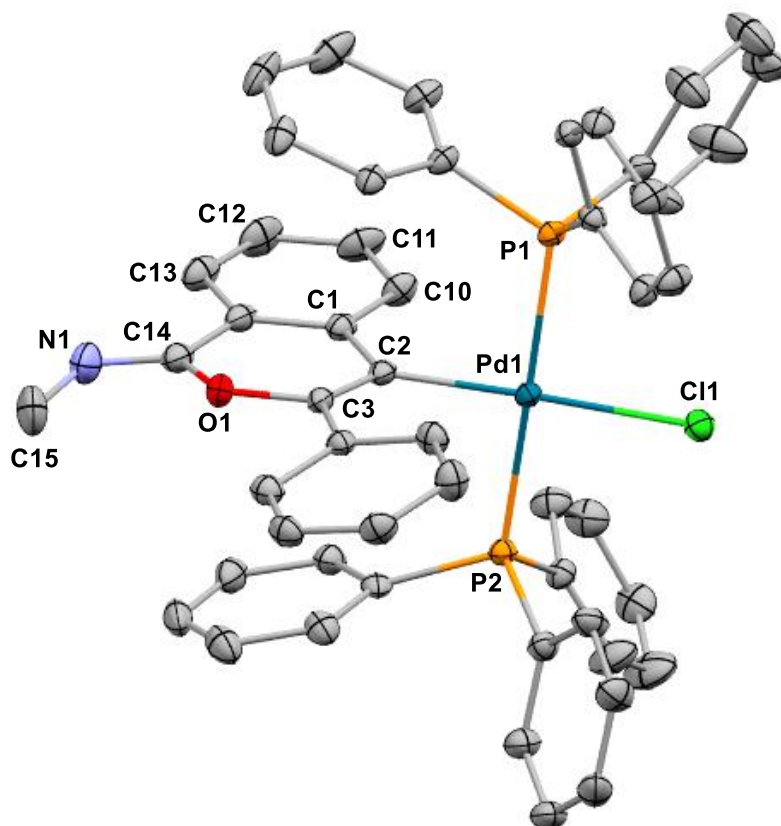


Empirical formula	C <sub>18</sub> H <sub>18</sub> F <sub>6</sub> NO <sub>4</sub> Sb
Formula weight	548.08
Temperature/K	100.01
Crystal system	monoclinic
Space group	P2 <sub>1</sub> /c
a/Å	11.4656(9)
b/Å	8.2017(7)
c/Å	22.0255(14)
α/°	90
β/°	102.279(3)
γ/°	90
Volume/Å <sup>3</sup>	2023.8(3)
Z	4
ρ <sub>calc</sub> /cm <sup>3</sup>	1.799
μ/mm <sup>-1</sup>	1.442
F(000)	1080.0
Crystal size/mm <sup>3</sup>	0.317 × 0.062 × 0.037
Radiation	MoKα (λ = 0.71073)
2θ range for data collection/°	4.658 to 61.09
Index ranges	-16 ≤ h ≤ 16, -11 ≤ k ≤ 11, -31 ≤ l ≤ 30
Reflections collected	42342
Independent reflections	6203 [R <sub>int</sub> = 0.0261, R <sub>sigma</sub> = 0.0165]
Data/restraints/parameters	6203/3/282
Goodness-of-fit on F <sup>2</sup>	1.067
Final R indexes [I ≥ 2σ (I)]	R <sub>1</sub> = 0.0189, wR <sub>2</sub> = 0.0462

Final R indexes [all data]  $R_1 = 0.0213$ ,  $wR_2 = 0.0476$   
Largest diff. peak/hole / e Å<sup>-3</sup> 0.68/-0.52



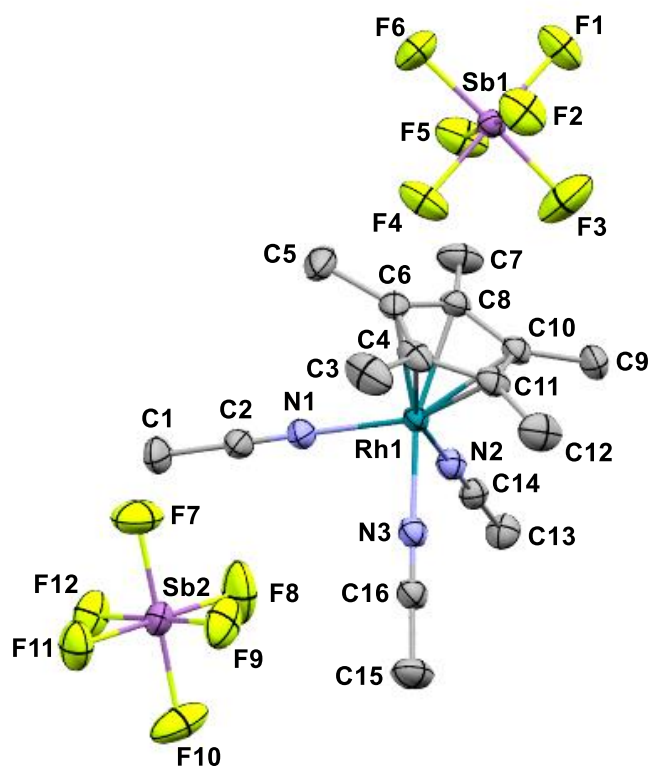
**(Z)-(1-(methylimino)-3-phenyl-1*H*-isochromen-4-yl)-bis(triphenylphosphine)palladium(IV) chloride (235):**



Empirical formula	C <sub>52</sub> H <sub>42</sub> Cl <sub>0.79</sub> I <sub>0.22</sub> NOP <sub>2</sub> Pd
Formula weight	921.00
Temperature/K	99.99
Crystal system	orthorhombic
Space group	P2 <sub>1</sub> 2 <sub>1</sub> 2 <sub>1</sub>
a/Å	10.9339(7)
b/Å	17.1794(8)
c/Å	22.2028(9)
α/°	90
β/°	90
γ/°	90
Volume/Å <sup>3</sup>	4170.5(4)
Z	4
ρ <sub>calc</sub> /cm <sup>3</sup>	1.467
μ/mm <sup>-1</sup>	0.777
F(000)	1880.0
Crystal size/mm <sup>3</sup>	0.282 × 0.17 × 0.123
Radiation	MoKα (λ = 0.71073)
2θ range for data collection/°	4.152 to 62
Index ranges	-15 ≤ h ≤ 13, -24 ≤ k ≤ 19, -32 ≤ l ≤ 31
Reflections collected	33108

Independent reflections	13250 [ $R_{\text{int}} = 0.0356$ , $R_{\text{sigma}} = 0.0469$ ]
Data/restraints/parameters	13250/14/571
Goodness-of-fit on $F^2$	1.076
Final R indexes [ $I \geq 2\sigma(I)$ ]	$R_1 = 0.0335$ , $wR_2 = 0.0758$
Final R indexes [all data]	$R_1 = 0.0348$ , $wR_2 = 0.0765$
Largest diff. peak/hole / $e \text{ \AA}^{-3}$	0.60/-0.67
Flack parameter	0.091(12)

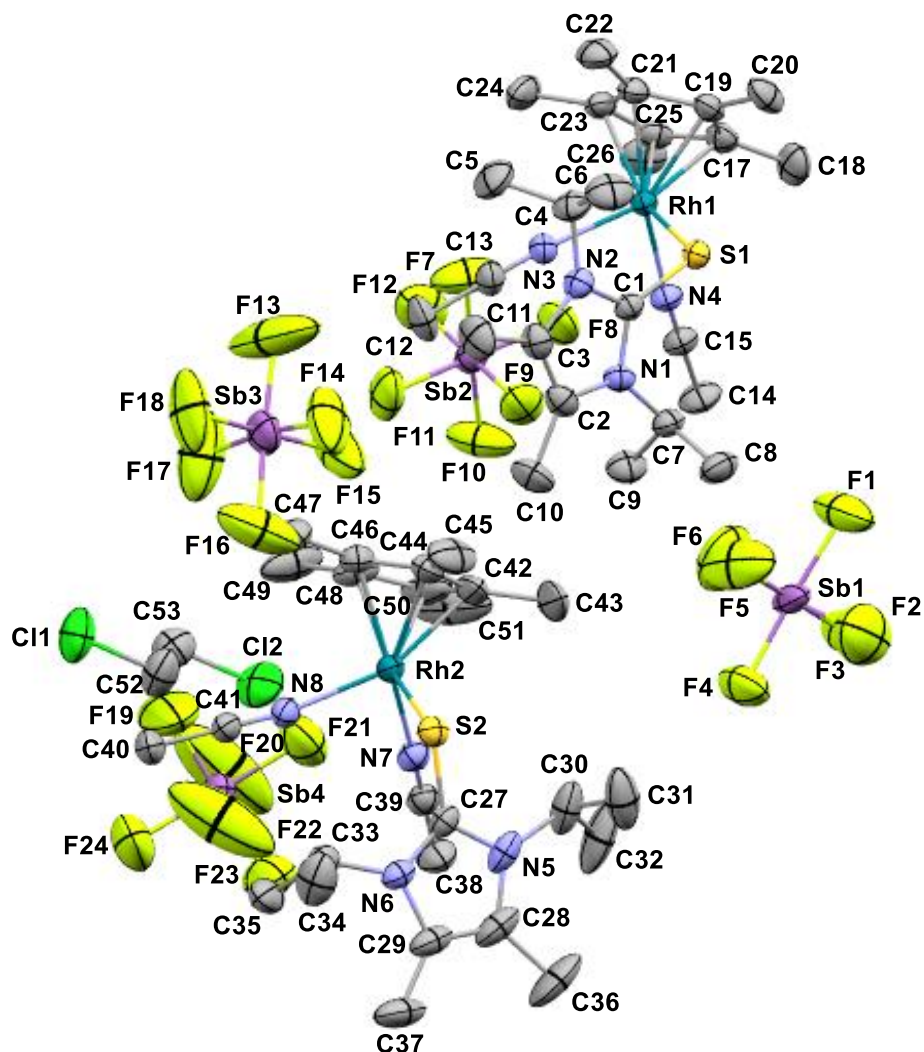
**RhCp\*(MeCN)<sub>3</sub>(SbF<sub>6</sub>)<sub>2</sub>:**



Empirical formula	C <sub>16</sub> H <sub>24</sub> F <sub>12</sub> N <sub>3</sub> RhSb <sub>2</sub>
Formula weight	832.79
Temperature/K	99.98
Crystal system	monoclinic
Space group	P2 <sub>1</sub> /c
a/Å	17.2400(6)
b/Å	9.7633(3)
c/Å	15.8635(6)
α/°	90
β/°	90.7400(10)
γ/°	90
Volume/Å <sup>3</sup>	2669.91(16)
Z	4
ρ <sub>calc</sub> /cm <sup>3</sup>	2.072
μ/mm <sup>-1</sup>	2.713
F(000)	1584.0
Crystal size/mm <sup>3</sup>	0.337 × 0.246 × 0.231
Radiation	MoKα (λ = 0.71073)
2θ range for data collection/°	4.726 to 63.068
Index ranges	-25 ≤ h ≤ 25, -14 ≤ k ≤ 14, -23 ≤ l ≤ 23
Reflections collected	55194
Independent reflections	8901 [R <sub>int</sub> = 0.0194, R <sub>sigma</sub> = 0.0130]

Data/restraints/parameters	8901/0/315
Goodness-of-fit on $F^2$	1.116
Final R indexes [ $I \geq 2\sigma(I)$ ]	$R_1 = 0.0399$ , $wR_2 = 0.1064$
Final R indexes [all data]	$R_1 = 0.0405$ , $wR_2 = 0.1068$
Largest diff. peak/hole / $e \text{ \AA}^{-3}$	3.86/-2.11

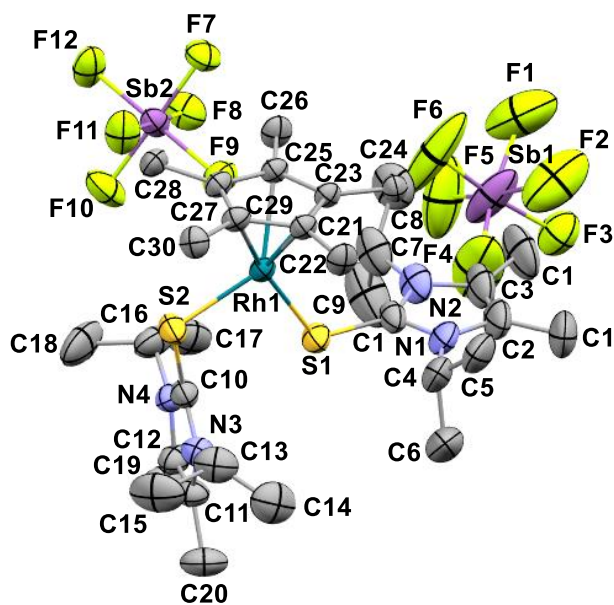
**Bis(acetonitrile){[(1,3-diisopropyl-4,5-dimethyl-1*H*-imidazol-3-ium-2-yl)thio](pentamethylcyclopentadienyl)rhodium(I) bis(hexafluoroantimonate) (236a):**



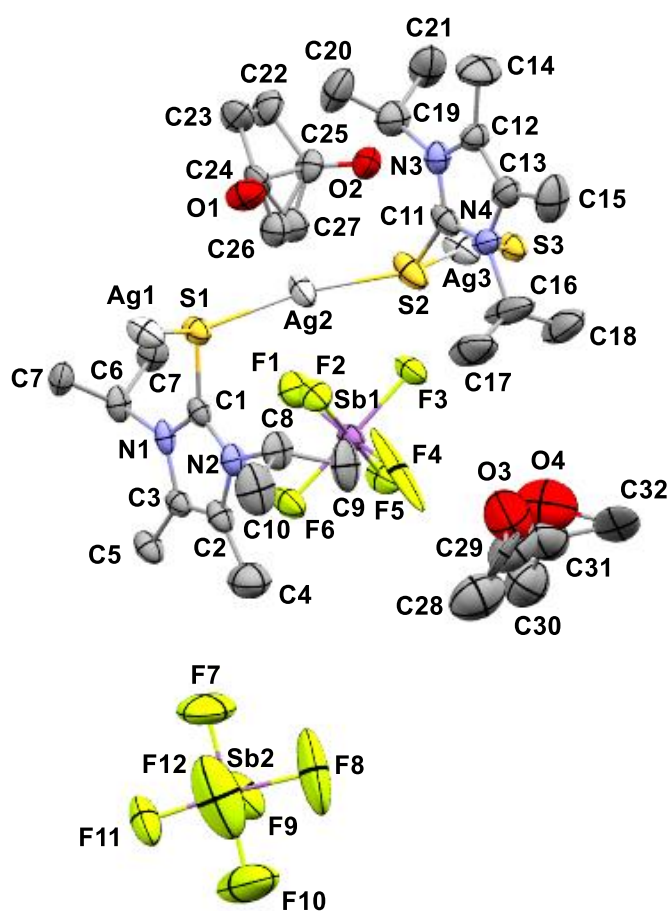
Empirical formula	C <sub>52</sub> H <sub>86</sub> Cl <sub>2</sub> F <sub>24</sub> N <sub>8</sub> Rh <sub>2</sub> S <sub>2</sub> Sb <sub>4</sub>
Formula weight	2107.12
Temperature/K	150.01
Crystal system	triclinic
Space group	P-1
a/Å	15.3226(8)
b/Å	15.8170(6)
c/Å	16.9991(8)
α/°	106.209(2)
β/°	92.527(2)
γ/°	101.649(2)
Volume/Å <sup>3</sup>	3852.4(3)
Z	2
ρ <sub>calc</sub> /g/cm <sup>3</sup>	1.816
μ/mm <sup>-1</sup>	2.021
F(000)	2060.0

Crystal size/mm <sup>3</sup>	0.347 × 0.313 × 0.172
Radiation	MoKα (λ = 0.71073)
2θ range for data collection/°	4.234 to 63.376
Index ranges	-22 ≤ h ≤ 22, -23 ≤ k ≤ 23, -25 ≤ l ≤ 25
Reflections collected	129927
Independent reflections	25784 [R <sub>int</sub> = 0.0262, R <sub>sigma</sub> = 0.0217]
Data/restraints/parameters	25784/189/873
Goodness-of-fit on F <sup>2</sup>	1.020
Final R indexes [I ≥ 2σ (I)]	R <sub>1</sub> = 0.0567, wR <sub>2</sub> = 0.1403
Final R indexes [all data]	R <sub>1</sub> = 0.0643, wR <sub>2</sub> = 0.1466
Largest diff. peak/hole / e Å <sup>-3</sup>	4.25/-3.96

Bis{[[(1,3-diisopropyl-4,5-dimethyl-1*H*-imidazol-3-ium-2-yl)thio](pentamethylcyclopentadienyl)rhodium(I) bis(hexafluoroantimonate) (236b):



**Ag-S-Im<sup>+</sup>-cluster (237):**

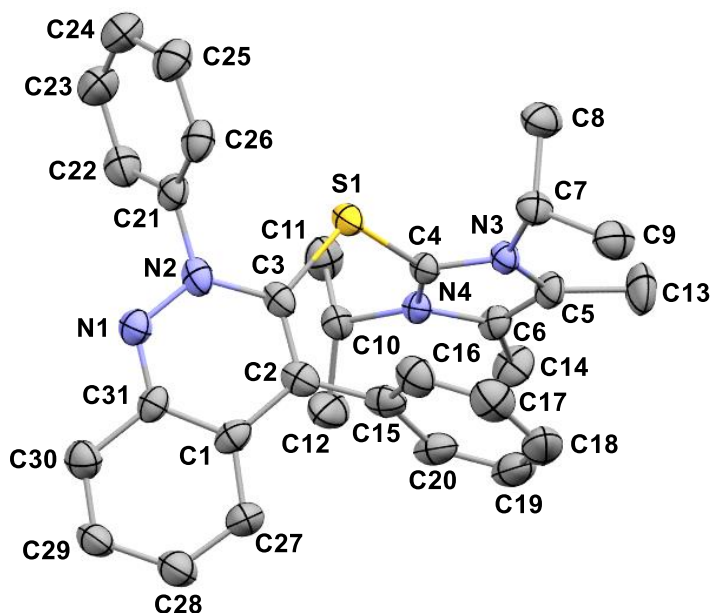


Empirical formula	C <sub>26.5</sub> H <sub>49</sub> Ag <sub>2</sub> F <sub>12</sub> N <sub>4</sub> O <sub>1.5</sub> S <sub>2</sub> Sb <sub>2</sub>
Formula weight	1199.05
Temperature/K	99.99
Crystal system	monoclinic
Space group	P2 <sub>1</sub> /m
a/Å	13.0611(6)
b/Å	8.7856(4)
c/Å	18.2908(9)
α/°	90
β/°	92.823(2)
γ/°	90
Volume/Å <sup>3</sup>	2096.31(17)
Z	2
ρ <sub>calc</sub> /cm <sup>3</sup>	1.900
μ/mm <sup>-1</sup>	2.376
F(000)	1168.0
Crystal size/mm <sup>3</sup>	0.254 × 0.045 × 0.026
Radiation	MoKα (λ = 0.71073)
2θ range for data collection/°	5.144 to 55.996
Index ranges	? ≤ h ≤ ?, ? ≤ k ≤ ?, ? ≤ l ≤ ?



Reflections collected	5379
Independent reflections	5379 [ $R_{\text{int}} = ?$ , $R_{\text{sigma}} = 0.0205$ ]
Data/restraints/parameters	5379/80/307
Goodness-of-fit on $F^2$	1.116
Final R indexes [ $I \geq 2\sigma(I)$ ]	$R_1 = 0.0787$ , $wR_2 = 0.1976$
Final R indexes [all data]	$R_1 = 0.0879$ , $wR_2 = 0.2080$
Largest diff. peak/hole / e $\text{\AA}^{-3}$	4.29/-2.88

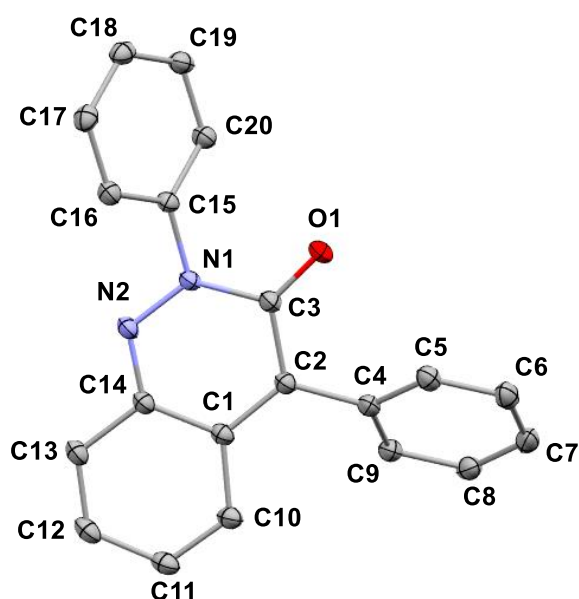
**3-[(1,3-Diisopropyl-4,5-dimethyl-1*H*-imidazol-3-ium-2-yl)thio]-2,4-diphenylcinnolin-2-ium hexafluoroantimonate (238) (AVK-AA-296):**



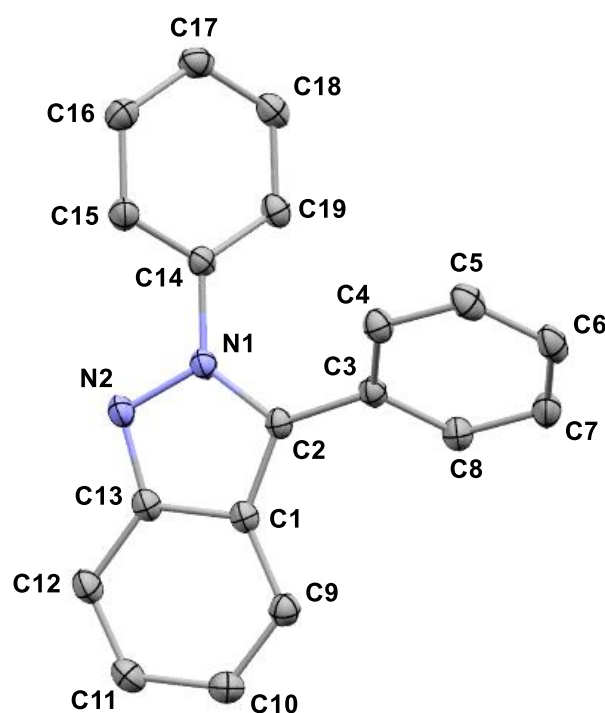
Empirical formula	C <sub>66</sub> H <sub>76</sub> F <sub>24</sub> N <sub>8</sub> OS <sub>2</sub> Sb <sub>4</sub>
Formula weight	2004.46
Temperature/K	100.02
Crystal system	monoclinic
Space group	P2 <sub>1</sub> /n
a/Å	11.3960(7)
b/Å	17.4009(9)
c/Å	20.1516(12)
α/°	90
β/°	105.418(2)
γ/°	90
Volume/Å <sup>3</sup>	3852.3(4)
Z	2
ρ <sub>calc</sub> /cm <sup>3</sup>	1.728
μ/mm <sup>-1</sup>	1.546
F(000)	1976.0
Crystal size/mm <sup>3</sup>	0.175 × 0.171 × 0.151
Radiation	MoKα (λ = 0.71073)
2θ range for data collection/°	4.384 to 63.184
Index ranges	-15 ≤ h ≤ 16, -25 ≤ k ≤ 20, -26 ≤ l ≤ 29
Reflections collected	35474
Independent reflections	12810 [R <sub>int</sub> = 0.0246, R <sub>sigma</sub> = 0.0316]
Data/restraints/parameters	12810/0/493
Goodness-of-fit on F <sup>2</sup>	1.013
Final R indexes [I ≥ 2σ (I)]	R <sub>1</sub> = 0.0553, wR <sub>2</sub> = 0.1334

Final R indexes [all data]  $R_1 = 0.0677$ ,  $wR_2 = 0.1412$   
Largest diff. peak/hole / e  $\text{\AA}^{-3}$  2.36/-1.32

**2,4-Diphenylcinnolin-3(2H)-one (241):**



Empirical formula	C <sub>20</sub> H <sub>14</sub> N <sub>2</sub> O
Formula weight	298.33
Temperature/K	100.0
Crystal system	monoclinic
Space group	P2 <sub>1</sub> /n
a/Å	9.5257(9)
b/Å	7.5502(7)
c/Å	20.3547(18)
α/°	90
β/°	97.113(3)
γ/°	90
Volume/Å <sup>3</sup>	1452.7(2)
Z	4
ρ <sub>calc</sub> /cm <sup>3</sup>	1.364
μ/mm <sup>-1</sup>	0.085
F(000)	624.0
Crystal size/mm <sup>3</sup>	0.46 × 0.281 × 0.215
Radiation	MoKα (λ = 0.71073)
2θ range for data collection/°	4.526 to 59.172
Index ranges	-12 ≤ h ≤ 13, -10 ≤ k ≤ 10, -28 ≤ l ≤ 28
Reflections collected	28596
Independent reflections	4070 [R <sub>int</sub> = 0.0208, R <sub>sigma</sub> = 0.0142]
Data/restraints/parameters	4070/0/208
Goodness-of-fit on F <sup>2</sup>	1.067
Final R indexes [I ≥ 2σ (I)]	R <sub>1</sub> = 0.0402, wR <sub>2</sub> = 0.1089
Final R indexes [all data]	R <sub>1</sub> = 0.0417, wR <sub>2</sub> = 0.1102
Largest diff. peak/hole / e Å <sup>-3</sup>	0.42/-0.17

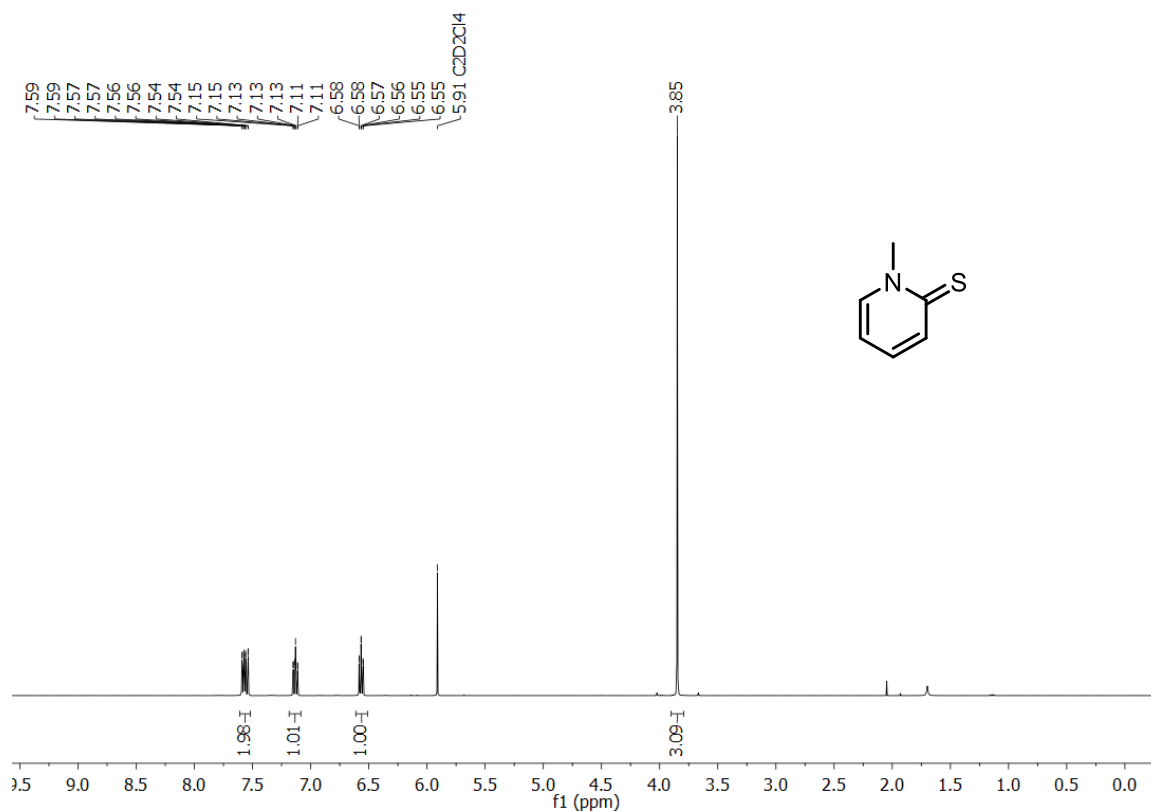
**2,3-Diphenyl-2*H*-indazole (242):**

Empirical formula	C <sub>19</sub> H <sub>14</sub> N <sub>2</sub>
Formula weight	270.32
Temperature/K	99.99
Crystal system	monoclinic
Space group	C2/c
<i>a</i> /Å	10.246(3)
<i>b</i> /Å	16.638(4)
<i>c</i> /Å	17.335(6)
$\alpha$ /°	90
$\beta$ /°	105.506(14)
$\gamma$ /°	90
Volume/Å <sup>3</sup>	2847.5(14)
<i>Z</i>	8
$\rho_{\text{calc}}$ /cm <sup>3</sup>	1.261
$\mu$ /mm <sup>-1</sup>	0.075
<i>F</i> (000)	1136.0
Crystal size/mm <sup>3</sup>	0.302 × 0.174 × 0.081
Radiation	MoK $\alpha$ ( $\lambda$ = 0.71073)
2 $\theta$ range for data collection/°	4.798 to 59.212
Index ranges	-14 ≤ <i>h</i> ≤ 14, -23 ≤ <i>k</i> ≤ 22, -23 ≤ <i>l</i> ≤ 24
Reflections collected	42375
Independent reflections	4007 [ <i>R</i> <sub>int</sub> = 0.0284, <i>R</i> <sub>sigma</sub> = 0.0137]
Data/restraints/parameters	4007/0/190
Goodness-of-fit on <i>F</i> <sup>2</sup>	1.051
Final <i>R</i> indexes [ <i>I</i> ≥ 2 $\sigma$ ( <i>I</i> )]	<i>R</i> <sub>1</sub> = 0.0416, <i>wR</i> <sub>2</sub> = 0.1056

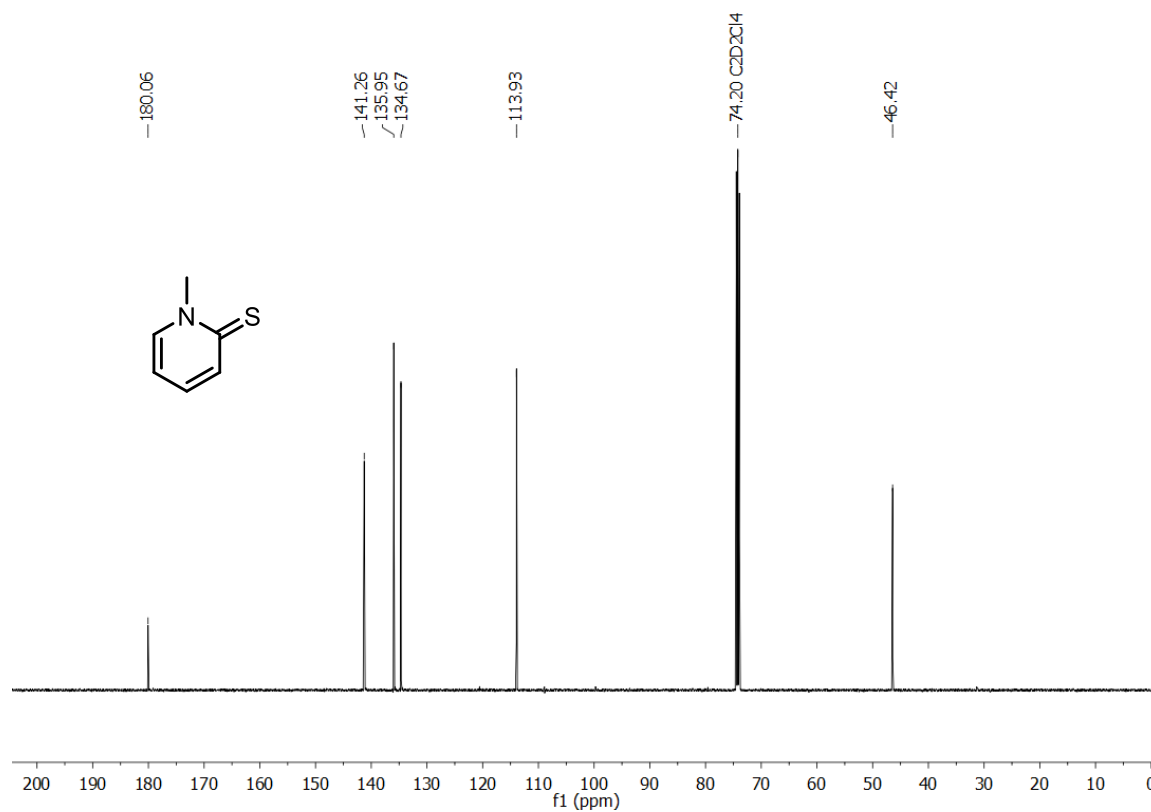
Final R indexes [all data]  $R_1 = 0.0447$ ,  $wR_2 = 0.1084$   
Largest diff. peak/hole / e  $\text{\AA}^{-3}$  0.40/-0.21

# SPECTRA

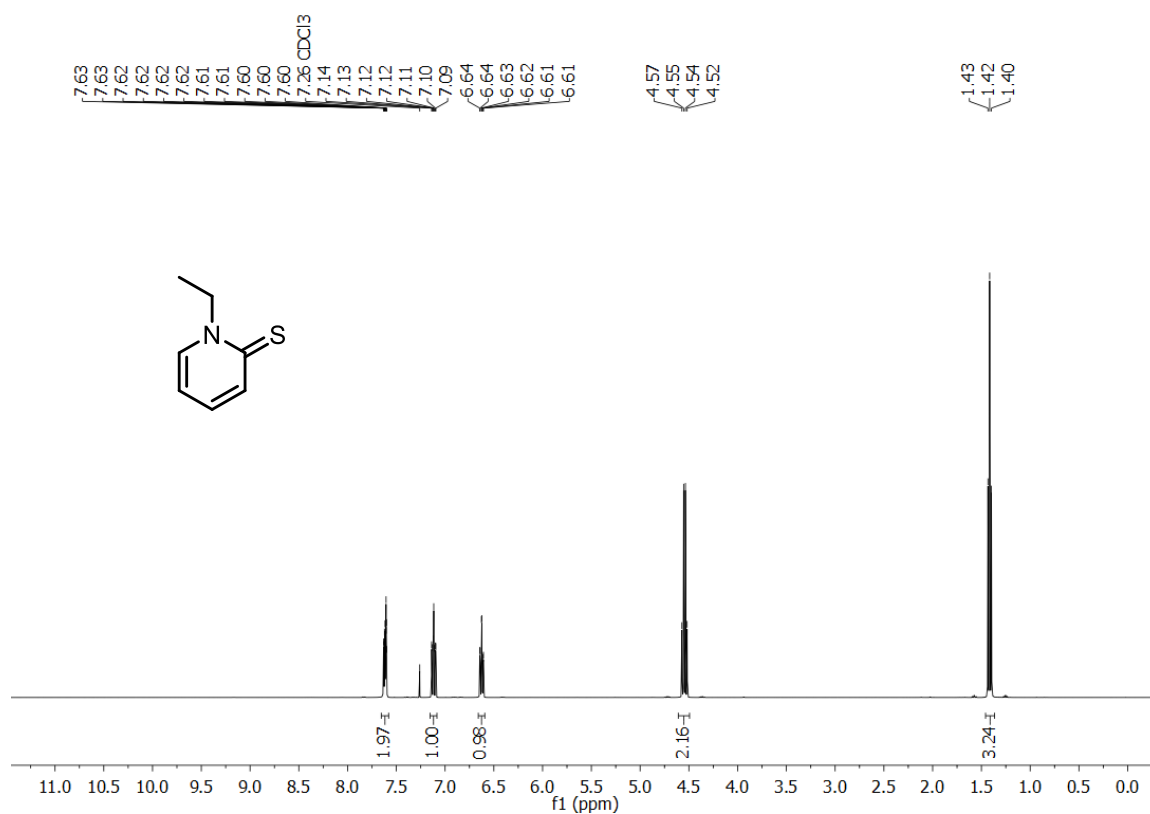
**<sup>1</sup>H NMR of compound 153a, 1-methylpyridine-2(1H)-thione, 400 MHz, C<sub>2</sub>D<sub>2</sub>Cl<sub>4</sub>, 298 K**



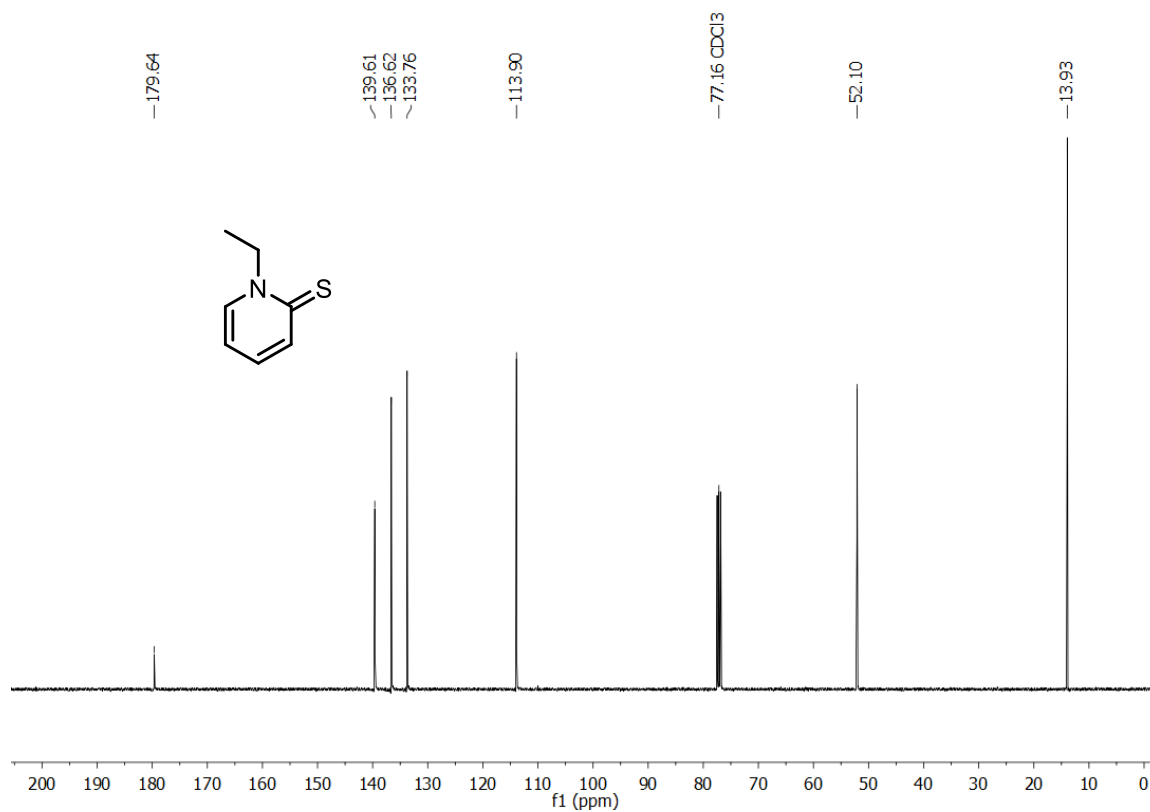
**<sup>13</sup>C NMR of compound 153a, 1-methylpyridine-2(1H)-thione, 101 MHz, C<sub>2</sub>D<sub>2</sub>Cl<sub>4</sub>, 298 K**



**$^1\text{H}$  NMR of compound 153b, 1-ethylpyridine-2(1*H*)-thione, 400 MHz,  $\text{CDCl}_3$ , 298 K**

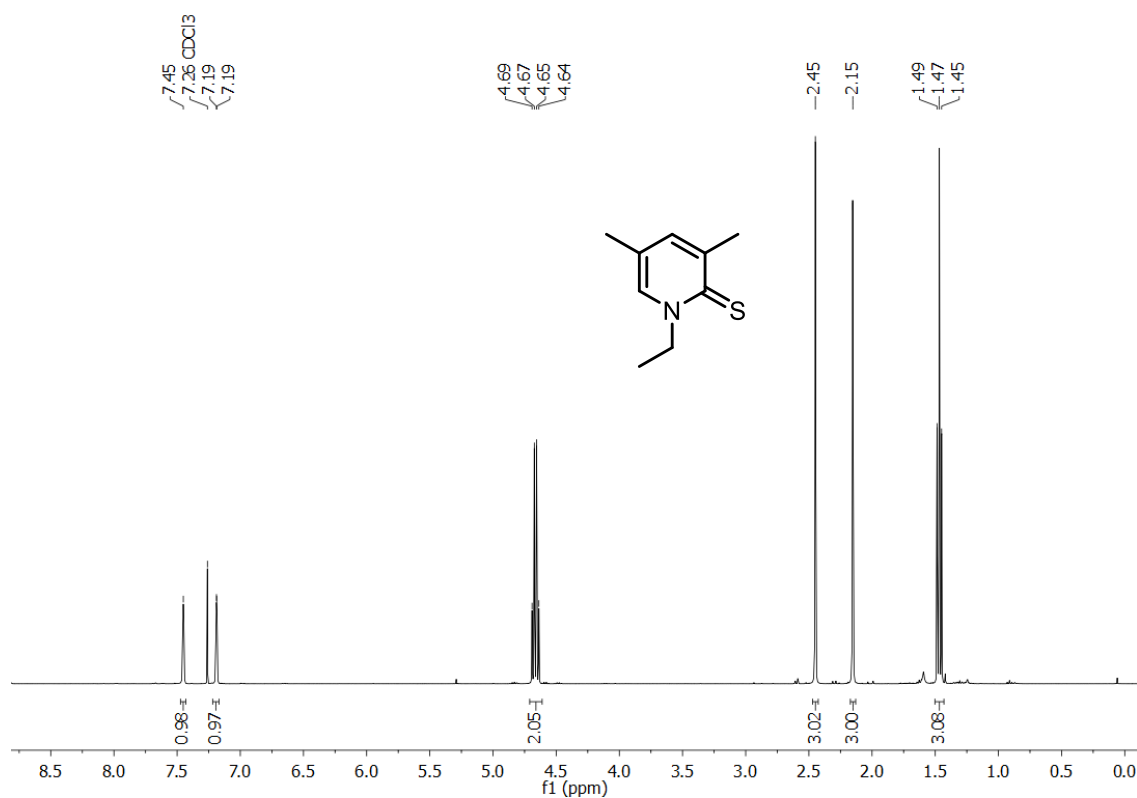


**$^{13}\text{C}$  NMR of compound 153b, 1-ethylpyridine-2(1*H*)-thione, 101 MHz,  $\text{CDCl}_3$ , 298 K**

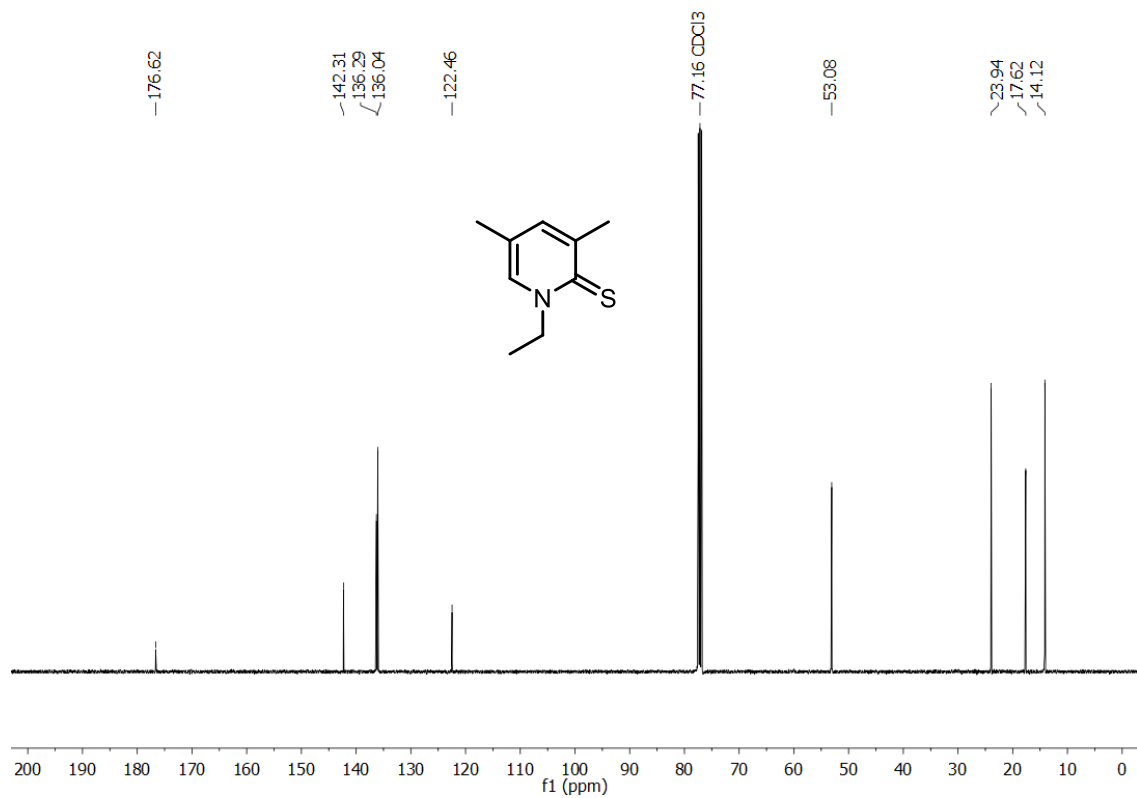




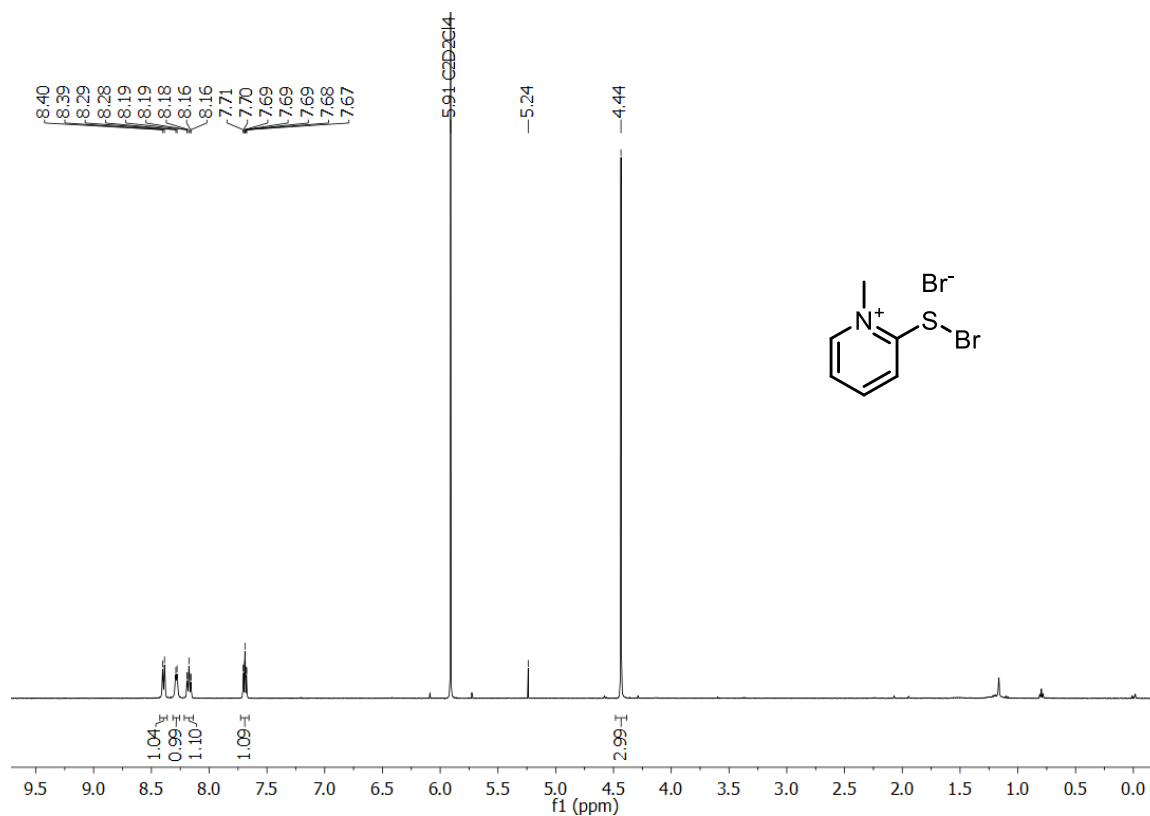
**<sup>1</sup>H NMR of compound 153c, 1-ethyl-3,5-dimethylpyridine-2(1H)-thione, 400 MHz, CDCl<sub>3</sub>, 298 K**



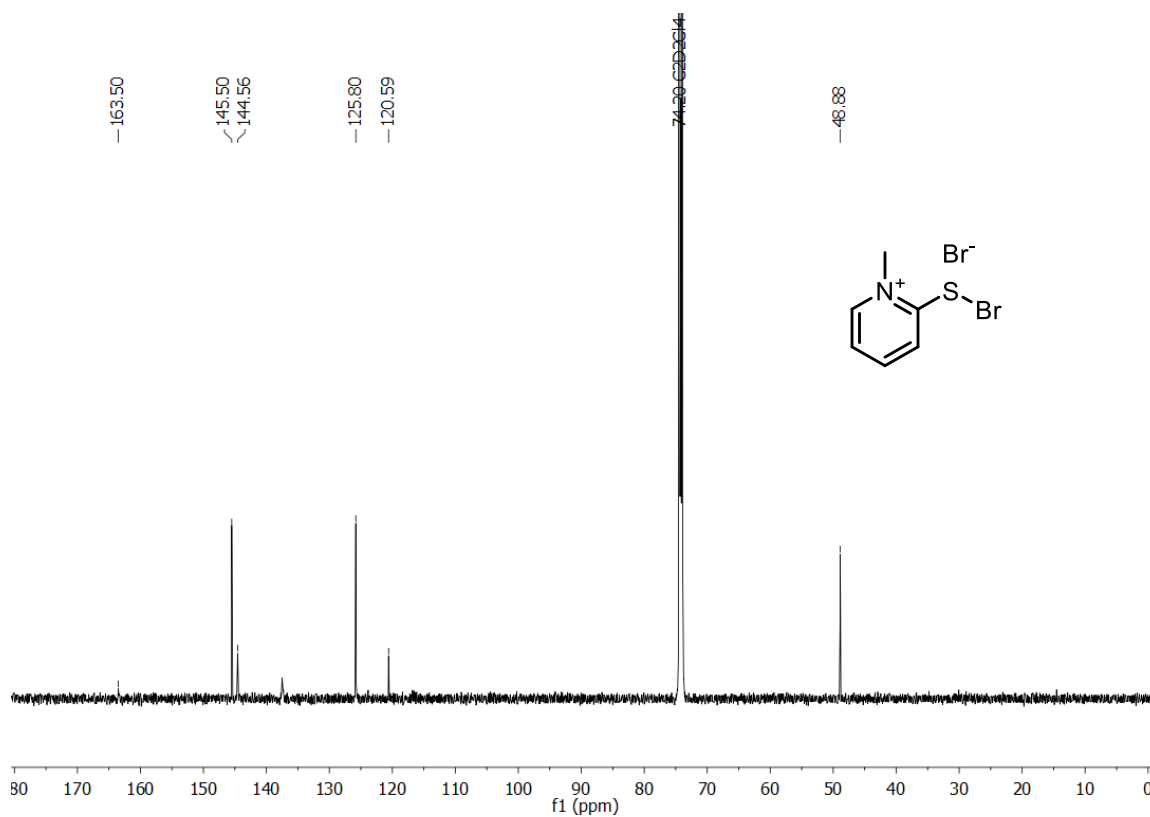
**<sup>13</sup>C NMR of compound 153c, 1-ethyl-3,5-dimethylpyridine-2(1H)-thione, 101 MHz, CDCl<sub>3</sub>, 298 K**



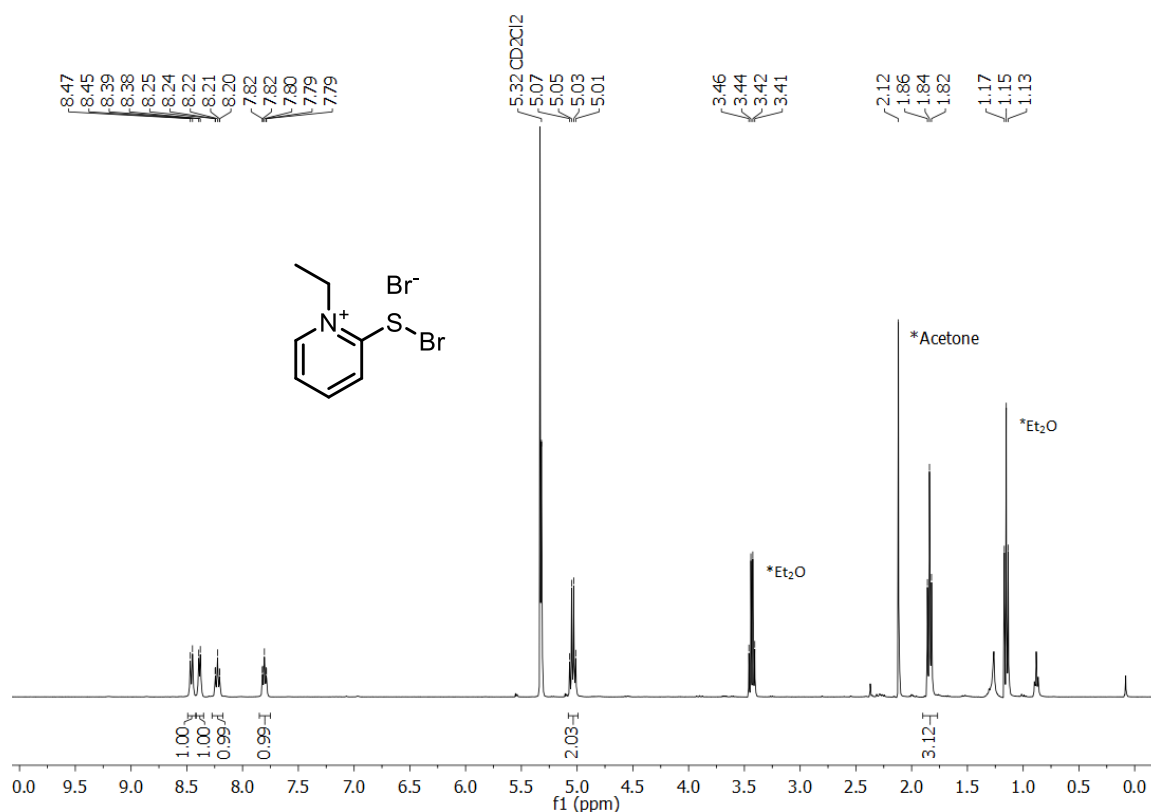
**$^1\text{H}$  NMR of compound 154a, 2-(bromothio)-1-methylpyridin-1-ium bromide, 500 MHz,  $\text{C}_2\text{D}_2\text{Cl}_4$ , 298 K**



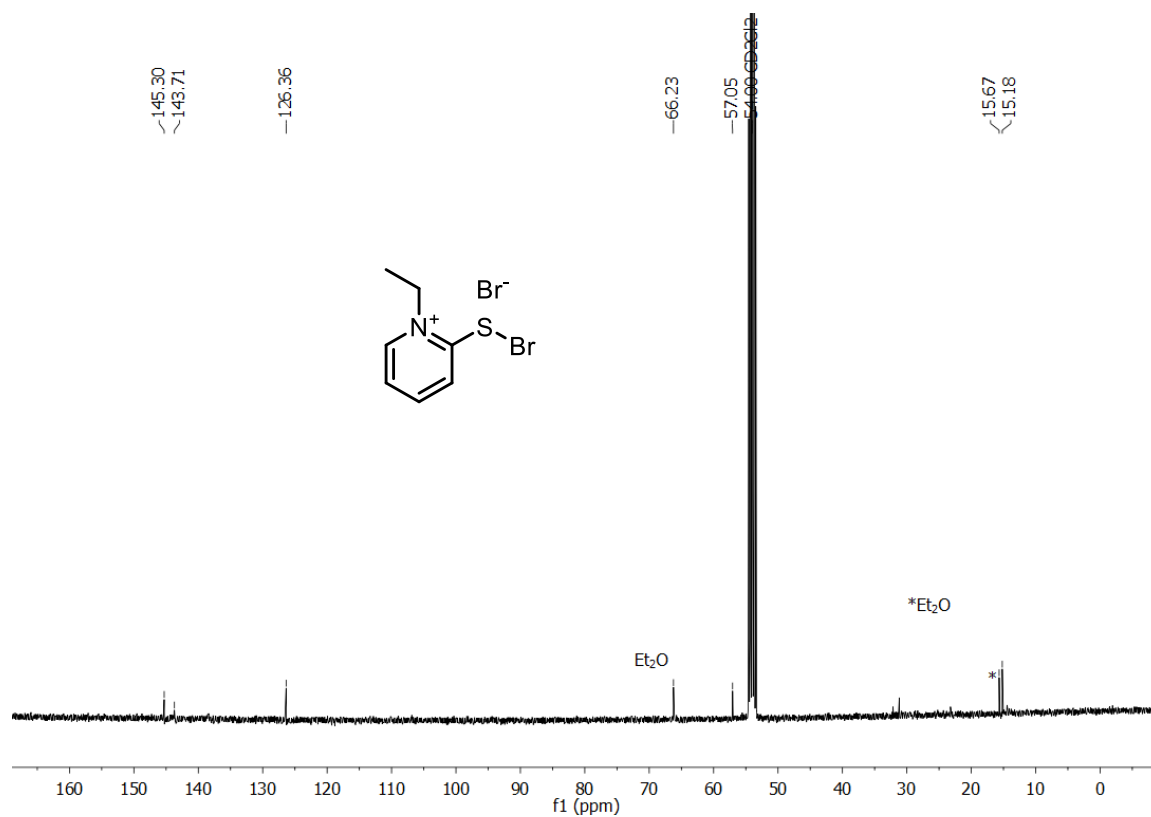
**$^{13}\text{C}$  NMR of compound 154a, 2-(bromothio)-1-methylpyridin-1-ium bromide, 126 MHz,  $\text{C}_2\text{D}_2\text{Cl}_4$ , 298 K**



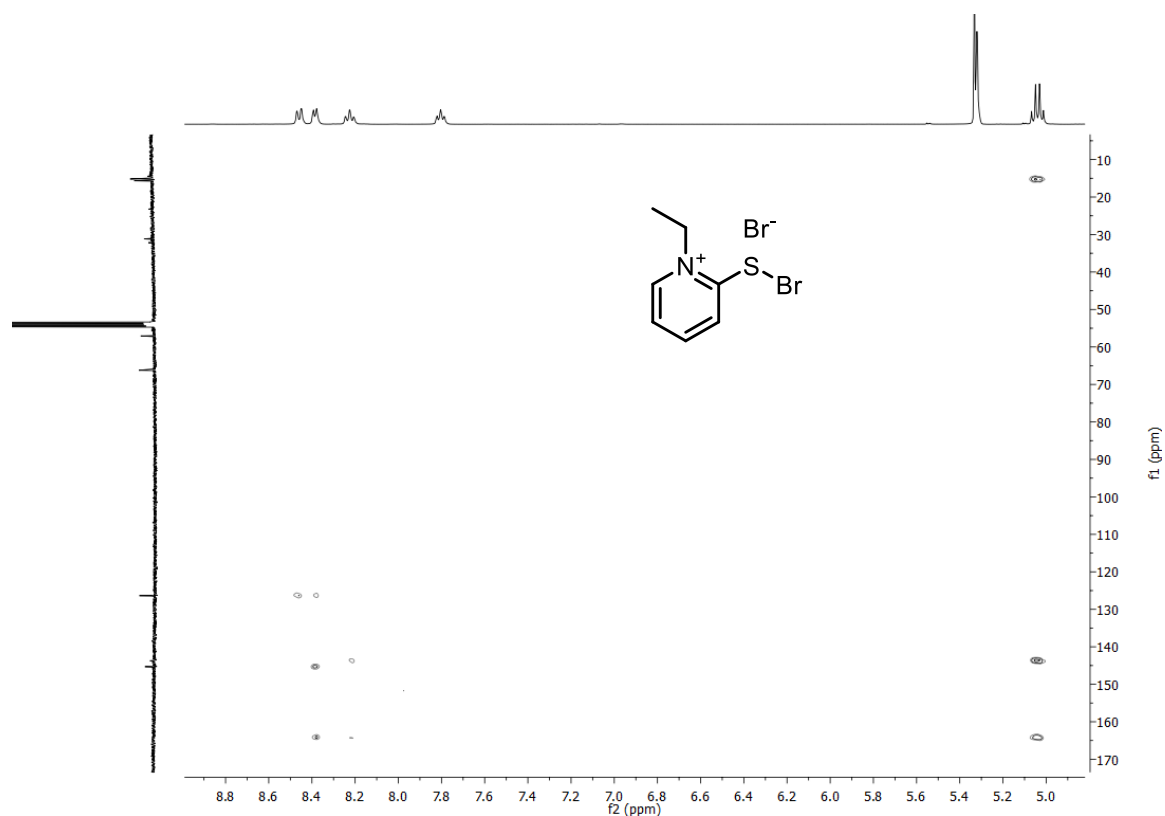
**<sup>1</sup>H NMR of compound 154ba, 2-(bromothio)-1-ethylpyridin-1-ium bromide, 400 MHz, CD<sub>2</sub>Cl<sub>2</sub>, 298 K**



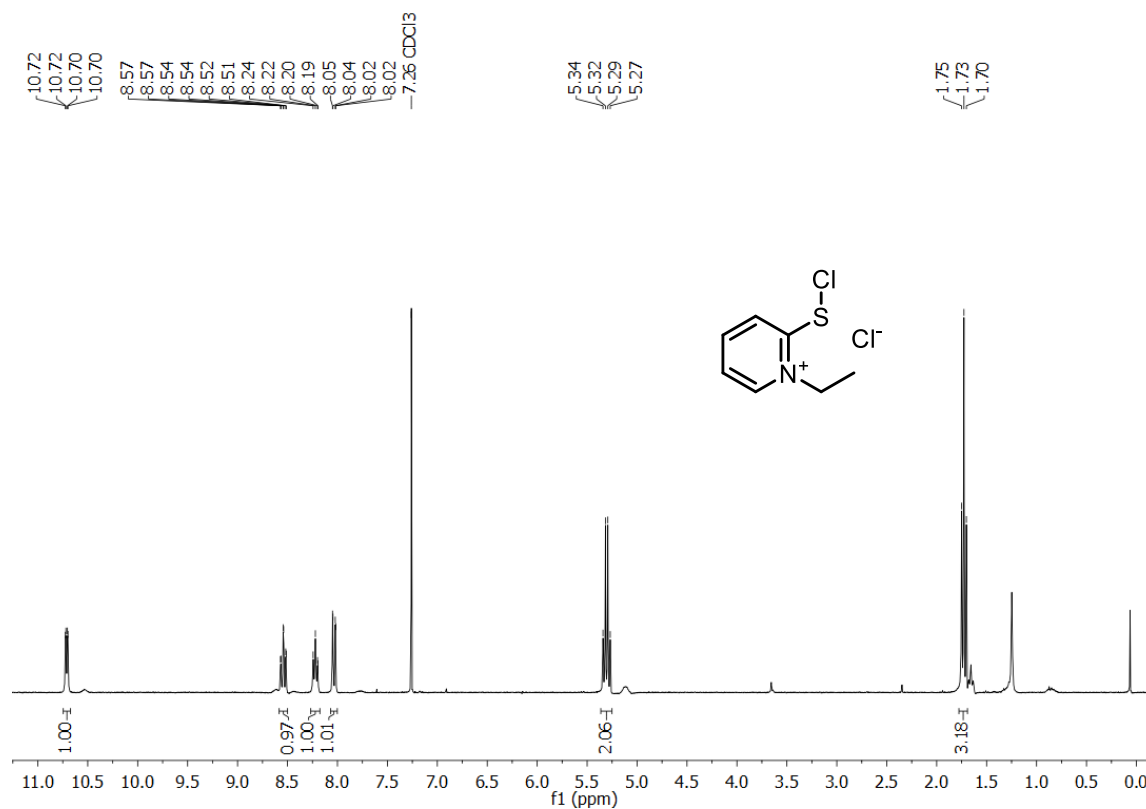
**<sup>13</sup>C NMR of compound 154ba, 2-(bromothio)-1-ethylpyridin-1-ium bromide, 101 MHz, CD<sub>2</sub>Cl<sub>2</sub>, 298 K**



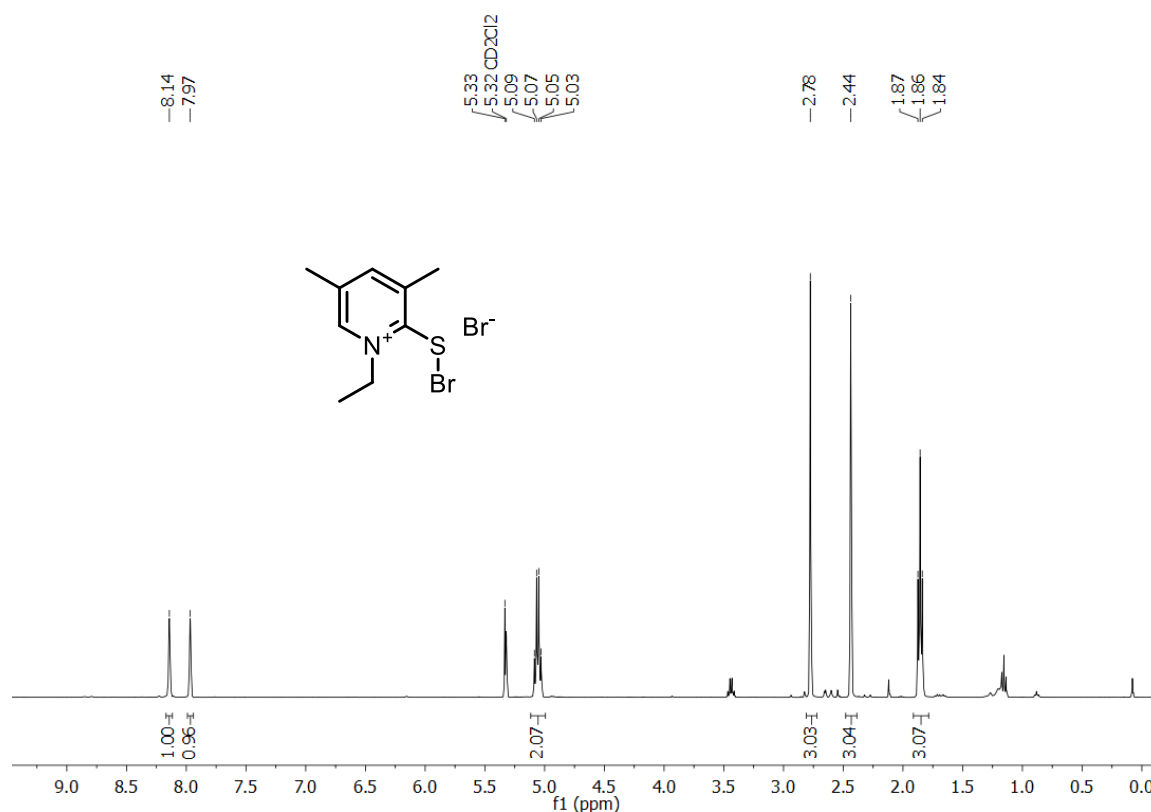
Selected region of HMBC for compound 154ba, 2-(bromothio)-1-ethylpyridin-1-ium bromide, 400 MHz / 101 MHz, CD<sub>2</sub>Cl<sub>2</sub>, 298 K



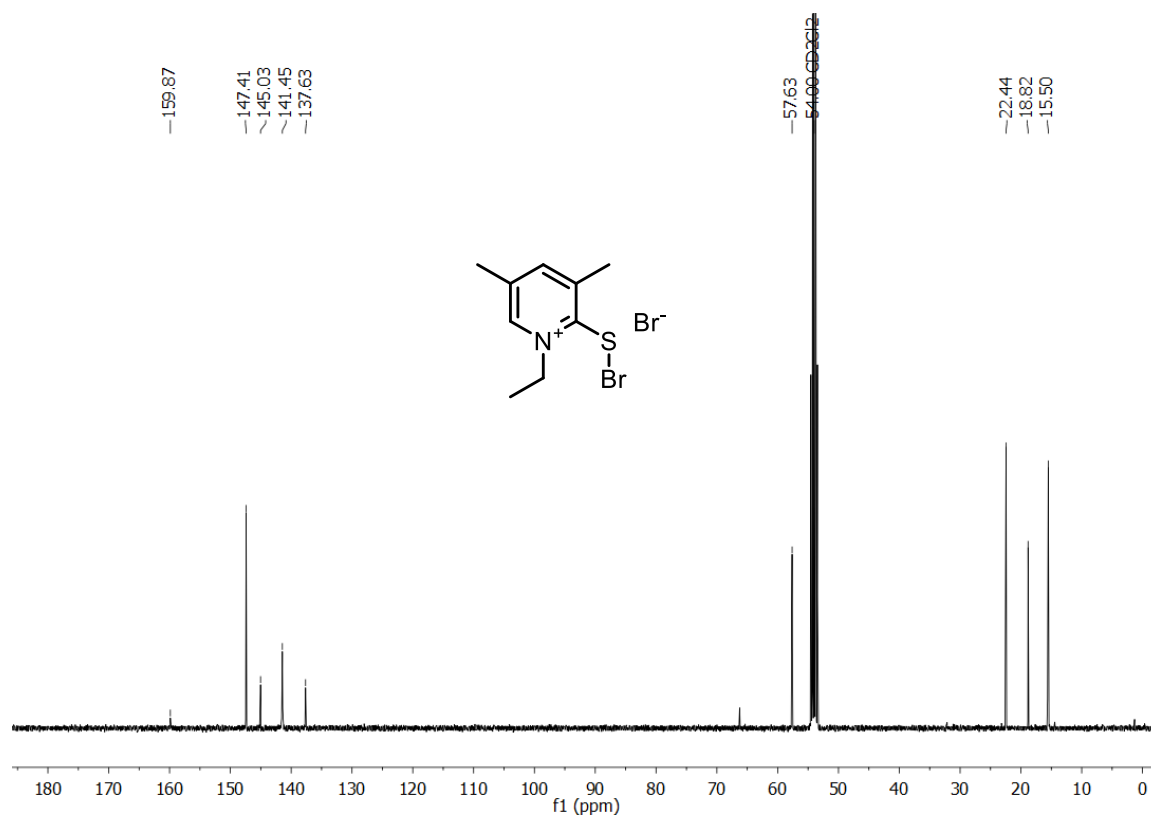
<sup>1</sup>H NMR of compound 154bb, 2-(chlorothio)-1-ethylpyridin-1-ium chloride, 300 MHz, CDCl<sub>3</sub>, 303 K



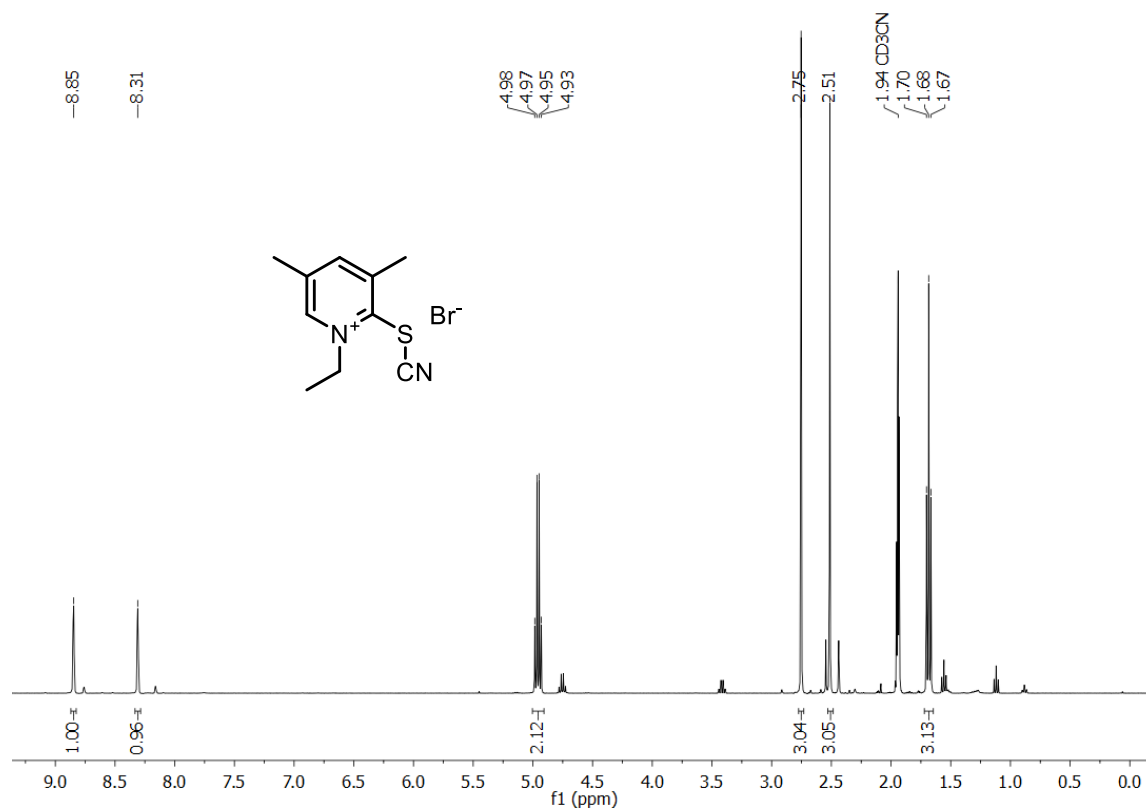
**<sup>1</sup>H NMR of compound 154c, 2-(bromothio)-1-ethyl-3,5-dimethylpyridin-1-ium bromide, 400 MHz, CD<sub>2</sub>Cl<sub>2</sub>, 298 K**



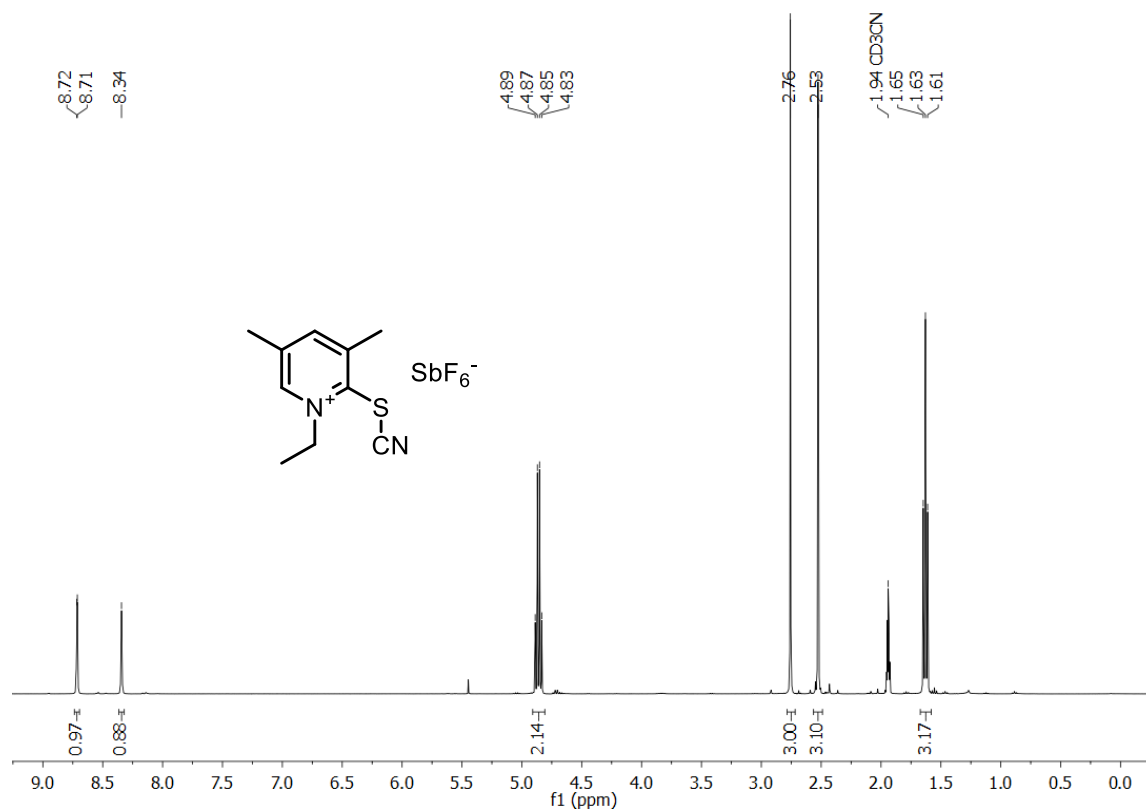
**<sup>13</sup>C NMR of compound 154c, 2-(bromothio)-1-ethyl-3,5-dimethylpyridin-1-ium bromide, 101 MHz, CD<sub>2</sub>Cl<sub>2</sub>, 298 K**



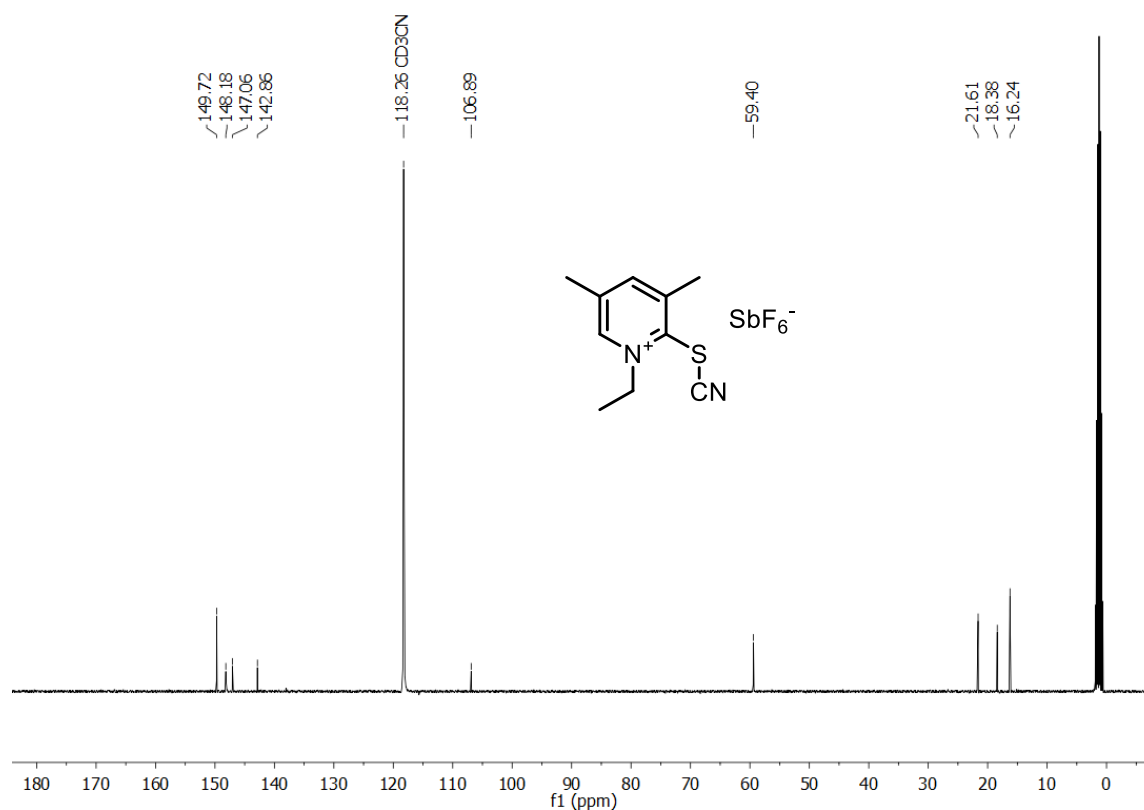
**$^1\text{H}$  NMR of compound 155a, 1-ethyl-3,5-dimethyl-2-thiocyanatopyridin-1-ium bromide, 400 MHz,  $\text{CD}_3\text{CN}$ , 300 K**



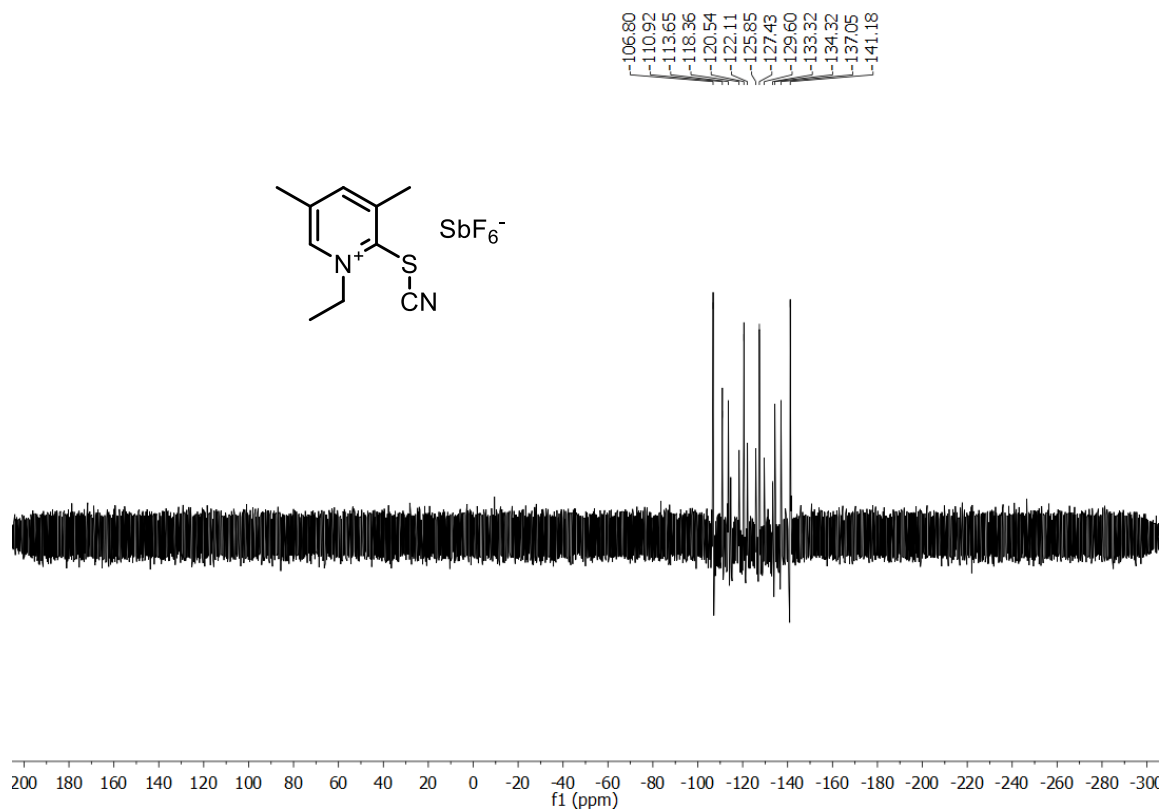
**$^1\text{H}$  NMR of compound 155b, 1-ethyl-3,5-dimethyl-2-thiocyanatopyridin-1-ium hexafluoroantimonate, 400 MHz,  $\text{CD}_3\text{CN}$ , 300 K**



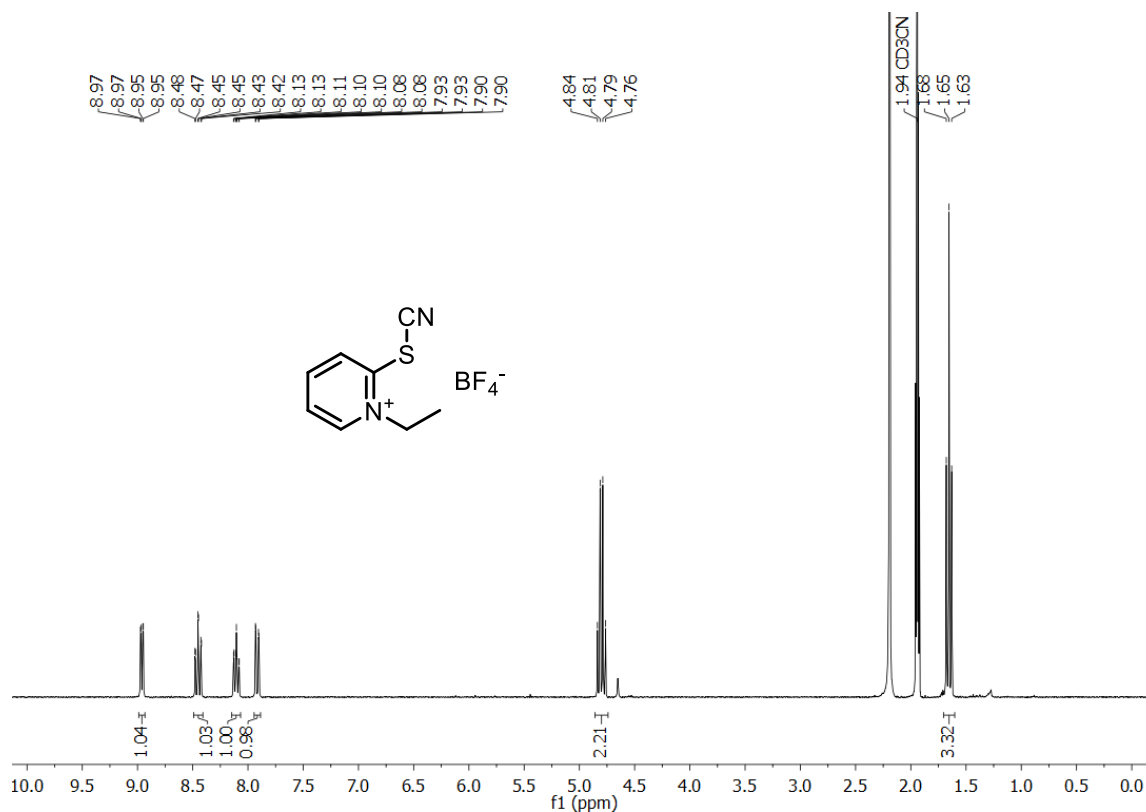
**$^{13}\text{C}$  NMR of compound 155b, 1-ethyl-3,5-dimethyl-2-thiocyanatopyridin-1-ium hexafluoroantimonate, 101 MHz,  $\text{CD}_3\text{CN}$ , 300 K**



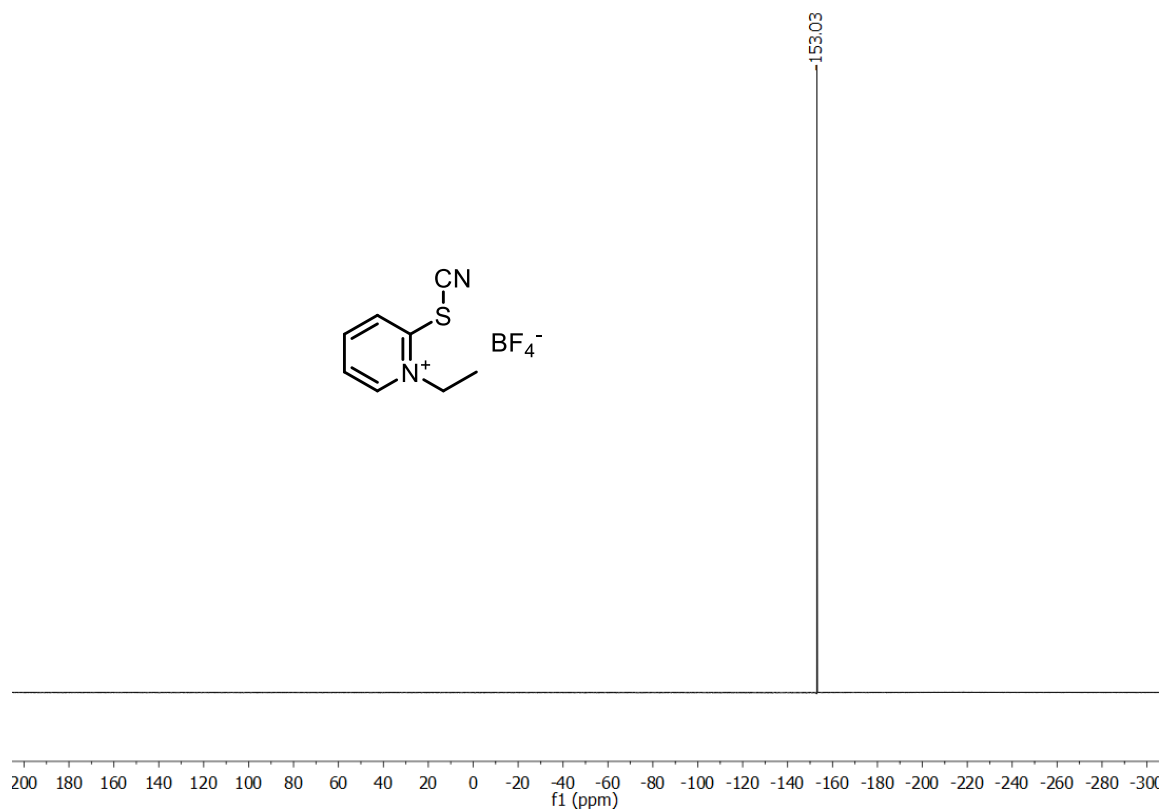
**$^{19}\text{F}$  NMR of compound 155b, 1-ethyl-3,5-dimethyl-2-thiocyanatopyridin-1-ium hexafluoroantimonate, 282 MHz,  $\text{CD}_3\text{CN}$ , 303 K**



**$^1\text{H}$  NMR of compound 155c, 1-ethyl-2-thiocyanatopyridin-1-ium tetrafluoroborate, 300 MHz,  $\text{CD}_3\text{CN}$ , 303 K**

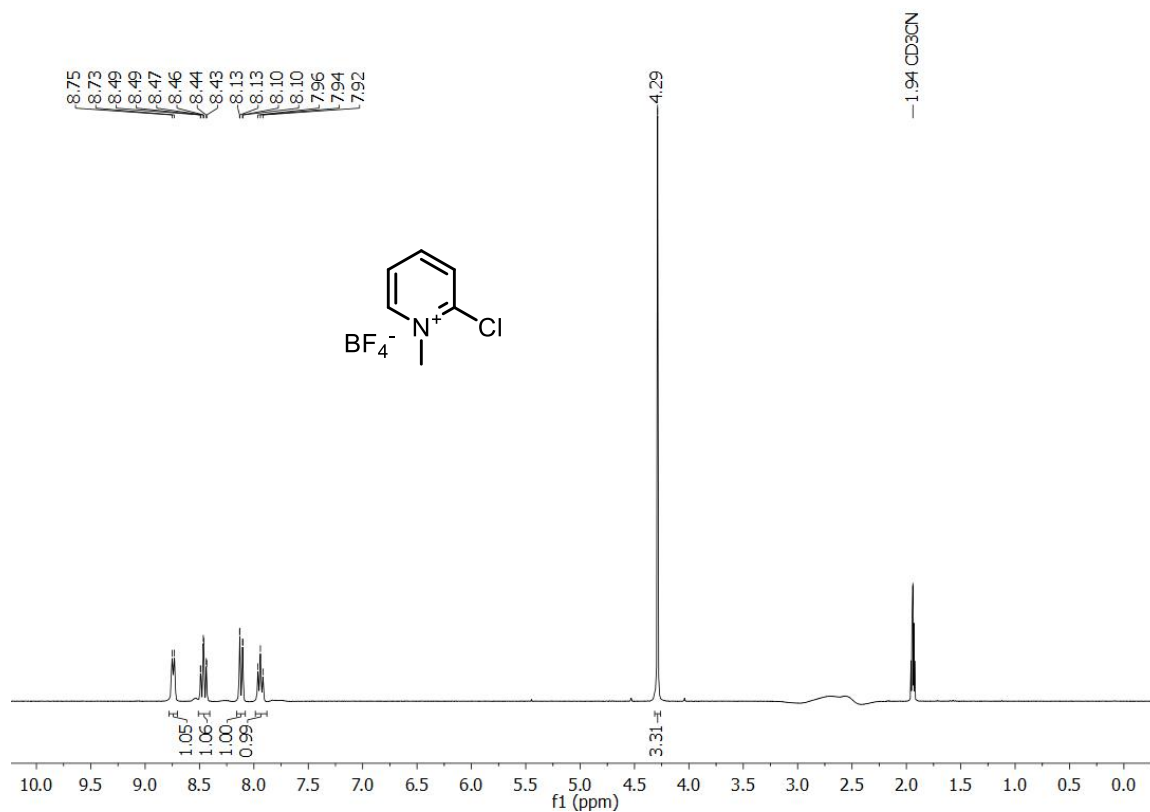


**$^{19}\text{F}$  NMR of compound 155c, 1-ethyl-2-thiocyanatopyridin-1-ium tetrafluoroborate, 282 MHz,  $\text{CD}_3\text{CN}$ , 303 K**

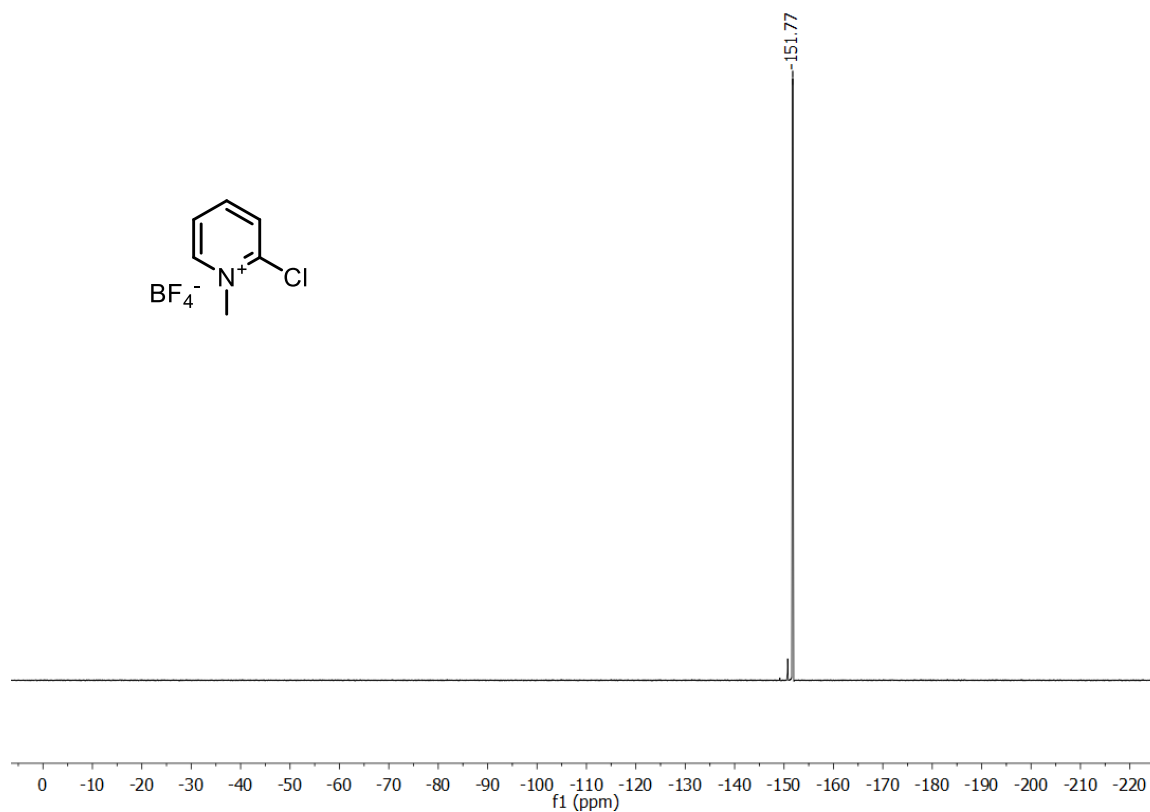




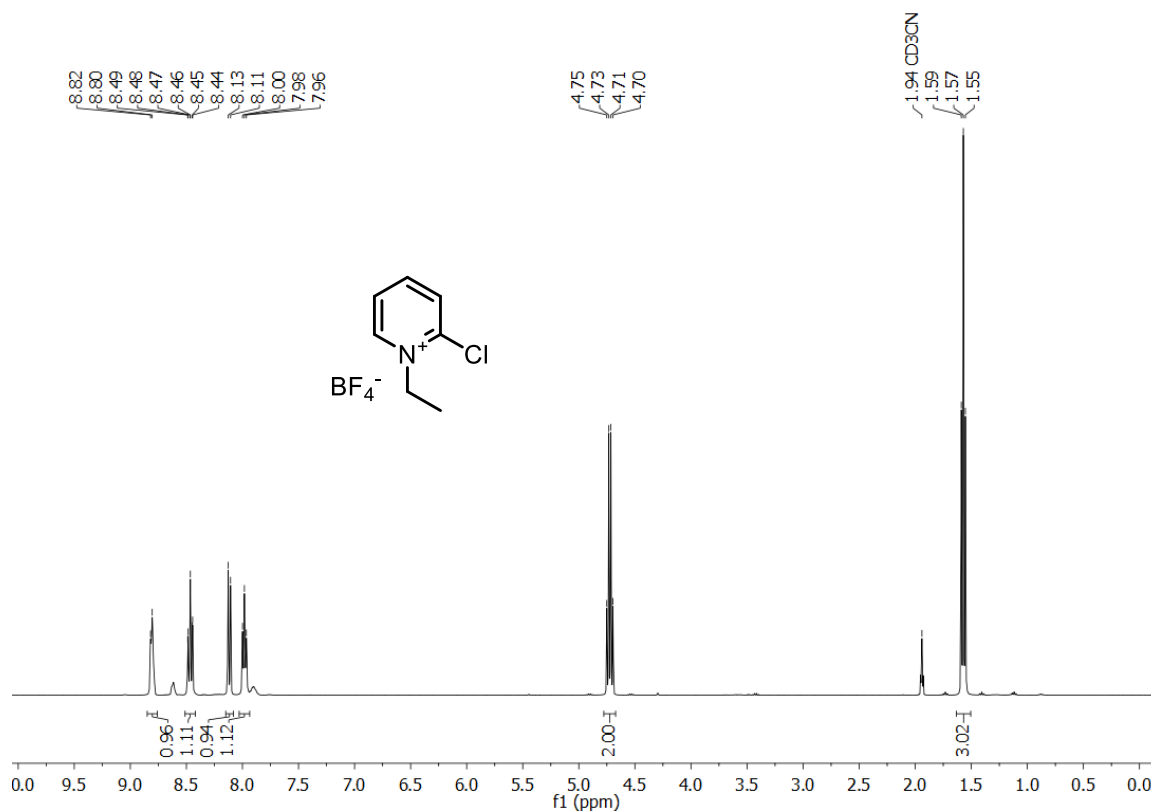
**<sup>1</sup>H NMR of compound 156a, 2-chloro-1-methylpyridin-1-ium tetrafluoroborate, 400 MHz, CD<sub>3</sub>CN, 298 K**



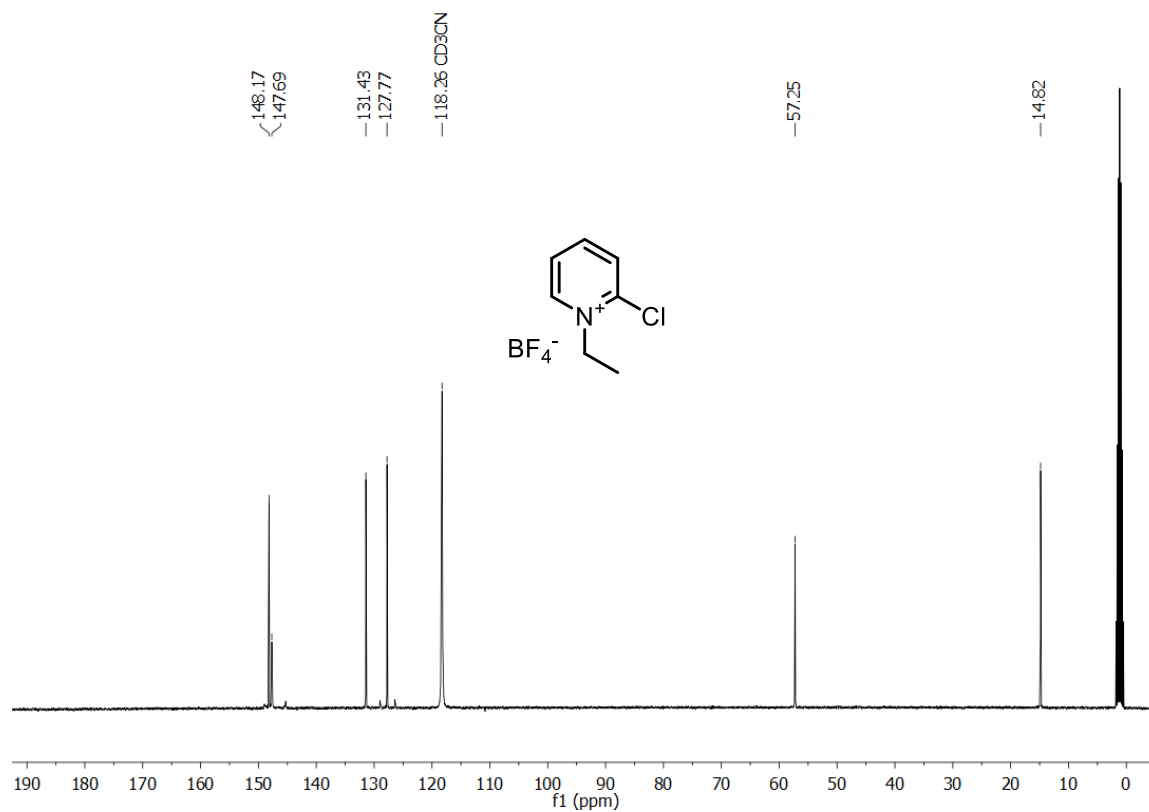
**<sup>19</sup>F NMR of compound 156a, 2-chloro-1-methylpyridin-1-ium tetrafluoroborate, 282 MHz, CD<sub>3</sub>CN, 298 K**



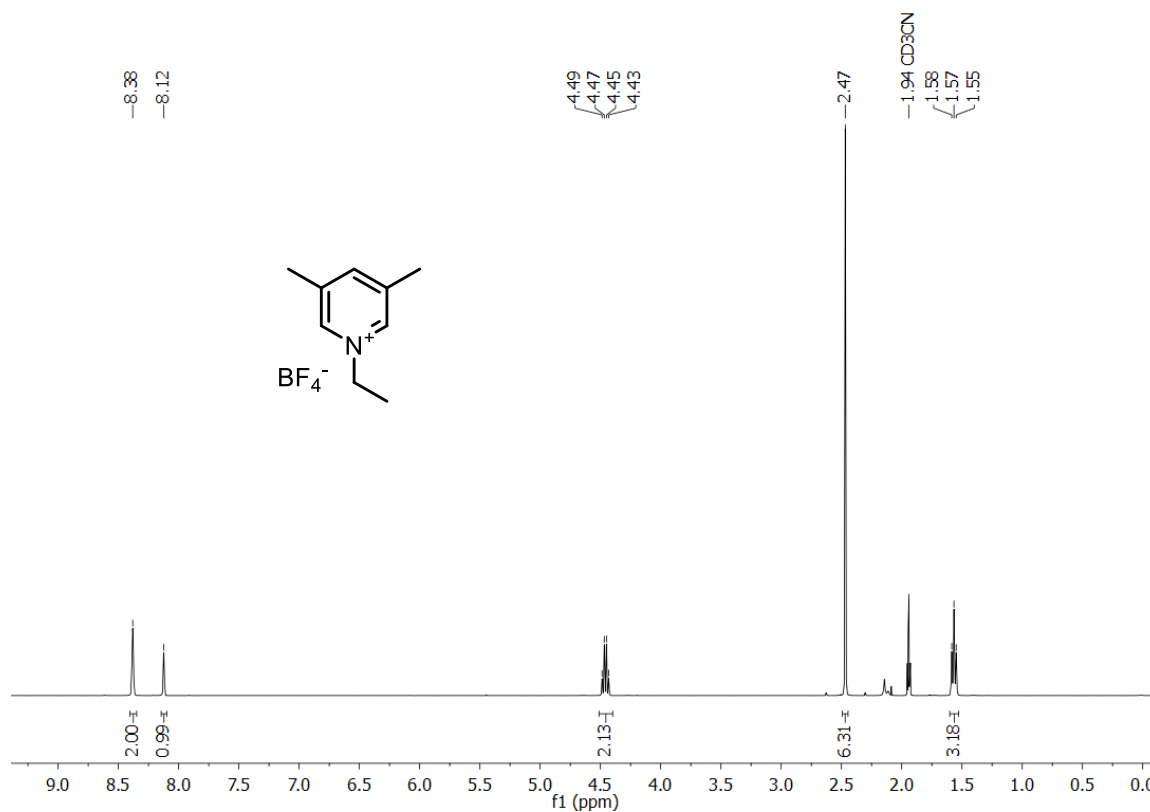
**$^1\text{H}$  NMR of compound 156b, 2-chloro-1-ethylpyridin-1-ium tetrafluoroborate, 400 MHz,  $\text{CD}_3\text{CN}$ , 298 K**



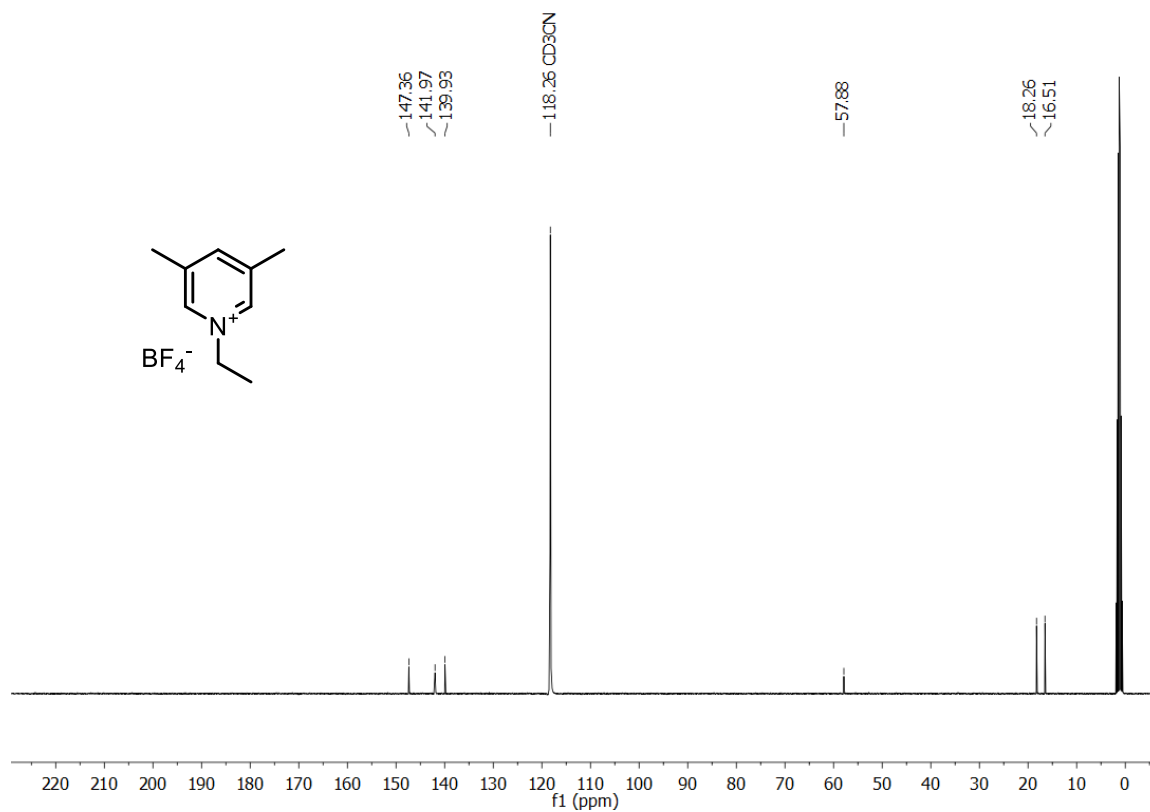
**$^{13}\text{C}$  NMR of compound 156b, 2-chloro-1-ethylpyridin-1-ium tetrafluoroborate, 101 MHz,  $\text{CD}_3\text{CN}$ , 298 K**



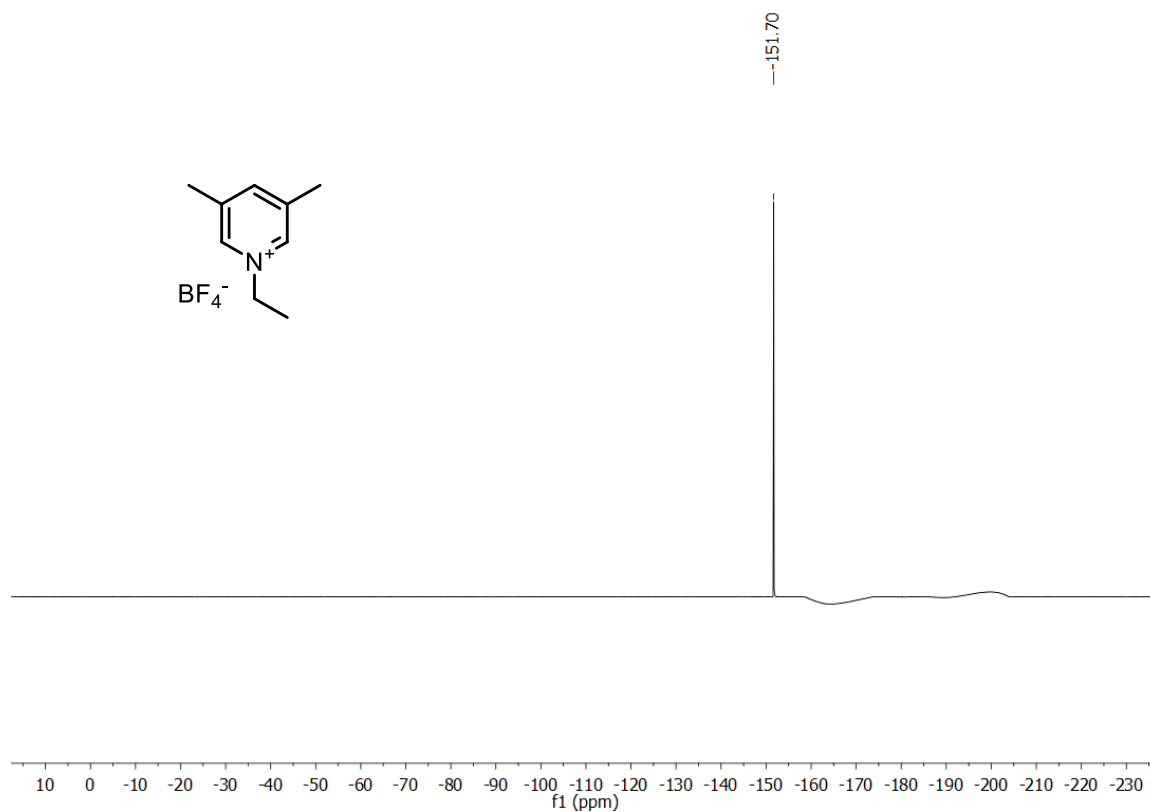
**$^1\text{H}$  NMR of compound 156c, 1-ethyl-3,5-dimethylpyridin-1-ium tetrafluoroborate, 400 MHz,  $\text{CD}_3\text{CN}$ , 298 K**



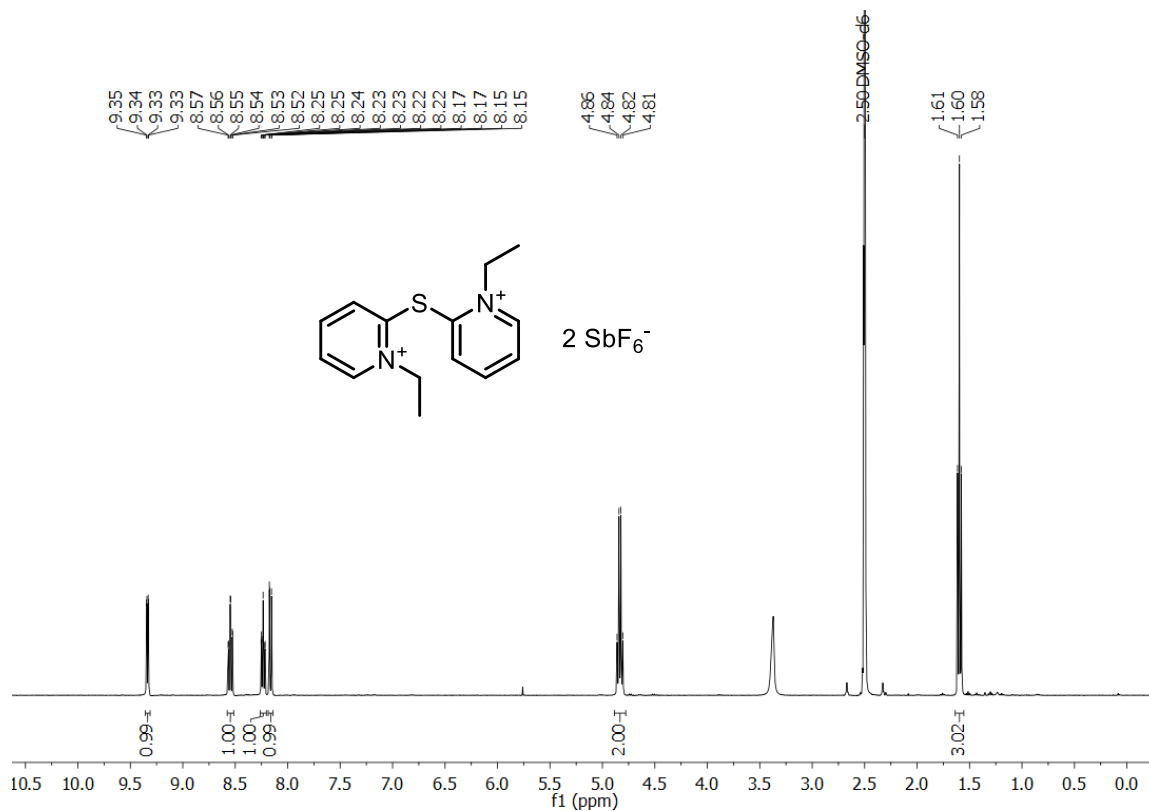
**$^{13}\text{C}$  NMR of compound 156c, 1-ethyl-3,5-dimethylpyridin-1-ium tetrafluoroborate, 101 MHz,  $\text{CD}_3\text{CN}$ , 298 K**



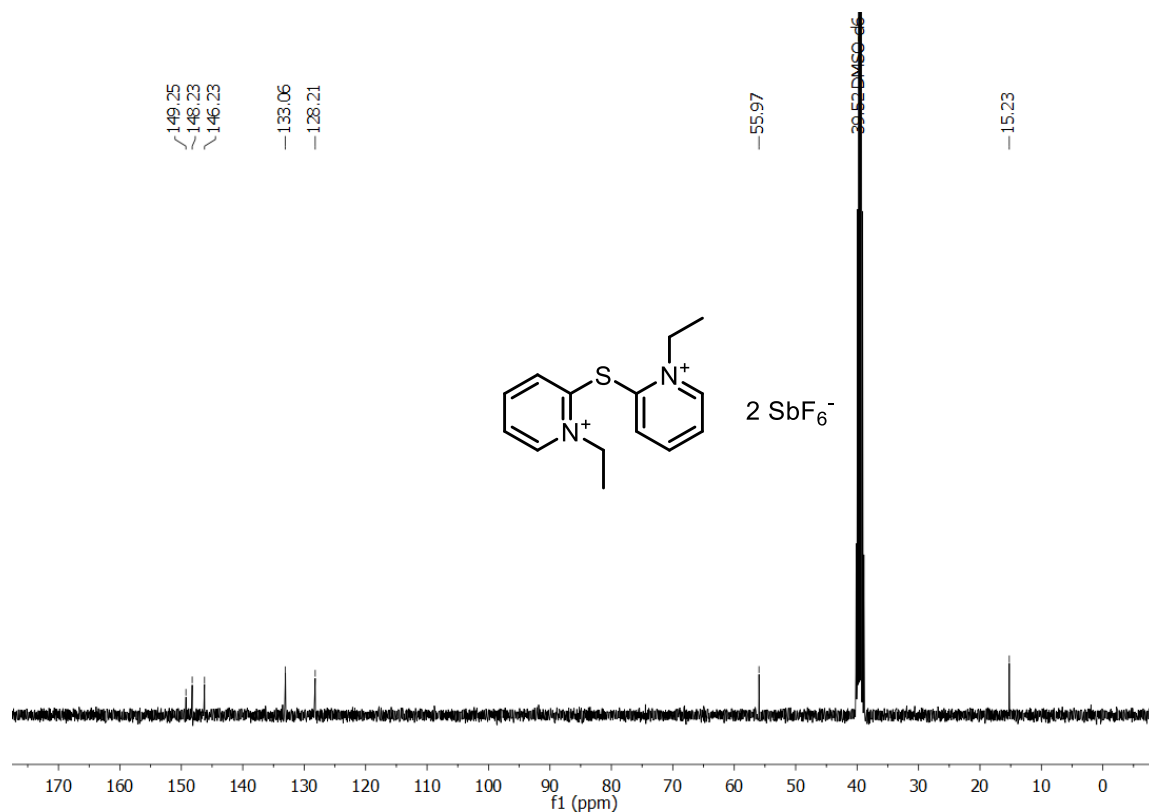
**$^{19}\text{F}$  NMR of compound 156c, 1-ethyl-3,5-dimethylpyridin-1-ium tetrafluoroborate, 377 MHz,  $\text{CD}_3\text{CN}$ , 298 K**



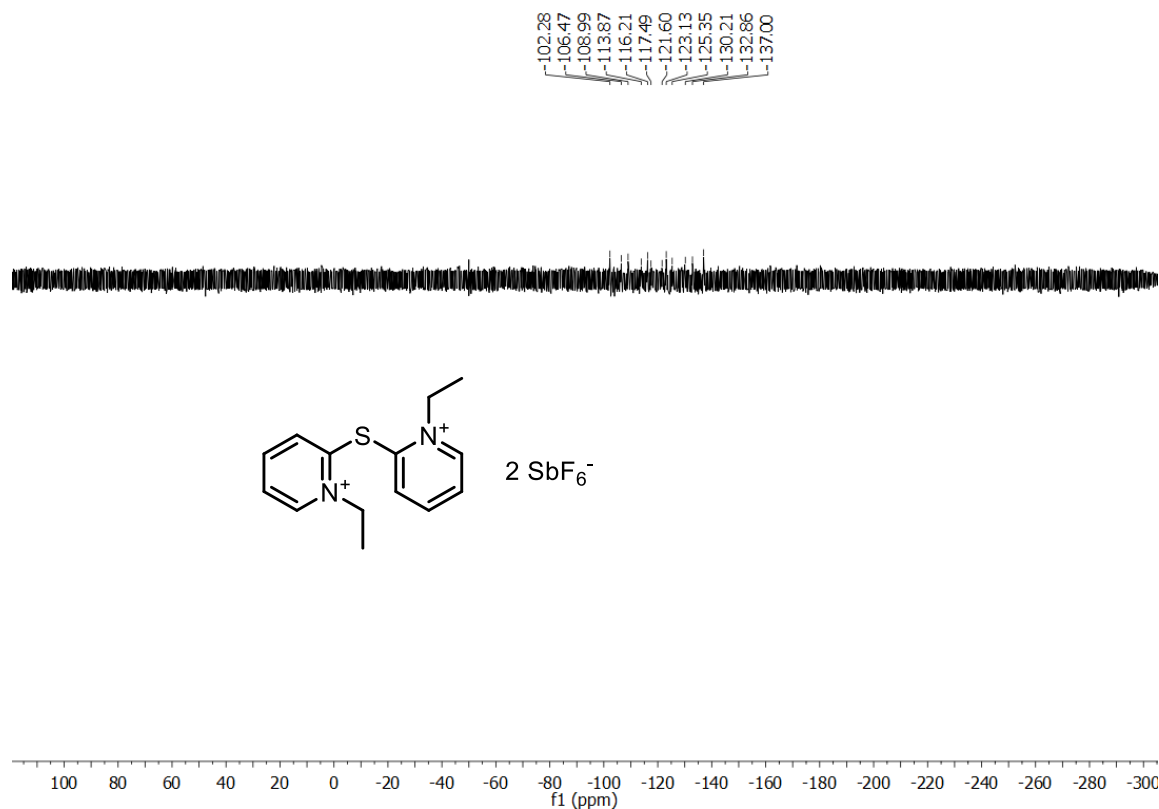
**$^1\text{H}$  NMR of compound 157, 2,2'-thiobis(1-ethylpyridin-1-ium) bis(hexafluoroantimonate), 400 MHz,  $\text{DMSO-d}_6$ , 300 K**



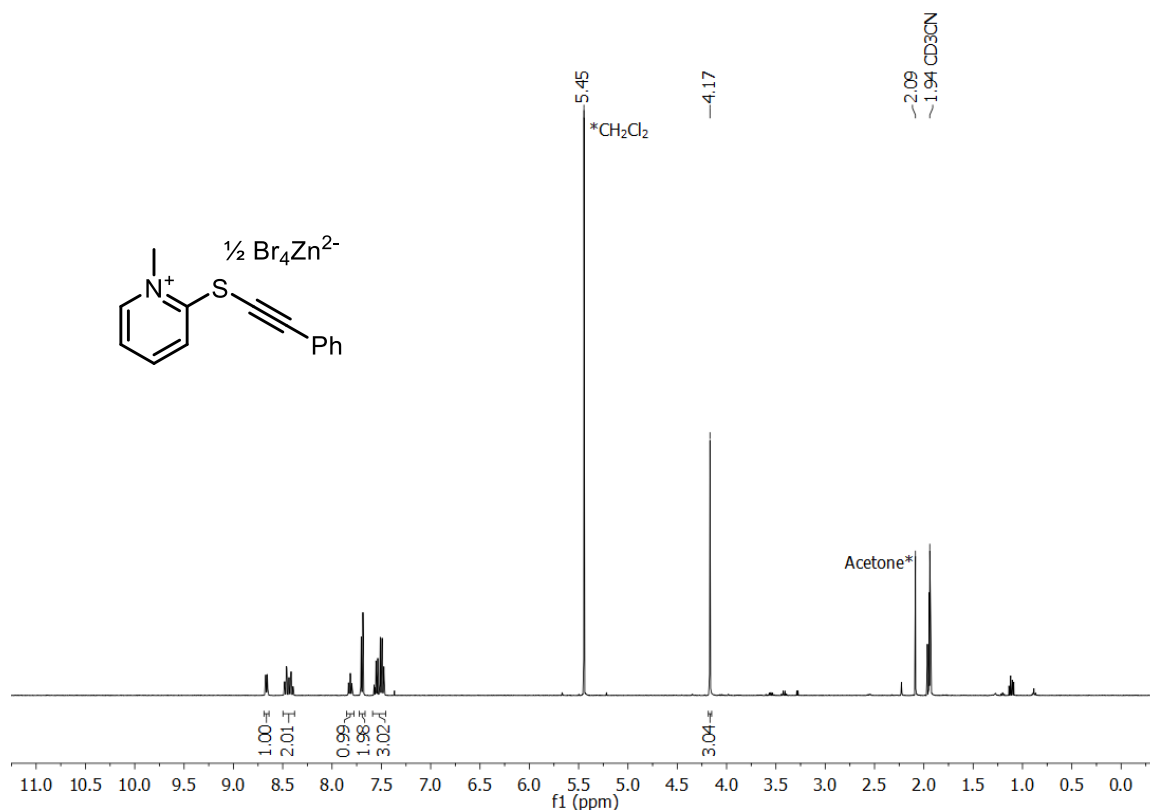
**$^{13}\text{C}$  NMR of compound 157, 2,2'-thiobis(1-ethylpyridin-1-ium) bishexafluoroantimonate, 101 MHz, DMSO- $d_6$ , 300 K**



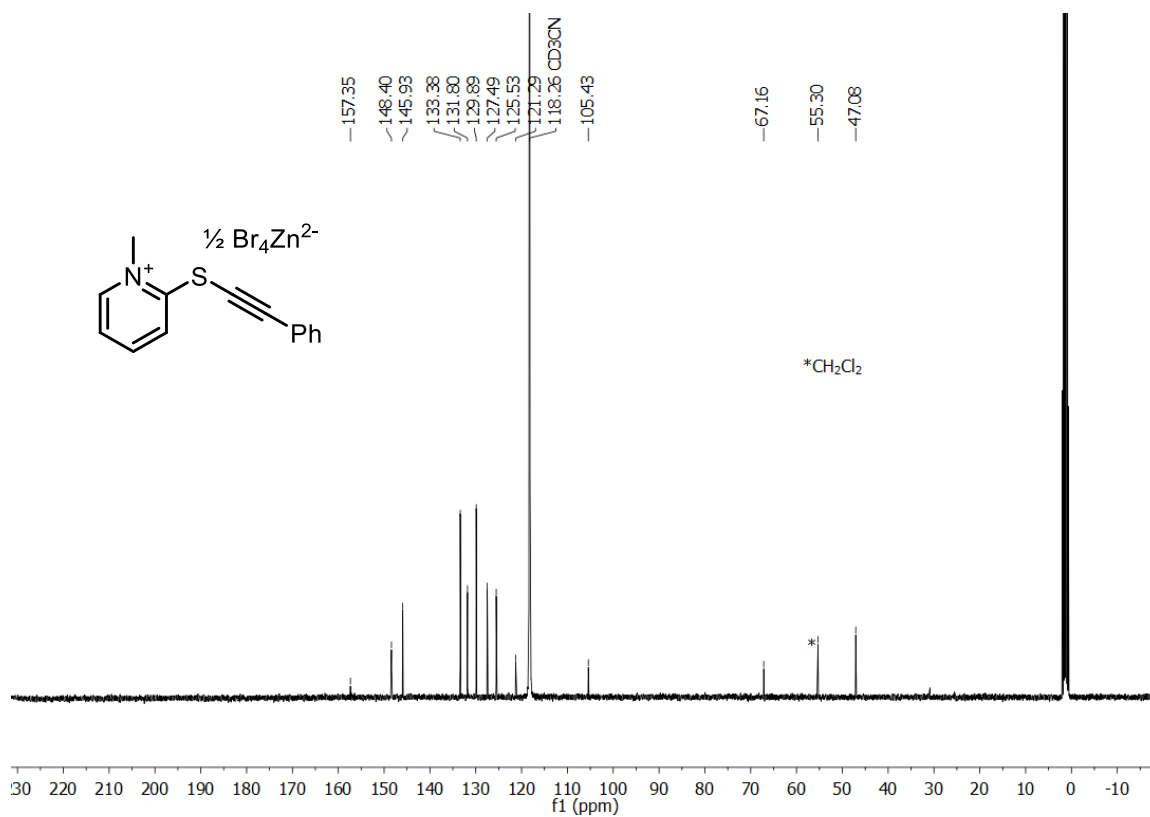
**$^{19}\text{F}$  NMR of compound 157, 2,2'-thiobis(1-ethylpyridin-1-ium) bishexafluoroantimonate, 282 MHz, DMSO- $d_6$ , 303 K**



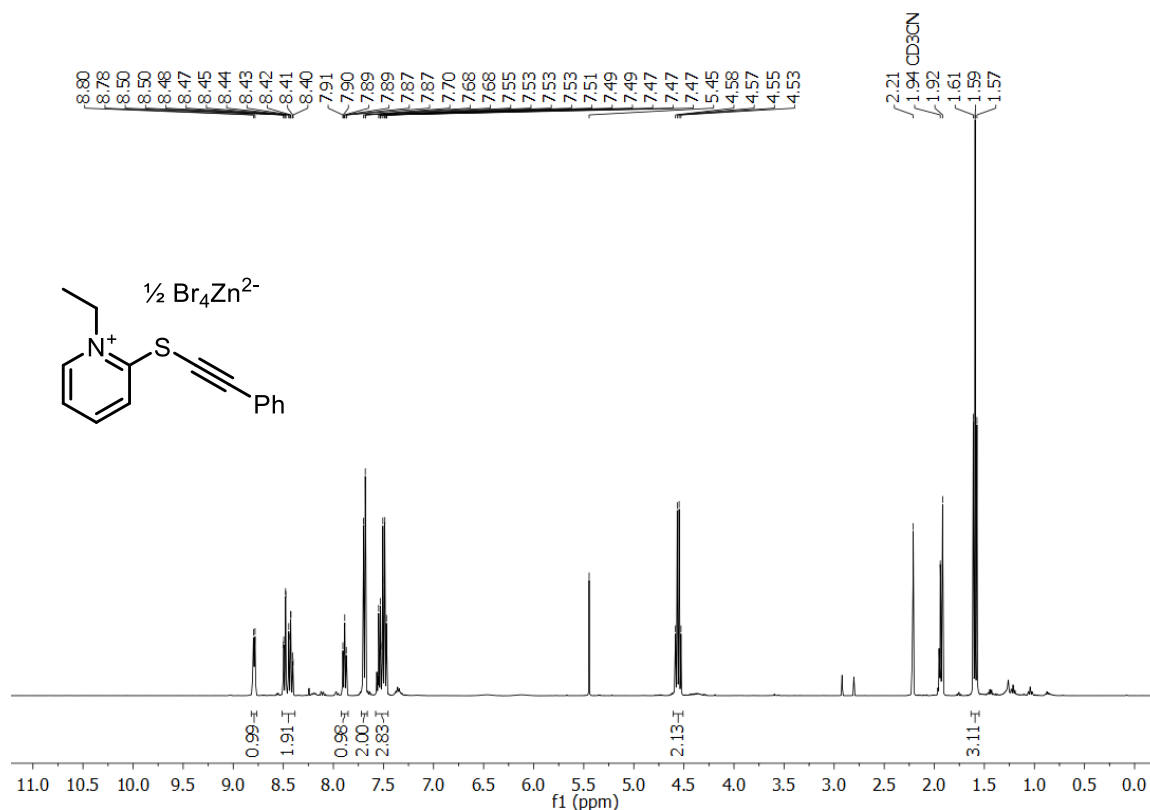
**$^1\text{H}$  NMR of compound 160a, 1-methyl-2-[(phenylethynyl)thio]pyridin-1-ium tetrabromozincate, 400 MHz,  $\text{CD}_3\text{CN}$ , 298 K**



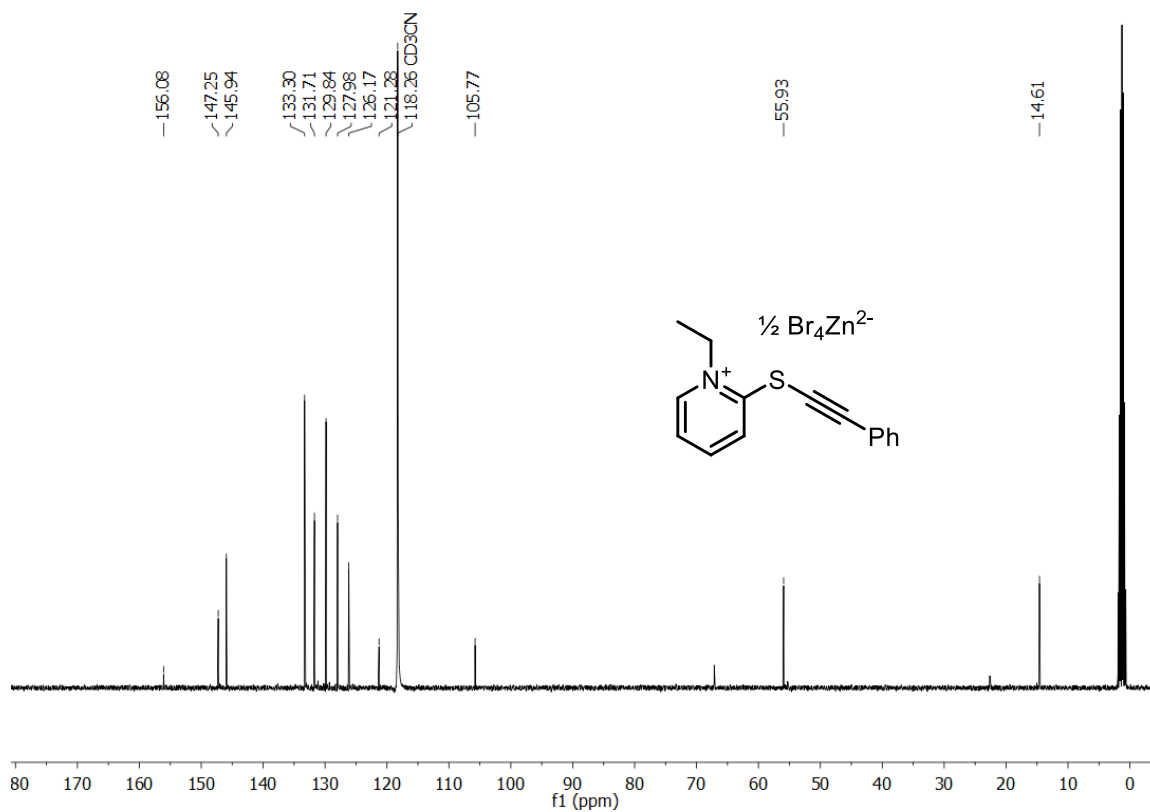
**$^{13}\text{C}$  NMR of compound 160a, 1-methyl-2-[(phenylethynyl)thio]pyridin-1-ium tetrabromozincate, 101,  $\text{CD}_3\text{CN}$ , 298 K**



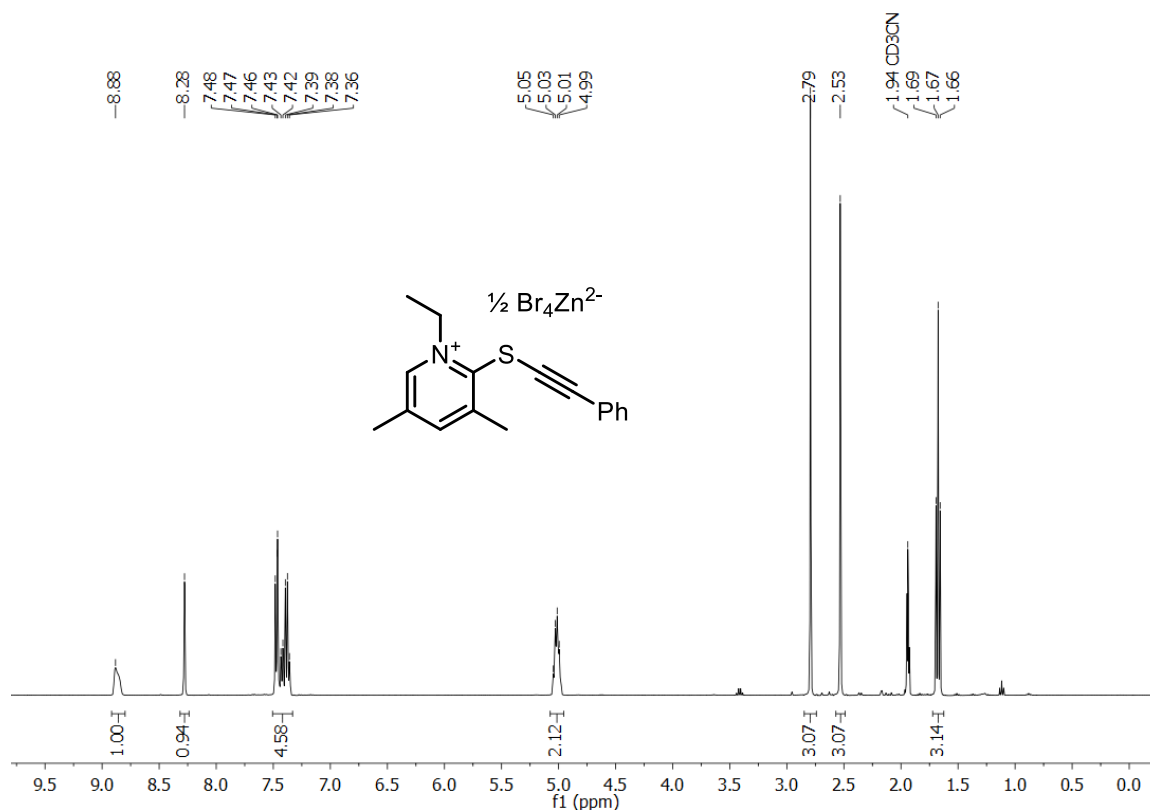
**$^1\text{H}$  NMR of compound 160b, 1-ethyl-2-[(phenylethynyl)thio]pyridin-1-ium tetrabromozincate, 400 MHz,  $\text{CD}_3\text{CN}$ , 300 K**



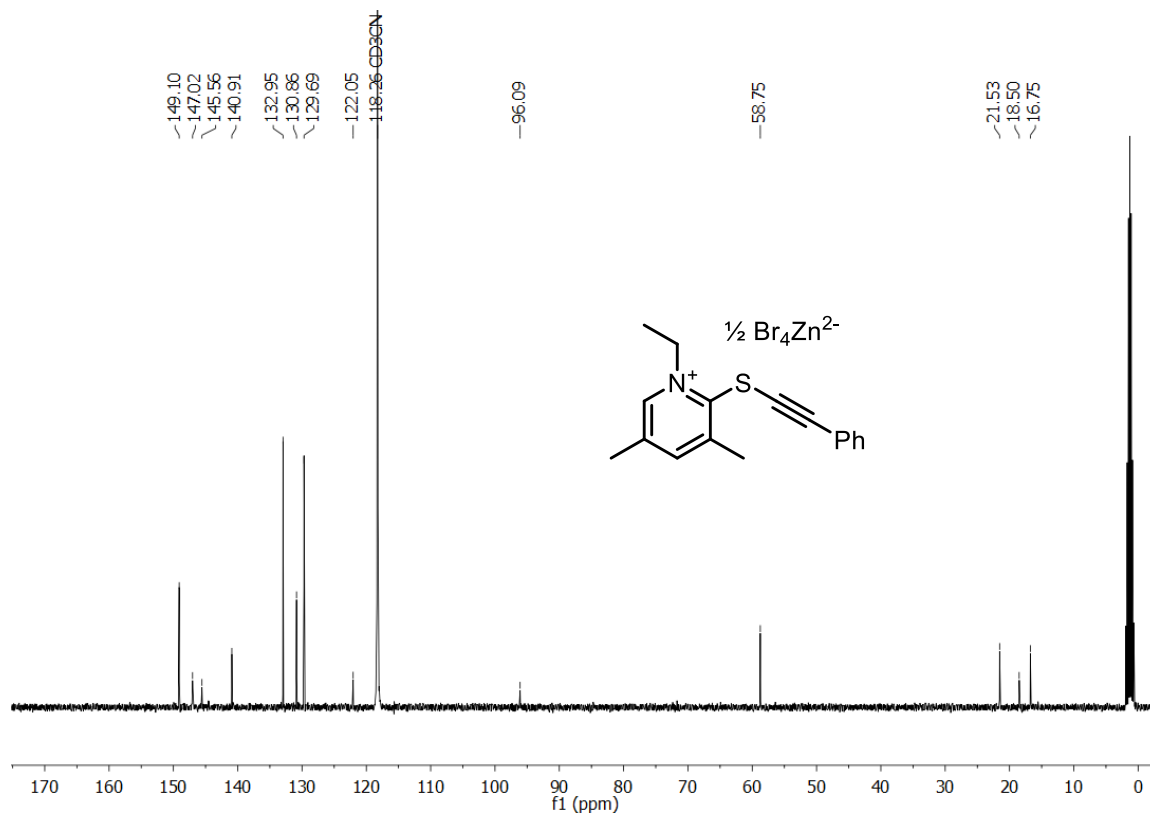
**$^{13}\text{C}$  NMR of compound 160b, 1-ethyl-2-[(phenylethynyl)thio]pyridin-1-ium tetrabromozincate, 101 MHz,  $\text{CD}_3\text{CN}$ , 300 K**



**$^1\text{H}$  NMR of compound 160c, 1-ethyl-3,5-dimethyl-2-[(phenylethynyl)thio]pyridin-1-ium tetrabromozincate, 400 MHz,  $\text{CD}_3\text{CN}$ , 300 K**

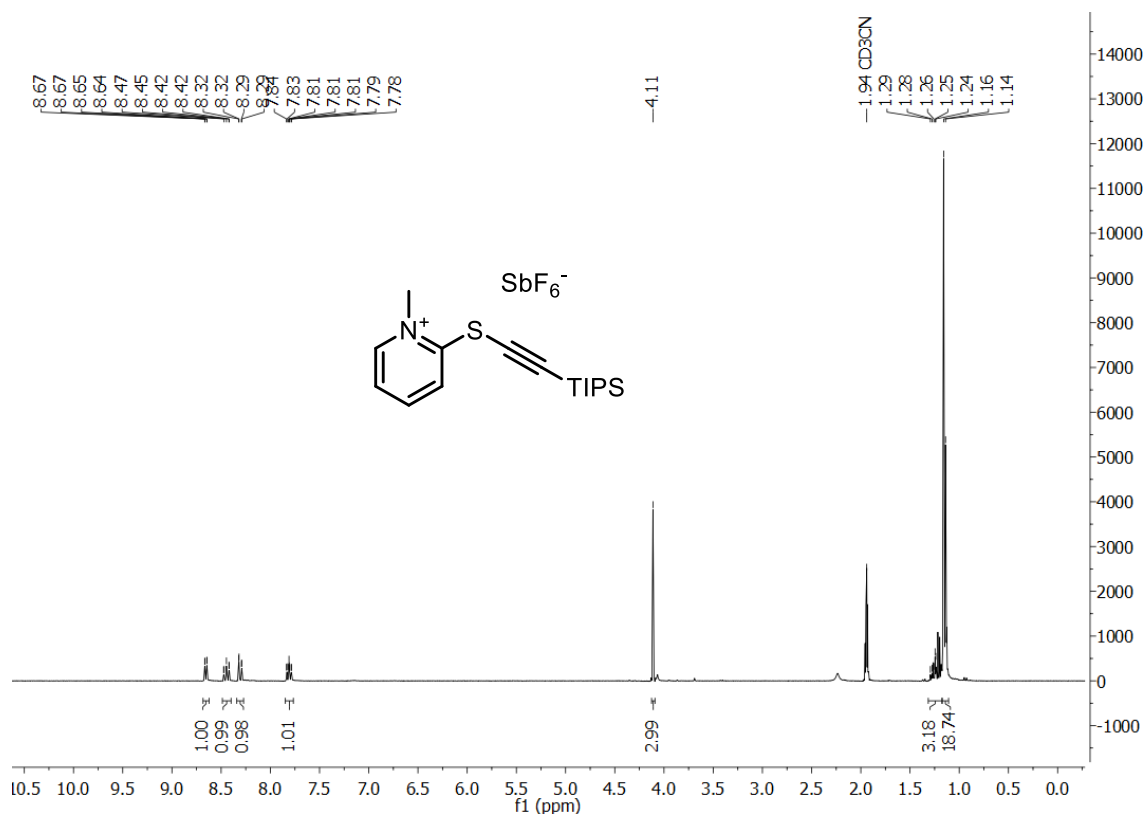


**$^{13}\text{C}$  NMR of compound 160c, 1-ethyl-3,5-dimethyl-2-[(phenylethynyl)thio]pyridin-1-ium tetrabromozincate, 101 MHz,  $\text{CD}_3\text{CN}$ , 300 K**

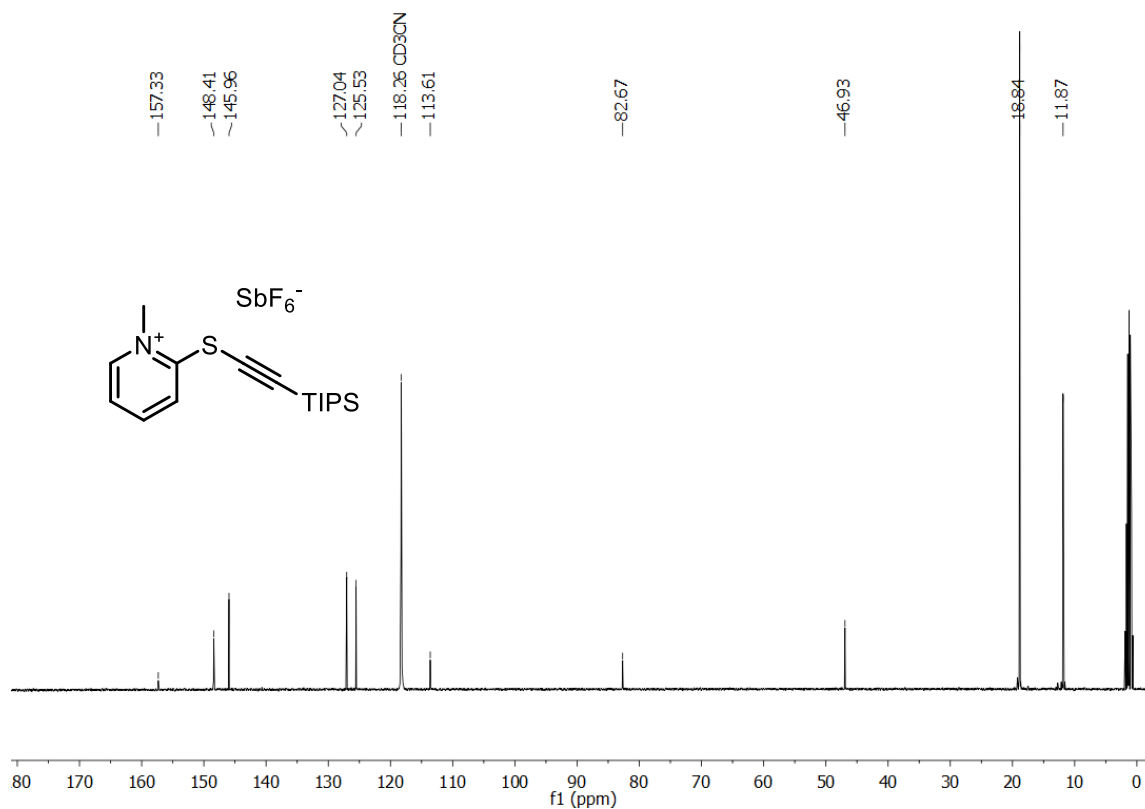




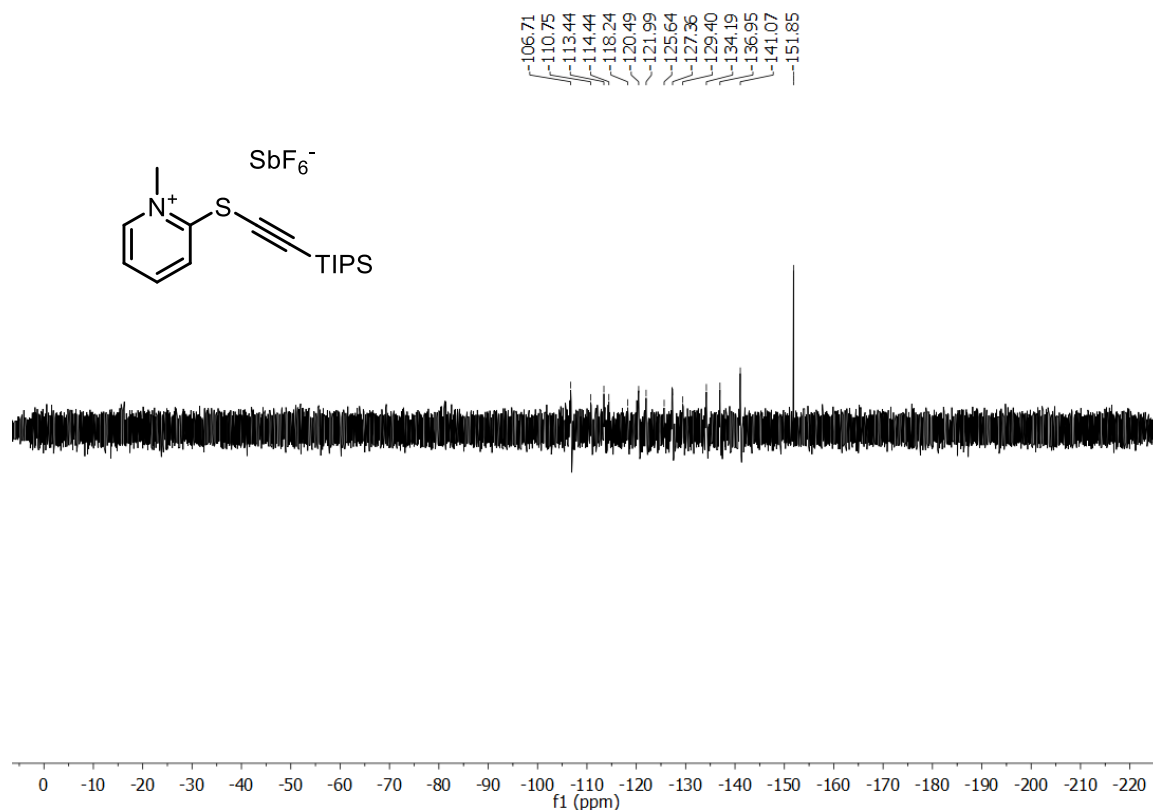
**$^1\text{H}$  NMR of compound 160d, 1-methyl-2-[[triisopropylsilyl]ethynyl]thio}pyridin-1-ium hexafluoroantimonate, 300 MHz,  $\text{CD}_3\text{CN}$ , 295 K**



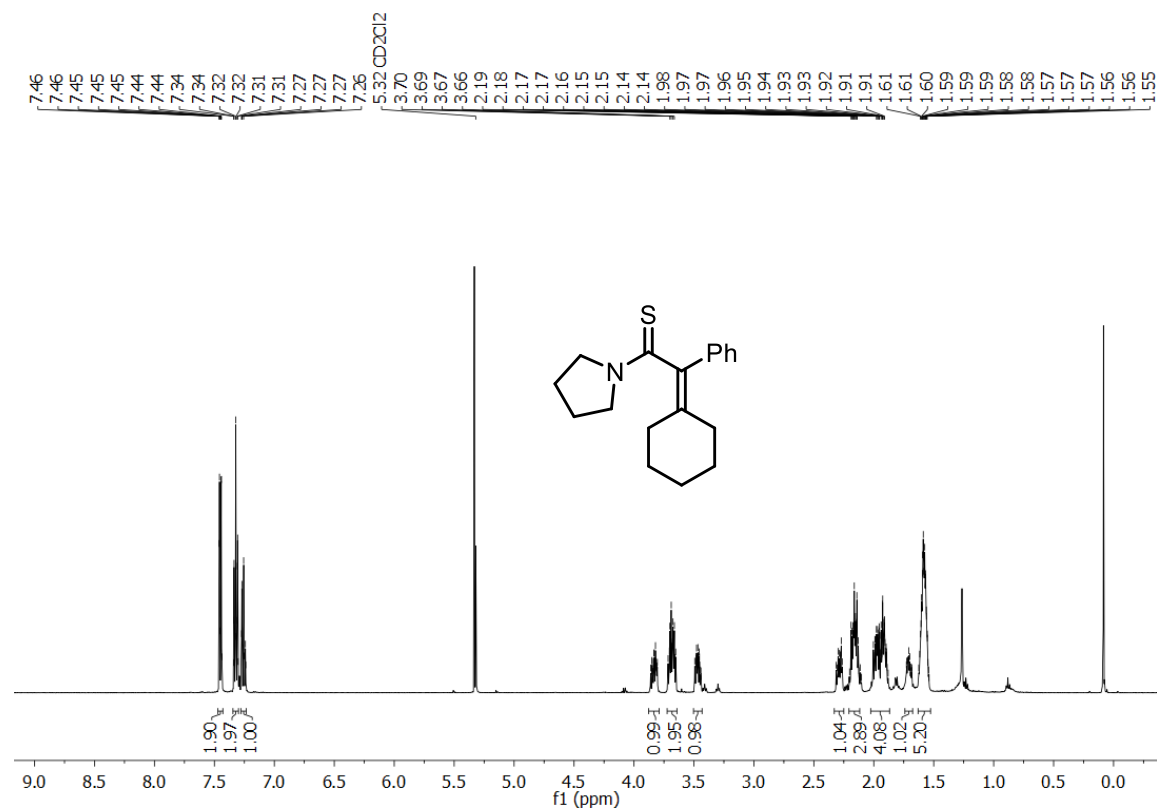
**$^{13}\text{C}$  NMR of compound 160d, 1-methyl-2-[[triisopropylsilyl]ethynyl]thio}pyridin-1-ium hexafluoroantimonate, 400 MHz,  $\text{CD}_3\text{CN}$ , 295 K**



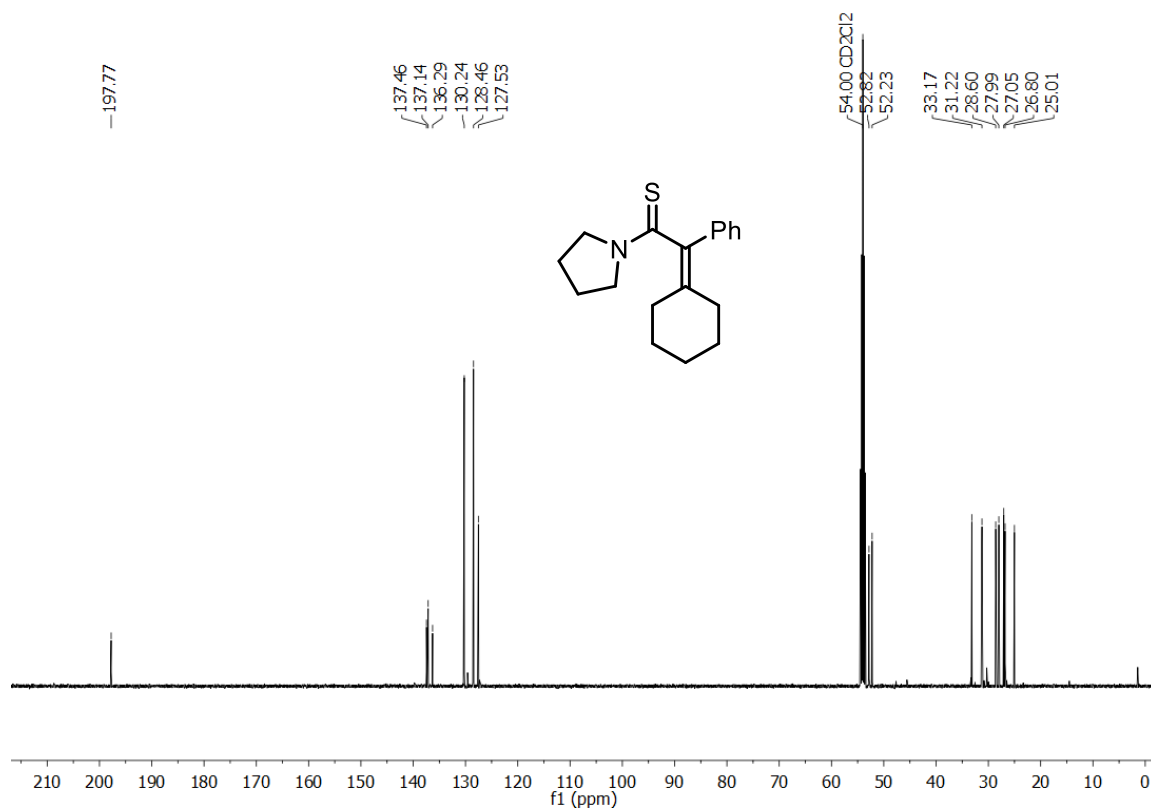
**$^{19}\text{F}$  NMR of compound 160d, 1-methyl-2-[[triisopropylsilyl]ethynyl]thio]pyridin-1-ium hexafluoroantimonate, 282 MHz,  $\text{CD}_3\text{CN}$ , 295 K**



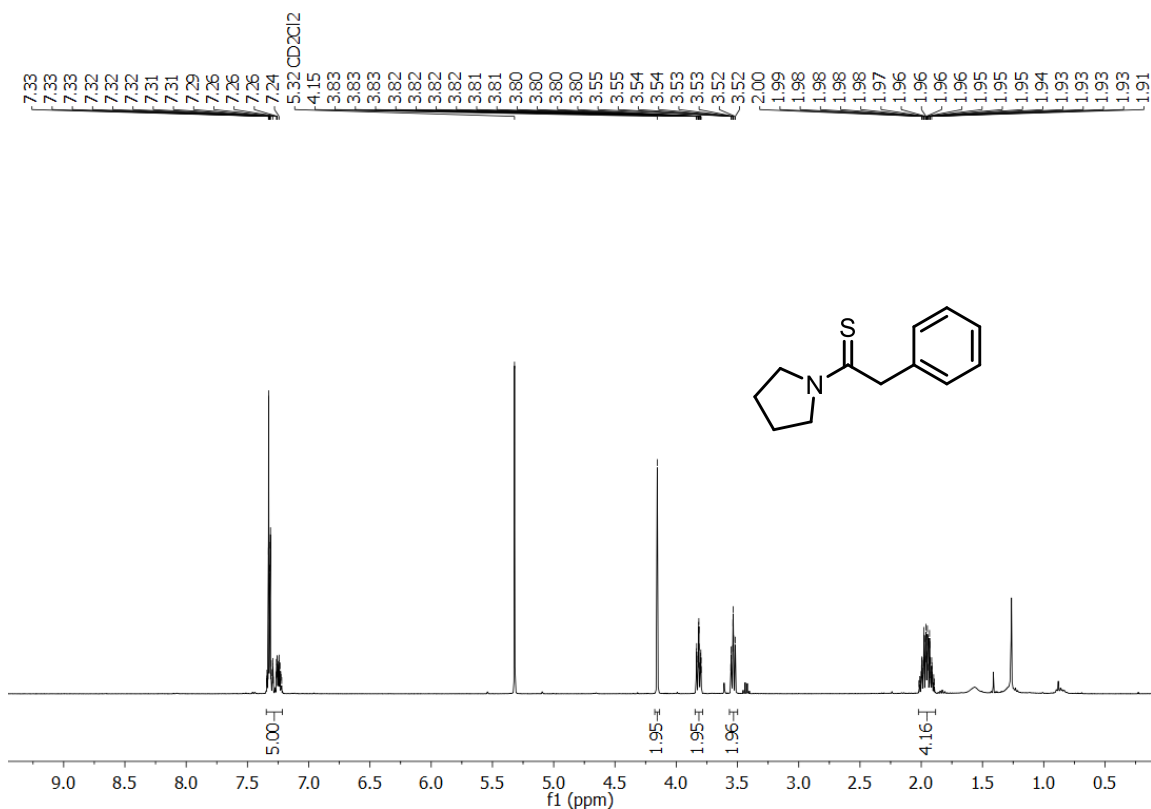
**$^1\text{H}$  NMR of compound 161a, 2-cyclohexylidene-2-phenyl-1-(pyrrolidin-1-yl)ethane-1-thione, 500 MHz,  $\text{CD}_2\text{Cl}_2$ , 298 K**



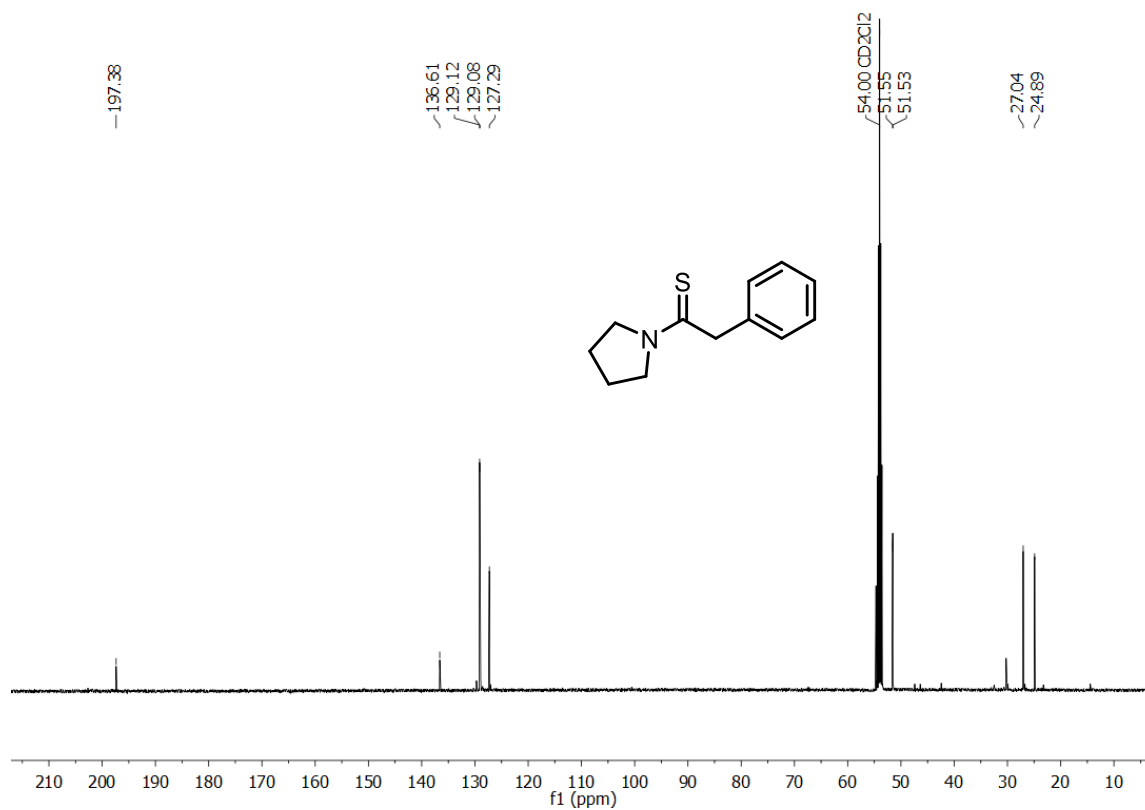
**$^{13}\text{C}$  NMR of compound 161a, 2-cyclohexylidene-2-phenyl-1-(pyrrolidin-1-yl)ethane-1-thione, 126 MHz,  $\text{CD}_2\text{Cl}_2$ , 300 K**



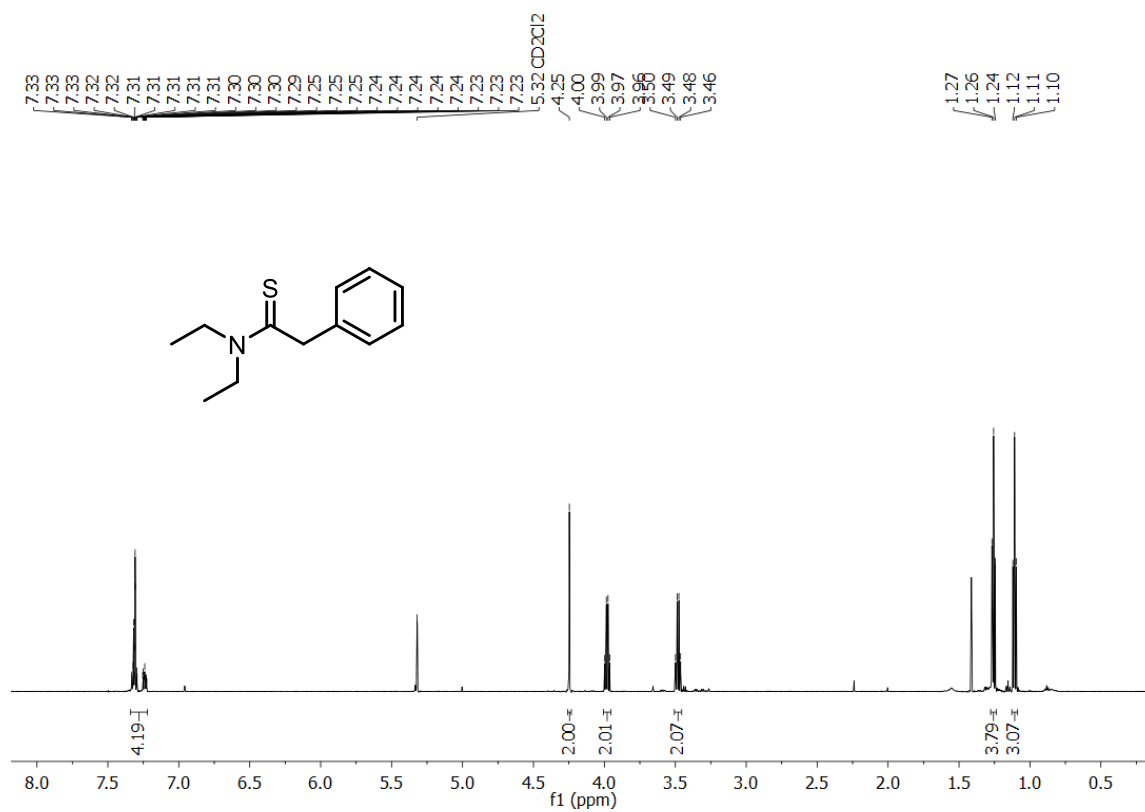
**$^1\text{H}$  NMR of compound 161b, 2-phenyl-1-(pyrrolidin-1-yl)ethane-1-thione, 400 MHz,  $\text{CD}_2\text{Cl}_2$ , 298 K**



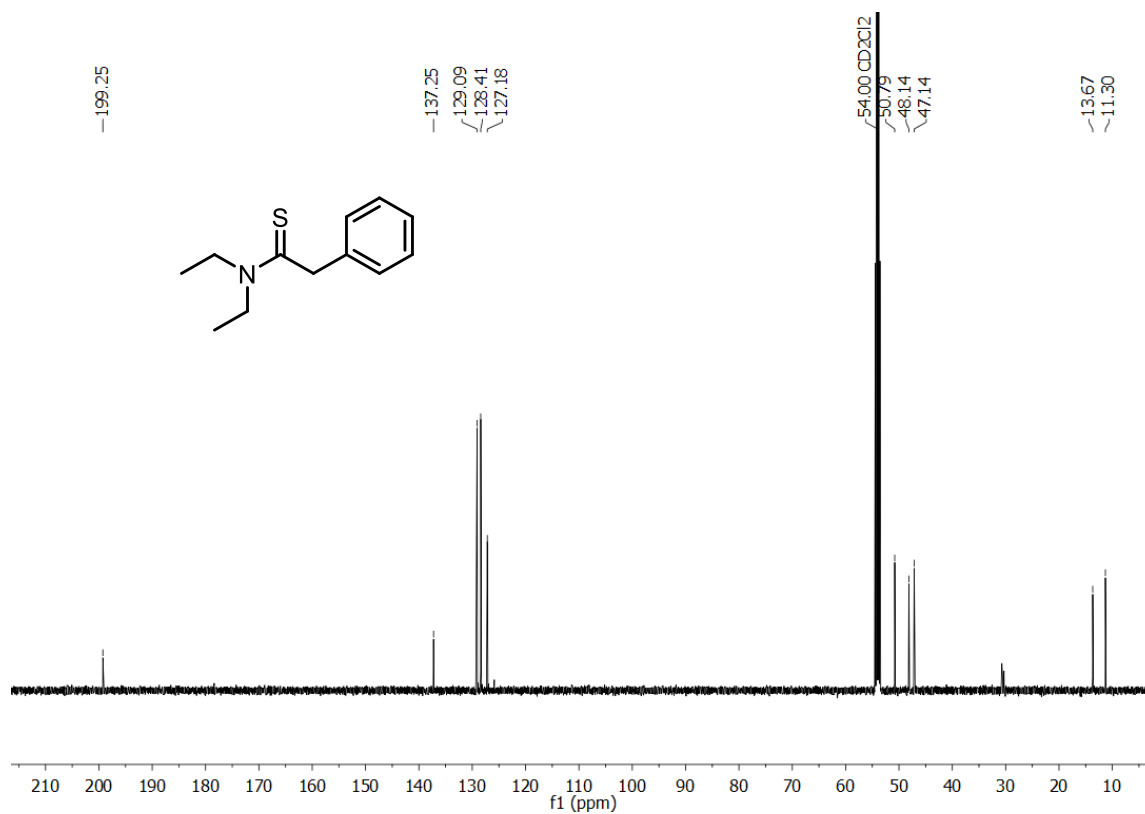
**$^{13}\text{C}$  NMR of compound 161b, 2-phenyl-1-(pyrrolidin-1-yl)ethane-1-thione, 126 MHz,  $\text{CD}_2\text{Cl}_2$ , 298 K**



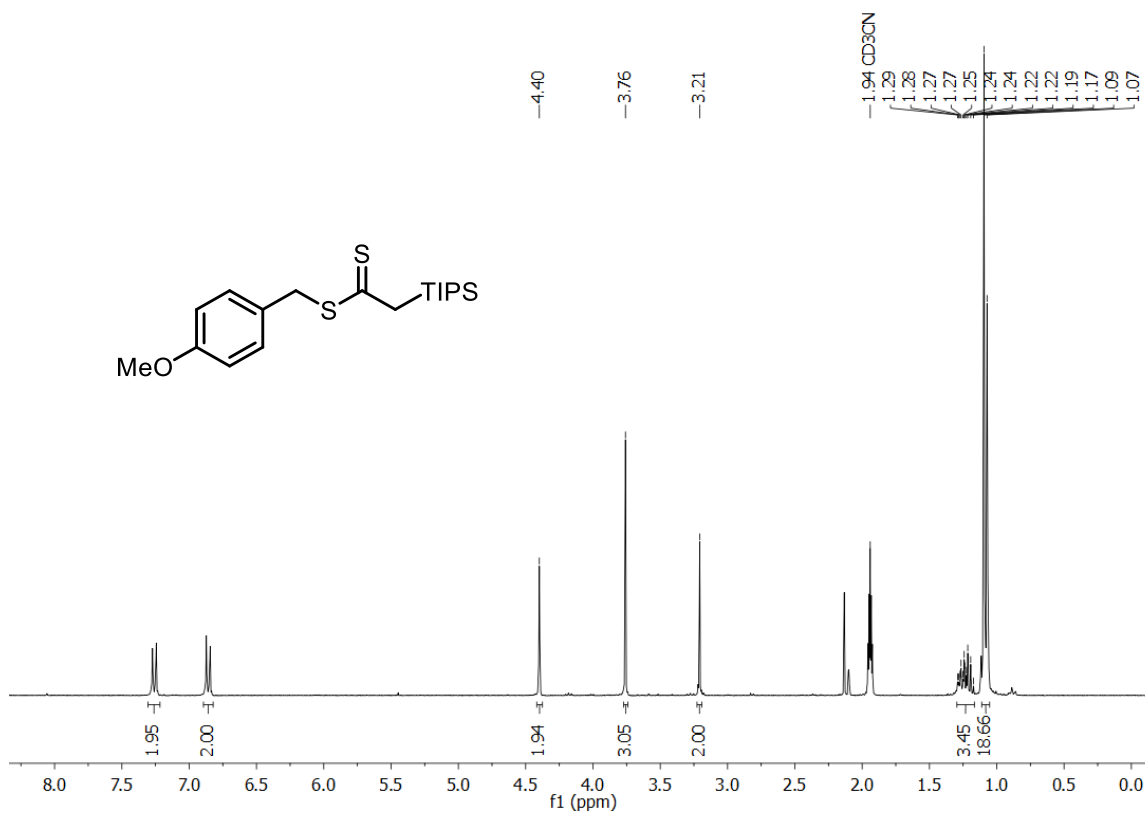
**$^1\text{H}$  NMR of compound 161c, *N,N*-diethyl-2-phenylethanethioamide, 600 MHz,  $\text{CD}_2\text{Cl}_2$ , 298 K**



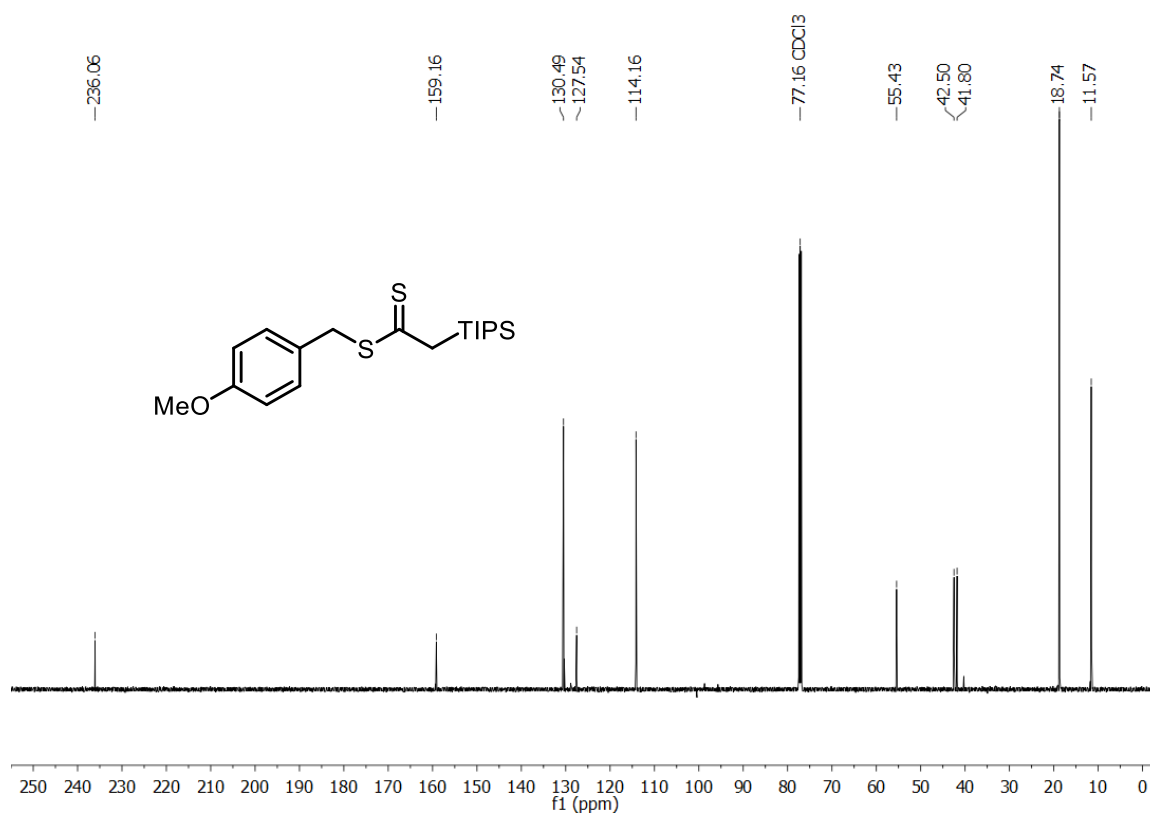
**<sup>13</sup>C NMR of compound 161c, *N,N*-diethyl-2-phenylethanethioamide, 126 MHz, CD<sub>2</sub>Cl<sub>2</sub>, 300 K**



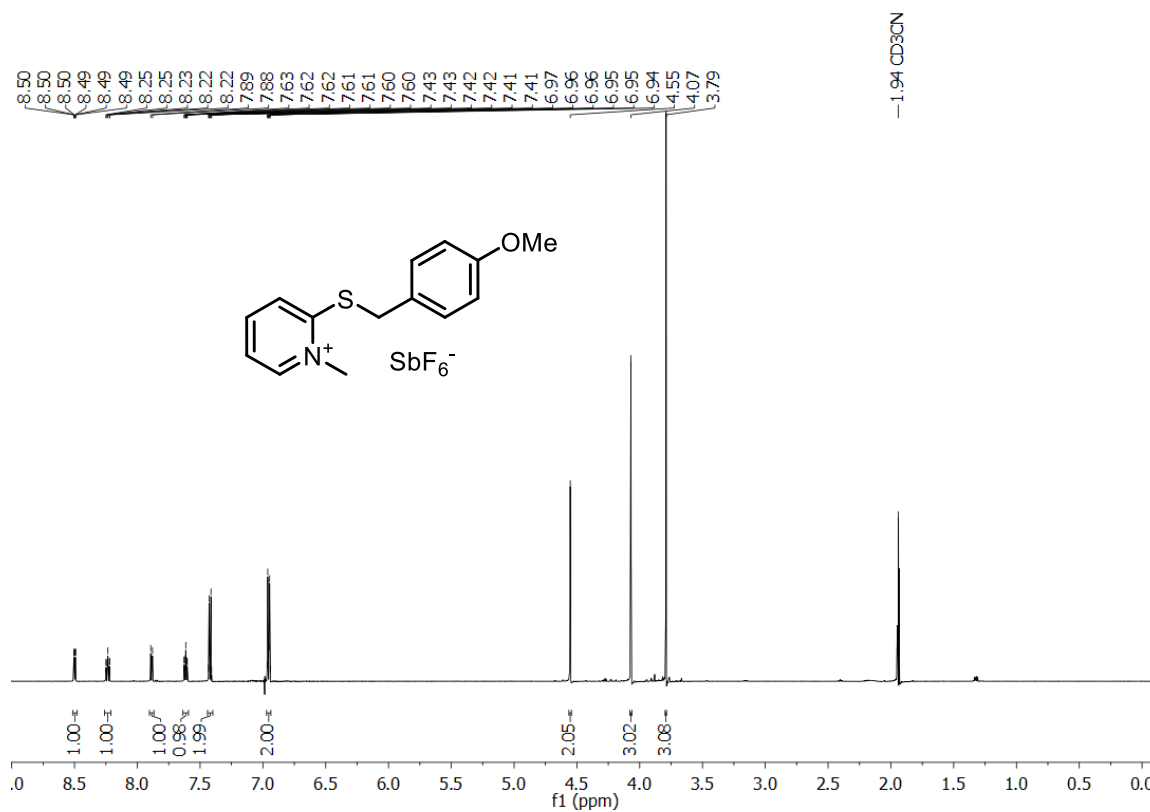
**<sup>1</sup>H NMR of compound 168a, 4-methoxybenzyl 2-(triisopropylsilyl)ethanedithioate, 300 MHz, CD<sub>3</sub>CN, 298 K**



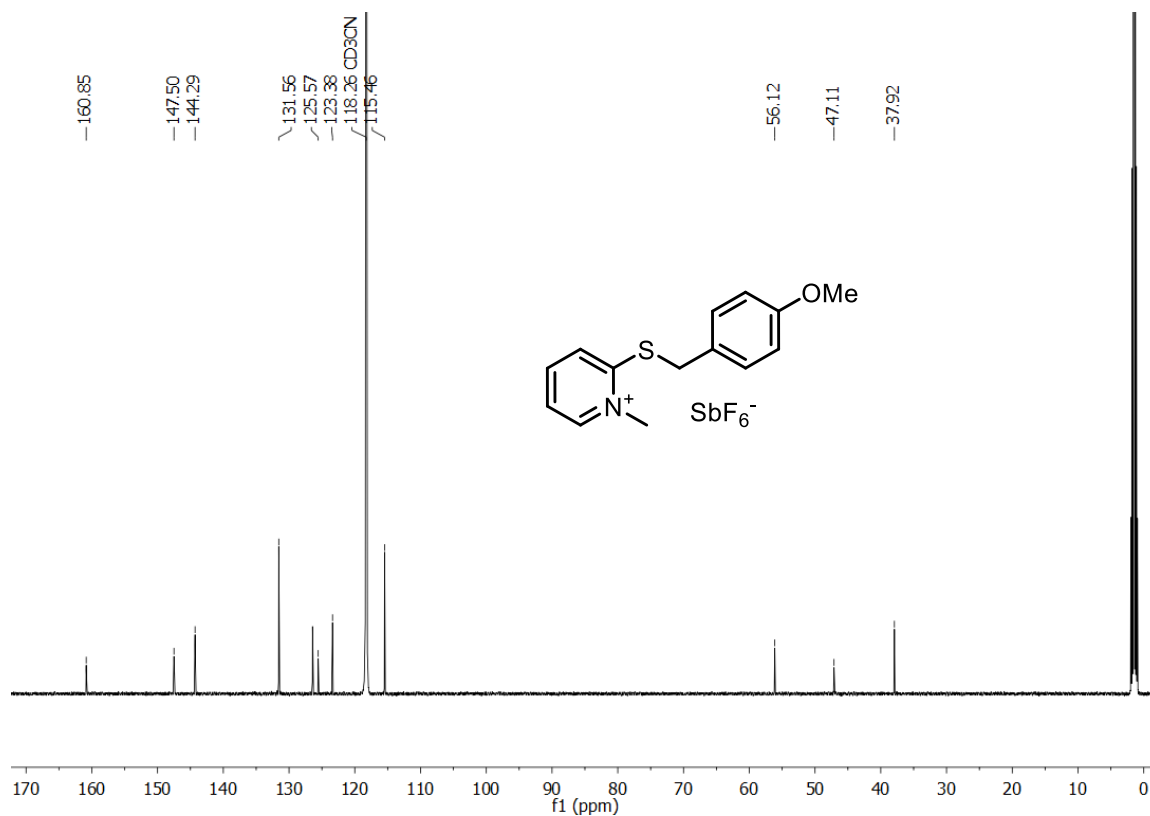
**<sup>13</sup>C NMR of compound 168a, 4-methoxybenzyl 2-(triisopropylsilyl)ethanedithioate, 126 MHz, CD<sub>3</sub>Cl, 298 K**



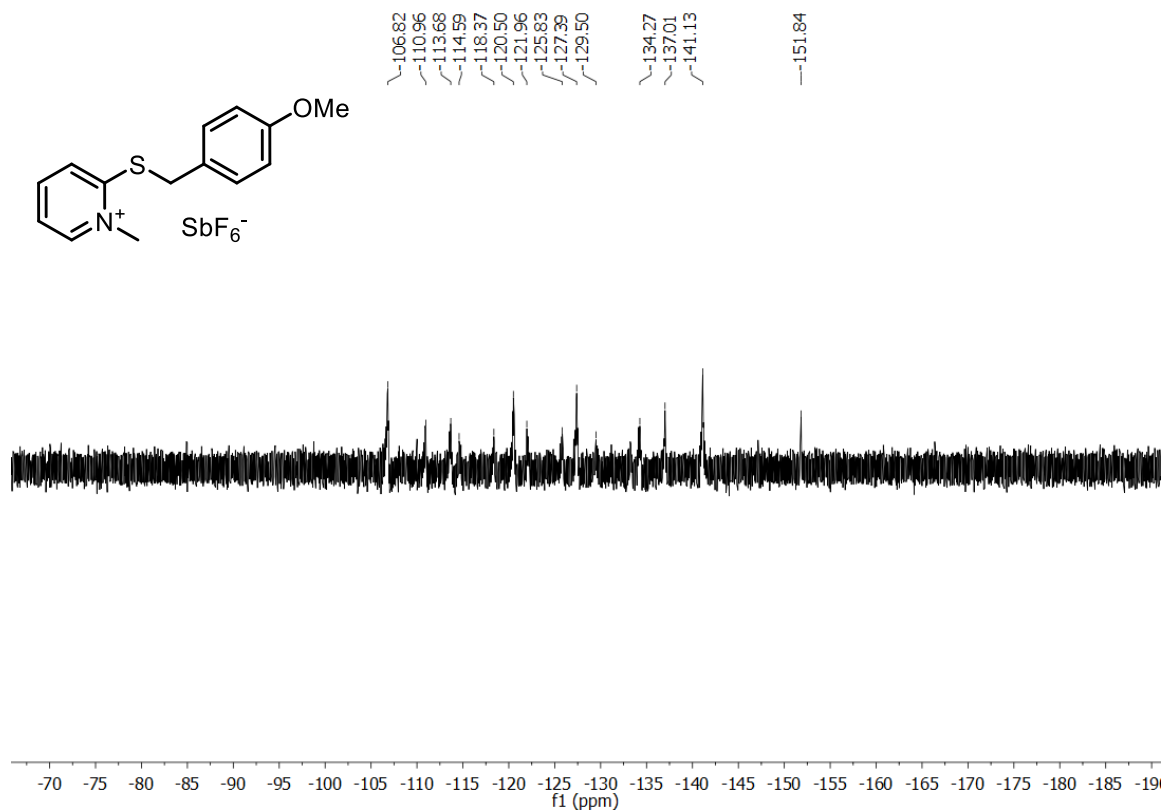
**<sup>1</sup>H NMR of compound 168b, 2-[(4-methoxybenzyl)thio]-1-methylpyridin-1-ium hexafluoroantimonate, 600 MHz, CD<sub>3</sub>CN, 298 K**



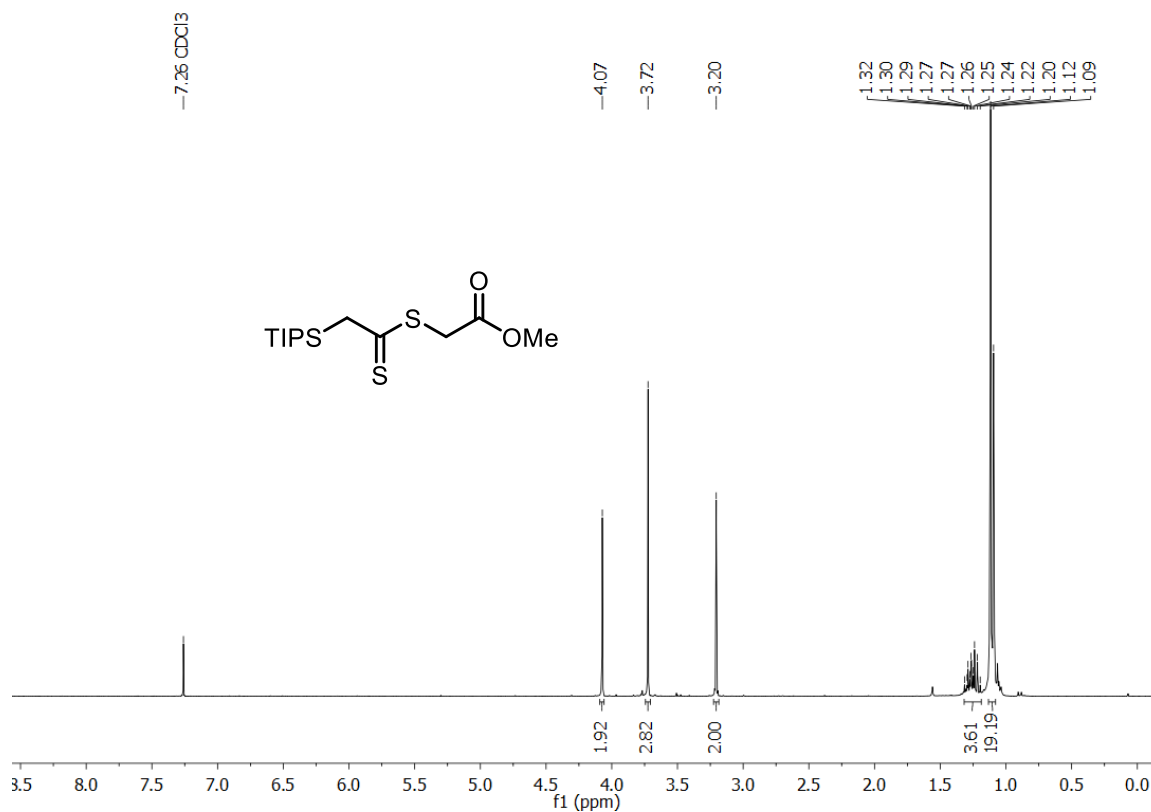
**$^{13}\text{C}$  NMR of compound 168b, 2-[(4-methoxybenzyl)thio]-1-methylpyridin-1-ium hexafluoroantimonate, 126 MHz,  $\text{CD}_3\text{CN}$ , 298 K**



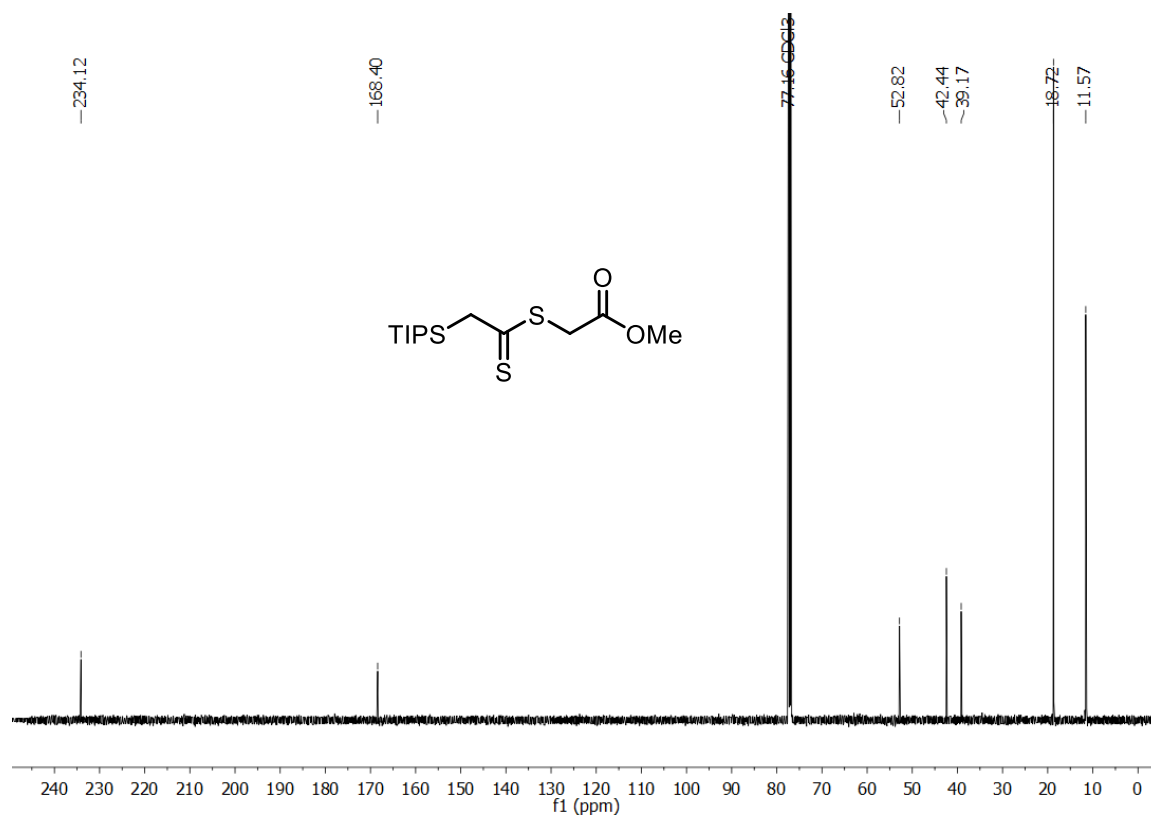
**$^{19}\text{F}$  NMR of compound 168b, 2-[(4-methoxybenzyl)thio]-1-methylpyridin-1-ium hexafluoroantimonate, 283 MHz,  $\text{CD}_3\text{CN}$ , 299 K**



**<sup>1</sup>H NMR of compound 169, methyl 2-[[2-(triisopropylsilyl)ethanethioyl]thio]acetate, 300 Mhz, CDCl<sub>3</sub>, 302 K**

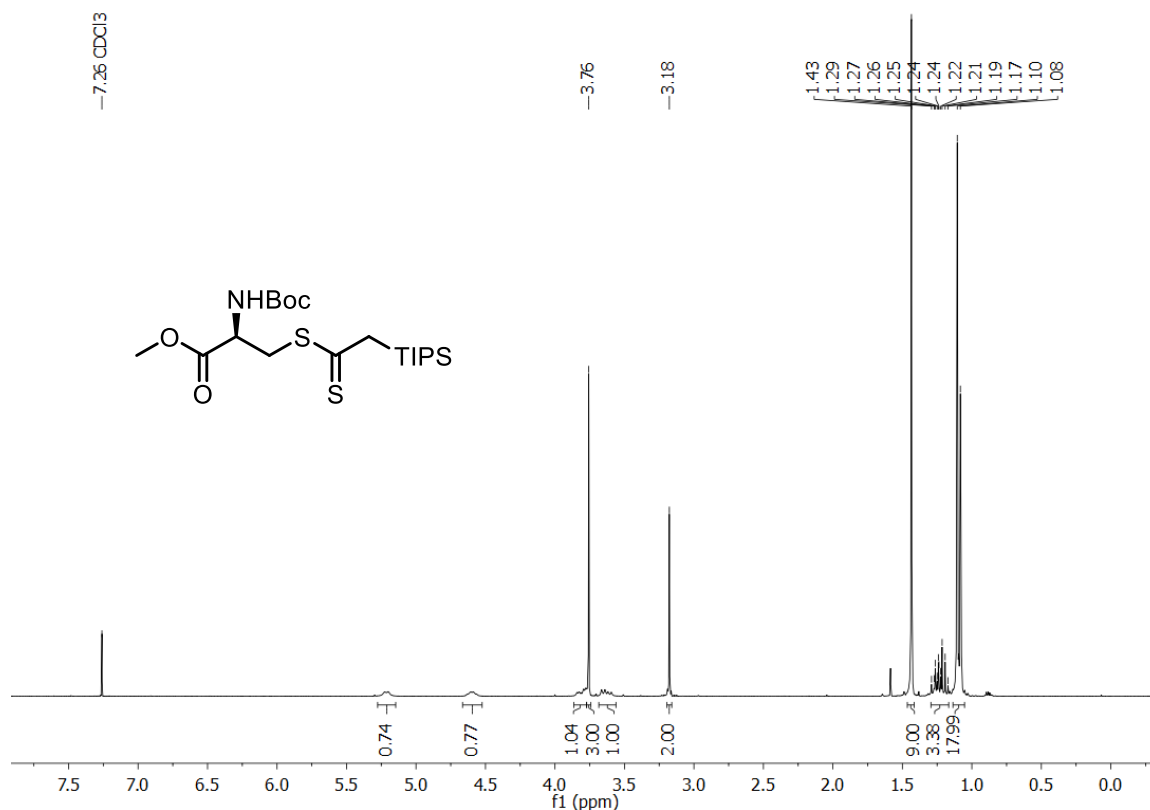


**<sup>13</sup>C NMR of compound 169, methyl 2-[[2-(triisopropylsilyl)ethanethioyl]thio]acetate, 126 Mhz, CDCl<sub>3</sub>, 302 K**

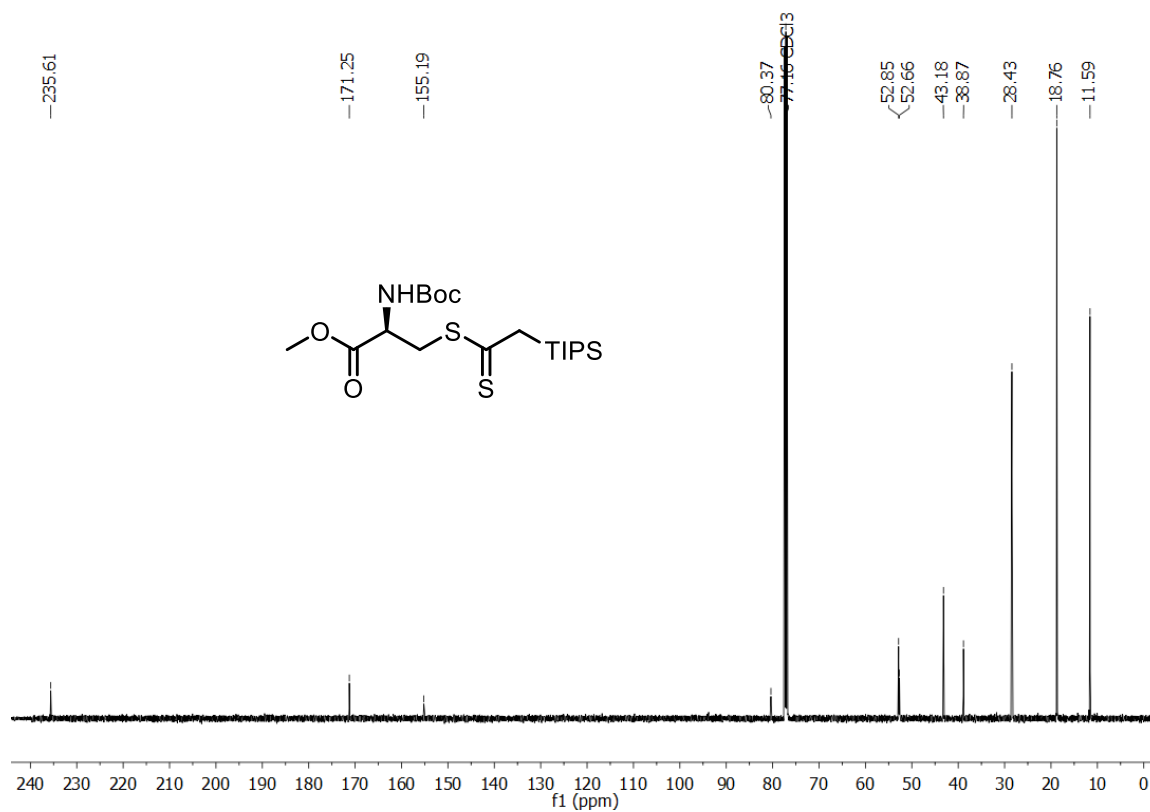




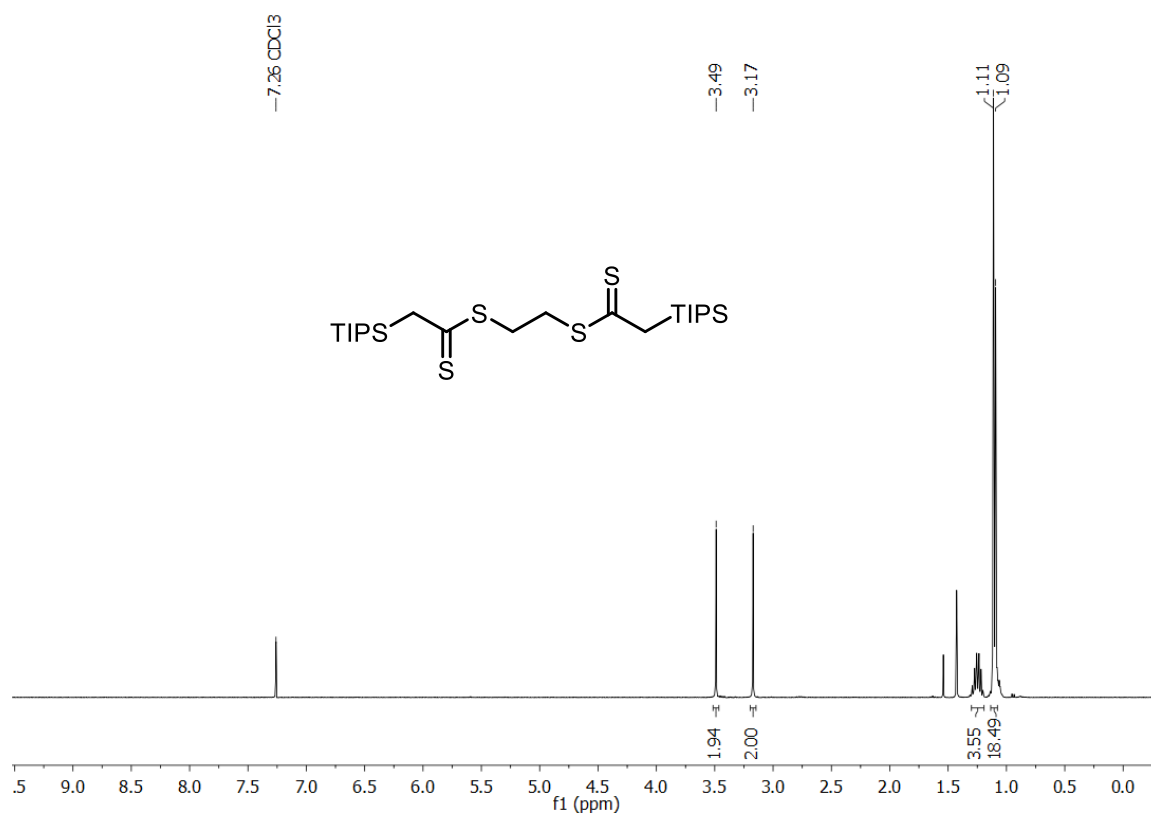
**<sup>1</sup>H NMR of compound 170, methyl *N*-(*tert*-butoxycarbonyl)-S-[2-(triisopropylsilyl)ethanethioyl]-L-cysteinate, 300 MHz, CDCl<sub>3</sub>, 302 K**



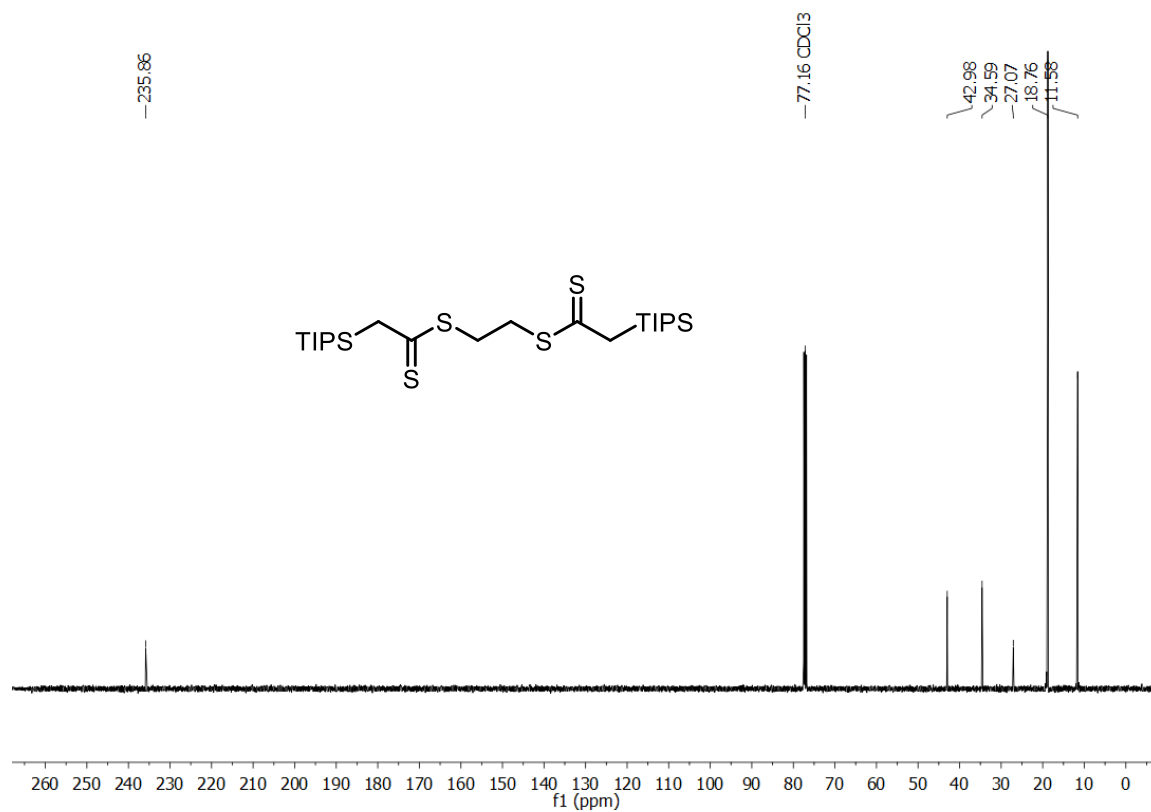
**<sup>13</sup>C NMR of compound 170, methyl *N*-(*tert*-butoxycarbonyl)-S-[2-(triisopropylsilyl)ethanethioyl]-L-cysteinate, 126 MHz, CDCl<sub>3</sub>, 298 K**



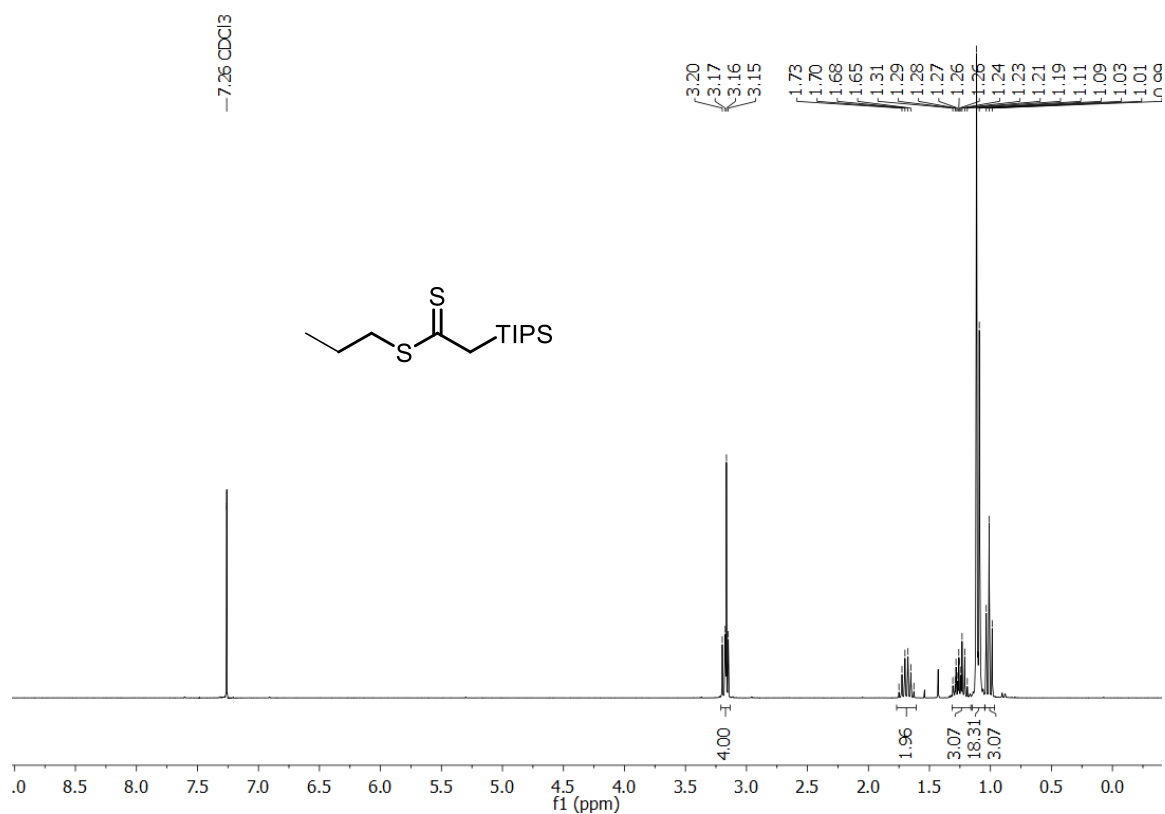
**$^1\text{H}$  NMR of compound 171, ethane-1,2-diyl bis[2-(triisopropylsilyl)ethanedithioate], 400 MHz,  $\text{CDCl}_3$ , 298 K**



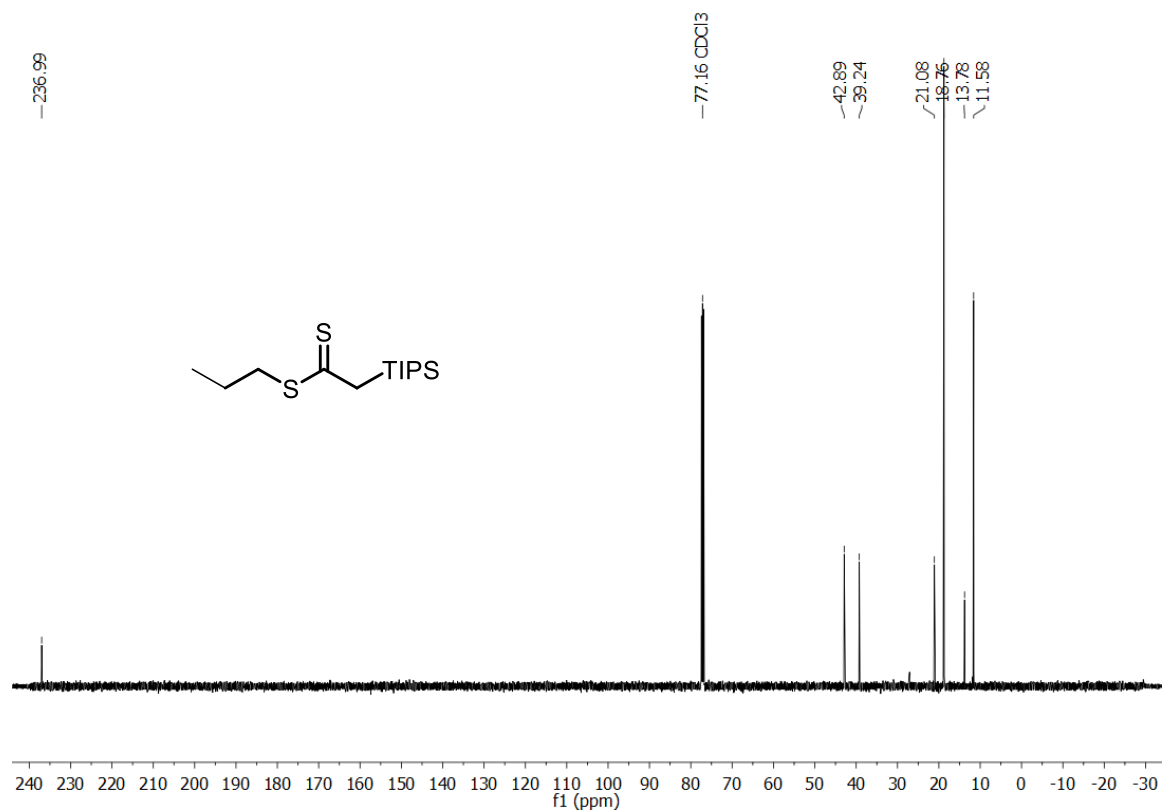
**$^{13}\text{C}$  NMR of compound 171, ethane-1,2-diyl bis[2-(triisopropylsilyl)ethanedithioate], 100 MHz,  $\text{CDCl}_3$ , 298 K**



**$^1\text{H}$  NMR of compound 172, propyl 2-(triisopropylsilyl)ethanedithioate, 300 MHz,  $\text{CDCl}_3$ , 302 K**



**$^{13}\text{C}$  NMR of compound 172, propyl 2-(triisopropylsilyl)ethanedithioate, 126 MHz,  $\text{CDCl}_3$ , 298 K**



Chemical structure of compound 10: COc1ccc(SCC(=S)C[Si](C)(C)C)cc1

<sup>1</sup>H NMR spectrum (CDCl<sub>3</sub>) data:

Chemical Shift (ppm)	Integration
7.25 (d, 2H)	2.17
3.85 (s, 3H)	3.00
0.1 (s, 9H)	18.61

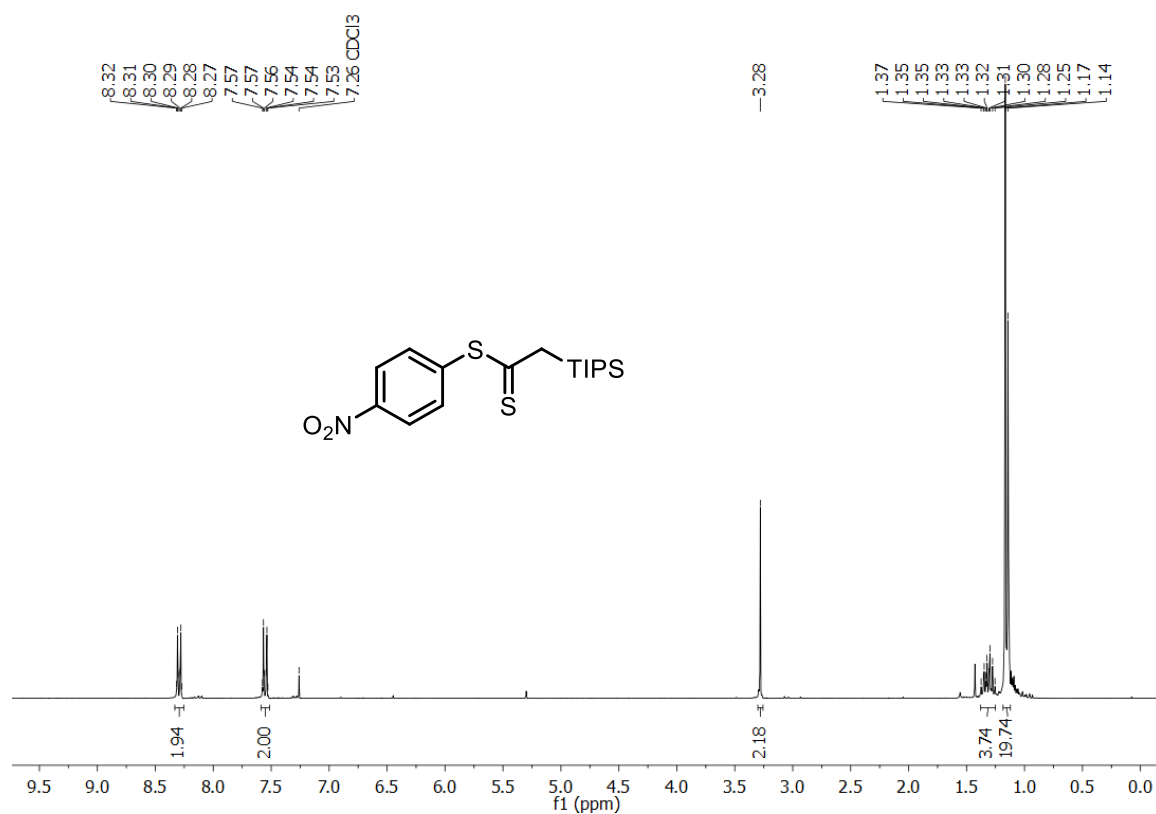
Chemical structure of the compound is shown above the spectrum:

COc1ccc(cc1)SC(=S)C[Si](C)(C)C(C)(C)C(C)(C)C

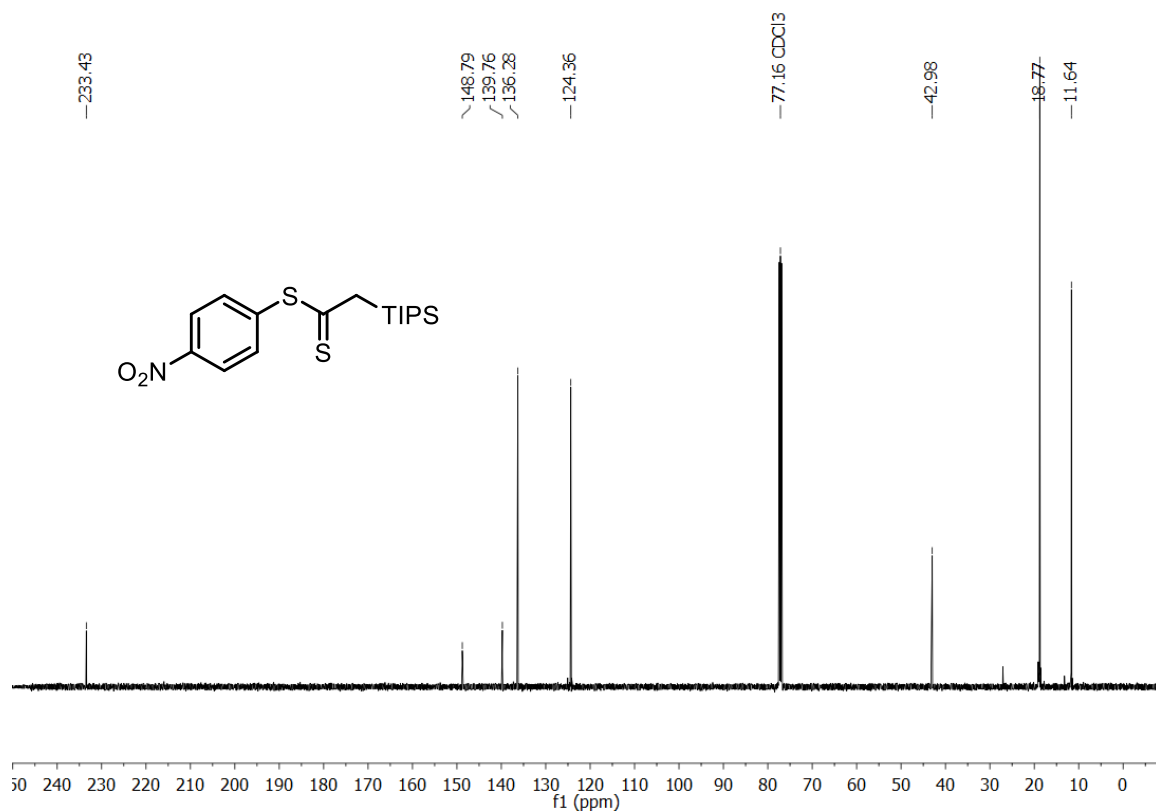
<sup>13</sup>C NMR spectrum (CDCl<sub>3</sub>) showing peaks at the following chemical shifts (ppm):

Chemical Shift (ppm)
237.87
161.20
136.74
123.48
115.13
77.16 (CDCl <sub>3</sub> )
55.47
41.92
18.81
11.64

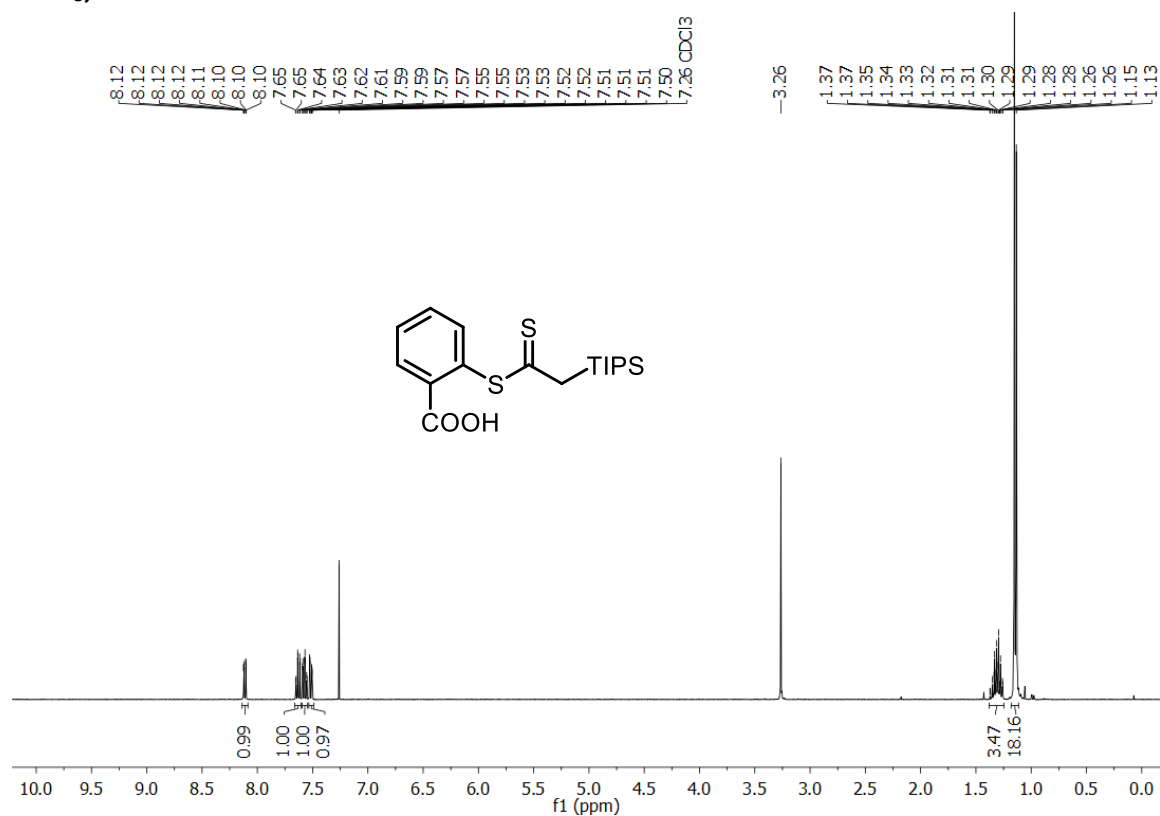
**<sup>1</sup>H NMR of compound 174, 4-nitrophenyl 2-(triisopropylsilyl)ethanedithioate, 300 MHz, CDCl<sub>3</sub>, 302 K**



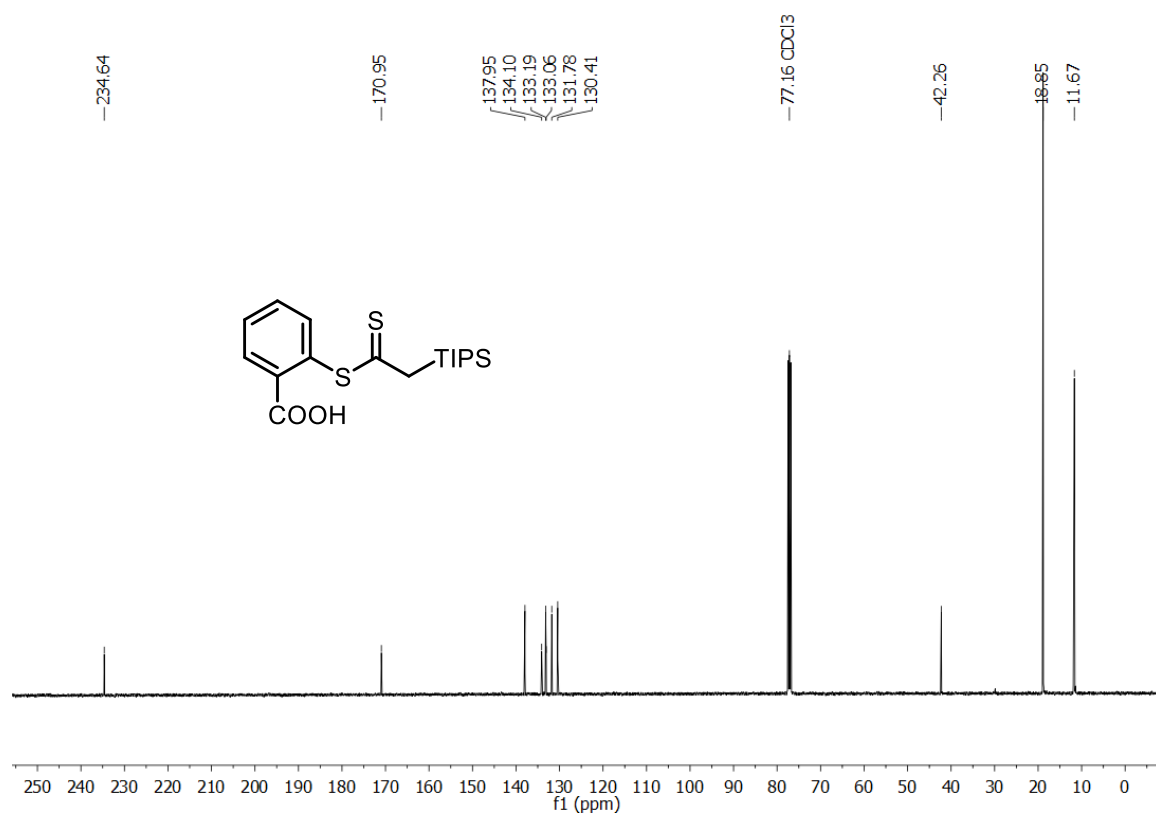
**<sup>13</sup>C NMR of compound 174, 4-nitrophenyl 2-(triisopropylsilyl)ethanedithioate, 126 MHz, CDCl<sub>3</sub>, 298 K**



**$^1\text{H}$  NMR of compound 175, 2-[[2-(triisopropylsilyl)ethanethioyl]thio]benzoic acid, 400 MHz,  $\text{CDCl}_3$ , 298 K**



**$^{13}\text{C}$  NMR of compound 175, 2-[[2-(triisopropylsilyl)ethanethioyl]thio]benzoic acid, 100 MHz,  $\text{CDCl}_3$ , 298 K**



Chemical structure: CC=C(Si(C)C)CC

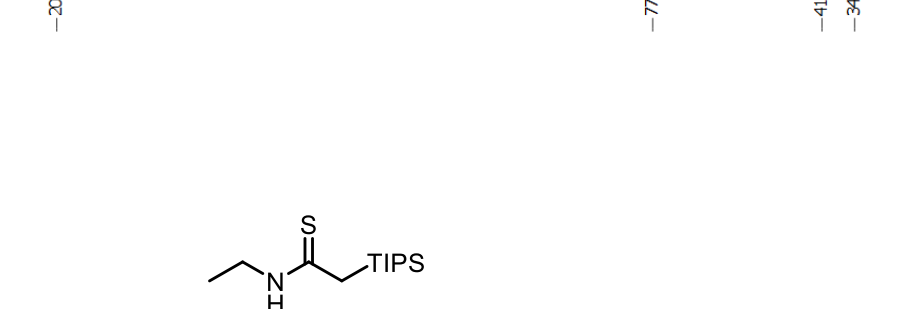
<sup>1</sup>H NMR spectrum (CDCl<sub>3</sub>) data:

Chemical Shift (ppm)	Integration
7.26	0.88
6.86	2.00
3.61-3.70	2.00
2.53	6.31
1.08-1.28	18.20

Chemical structure: CCNC(=S)C[Si](C)(C)C(C)(C)C

<sup>13</sup>C NMR spectrum (CDCl<sub>3</sub>) showing peaks at:

- 204.07
- 77.16 (CDCl<sub>3</sub>)
- 41.12
- 34.17
- 18.78
- 13.52
- 11.45



Chemical structure: CCNC(=S)C[Si](C)(C)C(C)(C)C

<sup>13</sup>C NMR spectrum (CDCl<sub>3</sub>) showing peaks at:

- 204.07
- 77.16 (CDCl<sub>3</sub>)
- 41.12
- 34.17
- 18.78
- 13.52
- 11.45

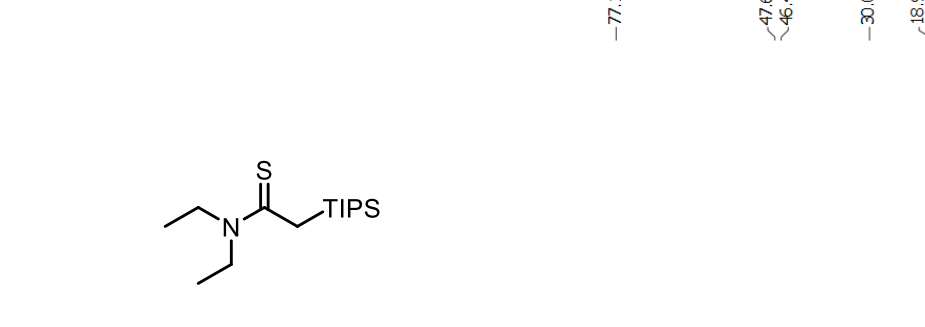
Chemical structure: CCN(CC)C(S)CC[Si](C)(C)C

<sup>1</sup>H NMR spectrum (CDCl<sub>3</sub>) showing peaks at 7.26 ppm (solvent), 4.05-4.00 ppm (N-CH<sub>2</sub>, 2H), 3.58-3.55 ppm (N-CH<sub>2</sub>, 2H), 2.69 ppm (CH<sub>3</sub>, 3H), and 1.33-1.09 ppm (TIPS, 9H). Integration values are 2.00, 2.00, 1.96, 9.18, and 18.14.

Chemical structure: CCN(CC)C(=S)C[Si](C)(C)C(C)(C)C (diethylthioacetamide derivative with a TIPS group).

<sup>13</sup>C NMR spectrum (CDCl<sub>3</sub>) showing peaks at:

- 201.80 ppm (C=O)
- 77.16 ppm (CDCl<sub>3</sub> solvent)
- 47.65 ppm (CH<sub>2</sub> of TIPS)
- 46.49 ppm (CH<sub>2</sub> of TIPS)
- 30.07 ppm (CH<sub>2</sub> of TIPS)
- 18.91 ppm (CH<sub>3</sub> of TIPS)
- 13.15 ppm (CH<sub>3</sub> of TIPS)
- 11.82 ppm (CH<sub>3</sub> of TIPS)
- 11.50 ppm (CH<sub>3</sub> of TIPS)



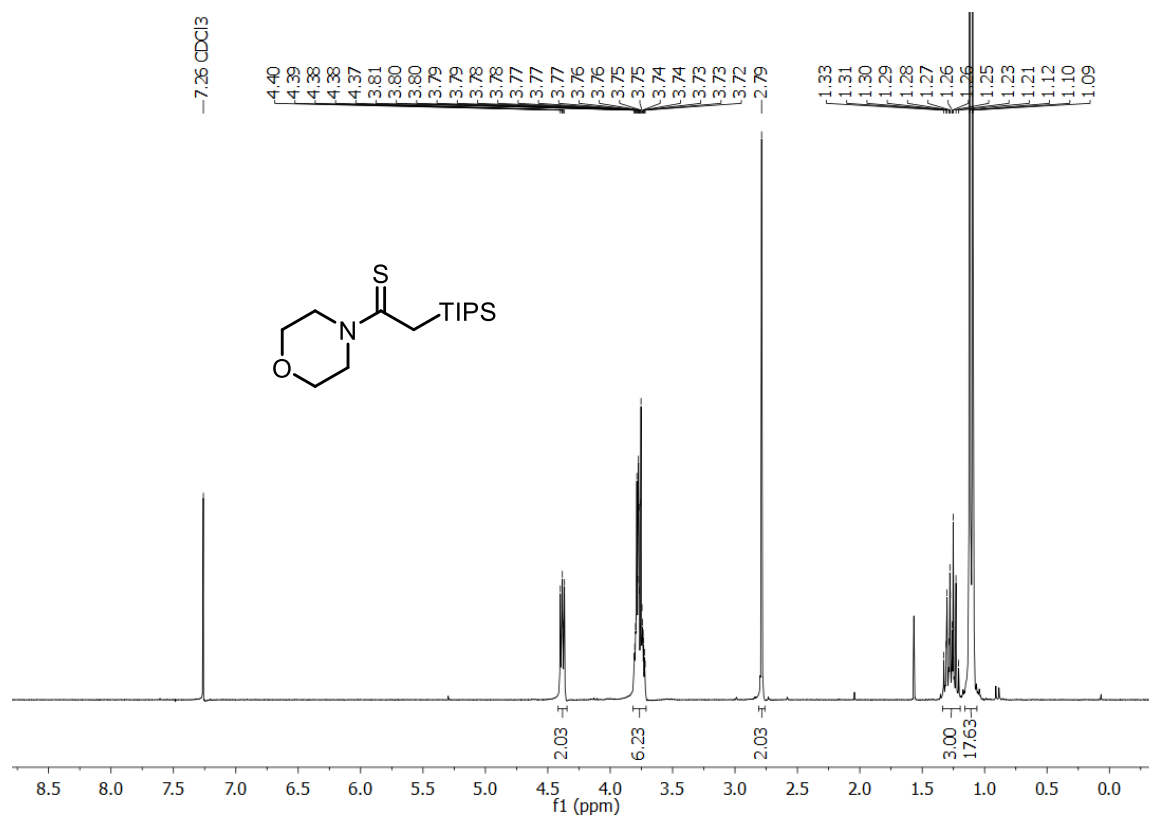
Chemical structure: CCN(CC)C(=S)C[Si](C)(C)C(C)(C)C

<sup>13</sup>C NMR spectrum (CDCl<sub>3</sub>) showing peaks at:

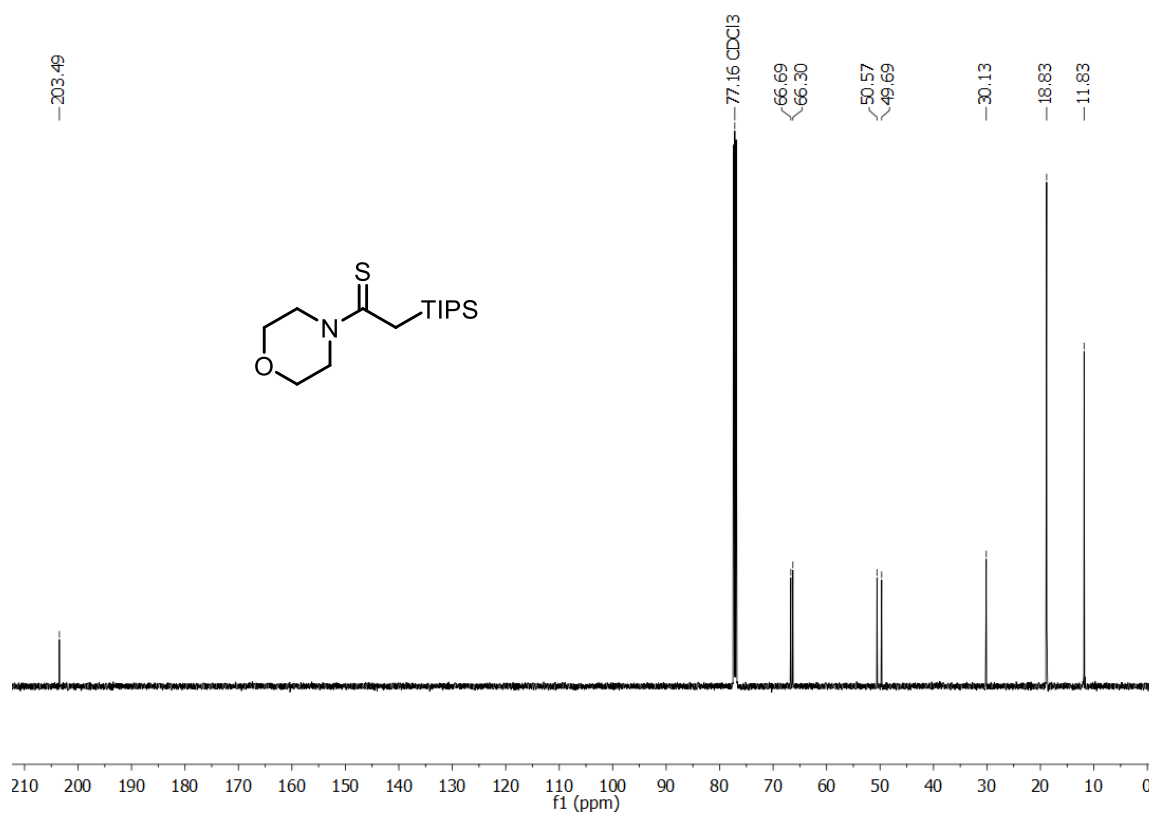
- 201.80
- 77.16 (CDCl<sub>3</sub>)
- 47.65
- 46.49
- 30.07
- 18.91
- 13.15
- 11.82
- 11.50



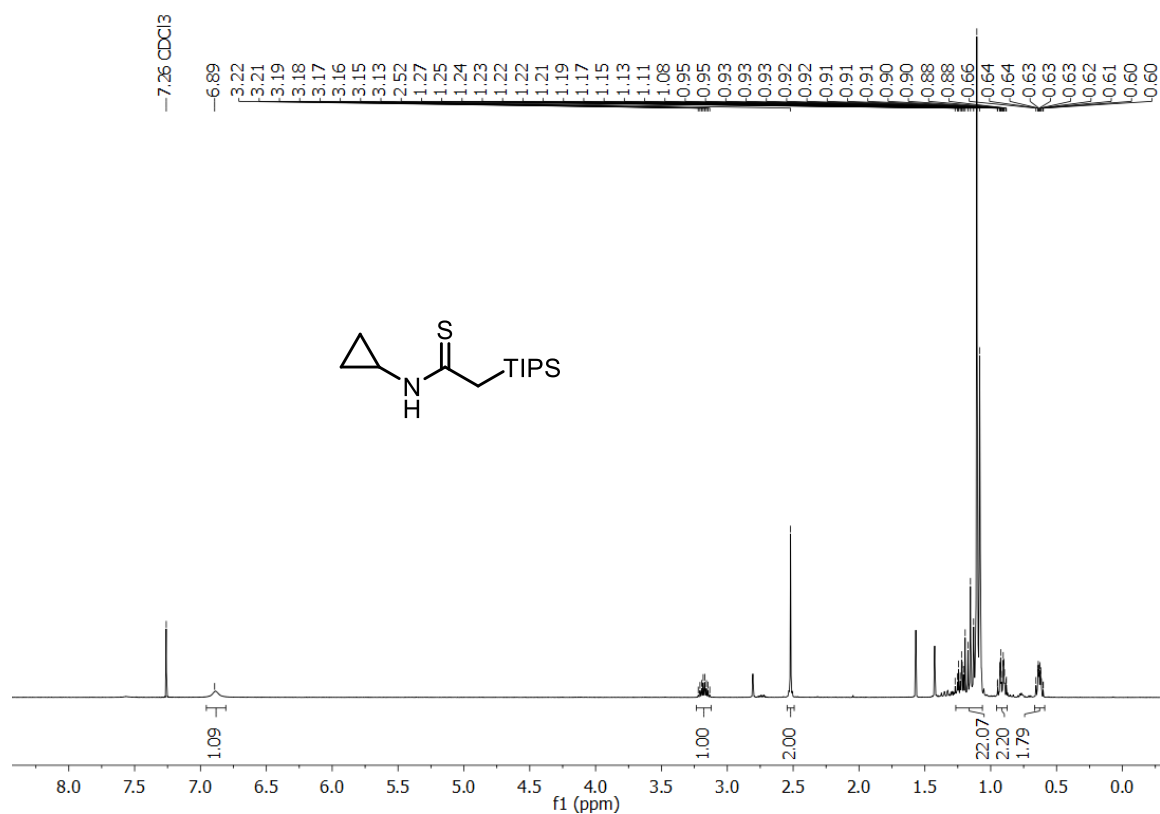
**$^1\text{H}$  NMR of compound 178, 1-morpholino-2-(triisopropylsilyl)ethane-1-thione, 300 MHz,  $\text{CDCl}_3$ , 302 K**



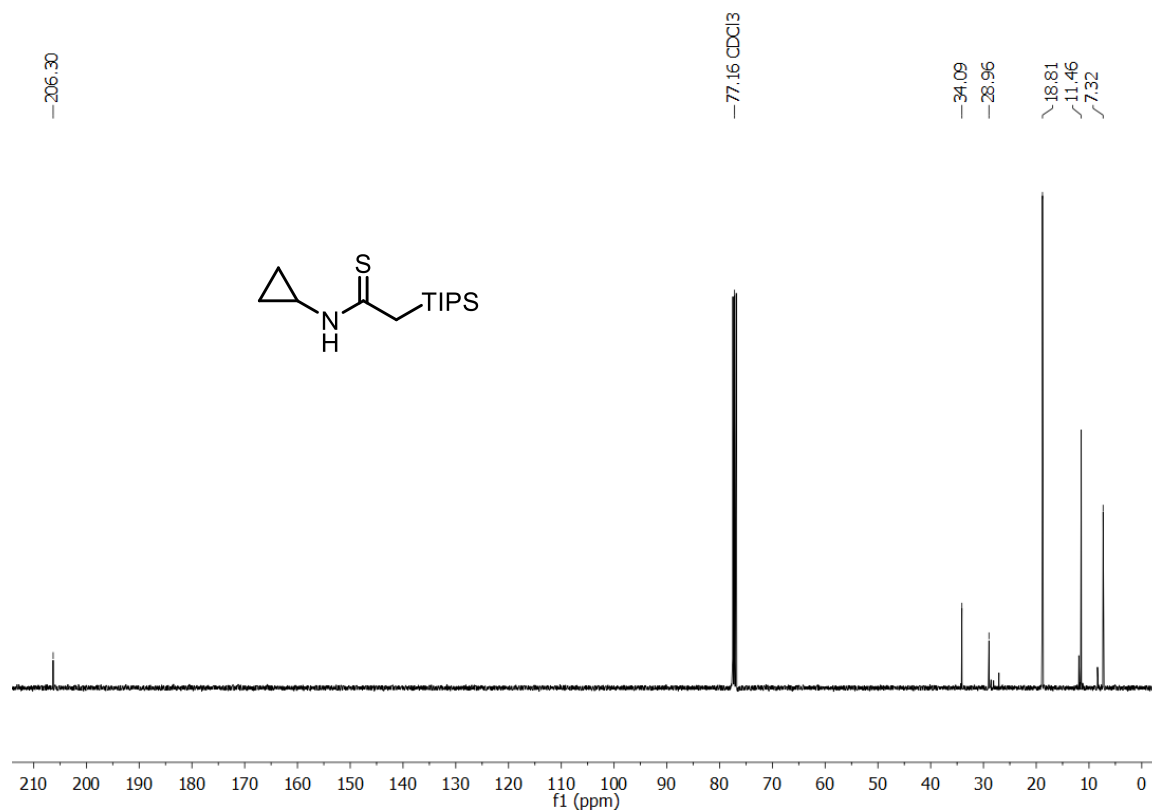
**$^{13}\text{C}$  NMR of compound 178, 1-morpholino-2-(triisopropylsilyl)ethane-1-thione, 126 MHz,  $\text{CDCl}_3$ , 298 K**



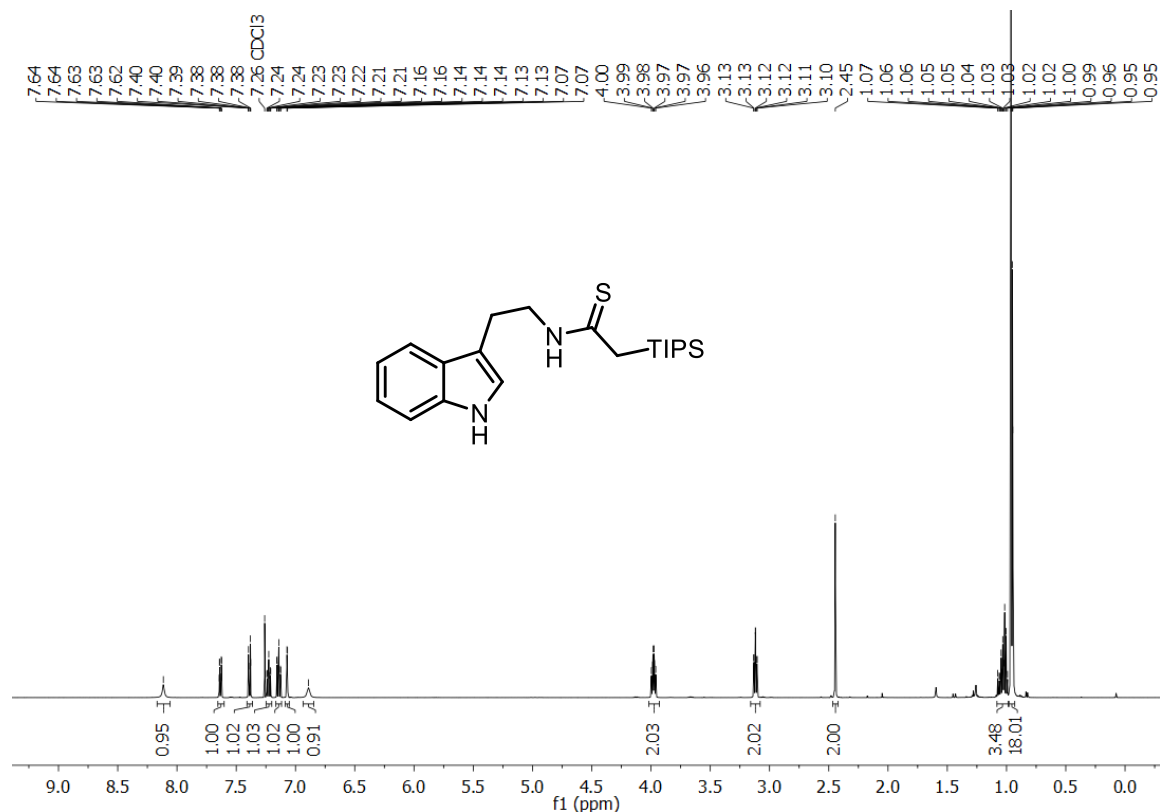
**<sup>1</sup>H NMR of compound 179, *N*-cyclopropyl-2-(triisopropylsilyl)ethanethioamide, 300 MHz, CDCl<sub>3</sub>, 302 K**



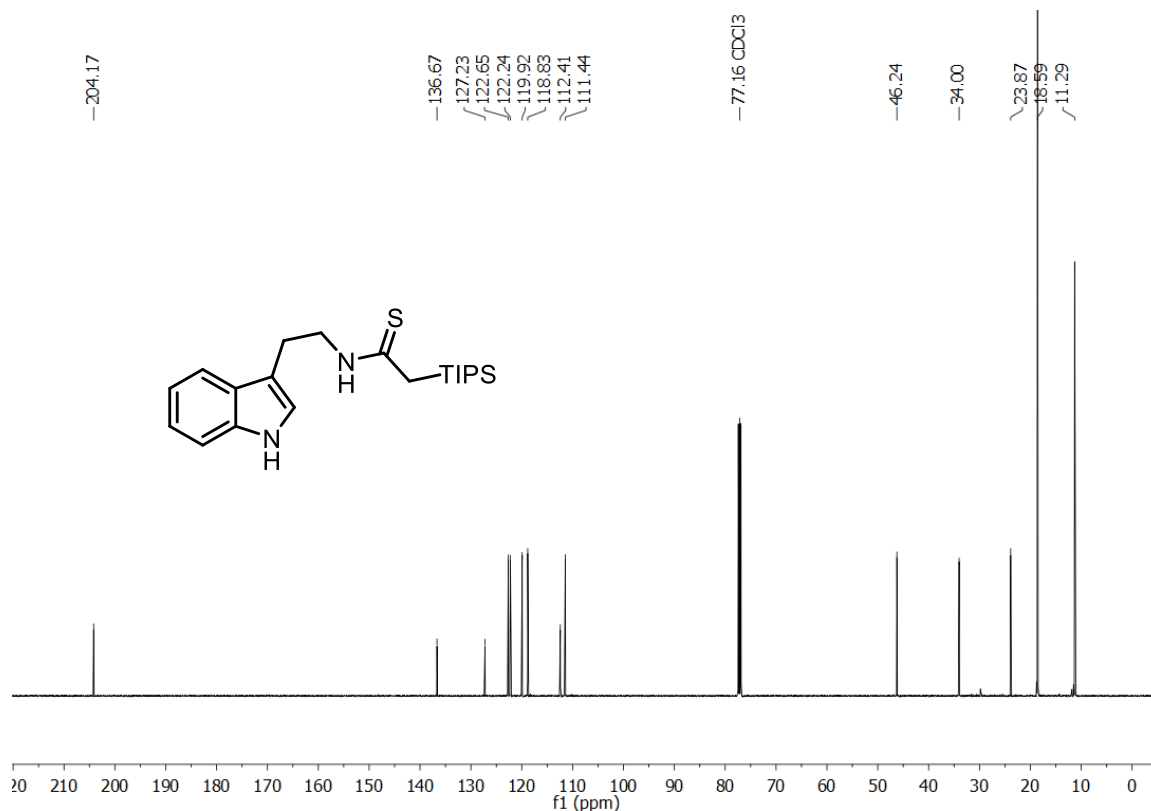
**<sup>13</sup>C NMR of compound 179, *N*-cyclopropyl-2-(triisopropylsilyl)ethanethioamide, 101 MHz, CDCl<sub>3</sub>; 298 K**



**<sup>1</sup>H NMR of compound 180, *N*-[2-(1*H*-indol-3-yl)ethyl]-2-(triisopropylsilyl)ethanethioamide, 500 MHz, CDCl<sub>3</sub>;298 K**



**<sup>13</sup>C NMR of compound 180, *N*-[2-(1*H*-indol-3-yl)ethyl]-2-(triisopropylsilyl)ethanethioamide, 126 MHz, CDCl<sub>3</sub>;298 K**



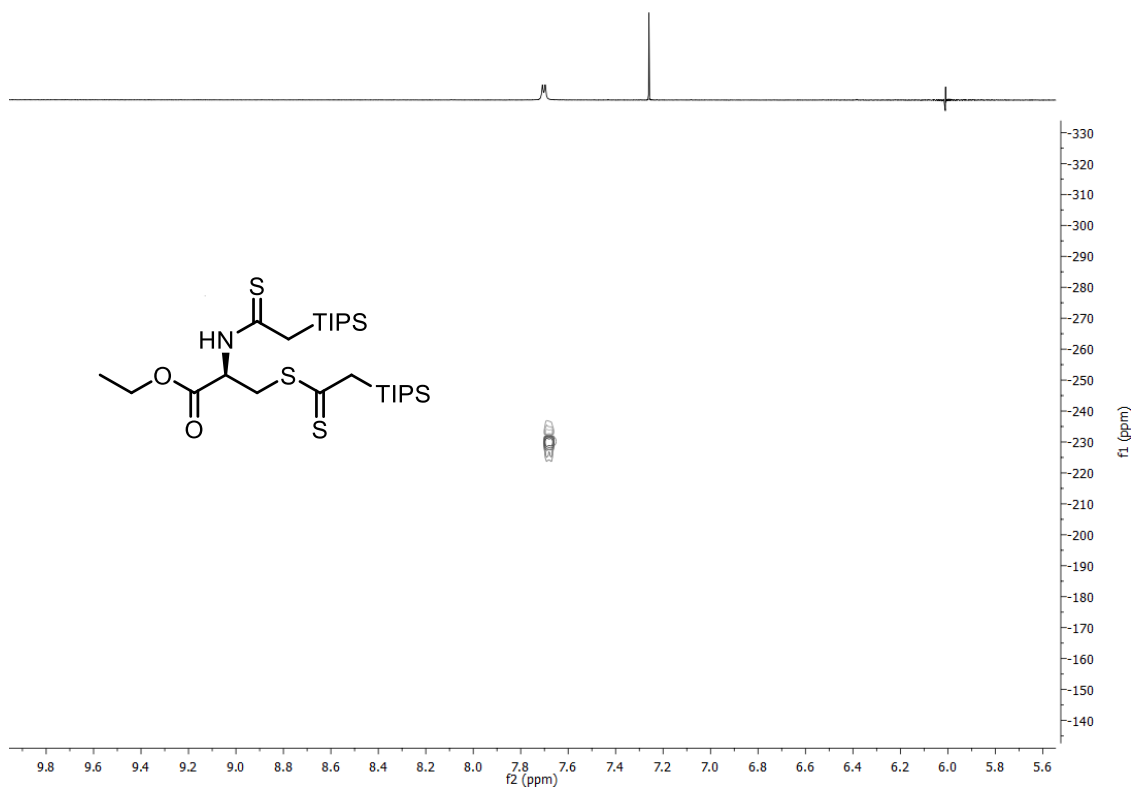
[illegible]

Chemical structure of the compound is shown above the spectrum. The structure is a thioether derivative of a thioamide, featuring a central carbon atom bonded to an ethyl ester group, a thioamide group, and a thioether group. The thioether group is substituted with a TIPS (triisopropylsilyl) group. The spectrum shows peaks corresponding to the chemical shifts of the various atoms in the molecule, with the most prominent peak at 77.46 ppm, likely representing the solvent CDCl<sub>3</sub>.

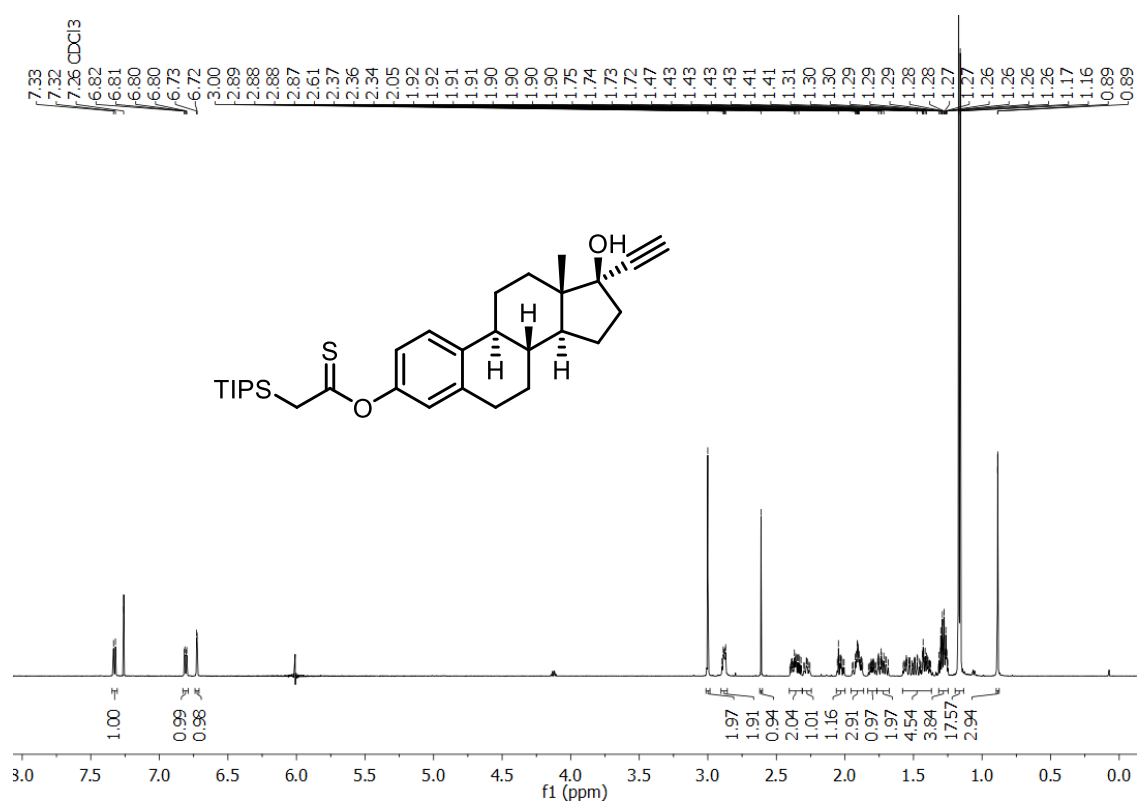
Chemical structure of the compound is shown above the spectrum. The structure is a thioether derivative of a thioamide, featuring a central carbon atom bonded to an ethyl ester group, a thioamide group, and a thioether group. The thioether group is substituted with a TIPS (triisopropylsilyl) group. The spectrum shows peaks corresponding to the chemical shifts of the various atoms in the molecule, with the most prominent peak at 77.46 ppm, likely representing the solvent CDCl<sub>3</sub>.

Chemical Shift (ppm)
236.18
205.63
169.65
77.46 (CDCl <sub>3</sub> )
62.38
57.99
43.41
37.88
34.40
18.86
18.78
14.26
11.65
11.49

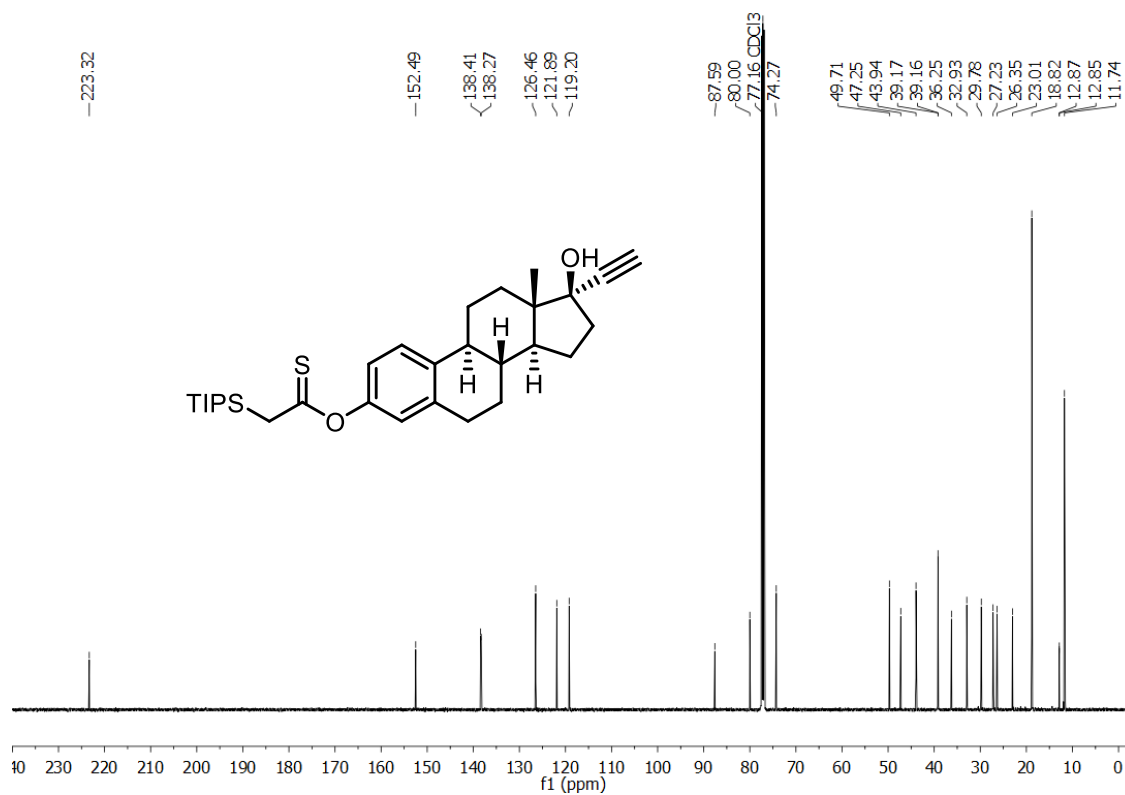
Selected region of NH-HSCQ for compound 181, methyl *N*-(*tert*-butoxycarbonyl)-*S*-[2-(triisopropylsilyl)ethanethioyl]-*L*-cysteinate, 600 MHz/126 MHz, CDCl<sub>3</sub>, 302 K



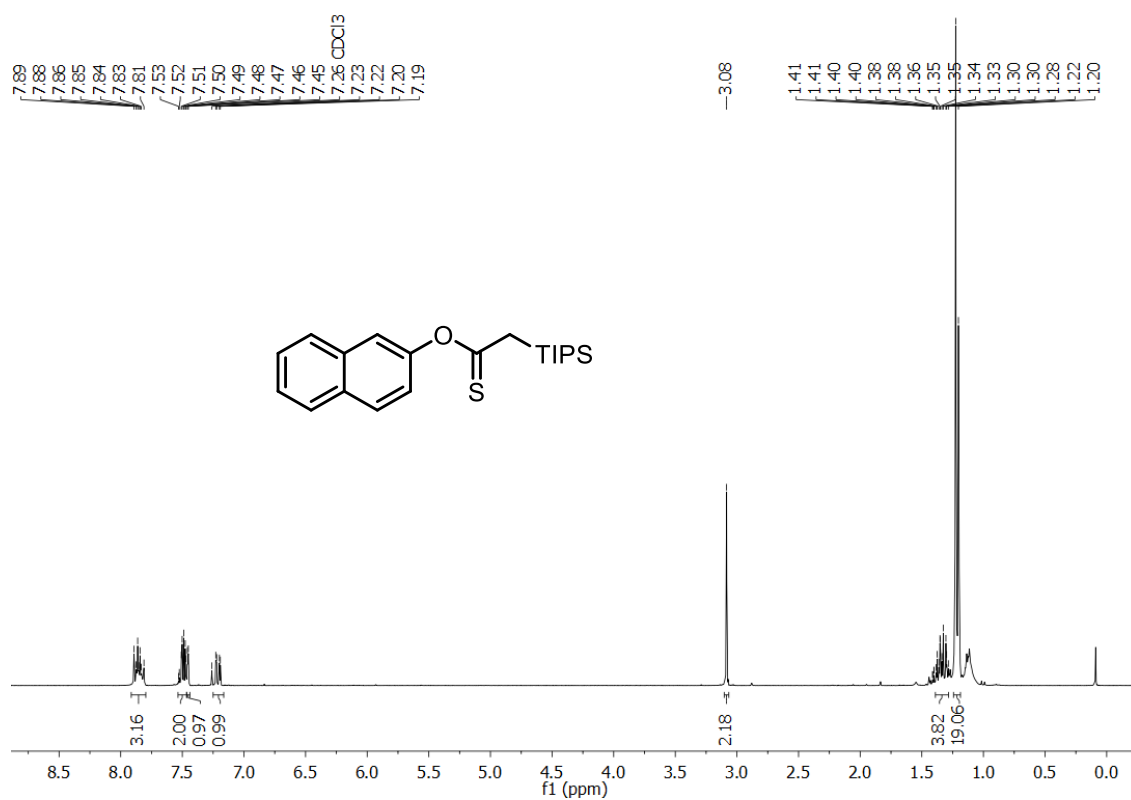
<sup>1</sup>H NMR of compound 182, *O*-[(8*R*,9*S*,13*S*,14*S*,17*R*)-17-Ethynyl-17-hydroxy-13-methyl-7,8,9,11,12,13,14,15,16,17-decahydro-6*H*-cyclopenta[*a*]phenanthren-3-yl] 2-(triisopropylsilyl)ethanethioate, 600 MHz, CD<sub>3</sub>Cl, 298 K



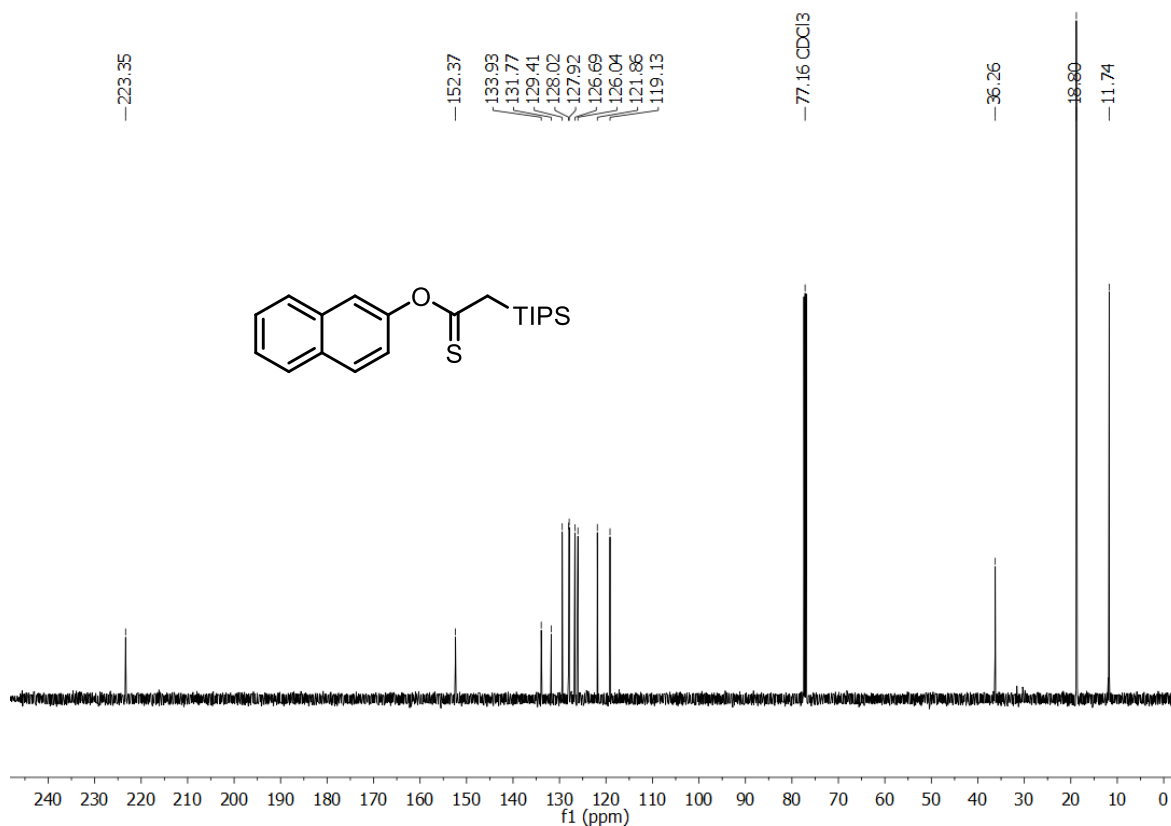
**$^{13}\text{C}$  NMR of compound 182, *O*-[(8*R*,9*S*,13*S*,14*S*,17*R*)-17-Ethynyl-17-hydroxy-13-methyl-7,8,9,11,12,13,14,15,16,17-decahydro-6*H*-cyclopenta[*a*]phenanthren-3-yl] 2-(triisopropylsilyl)ethanethioate, 126 MHz,  $\text{CD}_3\text{Cl}$ , 298 K**



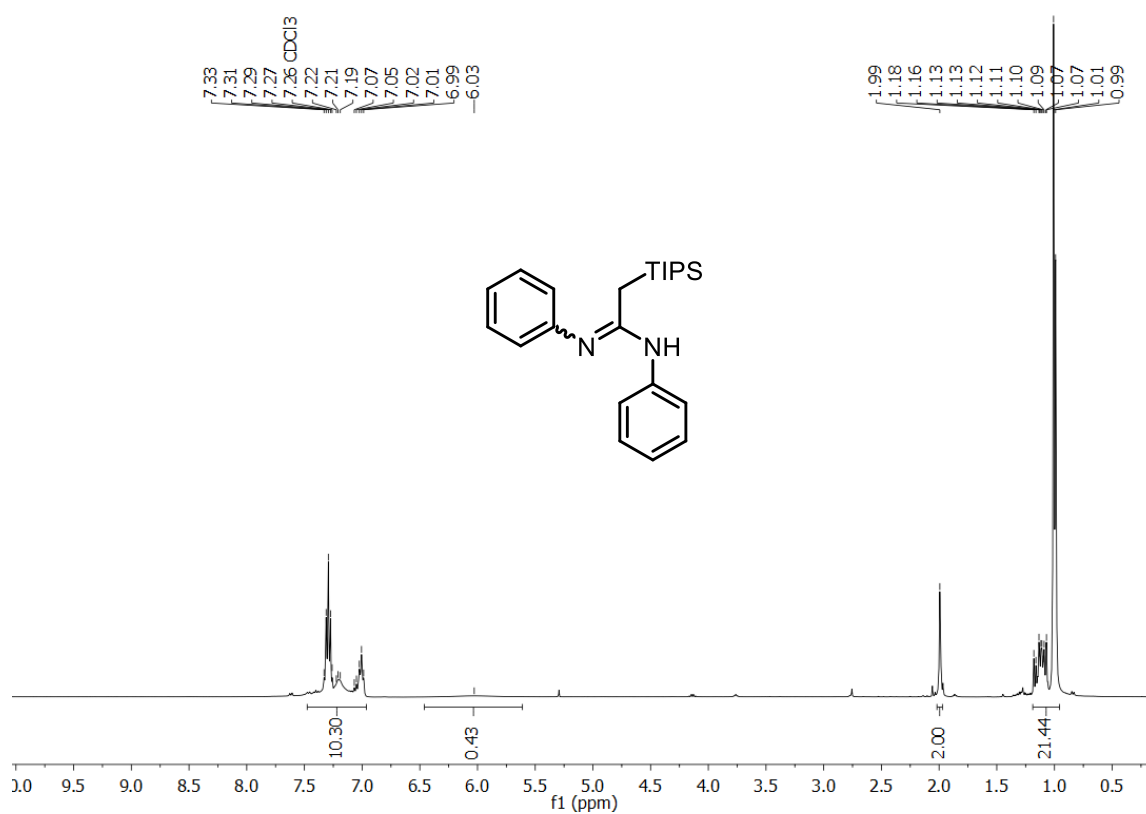
**$^1\text{H}$  NMR of compound 183, *O*-(naphthalen-2-yl) 2-(triisopropylsilyl)ethanethioate, 300 MHz,  $\text{CDCl}_3$ , 302 K**



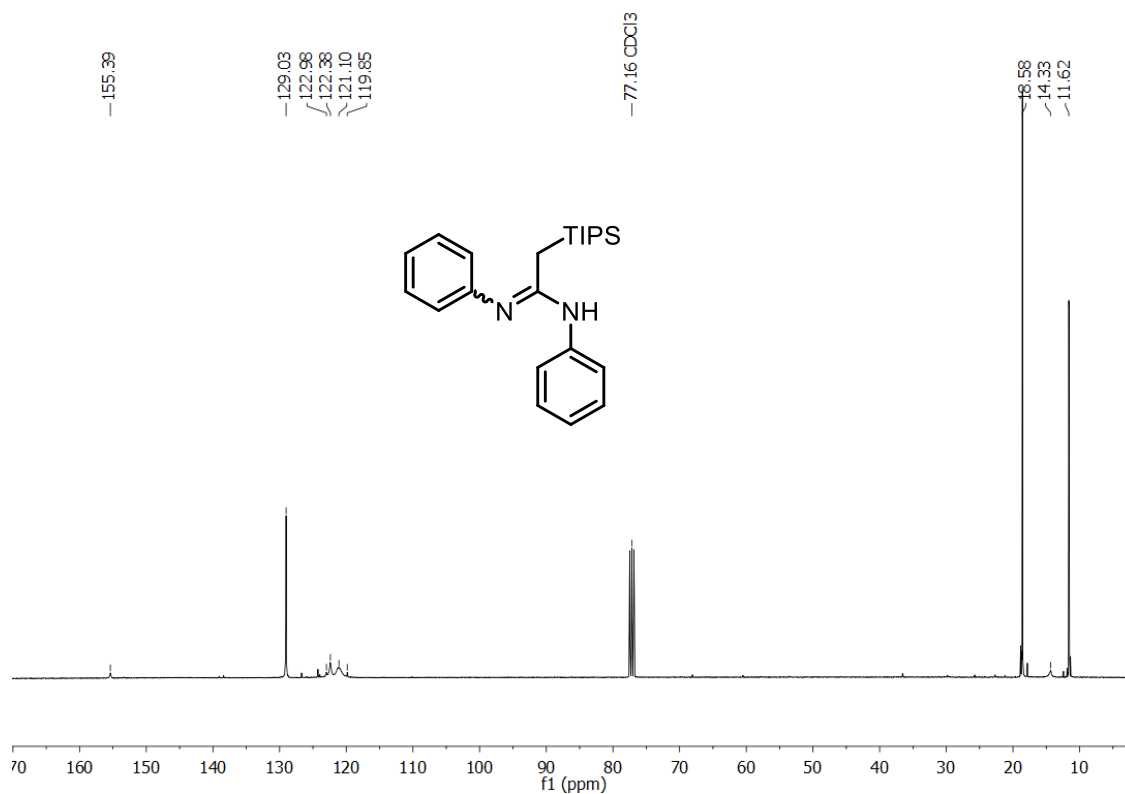
**$^{13}\text{C}$  NMR of compound 183, *O*-(naphthalen-2-yl) 2-(triisopropylsilyl)ethanethioate, 126 MHz,  $\text{CDCl}_3$ , 298 K**



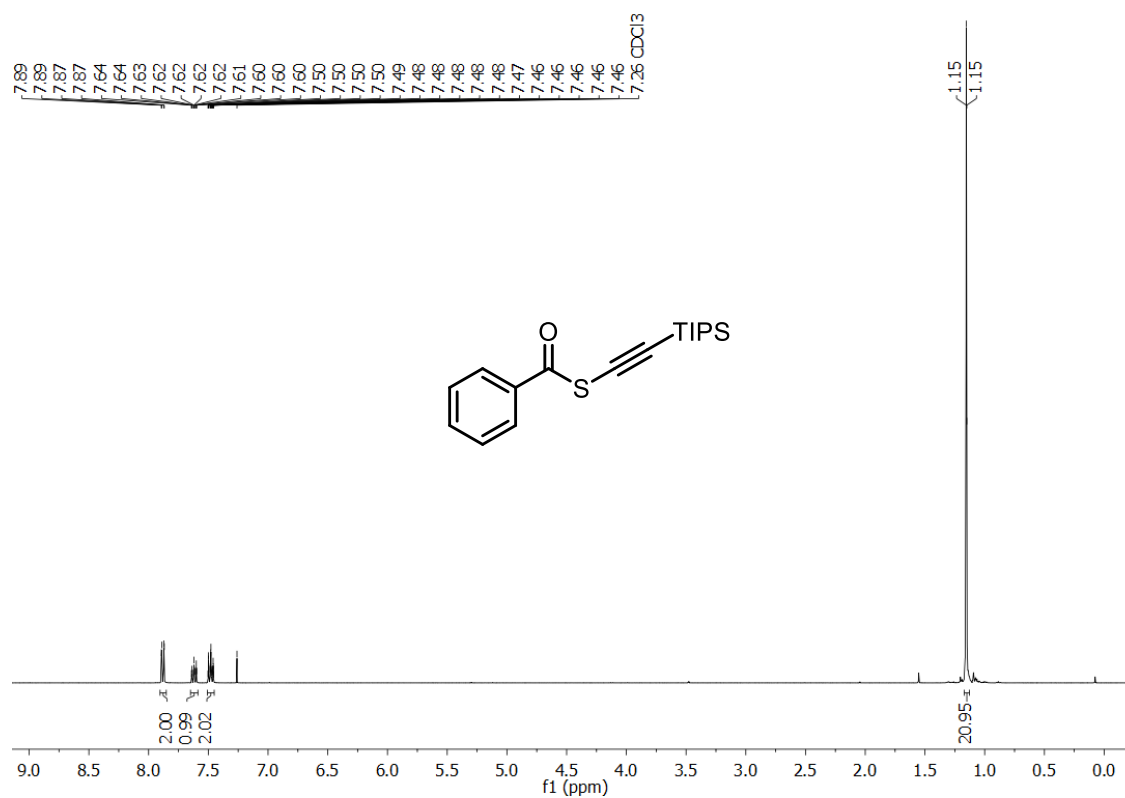
**$^1\text{H}$  NMR of compound 184, *N,N'*-diphenyl-2-(triisopropylsilyl)acetimidamide, 400 MHz,  $\text{CDCl}_3$ , 298 K**



**$^{13}\text{C}$  NMR of compound 184, *N,N'*-diphenyl-2-(triisopropylsilyl)acetimidamide, 101 MHz,  $\text{CDCl}_3$ , 298 K**

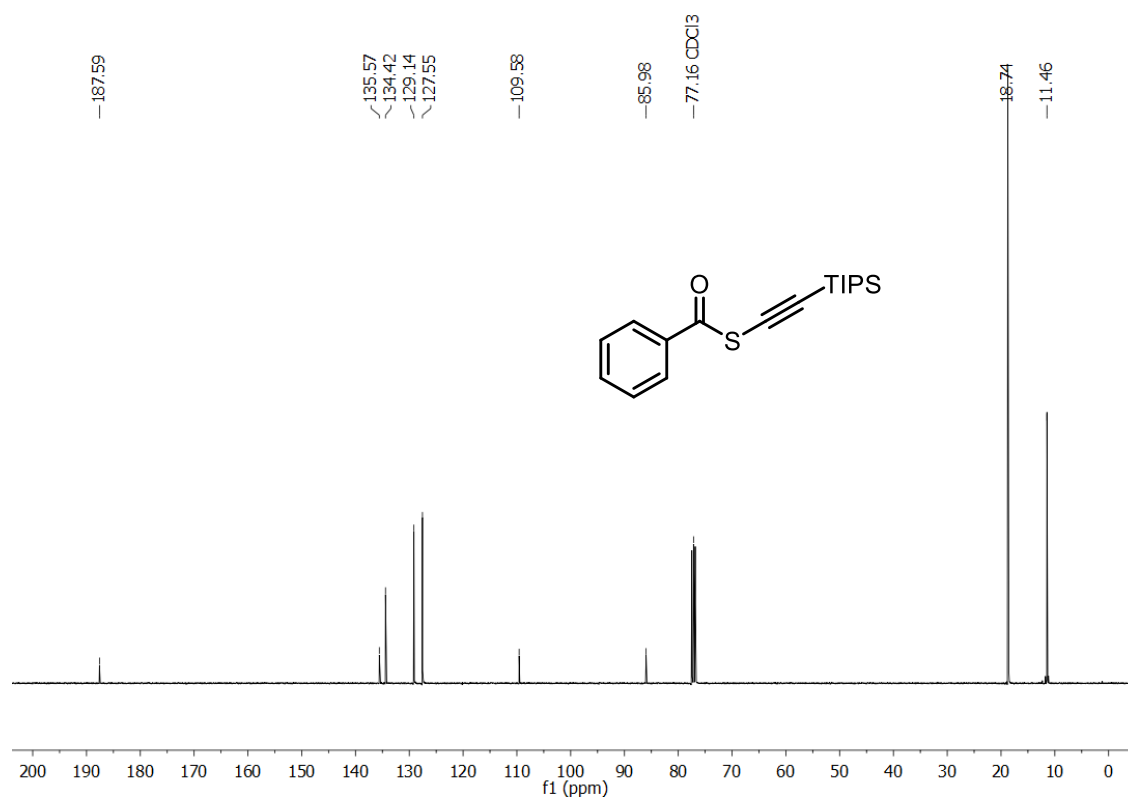


**$^1\text{H}$  NMR of compound 185, *S*-(triisopropylsilyl)ethynyl benzoate, 400 MHz,  $\text{CDCl}_3$ , 298 K**

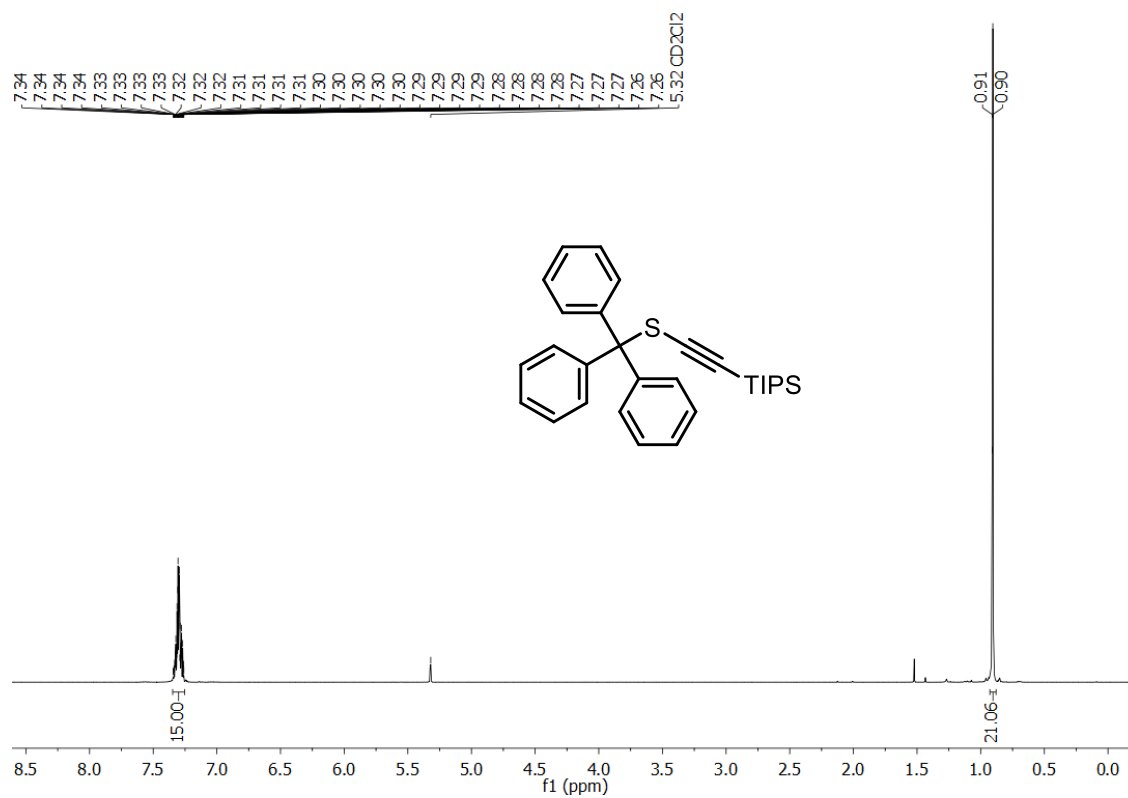




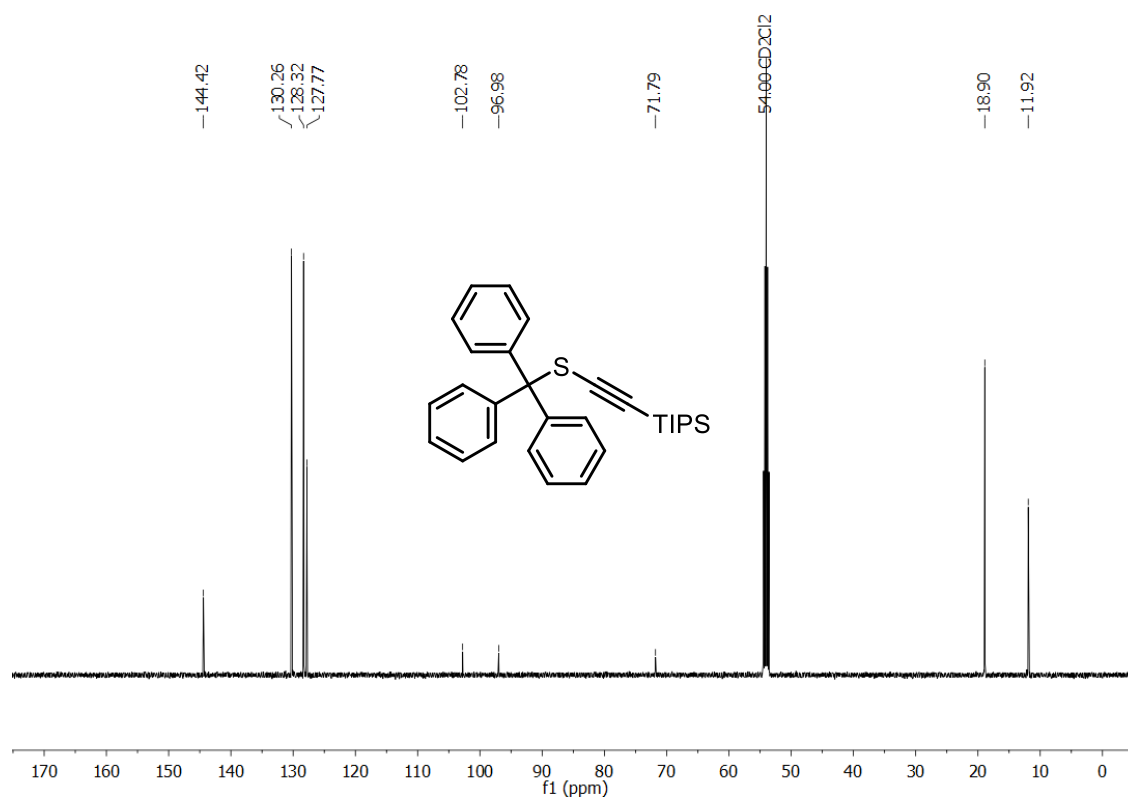
**<sup>1</sup>H NMR of compound 185, S-(triisopropylsilyl)ethynyl benzothioate, 100 MHz, CDCl<sub>3</sub>, 299 K**



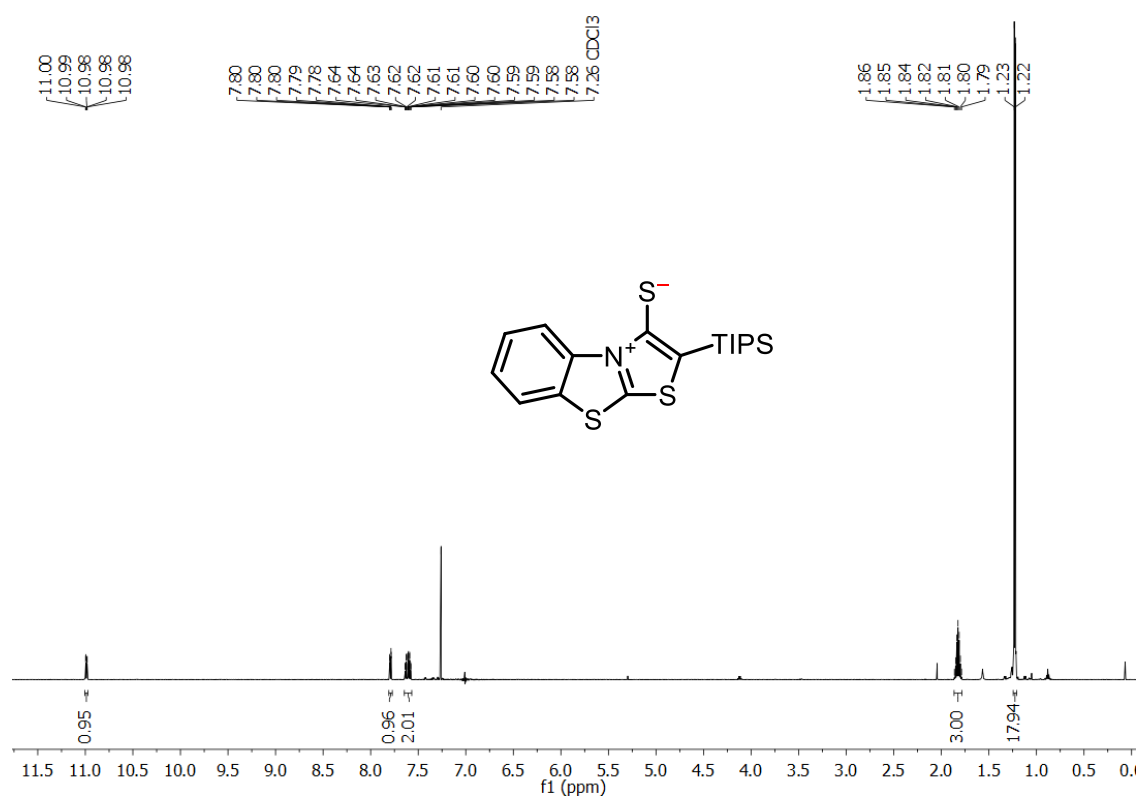
**<sup>1</sup>H NMR of compound 186, triisopropyl[(tritylthio)ethynyl]silane, 300 MHz, CD<sub>2</sub>Cl<sub>2</sub>, 302 K**



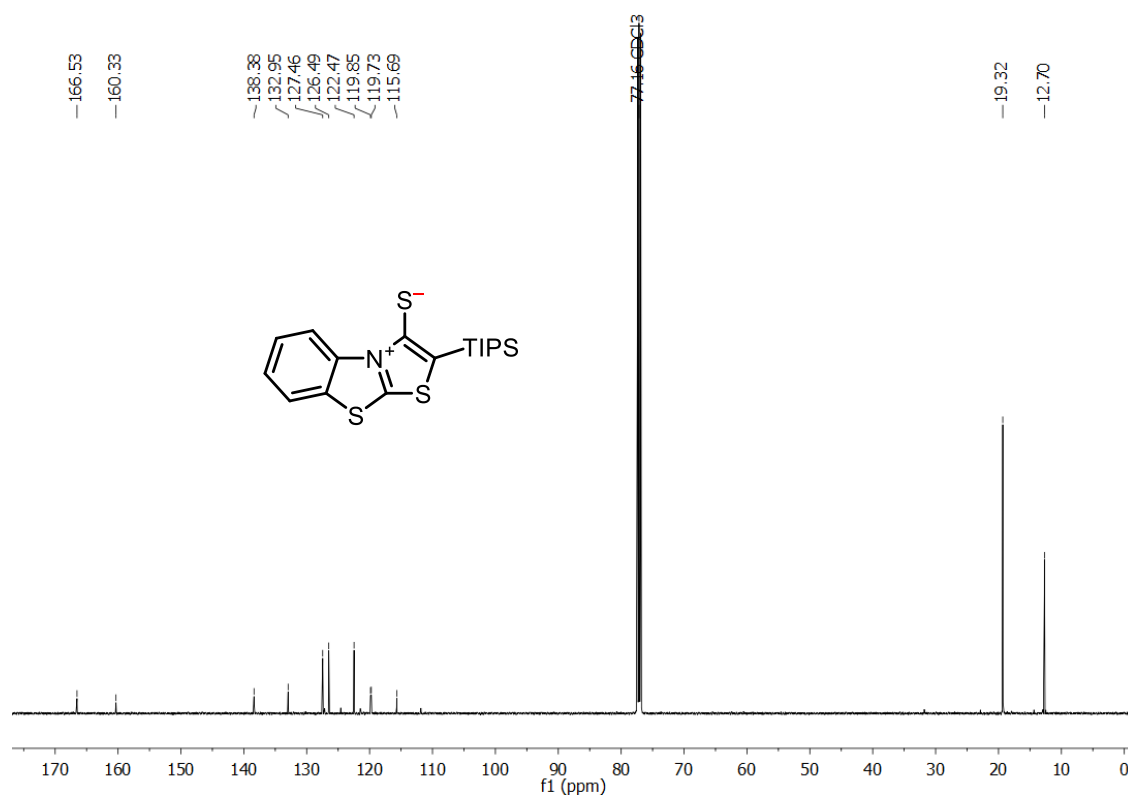
**$^{13}\text{C}$  NMR of compound 186, triisopropyl[(tritylthio)ethynyl]silane, 300 MHz,  $\text{CD}_2\text{Cl}_2$ , 298 K**



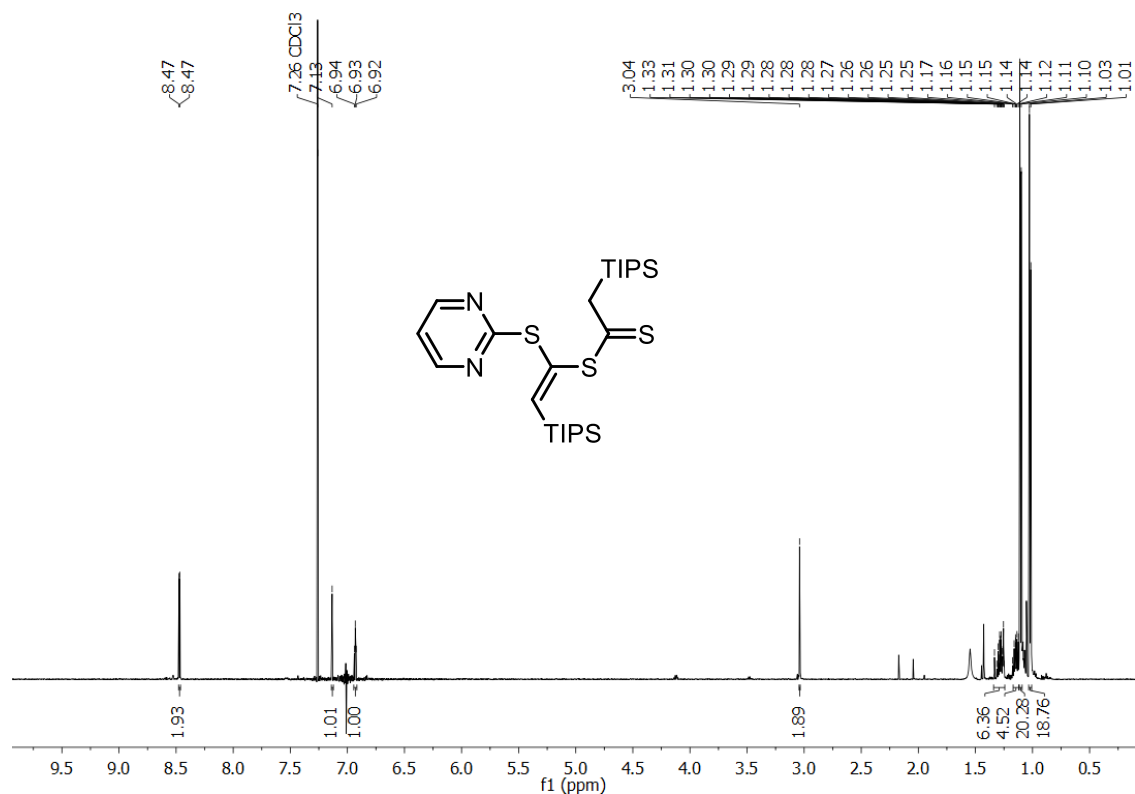
**$^1\text{H}$  NMR of compound 187, 2-(triisopropylsilyl)benzo[d]thiazolo[2,3-b]thiazol-4-ium-3-thiolate, 600 MHz,  $\text{CD}_3\text{Cl}$ , 298 K**



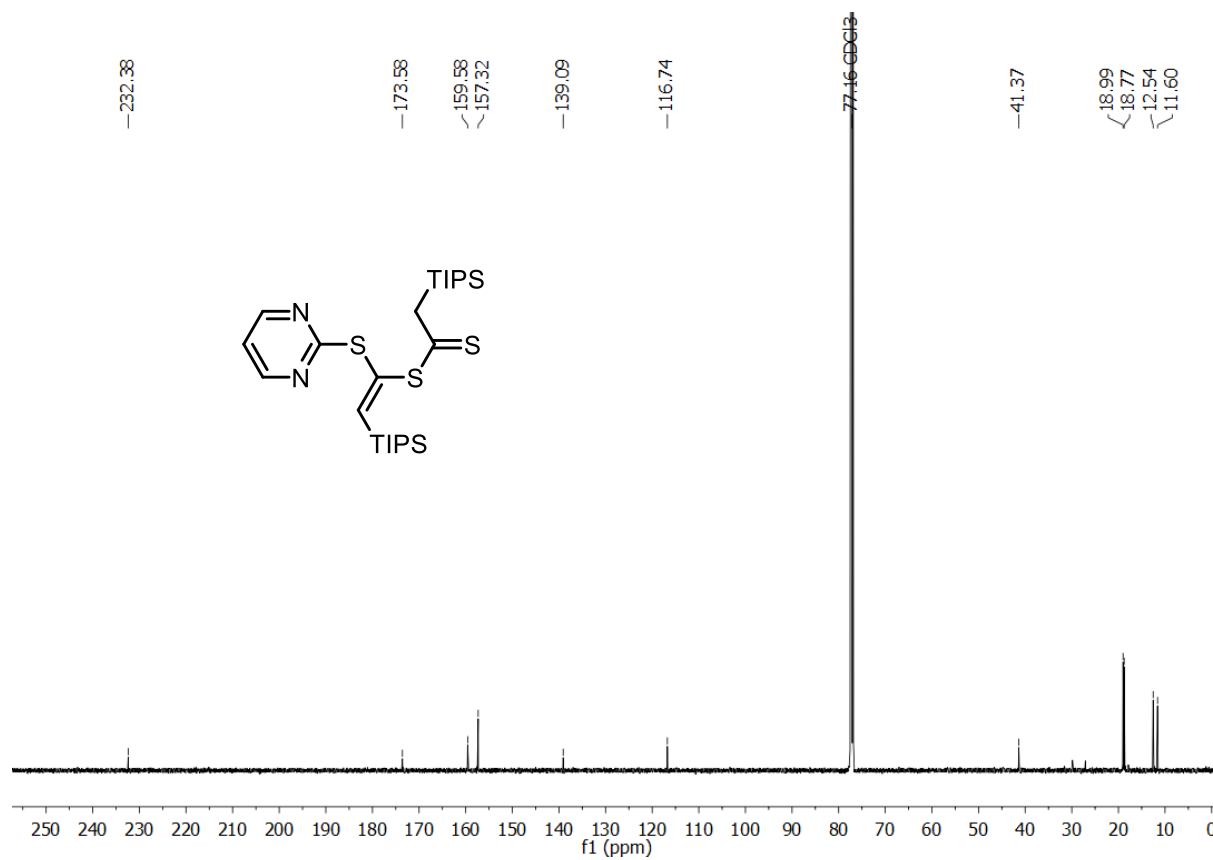
**$^{13}\text{C}$  NMR of compound 187, 2-(triisopropylsilyl)benzo[d]thiazolo[2,3-*b*]thiazol-4-ium-3-thiolate, 126 MHz,  $\text{CD}_3\text{Cl}$ , 298 K**



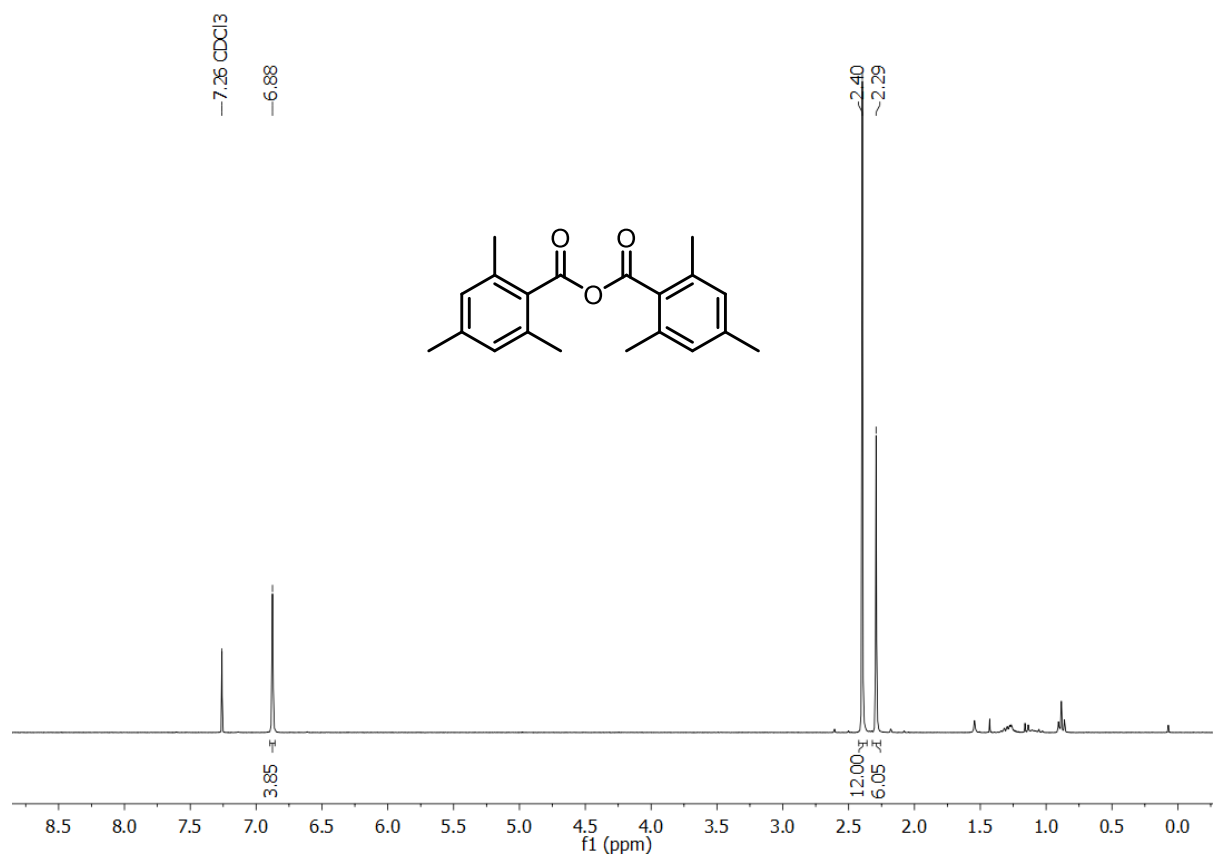
**$^1\text{H}$  NMR of compound 188, (Z)-1-(pyrimidin-2-ylthio)-2-(triisopropylsilyl)vinyl 2-(triisopropylsilyl)ethanedithioate, 600 MHz,  $\text{CD}_3\text{Cl}$ , 298 K**



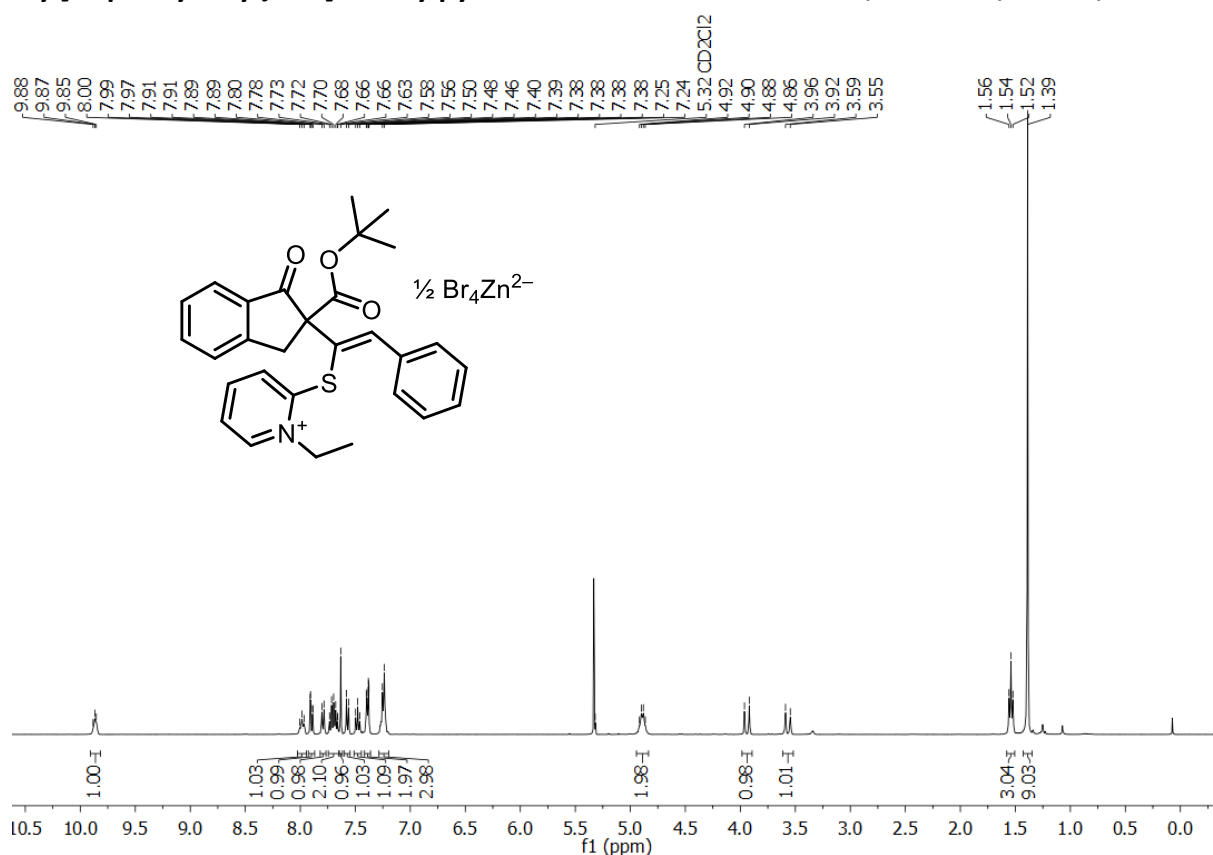
**$^{13}\text{C}$  NMR of compound 188, (Z)-1-(pyrimidin-2-ylthio)-2-(triisopropylsilyl)vinyl 2-(triisopropylsilyl)ethanedithioate, 126 MHz,  $\text{CD}_3\text{Cl}$ , 298 K**



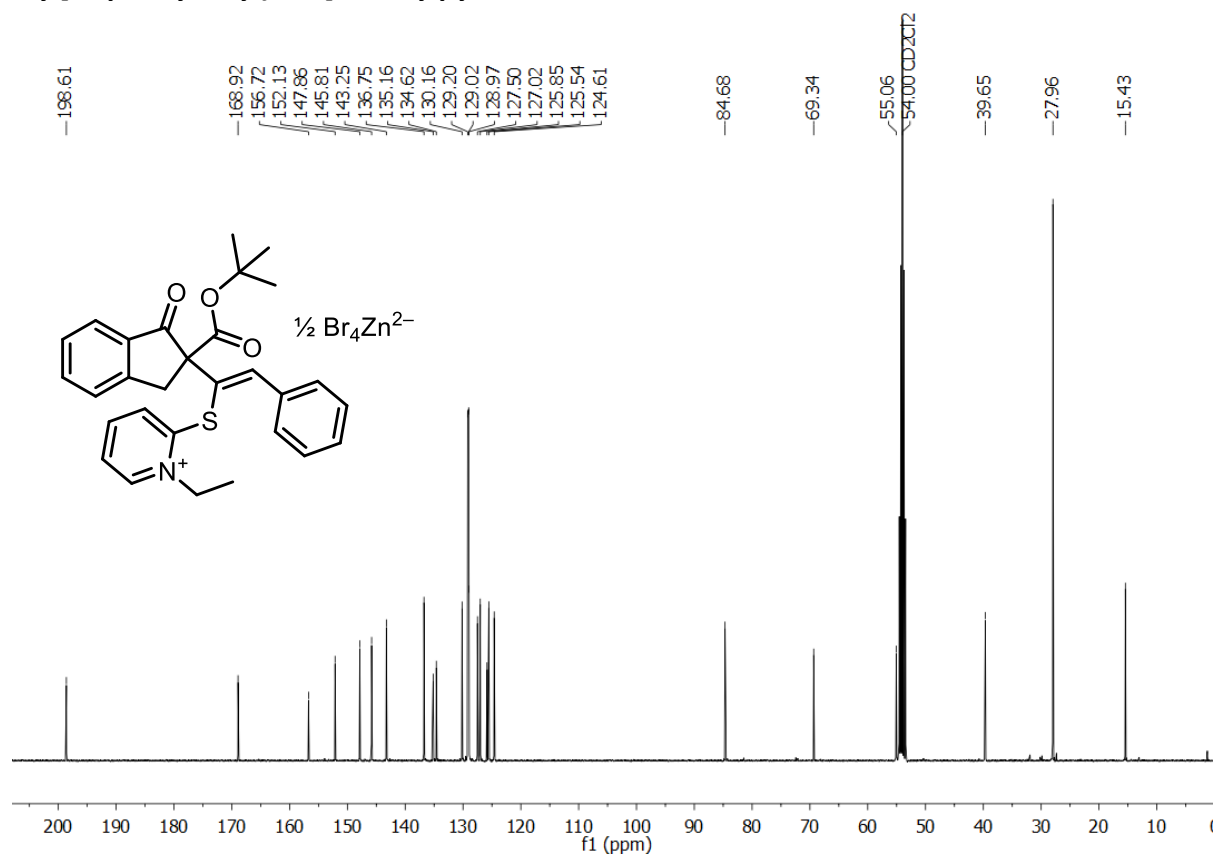
**$^1\text{H}$  NMR of compound 189, 2,4,6-trimethylbenzoic anhydride, 300 MHz,  $\text{CDCl}_3$ , 298 K**



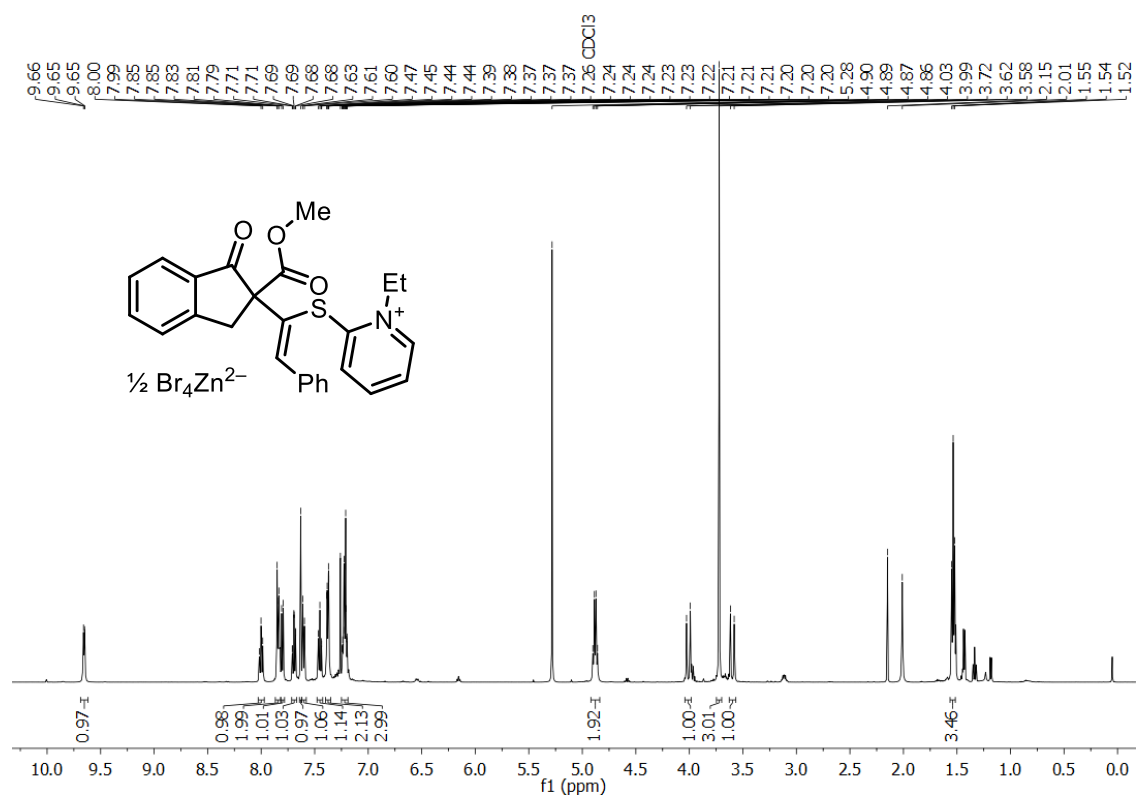
**<sup>1</sup>H NMR of compound 190a, (Z)-2-[[1-[2-(*tert*-butoxycarbonyl)-1-oxo-2,3-dihydro-1*H*-inden-2-yl]-2-phenylvinyl]thio]-1-ethylpyridin-1-ium tetrabromizincate, 500 MHz, CD<sub>2</sub>Cl<sub>2</sub>, 298 K**



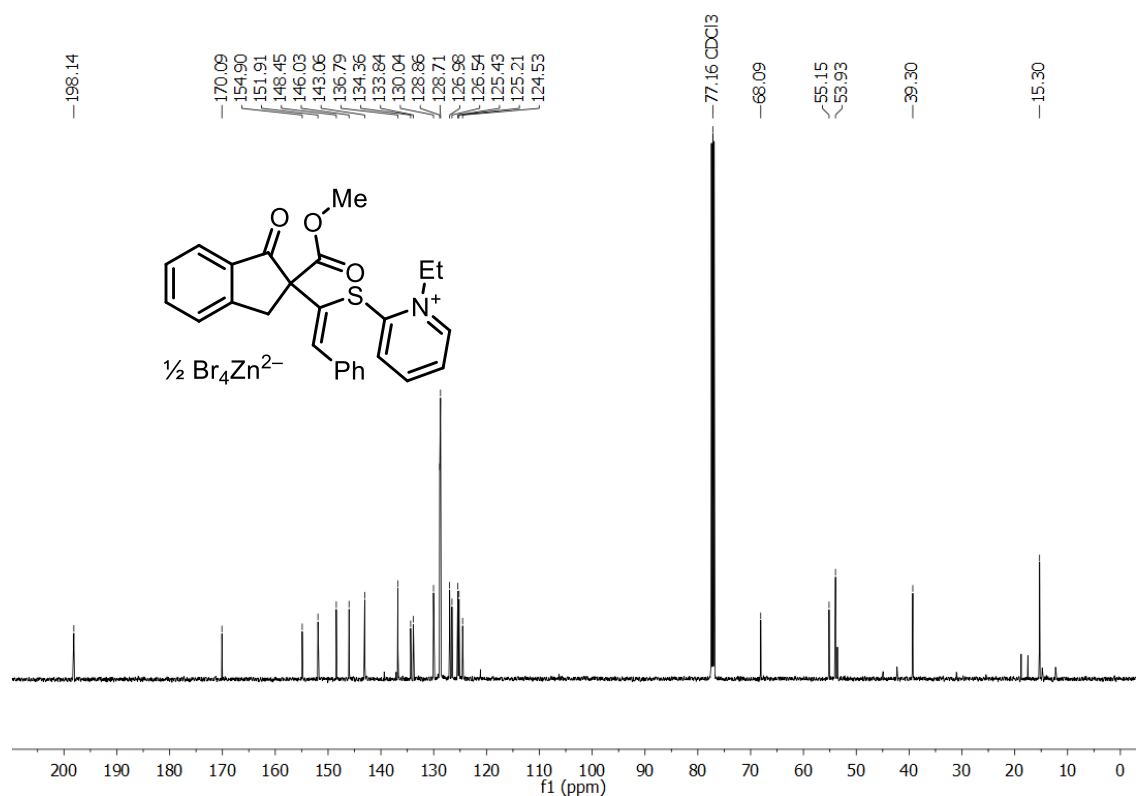
**<sup>13</sup>C NMR of compound 190, (Z)-2-[[1-[2-(*tert*-butoxycarbonyl)-1-oxo-2,3-dihydro-1*H*-inden-2-yl]-2-phenylvinyl]thio]-1-ethylpyridin-1-ium tetrabromozincate, 126 MHz, CD<sub>2</sub>Cl<sub>2</sub>, 298 K**



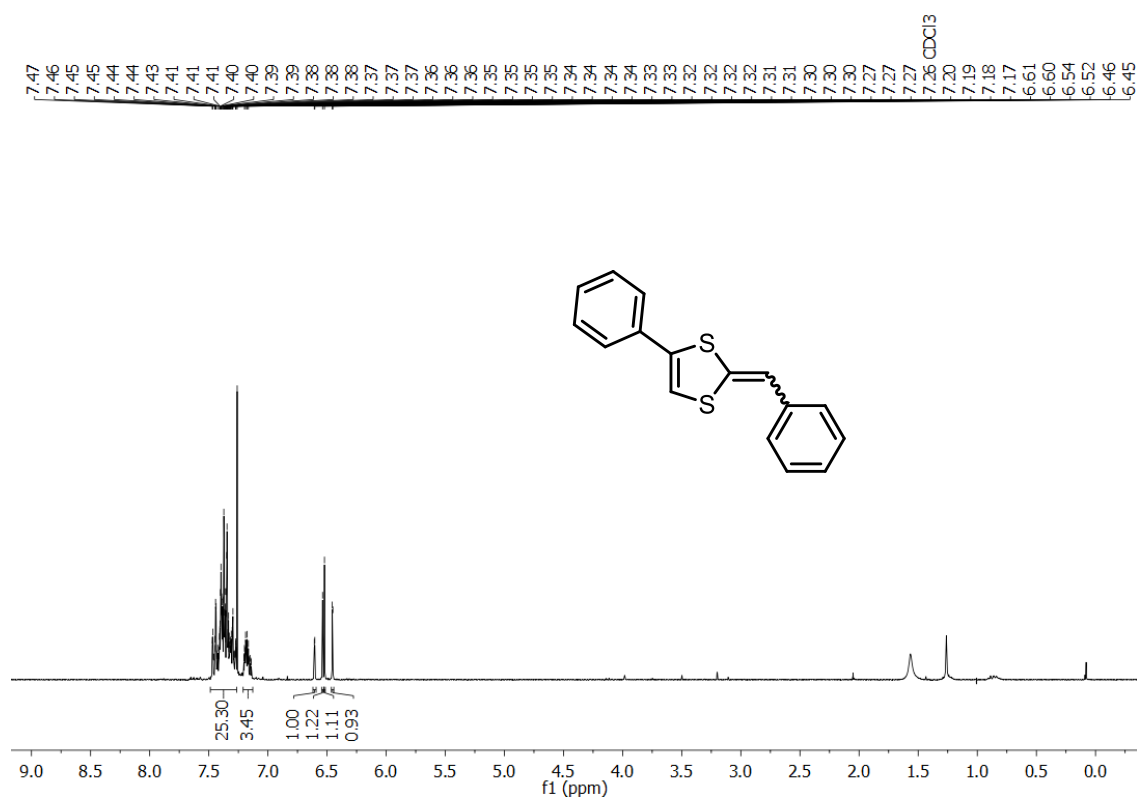
**<sup>1</sup>H NMR of compound 190b, (Z)-1-ethyl-2-[[1-[2-(methoxycarbonyl)-1-oxo-2,3-dihydro-1H-inden-2-yl]-2-phenylvinyl]thio]pyridin-1-ium tetrabromozincate, 500 MHz, CDCl<sub>3</sub>, 298 K**



**<sup>13</sup>C NMR of compound 190b, (Z)-1-ethyl-2-[[1-[2-(methoxycarbonyl)-1-oxo-2,3-dihydro-1H-inden-2-yl]-2-phenylvinyl]thio]pyridin-1-ium tetrabromozincate, 126 MHz, CDCl<sub>3</sub>, 298 K**



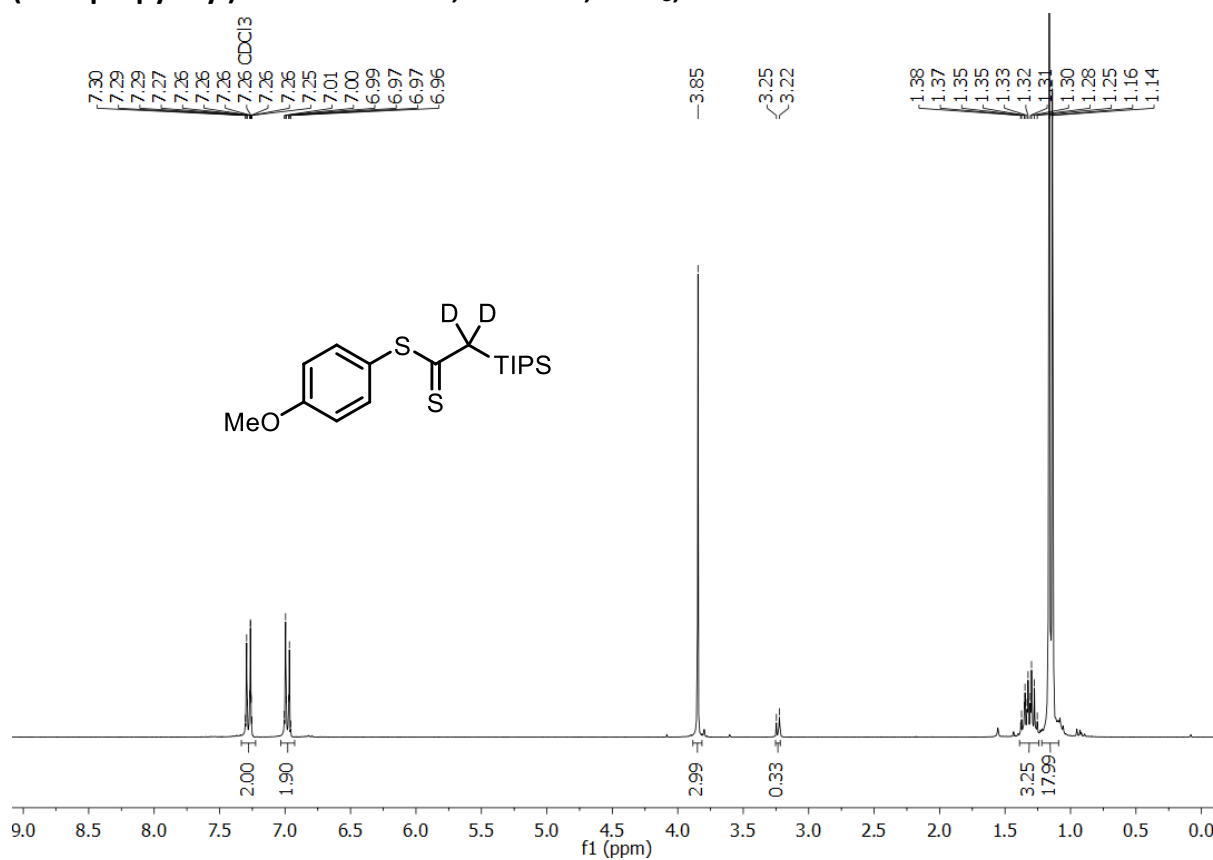
**<sup>1</sup>H NMR of compound 191, (*E/Z*)-2-benzylidene-4-phenyl-1,3-dithiole, 300 MHz, CDCl<sub>3</sub>, 298 K**



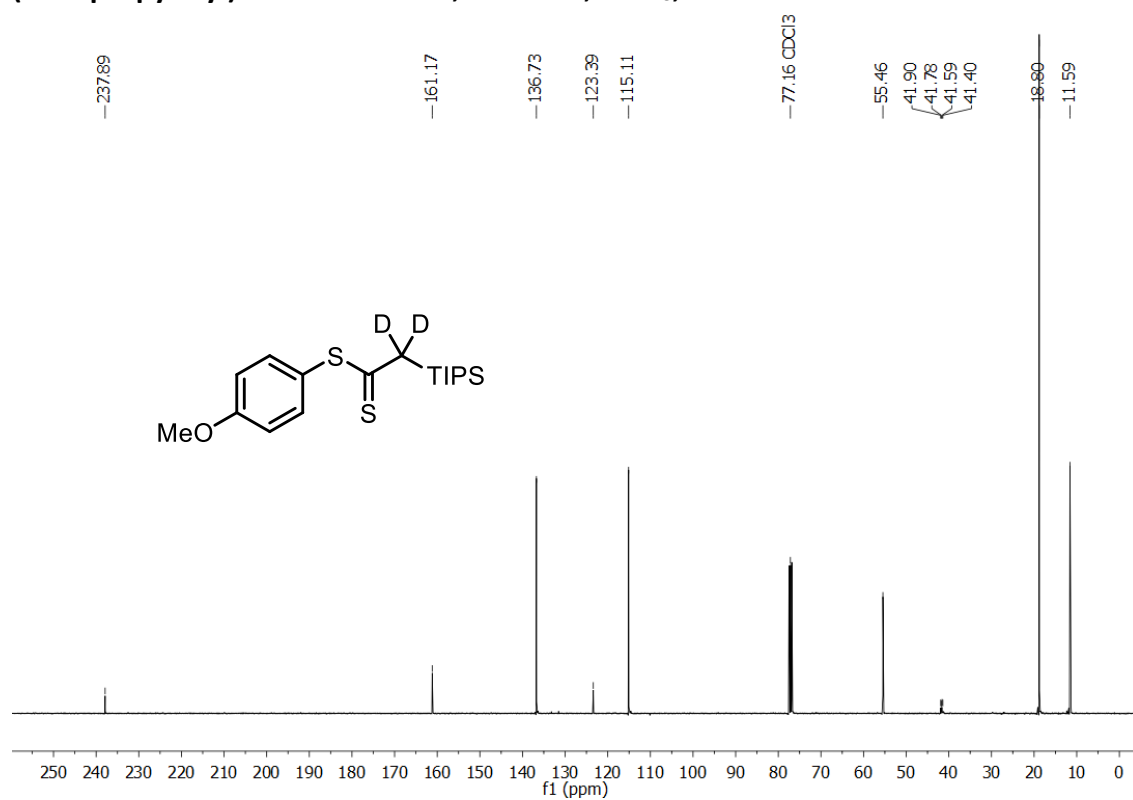
**<sup>13</sup>C NMR of compound 191, (*E/Z*)-2-benzylidene-4-phenyl-1,3-dithiole, 101 MHz, CDCl<sub>3</sub>, 298 K**



**$^1\text{H}$  NMR of compound 192, 4-methoxyphenyl 2,2-dideuterio-2-(triisopropylsilyl)ethanedithioate, 300 MHz,  $\text{CDCl}_3$ , 302 K**

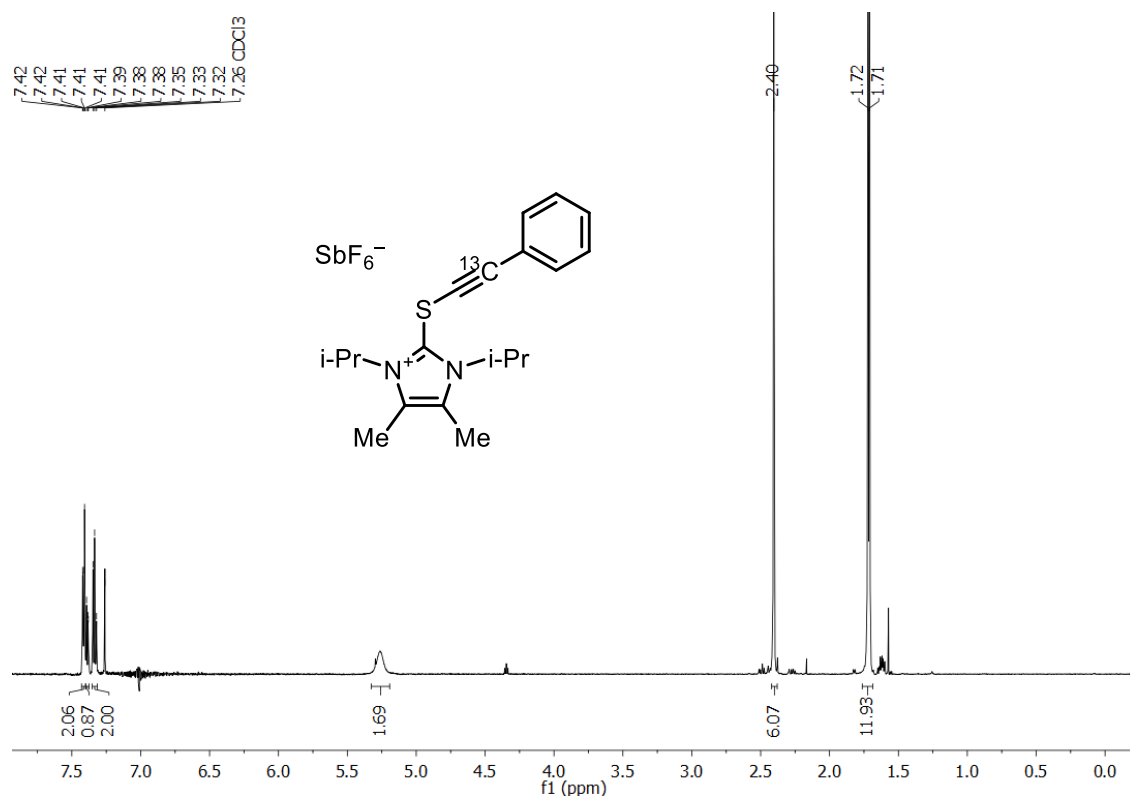


**$^{13}\text{C}$  NMR of compound 192, 4-methoxyphenyl 2,2-dideuterio-2-(triisopropylsilyl)ethanedithioate, 101 MHz,  $\text{CDCl}_3$ , 298 K**

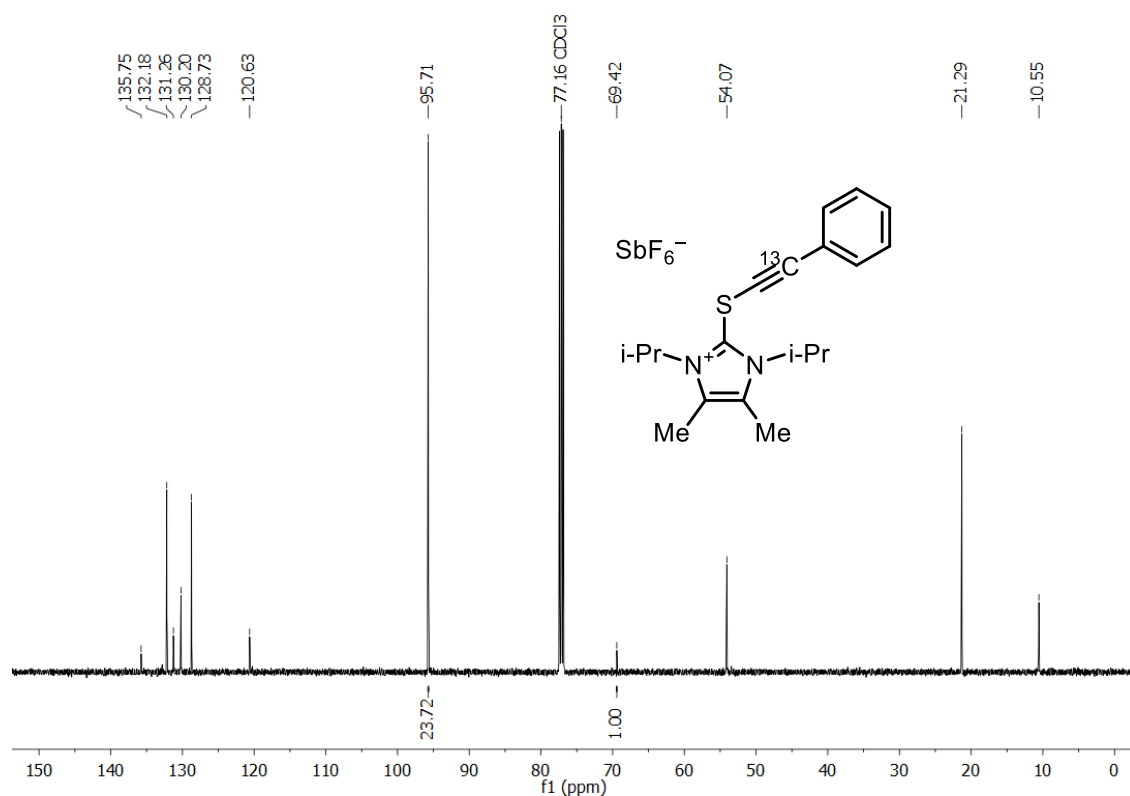




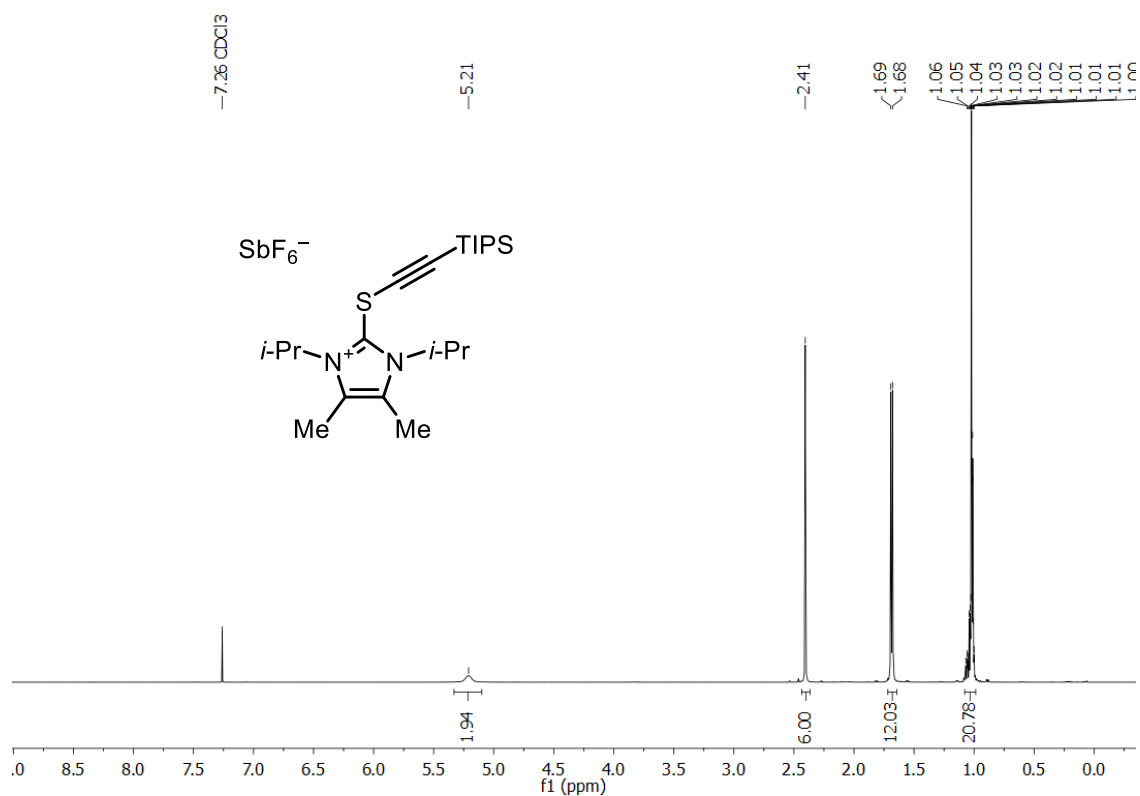
**$^1\text{H}$  NMR of compound  $\{^{13}\text{C}\}$ -197, 1,3-diisopropyl-4,5-dimethyl-2-[(phenylethynyl-2- $^{13}\text{C}$ )thio]-1*H*-imidazol-3-ium hexafluoroantimonate, 600 MHz,  $\text{CDCl}_3$ , 298 K**



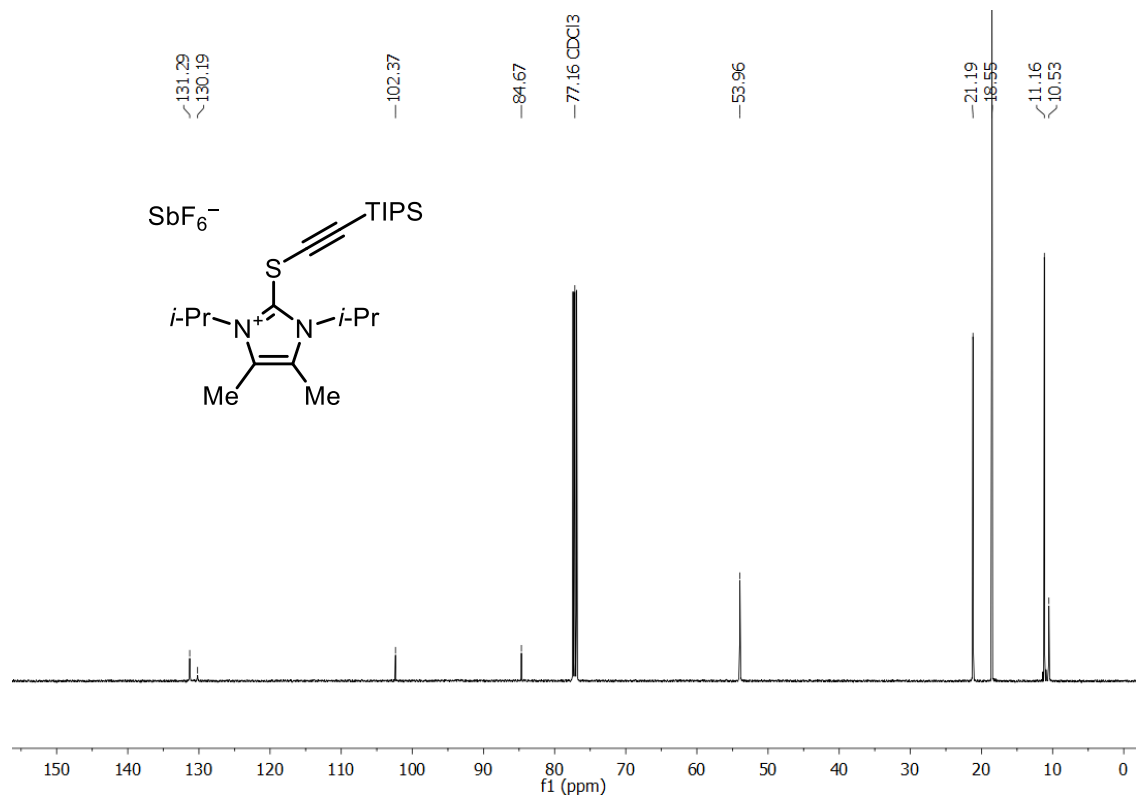
**$^{13}\text{C}$  NMR of compound  $\{^{13}\text{C}\}$ -197, 1,3-diisopropyl-4,5-dimethyl-2-[(phenylethynyl-2- $^{13}\text{C}$ )thio]-1*H*-imidazol-3-ium hexafluoroantimonate, 126 MHz,  $\text{CDCl}_3$ , 298 K**



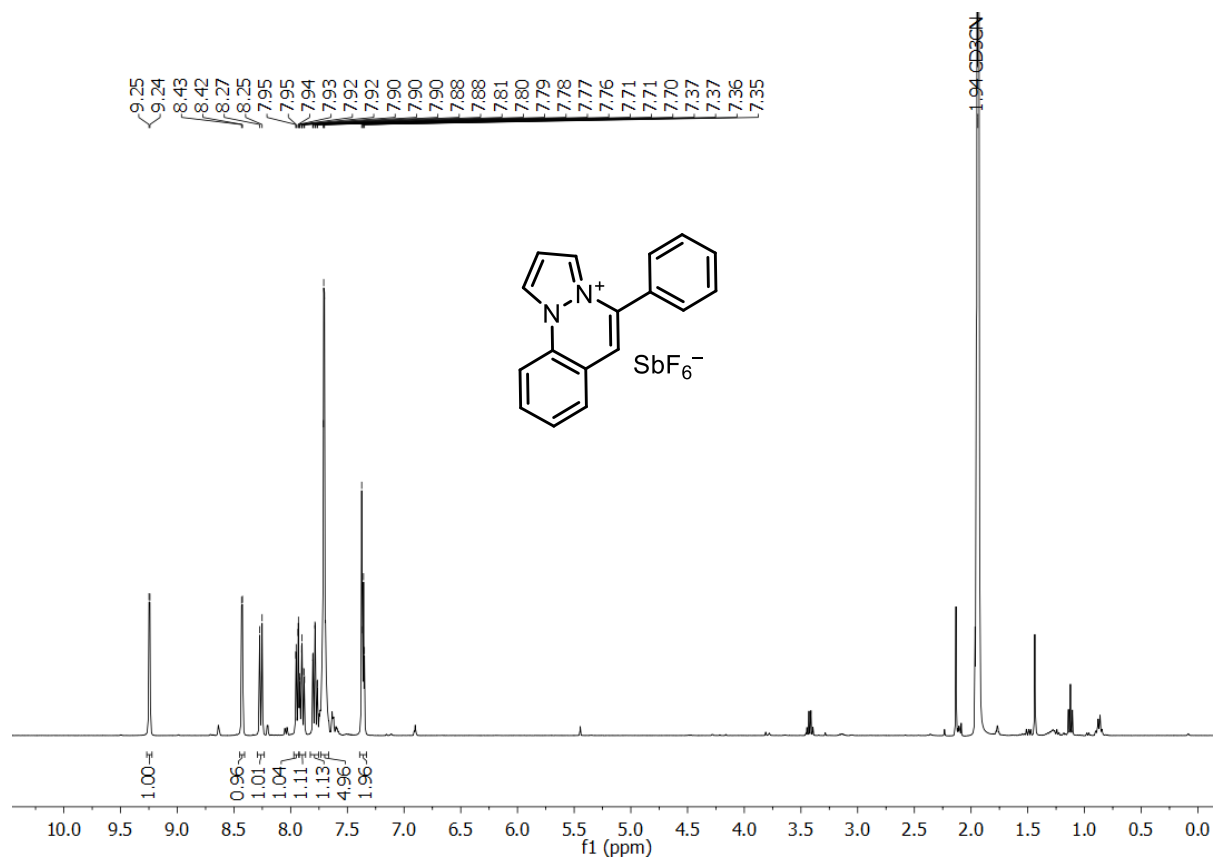
**$^1\text{H}$  NMR of compound 202, 1,3-diisopropyl-4,5-dimethyl-2-[[triisopropylsilyl]ethynyl]thio}-1*H*-imidazol-3-ium hexafluoroantimonate, 500 MHz,  $\text{CDCl}_3$ , 298 K**



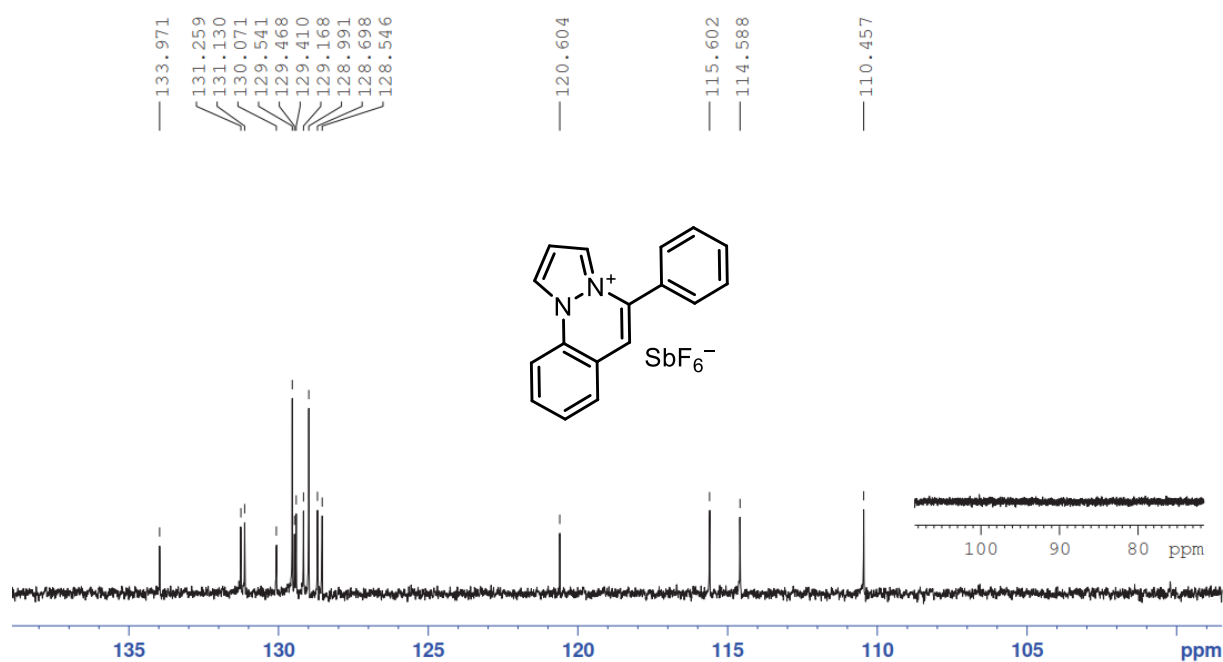
**$^{13}\text{C}$  NMR of compound 202, 1,3-diisopropyl-4,5-dimethyl-2-[[triisopropylsilyl]ethynyl]thio}-1*H*-imidazol-3-ium hexafluoroantimonate, 126 MHz,  $\text{CDCl}_3$ , 298 K**



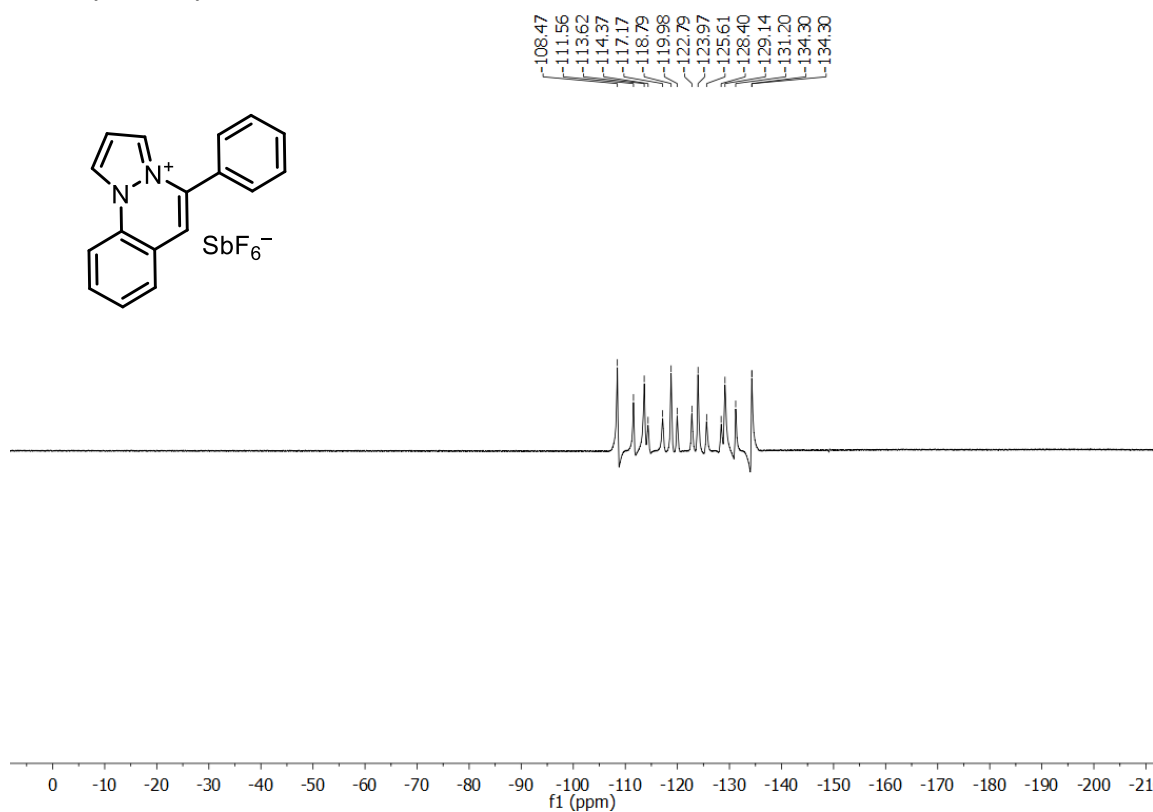
**$^1\text{H}$  NMR of compound 203, 5-phenylpyrazolo[1,2-*a*]cinnolin-4-ium hexafluoroantimonate, 400 MHz,  $\text{CD}_3\text{CN}$ , 298 K**



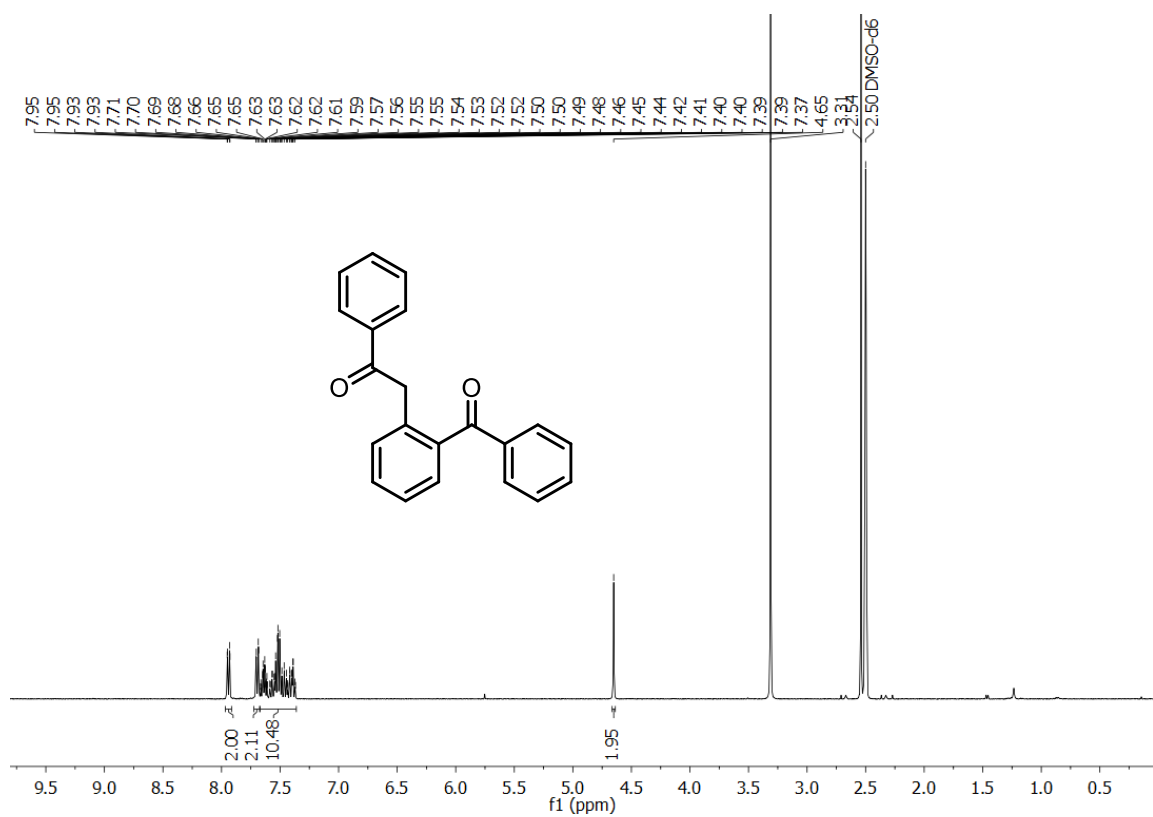
**$^{13}\text{C}$  NMR of compound 203, 5-phenylpyrazolo[1,2-*a*]cinnolin-4-ium hexafluoroantimonate, 151 MHz,  $\text{DMSO-d}_6$ , 303 K**



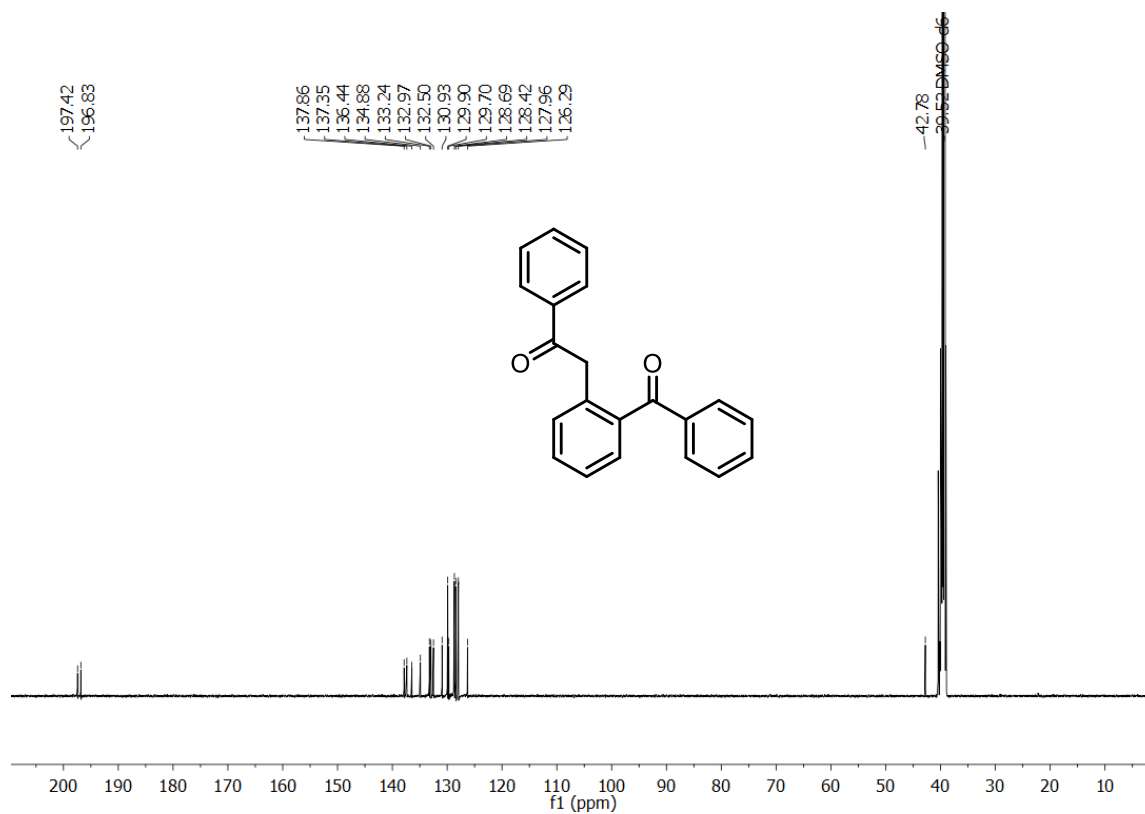
**$^{19}\text{F}$  NMR of compound 203, 5-phenylpyrazolo[1,2-*a*]cinnolin-4-ium hexafluoroantimonate, 377 MHz,  $\text{CD}_3\text{CN}$ , 298 K**



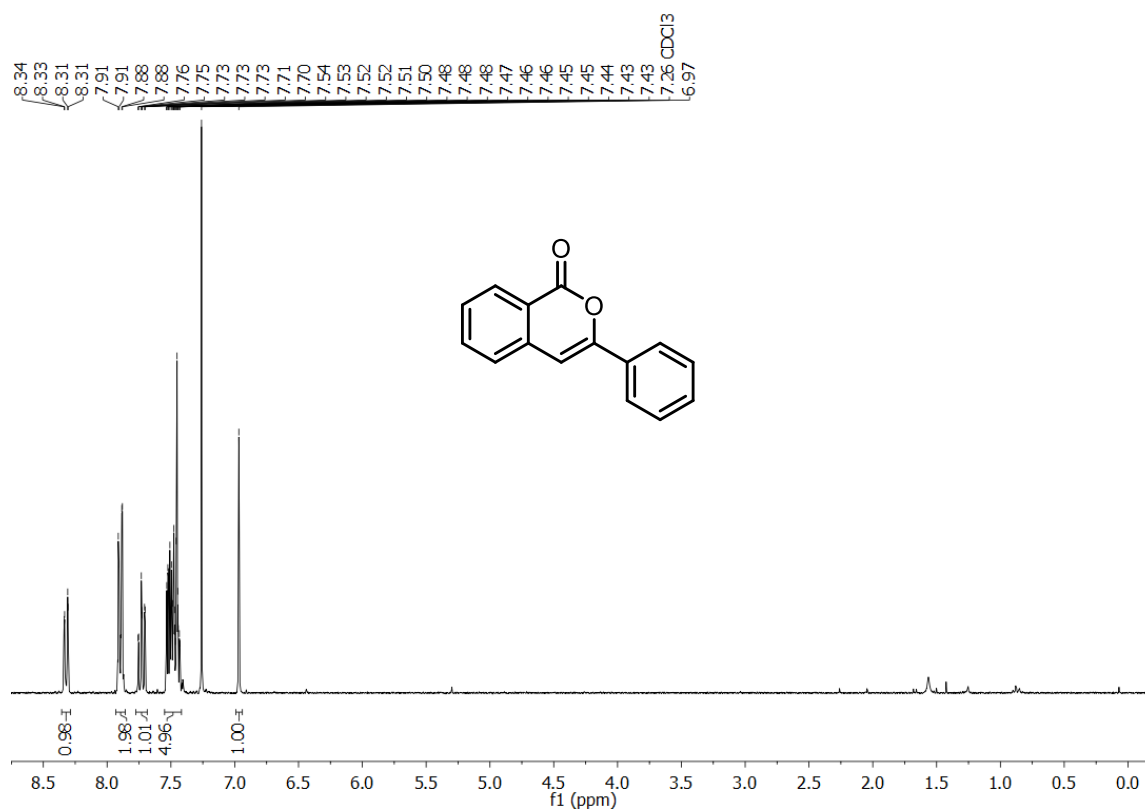
**$^1\text{H}$  NMR of compound 204, 2-(2-Benzoylphenyl)-1-phenylethan-1-one, 400 Mhz,  $\text{DMSO-}d_6$ , 300 K**



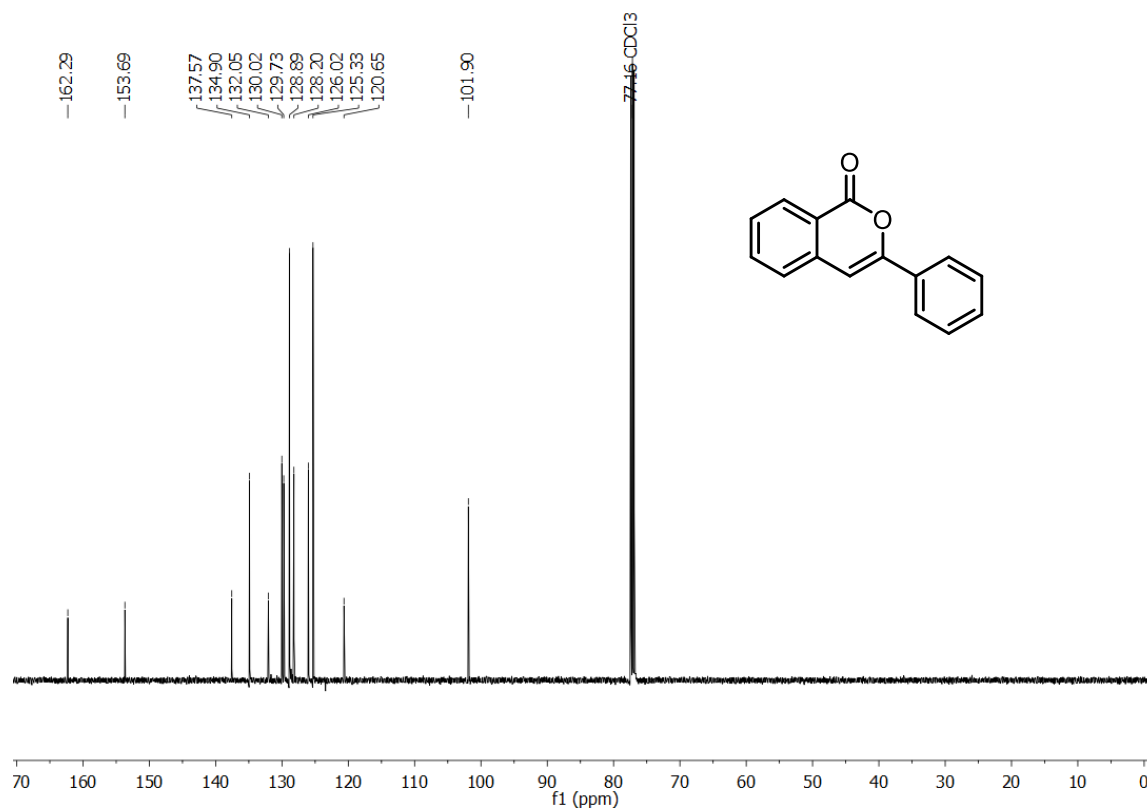
**$^{13}\text{C}$  NMR of compound 204, 2-(2-Benzoylphenyl)-1-phenylethan-1-one, 126 Mhz, DMSO- $d_6$ , 303 K**



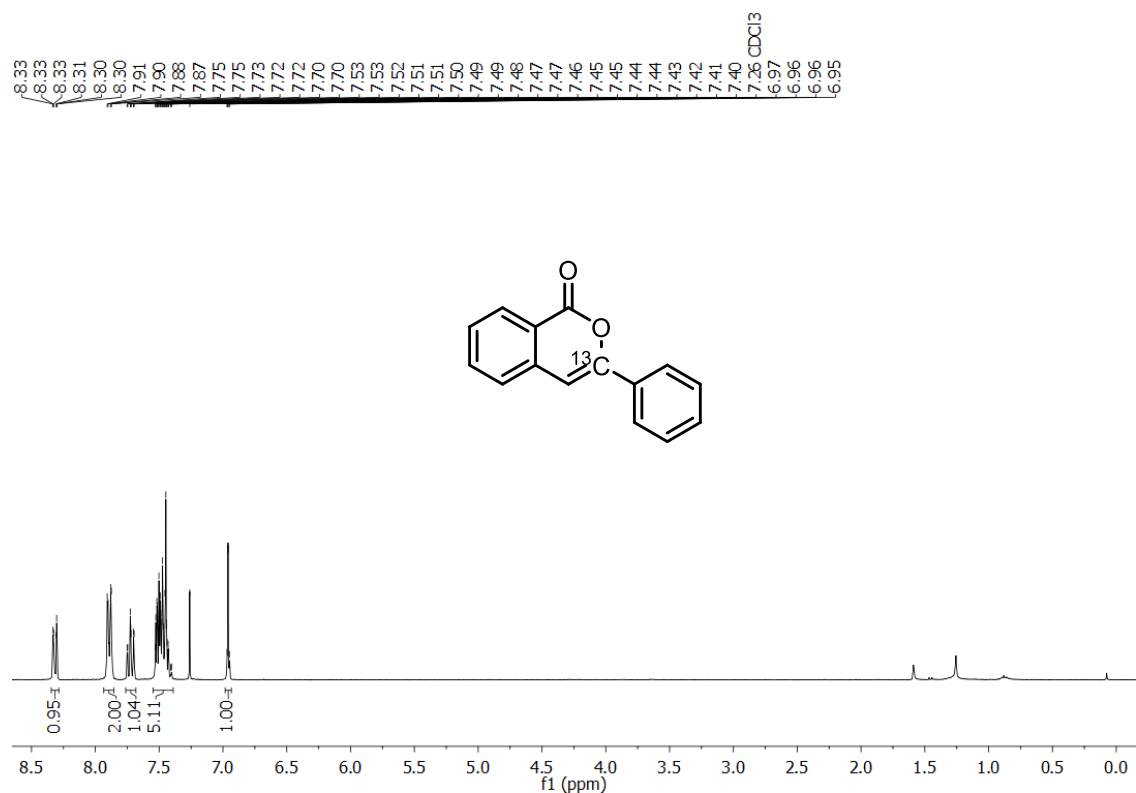
**$^1\text{H}$  NMR of compound 207, 3-phenyl-1H-isochromen-1-one (Homalicine), 300 MHz,  $\text{CDCl}_3$ , 300 K**



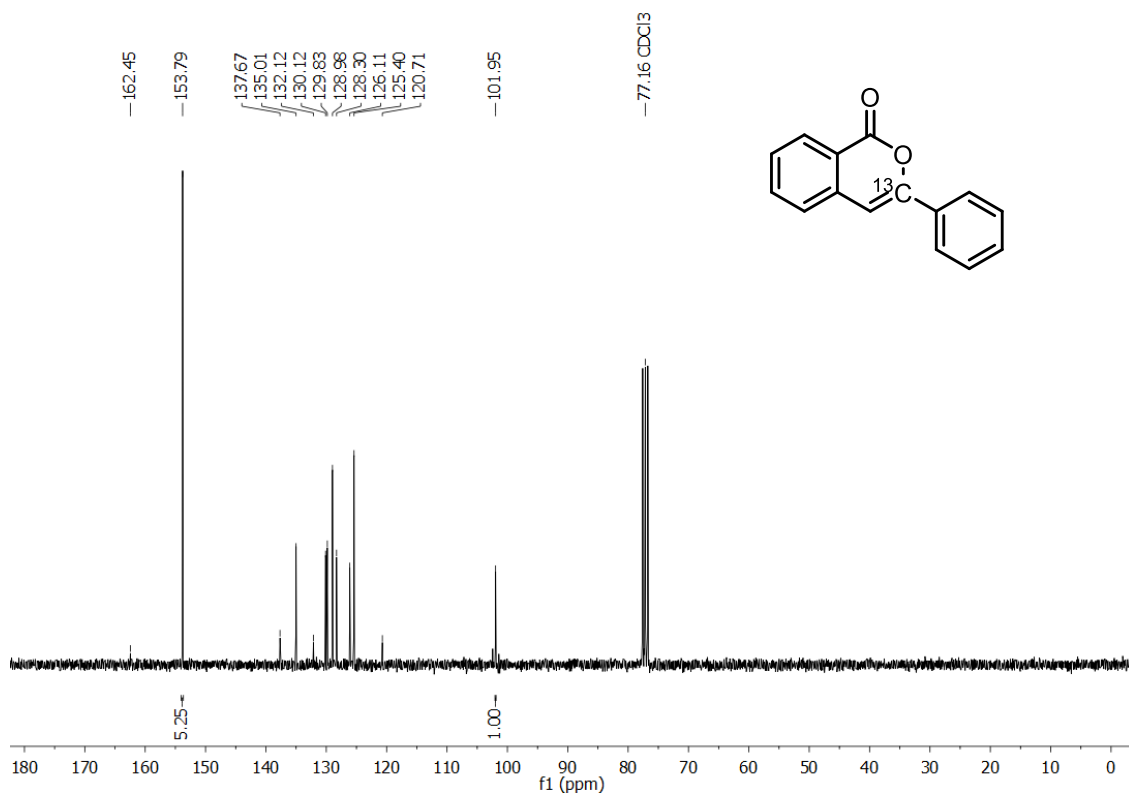
**$^{13}\text{C}$  NMR of compound 207, 3-phenyl-1*H*-isochromen-1-one (Homalicine), 126 MHz,  $\text{CDCl}_3$ , 300 K**



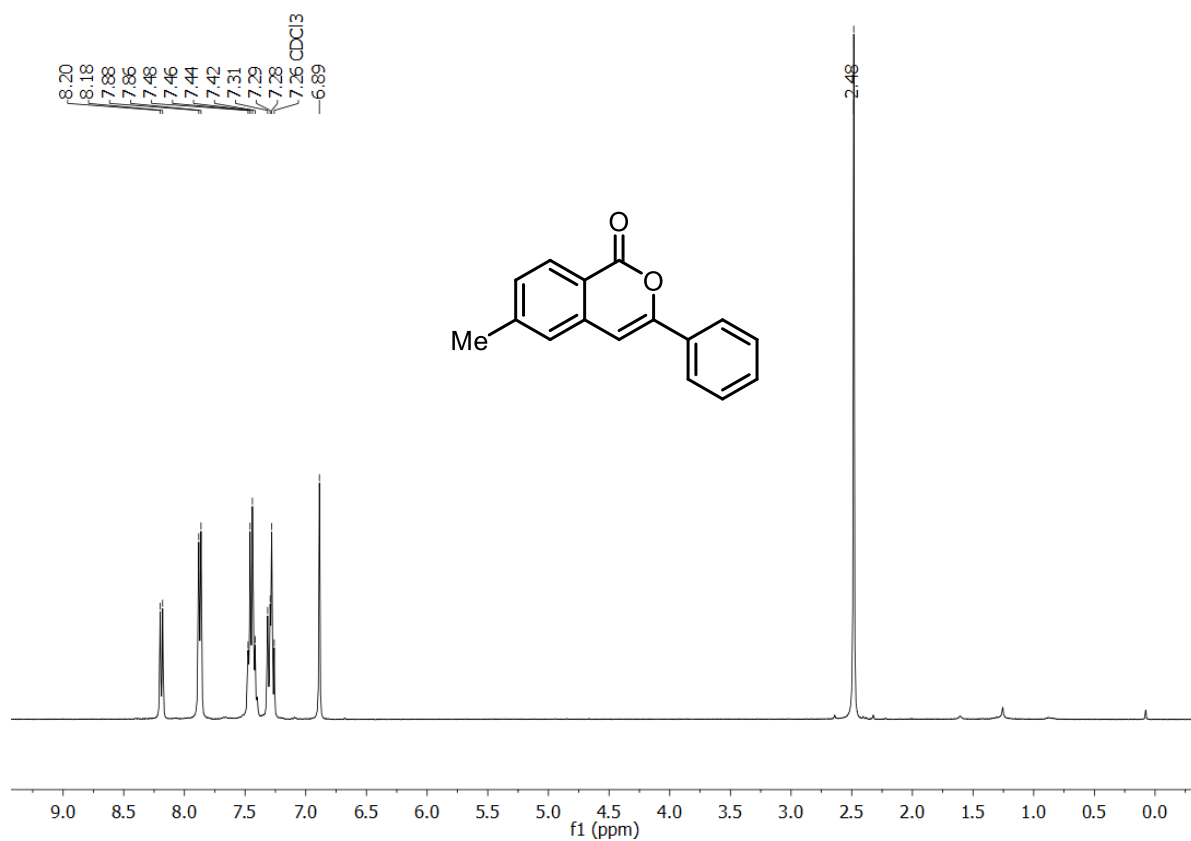
**$^1\text{H}$  NMR of compound  $\{^{13}\text{C}\}$ -207, 3- $\{^{13}\text{C}\}$ -3-phenyl-1*H*-isochromen-1-one (3- $\{^{13}\text{C}\}$ -Homalicine), 300 MHz,  $\text{CDCl}_3$ , 298 K**



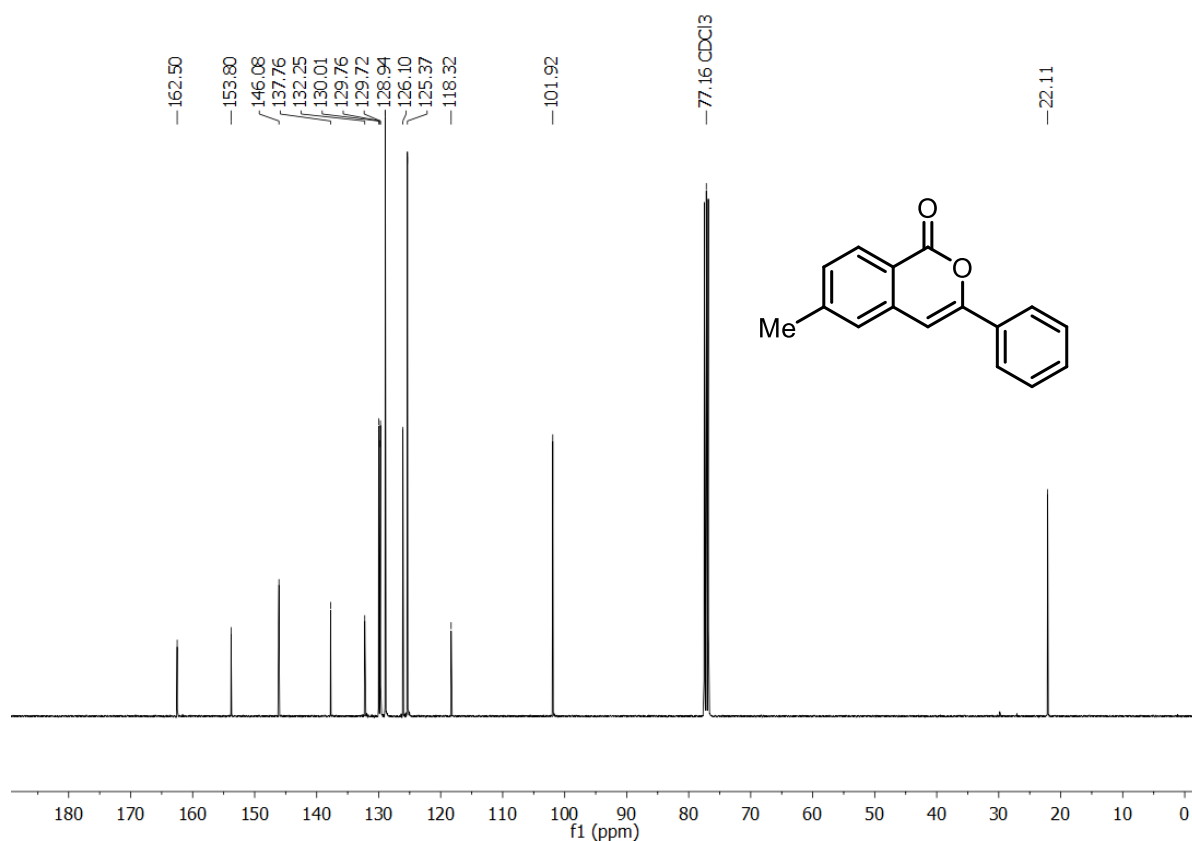
**$^{13}\text{C}$  NMR of compound  $\{^{13}\text{C}\}$ -207, 3- $\{^{13}\text{C}\}$ -3-phenyl-1*H*-isochromen-1-one (3- $\{^{13}\text{C}\}$ -Homalicine), 76 MHz,  $\text{CDCl}_3$ , 298 K**



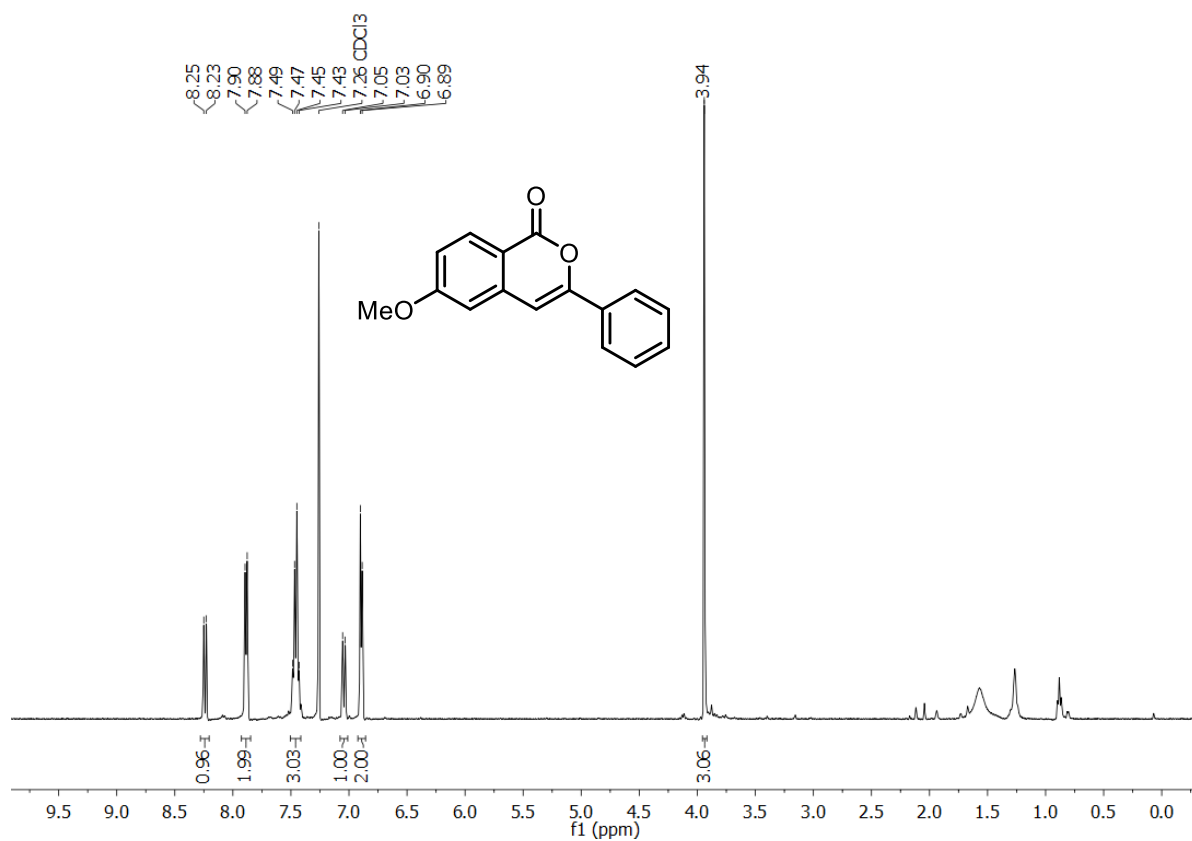
**$^1\text{H}$  NMR of compound 208, 6-methyl-3-phenyl-1*H*-isochromen-1-one, 400 MHz,  $\text{CDCl}_3$ , 299 K**



**$^{13}\text{C}$  NMR of compound 208, 6-methyl-3-phenyl-1*H*-isochromen-1-one, 300 MHz,  $\text{CDCl}_3$ , 300 K**

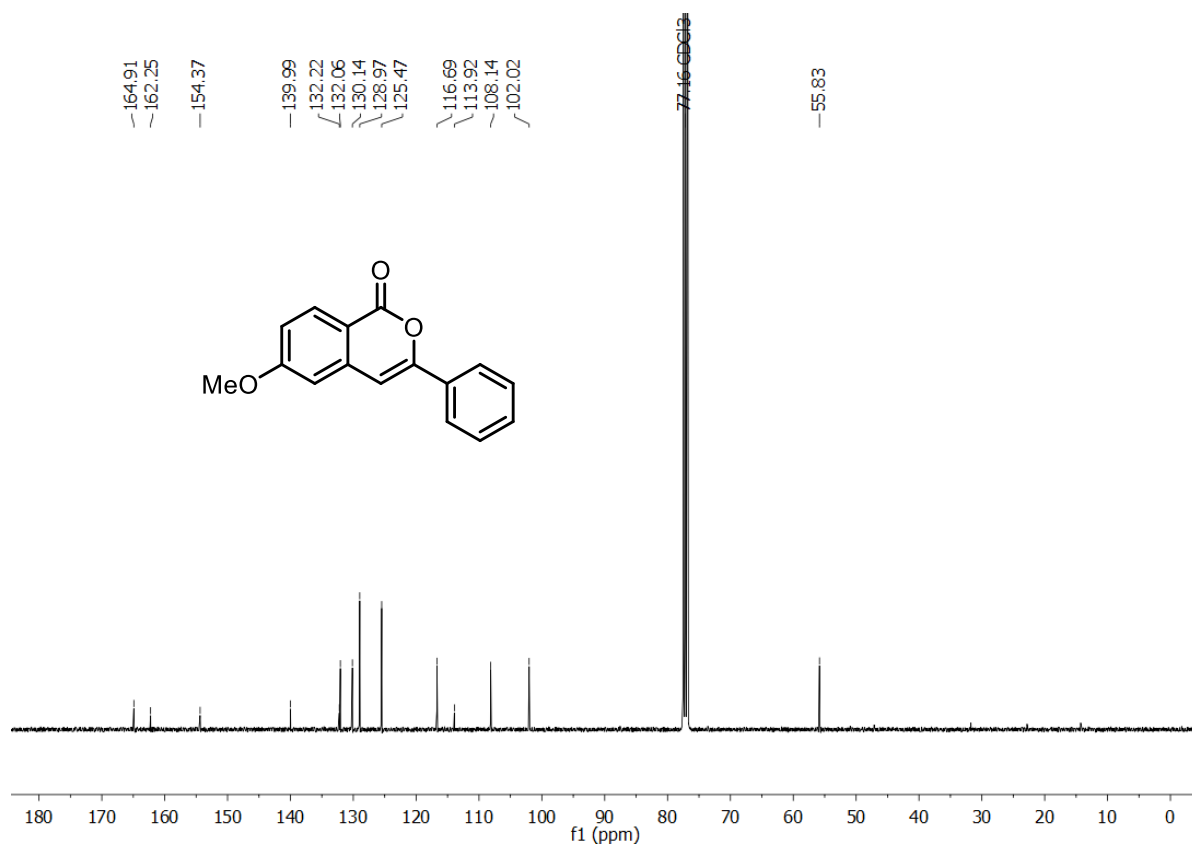


**$^1\text{H}$  NMR of compound 209, 6-methoxy-3-phenyl-1*H*-isochromen-1-one, 400 MHz,  $\text{CDCl}_3$ , 298 K**

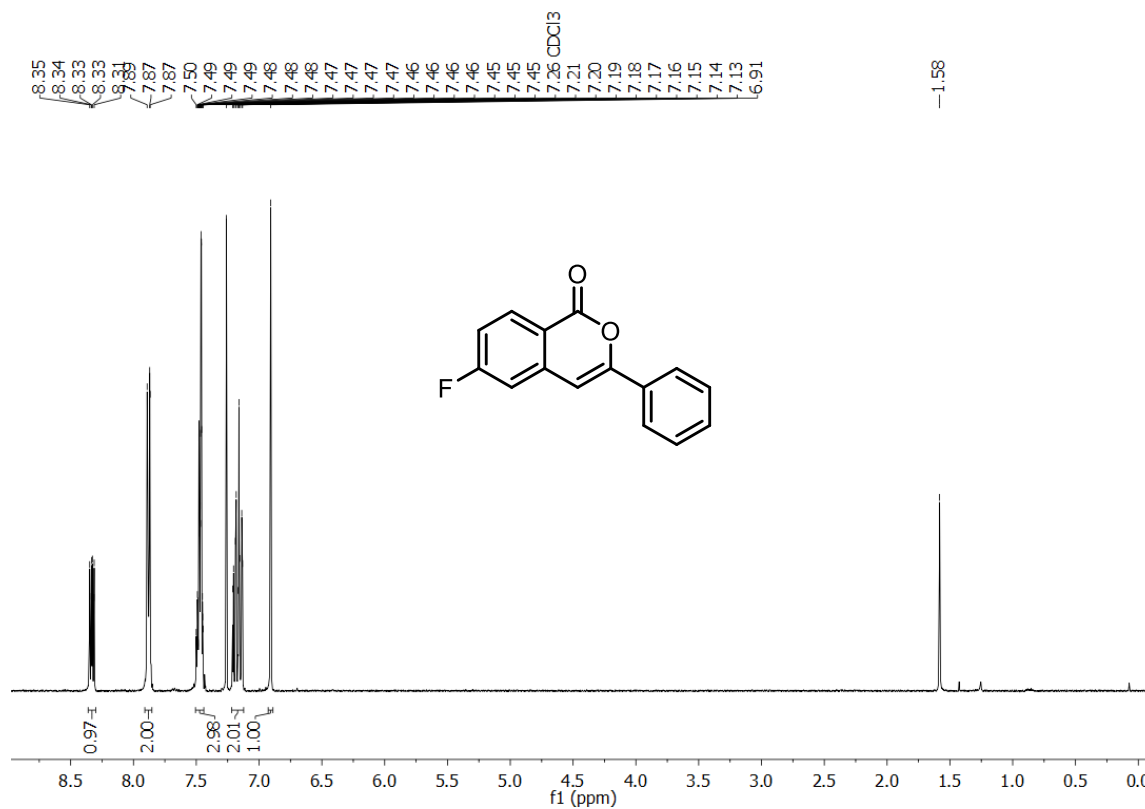




**$^{13}\text{C}$  NMR of compound 209, 6-methoxy-3-phenyl-1*H*-isochromen-1-one, 101 MHz,  $\text{CDCl}_3$ , 298 K**



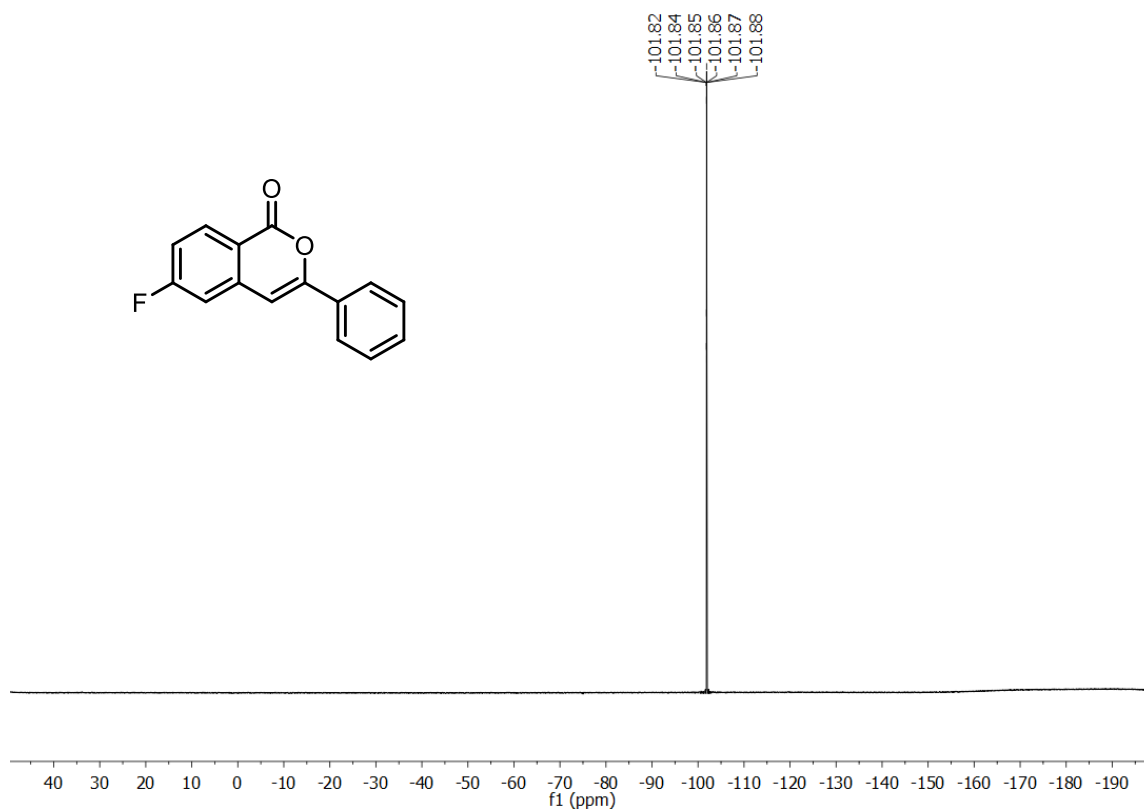
**$^1\text{H}$  NMR of compound 210, 6-fluoro-3-phenyl-1*H*-isochromen-1-one, 400 MHz,  $\text{CDCl}_3$ , 299 K**



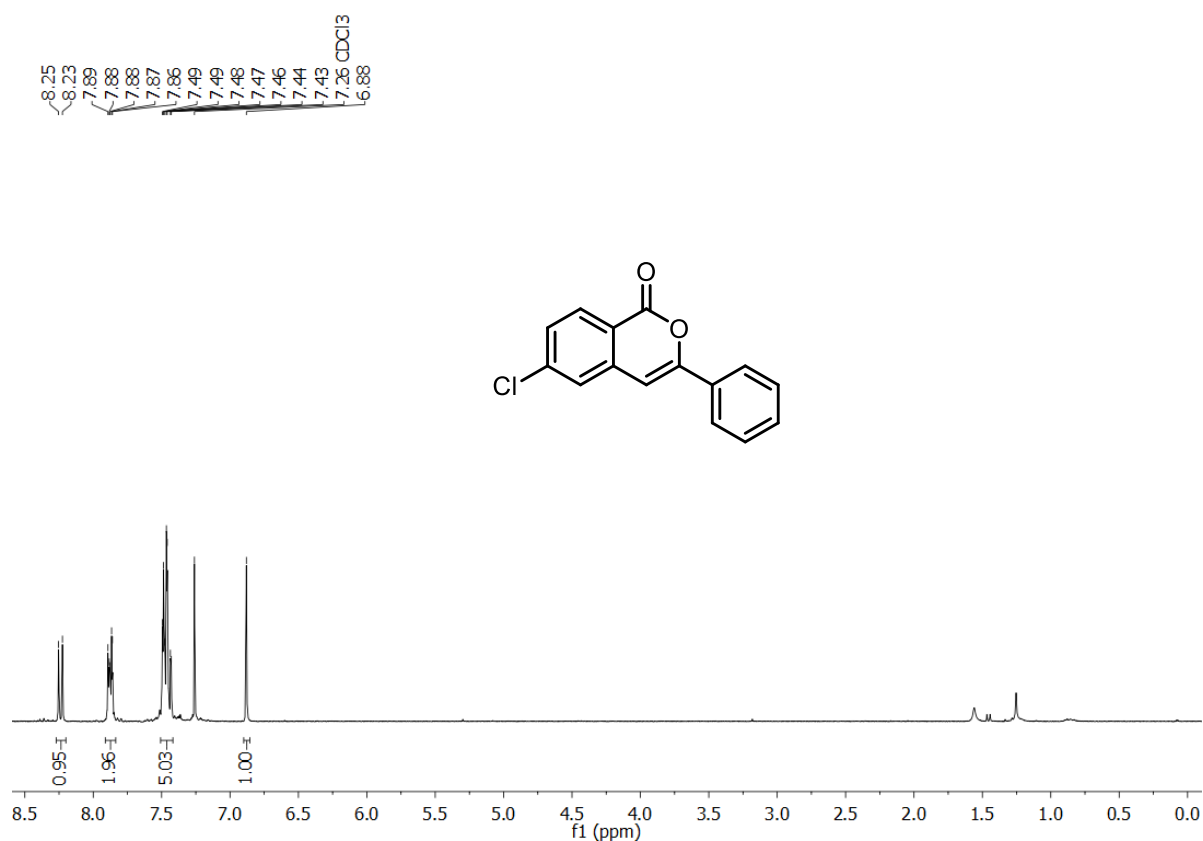
**$^{13}\text{C}$  NMR of compound 210, 6-fluoro-3-phenyl-1*H*-isochromen-1-one, 126 MHz,  $\text{CDCl}_3$ , 300 K**



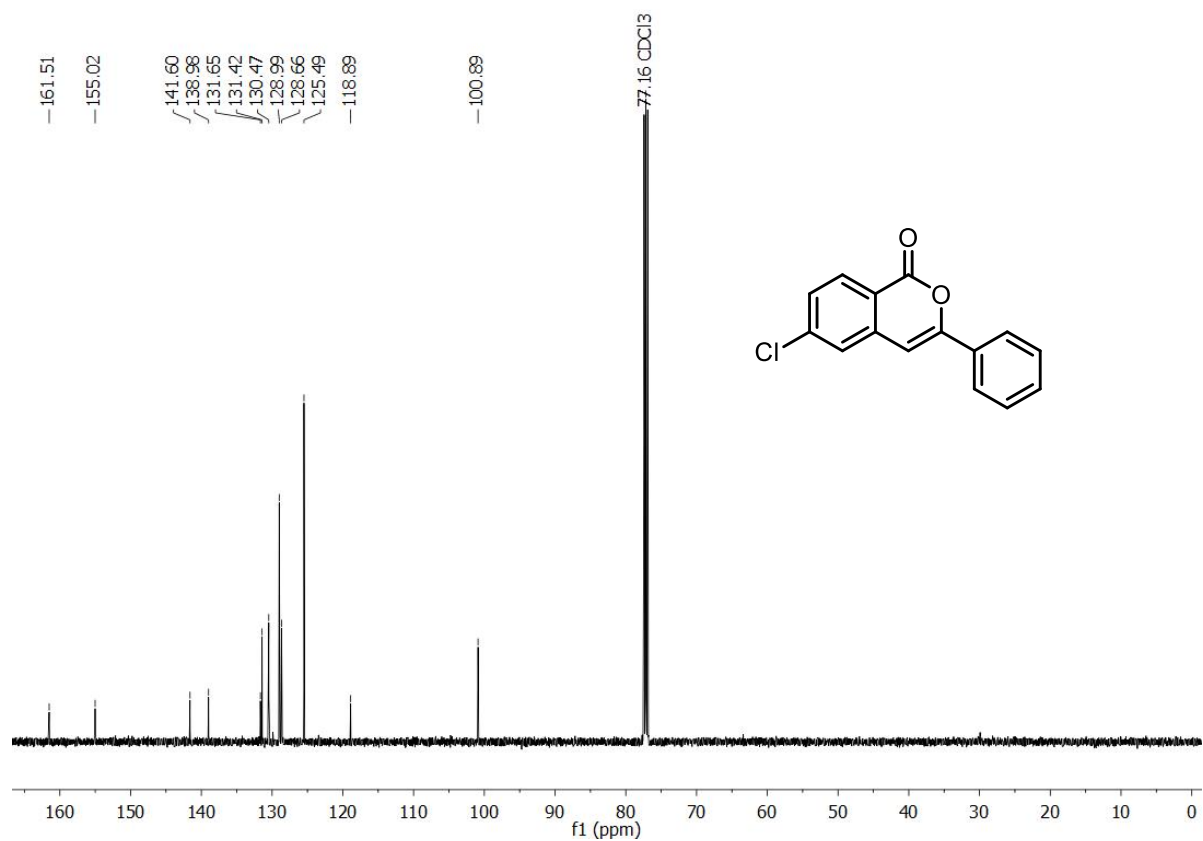
**$^{19}\text{F}$  NMR of compound 210, 6-fluoro-3-phenyl-1*H*-isochromen-1-one, 377 MHz,  $\text{CDCl}_3$ , 299 K**



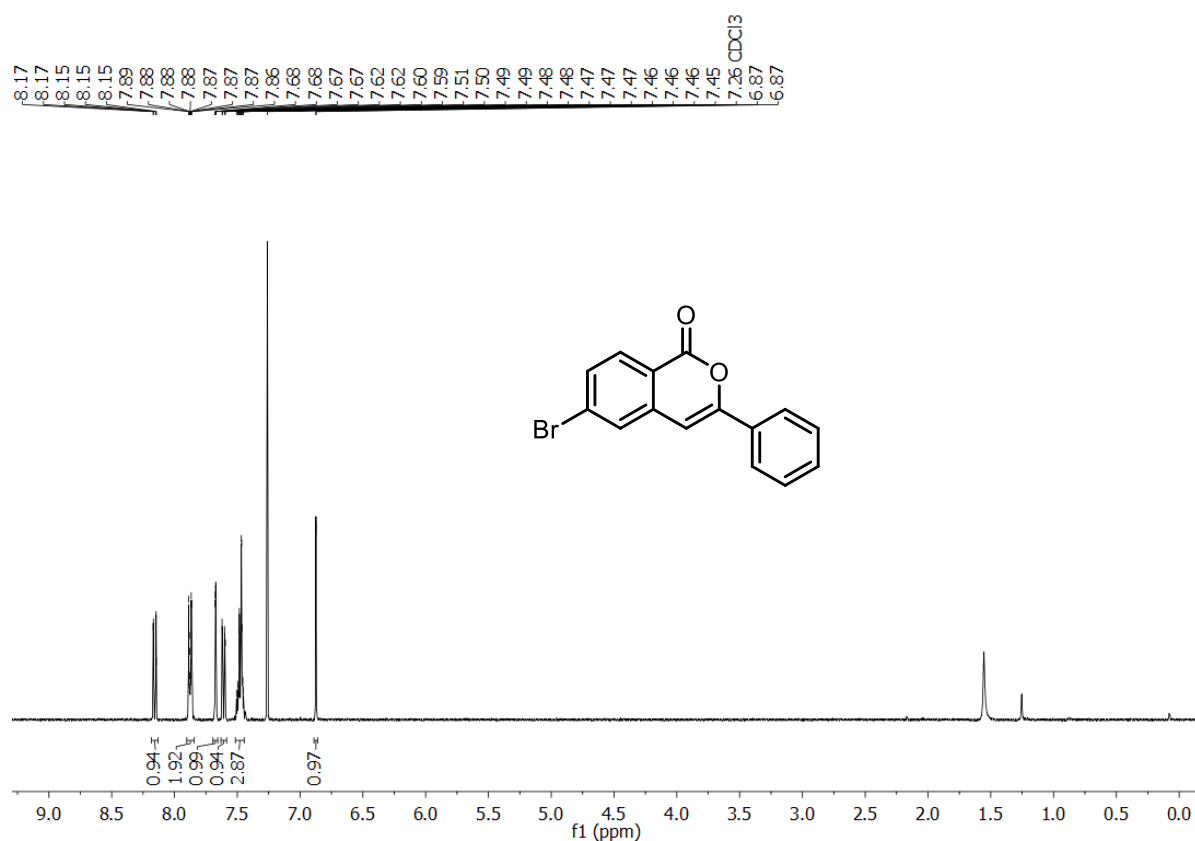
**<sup>1</sup>H NMR of compound 211, 6-chloro-3-phenyl-1*H*-isochromen-1-one, 300 MHz, CDCl<sub>3</sub>, 298 K**



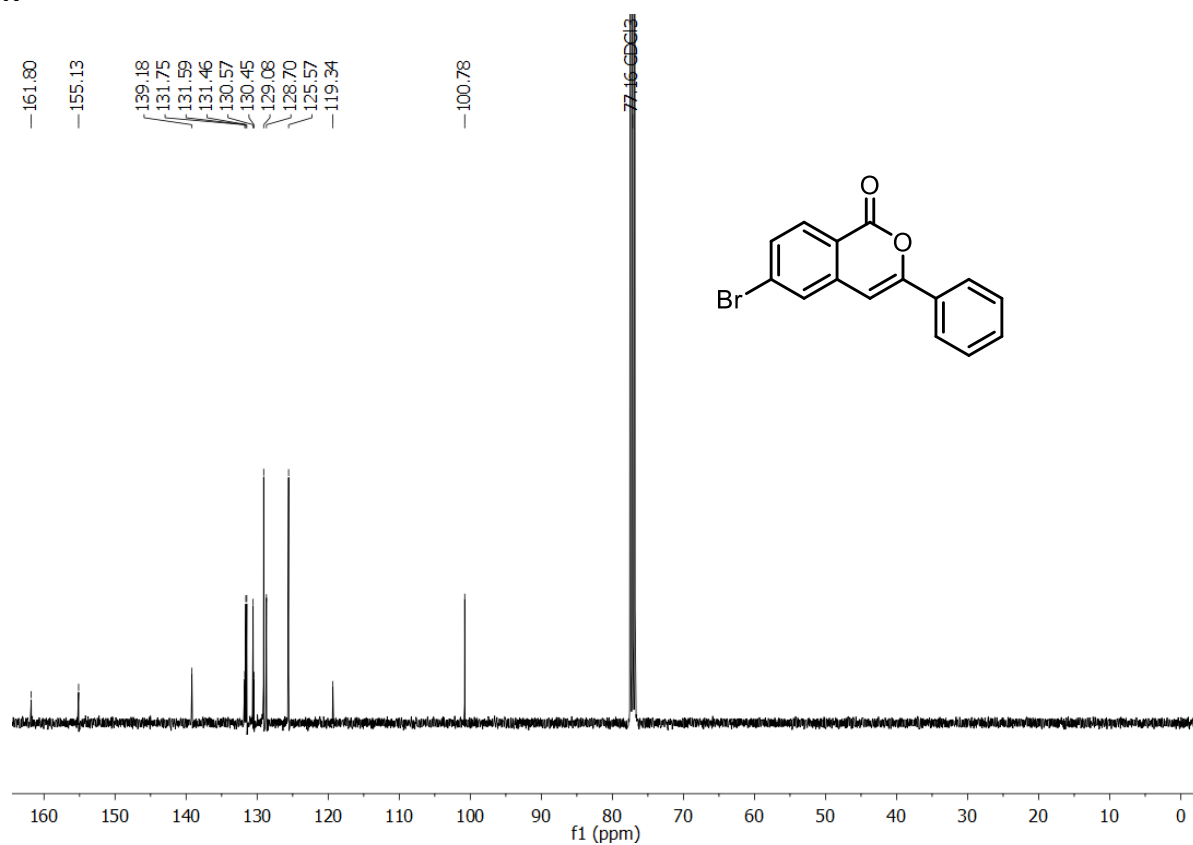
**<sup>13</sup>C NMR of compound 211, 6-chloro-3-phenyl-1*H*-isochromen-1-one, 126 MHz, CDCl<sub>3</sub>, 298 K**



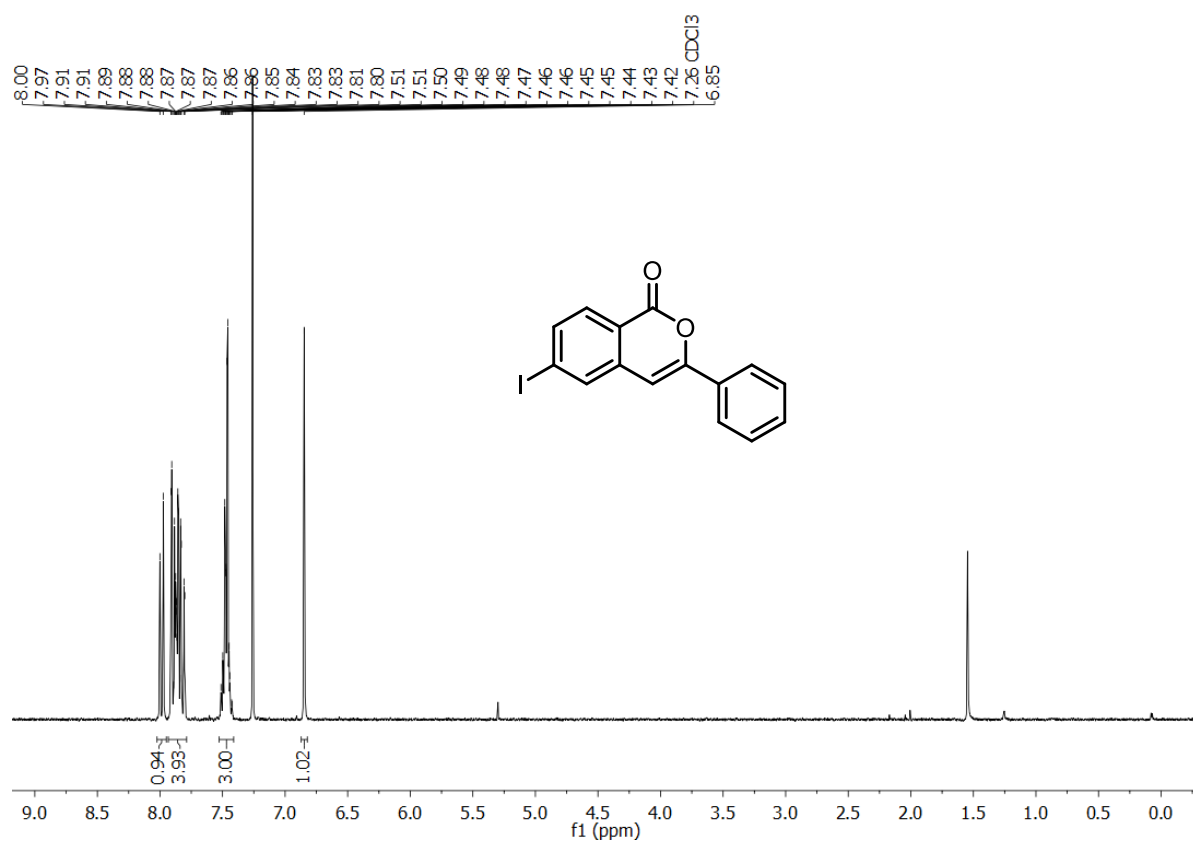
**<sup>1</sup>H NMR of compound 212, 6-bromo-3-phenyl-1*H*-isochromen-1-one, 400 MHz, CDCl<sub>3</sub>, 298 K**



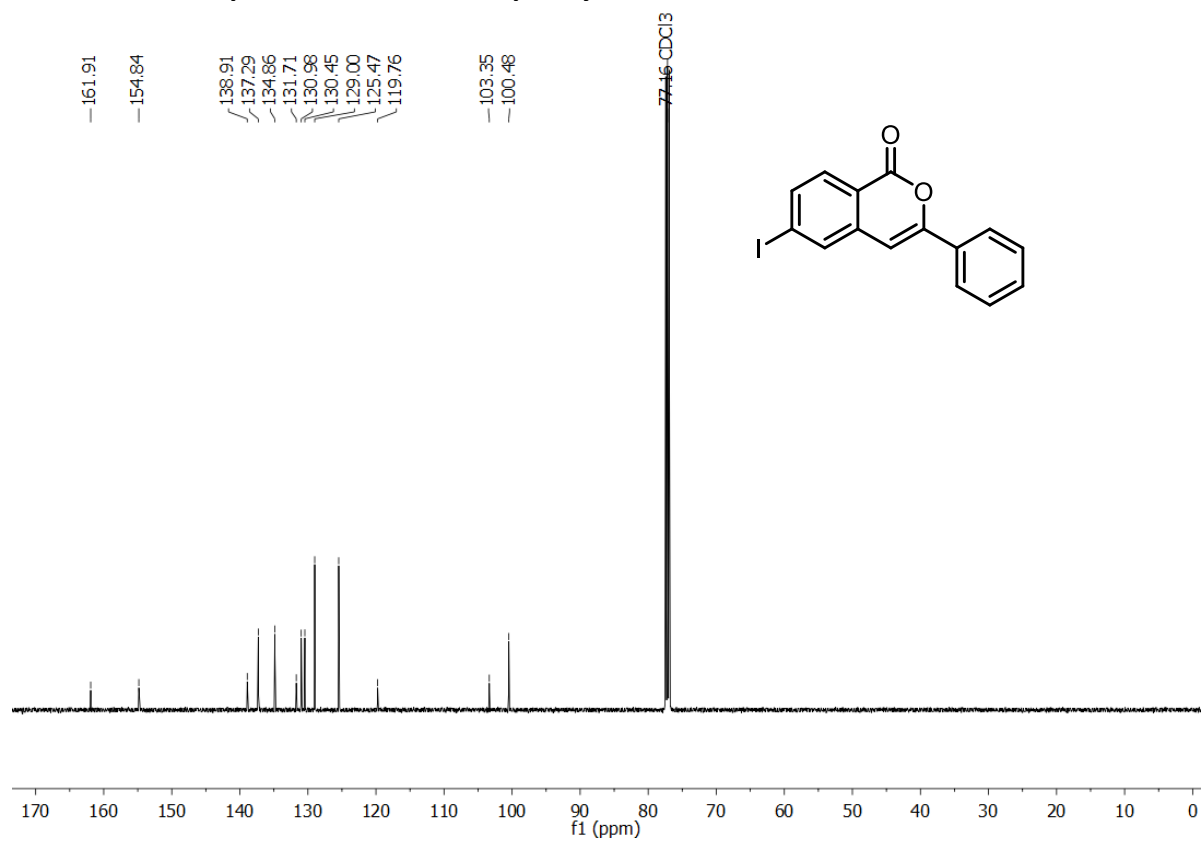
**<sup>13</sup>C NMR of compound 212, 6-bromo-3-phenyl-1*H*-isochromen-1-one, 101 MHz, CDCl<sub>3</sub>, 299 K**



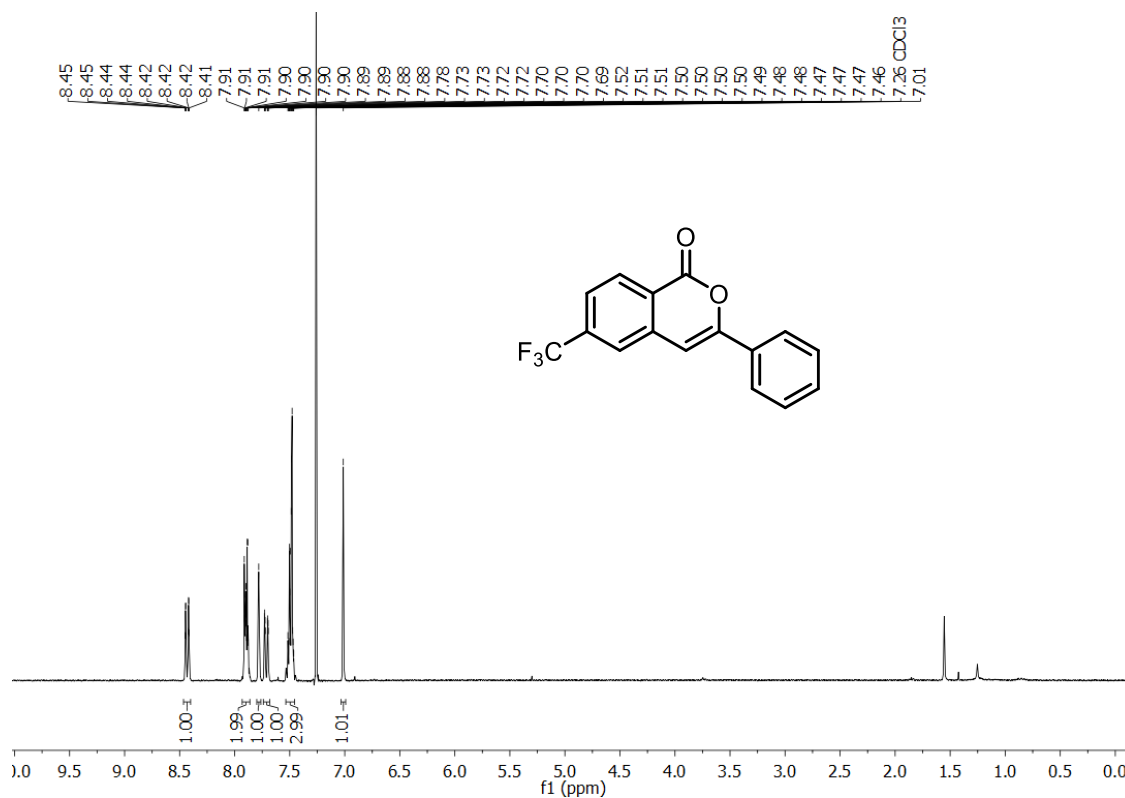
**<sup>1</sup>H NMR of compound 213, 6-iodo-3-phenyl-1*H*-isochromen-1-one, 300 MHz, CDCl<sub>3</sub>, 298 K**



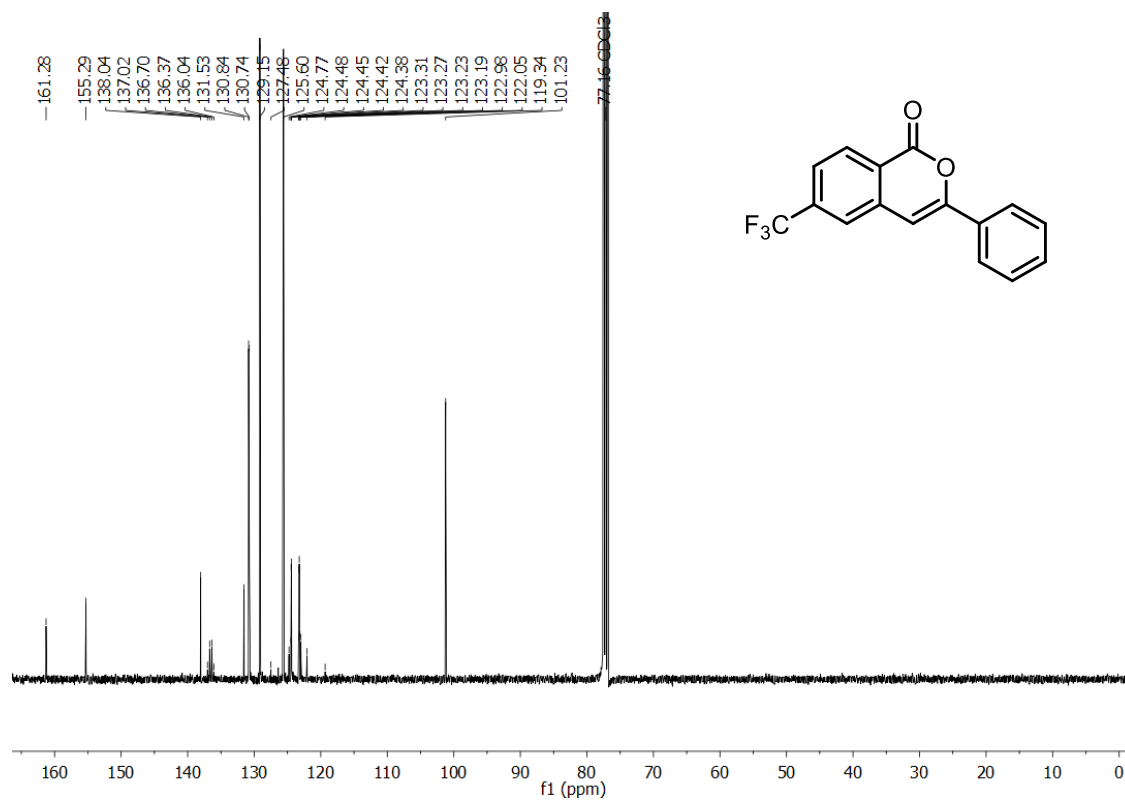
**<sup>13</sup>C NMR of compound 213, 6-iodo-3-phenyl-1*H*-isochromen-1-one, 126 MHz, CDCl<sub>3</sub>, 298 K**



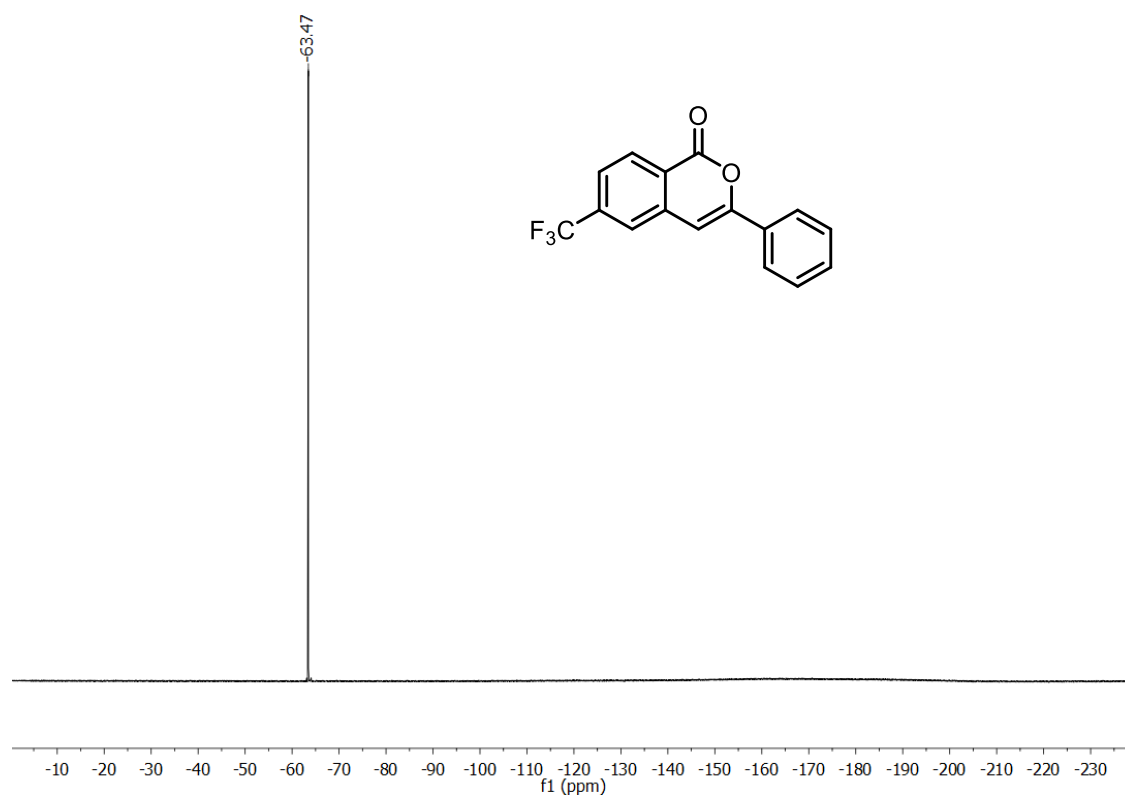
**<sup>1</sup>H NMR of compound 214, 3-phenyl-6-(trifluoromethyl)-1*H*-isochromen-1-one, 300 MHz, CDCl<sub>3</sub>, 300 K**



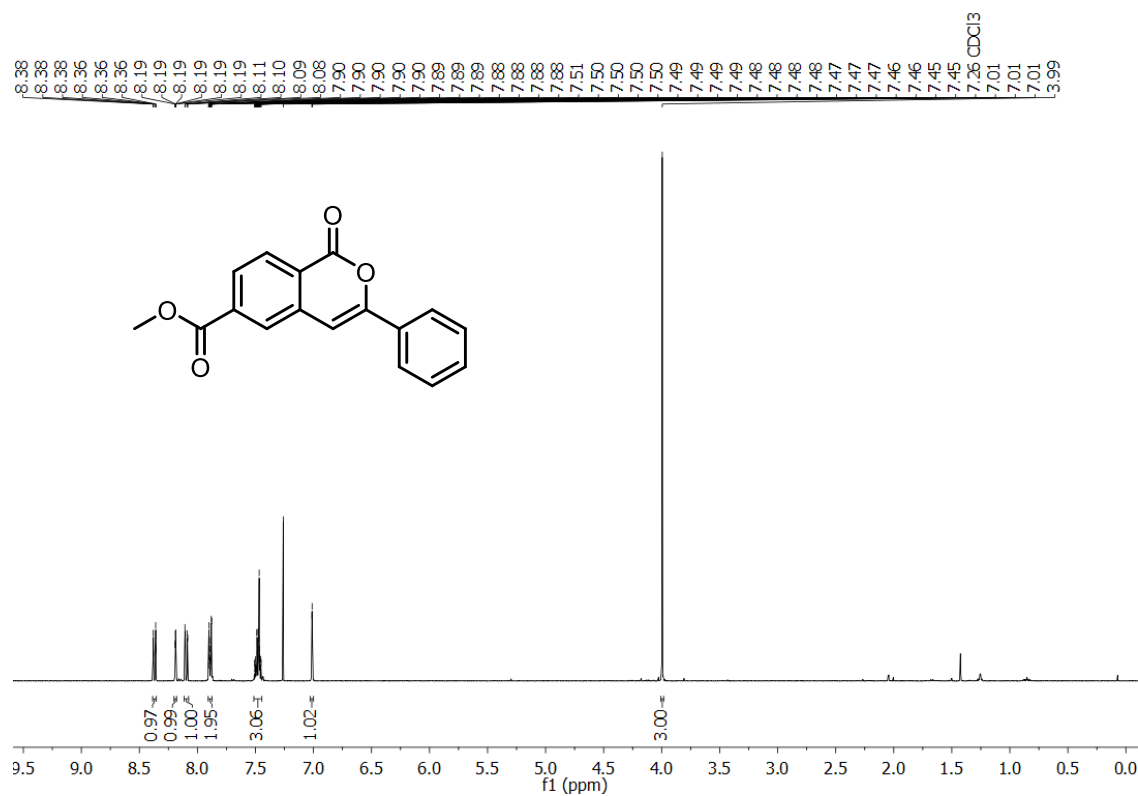
**<sup>13</sup>C NMR of compound 214, 3-phenyl-6-(trifluoromethyl)-1*H*-isochromen-1-one, 101 MHz, CDCl<sub>3</sub>, 298 K**



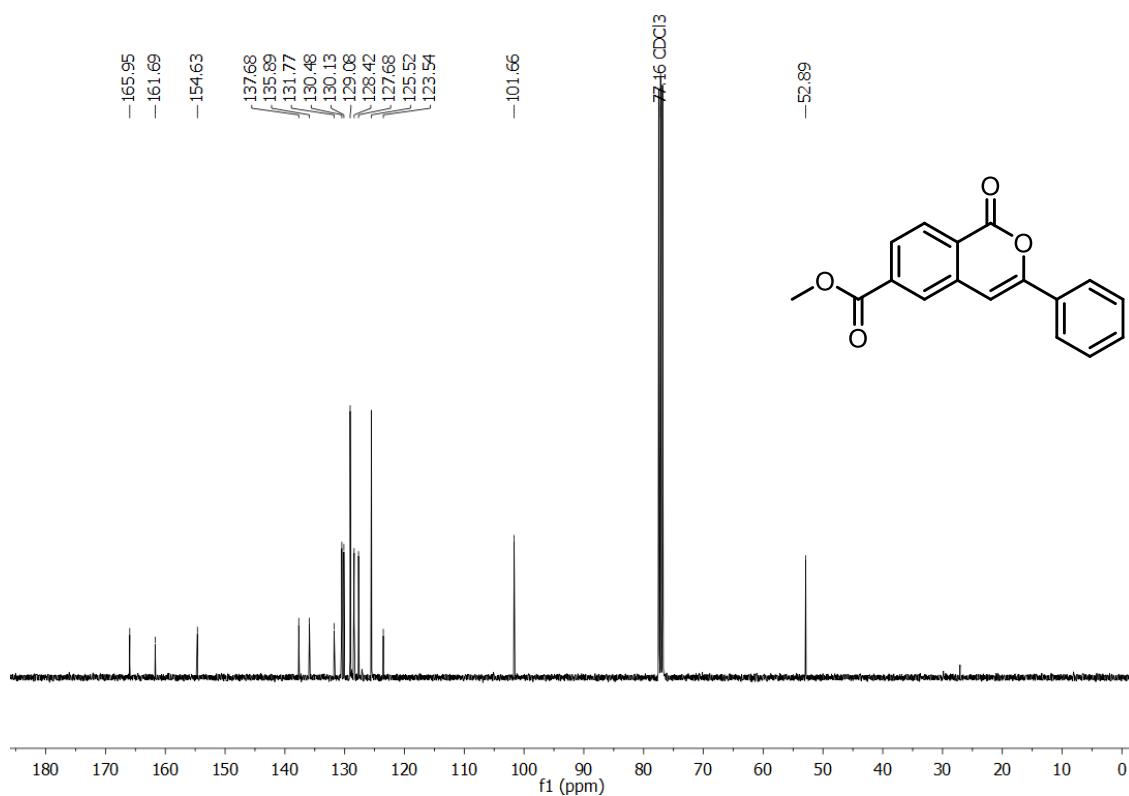
**$^{19}\text{F}$  NMR of compound 214, 3-phenyl-6-(trifluoromethyl)-1*H*-isochromen-1-one, 282 MHz,  $\text{CDCl}_3$ , 300 K**



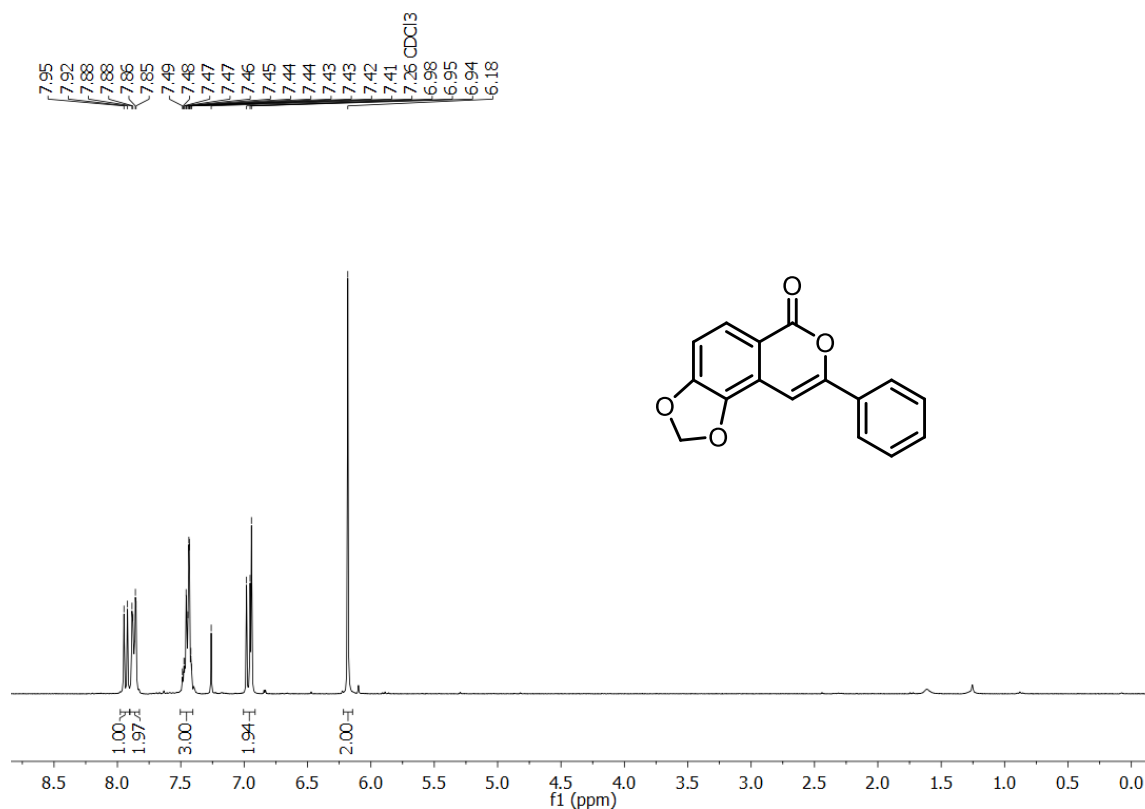
**$^1\text{H}$  NMR of compound 215, methyl 1-oxo-3-phenyl-1*H*-isochromene-6-carboxylate, 400 MHz,  $\text{CDCl}_3$ , 299 K**



**$^{13}\text{C}$  NMR of compound 215, methyl 1-oxo-3-phenyl-1*H*-isochromene-6-carboxylate, 101 MHz,  $\text{CDCl}_3$ , 300 K**

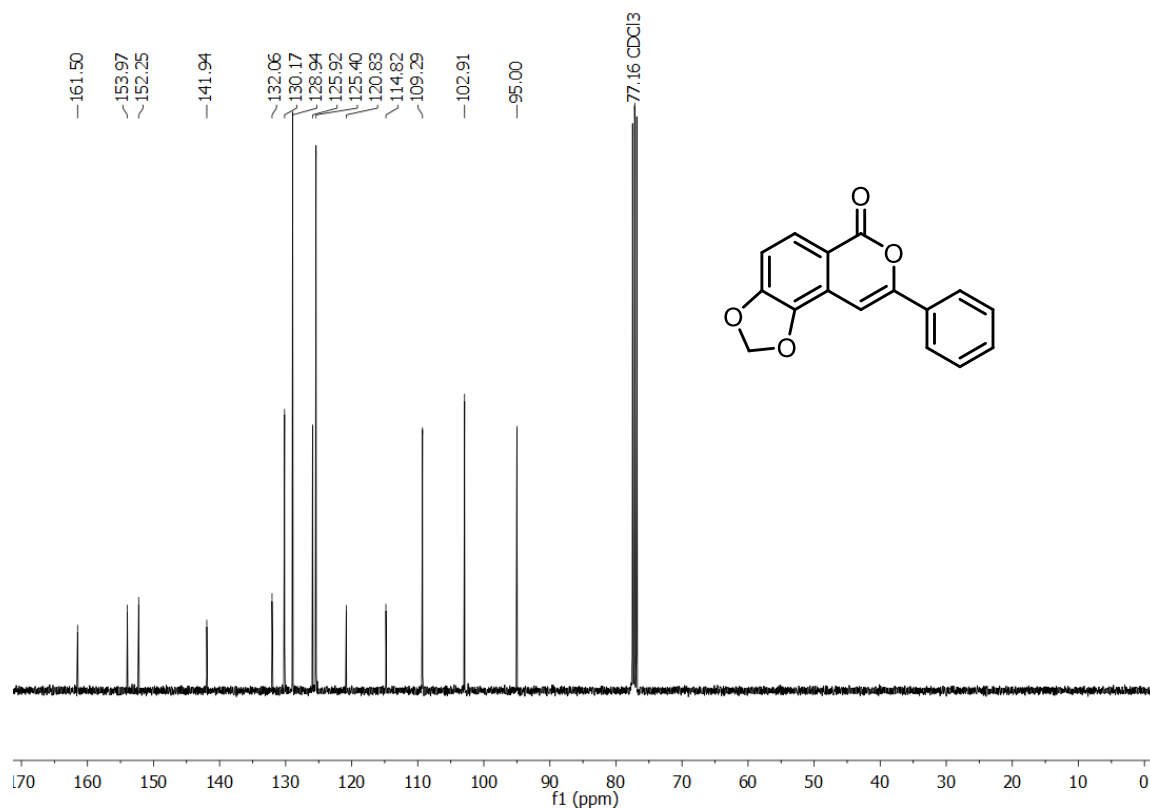


**$^1\text{H}$  NMR of compound 216, 8-phenyl-6*H*-[1,3]dioxolo[4,5-*f*]isochromen-6-one, 300 MHz,  $\text{CDCl}_3$ , 298 K**

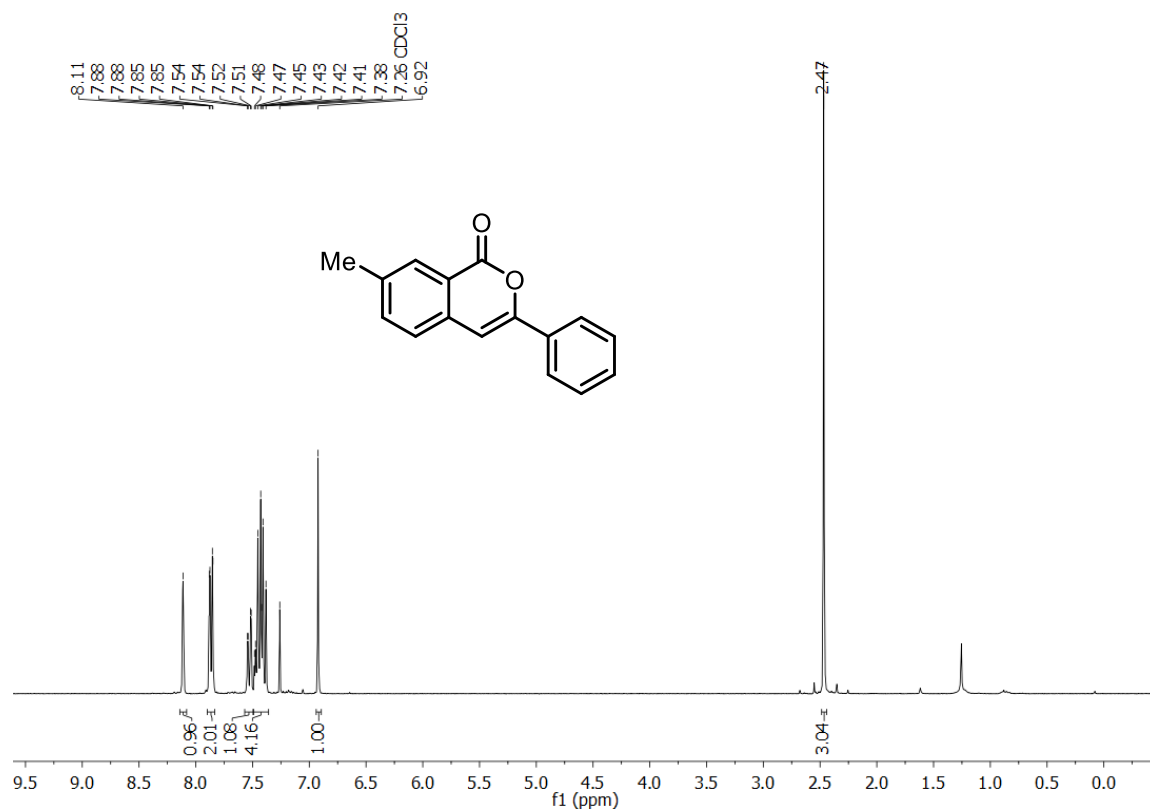




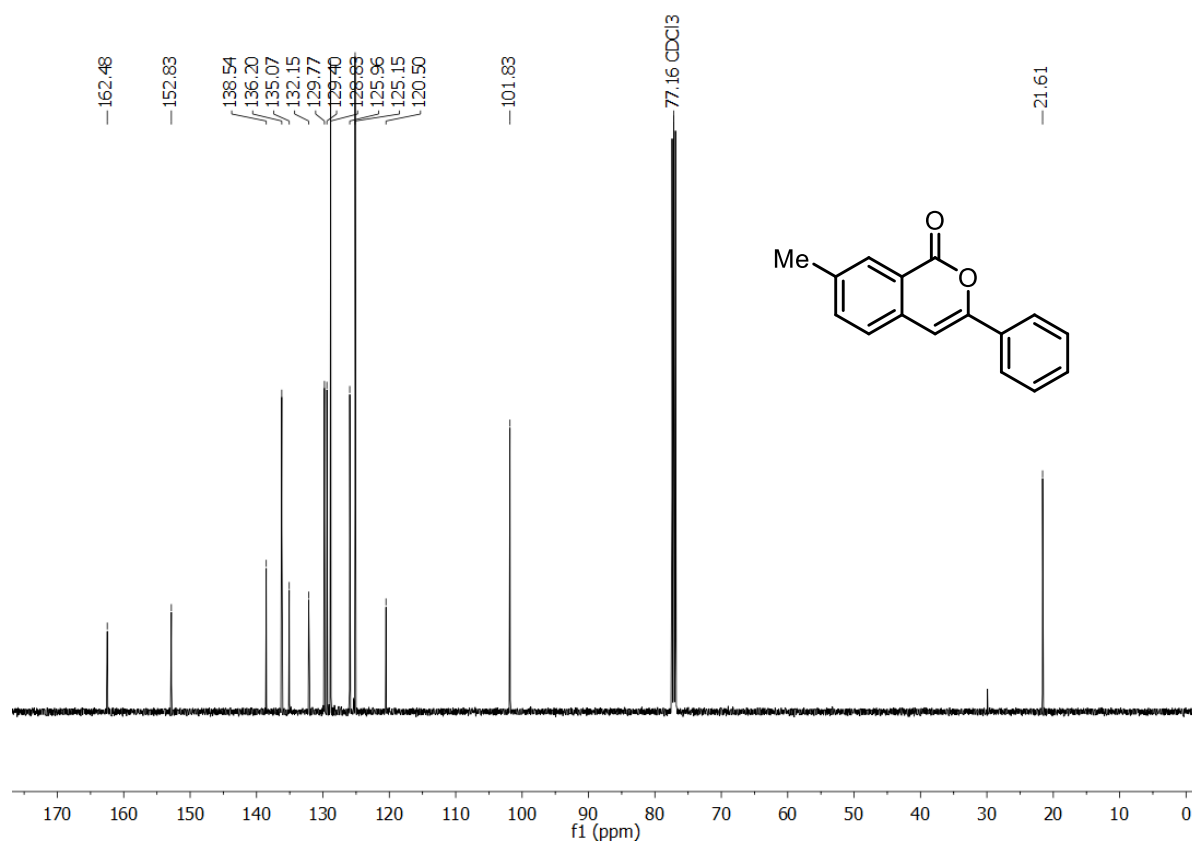
**$^{13}\text{C}$  NMR of compound 216, 8-phenyl-6*H*-[1,3]dioxolo[4,5-*f*]isochromen-6-one, 100 MHz,  $\text{CDCl}_3$ , 298 K**



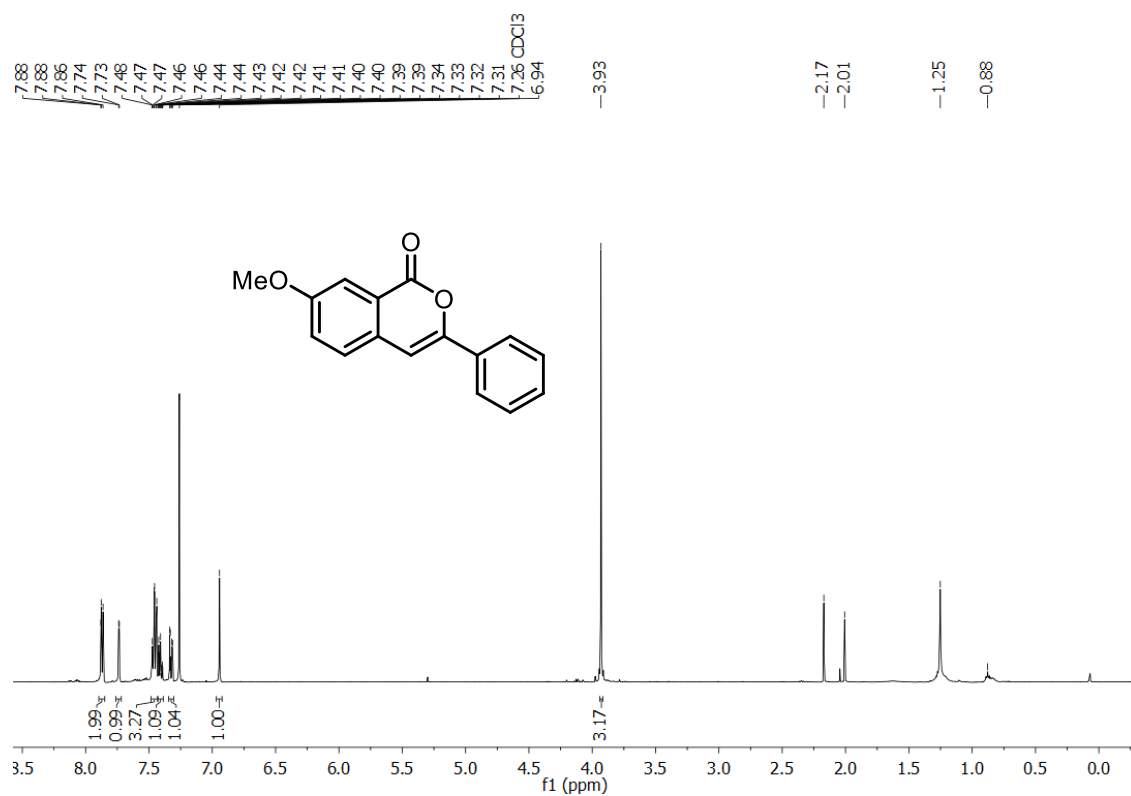
**$^1\text{H}$  NMR of compound 217, 7-methyl-3-phenyl-1*H*-isochromen-1-one, 300 MHz,  $\text{CDCl}_3$ , 298 K**



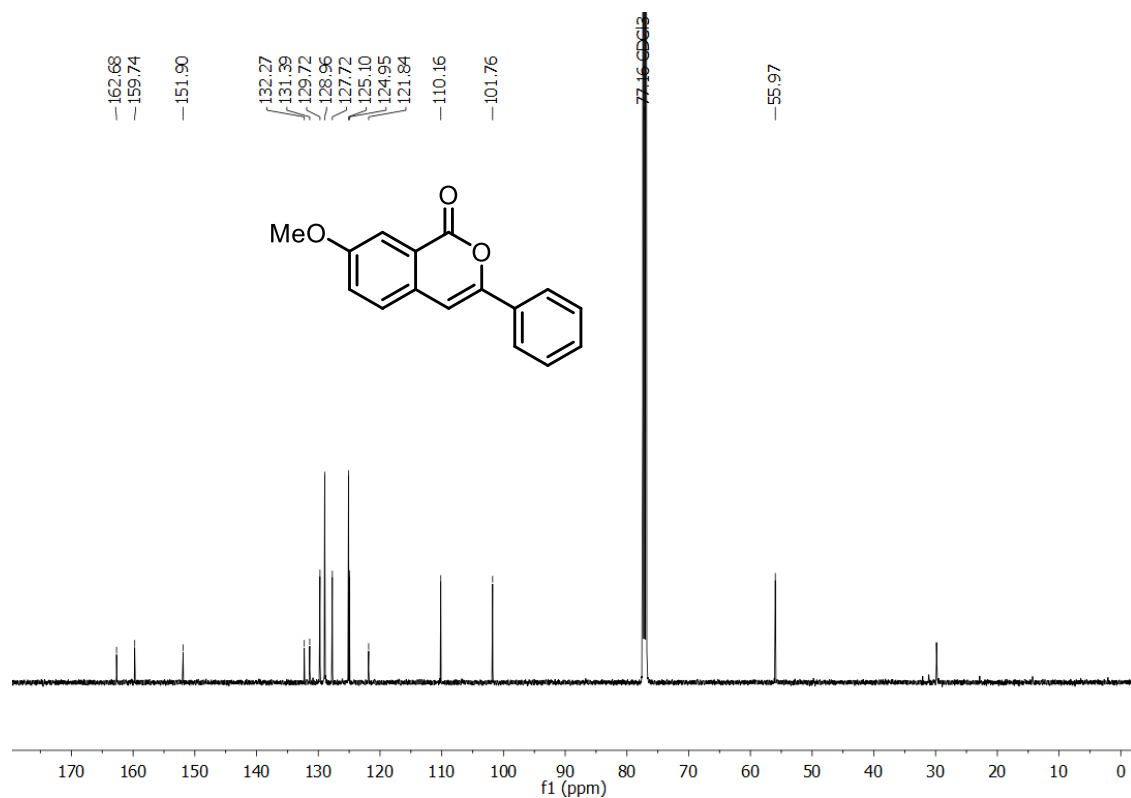
**$^{13}\text{C}$  NMR of compound 217, 7-methyl-3-phenyl-1*H*-isochromen-1-one, 300 MHz,  $\text{CDCl}_3$ , 298 K**



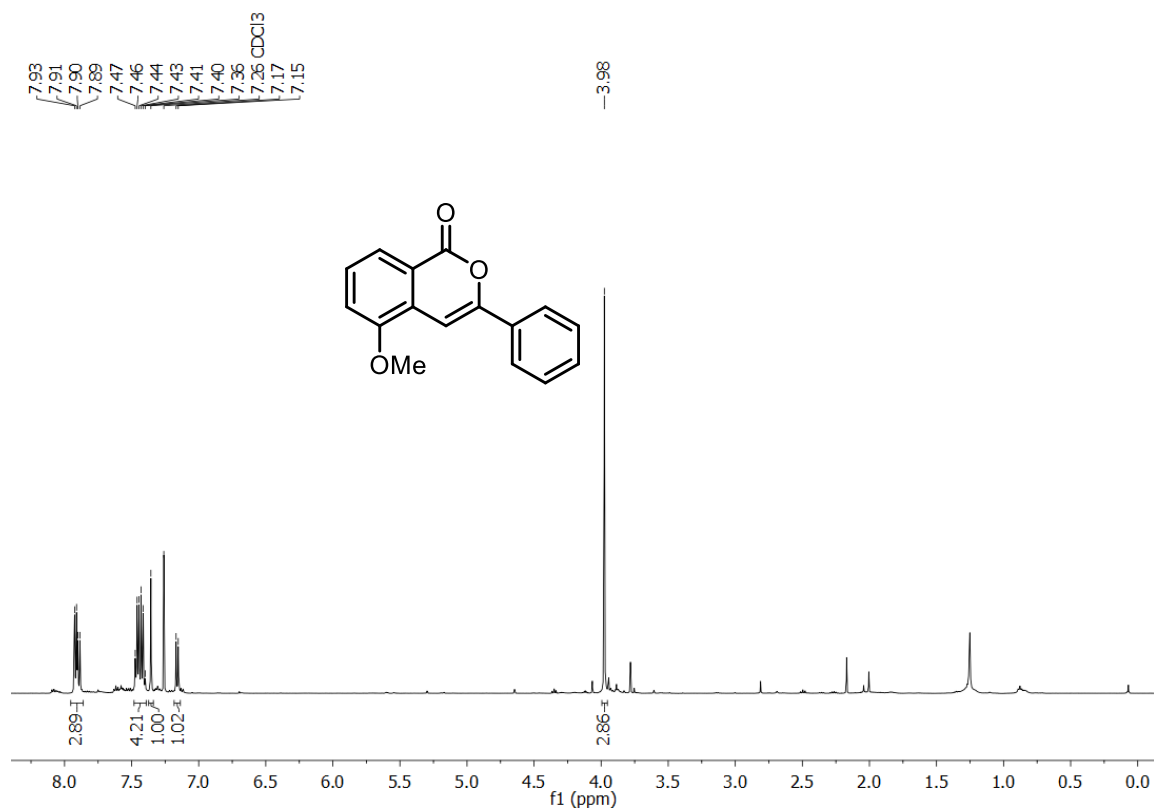
**$^1\text{H}$  NMR of compound 218a, 7-methoxy-3-phenyl-1*H*-isochromen-1-one, 500 MHz,  $\text{CD}_3\text{CN}$ , 298 K**



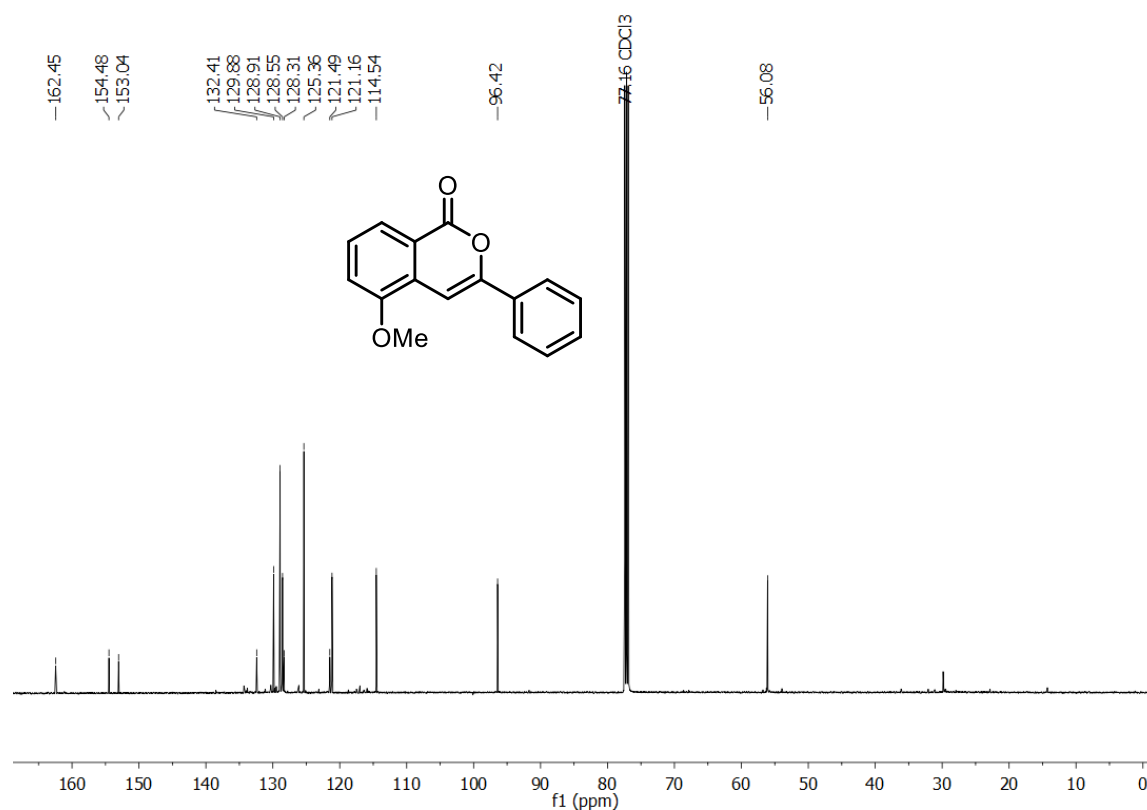
**$^{13}\text{C}$  NMR of compound 218a, 7-methoxy-3-phenyl-1*H*-isochromen-1-one, 126 MHz,  $\text{CD}_3\text{CN}$ , 298 K**



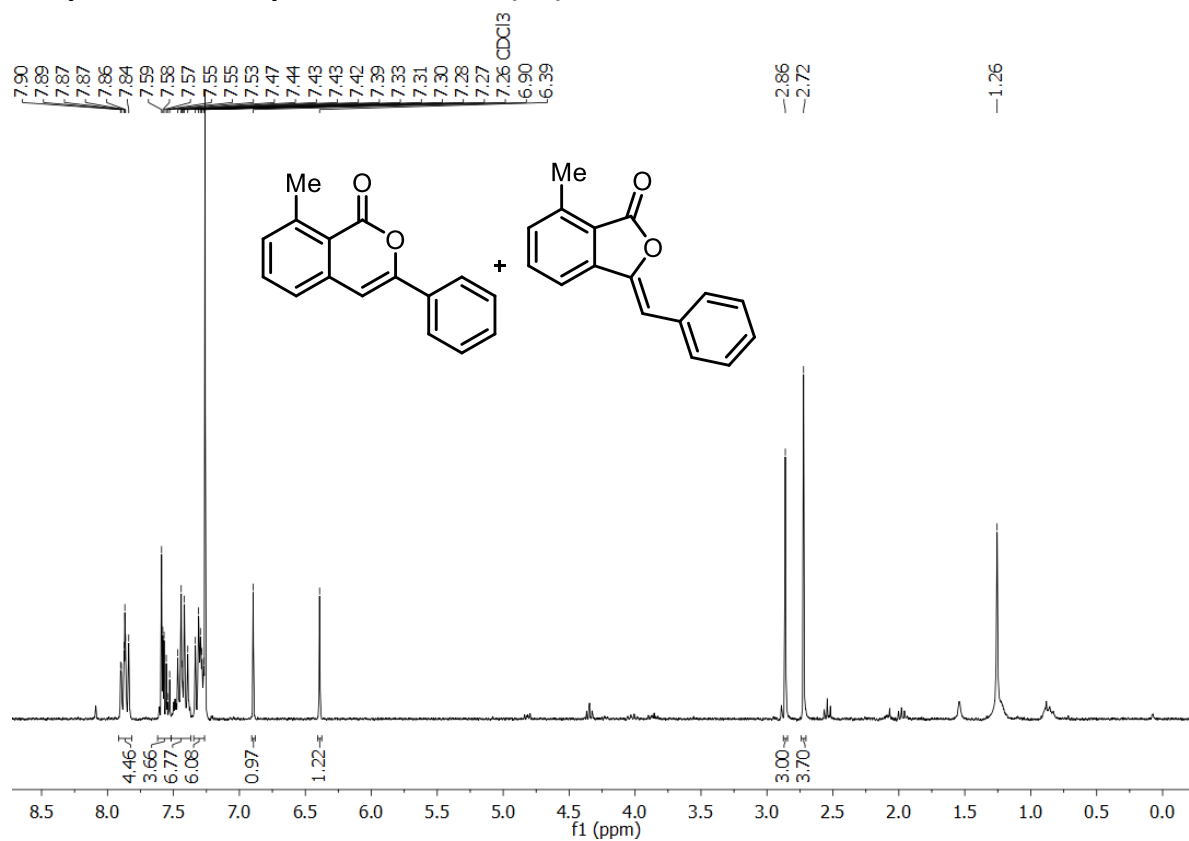
**$^1\text{H}$  NMR of compound 218b, 5-methoxy-3-phenyl-1*H*-isochromen-1-one, 500 MHz,  $\text{CDCl}_3$ , 298 K**



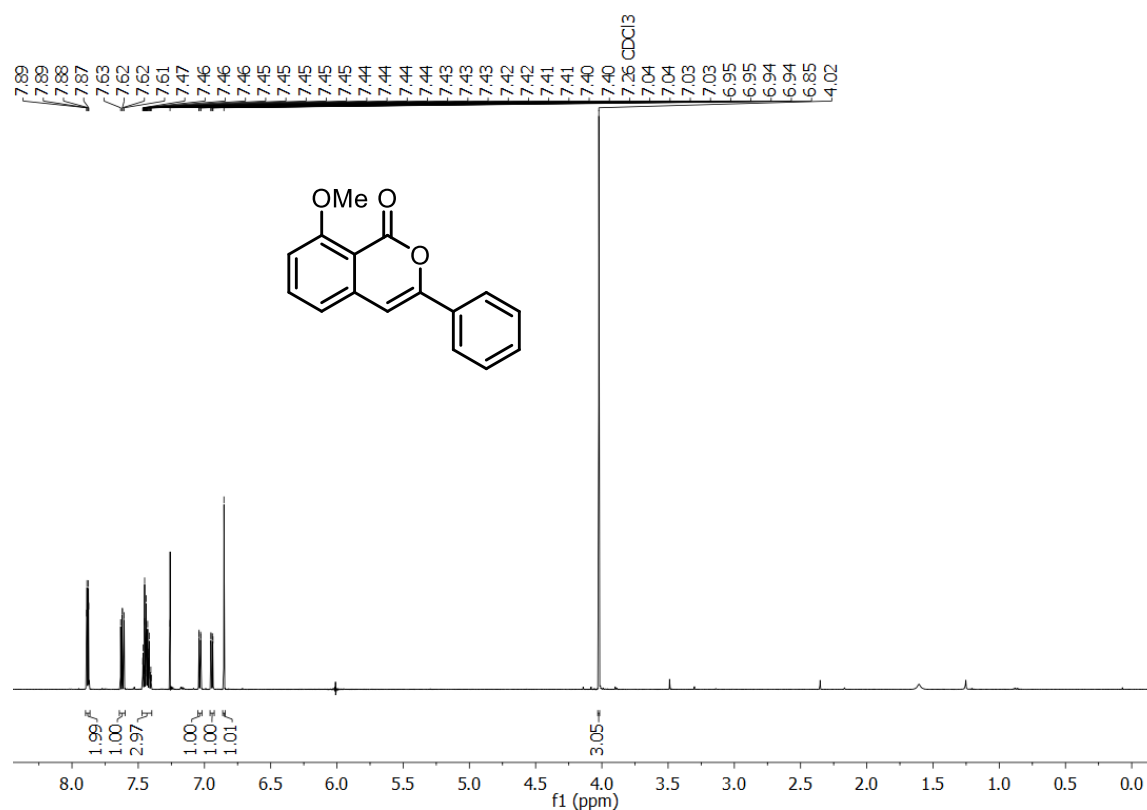
**$^{13}\text{C}$  NMR of compound 218b, 5-methoxy-3-phenyl-1*H*-isochromen-1-one, 126 MHz,  $\text{CDCl}_3$ , 298 K**



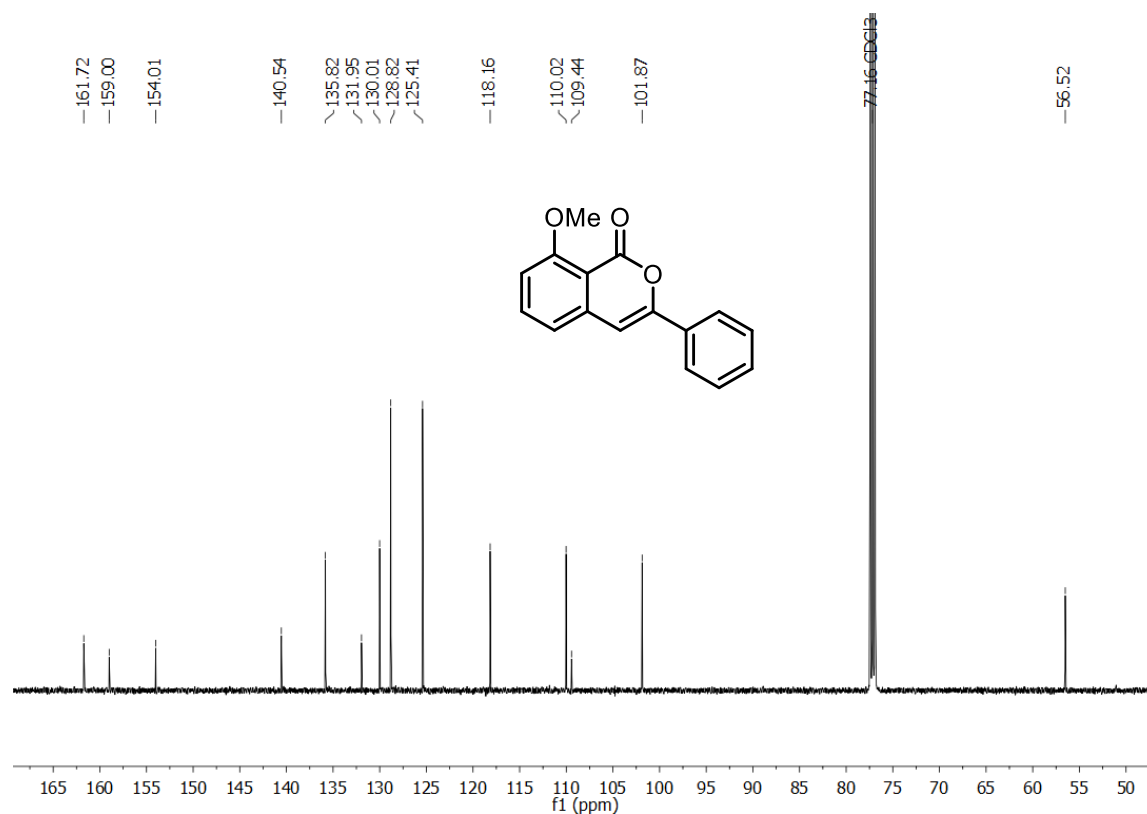
**$^1\text{H}$  NMR of compound 219a and 219b, 8-methyl-3-phenyl-1*H*-isochromen-1-one and (*Z*)-3-benzylidene-7-methylisobenzofuran-1(3*H*)-one, 300 MHz,  $\text{CDCl}_3$ , 298 K**



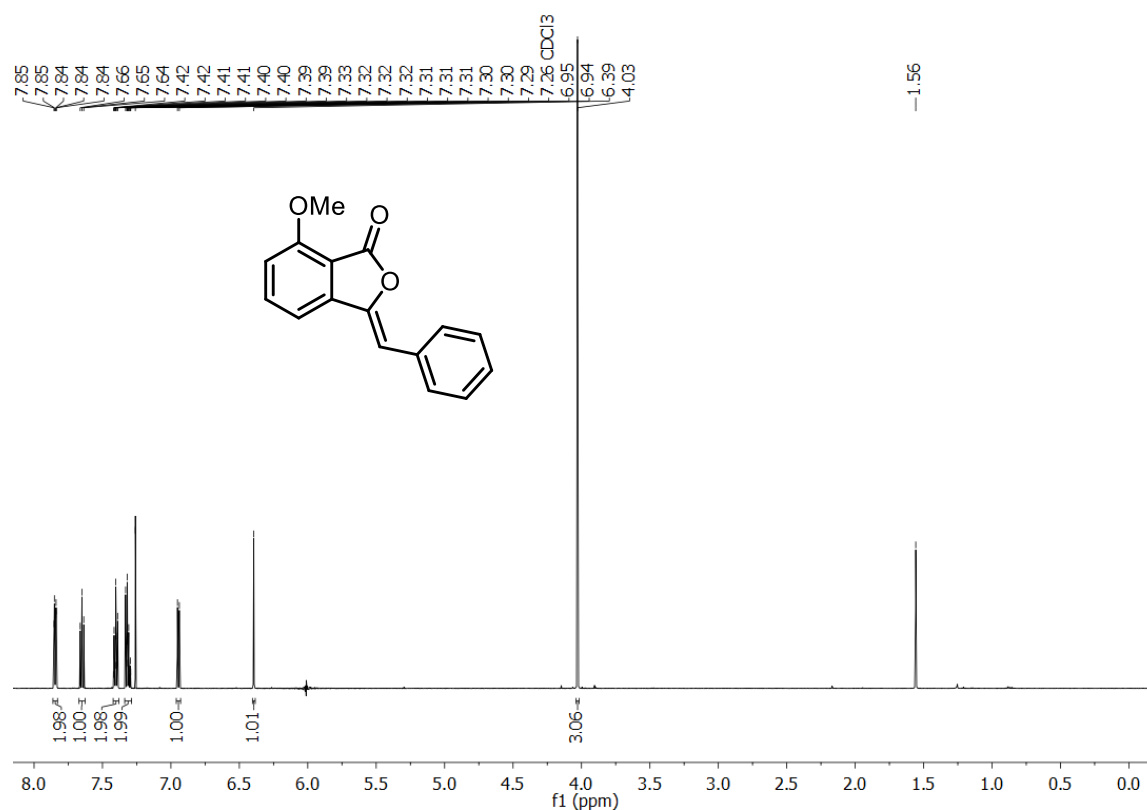
**<sup>1</sup>H NMR of compound 220a, 8-methoxy-3-phenyl-1*H*-isochromen-1-one, 600 MHz, CDCl<sub>3</sub>, 298 K**



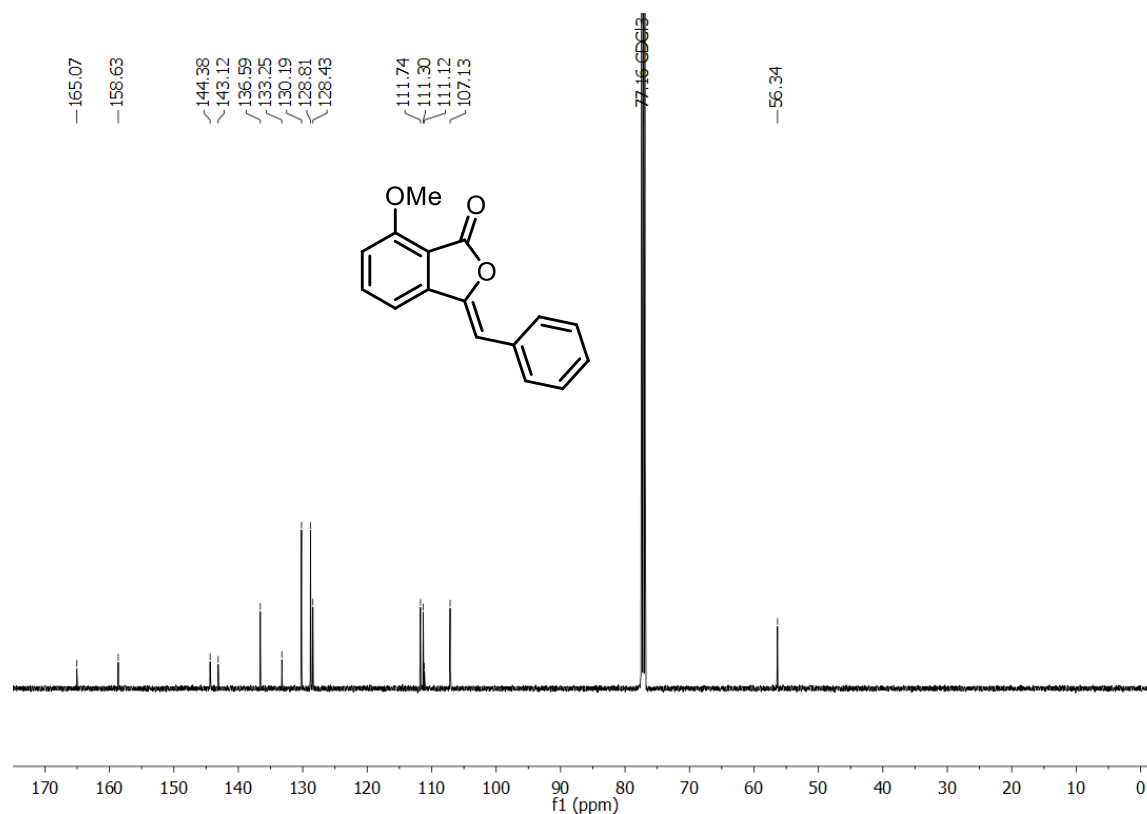
**<sup>13</sup>C NMR of compound 220a, 8-methoxy-3-phenyl-1*H*-isochromen-1-one, 126 MHz, CDCl<sub>3</sub>, 298 K**



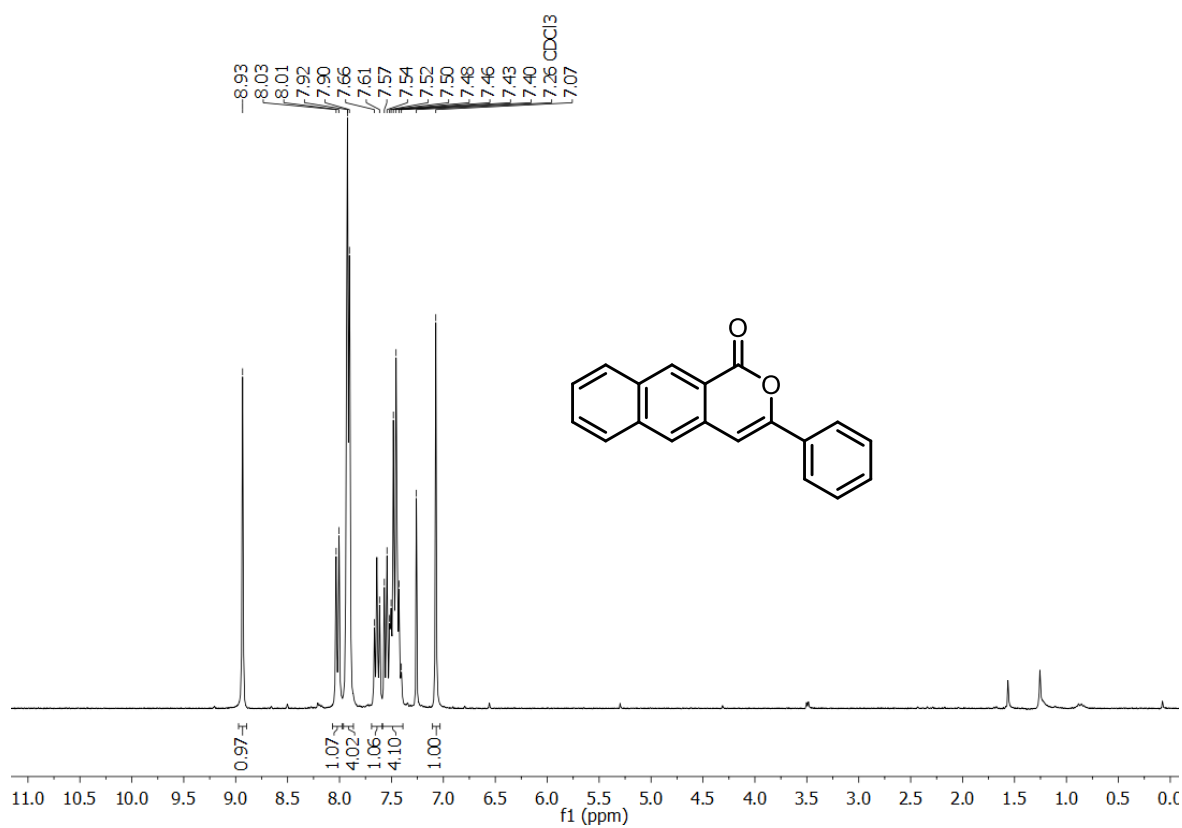
**<sup>1</sup>H NMR of compound 220b, (Z)-3-benzylidene-7-methoxyisobenzofuran-1(3H)-one, 600 MHz, CDCl<sub>3</sub>, 298 K**



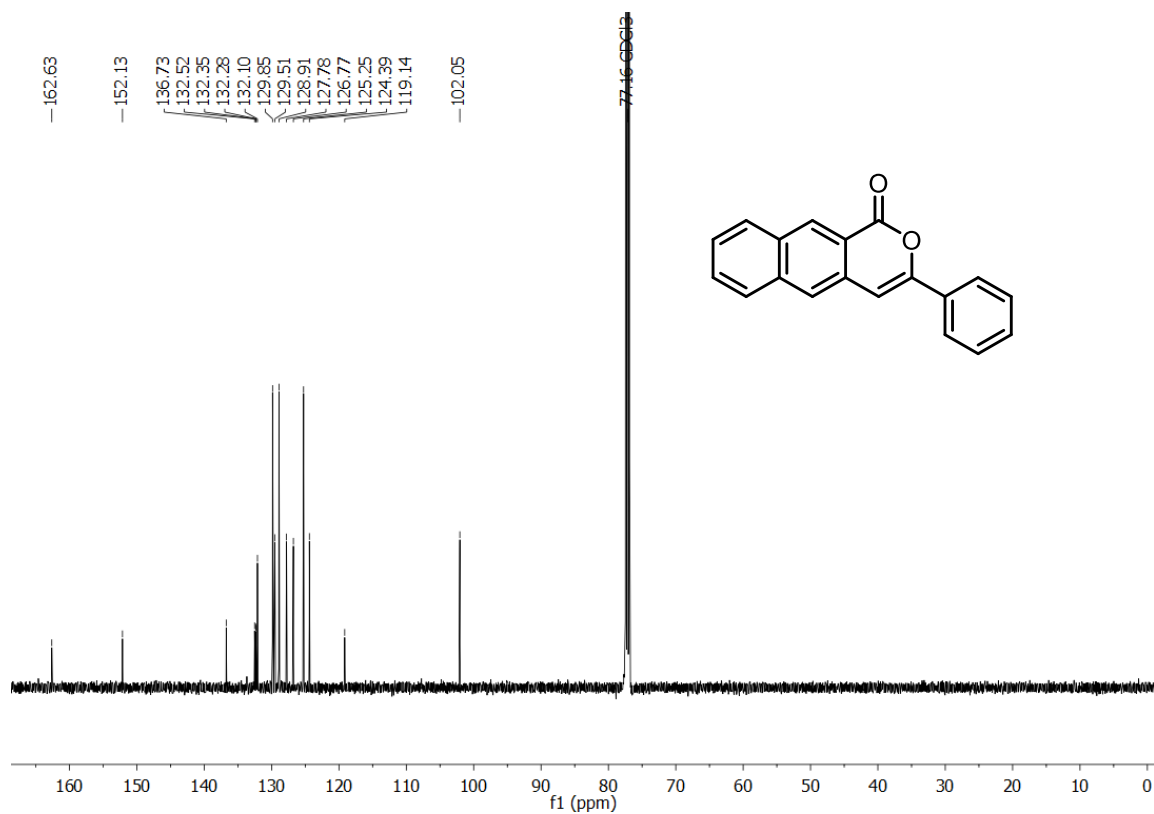
**<sup>13</sup>C NMR of compound 220b, (Z)-3-benzylidene-7-methoxyisobenzofuran-1(3H)-one, 126 MHz, CDCl<sub>3</sub>, 298 K**



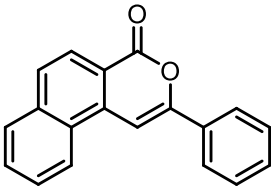
**<sup>1</sup>H NMR of compound 221a, 3-phenyl-1H-benzo[g]isochromen-1-one, 300 MHz, CDCl<sub>3</sub>, 298 K**



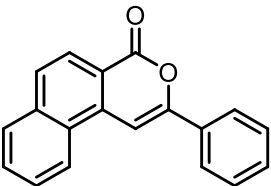
**<sup>13</sup>C NMR of compound 221a, 3-phenyl-1H-benzo[g]isochromen-1-one, 101 MHz, CDCl<sub>3</sub>, 298 K**



## K

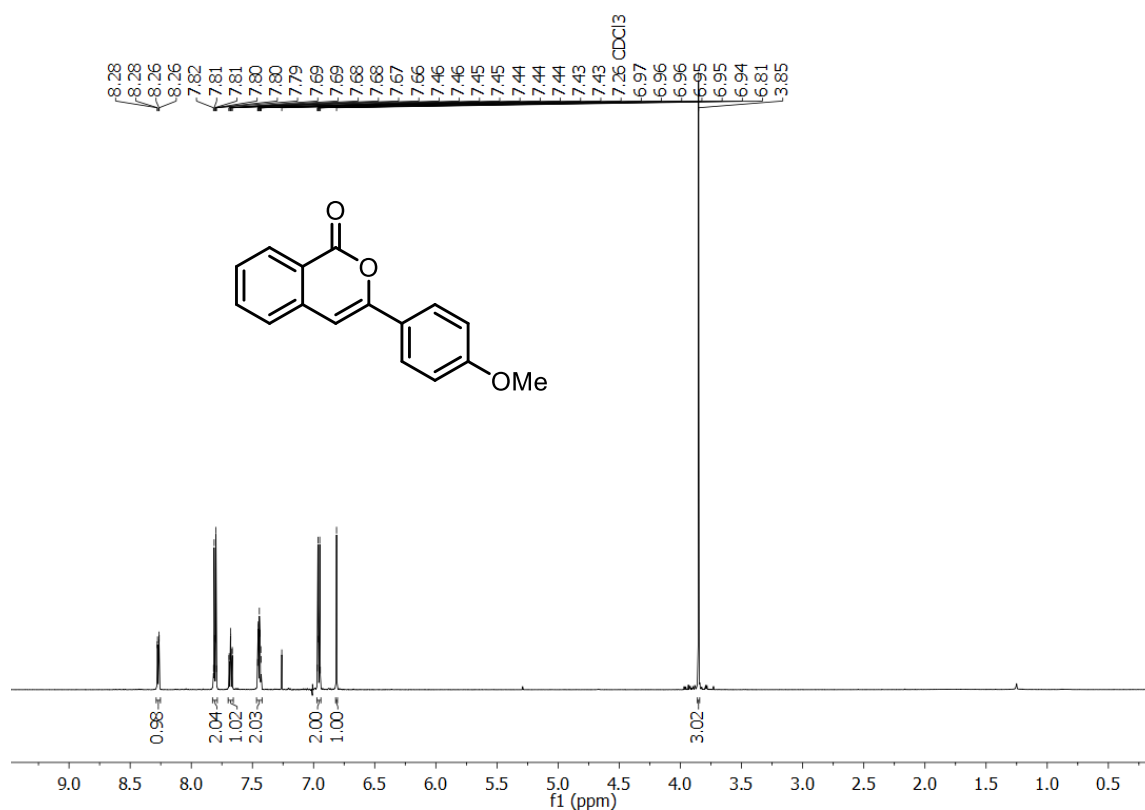


## K

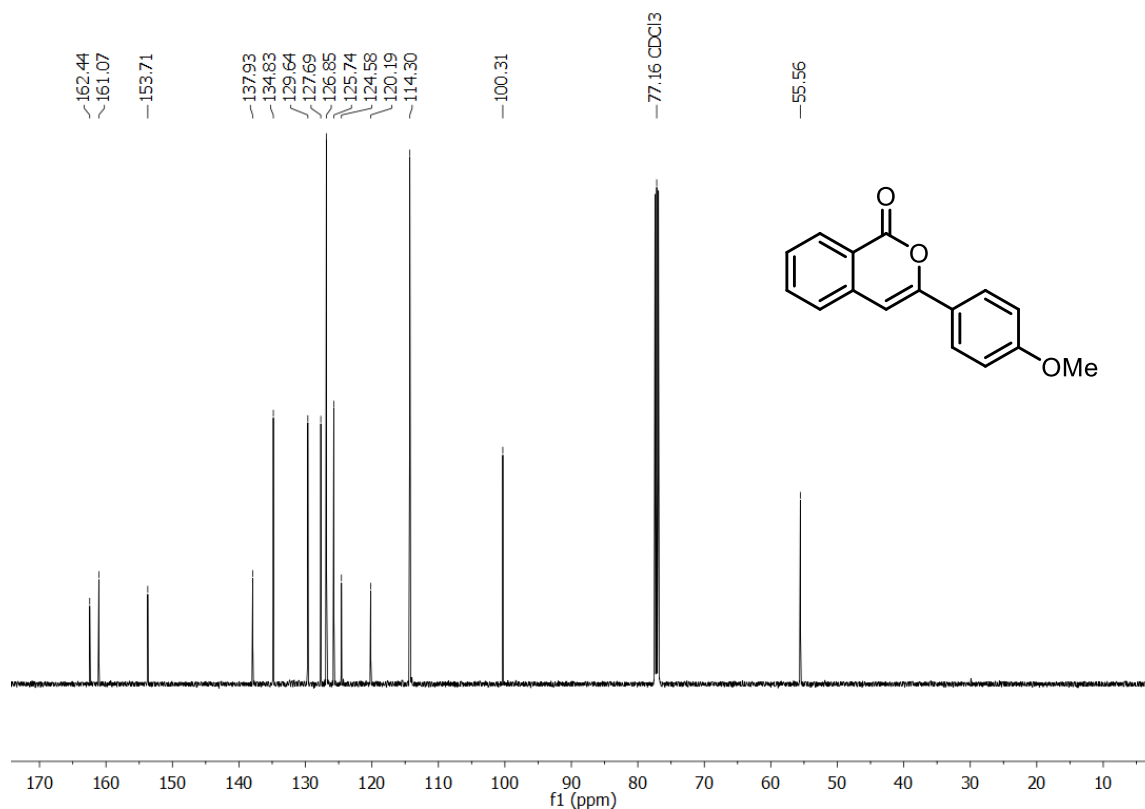




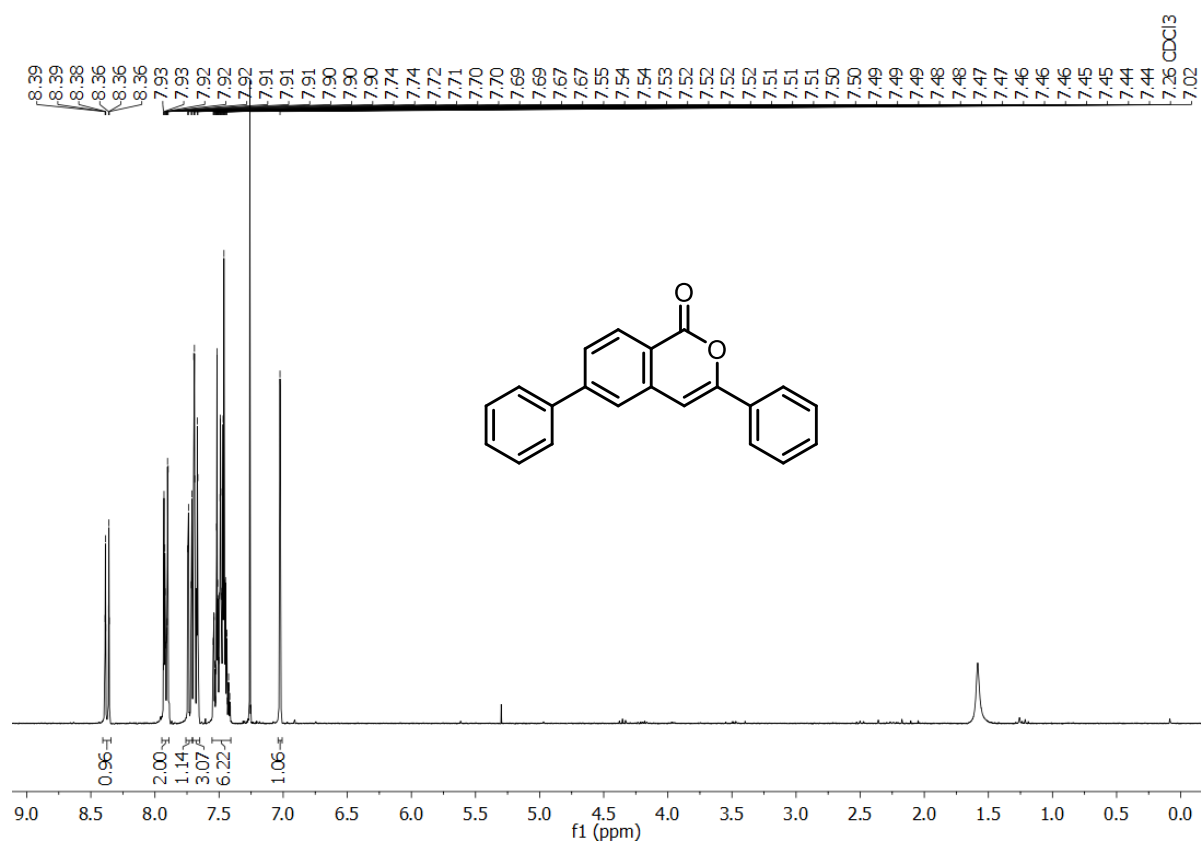
**<sup>1</sup>H NMR of compound 222, 3-(4-methoxyphenyl)-1*H*-isochromen-1-one, 600 MHz, CDCl<sub>3</sub>, 298 K**



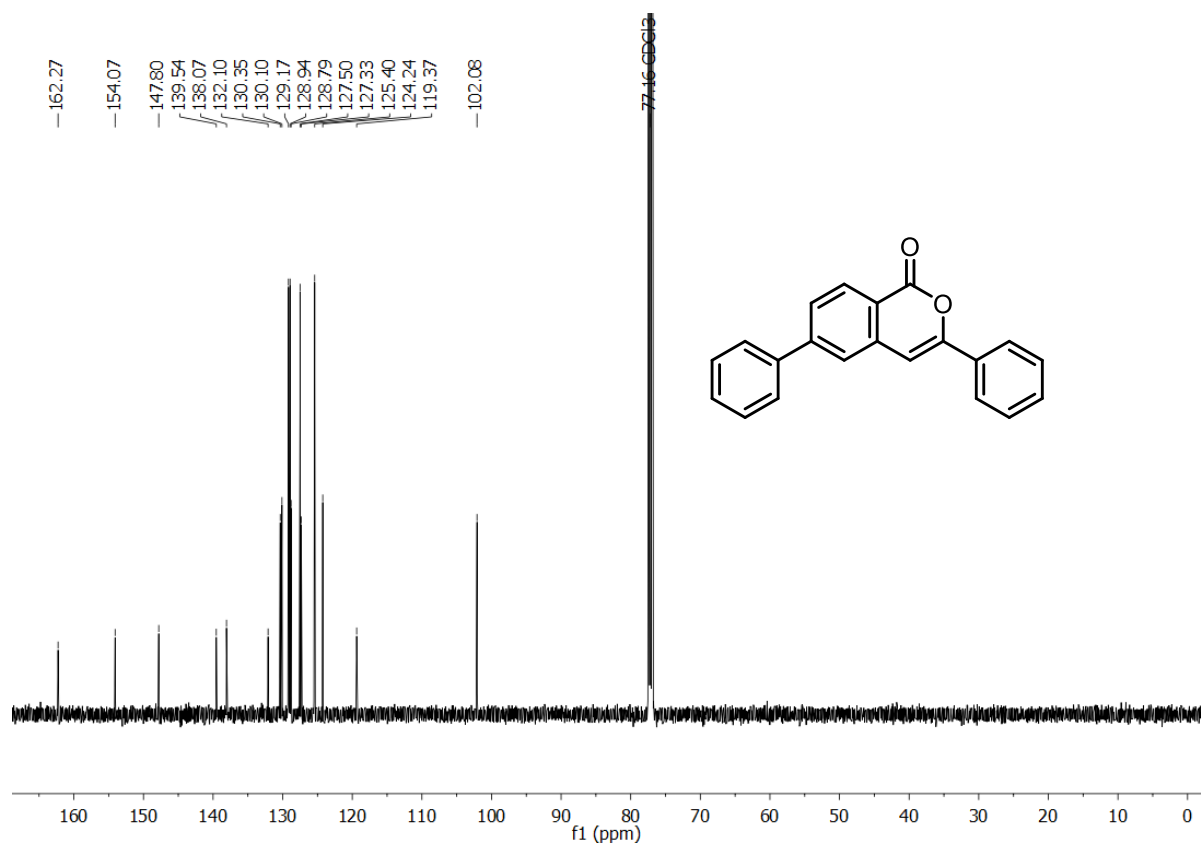
**<sup>13</sup>C NMR of compound 222, 3-(4-methoxyphenyl)-1*H*-isochromen-1-one, 126 MHz, CDCl<sub>3</sub>, 298 K**



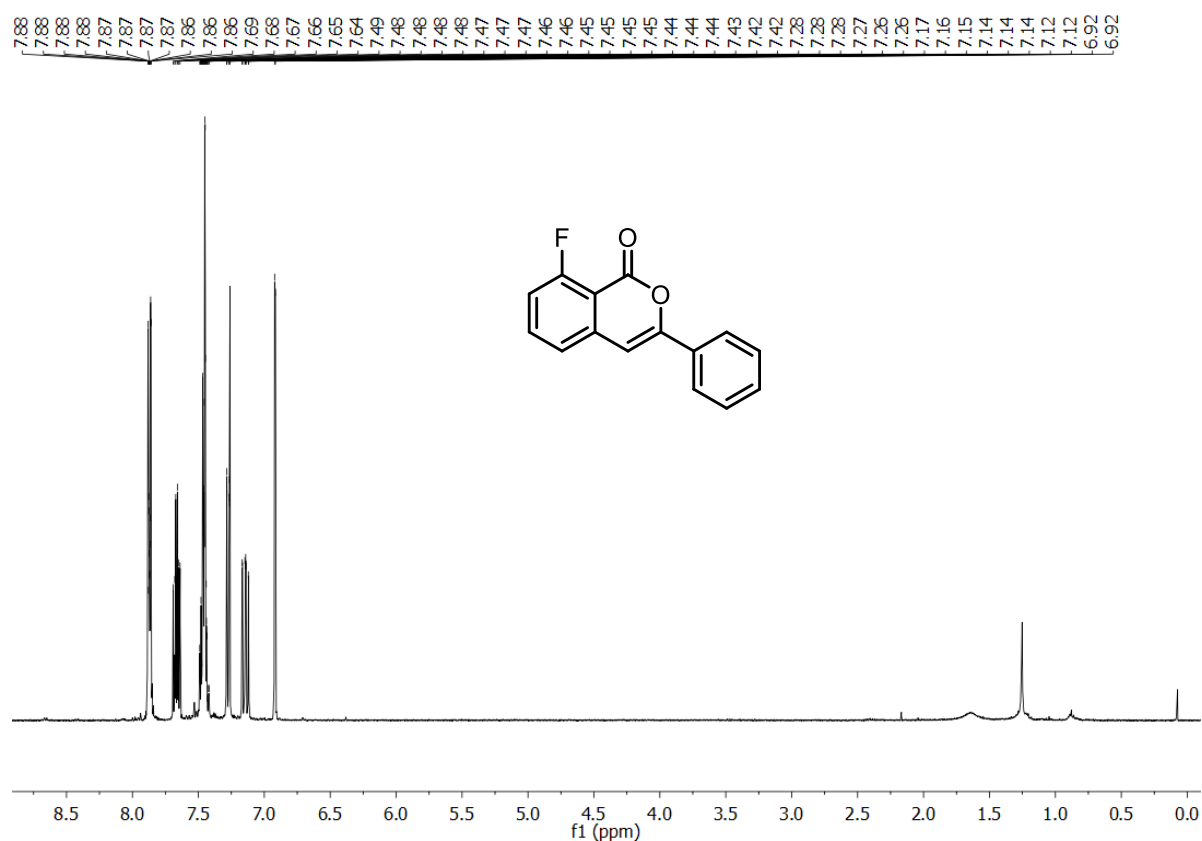
**<sup>1</sup>H NMR of compound 223, 3,6-diphenyl-1*H*-isochromen-1-one, 300 MHz, CDCl<sub>3</sub>, 302 K**



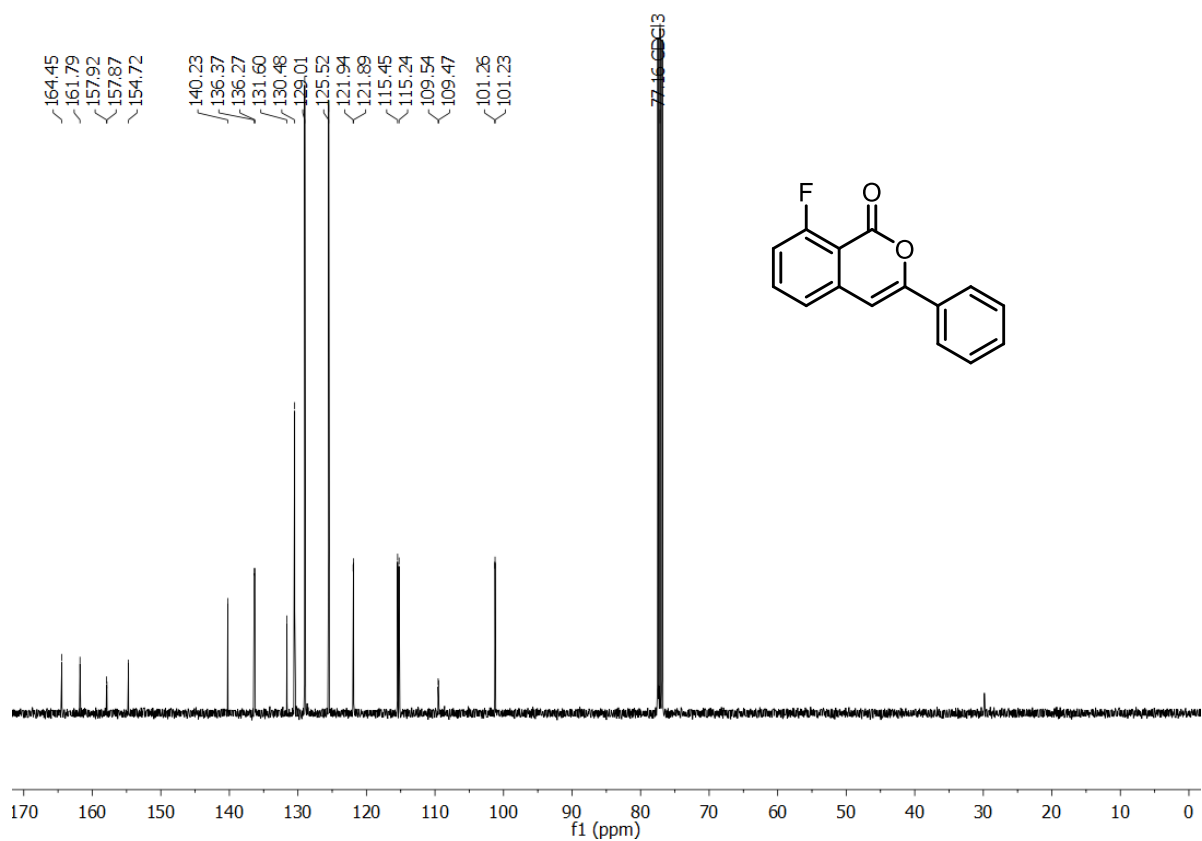
**<sup>13</sup>C NMR of compound 223, 3,6-diphenyl-1*H*-isochromen-1-one, 126 MHz, CDCl<sub>3</sub>, 298 K**



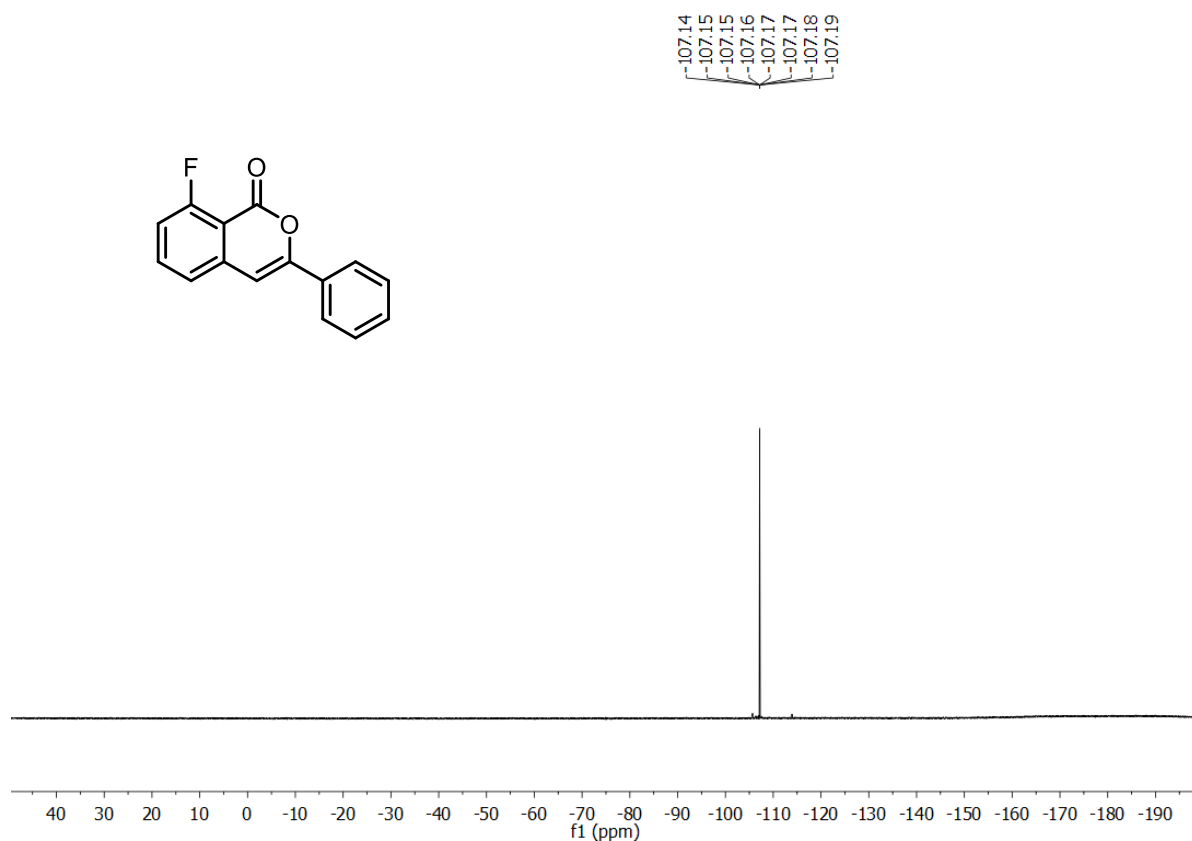
**<sup>1</sup>H NMR of compound 224, 8-fluoro-3-phenyl-1*H*-isochromen-1-one, 400 MHz, CDCl<sub>3</sub>, 298 K**



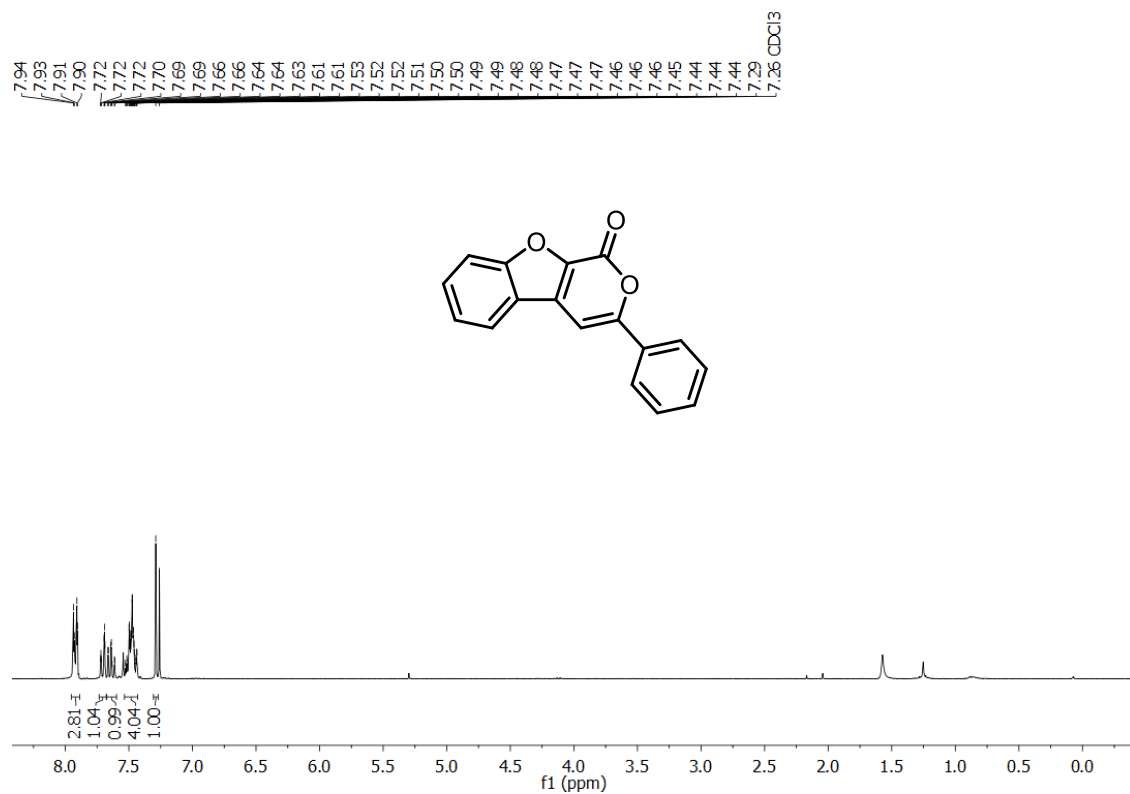
**<sup>13</sup>C NMR of compound 224, 8-fluoro-3-phenyl-1*H*-isochromen-1-one, 101 MHz, CDCl<sub>3</sub>, 300 K**



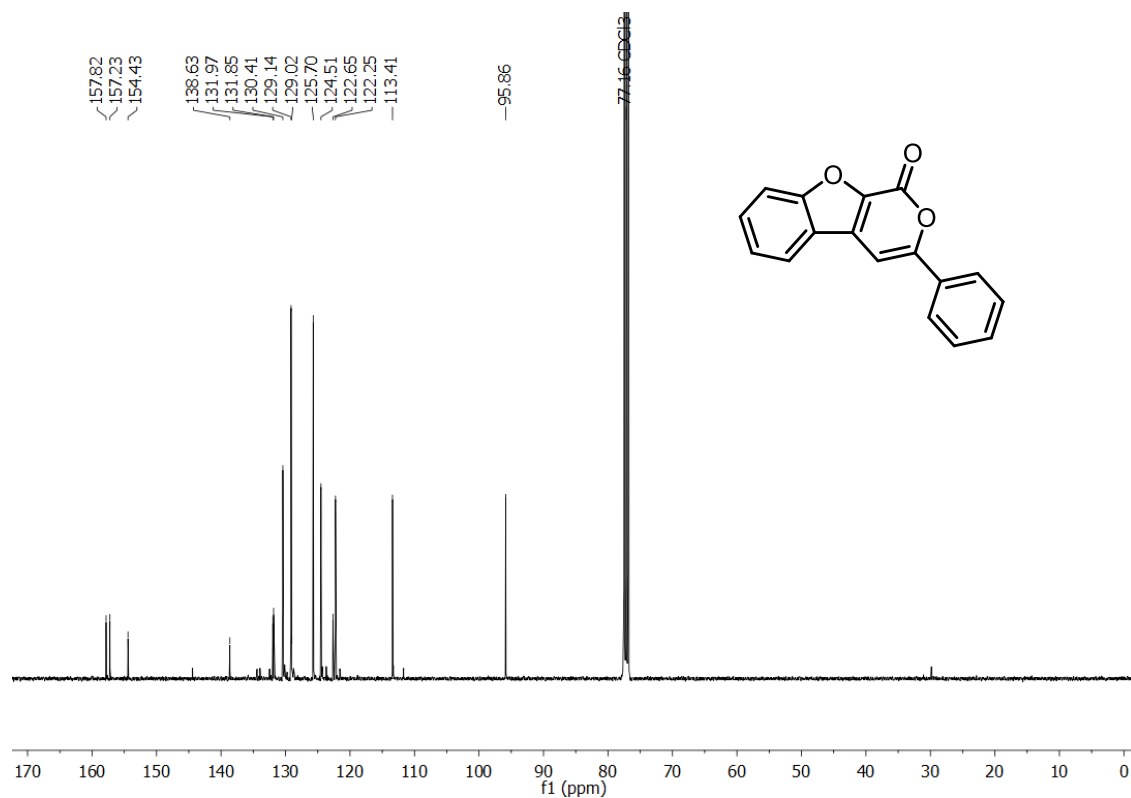
**$^{19}\text{F}$  NMR of compound 224, 8-fluoro-3-phenyl-1*H*-isochromen-1-one, 377 MHz,  $\text{CDCl}_3$ , 299 K**



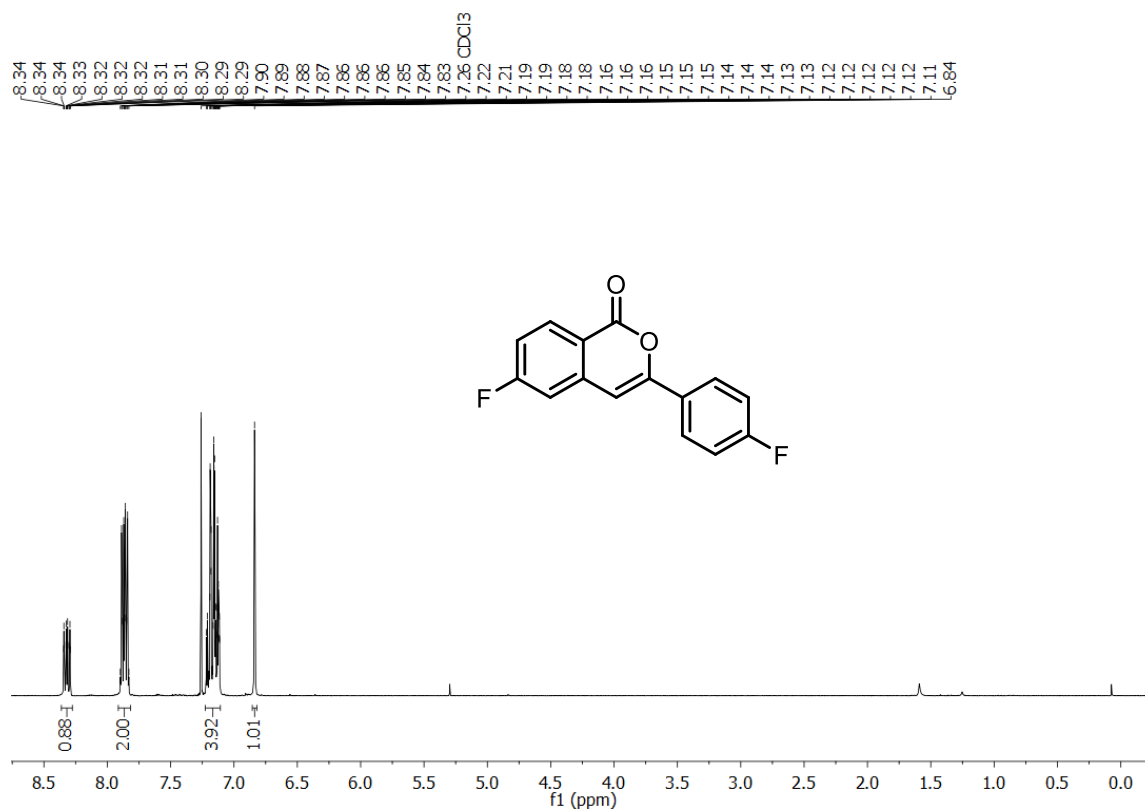
**$^1\text{H}$  NMR of compound 225, 3-phenyl-1*H*-pyrano[3,4-*b*]benzofuran-1-one, 300 MHz,  $\text{CDCl}_3$ , 298 K**



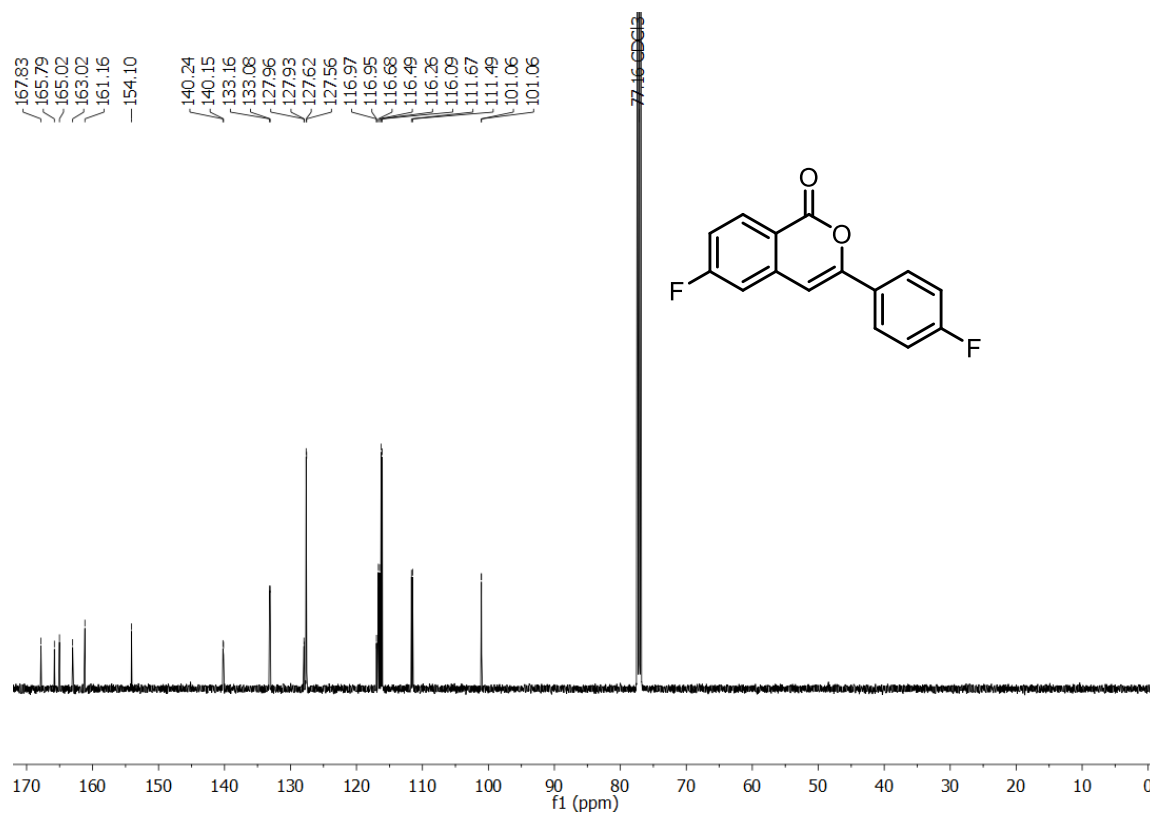
**$^{13}\text{C}$  NMR of compound 225, 3-phenyl-1*H*-pyrano[3,4-*b*]benzofuran-1-one, 101 MHz,  $\text{CDCl}_3$ , 299 K**



**$^1\text{H}$  NMR of compound 226, 6-fluoro-3-(4-fluorophenyl)-1*H*-isochromen-1-one, 300 MHz,  $\text{CDCl}_3$ , 300 K**



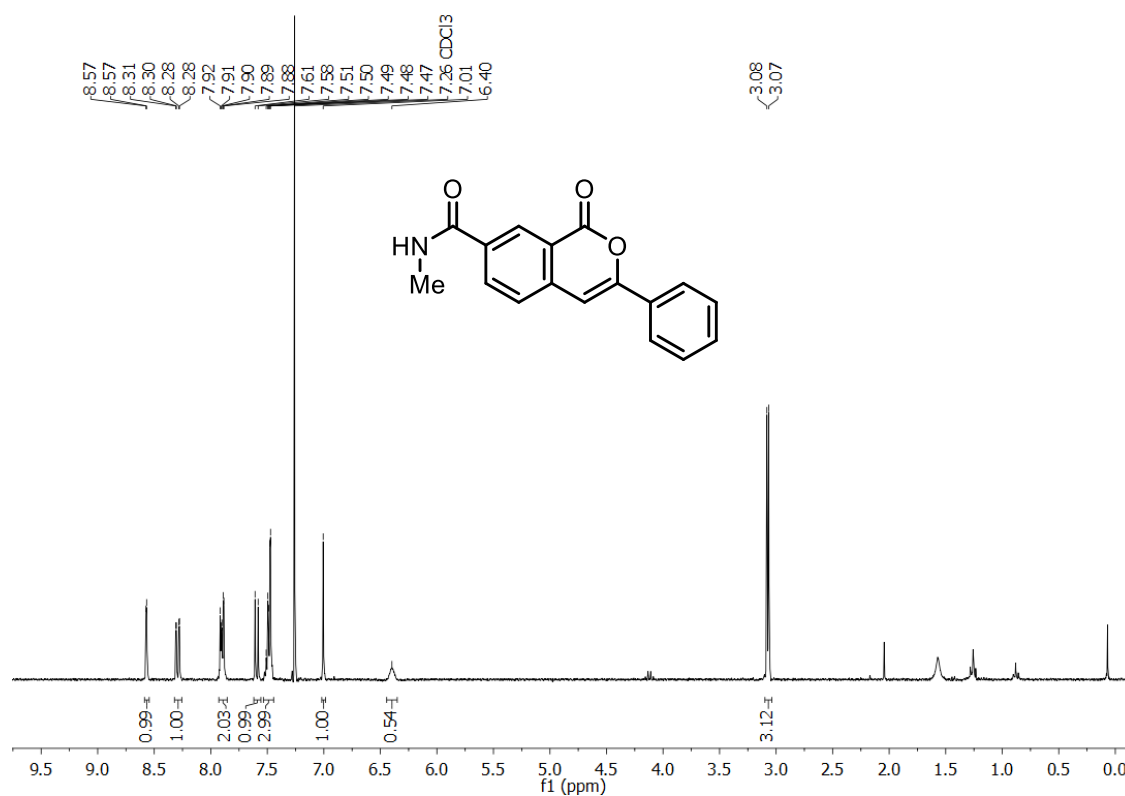
**$^{13}\text{C}$  NMR of compound 226, 6-fluoro-3-(4-fluorophenyl)-1*H*-isochromen-1-one, 126 MHz,  $\text{CDCl}_3$ , 300 K**



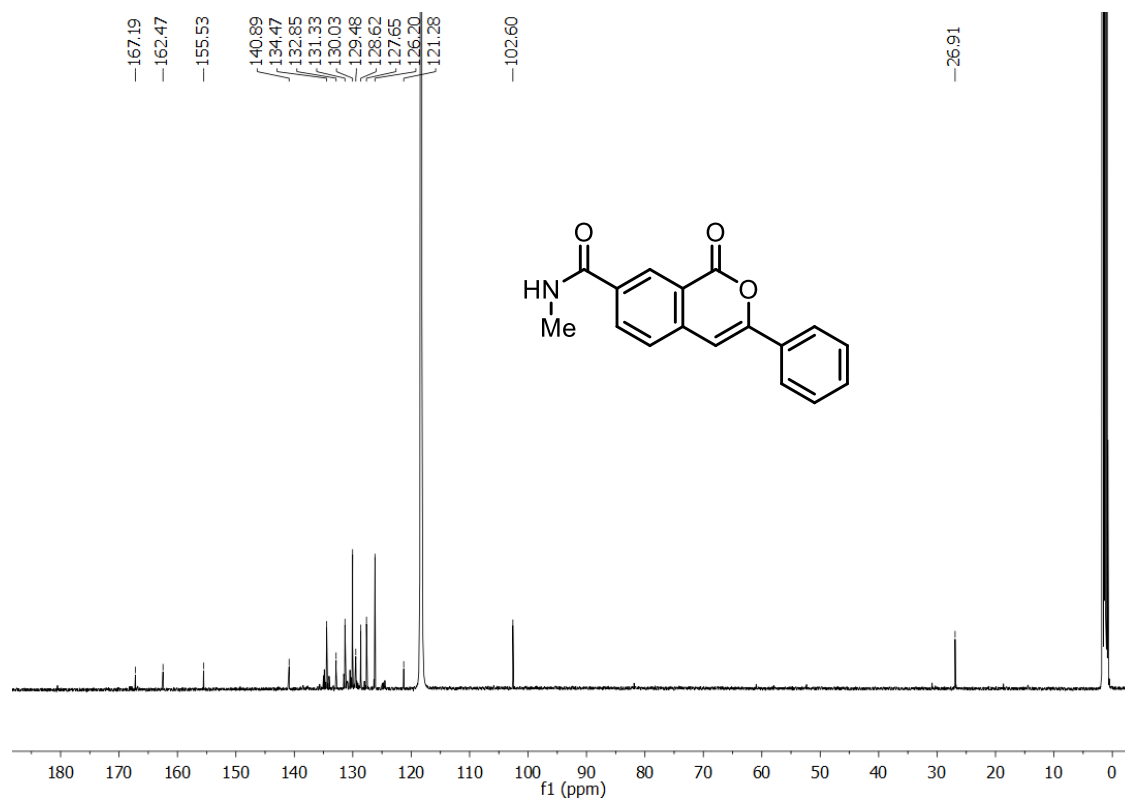
**$^{19}\text{F}$  NMR of compound 226, 6-fluoro-3-(4-fluorophenyl)-1*H*-isochromen-1-one, 282 MHz,  $\text{CDCl}_3$ , 308 K**



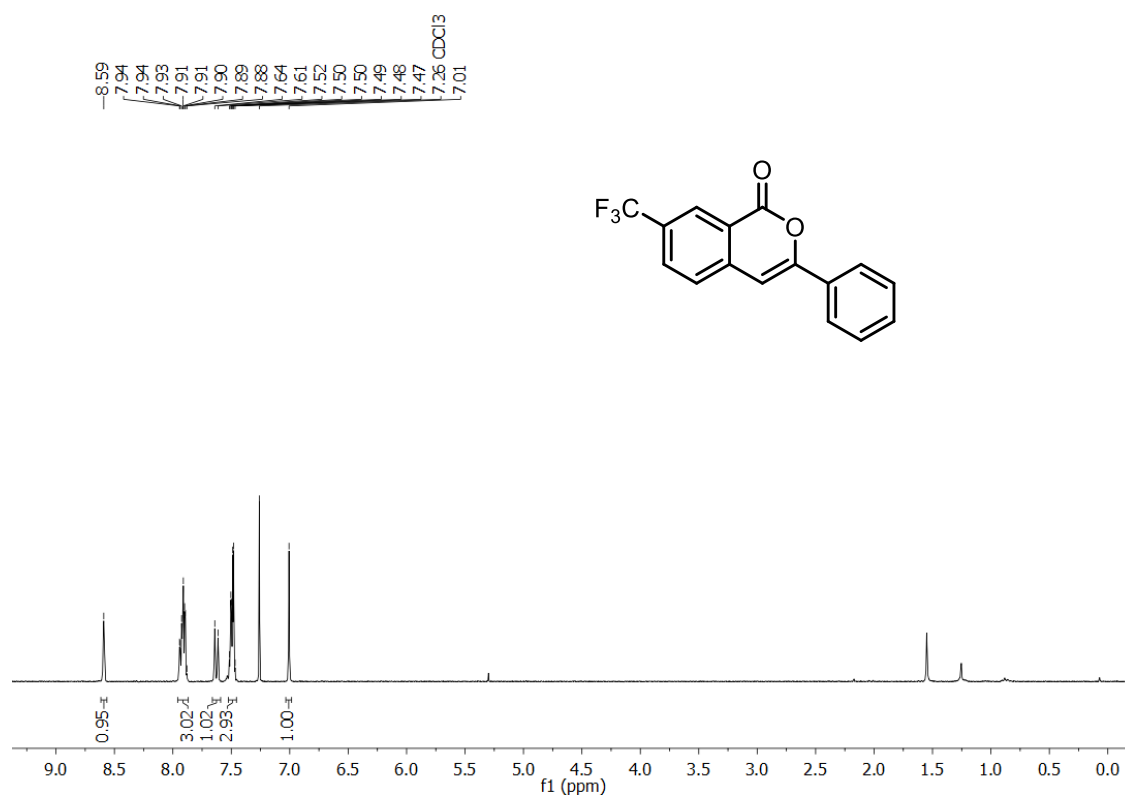
**<sup>1</sup>H NMR of compound 227, *N*-methyl-1-oxo-3-phenyl-1*H*-isochromene-7-carboxamide, 300 MHz, CDCl<sub>3</sub>, 298 K**



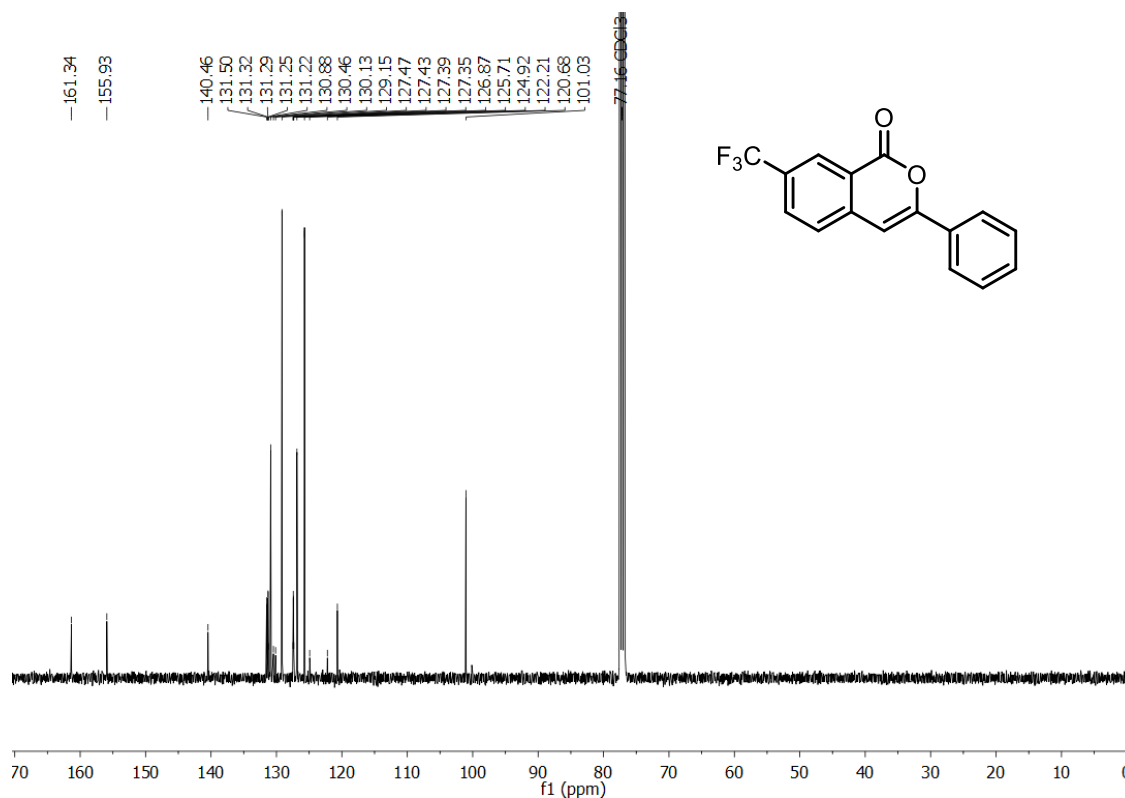
**<sup>13</sup>C NMR of compound 227, *N*-methyl-1-oxo-3-phenyl-1*H*-isochromene-7-carboxamide, 126 MHz, CDCl<sub>3</sub>, 298 K**



**<sup>1</sup>H NMR of compound 228, 3-phenyl-7-(trifluoromethyl)-1*H*-isochromen-1-one, 300 MHz, CDCl<sub>3</sub>, 298 K**

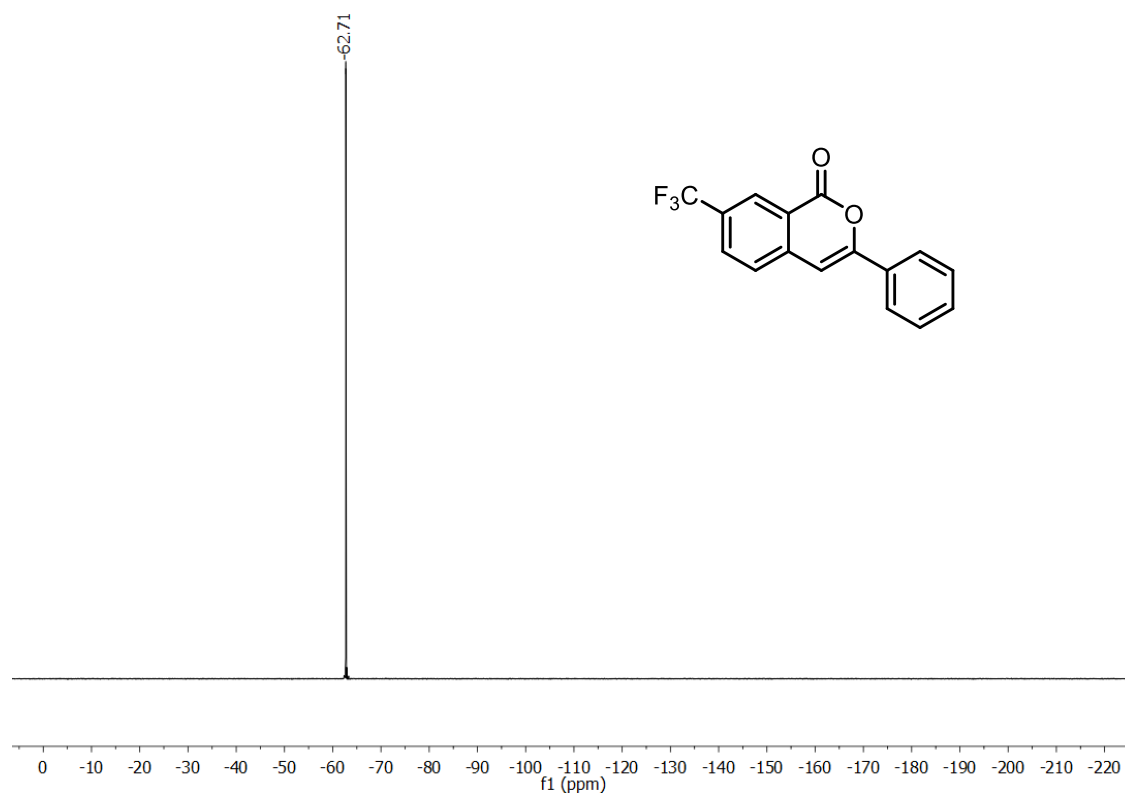


**<sup>13</sup>C NMR of compound 228, 3-phenyl-7-(trifluoromethyl)-1*H*-isochromen-1-one, 101 MHz, CDCl<sub>3</sub>, 299 K**

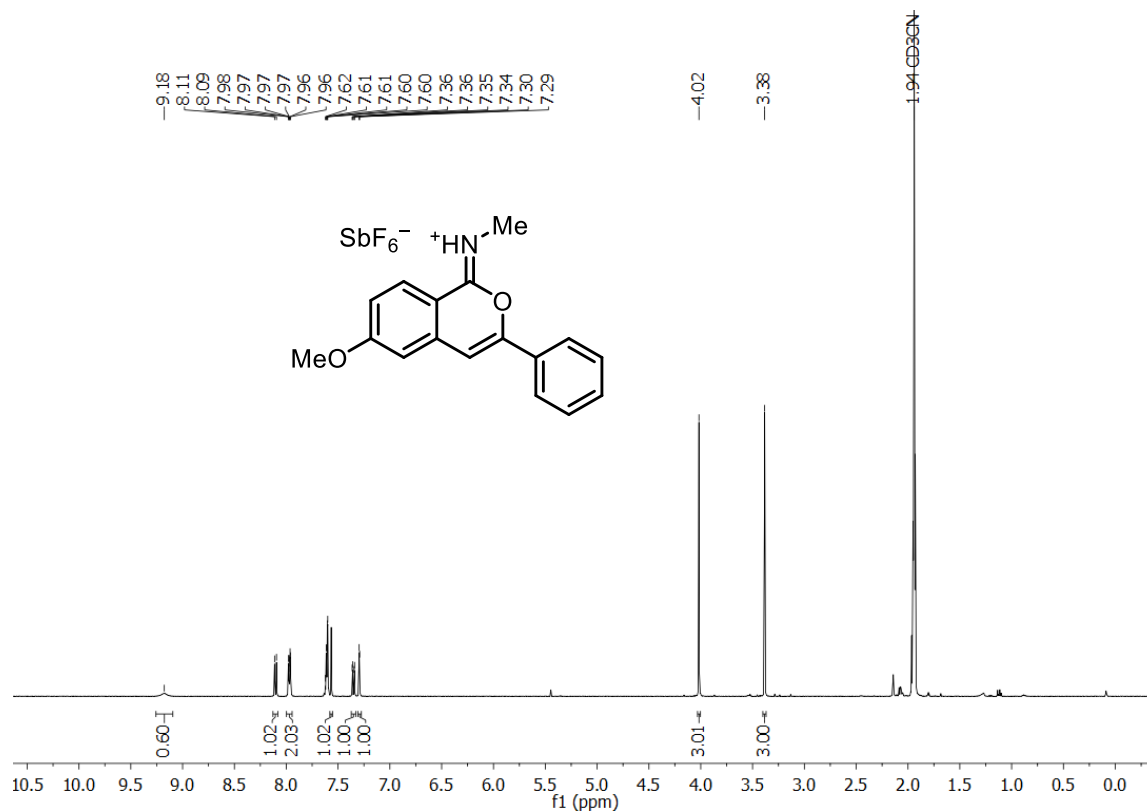




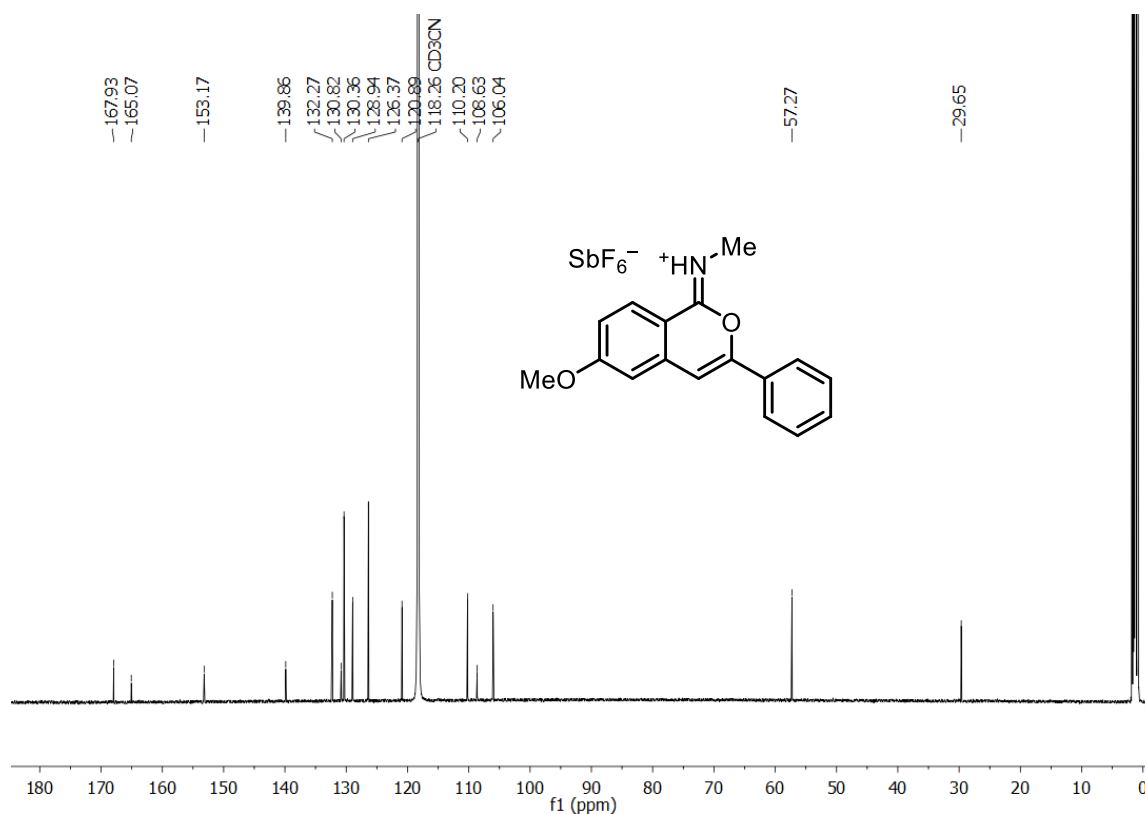
**$^{19}\text{F}$  NMR of compound 228, 3-phenyl-7-(trifluoromethyl)-1*H*-isochromen-1-one, 282 MHz,  $\text{CDCl}_3$ , 298 K**



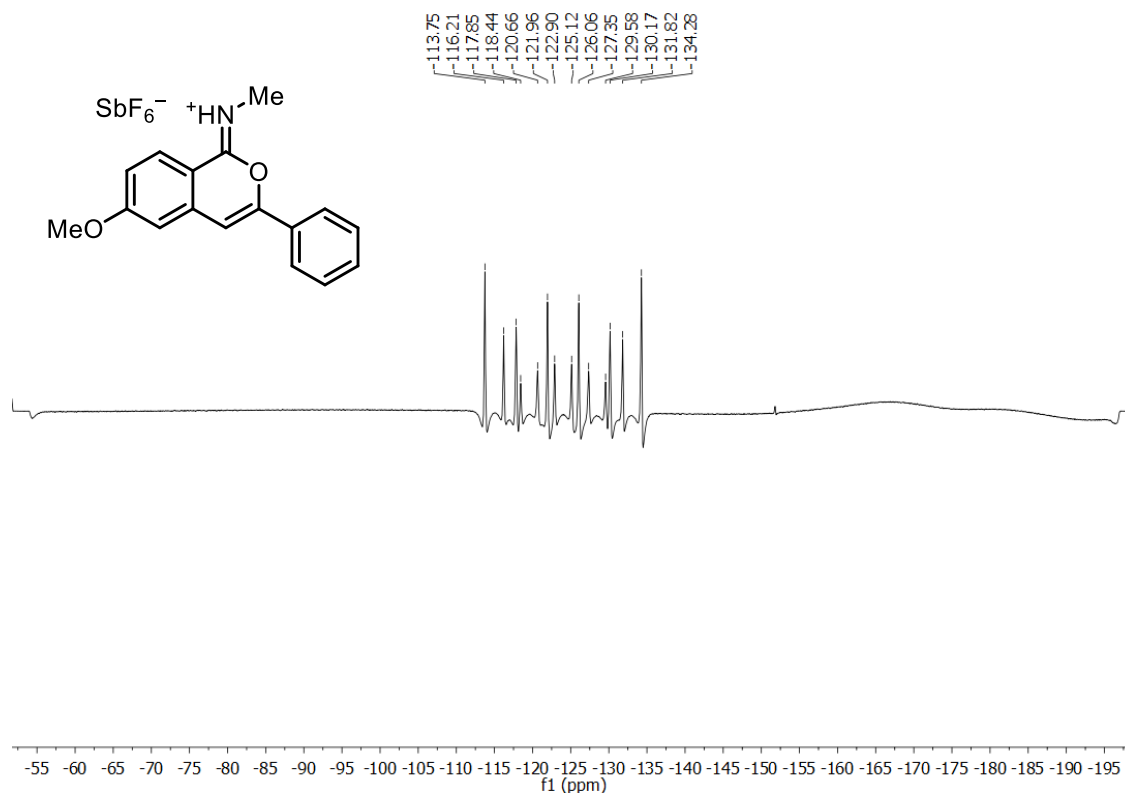
**$^1\text{H}$  NMR of compound 229, (*Z*)-*N*-(6-methoxy-3-phenyl-1*H*-isochromen-1-ylidene)methanaminium hexafluoroantimonate, 500 MHz,  $\text{CD}_3\text{CN}$ , 298 K**



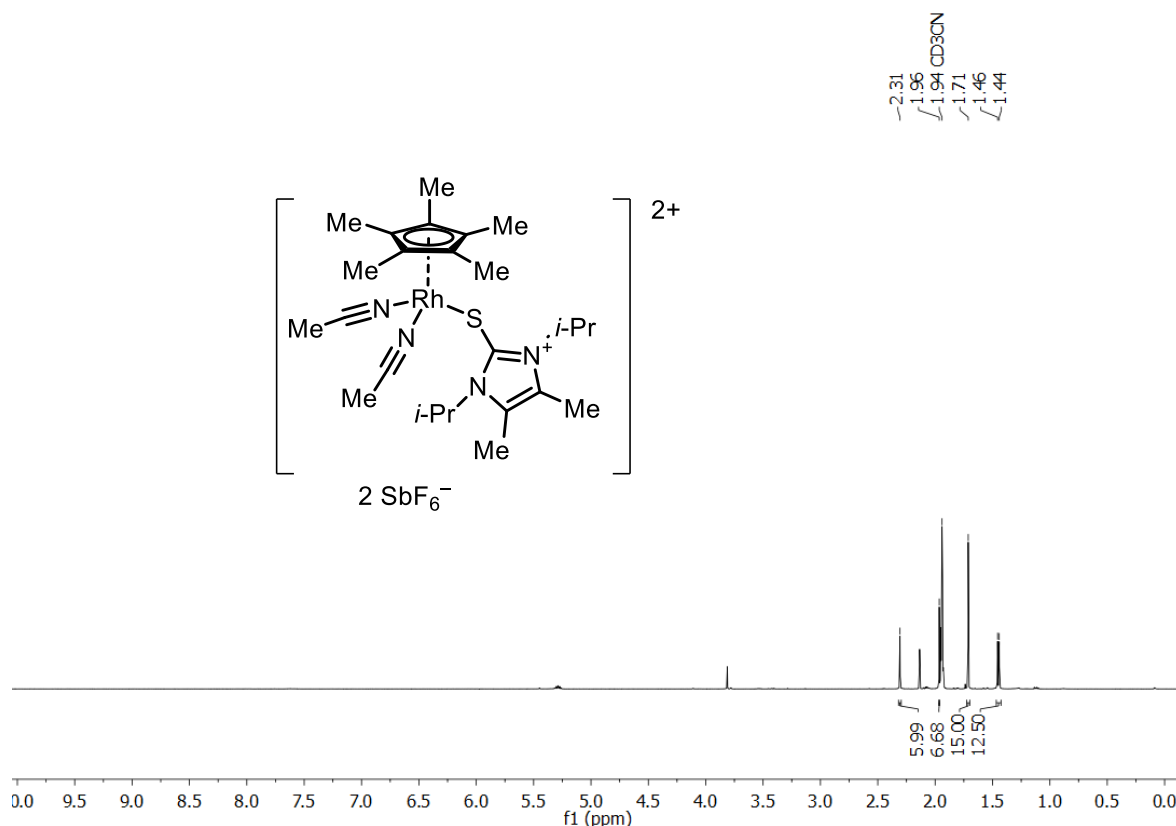
**$^{13}\text{C}$  NMR of compound 229, (Z)-N-(6-methoxy-3-phenyl-1*H*-isochromen-1-ylidene)methan-aminium hexafluoroantimonate, 126 MHz,  $\text{CD}_3\text{CN}$ , 298 K**



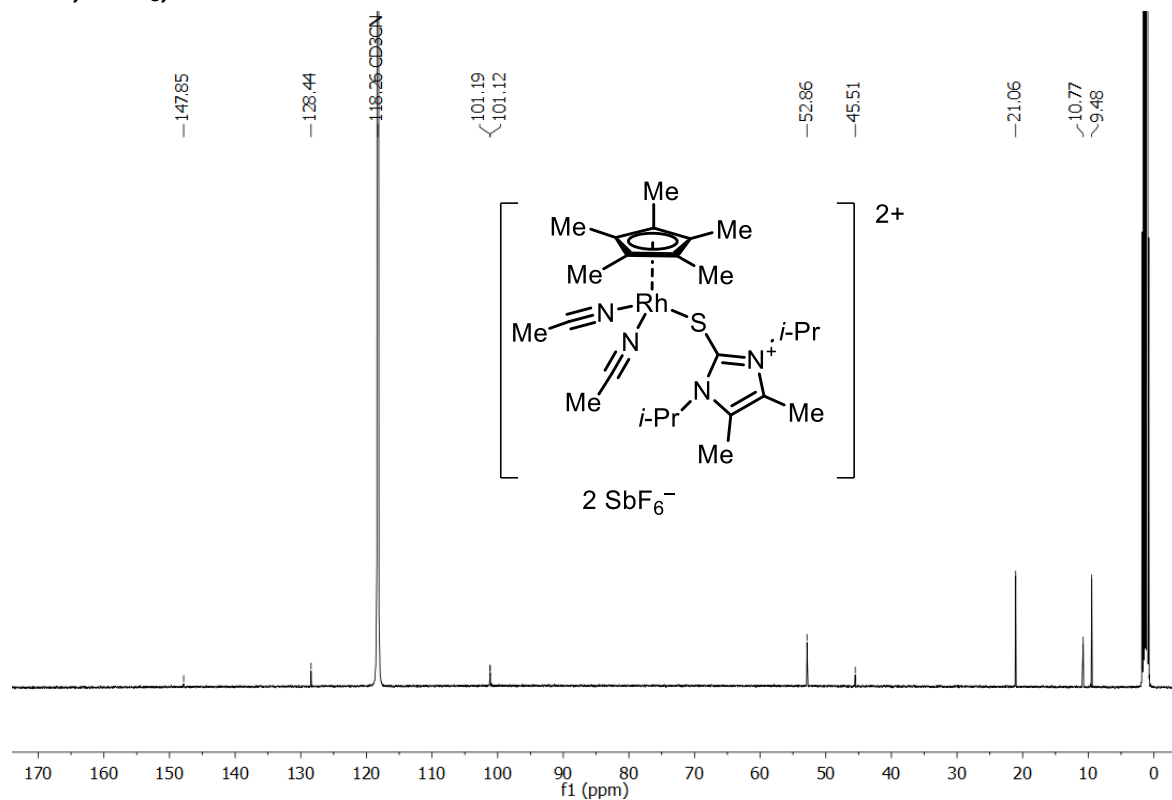
**$^{19}\text{F}$  NMR of compound 229, (Z)-N-(6-methoxy-3-phenyl-1*H*-isochromen-1-ylidene)methan-aminium hexafluoroantimonate, 471 MHz,  $\text{CD}_3\text{CN}$ , 298 K**



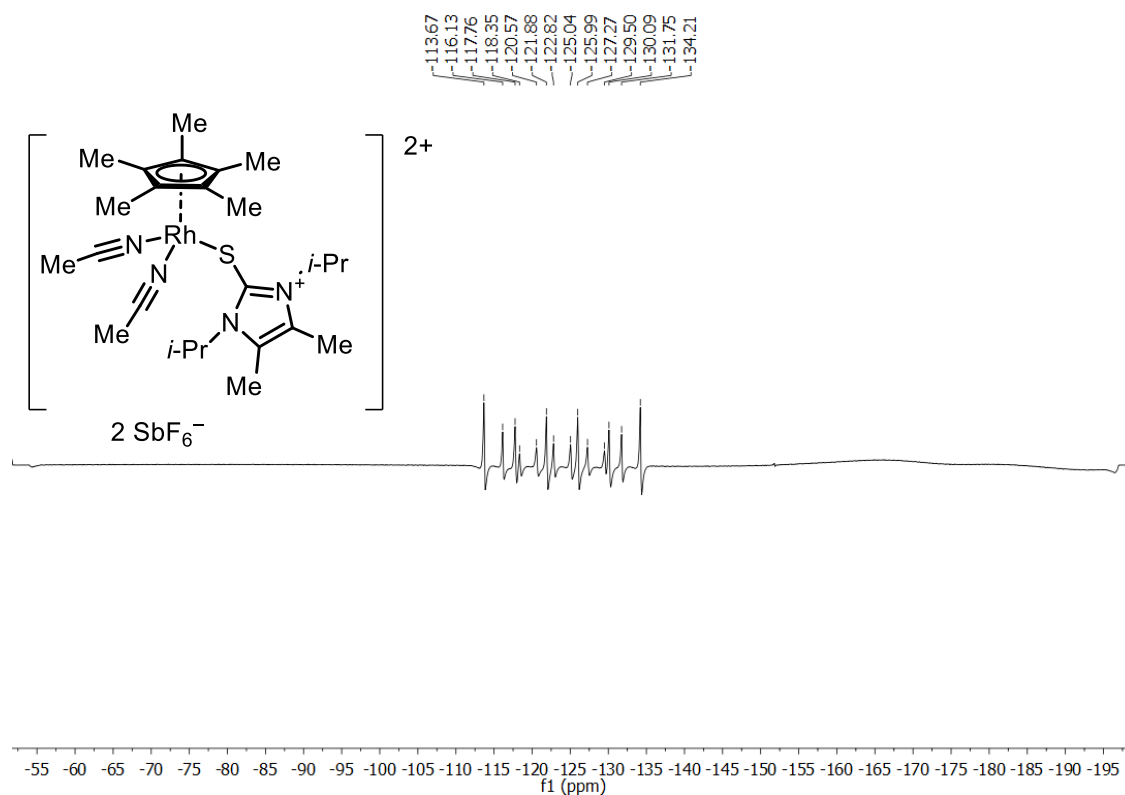
**$^1\text{H}$  NMR of compound 236, bis(acetonitrile){[(1,3-diisopropyl-4,5-dimethyl-1*H*-imidazol-3-ium-2-yl)thio](pentamethylcyclopentadienyl)rhodium(I) bis(hexafluoroantimonate), 500 MHz,  $\text{CDCl}_3$ , 298 K**



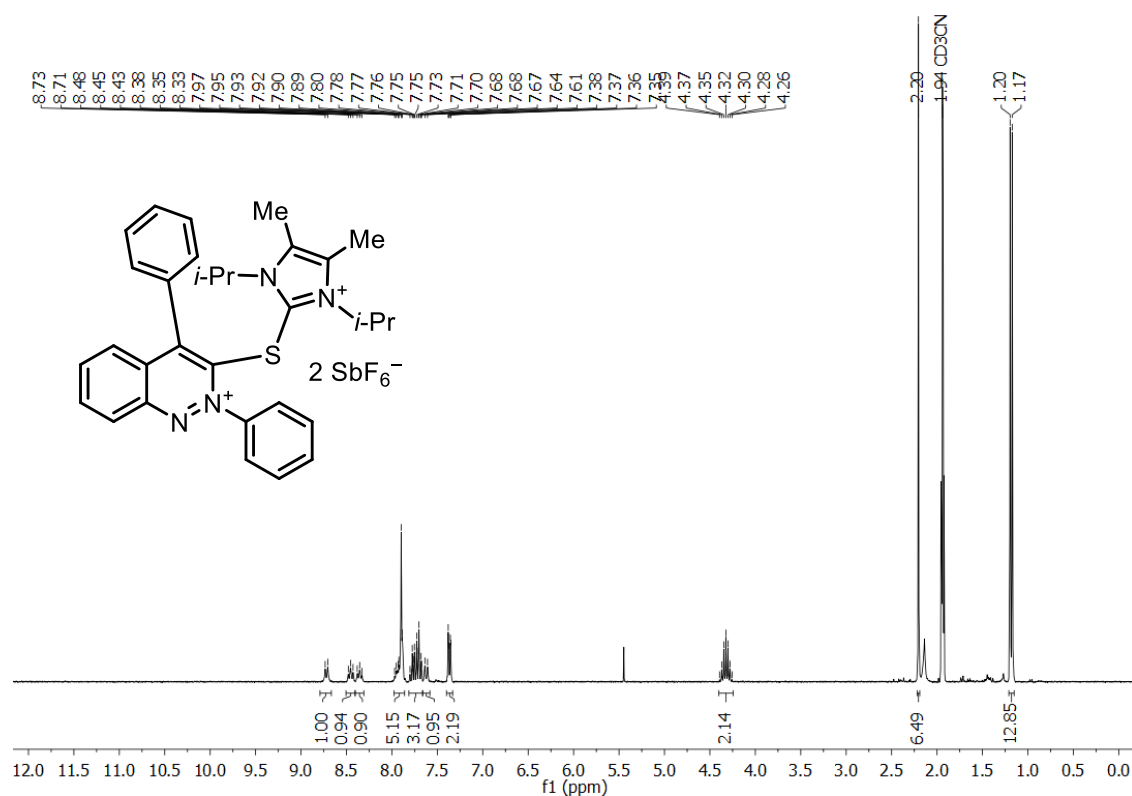
**$^{13}\text{C}$  NMR of compound 236, bis(acetonitrile){[(1,3-diisopropyl-4,5-dimethyl-1*H*-imidazol-3-ium-2-yl)thio](pentamethylcyclopentadienyl)rhodium(I) bis(hexafluoroantimonate), 126 MHz,  $\text{CDCl}_3$ , 298 K**



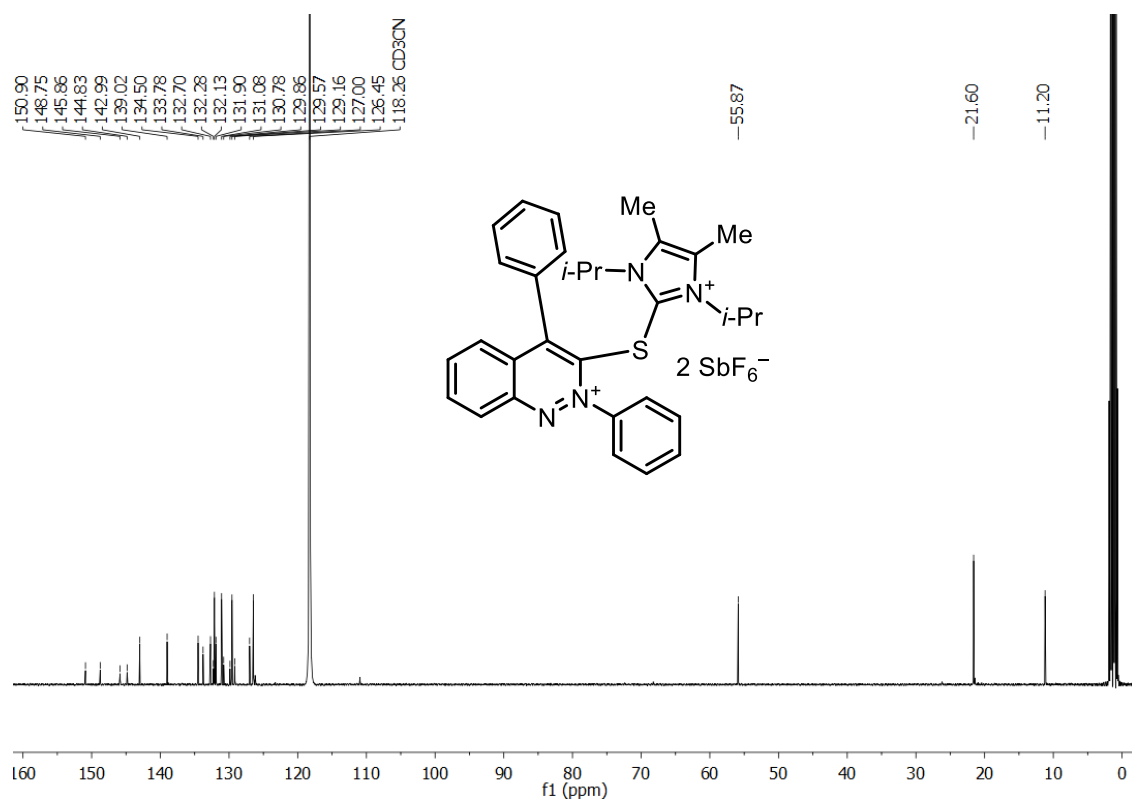
**$^{19}\text{F}$  NMR of compound 236, bis(acetonitrile){[(1,3-diisopropyl-4,5-dimethyl-1*H*-imidazol-3-ium-2-yl)thio](pentamethylcyclopentadienyl)rhodium(I) bis(hexafluoroantimonate), 471 MHz,  $\text{CDCl}_3$ , 298 K**



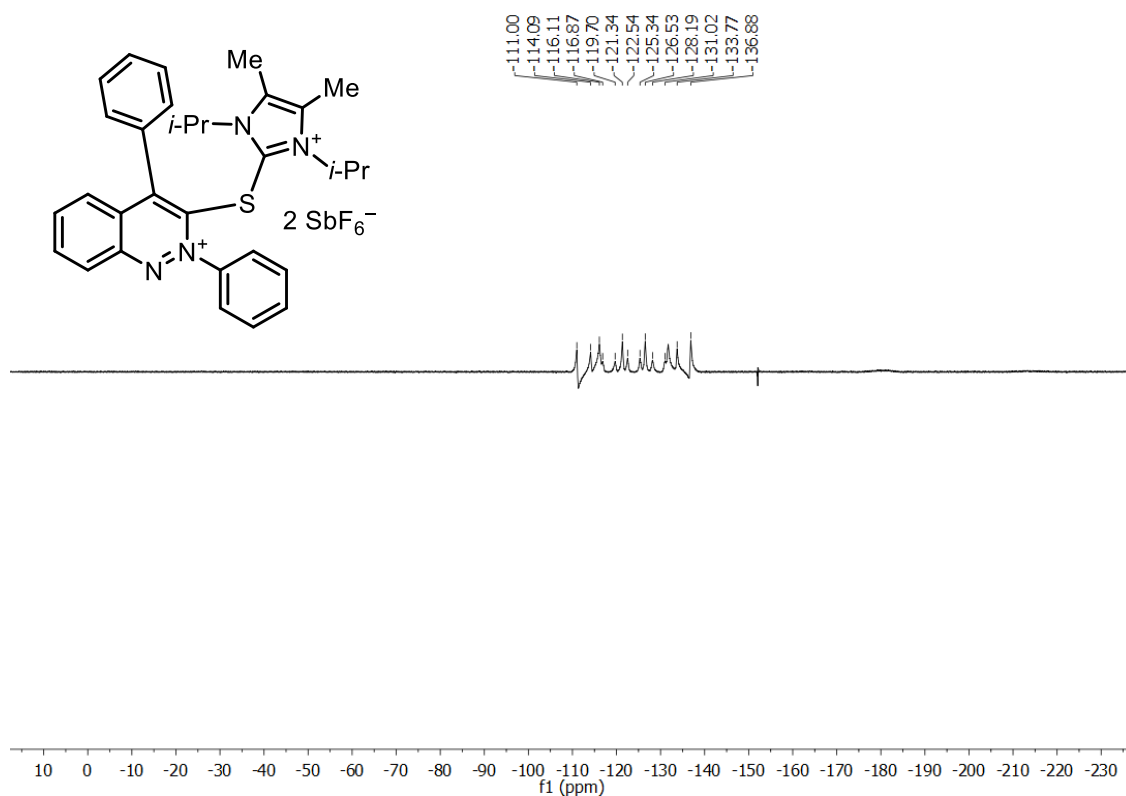
**$^1\text{H}$  NMR of compound 238, 3-[(1,3-diisopropyl-4,5-dimethyl-1*H*-imidazol-3-ium-2-yl)thio]-2,4-diphenylcinnolin-2-ium, 300 MHz,  $\text{CDCl}_3$ , 300 K**



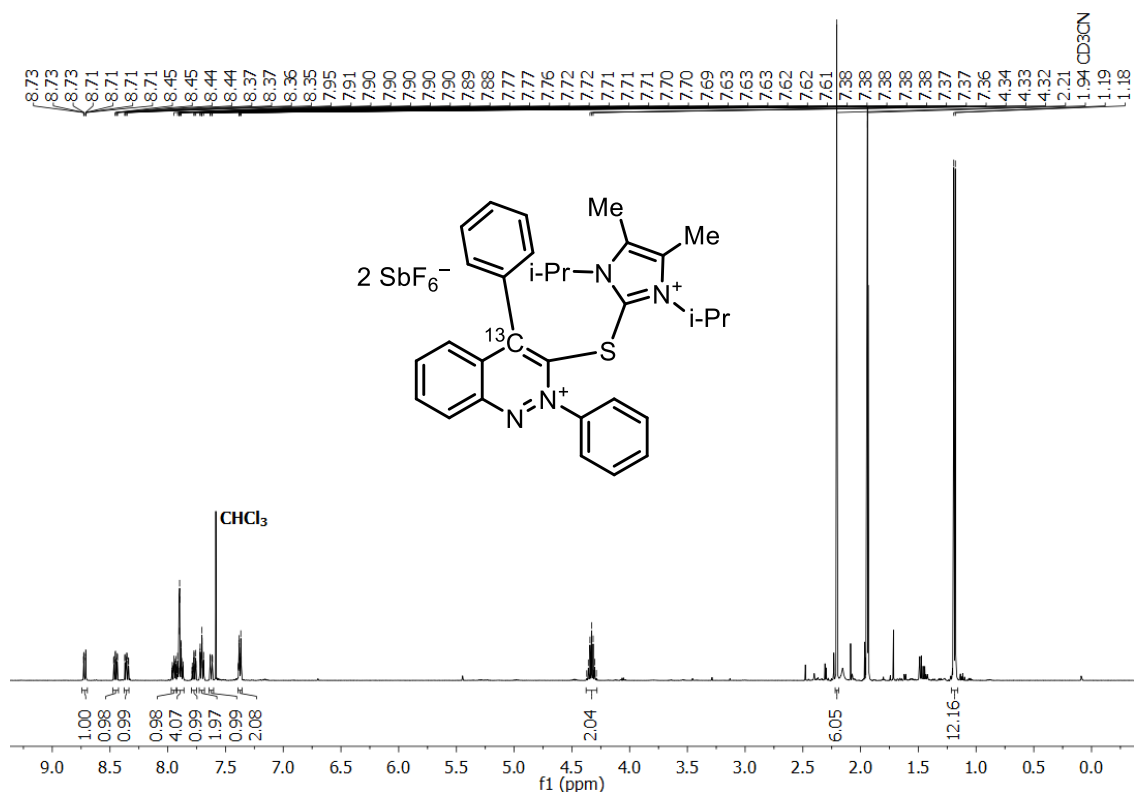
**$^{13}\text{C}$  NMR of compound 238, 3-[(1,3-diisopropyl-4,5-dimethyl-1*H*-imidazol-3-ium-2-yl)thio]-2,4-diphenylcinnolin-2-ium, 101 MHz,  $\text{CDCl}_3$ , 298 K**



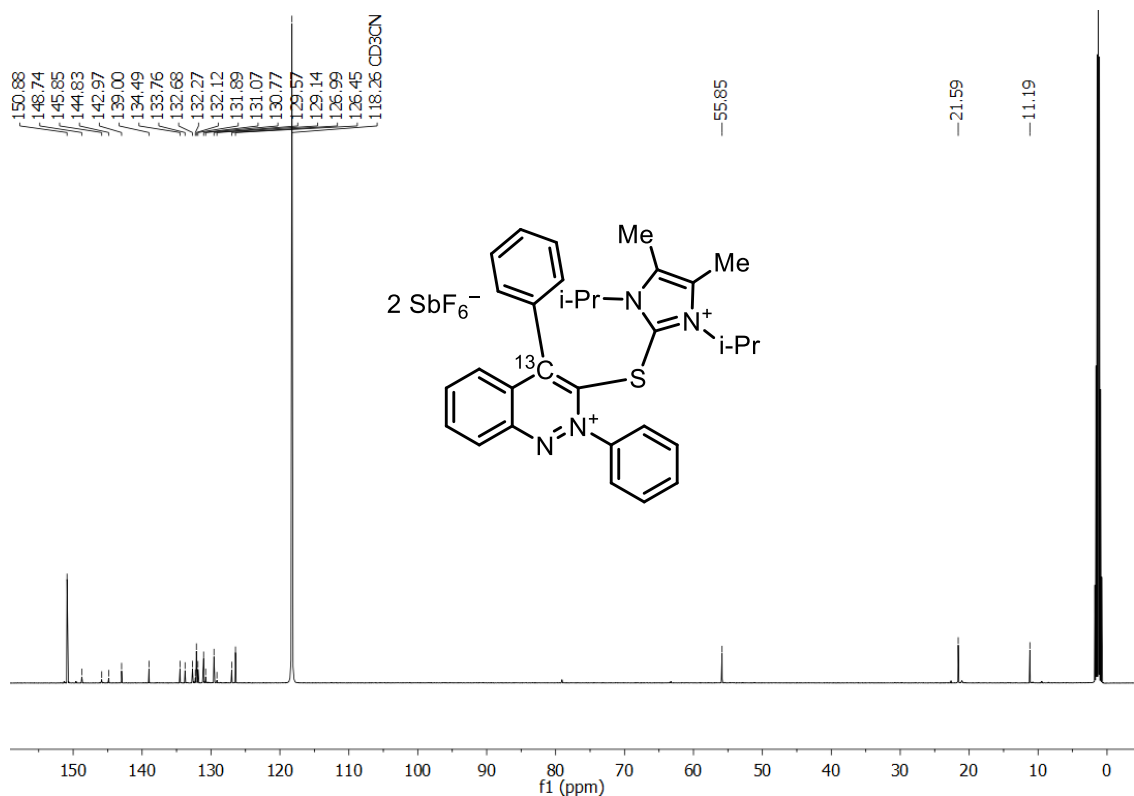
**$^{19}\text{F}$  NMR of compound 238, 3-[(1,3-diisopropyl-4,5-dimethyl-1*H*-imidazol-3-ium-2-yl)thio]-2,4-diphenylcinnolin-2-ium, 101 MHz,  $\text{CDCl}_3$ , 298 K**



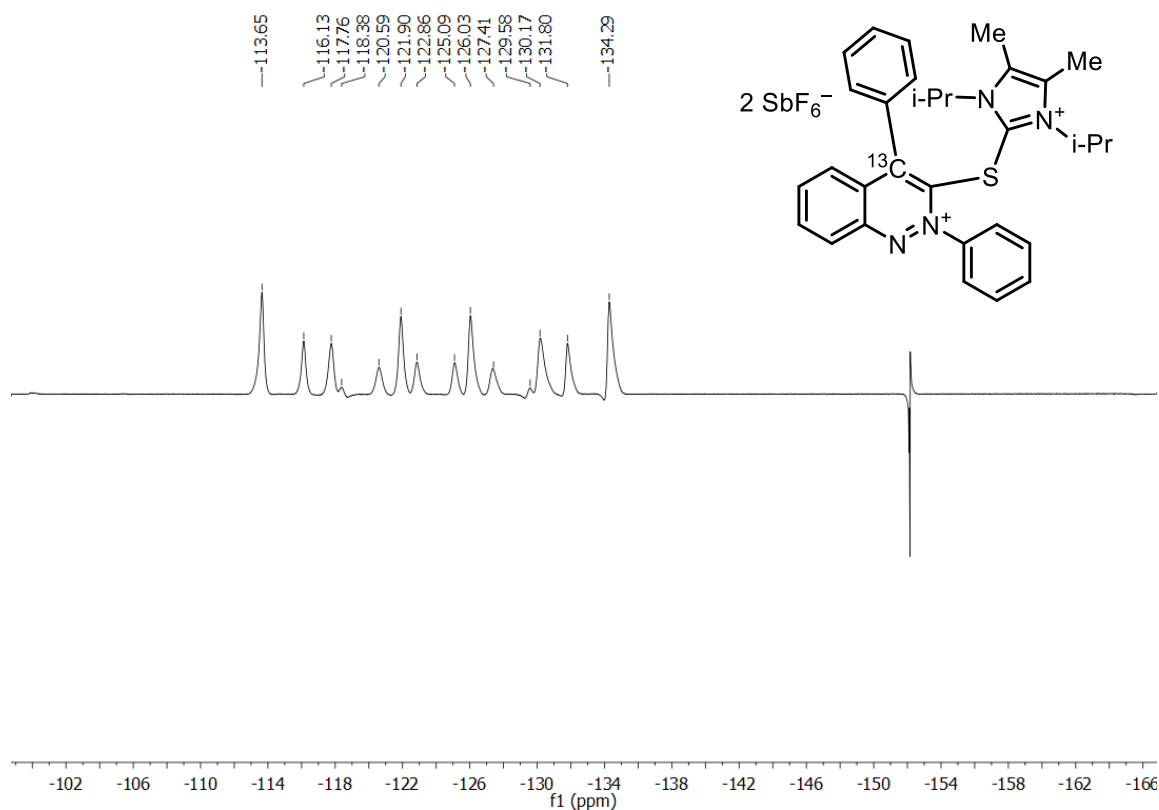
**$^1\text{H}$  NMR of compound  $\{^{13}\text{C}\}$ -238, 4- $\{^{13}\text{C}\}$ -3-[(1,3-diisopropyl-4,5-dimethyl-1*H*-imidazol-3-ium-2-yl)thio]-2,4-diphenylcinnolin-2-ium hexafluoroantimonate, 500 MHz,  $\text{CDCl}_3$ , 298 K**



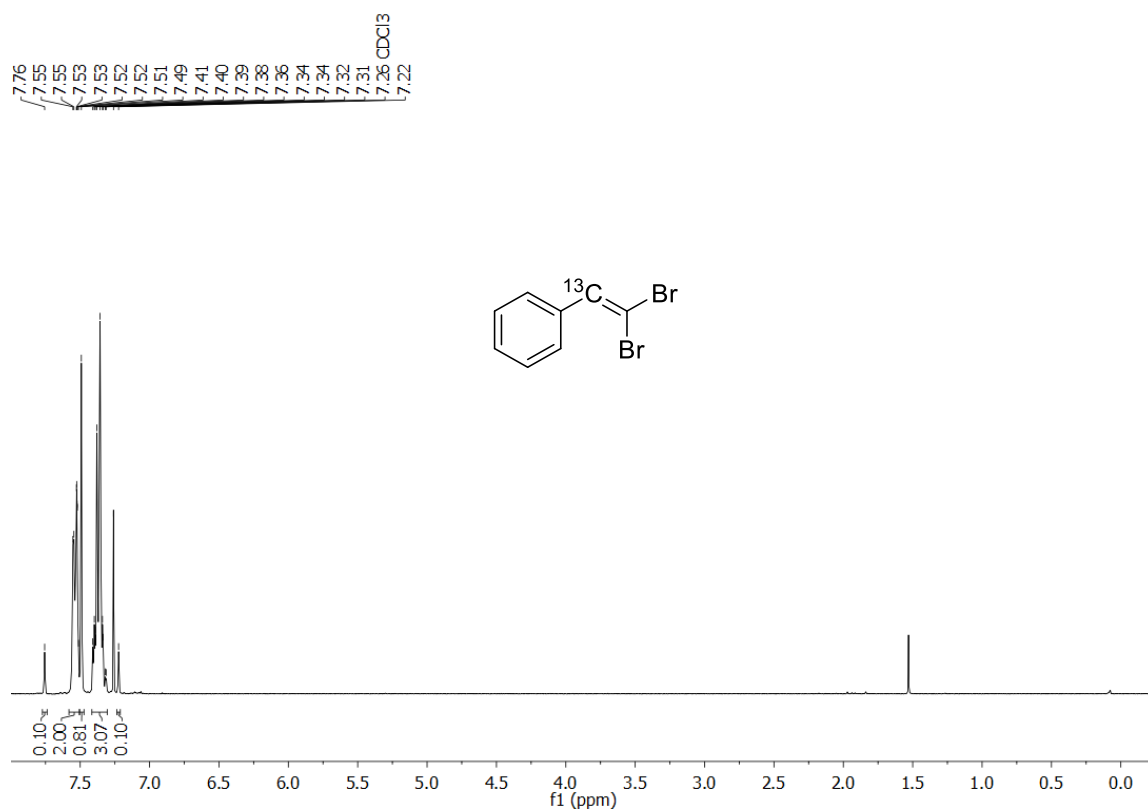
**$^{13}\text{C}$  NMR of compound  $\{^{13}\text{C}\}$ -238, 4- $\{^{13}\text{C}\}$ -3-[(1,3-diisopropyl-4,5-dimethyl-1*H*-imidazol-3-ium-2-yl)thio]-2,4-diphenylcinnolin-2-ium hexafluoroantimonate, 126 MHz,  $\text{CDCl}_3$ , 298 K**



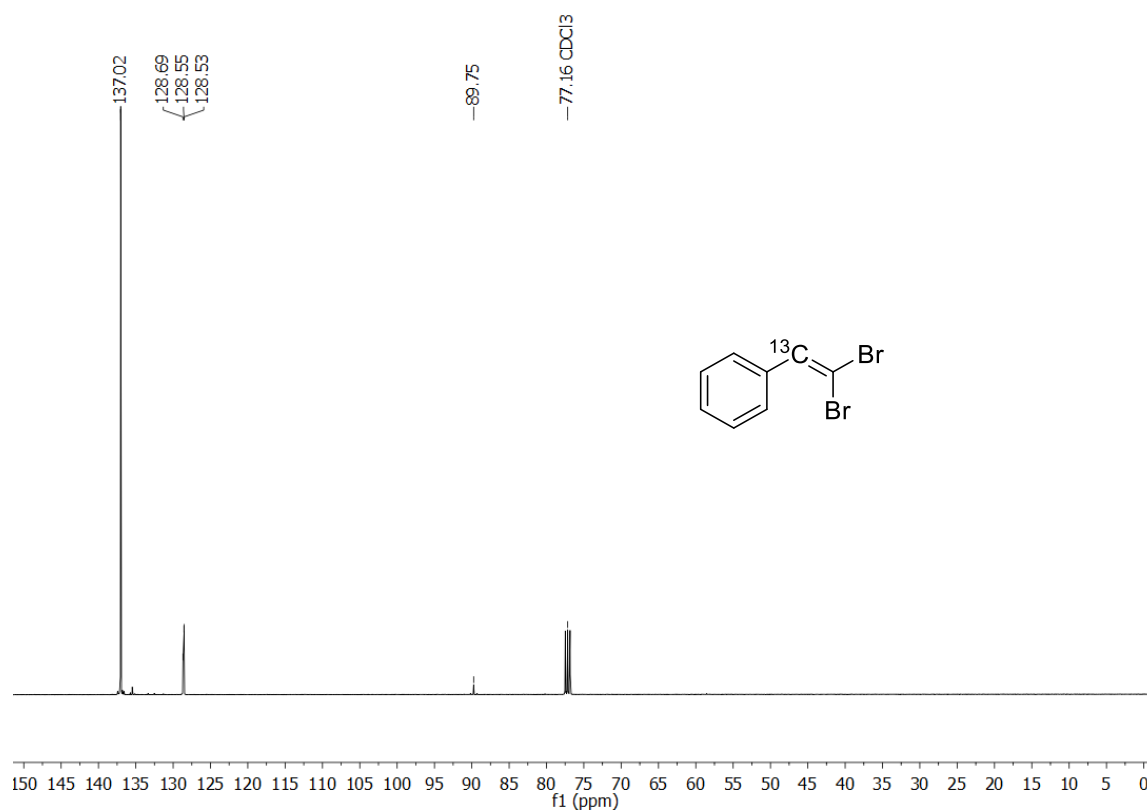
**$^{19}\text{F}$  NMR of compound  $\{^{13}\text{C}\}$ -238, 4- $\{^{13}\text{C}\}$ -3-[(1,3-diisopropyl-4,5-dimethyl-1*H*-imidazol-3-ium-2-yl)thio]-2,4-diphenylcinnolin-2-ium hexafluoroantimonate, 471 MHz,  $\text{CDCl}_3$ , 298 K**



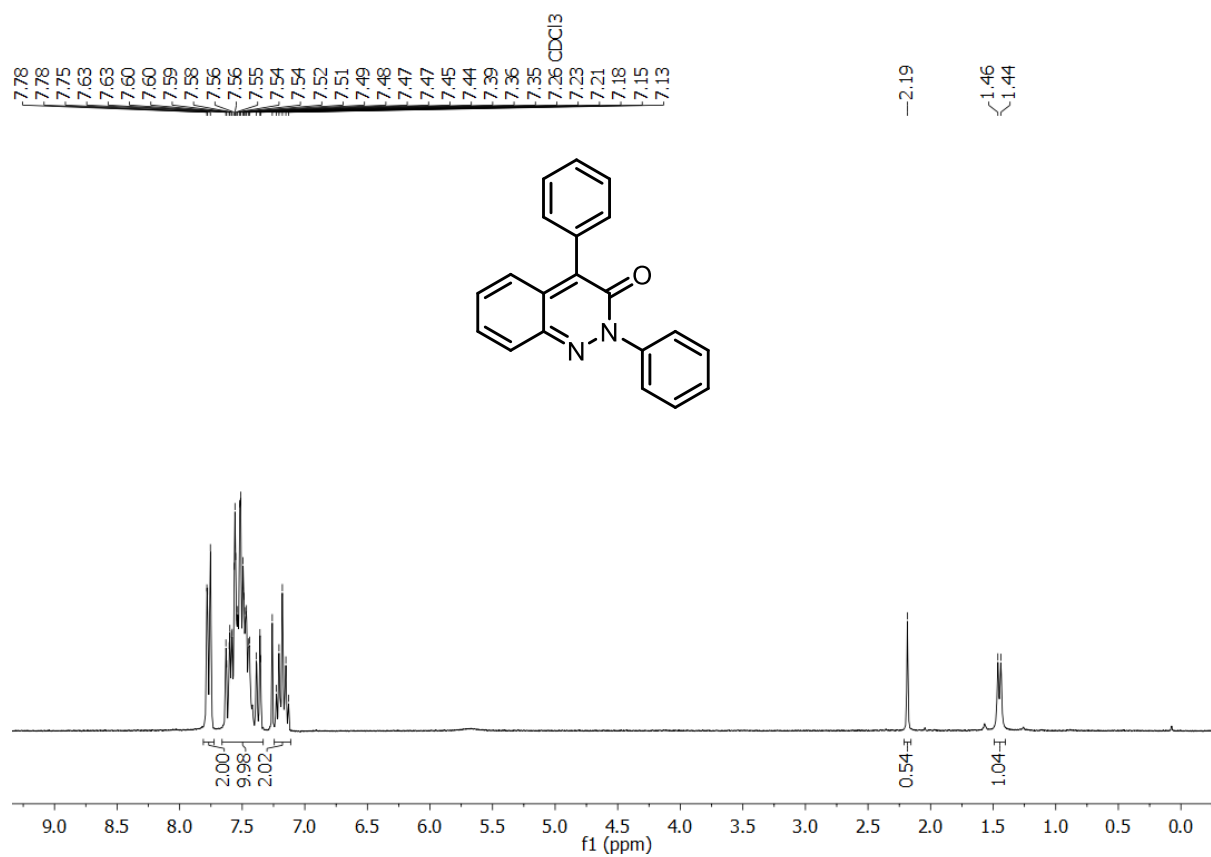
**$^1\text{H}$  NMR of compound 240, (1- $\{^{13}\text{C}\}$ -2,2-dibromovinyl)benzene, 300 MHz,  $\text{CDCl}_3$ , 298 K**



**$^{13}\text{C}$  NMR of compound 240, (1- $^{13}\text{C}$ )-2,2-dibromovinyl)benzene, 101 MHz,  $\text{CDCl}_3$ , 300 K**

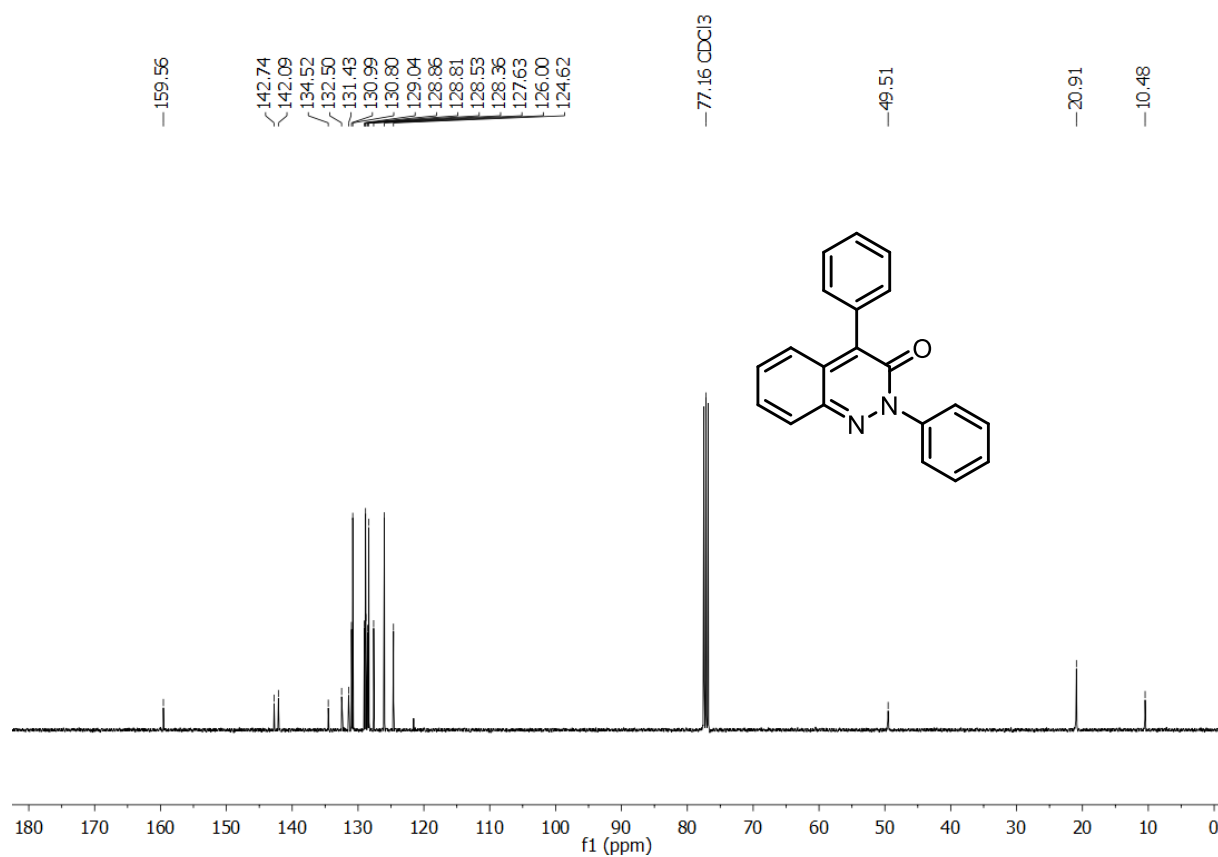


**$^1\text{H}$  NMR of compound 241, 2,4-diphenylcinnolin-3(2H)-one, 300 MHz,  $\text{CDCl}_3$ , 298 K**

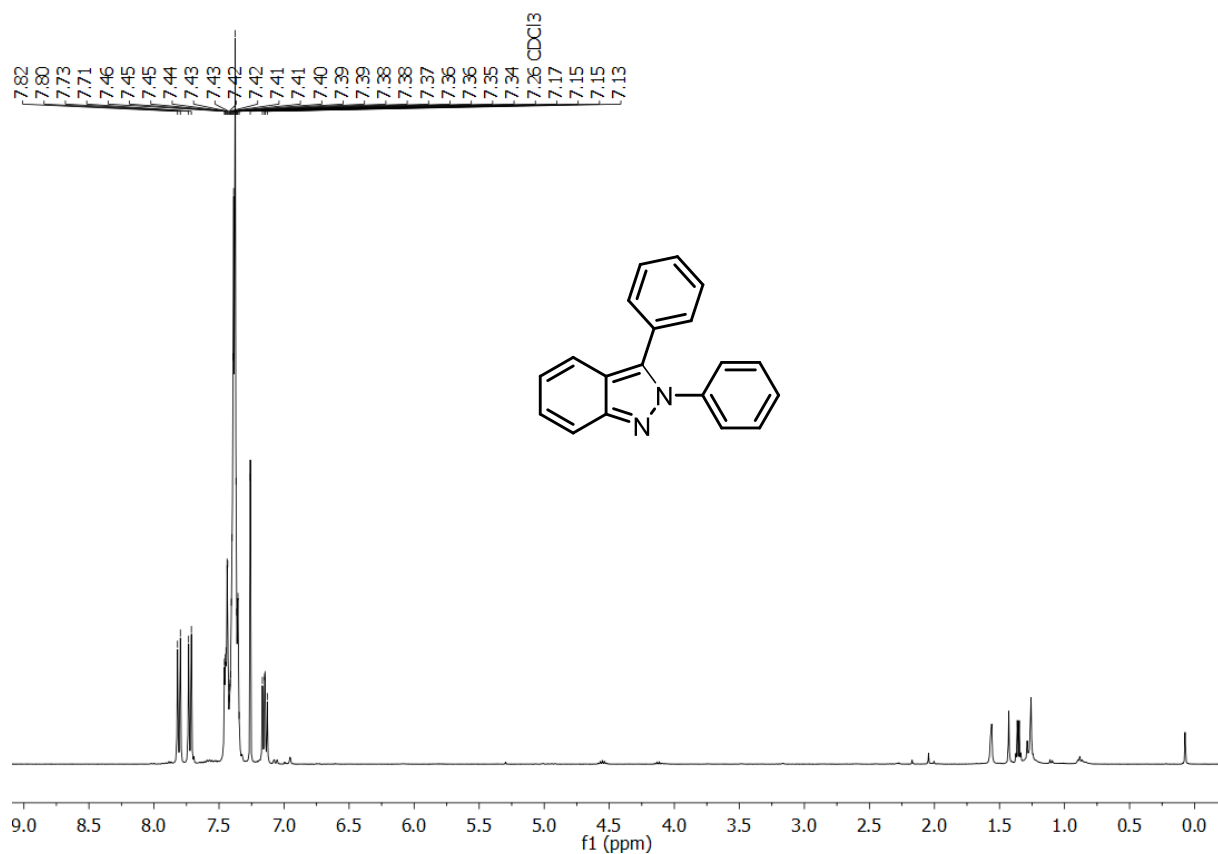




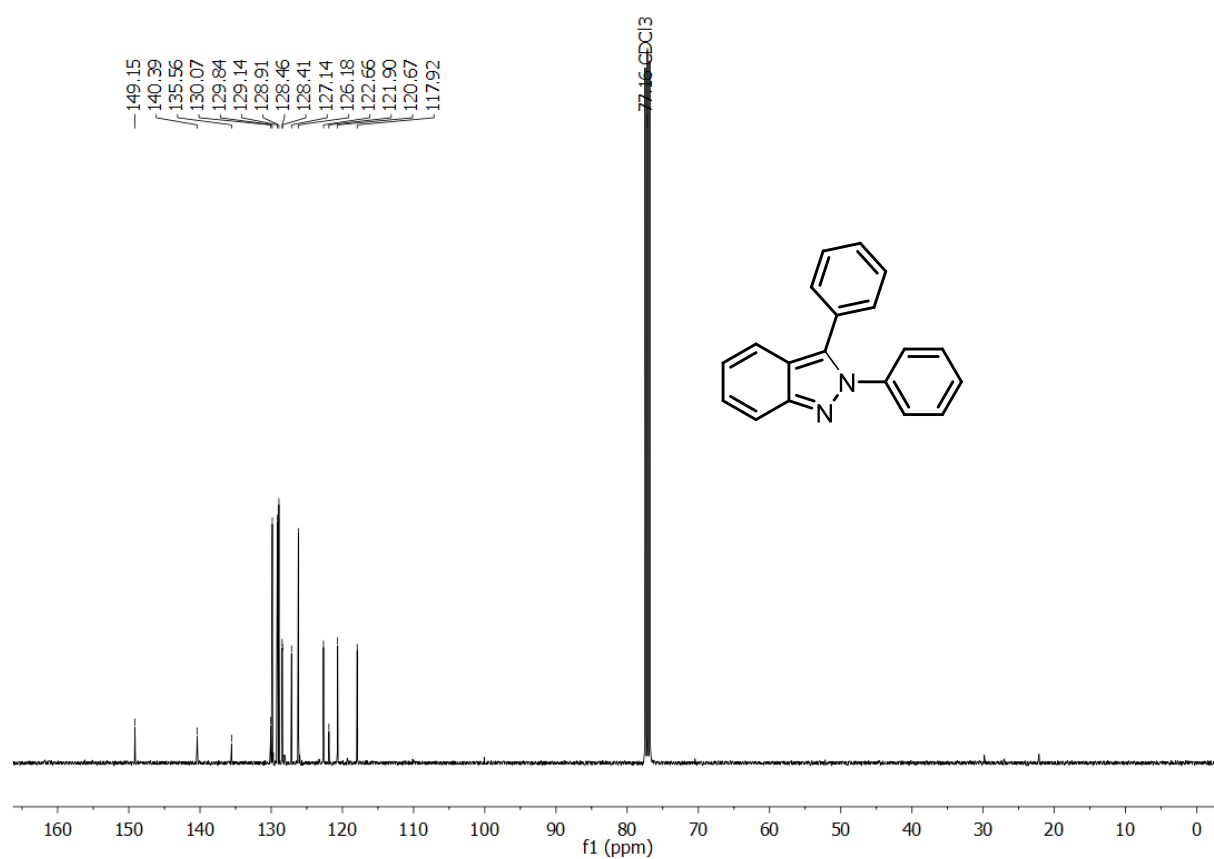
**$^{13}\text{C}$  NMR of compound 241, 2,4-diphenylcinnolin-3(2H)-one, 101 MHz,  $\text{CDCl}_3$ , 298 K**



**$^1\text{H}$  NMR of compound 242, 2,3-diphenyl-2H-indazole, 400 MHz,  $\text{CDCl}_3$ , 298 K**



**<sup>13</sup>C NMR of compound 242, 2,3-diphenyl-2*H*-indazole, 101 MHz, CDCl<sub>3</sub>, 298 K**



## CURRICULUM VITAE

### Personal Data:

Vogtei 20 B  
Kai Florian Gustav Averagesch 45239 Essen  
Born on the 3<sup>rd</sup> of July, 1988 in Essen Germany  
Family status: Single Ph.: +4915758506898  
Nationality: German kai.averesch@tu-dortmund.de

### Employment and Research History

---

<b>2016-2019</b>	PhD studies (continuation) at Georg August Universität Göttingen
<b>2016</b>	Internship at Bayer Research Center, Wuppertal
<b>2016</b>	Relocation with the research group to Georg August Universität Göttingen
<b>2015</b>	Commencement of PhD studies at the Max-Planck-Institut für Kohlenforschung with Prof. Dr. Manuel Alcarazo. On "Novel cationic Sulfur Reagents and their Application in Electrophilic Group Transfer Reactions"
<b>2014-2015</b>	Editorial work on supporting material and self-education of the book "Technische Biochemie – Die Biochemie und industrielle Nutzung von Naturstoffen" (eds. O. Kayser and N. Averagesch), ISBN: 978-3-658-05547-9
<b>2014</b>	Degree in Chemistry (Master of Science) from the TU Dortmund University, Germany (Prof. Dr. Arno Behr) on the "Ruthenium-catalyzed Tandem-reaction for the Synthesis of branched, primary higher Alcohols from 1-Alkenes"
<b>2013</b>	Internship at the Centre for Microbial Synthesis (CEMES) within the Advanced Water Management Centre (AWMC) at the University of Queensland, Australia
<b>2011</b>	Degree in Chemistry (Bachelor of Science) from the TU Dortmund University, Germany (Prof. Dr. Arno Behr) on the "Cooligomerization of Isobutene with Dienes"
<b>2011</b>	Student assistant at the chair for organic chemistry; supervision and assistance for undergraduate students in the degree-program chemistry or chemical biology at the TU Dortmund University

---

## Research Publications and Presentations

<b>2019</b>	K. F. G. Averesch, H. Pesch, C. Golz. M. Alcarazo, "Synthesis of Alkynylthiopyridinium Salts and Their Use as Thioketene Equivalents", <i>Chem. Eur.J.</i> <b>2019</b> , 25, 10472–10477.
<b>2013</b>	Attended 4th International Microbial Fuel Cell Conference (MFC4) in Cairns, Australia with a poster presentation

**Language Skills:** German (native), English (excellent command)